UNIVERSITÉ DE STRASBOURG

ÉCOLE DOCTORALE de Physique et chimie physique

ICPEES-UMR7515

THÈSE présentée par :

Alfred BAZIN

Soutenue le **16 Décembre 2021**

pour obtenir le grade de : **Docteur de l'université de Strasbourg**

Discipline/ Spécialité : Chimie des polymères

Développement de polyesters aromatiques biosourcés par catalyse enzymatique

THÈSE dirigée par :
Dr. POLLET Éric Maître de conférences, Université de Strasbourg

RAPPORTEURS :
Pr. HUMEAU Catherine Professeure, Université de Lorraine
Dr. PERUCH Frédéric Directeur de recherches CNRS, Bordeaux

AUTRES MEMBRES DU JURY :
Pr. JIERRY Loïc Professeur, Université de Strasbourg

MEMBRE INVITE :
Pr. AVÉROUS Luc Professeur, Université de Strasbourg

"*If you only do what you can do, you will never be more than who you are*."

Master Shifu

Remerciements

Mes premiers remerciements vont à mon directeur de thèse, Éric POLLET, pour m'avoir accueilli dans la BioTeam au sein de l'ICPESS (UMR7515). Je le remercie pour ses conseils ainsi que pour nos discussions grâce auxquelles j'ai beaucoup appris. Je le remercie enfin pour son encadrement durant toute la durée de ce projet ainsi que pour le temps qu'il m'a accordé notamment pour la correction et publication d'articles scientifiques.

Je remercie également madame Catherine HUMEAU, professeure au LRGP (UMR - 7274), ainsi que Frédéric PERUCH, directeur de recherche au LCPO (UMR – 5629) de m'avoir fait l'honneur d'être rapporteurs de ces travaux de thèse. J'exprime également ma gratitude au professeur Loïc JIERRY de l'ICS de Strasbourg (UPR22) qui a bien voulu être examinateur.

Je remercie le professeur Luc AVÉROUS pour son accueil au sein de son équipe, la BioTeam et le remercie également de participer comme membre invité du jury de cette thèse.

Je remercie ensuite tous mes collègues de la BioTeam et plus généralement de l'ICPEES pour leur sympathie et leur accompagnement tout au long de ce projet. Je remercie particulièrement Julien PEYRTON, mon collègue de bureau pour son accueil, ses conseils, nos nombreuses discussions, scientifiques ou non, et plus généralement son amitié. Je remercie également Sophie WENDELS pour son accueil au laboratoire et pour m'avoir aidé à mettre le pied à l'étrier. Je la remercie également chaleureusement pour l'amitié que nous avons construite durant ce projet. Je remercie chaleureusement Antoine DUVAL pour nos nombreuses discussions qui m'ont énormément enrichi et m'ont fait grandir durant ce projet. Bon courage pour ta vie de papa ! Je remercie l'ensemble des doctorants de la BioTeam avec qui j'ai pris un grand plaisir à travailler, mais également à lier des amitiés. Je remercie Alexis pour nos moments de jardinage et nos échanges, souvent culinaires, Agathe et Lisa pour leur bonne humeur qui, j'en suis sûr, leur permettront de surmonter les épreuves de la thèse.

Je souhaite également remercier les ex-doctorants et postdoctorants rencontrés durant mon projet. Je remercie Audrey pour nos nombreux échanges ainsi que pour avoir bien voulu me prêter son laboratoire de biologie. Je remercie Kim pour la bonne ambiance qu'elle a fait régner dans le laboratoire. Je remercie aussi Mohammad pour sa sympathie et son partage de la culture libanaise. Je remercie également Sébastien pour nos discussions qui m'ont beaucoup apporté (et pas seulement dans Fortnite). Je souhaite également remercier Marion et Mattéo avec qui j'ai pris grand plaisir à échanger, mais également à visiter les sentiers d'Alsace.

Je souhaite remercier Céline pour sa bonne humeur communicative. Je la remercie pour les nombreuses, très nombreuses analyses SEC. Un très grand merci à Christophe S. et Christophe M. pour leur gentillesse, pour nos échanges, mais également pour leur aide et leur expertise qui m'a été très

précieuse. Je remercie Catherine pour sa sympathie et pour m'avoir aidé à trouver mon chemin dans les méandres de l'administration.

Je souhaite remercier tout spécialement les membres du Jardin des Sciences et notamment Christelle et Marion. Grâce à leur expérience et aux activités qu'elles m'ont confiées, j'ai énormément appris sur la communication en science, mais également sur moi-même.

Je remercie mes amis que j'ai pour la plupart rencontrés à l'ECPM pour leur présence, même à distance lors des périodes de confinement. Je les remercie pour leur soutien, les weekends entre amis, les parties de jeu de rôle (notamment avec Eugénie, Laeranor, Lilithis et Krellian) et tout simplement leur amitié. Je souhaite notamment bon courage au docteur Fabien et aux futurs docteurs Alexandra, Camille, Cyrielle, Julia, Laure et Rodolphe.

Enfin, je remercie grandement ma famille et particulièrement ma maman pour son soutien. Je remercie également mes frères et sœurs Arthur, Albert et Juliette, ainsi que leurs pièces rapportées Étienne et Justine et mes neveux et nièces qui m'ont permis de sourire dans les étapes les plus difficiles.

Enfin, je remercie tout particulièrement Marine sans qui rien de tout cela n'aurait été possible.

Les chapitres de ce manuscrit de thèse sont rédigés sous la forme d'articles qui ont été ou vont prochainement être soumis à des revues relues par des pairs. Afin de rester fidèles au texte, ces articles sont donc rédigés en anglais et le reste du manuscrit est rédigé en français. Nous vous prions donc de bien vouloir être indulgent au regard du changement de langue et des répétitions que ce type de format pourrait engendrer.

Communications liées aux travaux de thèse

Publications

Les résultats présentés dans cette thèse font l'objet de 4 articles et d'une revue bibliographique.

Articles publiés :

- Bazin, A., Avérous, L. and Pollet, E. **(2021)** 'Lipase-catalyzed synthesis of furan-based aliphatic-aromatic biobased copolyesters: Impact of the solvent', *European Polymer Journal*, 159, p. 110717.
- Bazin, A., Avérous, L. and Pollet, E. (**2021**) 'Ferulic Acid as Building Block for the Lipase-Catalyzed Synthesis of Biobased Aromatic Polyesters', *Polymers*, 13(21), p. 3693.

Articles qui seront soumis ultérieurement :

- Bazin, A., Avérous, L. and Pollet, E. 'Enzymatic esterification, transesterification and polyesterification of aromatic acids from lignocellulosic biomass, a review'.
- Bazin, A., Steuer, M., Avérous, L. and Pollet, E. 'Photo-dimerization of ferulic derivatives for the CALB catalyzed synthesis of biobased cleavable polyesters'.
- Bazin, A., Duval, A., Avérous, L. and Pollet, E. 'Synthesis of biobased photo-crosslinkable polyesters based on caffeic acid through selective lipase-catalyzed polymerization'.

Article en collaboration :

- Magnin, A., Entzmann, L., Bazin, A., Pollet, E. and Avérous, L. **(2021)** 'Green Recycling Process for Polyurethane Foams by a Chem-Biotech Approach', *ChemSusChem*, 14(19), pp. 4234–4241.

Conférences

Les résultats présentés dans ce manuscrit on fait l'objet de communications orales dans des conférences nationales et internationales :

- Bazin, A., Pollet, E. **(3 juin 2021)** 'Enzymatic synthesis of biobased polyesters: Influence of aromatic furan-based monomers', *Soft Matter Meeting 2021*. Strasbourg.
- Bazin, A., Pollet, E. **(6 juillet 2021)** 'Enzymatic synthesis of biobased polyesters: Influence of aromatic furan-based monomers', *17e Journées Scientifiques du GFP-Section Est*. Strasbourg.

Liste des abréviations

A

AcFA	*p*-Acetyl ferulic acid
AFA	Arabinose ferulate
AnFaeA	*Aspergillus niger* Ferulic acid esterase A
AnFaeB	*Aspergillus niger* ferulic acid esterase B
AocFaeC	*Aspergillus ochraceus* ferulic acid esterase C
ATR-FTIR	Fourier transformed infrared spectroscopy with ATR module
a_w	Water activity

B

BDO	1,4-Butanediol
BTX	Benzene toluene xylene

C

CA	Caffeic acid
CALB	*Candida antarctica* lipase B
CD	Caffeic diol
$CDCl_3$	Deuterated chloroform
CLEA	Crosslinked enzyme aggregates
CRL	*Candida rugosa* lipase
CTAB	Cetyltrimethylammoniumbromide

D

Đ	Dispersity
DAcFA	Dimer of *p*-Acetyl ferulic acid
DCTB	2-[(2E)-3-(4-tert-Butylphenyl)-2-methylprop-2-enylidene]malononitrile
$DDeFA^{II}$	Dimer of diester of ferulic acid II
DEA	Diethyl adipate
DeDFA	Diester of dimer of ferulic acid
$DeFA^{I}$	Diester of ferulic acid I
$DeFA^{II}$	Diester of ferulic acid II
DES	Deep eutectic solvents
DIBAL-H	Diisobutyle aluminum hydride
DMF	Dimethyl formamide
DMFDC	dimethyl 2,5-furanedicarboxylate
DMSO-*d6*	Deuterated dimethyl sulfoxide
DP_n	Number degree of polymerization
DP_w	Mass degree of polymerization
DRX	Diffraction des rayons X
DSC	Differential scan calorimetry

F

FA	Ferulic acid
FAD^{I}	Ferulic acid-based diol I
FAD^{II}	Ferulic acid-based diol II
FAE	Ferulic acid esterase
FDA	Food and Drug Administration
FOE	*Fusarium oxysporum* Esterase
FoFAE-I	*Fusarium oxysporum* Ferulic acid esterase I
FoFAE-II	*Fusarium oxysporum* Ferulic acid esterase II
FSC	*Fusarium solani* cutinase
FTIR	Fourier transformed infrared spectroscopy

H

$H\text{-}DeFA^{I}$	Hydrogenated diester of ferulic acid I
$H\text{-}DeFA^{II}$	Hydrogenated diester of ferulic acid II
HDO	1,6-Hexanediol
HMF	Hydroxyméthyl furfural
HR-ESI-MS	High resolution electrospray ionization mass spectroscopy

I

I	Intensity
IL	Ionic liquids

IR	Infrared spectroscopy

L

Log P	Octanol/water partition coefficient

M

MDSC	Modulated Differential scan calorimetry
MeFA	Methyl ferulate
M_n	Number average molar mass
MSM	Memory shape materials
M_w	Mass average molecular mass

N

N435	Novozym 435
NMR	Nuclear magnetic resonance

O

ODO	1,8-Octanediol

P

PBAd	Poly(butylene adipate)
PBAd-co-PBF)	Poly(butylene adipate-co-furanoate)
PBF	poly(butylene furanoate)
PBS	Polybutylene succinate
PBSA	Polybutylene(adipate-co-succinate)
PBT	polybutylène terephthalate
PCL	Polycaprolactone
Pd/C	Palladium over activated charcoal
PDA	Photodiode array
$PDeFA^I$	Polymerized diester of ferulic acid I
$PDeFA^{II}$	Polymerized diester of ferulic acid II
PDO	1,3-Propanediol
PEF	Polyethylene furanoate
PEG	Polyethylene glycol
PET	Polyethylene terephthalate
PFA	Prenyl ferulate
$PFAD^I$	Polymerized ferulic acid-based diol I
$PFAD^{II}$	Polymerized ferulic acid-based diol II
PHA	Polyhydroxyalcanoate
PHAd	Poly(hexylene adipate)
PHAd-co-PHF	Poly(hexylene adipate-co-furanoate)
$PH\text{-}DeFA^I$	Polymerized hydrogenated diester of ferulic acid I
$PH\text{-}DeFA^{II}$	Polymerized hydrogenated diester of ferulic acid II
PHF	Poly(hexylene furanoate)
PLA	Polylactic acid
POC	Polymérisation par ouverture de cycle
PS	Polystyrene
PTT	Polypropylène téréphtalate

R

RI	Refractive Index
RML	*Rhizomucor miehei* lipase
RMN	Résonance magnétique nucléaire
RT	Room temperature

S

$ScCO_2$	Supercritical CO_2
SEC	Steric Exclusion Chromatography
SI	Supporting information
StFaeC	*Sporotrichum thermophile* ferulic acid esterase C

T

Tc	Crystallization temperature
$Td_{5\%}$	Temperature at 5% of mass loss
Td_{max}	Temperature of maximal mass loss rate
T_f	Température de fusion

X

TFA	Trifluoroacetic acid
T_g	Glass transition temperature
TGA	Thermogravimetric analysis
TLIM	Immobilised lipase from *Thermomyces lanuginosous*
T_m	Melting temperature

U

UV	Ultra-violet
UV-A	Light at $315 < \lambda < 400$ nm
UV-C	Light at $100 < \lambda < 280$ nm

W

wt %	Weight percent

X

XRD	X-ray diffraction

Sommaire

Remerciements III

Communications liées aux travaux de thèse VII
Publications VII
Conférences VII

Liste des abréviations IX

Sommaire XIII

Liste des illustrations XVII
Figures XVII
Schémas XXIV
Tableaux XXVI

Introduction générale 1
Références 5

Chapitre 1. Etat de l'art de l'utilisation de la catalyse enzymatique pour la fonctionnalisation, la modification ou la polymérisation de synthons aromatiques biosourcés. 7
Introduction chapitre 1 9
Sous-chapitre 1.1. Introduction à la synthèse de polyesters aromatiques biosourcés par catalyse enzymatique. 11
1. Les polyesters 13
2. Les polyesters biosourcés 14
3. La polymérisation enzymatique 19
3.1. La catalyse enzymatique 19
3.2. La lipase B de Candida antarctica 20
3.3. La synthèse de polyesters par la CALB 22
4. Références 26
Sous-chapitre 1.2. Enzymatic esterification, transesterification and polyesterification of aromatic acids from lignocellulosic biomass, a review 33
1. Introduction 35
2. Cinnamic and hydroxycinnamic derivatives 37
2.1. Impact of the substrate substitution and unsaturation 38
2.2. The screening of enzymes: 42
2.3. Impact of the solvent 51
3. Benzoic and hydroxybenzoic derivatives: 58
4. Gallic acid 63
4.1. Tannase 65
4.2. Other enzymes 69
5. Conclusion: 70
6. References 71
Conclusion chapitre 1 83

Chapitre 2. Synthèse de polyesters aromatiques à base de furane par catalyse enzymatique. . 85
Introduction chapitre 2 87
Chapitre 2 Lipase-catalyzed synthesis of furan-based aliphatic-aromatic biobased copolyesters: Impact of the solvent 89
1. Abstract 89
2. Introduction 89
3. Experimental part 91
3.1. Materials 91
3.2. Synthesis of the aliphatic-aromatic copolyesters 92
3.3. Influence of the solvent on the synthesis of PHF and PBF 93

3.4. Kinetics monitoring 93
3.5. Enzymatic activity assay 93
3.6. Characterizations 93
4. Results and discussions 94
4.1. Polyesters synthesis 94
4.2. Polyesters thermal properties 105
4.2.1. Thermal properties of PHAd-co-PHF and PBAd-co-PBF copolyesters 105
4.2.2. Thermal properties of the PHF and PBF synthesized in different solvents 108
5. Conclusion 108
6. References 109
Conclusion chapitre 2 115

Chapitre 3. L'acide férulique comme molécule plateforme pour la synthèse enzymatique de polyesters aromatiques biosourcés. 117
Introduction chapitre 3 119
Ferulic acid as building-block for the lipase-catalyzed synthesis of biobased aromatic polyesters 121
1. Abstract 121
2. Introduction 121
3. Materials and Methods 124
3.1. Materials 124
3.2. Characterization 124
3.3. Synthesis of ferulic diesters 125
3.4. Hydrogenation of the ferulic diesters 126
3.5. Synthesis of the ferulic diols 127
3.6. Enzymatic polymerization 127
*3.6.1. From ferulic-based diesters (**PDeFA**$^{I-II}$ and **PH-DeFA**$^{I-II}$): 127*
*3.6.2. From ferulic-based diols (**PFAD**$^{I-II}$): 128*
3.6.3. Recovery of the polyesters: 128
4. Results and discussion 128
4.1. Polyesters based on ferulic diesters. 128
4.2. Polyesters based on hydrogenated ferulic diesters. 131
4.3. Polyesters based on ferulic diols. 133
5. Conclusions 138
6. References 139
Conclusion chapitre 3 143

Chapitre 4. Dimères de dérivés d'acide férulique pour la synthèse enzymatique de polyesters aromatiques photo-dégradables. 145
Introduction chapitre 4 147
Sous-chapitre 4.1. Etude sur la dimérisation par irradiation UV de dérivés d'acide férulique 149
1. Introduction : 151
2. Etude de la réactivité en cycloaddition [2+2] de dérivés féruliques 153
2.1. Synthèse et caractérisation des dérivés de FA : 153
2.2. Essais de photo-dimérisation : 154
3. Conclusion : 160
4. Références 161
Sous-chapitre 4.2. Photo-dimerization of ferulic derivatives for the CALB catalyzed synthesis of biobased cleavable polyesters 165
1. Abstract 167
2. Introduction 167
3. Experimental section 170
3.1. Materials 170
3.2. Characterization 170
3.3. Synthesis of the monomers 171
*3.3.1. Acetyl ferulic acid (**AcFA**) 171*
*3.3.2. Diester of ferulic acid (**DeFA**^{II}) 172*
3.3.3. UV dimerization 172
*3.3.4. Diester of acetyl ferulic acid dimer (**DeDFA**): 173*
3.3.5. Enzymatic polymerization 173
3.3.6. Photo-depolymerization 173
4. Results and discussion 174
4.1. Synthesis of ferulic-based monomers for polymerization 174

4.2. Polymerization of ferulic-based dimers....179
4.3. Thermal properties of the polyesters....186
4.4. Photo-depolymerization of the polyester....188
5. Conclusion:....194
6. References....195
Conclusion chapitre 4....201

Chapitre 5. Synthèse par catalyse enzymatique de polyesters biosourcés photo-réticulables à partir d'acide caféique....203
Introduction chapitre 5....205
Synthesis of biobased photo-crosslinkable polyesters based on caffeic acid through selective lipase-catalyzed polymerization....207
1. Abstract....207
2. Introduction....207
3. Experimental section....209
3.1. Materials....209
3.2. Characterization....209
3.3. Ethyl caffeate....210
3.4. Ethyl 3,4-bis(hydroxyethyl)caffeate (CD)....211
3.5. Enzymatic Polymerization....211
3.6. UV irradiation of the polymers....211
3.7. Measurement of Gel Content....212
4. Results and discussion....212
4.1. Synthesis of the caffeic diol monomer....212
4.2. Synthesis of the polymer....213
4.3. Thermal properties:....218
4.4. Photo-crosslinking properties:....221
5. Conclusion....225
6. References....226
Conclusion chapitre 5....231

Conclusion générale et perspectives....233

Liste complète des références bibliographiques....241

Annexes....265
Annexes Chapitre 2 (supporting information)....267
Annexes Chapitre 3 (supporting information)....291
Annexes Chapitre 4 (supporting information)....305
Annexes Chapitre 5 (supporting information)....319

Liste des illustrations

Figures

Introduction

Figure 1: a) Répartition des polymères dans le packaging dans le monde en 2015 (Rabnawaz *et al.*, 2017) ; b) Production mondiale de fibres en 2018 (*Preferred Fiber & Materials, Market Report 2021*, 2021). 1

Figure 2: Capacités mondiales de production de matériaux plastiques biosourcés en 2020 (adapté de (*Bioplastics market data*, 2020)). 2

Chapitre 1

Sous-chapitre 1.1

Figure 1.1.1: représentation schématique de la synthèse du PET (adapté de (Ravindranath *et al.*, 1984)). 13

Figure 1.1.2: Capacités mondiales de production de matériaux plastiques biosourcés en 2020 (adapté de (*Bioplastics market data*, 2020)). 14

Figure 1.1.3: Représentation des polymères biosourcés PLA, PBS, PBSA et PHA. 16

Figure 1.1.4: Structure des polyesters aromatiques partiellement biosourcés PET, PTT et PBT. 17

Figure 1.1.5: Représentation du système clef-serrure de la catalyse enzymatique. 20

Figure 1.1.6: Représentation de la structure secondaire de la CALB. Les acides aminés du site actif sont représentés en bâtons. 20

Figure 1.1.7: Photo par microscopie électronique à balayage de billes de résine acrylique supportant la CALB ; b) Concentration relative en CALB au sein des billes acrylique du support (Mei *et al.*, 2003b)..... 21

Sous-chapitre 1.2

Figure 1.2.1: Count over the years of publications containing the word “ferulic acid”. From Web of Science, 2021..... 35

Figure 1.2.2: Examples of natural phenolics compounds investigated for the synthesis of high value-added products by enzyme-catalyzed esterification..... 37

Figure 1.2.3: Schematic representation of the most common natural cinnamic derivatives..... 37

Figure 1.2.4: Schematic representation of ferulic acid in its free, lignin-bound and crosslinked forms in hemicellulose. Adapted from (Oliveira et al., 2019; Terrett et al., 2019). 38

Figure 1.2.5: Conversion of the CALB-catalyzed transesterification of cinnamic methyl and ethyl ester derivatives with oleyl alcohol: a) ◇hydrogenated oleyl cinnamate, □ oleyl cinnamate; b) oleyl ◇ortho-hydroxycinnamate, □ meta-hydroxycinnamate and △ para-hydroxycinnamate; c) ◇hydrogenated oleyl caffeate, □ oleyl caffeate. Reproduced from (Weitkamp *et al.*, 2006). 40

Figure 1.2.6: Comparison of the conversion of benzyl cinnamate obtained by esterification of cinnamic acid with benzyl alcohol with different biocatalysts. Adapted from (Sun *et al.*, 2018a). 43

Figure 1.2.7: Evolution over time of the yield in PFA obtained by FAE-catalyzed esterification of prenol with various ferulic moieties: ● Vinyl ferulate, ○ Vinyl ferulate and stirring, ■ Methyl ferulate and □ Ferulic acid. Reproduced from (Antonopoulou et al., 2017)..... 48

Figure 1.2.8: Ratio of arabinose ferulate (AFA) and ferulic acid (FA) in the reaction medium for the transesterification of arabinose with vinyl ferulate catalyzed with different enzymes. Reproduced from (Antonopoulou *et al.*, 2018). 48

Figure 1.2.9: Binding of the methyl caffeate with the AnFaeA active site: a) catalytic energetically favorable orientation; b) non-catalytic also energetically favorable orientation. Reproduced from (Hunt *et al.*, 2017). 50

Figure 1.2.10: Effect of the solvent on the transesterification of ferulic acid with phosphatidylcholine. Reproduced from (Rychlicka *et al.*, 2020). 53

Figure 1.2.11: Yield of the lipase-catalyzed esterification of ferulic acid with butanol in common organic solvents and ionic liquids. The reaction was catalyzed by CALB (black symbols) or RML (white symbols). Reproduced from (Katsoura *et al.*, 2009)..... 55

Figure 1.2.12: Structures of the various IL employed for enzyme-catalyzed esterification and transesterification reactions. 56

Figure 1.2.13: Effect of vacuum on the CALB-catalyzed transesterification of ferulic acid with castor oil (EF: Ethyl ferulate). Reproduced from (Sun *et al.*, 2015). 57

Figure 1.2.14: AnFaeA-catalyzed transesterification of cinnamic derivatives with butanol: a) Free enzyme; b) Enzyme immobilized as CLEA. Reproduced from (Grajales-Hernández et al., 2020). 58

Figure 1.2.15: Schematic representation of the more common natural benzoic derivatives. 59

Figure 1.2.16: Yield of the CALB-catalyzed esterification of cinnamic and benzoic derivatives with glucose; Influence of the chain length, substitution of the aromatic ring and functionality of the acyl chain. “no rxn” stands for no product detected. Reproduced from (Otto *et al.*, 2000). 60

Figure 1.2.17: Structure of the main phytosterols present in the mixture employed by Tan *et al*. (Tan *et al.*, 2013). 61

Figure 1.2.18: Structure of the gallic acid. 64

Figure 1.2.19: Schematic structure of classified tannins (Sharma *et al.*, 2019) (de Hoyos-Martínez *et al.*, 2019). 64

Figure 1.2.20: Yield of propyl gallate obtained through the tannase-catalyzed esterification of gallic acid with propanol in solvents with different logP for 12 h. Data from (Yu *et al.*, 2004a). 67

Figure 1.2.21: Principle of the bio-imprinting. Adapted from (Rich et al., 2002). 68

Chapitre 2

Figure 2.1: Examples of polyesters synthesis from biobased aromatic building blocks. 90

Figure 2.2: CALB-catalyzed synthesis of poly(hexylene adipate)-co-(hexylene furanoate) and poly(butylene adipate)-co-(butylene furanoate) 91

Figure 2.3: ^{1}H NMR spectra of the enzymatically synthesized PHAd-co-PHF 95

Figure 2.4: Time evolution of the M_n values determined by NMR spectroscopy of the PHAd-co-PHF. ● PHAd, ▲ 10% of DMFDC, ▬ 30% of DMFDC, ○ 50% of DMFDC, ◊ 70% of DMFDC, ♦ 90% of DMFDC, ■ PHF . 98

Figure 2.5: Time evolution of the M_n values determined by NMR spectroscopy of the PBAd-co-PBF. ● PBAd, ▲ 10% of DMFDC, ▬ 30% of DMFDC, ○ 50% of DMFDC, ◊ 70% of DMFDC, ♦ 90% of DMFDC, ■ PBF.. 99

Figure 2.6: Determined ratios of aromatic moieties in the PHAd-co-PHF depending on time for different ratio of DMFDC..... 100

Figure 2.7: Determined ratios of aromatic moieties in the PBAd-co-PBF depending on time for different ratio of DMFDC..... 100

Figure 2.8: MALDI-TOF-MS spectra of PHF synthesized in a) diphenyl ether and b) acetophenone with c) corresponding end-groups identification..... 104

Figure 2.9: Assessment of the activity of CALB with diethyl adipate and 1-butanol..... 104

Figure 2.10: CALB catalyzed conversion of diethyl adipate with 1-butanol in various solvents: ▲ Diphenyl ether, ■ Acetophenone, ♦ Anisole. 105

Figure 2.11: Evolution of Tg of the PHAd-co-PHF with different proportions of DMFDC (experimental data compared to the theoretical ones from Fox equation) 106

Figure 2.12: Evolution of Tg of the PBAd-co-PBF with different proportions of DMFDC (experimental data compared to the theoretical ones from Fox equation) 107

Figure 2.13: TGA measurements of PHAd-co-PHF with different ration of DMFDC ▬ PHAd, ▬ 10% of DMFDC, ▬ 30% of DMFCD, ▬ 50% of DMFDC, ▬ 70% of DMFDC, ▬ 90% of DMFDC, ▬ PHF 107

Chapitre 3

Figure 3.1: NMR spectra in $CDCl_3$ of the ferulic-based diesters and their corresponding polyesters: (a) $DeFA^{I}$ and $PDeFA^{I}$; (b) $DeFA^{II}$ and $PDeFA^{II}$. 130

Figure 3.2: Molar mass of the polymers synthesized from the hydrogenated monomers. ■ $PH\text{-}DeFA^{I}$, ▲ $PH\text{-}DeFA^{II}$. 131

Figure 3.3: Thermal analysis of $PH\text{-}DeFA^{I}$ and $PH\text{-}DeFA^{II}$: (a) DSC measurement, heating rate 10 °C/min, data have been offset one from another by -0.5 $W.g^{-1}$; (b) TGA measurement, under air at a heating rate of 10 °C/min. 133

Figure 3.4: Molar masses of the polyesters synthesized from the ferulic-based diols. ■ $PFAD^{I}$, ▲ $PFAD^{II}$. ... 135

Figure 3.5: (a) MALDI-TOF MS spectrum of $PFAD^{I}$; (b) corresponding identified polymer structures. 135

Figure 3.6: Thermal analysis of $PFAD^{I}$ and $PFAD^{II}$: (a) DSC measurement, heating rate 10 °C/min, data have been offset one from another by -0.5 $W.g^{-1}$; (b) TGA measurement, under air at a heating rate of 10 °C/min. . 136

Chapitre 4

Sous-chapitre 4.1

Figure 4.1.1: Représentation schématique de l'arrangement des molécules d'acide cinnamique dans les formes cristallines α, β et γ . Adapté de (Ramamurthy *et al.*, 1987). 152

Figure 4.1.2: Représentation de la structure des acides truxillique et truxinique. 152

Figure 4.1.3 : Structure des dérivés de FA étudiés en photodimérisation. 153

Figure 4.1.4 : Spectres de RMN ^{1}H des produits issus de l'irradiation à 350 nm dans le cyclohexane des dérivés de FA : a) FA ; b) MeFA ; c) AcFA ; d) $DeFA^{I}$ et e) $DeFA^{II}$. 155

Figure 4.1.5 : Représentation de l'arrangement du FA sous forme cristalline. Adapté de (Nethaji *et al.*, 1988).156

Figure 4.1.6 : Proportions en produit de départ, isomère *cis* et dimère obtenus après irradiation des dérivés de FA sous UV (λ = 350 nm) pendant 24 heures dans le cyclohexane. 157

Figure 4.1.7 : Représentation de l'arrangement du AcFA sous forme cristalline. Adapté de (Lee *et al.*, 1988). 158

Figure 4.1.8 : Représentation des deux dimères possibles par cycloaddition du AcFA. 158

Figure 4.1.9 : Représentation de l'arrangement du $DeFA^{II}$ sous forme cristalline tel que déterminé par DRX. . 159

Figure 4.1.10: Représentation du dimère obtenu par cycloaddition du $DeFA^{II}$ sous UV dans le cyclohexane. a) Représentation tridimensionnelle issu de l'analyse par DRX, b) Représentation schématique. 160

Sous-chapitre 4.2

Figure 4.2.1: Yield of the dimer, *cis* isomer and starting product after exposition of AcFA to UV light (350 nm) for 24 hours in different solvents. All measurements were performed on triplicates. 175

Figure 4.2.2: Yield of the dimer, *cis* isomer and starting product after exposition of $DeFA^{II}$ to UV light (350 nm) for 24 hours in different solvents. All measurements were performed on triplicates. 177

Figure 4.2.3: Schematic representation of the two possible isomers resulting from the [2+2] cycloaddition reaction of $DeFA^{II}$. 178

Figure 4.2.4: Head-to-tail structure of $DDeFA^{II}$ determined by XRD analysis: a) Three-dimensional crystalline conformation; b) schematic representation. 179

Figure 4.2.5: NMR spectra of: a) $DDeFA^{II}$ and b) the polyester synthesized from $DDeFA^{II}$ and HDO. 180

Figure 4.2.6: Time evolution of Mn values during the polymerization of $DDeFA^{II}$ with diols of different length. Each measurement was performed in triplicates. 181

Figure 4.2.7: Calculated ratio of ester end-groups in the polyesters synthesized with diols of different lengths. Each measurement was performed in triplicates. 182

Figure 4.2.8: SEC analyses of the polyesters synthesized from $DDeFA^{II}$ and diols of different lengths (diphenyl ether, 90°C, partial vacuum): a) Time evolution of M_n values; b) Chromatogram at 48 hours of reaction, values calculated from PS calibration curve and normalized on the area, logarithmic scale. 183

Figure 4.2.9: Molar masses of the PDO and BDO-based polyester synthesized with and without an excess of diol: a) M_n, M_w measured by SEC and M_n measured by NMR after 48h of reaction; b) SEC elution profile, values calculated from PS calibration curve and normalized by area, logarithmic scale. 184

Figure 4.2.10: DSC second heating scans of polyesters synthesized from $DDeFA^{II}$ with different diols. Heating rate = 10°C.min^{-1}. Curves are offset by 0.3 W.g^{-1} from each other (Exo Up). 187

Figure 4.2.11: DSC second heating scans of polyesters synthesized from $DDeFA^{II}$ with PDO and BDO in different ratio. Heating rate = 10°C.min^{-1}. Curves are offset by 0.3 W.g^{-1} from each other (Exo Up). 187

Figure 4.2.12: TGA thermal weight loss analysis of polyesters synthesized from $DDeFA^{II}$ with different diols. Heating rate = 10°C.min^{-1}, under air. 188

Figure 4.2.13: Absorbance of the polyesters after various times of UV-C irradiation: a) Absorbance spectra between 250 and 500 nm of the HDO-based polyester; b) maximum of absorbance between 300 and 400 nm for the polyesters synthesized from diols of different lengths with exponential model fitting. 190

Figure 4.2.14: Yield in double bond formation measured from NMR analyses as a function of UV-C irradiation time for the polyester synthesized from $DDeFA^{II}$ and HDO. 191

Figure 4.2.15: Yield in double bond formation measured from NMR analyses after UV-C irradiation (600s, RT) for the polyester synthesized from $DDeFA^{II}$ and diols of different lengths. 191

Figure 4.2.16: Degree of polymerization as a function of UV-C irradiation time for the polyester synthesized from $DDeFA^{II}$ and HDO ♦ DP_w, ♦ $DP_{n(sec)}$, ♦ $DP_{n(NMR)}$. 193

Figure 4.2.17: SEC molar mass distribution as a function of UV-C irradiation time for the polyester synthesized from $DDeFA^{II}$ and HDO. Values given as PS equivalent and normalized by area, logarithmic scale. 193

Figure 4.2.18: Absorbance of the polyester photodegraded under UV-C and subsequently irradiated under UV-A: a) Absorbance spectra between 250 and 500 nm of the HDO-based at different UV-A irradiation times; b) maximum of absorbance between 300 and 400 nm as a function of UV-A irradiation time for the polyester synthesized from diols of different lengths and exponential model fitting. 194

Chapitre 5

Figure 5.1: ^{1}H NMR analysis of the ethyl 3,4-bis(hydroxyethyl)caffeate (CD) a) before UV irradiation; b) after irradiation at 350 nm for 24h in cyclohexane. 213

Figure 5.2: ^{1}H NMR analysis and interpretation of the polyester containing 50 % of CD (24 h, diphenyl ether, partial vacuum). 215

Figure 5.3: FTIR transmittance spectra of the polyesters containing 0, 10 and 50 of CD. Curves are offset by 30 % from each other. 216

Figure 5.4: SEC analysis results of the polyesters synthesized with various ratios of CD (20 %wt CALB, 24 h, diphenyl ether, partial vacuum). 218

Figure 5.5: DSC analysis of the polyesters synthesized with various ratios of CD. Second heating scan, heating rate: 10 °C.min^{-1}. 219

Figure 5.6: Glass transition temperature of the polyesters synthesized with various ratios of CD fitted with Fox laws calculated on all experimental data or extrapolated from first measurements. 220

Figure 5.7: TGA analysis under air of the polyesters synthesized with various ratio of CD. Heating rate: 20 °C.min^{-1}. 221

Figure 5.8: Measurement of the absorbance of the polyester containing 10 % of CD. a) Absorption spectra between 500 and 200 nm for various times of UV-A irradiation and b) Evolution of the maximum of absorption against UV-A irradiation time. 222

Figure 5.9: Soluble (in THF) and insoluble fractions of polyesters synthesized with various ratios of CD after crosslinking under UV light at 350 nm and swelling in THF for 48h. 223

Figure 5.10: Absorption spectra of the polyester containing 10 % of CD before irradiation, after irradiation under UV-A (250 min at 350 nm) and after subsequent irradiation under UV-C (5 min at 254 nm). 224

Annexes

Annexes chapitre 2

Figure S2.1: NMR spectrum of PHAd in $CDCl_3$ ... 267
Figure S2.2: NMR spectrum of PHF10 in $CDCl_3$ ... 267
Figure S2.3: NMR spectrum of PHF30 in $CDCl_3$ ... 268
Figure S2.4: NMR spectrum of PHF50 in $CDCl_3$ ... 268
Figure S2.5: NMR spectrum of PHF70 in $CDCl_3$ ... 269
Figure S2.6: NMR spectrum of PHF90 in $CDCl_3$ ... 269
Figure S2.7: NMR spectrum of PHF in $CDCl_3$ ... 270
Figure S2.8: COSY NMR analysis of PHF50 in $CDCl_3$ ... 270
Figure S2.9: HSQC NMR analysis of PHF50 in $CDCl_3$ ... 271
Figure S2.10: HMBC NMR analysis of PHF50 in $CDCl_3$ ... 271
Figure S2.11: NMR spectrum of PBAd in $CDCl_3$ ... 272
Figure S2.12: NMR spectrum of PBF10 in $CDCl_3$ ... 272
Figure S2.13: NMR spectrum of PBF30 in $CDCl_3$ ... 273
Figure S2.14: NMR spectrum of PBF50 in $CDCl_3$ ... 273
Figure S2.15: NMR spectrum of PBF70 in $CDCl_3$ ... 274
Figure S2.16: NMR spectrum of PBF90 in $CDCl_3$ ... 274
Figure S2.17: NMR spectrum of PBF in $CDCl_3$ ... 275
Figure S2.18: SEC elution curves of the PHAd-co-PHF. The intensities have been normalised by area. ... 275
Figure S2.19: SEC elution curves of the PBAd-co-PBF. The intensities have been normalised by area. ... 276
Figure S2.20: Stacked representation of the DSC analyses of the PHAd-co-PHF with various proportions of DMFDC. The heating was 10°C/min and the cooling rate 5°C/min. ... 277
Figure S2.21: Stacked representation of the MDSC analyses of the PHAd-co-PHF with various proportions of DMFDC. The heating rate was 2°C/min modulated with an amplitude of 1.20°C every 60 seconds. ... 277
Figure S2.22: Stacked representation of the DSC analyses of the PBAd-co-PBF with various proportions of DMFDC. The heating was 10°C/min and the cooling rate 5°C/min. ... 278
Figure S2.23: Stacked representation of the MDSC analyses of the PBAd-co-PBF with various proportions of DMFDC. The heating rate was 2°C/min modulated with an amplitude of 1.20°C every 60 seconds. ... 278
Figure S2.24: Weight loss curves of the PHAd-co-PHF with various proportions of DMFDC from TGA with a heating rate of 10°C/min. Each curve is offset by 4 wt.% from the previous one. ... 279
Figure S2.25: Derivative weight loss curves of the PHAd-co-PHF with various proportions of DMFDC from TGA with a heating rate of 10°C/min. Each curve is offset by 1 unit from the previous one. ... 279
Figure S2.26: Weight loss curves of the PBAd-co-PBF with various proportions of DMFDC from TGA with a heating rate of 10°C/min. Each curve is offset by 4 wt.% from the previous one. ... 280
Figure S2.27: Derivative weight loss curves of the PHAd-co-PHF with various proportions of DMFDC from TGA with a heating rate of 10°C/min. Each curve is offset by 1 unit from the previous one. ... 280
Figure S2.28: Stacked representation of the MDSC analyses of the PHF synthesized in different solvents. The heating rate was 2°C/min modulated with an amplitude of 1.20°C every 60 seconds. ... 281
Figure S2.29: Stacked representation of the MDSC analyses of the PBF synthesized in different solvents. The heating rate was 2°C/min modulated with an amplitude of 1.20°C every 60 seconds. ... 281
Figure S2.30: Stacked representation of the DSC analyses of the PHF synthesized in different. The heating was 10°C/min and the cooling rate 5°C/min. ... 282

Figure S2.31: Stacked representation of the DSC analyses of the PBF synthesized in different. The heating was 10°C/min and the cooling rate 5°C/min. 282
Figure S2.32: NMR spectrum of PHF synthesized in diphenyl ether in $CDCl_3$. 283
Figure S2.33: NMR spectrum of PHF synthesized in toluene in $CDCl_3$. 283
Figure S2.34: NMR spectrum of PHF synthesized in phenetole in $CDCl_3$ 284
Figure S2.35: NMR spectrum of PHF synthesized in anisole in $CDCl_3$ 284
Figure S2.36: NMR spectrum of PHF synthesized in acetophenone in $CDCl_3$. 285
Figure S2.37: NMR spectrum of PHF synthesized in cyclohexanone in $CDCl_3$. 285
Figure S2.38: NMR spectrum of PBF synthesized in diphenyl ether in $CDCl_3$ 286
Figure S2.39: NMR spectrum of PBF synthesized in toluene in $CDCl_3$. 286
Figure S2.40: NMR spectrum of PBF synthesized in phenetole in $CDCl_3$. 287
Figure S2.41: NMR spectrum of PBF synthesized in anisole in $CDCl_3$. 287
Figure S2.42: NMR spectrum of PBF synthesized in acetophenone in $CDCl_3$ 288
Figure S2.43: NMR spectrum of PBF synthesized in cyclohexanone in $CDCl_3$ 288
Figure S2.44: Reaction medium of the PHF synthesis in acetophenone after 24h of reaction. 289
Figure S2.45: MALDI-TOF-MS analysis of PHF synthesized in anisole. 289
Figure S2.46: MALDI-TOF-MS analysis of PBF synthesized in diphenyl ether. 289
Figure S2.47: MALDI-TOF-MS analysis of PBF synthesized in anisole. a: full view, b: zoom. 290
Figure S2.48: MALDI-TOF-MS analysis of PBF synthesized in acetophenone. a: full view, b: zoom. 290

Annexes chapitre 3

Figure S.3.1: ^{1}H NMR analysis of methyl ferulate (MeFA). 291
Figure S.3.2: ^{1}H NMR analysis of methyl 4-(methyl ethanoate-oxy)-ferulate ($DeFA^{I}$) 291
Figure S.3.3: ^{1}H NMR analysis of methyl 4-(methyl butanoate-oxy)-ferulate ($DeFA^{II}$). 292
Figure S.3.4: ^{1}H NMR analysis of methyl 3-(3-methoxy-4-(2-methoxy-2-oxoethoxy)phenyl)propanoate (H-$DeFA^{I}$). 292
Figure S.3.5: ^{1}H NMR analysis of methyl 4-(2-methoxy-4-(3-methoxy-3-oxopropyl)phenoxy)butanoate (H-$DeFA^{II}$). 293
Figure S.3.6: ^{1}H NMR analysis of 4-(hydroxyethoxy)-coniferyl alcohol (FAD^{I}) 293
Figure S.3.7: ^{1}H NMR analysis of 4-(hydroxybutoxy)-coniferyl alcohol (FAD^{II}) 294
Figure S.3.8: ^{13}C NMR analysis of Methyl ferulate (MeFA) 295
Figure S.3.9: ^{13}C NMR analysis of methyl 4-(methyl ethanoate-oxy)-ferulate ($DeFA^{I}$) 295
Figure S.3.10: ^{13}C NMR analysis of methyl 4-(methyl butanoate-oxy)-ferulate ($DeFA^{II}$) 296
Figure S.3.11: ^{13}C NMR analysis of methyl 3-(3-methoxy-4-(2-methoxy-2-oxoethoxy)phenyl)propanoate (H-$DeFA^{I}$). 296
Figure S.3.12: ^{13}C NMR analysis of methyl 4-(2-methoxy-4-(3-methoxy-3-oxopropyl)phenoxy)butanoate (H-$DeFA^{II}$). 297
Figure S.3.13: ^{13}C NMR analysis of 4-(hydroxyethoxy)-coniferyl alcohol (FAD^{I}) 297
Figure S.3.14: ^{13}C NMR analysis of 4-(hydroxybutoxy)-coniferyl alcohol (FAD^{II}) 298
Figure S.3.15: HMBC NMR analysis of methyl 4-(methyl butanoate-oxy)-ferulate ($DeFA^{II}$) in $CDCl_3$ 299
Figure S.3.16: HSQC NMR analysis of methyl 4-(methyl butanoate-oxy)-ferulate ($DeFA^{II}$) in $CDCl_3$ 299
Figure S.3.17: ^{1}H NMR analysis of poly(butylene-co-4-(methyl ethanoate-oxy)-ferulate) ($PDeFA^{I}$) 300
Figure S.3.18: ^{1}H NMR analysis of poly(butylene-co-4-(methyl butanoate-oxy)-ferulate) ($PDeFA^{II}$) 300

Figure S.3.19: ^{1}H NMR analysis of poly(butylene-co-3-(3-methoxy-4-(2-methoxy-2-oxoethoxy)phenyl)propanoate) (PH-DeFA^{I})..... 301

Figure S.3.20: ^{1}H NMR analysis of poly(butylene-co-4-(2-methoxy-4-(3-methoxy-3-oxopropyl)phenoxy)butanoate) (PH-DeFA^{II})..... 301

Figure S.3.21: ^{1}H NMR analysis of poly(4-(hydroxyethoxy)-coniferylene -co-adipate) (PFAD^{I})..... 302

Figure S.3.22: ^{1}H NMR analysis of poly(4-(hydroxybutoxy)-coniferylene-co-adipate) (PFAD^{II})..... 302

Figure S.3.23: SEC analyses in THF of the ferulic diester-based polyesters PDeFA^{I} and PDeFA^{II} (curves were normalised by their area)..... 303

Figure S.3.24: SEC analyses in THF of the hydrogenated ferulic diester-based polyesters PH-DeFA^{I} and PH-DeFA^{II} (curves were normalised by their area)..... 303

Figure S.3.25: SEC analyses in THF of ferulic diol-based polyesters PFAD^{I} and PFAD^{II} (curves were normalised by their area)..... 303

Figure S.3.26: MALDI-TOF MS analysis of PFAD^{I} obtained with 1.1 equivalent of diol in comparison to the diester after 24hours of synthesis in acetophenone at 90°C and under reduced pressure (a) MALD^{I}-TOF MS analysis, (b) mass of the corresponding end-groups..... 304

Figure S.3.27: SEC analyses in THF of ferulic diol-based polyesters PFAD^{I} with and without excess of diol (curves were normalized by their area)..... 304

Annexes chapitre 4

Figure S4.1: ^{1}H NMR analysis of the *p*-acetyl ferulic acid (AcFA)..... 305

Figure S4.2: ^{13}C NMR analysis the *p*-acetyl ferulic acid (AcFA)..... 305

Figure S4.3: ^{1}H NMR analyses of AcFA exposed to UV light at a wavelength of 350 nm for 24 hours in different solvents. a) cyclohexane, b) ethyl acetate, c) acetonitrile, d) water. 306

Figure S4.4: ^{1}H NMR analysis of the dimer of *p*-acetyl ferulic (DAcFA) synthesized in water..... 307

Figure S4.5: ^{13}C NMR analysis of the dimer of *p*-acetyl ferulic (DAcFA) synthesized in water..... 307

Figure S4.6: ^{1}H NMR analysis of the dimer of ethyl ferulate (DeDFA). 308

Figure S4.7: ^{13}C NMR analysis of the dimer of ethyl ferulate (DeDFA). 308

Figure S4.8: NMR analyses of methyl 4-(methyl butanoate-oxy)-ferulate (DeFA^{II}) exposed to UV light (350 nm) for 24 hours in different solvents. a) cyclohexane, b) ethyl acetate, c) acetonitrile, d) water..... 309

Figure S4.9: Vials containing DeFA^{II} solubilized or suspended is different solvent 309

Figure S4.10: ^{1}H NMR analysis of the dimer of methyl 4-(methyl butanoate-oxy)-ferulate (DDeFA^{II}) synthesized in water..... 310

Figure S4.11: ^{13}C NMR analysis of the dimer of methyl 4-(methyl butanoate-oxy)-ferulate (DDeFA^{II}) synthesized in water..... 310

Figure S4.12: XRD analysis of DDeFA^{II}..... 311

Figure S4.13: XRD analysis of DeFA^{II}..... 312

Figure S4.14: ^{1}H NMR analysis of the medium of reaction of DeDFA with an excess of butanol (CALB, in diphenyl ether, 90°C, 16 h). 313

Figure S4.15: ^{1}H NMR analyses of polyesters synthesized from DDeFA^{II} and diols of different lengths through CALB-catalyzed polymerization (diphenyl ether, 90°C, 48h, partial vacuum). Diols employed for the reaction: a) PDO; b) BDO; c) HDO; d) ODO. 313

Figure S4.16: SEC chromatogram of polyesters synthesized from DDeFA^{II} with different ratio of PDO through CALB catalyzed polymerization (diphenyl ether, 90°C, 48h, partial vacuum) 314

Figure S4.17: ^{1}H NMR analyses of the polyester synthesized from DDeFA^{II} and HDO after different times of UV-C light irradiation..... 314

Figure S4.18: ^{1}H NMR analyses of polyesters synthesized from DDeFA^{II} and diols of different length after UV-C irradiation (600 seconds, RT) : a) PDO; b) BDO; c) HDO; d) ODO..... 315

Figure S4.19: SEC chromatograms of polyesters synthesized from DDeFA^{II} and diols of different length after UV-C irradiation under (600 seconds, RT): a) PDO; b) BDO; c) HDO; d) ODO. 315

Figure S4.20: Detail of the calculation of the DP_n of the oligo-esters after photo-depolymerization. 316

Figure S4.21: NMR analysis of the polyester synthesized from DDeFA^{II} and HDO, initially photodepolymerized under UV-C irradiation for 600s and subsequently repolymerized under UV-A light for 120 minutes. 317

Annexes chapitre 5

Figure S5.1: ^{1}H NMR analysis of ethyl caffeate. 319

Figure S5.2: ^{13}C NMR analysis of ethyl caffeate. 319

Figure S5.3: ^{1}H NMR analysis of ethyl 3,4-bis(hydroxyethyl) caffeate (CD). 320

Figure S5.4: ^{13}C NMR analysis of ethyl 3,4-bis(hydroxyethyl) caffeate (CD). 320

Figure S5.5: NMR analyses of polyesters synthesised with different CD ratios (CALB in diphenyl ether, 90 °C, 24 h under partial vacuum). 321

Figure S5.6: FTIR analyses of polyesters synthesised with different CD ratios (CALB in diphenyl ether, 90 °C, 24 h under partial vacuum). 321

Figure S5.7: Integration of the FTIR bands attributed to the CD in the polyesters against the ratio of CD. 322

Figure S5.8:.SEC analyses of polyesters synthesised with different CD ratios (CALB in diphenyl ether, 90 °C, 24 h under partial vacuum). a: refractive index detector, intensity normalised by area, b: UV detector, intensity normalised according to area in RI detection. 322

Figure S5.9: Measurement of the absorbance of the polyester containing 50 % of CD. a) Absorption spectra between 500 and 200 nm for various times of UV-A irradiation. b) Evolution of the maximum of absorption against UV-A irradiation time. 322

Figure S5.10: Absorption spectra of the polyester containing 10 % of CD before and after sunlight irradiation (7 h exposure). 323

Figure S5.11: Visual aspect of the polyester containing 20 %CD irradiated under UV-A light after swelling in THF for 48 h. 323

Figure S5.12: ^{1}H NMR analyses of the soluble fraction (in THF) recovered from gel content tests of the polyesters containing 10 % and 20 % of CD before and after irradiation under UV-A light. 323

Figure S5.13: SEC analyses of the soluble fraction (in THF) recovered from the polyesters containing different ratio of CD before and after irradiation under UV-A light. a) 10 % of CD, b) 20 % of CD. Intensity normalised by the curve area. 324

Figure S5.14: FTIR transmittance spectra of the polyester containing 10 % of CD before and after irradiation under UV-A (insoluble fraction), data offset by 30 % from each other. 324

Figure S5.15: Absorption spectra of the polyester containing 50 % of CD before irradiation, after irradiation under UV-A (250 min at 350 nm) and after subsequent irradiation under UV-C (5 min at 254 nm). 325

Figure S5.16: FTIR analyses of the insoluble fraction of the polyester containing 10, 20 and 50 % of CD induced by UV-A irradiation after exposure to UV-C light (10 minutes) 325

Schémas

Chapitre 1

Sous-chapitre 1.1

Schéma 1.1.1: Synthèse de PEF à partir FDCA provenant de la biomasse (Sajid *et al.*, 2018)..... 17

Schéma 1.1.2: Synthèse du poly(éthylène vanillate) : a) à partir d'acide p-hydroxyethoxyvanillique (Xanthopoulou *et al.*, 2021) ; b) à partir d'acide vanillique estérifié et de carbonate d'éthylène (Gioia *et al.*, 2016). 18

Schéma 1.1.3: Synthèse de copolyesters semi-aromatiques à base d'acide férulique, d'ε-caprolactone et de lactide. 18

Schéma 1.1.4: Mécanisme de la transestérification catalysé par la triade catalytique de la CALB. 21

Schéma 1.1.5: Réactions se produisant au cours de la polymérisation enzymatique par polycondensation (adapté de (Jiang *et al.*, 2016)) 23

Schéma 1.1.6: a) Synthèse enzymatique de PBS (Azim *et al.*, 2006), b) synthèse enzymatique de polyesters à base d'isosorbide, 1 < x < 9 (Juais *et al.*, 2010). 24

Schéma 1.1.7: Synthèse enzymatique de polyester à partir de diméthyle ester de FDCA (Jiang *et al.*, 2015). 25

Schéma 1.1.8: Synthèse enzymatique de polyesters à base de diester de FDCA par POC (Flores *et al.*, 2019). .. 25

Schéma 1.1.9: Synthèse de précurseurs à base d'hydroxyméthylfurfural pour la synthèse enzymatique de polyesters biosourcés (Muthusamy et al., 2018). 26

Sous-chapitre 1.2

Scheme 1.2.1: Aromatic acids and alcohols tested in the CALB-catalyzed esterification for the synthesis of biobased antimicrobial compounds. Adapted from (Stevenson et al., 2007). 41

Scheme 1.2.2: Synthesis of feruloylated chromogenic compounds by TLIM-catalyzed transesterification: a) study of the impact of the alcohol structure on the enzyme reactivity; b) Selective synthesis of a chromogenic compound from a diol. Adapted from (Gherbovet *et al.*, 2020) 44

Scheme 1.2.3: FAE catalyzed esterification and transesterification of ferulic moieties with prenol. Adapted from (Antonopoulou et al., 2017) 47

Scheme 1.2.4: FAE catalyzed esterification and transesterification of vinyl ferulate with L-arabinose. Adapted from (Antonopoulou *et al.*, 2018). 48

Scheme 1.2.5: Transesterification of ethyl ferulate with phosphatidylcholine (Yang *et al.*, 2013; Rychlicka *et al.*, 2020). 53

Scheme 1.2.6: Comparison of the transesterification of cinnamic and benzoic vinyl esters with arbutin catalyzed by the lipase from *Penicillium expansum*. Adapted from (Yang et al., 2010). 61

Scheme 1.2.7: CALB-catalyzed polymerization of a benzoic acid derivative. Adapted from (Fodor *et al.*, 2017). 63

Chapitre 3

Scheme 3.1: Representation of the synthesis of polyesters from ferulic derivatives of different length as well as with and without hydrogenation. Adapted from (Nguyen *et al.*, 2015). 123

Scheme 3.2: Synthesis and polymerization of the ferulic diesters $DeFA^{I}$ and $DeFA^{II}$, i: MeOH, H_2SO_4, 70 °C 16h. ii(a): Methyl chloroacetate, K_2CO_3, KI, acetonitrile, 85 °C 16h. ii(b): Methyl 4-chlorobutyrate, K_2CO_3, KI, acetonitrile, 85 °C 16h. 129

Scheme 3.3: Synthesis and polymerization of the hydrogenated ferulic diesters $H\text{-}DeFA^{I}$ and $H\text{-}DeFA^{II}$ 131

Scheme 3.4: Synthesis and polymerization of the ferulic-based diols FAD^{I} and FAD^{II}. 134

Chapitre 4

Sous-chapitre 4.1

Schéma 4.1.1: Dimérisation et polymérisation de l'acide p-acétyle férulique. Adapté de (Castillo *et al.*, 2004). 153

Sous-chapitre 4.2

Scheme 4.2.1: Synthesis of the $DeFA^{II}$ from ferulic acid (Bazin *et al.*, 2021a) 169

Scheme 4.2.2: Synthesis and dimerization of p-acetyl ferulic acid. 174

Scheme 4.2.3: Esterification of the DAcFA to produce DeDFA. 176

Scheme 4.2.4: Synthesis and dimerization of $DeFA^{II}$ into $DDeFA^{II}$. 176

Scheme 4.2.5: CALB catalyzed polymerization of $DDeFA^{II}$ with diols of different lengths. 180

Scheme 4.2.6: Reversible reaction of [2+2] cycloaddition of the cyclobutane ring within the polymeric chain. 189

Chapitre 5

Scheme 5.1: Synthesis of the caffeic diol from caffeic acid 213

Scheme 5.2: Copolymerization of the CD with HDO and DEA as co-monomers..... 214

Scheme 5.3: Reversible photo-crosslinking of the CD-based polyesters under UV light. 221

Tableaux

Chapitre 1

Sous-chapitre 1.1

Table 1.2.1: Effect of cinnamic derivative structure on the reaction rate and conversion yields for esterification in octanol catalyzed by the lipase from *Candida Antarctica* (CALB) and *Rhizomucor miehei* (RML)for 12 days. Adapted from (Stamatis *et al.*, 1999)..... 39

Sous-chapitre 1.2

Table 1.2.2: study of the impact of the alcohol structure on the reaction yield in the synthesis of feruloylated chromogenic compounds by TLIM-catalyzed transesterification. Reproduced from (Gherbovet *et al.*, 2020). ... 45

Chapitre 2

Table 2.1: Compositions and molar masses values of the PHAd-co-PHF, as determined by NMR spectroscopy and SEC..... 97

Table 2.2: Compositions and molar masses values of the PBAd-co-PBF as determined by NMR spectroscopy and SEC..... 98

Table 2.3: Influence of solvents on molar masses of PHF and PBF (CALB 20 wt.%, solvent 300 wt.%, 90°C 72 h) 102

Table 2.4: Thermal properties of PHAd-co-PHF and PBAd-co-PBF 105

Table 2.5: Thermal properties of the PHF and PBF synthesized in different solvents..... 108

Chapitre 3

Table 3.1: Main properties of the enzymatically synthesized polyesters. 137

Chapitre 4

Sous-chapitre 4.1

Table 4.2.1: Molecular parameters of the polyesters synthesized from DDeFA^{II} with diol of different lengths and different ratios..... 186

Sous-chapitre 4.2

Table 4.2.2: Thermal properties of the polyesters synthesized from DDeFA^{II} with different diols (90°C, 24h, 40 % CALB)..... 188

Chapitre 5

Table 5.1: Feed and incorporated ratio of CD in relation to HDO. 215

Table 5.2: Thermal properties of the polyester synthesized with various ratios of CD as determined from TGA and DSC analyses. 219

Annexes

Annexes chapitre 2

Table S2.1: Results of SEC analysis for the PHAd-co-PHF containing from 0 to 100 % of DMFDC..... 276

Table S2.2: Results of SEC analysis for the PBAd-co-PBF containing from 0 to 100 % of DMFDC. 276

Introduction générale

Les matériaux polymères sont omniprésents dans notre quotidien. Cette notoriété résulte de leur grande facilité de mise en œuvre, leurs bonnes propriétés mécaniques ainsi que leur prix attractif (Feldman, 2008). Ils permettent également d'importants progrès technologiques par exemple dans le domaine de l'automobile et de l'aéronautique. Leur utilisation permet une réduction du poids des véhicules, entrainant une diminution de leur consommation et émissions de gaz à effet de serre (Heuss *et al.*, 2012). De plus, ils ont montré leur importance lors de la crise sanitaire du COVID-19, garantissant la stérilité du matériel hospitalier et la protection des personnes par l'usage de masques ou de panneaux transparents (Singh, 2020). Le revers de la médaille est cependant l'important impact environnemental des matériaux plastiques. La pollution engendrée par les plastiques est un phénomène complexe rencontré à plusieurs niveaux, de la production à la fin de vie du matériau. Ainsi, la pollution de grande ampleur de l'environnement et notamment celle des océans est au cœur des préoccupations (Chae *et al.*, 2018). De plus, du fait de leur origine fossile, les matériaux plastiques actuels peuvent difficilement s'inscrire dans une dynamique renouvelable ou d'économie circulaire (Kakadellis *et al.*, 2021). La production de polymères issus de ressources renouvelables semble une alternative intéressante pour la production de matériaux plus respectueux de l'environnement. Certains rapports prédisent que la production de polyesters sera multipliée par 1,4 entre 2019 et 2025, attestant de l'engouement général pour ce type de matériaux (*Bioplastics market data*, 2020).

Les polyesters sont au cœur de la problématique environnementale liée aux plastiques, notamment du fait de leur large production. Ils représentent en effet 8 % de la demande de polymères en Europe en 2019 (*Platics - the Facts 2020*, 2020) et sont utilisés en particulier dans le domaine du packaging où ils représentent 23 % des polymères utilisés (Rabnawaz *et al.*, 2017). Ils se retrouvent également dans l'industrie du textile dans laquelle ils constituent 52 % des fibres produites (*Preferred Fiber & Materials, Market Report 2021*, 2021). Les proportions des polyesters utilisés dans ces deux domaines par rapport aux autres polymères sont présentées dans la Figure 1.

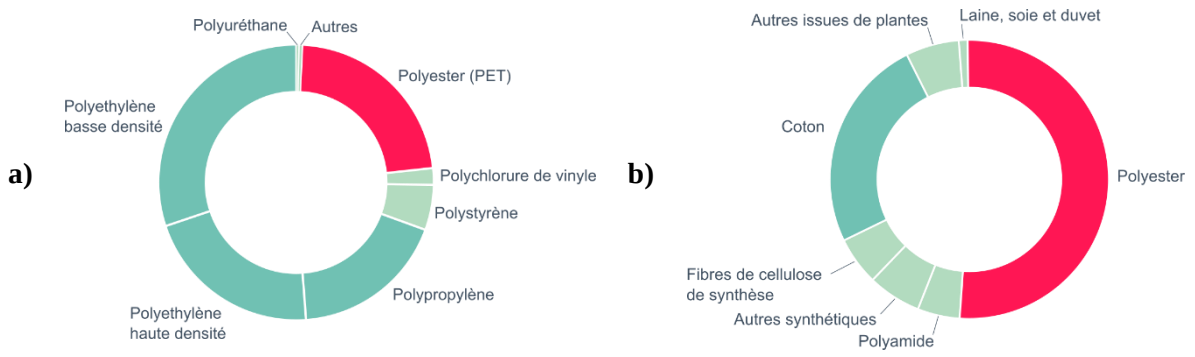

Figure 1: a) Répartition des polymères dans le packaging dans le monde en 2015 (Rabnawaz *et al.*, 2017) ; b) Production mondiale de fibres en 2018 (*Preferred Fiber & Materials, Market Report 2021*, 2021).

Les polyesters présentent des liaisons facilement hydrolysables par voie chimique ou biochimique, leur donnant de bonnes propriétés potentielles de recyclage. Ceci renforce d'autant plus l'intérêt de leur étude dans le cadre du développement d'une économie circulaire et environnementale (Tournier *et al.*, 2020; Kakadellis *et al.*, 2021). Enfin, une très grande diversité de structures polyesters issues de la biomasse a déjà été développée. Cette grande variété découle du nombre important de molécules plateforme facilement productibles à partir de la biomasse et pouvant être converties en polyesters. Ainsi, les polyesters représentent plus de la moitié des polymères biosourcés produits dans le monde en 2020 comme le montrent les chiffres de la Figure 2.

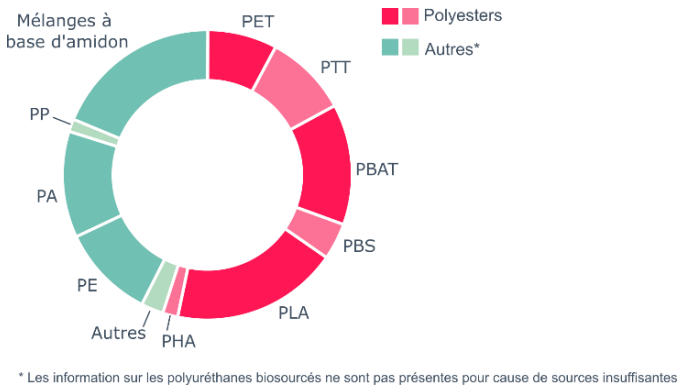

Figure 2: Capacités mondiales de production de matériaux plastiques biosourcés en 2020 (adapté de (*Bioplastics market data*, 2020)).

Comme indiqué sur la Figure 2, une large proportion des polyesters biosourcés présente des structures distinctes des polymères pétrosourcés classiques. Ils sont synthétisés à partir de molécules plateforme qui peuvent facilement être produites à partir de la biomasse (Pellis *et al.*, 2016b). Cette stratégie conduit à la synthèse de polymères avec des structures originales présentant des propriétés pouvant être identiques voir supérieures à celles des polymères pétrosourcés (Gandini *et al.*, 2009). Cette stratégie permet également le développement de polymères de spécialité avec des propriétés avancées comme la biodégradabilité, la biocompatibilité, une dégradation chimique contrôlée ou encore une réactivité vis-à-vis de rayonnements UV (Dong *et al.*, 2011; Zia *et al.*, 2016; Nakajima *et al.*, 2017; Wang *et al.*, 2020a). Ces nouvelles propriétés viennent concurrencer les propriétés des polymères non renouvelables et apportent une justification aux couts de production pour le moment généralement plus élevés des polyesters biosourcés. Dans un souci de préservation de l'environnement, des méthodes douces de production de ces polymères doivent également être envisagées. Une alternative intéressante étudiée dans cette thèse est l'utilisation de la catalyse enzymatique. Cette voie de catalyse est en effet plus douce et plus respectueuse de l'environnement que les méthodes couramment employées pour la synthèse de polyesters faisant notamment appel à de hautes températures et à des catalyseurs à base de métaux.

Cette thèse a été financée par une bourse obtenue auprès de l'école doctorale de physique et chimie physique de Strasbourg (ED182) et elle a été dirigée par le Dr Éric Pollet. Le travail de recherche

de cette thèse a été réalisé dans l'équipe BioTeam, dirigée par le Pr. Luc Avérous, au sein de l'Institut de Chimie et Procédés pour l'Énergie, l'Environnement et la Santé (ICPEES-UMR7515).

Ce projet s'inscrit dans la continuée des recherches effectuées au sein de la BioTeam qui portent sur l'élaboration de polymères biosourcés. Plusieurs études récentes ont été réalisées, dans le cadre de différentes thèses de doctorat, sur la synthèse enzymatique de polyesters, ainsi que sur la dégradation enzymatique de matériaux polymères. L'étude la plus récente portait sur la synthèse de polyesters aliphatiques à partir de synthons biosourcés. Ce travail avait permis de montrer l'efficacité de la catalyse enzymatique et notamment de la lipase B de *Candida antarctica* (CALB) pour l'élaboration de matériaux polyesters biosourcés. Les conclusions de cette précédente thèse soulignaient cependant les faibles propriétés, notamment thermiques, de ces matériaux. Parmi les perspectives évoquées, l'utilisation de monomères biosourcés aromatiques était notamment envisagée afin d'améliorer les propriétés thermiques des matériaux obtenus.

Le sujet de recherche de cette thèse s'intéresse donc au cas spécifique de la synthèse de polyesters aromatiques par catalyse enzymatique. Plusieurs monomères issus de ressources différentes ont été étudiés pour la synthèse de ces polyesters. La modification ou fonctionnalisation des monomères a parfois été investiguée afin de maximiser leur réactivité vis-à-vis de l'enzyme. Afin d'obtenir des résultats comparables aux études citées précédemment ainsi que pour des raisons exprimées plus loin dans ce manuscrit l'enzyme utilisée dans cette étude est la CALB. Les propriétés, notamment thermiques, des polyesters aromatiques biosourcés obtenus ont été étudiées et comparées à celles de leurs homologues aliphatiques.

Organisation du manuscrit :

Ce manuscrit est constitué de 5 chapitres constitués essentiellement d'articles scientifiques, déjà publiés ou à soumettre prochainement, encadrés par des introductions et des conclusions rédigées en français. Certains chapitres comportent également des sous-chapitres rédigés en français qui introduisent plus en détail un volet de la problématique abordée dans le chapitre en question.

Le premier chapitre de ce manuscrit vise à présenter un état de l'art du sujet abordé dans cette thèse. Il est constitué d'un premier sous-chapitre bibliographique qui aborde les points clefs de ce travail de thèse et en particulier la synthèse enzymatique de polyesters biosourcés. La suite de ce chapitre est constituée d'une étude bibliographique sous la forme d'un article de review portant sur la réactivité en estérification et en transestérification de synthons aromatiques biosourcés issus de la biomasse lignocellulosique. Ce chapitre bibliographique permet ainsi de mieux appréhender la réactivité particulière de ces synthons aromatiques naturels engagés dans des réactions catalysées par des enzymes.

Le second chapitre de ce manuscrit s'intéresse à la synthèse par catalyse enzymatique de polyesters à partir d'un diester de furane. Les furanes sont des molécules plateformes biosourcées à fort potentiel. Ils permettent déjà la synthèse de polyesters aux propriétés proches des polyesters employés

couramment aujourd'hui. Ce chapitre porte plus spécifiquement sur la mise en lumière du phénomène responsable des faibles masses molaires obtenues lors de la synthèse enzymatique de polyesters présentant des taux élevés de dérivés de furanes. La solubilité du substrat dans le milieu réactionnel et l'emploi de solvants facilitant cette solubilité ont été étudiés et notamment leur influence sur les masses molaires des polyesters obtenus.

Dans le troisième chapitre de ce manuscrit, un autre synthon aromatique issu de la biomasse est étudié : l'acide férulique. La synthèse de polyesters dérivés d'acide férulique par catalyse enzymatique avec une hydrolase n'avait, à notre connaissance, encore jamais été étudiée. Fort des connaissances acquises dans le chapitre 1, l'acide férulique a été modifié de différentes manières afin d'optimiser sa réactivité vis-à-vis de l'enzyme et d'obtenir des polyesters de hautes masses molaires. Les relations structure-propriété de ces polyesters ont été étudiées avec une attention particulière portée aux propriétés thermiques des matériaux ainsi obtenus.

Le quatrième chapitre porte également sur l'acide férulique et s'appuie sur certaines observations décrites dans le chapitre 3. En tirant parti des propriétés de cycloadditions de dérivés d'acide férulique, il est possible, via l'irradiation par les UV, de synthétiser des dimères d'acide férulique particulièrement intéressants pour l'élaboration de polyesters aromatiques. Ce chapitre est d'abord constitué d'un sous-chapitre dans lequel la réactivé en photo-dimérisation pas cycloaddition de plusieurs monomères, issus de la littérature et du chapitre précédent, sont étudiés. Le sous-chapitre suivant est un article s'intéressant à la réactivité en polymérisation enzymatique des monomères capables de dimériser par cycloaddition. Cette étude conduit ainsi à la synthèse de polyesters avec une structure singulière, les chaînes présentant des groupements esters pendants. De plus, les matériaux présentent de bonnes propriétés de rétropolymérisation via irradiation UV à une longueur d'onde plus faible. Ce chapitre montre ainsi comment tirer parti de la sélectivité de la catalyse enzymatique pour synthétiser de polyesters possédant une structure et des propriétés innovantes.

Cet aspect de la polymérisation enzymatique est étudié plus en détail dans le cinquième et dernier chapitre de cette thèse. Le chapitre 5 porte sur l'utilisation de l'acide caféique pour la synthèse de matériaux polyesters par catalyse enzymatique. Cette molécule plateforme est structurellement proche de l'acide férulique. Elle a été modifiée par l'éthylène carbonate en un diol. La réactivité particulière des dérivés d'acide caféique vis-à-vis de l'enzyme a ainsi permis l'élaboration de polyesters possédants des chaines pendantes constituées d'esters α,β-insaturés. Ces groupements permettent ainsi une réticulation du polymère par irradiation sous rayonnement UV qui s'avère être partiellement réversible quand irradié à une longueur d'onde plus faible. Ce chapitre constitue donc une ouverture vers un élargissement des utilisations potentielles de la catalyse enzymatique pour sa capacité à produire des polyesters aux propriétés innovantes pouvant concurrencer, à terme, les polymères pétrosourcés.

Références

Bioplastics market data (**2020**) *European bioplastics*. Available at: https://www.european-bioplastics.org/market/ (Accessed: 2 September 2021).

Chae, Y. and An, Y.-J. (**2018**) 'Current research trends on plastic pollution and ecological impacts on the soil ecosystem: A review', *Environmental Pollution*, 240, pp. 387–395.

Dong, W., Li, H., Chen, M., Ni, Z., Zhao, J., Yang, H. and Gijsman, P. (**2011**) 'Biodegradable bio-based polyesters with controllable photo-crosslinkability, thermal and hydrolytic stability', *Journal of Polymer Research*, 18(6), pp. 1239–1247.

Feldman, D. (**2008**) 'Polymer History', *Designed Monomers and Polymers*, 11(1), pp. 1–15.

Gandini, A., Silvestre, A. J. D., Neto, C. P., Sousa, A. F. and Gomes, M. (**2009**) 'The furan counterpart of poly(ethylene terephthalate): An alternative material based on renewable resources', *Journal of Polymer Science Part A: Polymer Chemistry*, 47(1), pp. 295–298.

Heuss, R., Müller, N., Van Sintern, W., Starke, A. and Tschiesner, A. (**2012**) *Lightweight, heavy impact*. McKinsey & Comapny. Available at: https://www.mckinsey.com/~/media/mckinsey/dotcom/client_service/automotive%20and%20assembly/pdfs/lightweight_heavy_impact.ashx (Accessed: 1 September 2021).

Kakadellis, S. and Rosetto, G. (**2021**) 'Achieving a circular bioeconomy for plastics', *Science*, 373(6550), pp. 49–50.

Nakajima, H., Dijkstra, P. and Loos, K. (**2017**) 'The Recent Developments in Biobased Polymers toward General and Engineering Applications: Polymers that are Upgraded from Biodegradable Polymers, Analogous to Petroleum-Derived Polymers, and Newly Developed', *Polymers*, 9(12), p. 523.

Pellis, A., Herrero Acero, E., Gardossi, L., Ferrario, V. and Guebitz, G. M. (**2016**)**b** 'Renewable building blocks for sustainable polyesters: new biotechnological routes for greener plastics: Renewable building blocks for sustainable polyesters', *Polymer International*, 65(8), pp. 861–871.

Platics - the Facts 2020 (**2020**). Platics Europe. Available at: https://www.plasticseurope.org/application/files/5716/0752/4286/AF_Plastics_the_facts-WEB-2020-ING_FINAL.pdf.

Preferred Fiber & Materials, Market Report 2021 (**2021**). Textile Exchange. Available at: https://textileexchange.org/wp-content/uploads/2021/08/Textile-Exchange_Preferred-Fiber-and-Materials-Market-Report_2021.pdf.

Rabnawaz, M., Wyman, I., Auras, R. and Cheng, S. (**2017**) 'A roadmap towards green packaging: the current status and future outlook for polyesters in the packaging industry', *Green Chem.*, 19(20), pp. 4737–4753.

Singh, R. (**2020**) 'The New Normal for Bioplastics Amid the COVID-19 Pandemic', *Industrial Biotechnology*, 16(4), pp. 215–217.

Tournier, V., Topham, C. M., Gilles, A., David, B., Folgoas, C., Moya-Leclair, E., Kamionka, E., Desrousseaux, M.-L., Texier, H., Gavalda, S., Cot, M., Guémard, E., Dalibey, M., Nomme, J., Cioci, G., Barbe, S., Chateau, M., André, I., Duquesne, S. and Marty, A. (**2020**) 'An engineered PET depolymerase to break down and recycle plastic bottles', *Nature*, 580(7802), pp. 216–219.

Wang, B., Ma, S., Li, Q., Zhang, H., Liu, J., Wang, R., Chen, Z., Xu, X., Wang, S., Lu, N., Liu, Y., Yan, S. and Zhu, J. (**2020**)**a** 'Facile synthesis of "digestible", rigid-and-flexible, bio-based building block for high-performance degradable thermosetting plastics', *Green Chemistry*, 22(4), pp. 1275–1290.

Zia, K. M., Noreen, A., Zuber, M., Tabasum, S. and Mujahid, M. (**2016**) 'Recent developments and future prospects on bio-based polyesters derived from renewable resources: A review', *International Journal of Biological Macromolecules*, 82, pp. 1028–1040.

Chapitre 1. Etat de l'art de l'utilisation de la catalyse enzymatique pour la fonctionnalisation, la modification ou la polymérisation de synthons aromatiques biosourcés.

- **Sous-Chapitre 1.1 : Introduction à la synthèse de polyesters aromatiques biosourcés par catalyse enzymatique.**

- **Sous-Chapitre 1.2 : Enzymatic esterification, transesterification and polyesterification of aromatic acids from lignocellulosic biomass, a review.**

Introduction chapitre 1

L'introduction générale de ce manuscrit a permis d'exposer le contexte de ce travail de thèse. Le premier chapitre s'attachera à introduire plus en détail les différentes notions qui seront abordées dans cette thèse et à présenter l'état de l'art actuel dans le domaine. Il se compose de deux sous-chapitres distincts. Le premier sous-chapitre consiste en une introduction sur les polyesters où leur historique et les méthodes les plus courantes de production de ces matériaux y sont décrits. L'état de l'art sur les polyesters biosourcés est ensuite exposé plus en détail en s'attardant sur ceux qui sont le plus couramment étudiés aujourd'hui. La synthèse de polyesters biosourcés aromatiques y est notamment mise en avant. L'étude de la bibliographie se porte ensuite sur la catalyse enzymatique et plus particulièrement l'utilisation de l'enzyme utilisée pour ce travail de thèse, à savoir la lipase B de *Candida antarctica* (CALB). Après une description de son mécanisme d'action, ses utilisations pour la synthèse de polyesters sont passées en revue. La présentation de cet état de l'art s'attardera plus particulièrement sur la synthèse enzymatique de polyesters biosourcés. Enfin, la littérature portant sur l'utilisation de la CALB pour la synthèse de polyesters aromatiques biosourcés est présentée.

La biomasse lignocellulosique est une source importante de synthons aromatiques. Bien que certains de ces synthons aient déjà été utilisés pour la synthèse de polyesters, la polymérisation par voie enzymatique n'a que très rarement été étudiée. Le sous-chapitre 1.2 est une étude bibliographique portant sur la réactivité de ces synthons dans des réactions d'estérification et de transestérification catalysées par les enzymes. Il est présenté sous la forme d'un article de review intitulé « Enzymatic esterification, transesterification and polyesterification of aromatic acids from lignocellulosic biomass, a review ». Ce travail bibliographique porte plus particulièrement sur les synthons phénoliques naturels tels que les dérivés des acides cinnamique et benzoïque. Les sources de ces synthons, leur utilisation ainsi que leur modification par catalyse enzymatique y sont décrites en détail. L'influence du milieu réactionnel, de la nature de l'enzyme employée ainsi que de la structure du substrat sur le rendement de réaction sont notamment discutées dans ce sous-chapitre sur base des résultats de la littérature. Ce travail de recherche bibliographique a pour objectif de donner une base de connaissances large et solide pour une meilleure compréhension de l'activité catalytique des lipases telles que CALB vis-à-vis de synthons aromatiques biosourcés.

Sous-chapitre 1.1. Introduction à la synthèse de polyesters aromatiques biosourcés par catalyse enzymatique.

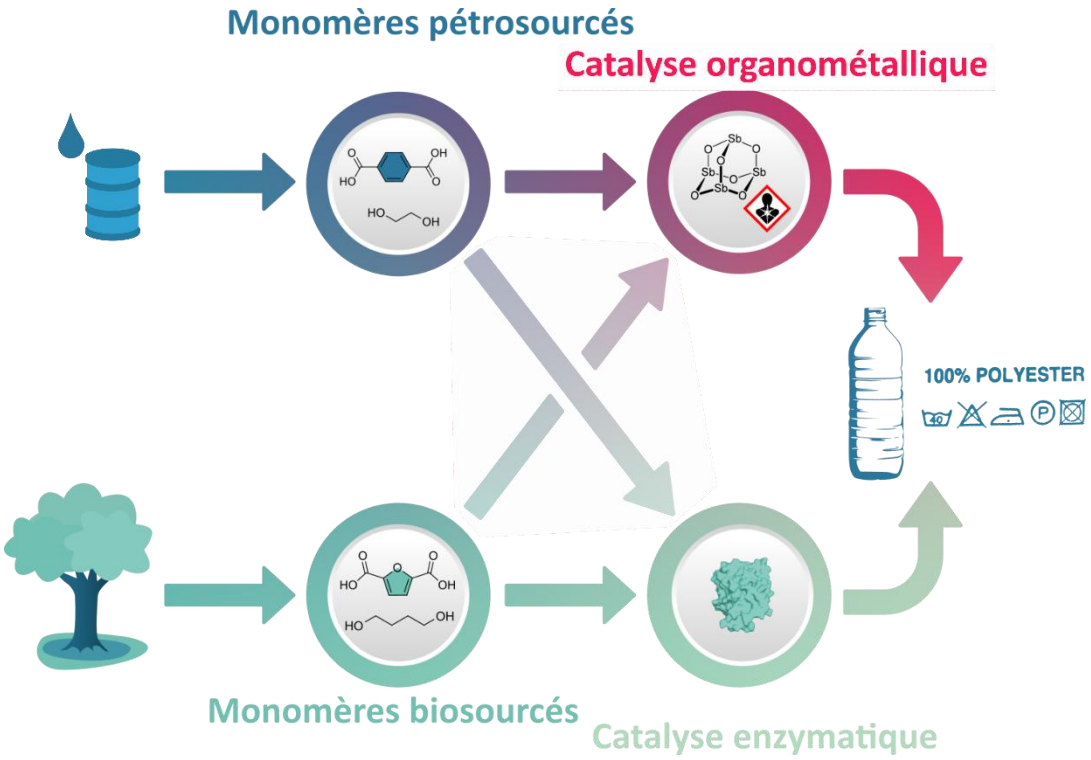

1. Les polyesters

Les polyesters sont omniprésents dans notre quotidien notamment dans les domaines du packaging où ils représentent 23 % des polymères utilisés (Rabnawaz *et al.*, 2017) . On les retrouve également dans l'industrie du textile dans laquelle 52 % des fibres produites sont en polyester (*Preferred Fiber & Materials, Market Report 2021*, 2021). Les polyesters sont synthétisés pour la première fois par W. H. Carothers en 1929, alors employé chez DuPont. Il découvre alors que la réaction de diols et de diacides carboxyliques permet la synthèse de fibres (McIntyre, 2004; Feldman, 2008). Carothers étudiera ainsi la synthèse de nombreux polyesters aliphatiques.

Aujourd'hui, trois voies de synthèse sont les plus couramment employées pour la synthèse de polyesters. La première est la polycondensation entre un diol et un diacide carboxylique (on parle de monomères A-A et B-B). Cette méthode utilise donc un diol et un diacide de structures différentes pour obtenir un copolymère. La seconde méthode est la polycondensation par homopolymérisation d'un hydroxyacide carboxylique (on parle de monomère A-B) sur lui-même. Il est également possible de synthétiser des polyesters par polymérisation par ouverture de cycle (POC) de lactones. Enfin, d'autres voies de synthèse existent comme l'utilisation de chlorure d'acyle ou d'anhydride. Cette thèse se concentre essentiellement sur la polymérisation par polycondensation de monomères A-A avec des monomères B-B.

Sur la base des travaux de Carothers, J. R. Whinfield et J. T. Dickson étudient et décrivent pour la première fois en 1941 la synthèse du polyéthylène téréphtalate (PET) (McIntyre, 2004) et ils déposeront le premier brevet sur ce polymère (Dickson *et al.*, 1946). Le PET a ensuite été produit industriellement en grande quantité à partir de 1953 (Feldman, 2008) et représente aujourd'hui la grande majorité des polyesters produits à l'échelle mondiale. Il est produit à partir d'éthylène glycol et d'acide téréphtalique ou de son diester méthylique. La réaction se fait en quatre étapes et nécessite l'aide de catalyseurs organométalliques telle que le trioxyde d'antimoine à des températures supérieures à 280°C (Figure 1.1.) (Ravindranath *et al.*, 1984; Mandal *et al.*, 2019).

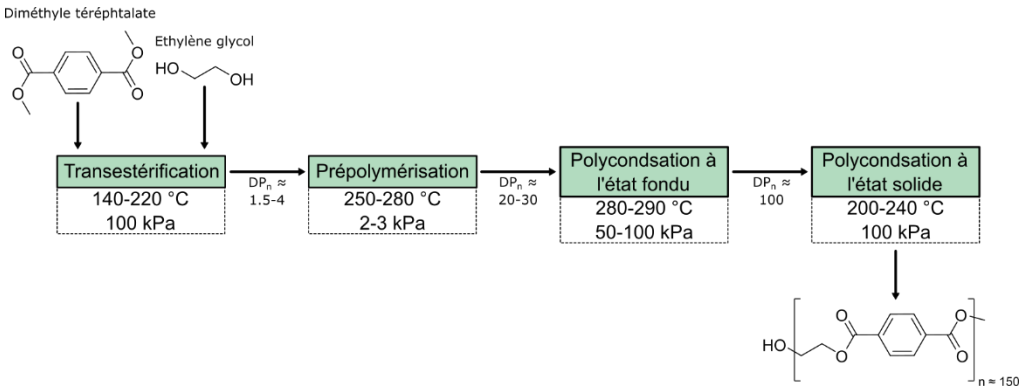

Figure 1.1.1: représentation schématique de la synthèse du PET (adapté de (Ravindranath *et al.*, 1984)).

Le diméthyle téréphtalate est produit par estérification de l'acide téréphtalique couramment produit selon le procédé Amoco à partir de *p*-xylène, lui-même produit à partir de naphta issu du pétrole (Tomás *et al.*, 2013). L'éthylène glycol est produit industriellement par oxydation de l'éthylène, lui-même pétrosourcé (Yang *et al.*, 2019). Ainsi, le PET et la plupart des polyesters produits aujourd'hui sont issus de ressources fossiles. Plusieurs techniques de recyclage physique, chimique ou biochimique de polyesters et plus particulièrement du PET ont été développées afin de réduire l'empreinte écologique de ce polyester (Tournier *et al.*, 2020; Devi Salam *et al.*, 2021; Schyns *et al.*, 2021). Le développement d'alternatives biosourcées représente cependant un important champ de la recherche actuelle.

2. Les polyesters biosourcés

Les polyesters sont au cœur de la problématique environnementale liée au plastique, notamment du fait de leur large utilisation. De plus, ils présentent des liaisons facilement hydrolysables par voie chimie ou biochimique, leur donnant de bonnes propriétés potentielles de recyclage et augmentant leur intérêt dans le cadre d'une économie circulaire (Kakadellis *et al.*, 2021). Enfin, les polyesters biosourcés existent en une très grande variété et sont déjà produits à échelle industrielle. Ainsi, ils représentent plus de la moitié des polymères biosourcés produits en 2020 comme le montrent les chiffres de la Figure 1.1.2.

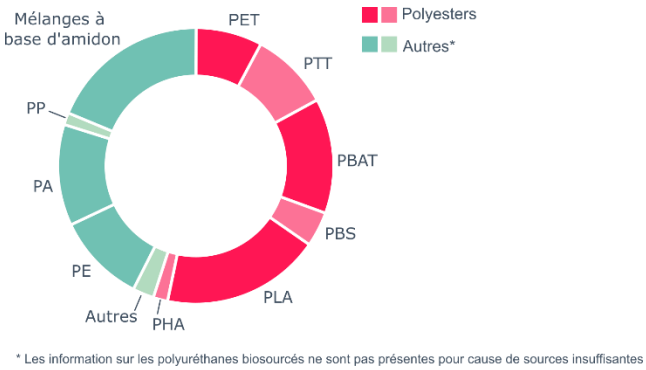

Figure 1.1.2: Capacités mondiales de production de matériaux plastiques biosourcés en 2020 (adapté de (*Bioplastics market data*, 2020)).

Les polymères biosourcés produits aujourd'hui à une échelle industrielle peuvent être classés en trois catégories. La première catégorie correspond aux polymères produits à partir d'amidon plastifié. La seconde catégorie correspond aux polymères comme le bio-PE, bio-PP ou du bio-PET qui sont produits à partir de synthons issus de ressources renouvelables, mais ayant une structure identique à leur version pétrosourcée. Ils possèdent ainsi des propriétés identiques à leurs homologues pétrosourcés (Siracusa *et al.*, 2020). La troisième catégorie correspond aux « nouveaux polymères » issus de synthons biosourcés. En effet, une très grande diversité de synthons de base issue de la biomasse (appelés aussi « building-blocks ») a été identifiée pour la synthèse de polymères et notamment de polyesters (Jang *et al.*, 2012; Becker *et al.*, 2015). Cette large diversité de molécules biosourcées explique la grande variété de polyesters biosourcés présentés dans la Figure 1.1.2. Par exemple, plusieurs diols utiles à la synthèse

de polyesters peuvent être produits à partir de glucose comme l'éthylène glycol, le 1,3-propanediol, le 1,4-butanediol ou le 1,6-hexanediol. Il est également possible de produire plusieurs diacides, qui sont à la base de la synthèse de nombreux polyesters, comme les acides succinique, adipique, maléique, muconique, itaconique, téréphtalique ou 2,5-furandicarboxylique. La synthèse de ces monomères bisourcés repose essentiellement sur la transformation de cellulose, d'hémicellulose ou encore d'amidon (Jang *et al.*, 2012; Becker *et al.*, 2015). D'autres ressources issues de la biomasse peuvent également être converties en molécules d'intérêt pour la synthèse de polyesters. C'est le cas par exemple de la lignine qui permet de produire par différents procédés chimiques ou biochimiques des molécules d'intérêt tel que l'acide vanillique (Llevot *et al.*, 2016).

Le polyester biosourcé le plus connu et le plus courant est certainement l'acide polylactique (PLA) (Figure 1.1.3). L'acide lactique produit à partir de de sucres, d'amidon ou même de biomasse lignocellulosique (Abdel-Rahman *et al.*, 2013) peut être transformé en lactide (son diester cyclique) puis polymérisé par POC en PLA. Le PLA peut être utilisé dans le secteur de l'emballage. Il est notamment approuvé par la Food and Drug Administration (FDA) des Etats-Unis d'Amérique pour le contact alimentaire (Rabnawaz *et al.*, 2017). Grâce à une mise en œuvre facilitée par une température de fusion (T_f) relativement modérée entre 160-180°C, le PLA est le polymère le plus utilisé dans le domaine de l'impression 3D par dépôt de filament fondu (Tümer *et al.*, 2021). Sa température de transition vitreuse (T_g) se situe entre 60 et 65°C, donc proche de celle du PET, ce qui lui confère une très bonne rigidité à température ambiante (Tümer *et al.*, 2021). Enfin, il présente de bonnes propriétés de biodégradabilité et de compostabilité (en condition de compostage industriel) (Rabnawaz *et al.*, 2017). Pour toutes ces raisons, le PLA représente plus de 18 % de la production de polymères biosourcés avec plus de 394 milliers de tonnes produites en 2020 (*Bioplastics market data*, 2020).

Le 1,4-butanediol et l'acide succinique évoqués précédemment en tant que synthons biosourcés peuvent être combinés pour synthétiser le poly(butylène succinate) (PBS) (Figure 1.1.3). Ce polymère aliphatique représente un peu plus de 4 % de la production mondiale de polymères biosourcés (*Bioplastics market data*, 2020). Il présente une T_f comprise entre 90 et 120 °C, une T_g entre -45 et -10°C (Mochane *et al.*, 2021). Le PBS possède une résistance à la traction qui peut atteindre entre 30 et 35 MPa (Rafiqah *et al.*, 2021) et des propriétés mécaniques et thermiques comparables à celles du polypropylène (Grebowicz *et al.*, 2007; Arrakhiz *et al.*, 2012). Le PBS, en plus de pouvoir être issu de carbone renouvelable à 100 %, présente d'excellentes propriétés de biodégradabilité (Rafiqah *et al.*, 2021). Il est notamment utilisé dans l'agriculture pour l'élaboration de films de paillage (Rafiqah *et al.*, 2021). Des études ont également montré que l'acide succinique pouvait être substitué partiellement par l'acide adipique pour former le polybutylène(adipate-co-succinate) (PBSA) ou en totalité pour former le poly(butylène adipate) (PBAd). L'insertion de ces unités adipate tend à diminuer les propriétés thermiques et mécaniques par rapport au PBS, mais en améliore cependant les propriétés de biodégradabilité (Tserki *et al.*, 2006).

Les polyhydroxyalcanoates (PHA) (Figure 1.1.3) sont des polyesters synthétisés naturellement par des bactéries. Ils sont composés d'hydroxyacides, dont la longueur et les substituants peuvent varier en fonction de la souche bactérienne employée. Des bactéries provenant d'une grande diversité de sources et de plusieurs genres tels que *Bacillus*, *Myctobacterium* ou *Pseudomonas* ont été identifiées comme capables de produire des PHA (Kalia *et al.*, 2021). De plus, certaines bactéries comme *Escherichia coli* peuvent être modifiées génétiquement afin de produire des PHA (Chen *et al.*, 2017). Ces bactéries peuvent convertir des sucres issus de la biomasse, mais également des déchets organiques tels que l'huile de cuisine usagée ou les co-produits de la production de cidre (Kalia *et al.*, 2021). Les PHA, grâce à leur diversité de structure possèdent des propriétés thermiques variables avec par exemple des T_g allant de -50 à -4 °C (Chen, 2010). Ces polyesters biodégradables peuvent être utilisés dans le domaine du packaging ou pour des applications biomédicales (Chen, 2010).

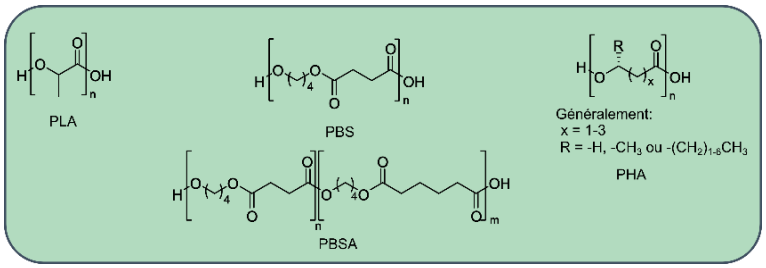

Figure 1.1.3: Représentation des polymères biosourcés PLA, PBS, PBSA et PHA.

Les polyesters biosourcés présentés jusqu'à maintenant partagent la particularité d'être tous aliphatiques. Cela entraine des limitations en termes de propriétés mécaniques et thermiques qui peuvent restreindre leur champ d'application. Par ailleurs, il est largement établi et connu que l'insertion d'unités aromatiques dans la chaîne polymère est un moyen efficace d'améliorer les propriétés thermiques, mécaniques et barrière d'un polyester (Albanese *et al.*, 2016; Hu *et al.*, 2018). L'aromaticité élevée du PET explique ainsi ses excellentes propriétés et donc sa très large utilisation (Albanese *et al.*, 2016). Les polyesters aliphatiques tels que le PBS ou les PHA présentent des températures de transitions et des modules très bas en comparaison du PET. Le PLA possède quant à lui une T_g comparable au PET, mais des propriétés barrières bien plus basses (Hu *et al.*, 2018). Face à cette difficulté pour concurrencer et remplacer le PET pétrosourcé, une attention particulière a été portée au développement de polyesters biosourcés aromatiques.

Les polyesters aromatiques biosourcés présents sur le marché ne présentent cependant généralement que la partie diol qui est issue de ressources renouvelables. L'aromaticité est généralement apportée, comme pour le PET, par de l'acide téréphtalique d'origine fossile. L'éthylène glycol, le 1,3-propanediol et le 1,4-butanediol peuvent ainsi être produit à partir de biomasse comme la cellulose et associés à l'acide téréphtalique pour la synthèse de polyesters que sont le bio-PET, le polypropylène téréphtalate (PTT) et le polybutylène téréphtalate (PBT), respectivement (Figure 1.1.4). Ces polyesters possèdent des propriétés mécaniques et thermiques supérieures aux polymères aliphatiques cités

précédemment, mais ne sont que partiellement biosourcés (Albanese *et al.*, 2016). Ils sont notamment mis en avant par des entreprises comme Coca-cola dans leur gamme « plant-bottle » (*Coca-Cola Expands Access to PlantBottle IP*). Des recherches sont cependant menées depuis quelques années pour produire de l'acide téréphtalique à partir de molécules issues de la biomasse tels que des dérivés de furanes, de terpènes ou de la lignine (Pellis *et al.*, 2016b; Volanti *et al.*, 2019).

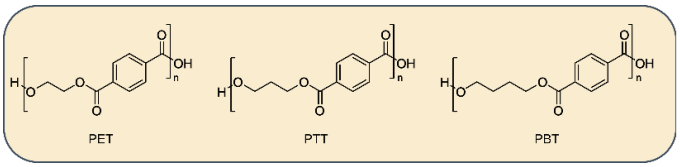

Figure 1.1.4: Structure des polyesters aromatiques partiellement biosourcés PET, PTT et PBT.

Des alternatives au PET entièrement biosourcées sont en cours de développement. C'est notamment le cas des polyesters à base de furane. L'acide 2,5-furandicarboxylique (FDCA) peut être produit à partir d'hydroxyméthyl furfural (HMF), une importante molécule plateforme produite à partir de cellulose (Sajid *et al.*, 2018; Rajesh *et al.*, 2020) (Schéma 1.1.1). Le FDCA possède des propriétés proches de l'acide téréphtalique et permet de former, avec l'éthylène glycol, le polyéthylène furanoate (PEF) (Papageorgiou *et al.*, 2016; Terzopoulou *et al.*, 2020). Le PEF en plus d'être entièrement biosourcé possède des propriétés thermiques et mécaniques identiques au PET et des propriétés barrières supérieures (Gandini *et al.*, 2009; Loos *et al.*, 2020). Des plateformes de production de PEF sont actuellement en cours de développement par diverses entreprises et notamment Avantium ('YXY® Technology', 2021).

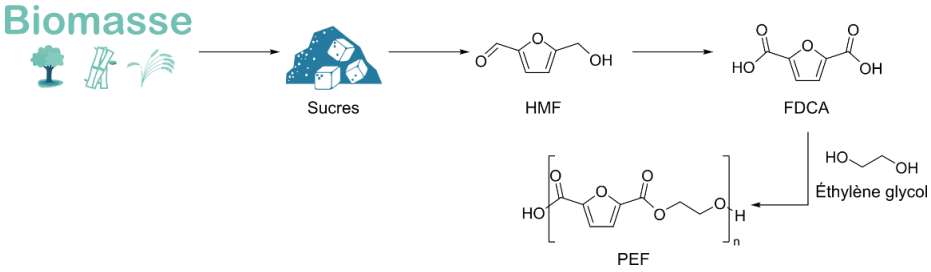

Schéma 1.1.1: Synthèse de PEF à partir FDCA provenant de la biomasse (Sajid *et al.*, 2018).

D'autres alternatives biosourcées au PET sont actuellement étudiées notamment des polyesters synthétisés à partir de monomères issus de la lignine ou de l'hémicellulose. Par exemple, l'acide vanillique est un acide hydroxybenzoïque qui peut être produit à partir de lignine (Li *et al.*, 2021; Poveda-Giraldo *et al.*, 2021). Après modification de son hydroxyle, l'acide vanillique peut être homopolymérisé ou copolymérisé pour former un polyester aromatique aux propriétés comparables au PET (Fache *et al.*, 2015; Pang *et al.*, 2015; Xanthopoulou *et al.*, 2021) (Schéma 1.1.2.a). Gioia *et al.* (Gioia *et al.*, 2016, 2018) ont également montré que l'acide vanillique, après estérification, pouvait réagir avec l'éthylène carbonate (un synthon lui aussi biosourcé) pour former ce même poly(éthylène vanillate) (Schéma 1.1.2.b). La dimérisation de l'acide vanillique par des procédés enzymatiques

(employant des peroxydases) est également présentée comme une voie intéressante pour la production de polyesters aromatiques biosourcés présentant une rigidité élevée (Llevot *et al.*, 2015).

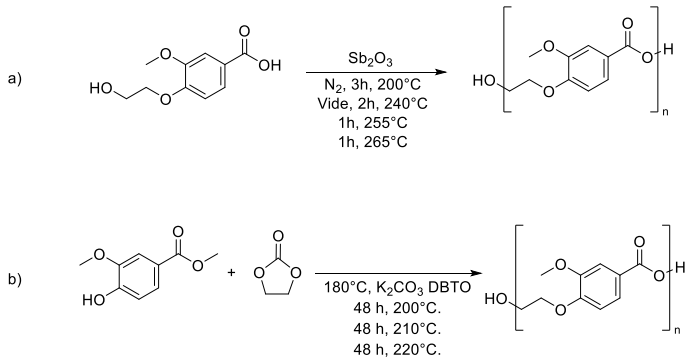

Schéma 1.1.2: Synthèse du poly(éthylène vanillate) : a) à partir d'acide p-hydroxyethoxyvanillique (Xanthopoulou *et al.*, 2021) ; b) à partir d'acide vanillique estérifié et de carbonate d'éthylène (Gioia *et al.*, 2016).

Les dérivés cinnamiques comme l'acide férulique sont des synthons biosourcés aromatiques qui ont également été étudiés pour la synthèse de polyesters aromatiques. Ils peuvent être directement extraits de sources naturelles comme le son de blé ou de riz (Flourat *et al.*, 2021). L'acide férulique permet la synthèse de polyesters avec des T_g pouvant atteindre 113°C (Elias *et al.*, 1985). L'acide férulique est cependant souvent modifié ou copolymérisé afin de permettre l'obtention de matériaux aux propriétés modulables, facilitant la mise en forme du matériau (Nguyen *et al.*, 2015, 2017; Llevot *et al.*, 2016; Kurt *et al.*, 2020). Par exemple, Nguyen *et al.* (Nguyen *et al.*, 2017) ont étudié la copolymérisation d'un synthon issu de l'acide férulique avec le lactide et l'ε-caprolactone (Schéma 1.1.3). Des matériaux avec des T_g allant de -60 à 113 °C ont ainsi été obtenus. D'autres dérivés cinnamiques comme l'acide caféique ont également été évalués en tant que molécules plateformes pour la synthèse de polyesters à hautes propriétés thermiques.

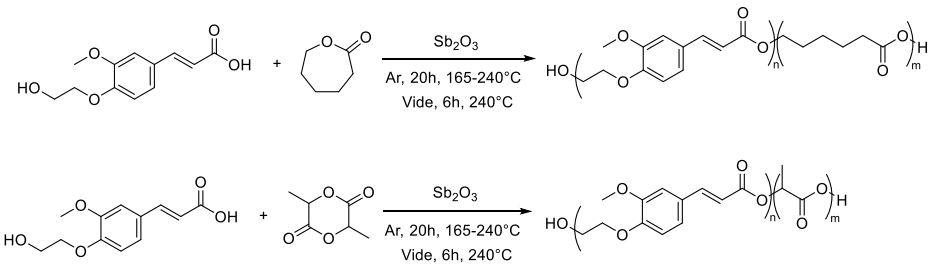

Schéma 1.1.3: Synthèse de copolyesters semi-aromatiques à base d'acide férulique, d'ε-caprolactone et de lactide.

La synthèse de polyesters biosourcés aux propriétés thermiques élevées a été passée en revue par Nguyen *et al.* (Nguyen *et al.*, 2018) en 2018. La synthèse de ces polyesters se fait à haute température et par catalyse organométallique. Les catalyseurs employés sont généralement à base de titane comme le butoxyde de titane ou l'isopropylate de titane, à base d'antimoine comme le trioxyde d'antimoine ou

à base d'étain comme l'oxyde de dibutylétain (Terzopoulou *et al.*, 2017; Xanthopoulou *et al.*, 2021). Certains de ces catalyseurs présentent toutefois des risques importants pour l'environnement et la santé. De plus, ces derniers peuvent se retrouver dans le matériau polymère final, limitant ainsi les possibilités d'utilisations dans le domaine médical ou au contact alimentaire. L'emploi de ces catalyseurs n'est donc pas en phase avec certains des principes de la chimie verte (Anastas *et al.*, 2010) et l'utilisation d'enzymes comme catalyseurs représente aujourd'hui une alternative plus verte particulièrement prometteuse (Shoda *et al.*, 2016).

3. La polymérisation enzymatique

3.1. La catalyse enzymatique

Les enzymes sont des protéines ayant la particularité de présenter une activité catalytique. Elles permettent la réalisation de réactions dans des conditions douces et présentent généralement une grande sélectivité de substrat. Cette sélectivité permet par exemple de se passer de groupements protecteurs dans certaines réactions (Chapman *et al.*, 2018). Les enzymes sont également des catalyseurs biosourcés, non polluants, et sont donc en parfaite adéquation avec plusieurs des principes de la chimie verte (Anastas *et al.*, 2010). Grâce à ces propriétés, les enzymes trouvent de nombreuses applications industrielles notamment dans le secteur agroalimentaire, le textile ou l'industrie pharmaceutique (Kirk *et al.*, 2002; Parlement Européen, 2008; Chapman *et al.*, 2018). Les protéases représentent ainsi la plus grande proportion des enzymes utilisées dans l'industrie notamment dans les lessives. En effet, leur sélectivité permet la dégradation des taches issues de protéines dans des conditions douces sans abimer les fibres. De plus, elles sont moins toxiques et polluantes que leurs équivalents issus de la (pétro)chimie.

Les lipases sont également des enzymes couramment employées par l'industrie. Elles sont classées dans la catégorie des hydrolases et présentent une affinité particulière pour l'hydrolyse d'acide gras. Elles sont ainsi utilisées communément dans les lessives pour la dégradation de lipides (Kirk *et al.*, 2002; Chapman *et al.*, 2018) ainsi que pour la synthèse de biocarburants (Amini *et al.*, 2017). Placées en conditions hydrophobes, certaines lipases permettent également d'effectuer des réactions d'estérification et de transestérification (Stergiou *et al.*, 2013).

La réactivité d'une enzyme est intrinsèquement liée à sa structure. La structure d'une enzyme est imposée par sa séquence d'acides aminés ainsi que les interactions entre ces acides aminés. L'enzyme se retrouve ainsi structurée à plusieurs échelles (structures primaire, secondaire, tertiaire…). La capacité du substrat à se loger correctement dans le site actif de l'enzyme conditionne la faisabilité et la cinétique de la réaction (Yagi *et al.*, 2018; Santos *et al.*, 2019; Silvestrini *et al.*, 2020). On parle alors de système clef-serrure dans lequel le substrat représente la clef, l'enzyme la serrure et le déverrouillage de la serrure la réaction (Figure 1.1.5). Différents facteurs propres au milieu tels que la température, le pH ou l'activité de l'eau peuvent entraîner la perte ou la déformation de la structure tridimensionnelle de l'enzyme modifiant ainsi les interactions substrat-enzyme et impactant la cinétique de la réaction

(Stergiou *et al.*, 2013; Yagi *et al.*, 2018). Si l'enzyme se retrouve inactive, on parle de dénaturation. Cette dénaturation peut être réversible ou non.

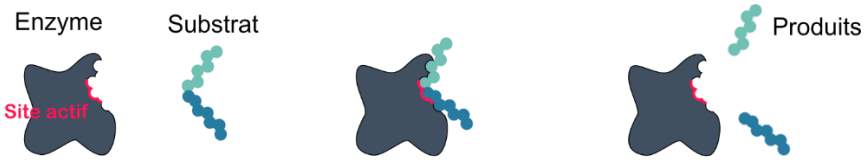

Figure 1.1.5: Représentation du système clef-serrure de la catalyse enzymatique.

3.2. La lipase B de Candida antarctica

La lipase B provenant du champignon *Candida antarctica* (CALB) est une lipase constituée de 317 acides aminés pour une masse de 33 kDa (Brito e Cunha *et al.*, 2019). Sa structure est représentée en Figure 1.1.6. Son site actif en forme d'entonnoir permet l'introduction d'une grande variété de substrats (Pleiss *et al.*, 1998). Afin de mieux comprendre les interactions substrat-enzyme de la CALB, plusieurs études de modélisation ont été menées (Dettori *et al.*, 2018; Yagi *et al.*, 2018; Silvestrini *et al.*, 2020). Le site actif de la CALB, comme pour les de nombreuses lipases, est constitué de la triade catalytique serine, histidine et aspartate.

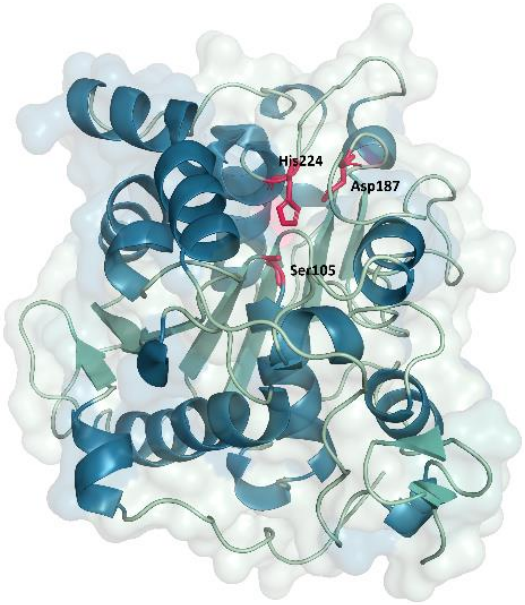

Figure 1.1.6: Représentation de la structure secondaire de la CALB. Les acides aminés du site actif sont représentés en bâtons.

Le mécanisme de la réaction de transestérification catalysée par CALB est résumé dans le Schéma 1.1.4. La première étape est la déprotonation de la serine par l'histidine. Cette dernière est alors stabilisée par l'anion de l'aspartate. L'alcoolate de la serine peut alors attaquer le carbonyle du substrat, formant un composé cyclique intermédiaire. Ce composé est instable et un alcool est alors éliminé, laissant la serine sous une forme estérifiée. Un alcool présent dans le milieu peut alors être attaqué par l'histidine, formant de nouveau un composé intermédiaire cyclique. L'alcoolate ainsi formé peut

attaquer le carbonyle de la serine. En libérant un ester, la serine récupère son proton, régénérant ainsi le site actif de l'enzyme qui se retrouve de nouveau prêt à réagir.

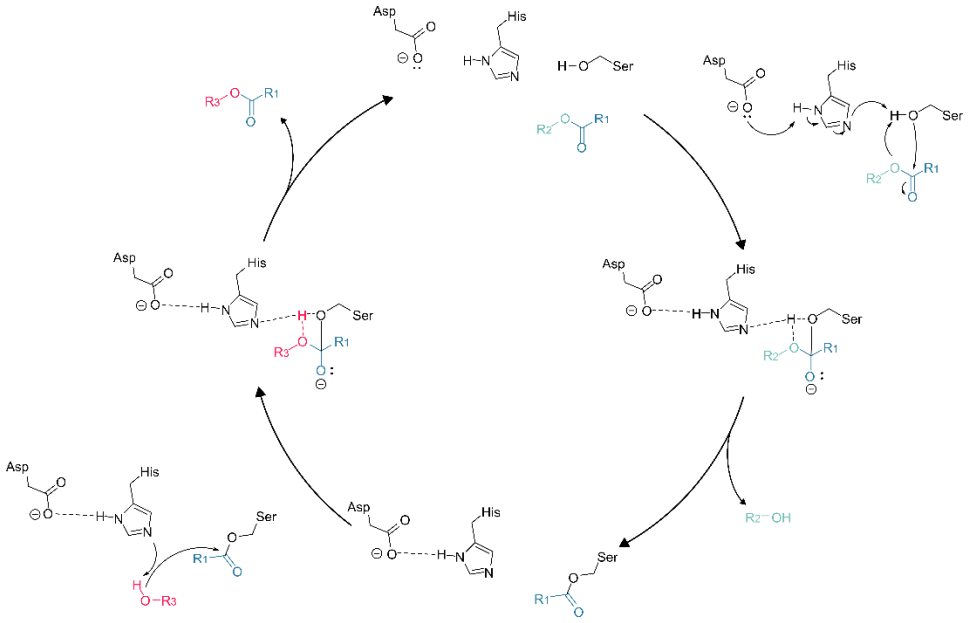

Schéma 1.1.4: Mécanisme de la transestérification catalysé par la triade catalytique de la CALB.

La CALB est largement employée dans la recherche, mais également en industrie. Elle doit cette popularité à sa bonne résistance en température et aux solvants, à sa stéréosélectivité, notamment au contact d'alcools secondaires, et à sa grande versatilité (Nielsen *et al.*, 1999; Yagi *et al.*, 2018). La forme immobilisée de l'enzyme sur des billes acryliques portant le nom commercial Novozym 435 (ou N435) commercialisée par Novozymes est la forme la plus populaire (Heldt-Hansen *et al.*, 1989; Ortiz *et al.*, 2019) (Figure 1.1.7). En effet, l'immobilisation de l'enzyme améliore sa résistance aux solvants et en température (Poojari *et al.*, 2013; Stergiou *et al.*, 2013). Elle permet également une récupération aisée du catalyseur et une plus grande réutilisabilité. Ces deux points favorisent son utilisation industrielle et sont en accord avec les principes de la chimie verte. La CALB immobilisée existe également sous d'autres formes commerciales comme Fermase CALB™ 10000 (Sonseca *et al.*, 2017), SP435 (Nielsen *et al.*, 1999) ou CalB immo Plus (*Purolite Life Sciences Product: Lifetech™ CalB immo Plus - Immobilized Lipase - Purolite*, 2021).

a)

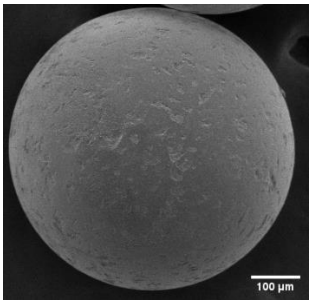

b)

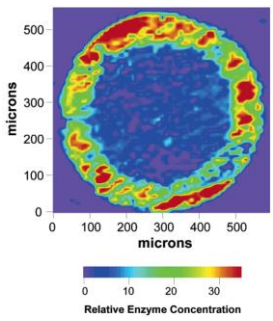

Figure 1.1.7: Photo par microscopie électronique à balayage de billes de résine acrylique supportant la CALB ; b) Concentration relative en CALB au sein des billes acrylique du support (Mei *et al.*, 2003b).

3.3. La synthèse de polyesters par la CALB

Il a été montré que l'utilisation de CALB immobilisée est une méthode de catalyse efficace pour la synthèse de polyesters (Varma *et al.*, 2005; Douka *et al.*, 2018). La synthèse de polyesters catalysée par la CALB peut se faire par POC, par polycondensation ou en combinant ces deux méthodes. La POC catalysée par CALB permet par exemple la synthèse du polyester polycaprolactone (PCL) présentant de hautes masses molaires (jusqu'à 44 800 $g.mol^{-1}$) (Dong *et al.*, 1999; Kumar *et al.*, 2000; Mei *et al.*, 2003a). La structure de la CALB a même été optimisée pour la synthèse de PCL (Montanier *et al.*, 2017). La synthèse par POC d'autres polyesters biosourcés comme le PLA à partir du lactide a également été étudiée (Lassalle *et al.*, 2008; Omay *et al.*, 2013; Duchiron *et al.*, 2015). La littérature dans ce domaine de la synthèse de polyesters par POC catalysée par CALB est particulièrement riche et ne sera pas détaillée plus avant ici. En effet, plusieurs articles de la littérature présentent les progrès dans le domaine de la POC par catalyse enzymatique (Shoda *et al.*, 2016; Engel *et al.*, 2019; Nikulin *et al.*, 2021).

Cette thèse s'intéressera ainsi plus spécifiquement à la synthèse de polyesters par polycondensation. En effet, cette voie présente l'avantage de concerner une plus large gamme de substrats biosourcés (Jiang *et al.*, 2016). La première étape de cette polycondensation peut se faire soit par estérification directe ou par transestérification. La polymérisation se poursuit ensuite par transestérification et interestérification. Ces deux phénomènes entrainent une randomisation de la structure du polymère (Takamoto *et al.*, 2001; Varma *et al.*, 2005). La polymérisation par polycondensation entraine la production d'un adduit au cours de la réaction. Cet adduit est une molécule d'eau dans le cas de l'estérification et un alcool ou un acide dans le cas de la transestérification. L'élimination de cet adduit favorise la croissance des chaînes polymères (par déplacement de l'équilibre de la réaction) et peut se faire par distillation azéotropique (Juais *et al.*, 2010), à l'aide de tamis moléculaire (Vouyiouka *et al.*, 2013; Debuissy *et al.*, 2016) ou par distillation sous pression réduite (Debuissy *et al.*, 2017b). Les étapes de la synthèse de polyesters par polycondensation enzymatique sont résumées dans le Schéma 1.1.5. Il a été montré à plusieurs reprises dans la littérature que la polymérisation initiée par la transestérification (impliquant donc un dérivé ester du substrat acide carboxylique) permettait d'atteindre de plus hautes masses molaires que par estérification. En effet, l'adduit alcool produit par la réaction est plus facile à éliminer que l'eau. Il est également possible d'employer des esters dits « activés » comme les esters vinyliques (Taresco *et al.*, 2016). L'alcoolyse des esters vinyliques produit de l'alcool vinylique qui par tautomérisation se transforme en acétaldéhyde, un composé toxique, mais très facilement éliminable.

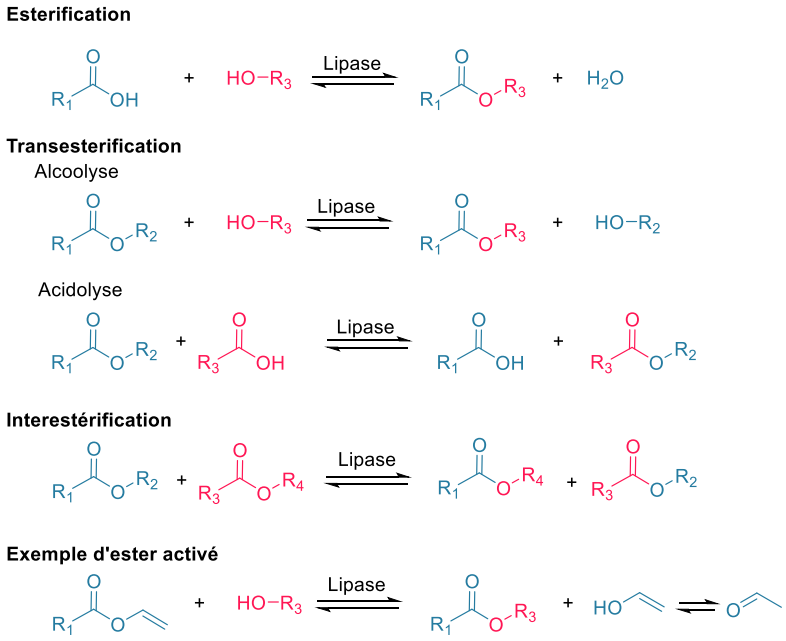

Schéma 1.1.5: Réactions se produisant au cours de la polymérisation enzymatique par polycondensation (adapté de (Jiang *et al.*, 2016)).

La synthèse de polyesters par polycondensation catalysée par la CALB peut se faire avec ou sans présence de solvant. Les procédés sans solvant sont plus avantageux d'un point de vue économique et environnemental. La croissance des chaînes polymères peut cependant entrainer une augmentation importante de la viscosité qui limite la diffusion des espèces et réduit le rendement de la réaction (Mahapatro *et al.*, 2003). De nombreux solvants ont été évalués pour la synthèse de polyesters catalysés par la CALB. Les solvants avec un coefficient de partage octanol-eau (LogP) supérieur à 1.9 (Dong *et al.*, 1999; Kumar *et al.*, 2000; Laane *et al.*) semblent favoriser l'activité de l'enzyme et limitent l'hydrolyse du polymère au cours de la réaction. Le toluène (LogP = 2,5 (Dong *et al.*, 1999)) est ainsi couramment employé pour la synthèse de polyesters. Le diphényle éther (LogP = 4,2) est cependant employé préférentiellement lorsque la réaction est réalisée sous pression réduite grâce à son haut point d'ébullition (259°C) ainsi que la grande stabilité de la CALB dans ce dernier. L'évaluation de l'impact du milieu réactionnel sur l'activité de l'enzyme doit cependant être considérée de manière holistique et le LogP du solvant n'en est qu'un élément. En effet, d'autres paramètres comme la mesure des interactions de surface entre solvant et substrat ont également été considérés (Pellis *et al.*, 2019a).

Comme pour les polyesters synthétisés par catalyse organométallique, la recherche s'est d'abord intéressée à la synthèse de polyesters aliphatiques (Varma *et al.*, 2005). La synthèse de polyesters aliphatiques catalysée par la CALB à partir d'une grande variété de diacides (ou diesters) et de diols a ainsi été étudiée (Pellis *et al.*, 2016a, 2016b). Il est ainsi possible de synthétiser des polyesters biosourcé à partir de synthons biosourcés comme le BDO et le diméthyle succinate pour la synthèse de PBS avec une masse molaire moyenne en nombre (M_n) autour de 12 000 g.mol^{-1} en conditions douces (Azim *et al.*, 2006; Debuissy *et al.*, 2017b) (Schéma 1.1.6.a). Plusieurs auteurs ont cependant montré que le type

de substrat et notamment sa longueur impactait fortement l'activité de l'enzyme. Il a ainsi été montré que pour des polymères aliphatiques, l'activité de l'enzyme vis-à-vis du substrat suivait l'ordre : 1,6-hexanediol > 1,4-butenadiol > 1,3-propanol (Mahapatro *et al.*, 2003; Pellis *et al.*, 2018). De même, les diacides employés présentent une réactivité qui suit l'ordre suivant : acide adipique > sébacique > octanoïque > dodécanoïque > succinique (Mahapatro *et al.*, 2003; Pellis *et al.*, 2018). Des monomères de structures plus complexes ont également été étudiés, notamment la polymérisation de l'isosorbide avec des esters de différentes longueurs donnant des polyesters avec des M_n allant jusqu'à 21 400 g.mol^{-1} (Juais *et al.*, 2010) (Schéma 1.1.6.b). Enfin, plusieurs études ont montré la faisabilité de la synthèse enzymatique de polyesters aliphatiques à l'échelle de la centaine de grammes jusqu'à la tonne (Binns *et al.*, 1999; Korupp *et al.*, 2010). L'état de l'art sur la synthèse enzymatique de polyesters aliphatiques a été plusieurs fois passé en revue dans la littérature (Varma *et al.*, 2005; Jiang *et al.*, 2016; Shoda *et al.*, 2016; Douka *et al.*, 2018; Kobayashi *et al.*, 2019; Nikulin *et al.*, 2021).

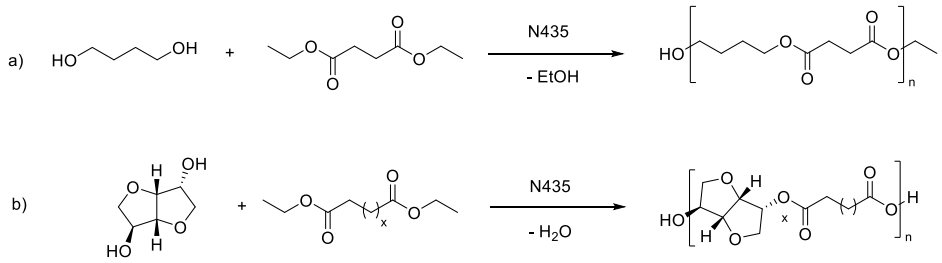

Schéma 1.1.6: a) Synthèse enzymatique de PBS (Azim *et al.*, 2006), b) synthèse enzymatique de polyesters à base d'isosorbide, 1 < x < 9 (Juais *et al.*, 2010).

La forte dépendance de l'activité des enzymes en fonction du substrat et la grande différence de structure entre les composés aromatiques et les triglycérides est sans doute l'une des raisons expliquant la plus faible proportion d'études portant sur la synthèse enzymatique de polyesters aromatiques (Jiang *et al.*, 2016; Douka *et al.*, 2018) que sur leurs homologues aliphatiques. Cependant, comme évoqué précédemment, les propriétés limitées de ces derniers font que de plus en plus d'études récentes s'intéressent à la synthèse enzymatique de polyesters aromatiques biosourcés pour lesquels l'aromaticité permet notamment d'améliorer les propriétés mécaniques et thermiques.

Comme dans le cadre de la synthèse par catalyse organométallique, la synthèse enzymatique de polyesters à base de FDCA a ainsi été assez largement étudiée. La synthèse d'oligomères à partir de diester de FDCA et de diols de plusieurs longueurs (2 < n < 12) a été étudiée (Cruz-Izquierdo *et al.*, 2015). Le degré de polymérisation (DP_n) le plus élevé (DP_n = 6) a été obtenu avec le HDO. Les auteurs n'ont pas observé d'inhibition de l'enzyme due à la présence du monomère aromatique. D'autres auteurs ont également étudié la polymérisation du diester méthylique du FDCA catalysée par la CALB (Jiang *et al.*, 2015)(Schéma 1.1.7). Des M_n entre 1 000 et 51 600 g.mol^{-1} ont ainsi été obtenues. Les synthèses ont cependant été réalisées à des températures élevées pour de la biocatalyse (140°C) ce qui peut soulever la question d'une possible dénaturation de l'enzyme et une activité catalytique autre

qu'enzymatique. Par ailleurs, les masses molaires les plus élevées ont été obtenues avec des diols particulièrement longs comme le 1,10-decanediol ou le 1,8-octanediol. La souplesse apportée par ces longs diols entraine une forte diminution des propriétés mécaniques et thermiques. Des études ont également montré que la catalyse enzymatique permettait la copolymérisation du FDCA avec l'acide itaconique (Aparaschivei *et al.*, 2019), le 1,4-cyclohexanediméthanol et le diéthylène glycol (Skoczinski *et al.*, 2020). Dans ces études, des polyesters aromatiques de masses molaires faibles (M_n < 3000 g.mol^{-1}) en comparaison de celles des polymères aliphatiques ont systématiquement été obtenues.

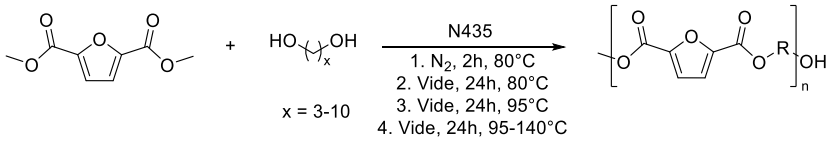

Schéma 1.1.7: Synthèse enzymatique de polyester à partir de diméthyle ester de FDCA (Jiang *et al.*, 2015).

Des auteurs ont également étudié la synthèse de polyesters à base de FDCA, diméthyle succinate et BDO par POC catalysée par la CALB de macrocycles formés préalablement (Morales-Huerta *et al.*, 2017). Récemment, Flores *et al*.(Flores *et al.*, 2019) ont étudié la synthèse de polyesters à base de diester de FDCA et HDO également par POC (Schéma 1.1.8). À la différence de l'étude précédente, la cyclisation préalable des monomères a également été effectuée par catalyse enzymatique. Un polyester de M_n supérieure à 9 000 g.mol^{-1} a ainsi été obtenu.

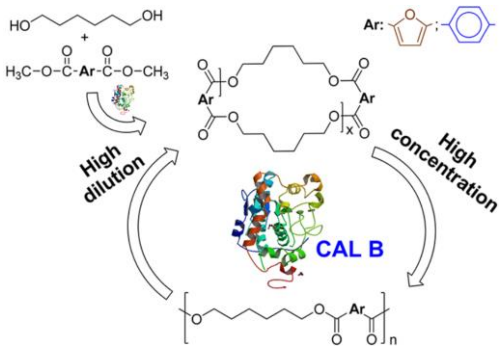

Schéma 1.1.8: Synthèse enzymatique de polyesters à base de diester de FDCA par POC (Flores *et al.*, 2019).

D'autres dérivés de furanes que le FDCA ont également été étudiés pour la synthèse de polyesters par la CALB. Des auteurs ont étudiés la synthèse de polyesters à partir du 2,5-bis-hydroxyméthyle furane avec différent diesters aliphatiques (Jiang *et al.*, 2014). La présence de réactions secondaires a cependant conduit à l'obtention de masses molaires inférieures à 2 400 g.mol^{-1}. D'autres auteurs ont synthétisé trois dérivés de l'hydroxyméthylfurfural (HMF) condensé avec des cétones dérivées du D-glucose (G-HMF), de l'acide succinique (S-HMF) et de l'acide malonique (M-HMF) (Schéma 1.1.9) (Muthusamy *et al.*, 2018). Le G-HMF a ensuite été copolymérisé avec l'acide succinique par catalyse enzymatique. Les autres dérivés ont été homopolymérisés. Dans tous les cas, seuls des oligomères ont été obtenus avec des M_n inférieures à 700 g.mol^{-1}.

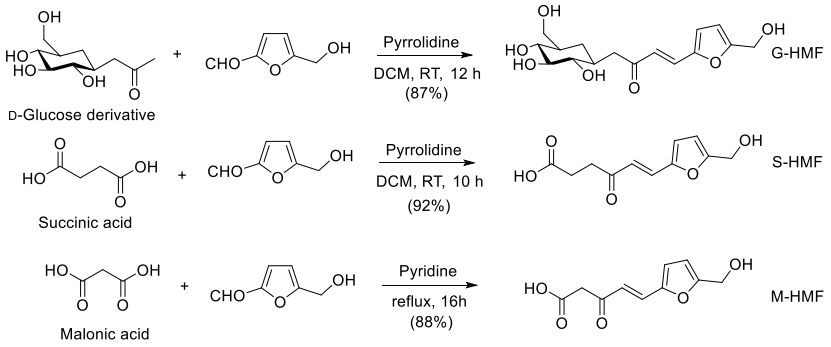

Schéma 1.1.9: Synthèse de précurseurs à base d'hydroxyméthylfurfural pour la synthèse enzymatique de polyesters biosourcés (Muthusamy et al., 2018).

La biomasse lignocellulosique représente la plus grande source potentielle de composés aromatiques biosourcés. Toutefois, les synthons issus de cette ressource n'ont que peu été utilisés pour la synthèse enzymatique de polyesters aromatiques. Pellis *et al.* ont étudié la synthèse de polyesters à partir de diols et de diacides aromatiques produits à partir de la lignine comme la 2,6-bis-hydroxyméthyle pyridine et le 2,4-pyridinedicarboxylate de diéthyle (Pellis *et al.*, 2019b, 2020; Comerford *et al.*, 2020). Des polyesters de M_n supérieures à 14 000 g.mol^{-1} ont ainsi été obtenus avec des T_g allant jusqu'à 30 °C.

D'autres composés tels que les phénols naturels issus de la biomasse lignocellulosique pourraient représenter une source intéressante de monomères aromatiques pour la synthèse de polyesters. Cependant, la réactivité en polymérisation enzymatique de ces composés n'a que rarement été étudiée (Fodor *et al.*, 2017). Le chapitre suivant s'attachera donc à établir un état de l'art complet portant sur la réactivité de ces dérivés phénoliques naturels dans des réactions d'estérification et transestérification catalysées par des enzymes. En effet, comprendre la réactivité de ces substrat engagés dans des réactions d'estérification et de transestérification est crucial afin d'évaluer leur potentielle utilisation en tant que monomères ou molécules plateforme pour la synthèse de polyesters.

4. Références

Abdel-Rahman, M. A., Tashiro, Y. and Sonomoto, K. (**2013**) 'Recent advances in lactic acid production by microbial fermentation processes', *Biotechnology Advances*, 31(6), pp. 877–902.

Albanese, M., Boyenval, J., Marchese, P., Sullalti, S. and Celli, A. (**2016**) 'The aliphatic counterpart of PET, PPT and PBT aromatic polyesters: effect of the molecular structure on thermo-mechanical properties', *AIMS Molecular Science*, 3(1), pp. 32–51.

Amini, Z., Ilham, Z., Ong, H. C., Mazaheri, H. and Chen, W.-H. (**2017**) 'State of the art and prospective of lipase-catalyzed transesterification reaction for biodiesel production', *Energy Conversion and Management*, 141, pp. 339–353.

Anastas, P. and Eghbali, N. (**2010**) 'Green Chemistry: Principles and Practice', *Chem. Soc. Rev.*, 39(1), pp. 301–312.

Aparaschivei, D., Todea, A., Frissen, A. E., Badea, V., Rusu, G., Sisu, E., Puiu, M., Boeriu, C. G. and Peter, F. (**2019**) 'Enzymatic synthesis and characterization of novel terpolymers from renewable sources', *Pure and Applied Chemistry*, 91(3), pp. 397–408.

Arrakhiz, F. Z., Elachaby, M., Bouhfid, R., Vaudreuil, S., Essassi, M. and Qaiss, A. (**2012**) 'Mechanical and thermal properties of polypropylene reinforced with Alfa fiber under different chemical treatment', *Materials & Design*, 35, pp. 318–322.

Azim, H., Dekhterman, A., Jiang, Z. and Gross, R. A. (**2006**) '*Candida antarctica* Lipase B-Catalyzed Synthesis of Poly(butylene succinate): Shorter Chain Building Blocks Also Work', *Biomacromolecules*, 7(11), pp. 3093–3097.

Becker, J., Lange, A., Fabarius, J. and Wittmann, C. (**2015**) 'Top value platform chemicals: bio-based production of organic acids', *Current Opinion in Biotechnology*, 36, pp. 168–175.

Binns, F., Harffey, P., Roberts, S. M. and Taylor, A. (**1999**) 'Studies leading to the large scale synthesis of polyesters using enzymes', *Journal of the Chemical Society, Perkin Transactions 1*, (19), pp. 2671–2676.

Bioplastics market data (**2020**) *European bioplastics*. Available at: https://www.european-bioplastics.org/market/ (Accessed: 2 September 2021).

Brito e Cunha, D. A., Bartkevihi, L., Robert, J. M., Cipolatti, E. P., Ferreira, A. T. S., Oliveira, D. M. P., Gomes-Neto, F., Almeida, R. V., Fernandez-Lafuente, R., Freire, D. M. G. and Anobom, C. D. (**2019**) 'Structural differences of commercial and recombinant lipase B from Candida antarctica: An important implication on enzymes thermostability', *International Journal of Biological Macromolecules*, 140, pp. 761–770.

Chapman, J., Ismail, A. and Dinu, C. (**2018**) 'Industrial Applications of Enzymes: Recent Advances, Techniques, and Outlooks', *Catalysts*, 8(6), p. 238.

Chen, G.-Q. (ed.) (**2010**) *Plastics from Bacteria*. Berlin, Heidelberg: Springer (Microbiology Monographs).

Chen, G.-Q. and Jiang, X.-R. (**2017**) 'Engineering bacteria for enhanced polyhydroxyalkanoates (PHA) biosynthesis', *Synthetic and Systems Biotechnology*, 2(3), pp. 192–197.

Coca-Cola Expands Access to PlantBottle IP , *The Coca-Cola Company*. Available at: http://www.coca-colacompany.com/news/coca-cola-expands-access-to-plantbottle-ip (Accessed: 14 September 2021).

Comerford, J. W., Byrne, F. P., Weinberger, S., Farmer, T. J., Guebitz, G. M., Gardossi, L. and Pellis, A. (**2020**) 'Thermal Upgrade of Enzymatically Synthesized Aliphatic and Aromatic Oligoesters', *Materials*, 13(2), p. 368.

Cruz-Izquierdo, Á., van den Broek, L. A. M., Serra, J. L., Llama, M. J. and Boeriu, C. G. (**2015**) 'Lipase-catalyzed synthesis of oligoesters of 2,5-furandicarboxylic acid with aliphatic diols', *Pure and Applied Chemistry*, 87(1), pp. 59–69.

Debuissy, T., Pollet, E. and Avérous, L. (**2016**) 'Enzymatic Synthesis of a Bio-Based Copolyester from Poly(butylene succinate) and Poly((*R*)-3-hydroxybutyrate): Study of Reaction Parameters on the Transesterification Rate', *Biomacromolecules*, 17(12), pp. 4054–4063.

Debuissy, T., Pollet, E. and Avérous, L. (**2017**)**b** 'Lipase-catalyzed synthesis of biobased and biodegradable aliphatic copolyesters from short building blocks. Effect of the monomer length', *European Polymer Journal*, 97, pp. 328–337.

Dettori, L., Jelsch, C., Guiavarc'h, Y., Delaunay, S., Framboisier, X., Chevalot, I. and Humeau, C. (**2018**) 'Molecular rules for selectivity in lipase-catalysed acylation of lysine', *Process Biochemistry*, 74, pp. 50–60.

Devi Salam, M., Varma, A., Prashar, R. and Choudhary, D. (**2021**) 'Review on Efficacy of Microbial Degradation of Polyethylene Terephthalate and Bio-upcycling as a Part of Plastic Waste Management', *Applied Ecology and Environmental Sciences*, 9(7), pp. 695–703.

Dickson, J. T. and Whinfield, J. R. (**1946**) 'Improvements relating to the manufacture of highly polymeric substances', GB578079A.

Dong, H., Cao, S.-G., Li, Z.-Q., Han, S.-P., You, D.-L. and Shen, J.-C. (**1999**) 'Study on the enzymatic polymerization mechanism of lactone and the strategy for improving the degree of polymerization', *Journal of Polymer Science Part A: Polymer Chemistry*, 37(9), pp. 1265–1275.

Douka, A., Vouyiouka, S., Papaspyridi, L.-M. and Papaspyrides, C. D. (**2018**) 'A review on enzymatic polymerization to produce polycondensation polymers: The case of aliphatic polyesters, polyamides and polyesteramides', *Progress in Polymer Science*, 79, pp. 1–25.

Duchiron, S. W., Pollet, E., Givry, S. and Avérous, L. (**2015**) 'Mixed systems to assist enzymatic ring opening polymerization of lactide stereoisomers', *RSC Advances*, 5(103), pp. 84627–84635.

Elias, H.-G. and Palacios, J. A. (**1985**) 'Poly(ferulic acid) by Thionyl Chloride Activated Polycondensation', *Die Makromolekulare Chemie*, 186(5), pp. 1027–1045.

Engel, J., Cordellier, A., Huang, L. and Kara, S. (**2019**) 'Enzymatic Ring Opening Polymerization of Lactones: Traditional Approaches and Alternative Strategies', *ChemCatChem*, 11(20), pp. 4983–4997.

Fache, M., Boutevin, B. and Caillol, S. (**2015**) 'Vanillin, a key-intermediate of biobased polymers', *European Polymer Journal*, 68, pp. 488–502.

Feldman, D. (**2008**) 'Polymer History', *Designed Monomers and Polymers*, 11(1), pp. 1–15.

Flores, I., Martínez de Ilarduya, A., Sardon, H., Müller, A. J. and Muñoz-Guerra, S. (**2019**) 'Synthesis of Aromatic–Aliphatic Polyesters by Enzymatic Ring Opening Polymerization of Cyclic Oligoesters and their Cyclodepolymerization for a Circular Economy', *ACS Applied Polymer Materials*, 1(3), pp. 321–325.

Flourat, A. L., Combes, J., Bailly-Maitre-Grand, C., Magnien, K., Haudrechy, A., Renault, J. and Allais, F. (**2021**) 'Accessing *p*-Hydroxycinnamic Acids: Chemical Synthesis, Biomass Recovery, or Engineered Microbial Production?', *ChemSusChem*, 14(1), pp. 118–129.

Fodor, C., Golkaram, M., Woortman, A. J. J., van Dijken, J. and Loos, K. (**2017**) 'Enzymatic approach for the synthesis of biobased aromatic–aliphatic oligo-/polyesters', *Polymer Chemistry*, 8(44), pp. 6795–6805.

Gandini, A., Silvestre, A. J. D., Neto, C. P., Sousa, A. F. and Gomes, M. (**2009**) 'The furan counterpart of poly(ethylene terephthalate): An alternative material based on renewable resources', *Journal of Polymer Science Part A: Polymer Chemistry*, 47(1), pp. 295–298.

Gioia, C., Banella, M. B., Marchese, P., Vannini, M., Colonna, M. and Celli, A. (**2016**) 'Advances in the synthesis of bio-based aromatic polyesters: novel copolymers derived from vanillic acid and ε-caprolactone', *Polymer Chemistry*, 7(34), pp. 5396–5406.

Gioia, C., Banella, M. B., Totaro, G., Vannini, M., Marchese, P., Colonna, M., Sisti, L. and Celli, A. (**2018**) 'Biobased Vanillic Acid and Ricinoleic Acid: Building Blocks for Fully Renewable Copolyesters', *Journal of Renewable Materials*, 6(1), pp. 126–135.

Grebowicz, J., Lau, S.-F. and Wunderlich, B. (**2007**) 'The thermal properties of polypropylene', *Journal of Polymer Science: Polymer Symposia*, 71(1), pp. 19–37.

Heldt-Hansen, H. P., Ishii, M., Patkar, S. A., Hansen, T. T. and Eigtved, P. (**1989**) 'A New Immobilized Positional Nonspecific Lipase for Fat Modification and Ester Synthesis', in Whitaker, J. R. and Sonnet, P. E. (eds) *Biocatalysis in Agricultural Biotechnology*. Washington, DC: American Chemical Society, pp. 158–172.

Hu, H., Zhang, R., Wang, J., Ying, W. B. and Zhu, J. (**2018**) 'Fully bio-based poly(propylene succinate-co-propylene furandicarboxylate) copolyesters with proper mechanical, degradation and barrier properties for green packaging applications', *European Polymer Journal*, 102, pp. 101–110.

Jang, Y.-S., Kim, B., Shin, J. H., Choi, Y. J., Choi, S., Song, C. W., Lee, J., Park, H. G. and Lee, S. Y. (**2012**) 'Bio-based production of C2-C6 platform chemicals', *Biotechnology and Bioengineering*, 109(10), pp. 2437–2459.

Jiang, Y. and Loos, K. (**2016**) 'Enzymatic Synthesis of Biobased Polyesters and Polyamides', *Polymers*, 8(7), p. 243.

Jiang, Y., Woortman, A. J. J., Alberda van Ekenstein, G. O. R. and Loos, K. (**2015**) 'A biocatalytic approach towards sustainable furanic–aliphatic polyesters', *Polymer Chemistry*, 6(29), pp. 5198–5211.

Jiang, Y., Woortman, A. J. J., Alberda van Ekenstein, G. O. R., Petrović, D. M. and Loos, K. (**2014**) 'Enzymatic Synthesis of Biobased Polyesters Using 2,5-Bis(hydroxymethyl)furan as the Building Block', *Biomacromolecules*, 15(7), pp. 2482–2493.

Juais, D., Naves, A. F., Li, C., Gross, R. A. and Catalani, L. H. (**2010**) 'Isosorbide Polyesters from Enzymatic Catalysis', *Macromolecules*, 43(24), pp. 10315–10319.

Kakadellis, S. and Rosetto, G. (**2021**) 'Achieving a circular bioeconomy for plastics', *Science*, 373(6550), pp. 49–50.

Kalia, V. C., Singh Patel, S. K., Shanmugam, R. and Lee, J.-K. (**2021**) 'Polyhydroxyalkanoates: Trends and advances toward biotechnological applications', *Bioresource Technology*, 326, p. 124737.

Kirk, O., Borchert, T. V. and Fuglsang, C. C. (**2002**) 'Industrial enzyme applications', *Current Opinion in Biotechnology*, 13(4), pp. 345–351.

Kobayashi, S. and Uyama, H. (**2019**) 'Synthesis of Polyesters I: Hydrolase as Catalyst for Polycondensation (Condensation Polymerization)', in Kobayashi, S., Uyama, H., and Kadokawa, J. (eds) *Enzymatic Polymerization towards Green Polymer Chemistry*. Singapore: Springer Singapore (Green Chemistry and Sustainable Technology), pp. 105–163.

Korupp, C., Weberskirch, R., Müller, J. J., Liese, A. and Hilterhaus, L. (**2010**) 'Scaleup of Lipase-Catalyzed Polyester Synthesis', *Organic Process Research & Development*, 14(5), pp. 1118–1124.

Kumar, A. and Gross, R. A. (**2000**) '*Candida antartica* Lipase B Catalyzed Polycaprolactone Synthesis: Effects of Organic Media and Temperature', *Biomacromolecules*, 1(1), pp. 133–138.

Kurt, G. and Gokturk, E. (**2020**) 'Synthesis of polyesters mimicking polyethylene terephthalate and their thermal and mechanical properties', *Journal of Polymer Research*, 27(10), p. 314.

Laane, C., Boeren, S., Vos, K. and Veeger, C. , 'Rules for optimization of biocatalysis in organic solvents', p. 8.

Lassalle, V. L. and Ferreira, M. L. (**2008**) 'Lipase-catalyzed synthesis of polylactic acid: an overview of the experimental aspects', *Journal of Chemical Technology & Biotechnology*, 83(11), pp. 1493–1502.

Li, M. and Wilkins, M. (**2021**) 'Lignin bioconversion into valuable products: fractionation, depolymerization, aromatic compound conversion, and bioproduct formation', *Systems Microbiology and Biomanufacturing*, 1(2), pp. 166–185.

Llevot, A., Grau, E., Carlotti, S., Grelier, S. and Cramail, H. (**2015**) 'Renewable (semi)aromatic polyesters from symmetrical vanillin-based dimers', *Polymer Chemistry*, 6(33), pp. 6058–6066.

Llevot, A., Grau, E., Carlotti, S., Grelier, S. and Cramail, H. (**2016**) 'From Lignin-derived Aromatic Compounds to Novel Biobased Polymers', *Macromolecular Rapid Communications*, 37(1), pp. 9–28.

Loos, K., Zhang, R., Pereira, I., Agostinho, B., Hu, H., Maniar, D., Sbirrazzuoli, N., Silvestre, A. J. D., Guigo, N. and Sousa, A. F. (**2020**) 'A Perspective on PEF Synthesis, Properties, and End-Life', *Frontiers in Chemistry*, 8, p. 585.

Mahapatro, A., Kalra, B., Kumar, A. and Gross, R. A. (**2003**) 'Lipase-Catalyzed Polycondensations: Effect of Substrates and Solvent on Chain Formation, Dispersity, and End-Group Structure', *Biomacromolecules*, 4(3), pp. 544–551.

Mandal, S. and Dey, A. (**2019**) 'PET Chemistry', in *Recycling of Polyethylene Terephthalate Bottles*. Elsevier, pp. 1–22.

McIntyre, J. E. (**2004**) 'The Historical Development of Polyesters', in Scheirs, J. and Long, T. E. (eds) *Wiley Series in Polymer Science*. Chichester, UK: John Wiley & Sons, Ltd, pp. 1–28.

Mei, Y., Kumar, A. and Gross, R. (**2003**)**a** 'Kinetics and Mechanism of *Candida a ntarctica* Lipase B Catalyzed Solution Polymerization of ε-Caprolactone', *Macromolecules*, 36(15), pp. 5530–5536.

Mei, Y., Miller, L., Gao, W. and Gross, R. A. (**2003**)**b** 'Imaging the Distribution and Secondary Structure of Immobilized Enzymes Using Infrared Microspectroscopy', *Biomacromolecules*, 4(1), pp. 70–74.

Mochane, M. J., Magagula, S. I., Sefadi, J. S. and Mokhena, T. C. (**2021**) 'A Review on Green Composites Based on Natural Fiber-Reinforced Polybutylene Succinate (PBS)', *Polymers*, 13(8), p. 1200.

Montanier, C. Y., Chabot, N., Emond, S., Guieysse, D., Remaud-Siméon, M., Peruch, F. and André, I. (**2017**) 'Engineering of Candida antarctica lipase B for poly(ε-caprolactone) synthesis', *European Polymer Journal*, 95, pp. 809–819.

Morales-Huerta, J. C., Ciulik, C. B., de Ilarduya, A. M. and Muñoz-Guerra, S. (**2017**) 'Fully bio-based aromatic–aliphatic copolyesters: poly(butylene furandicarboxylate-co-succinate)s obtained by ring opening polymerization', *Polymer Chemistry*, 8(4), pp. 748–760.

Muthusamy, K., Lalitha, K., Prasad, Y. S., Thamizhanban, A., Sridharan, V., Maheswari, C. U. and Nagarajan, S. (**2018**) 'Lipase-Catalyzed Synthesis of Furan-Based Oligoesters and their Self-Assembly-Assisted Polymerization', *ChemSusChem*, 11(14), pp. 2453–2463.

Nguyen, H. T. H., Qi, P., Rostagno, M., Feteha, A. and Miller, S. A. (**2018**) 'The quest for high glass transition temperature bioplastics', *Journal of Materials Chemistry A*, 6(20), pp. 9298–9331.

Nguyen, H. T. H., Reis, M. H., Qi, P. and Miller, S. A. (**2015**) 'Polyethylene ferulate (PEF) and congeners: polystyrene mimics derived from biorenewable aromatics', *Green Chemistry*, 17(9), pp. 4512–4517.

Nguyen, H. T. H., Short, G. N., Qi, P. and Miller, S. A. (**2017**) 'Copolymerization of lactones and bioaromatics via concurrent ring-opening polymerization/polycondensation', *Green Chemistry*, 19(8), pp. 1877–1888.

Nielsen, T. B., Ishii, M. and Kirk, O. (**1999**) 'Lipases A and B from the yeast Candida antarctica', in *Biotechnological Application of Cold-Adapted Organisms*. Springer Berlin Heidelberg, pp. 49–61.

Nikulin, M. and Švedas, V. (**2021**) 'Prospects of Using Biocatalysis for the Synthesis and Modification of Polymers', *Molecules*, 26(9), p. 2750.

Omay, D. and Guvenilir, Y. (**2013**) 'Synthesis and characterization of poly(d,l-lactic acid) via enzymatic ring opening polymerization by using free and immobilized lipase', *Biocatalysis and Biotransformation*, 31(3), pp. 132–140.

Ortiz, C., Ferreira, M. L., Barbosa, O., dos Santos, J. C. S., Rodrigues, R. C., Berenguer-Murcia, Á., Briand, L. E. and Fernandez-Lafuente, R. (**2019**) 'Novozym 435: the "perfect" lipase immobilized biocatalyst?', *Catalysis Science & Technology*, 9(10), pp. 2380–2420.

Pang, C., Zhang, J., Zhang, Q., Wu, G., Wang, Y. and Ma, J. (**2015**) 'Novel vanillic acid-based poly(ether–ester)s: from synthesis to properties', *Polymer Chemistry*, 6(5), pp. 797–804.

Papageorgiou, G. Z., Papageorgiou, D. G., Terzopoulou, Z. and Bikiaris, D. N. (**2016**) 'Production of bio-based 2,5-furan dicarboxylate polyesters: Recent progress and critical aspects in their synthesis and thermal properties', *European Polymer Journal*, 83, pp. 202–229.

Parlement Européen (**2008**) *Concernant les enzymes alimentaires*, *Parlement Européen et du Conseil*. Available at: https://eur-lex.europa.eu/legal-content/FR/TXT/HTML/?uri=CELEX:32008R1332&from=EN.

Pellis, A., Byrne, F. P., Sherwood, J., Vastano, M., Comerford, J. W. and Farmer, T. J. (**2019**)**a** 'Safer bio-based solvents to replace toluene and tetrahydrofuran for the biocatalyzed synthesis of polyesters', *Green Chemistry*, 21(7), pp. 1686–1694.

Pellis, A., Comerford, J. W., Maneffa, A. J., Sipponen, M. H., Clark, J. H. and Farmer, T. J. (**2018**) 'Elucidating enzymatic polymerisations: Chain-length selectivity of Candida antarctica lipase B towards various aliphatic diols and dicarboxylic acid diesters', *European Polymer Journal*, 106, pp. 79–84.

Pellis, A., Comerford, J. W., Weinberger, S., Guebitz, G. M., Clark, J. H. and Farmer, T. J. (**2019**)**b** 'Enzymatic synthesis of lignin derivable pyridine based polyesters for the substitution of petroleum derived plastics', *Nature Communications*, 10(1).

Pellis, A., Herrero Acero, E., Ferrario, V., Ribitsch, D., Guebitz, G. M. and Gardossi, L. (**2016**)**a** 'The Closure of the Cycle: Enzymatic Synthesis and Functionalization of Bio-Based Polyesters', *Trends in Biotechnology*, 34(4), pp. 316–328.

Pellis, A., Herrero Acero, E., Gardossi, L., Ferrario, V. and Guebitz, G. M. (**2016**)**b** 'Renewable building blocks for sustainable polyesters: new biotechnological routes for greener plastics: Renewable building blocks for sustainable polyesters', *Polymer International*, 65(8), pp. 861–871.

Pellis, A., Weinberger, S., Gigli, M., Guebitz, G. M. and Farmer, T. J. (**2020**) 'Enzymatic synthesis of biobased polyesters utilizing aromatic diols as the rigid component', *European Polymer Journal*, 130, p. 109680.

Pleiss, J., Fischer, M. and Schmid, R. D. (**1998**) 'Anatomy of lipase binding sites: the scissile fatty acid binding site', *Chemistry and Physics of Lipids*, 93(1–2), pp. 67–80.

Poojari, Y. and Clarson, S. J. (**2013**) 'Thermal stability of Candida antarctica lipase B immobilized on macroporous acrylic resin particles in organic media', *Biocatalysis and Agricultural Biotechnology*, 2(1), pp. 7–11.

Poveda-Giraldo, J. A., Solarte-Toro, J. C. and Cardona Alzate, C. A. (**2021**) 'The potential use of lignin as a platform product in biorefineries: A review', *Renewable and Sustainable Energy Reviews*, 138, p. 110688.

Preferred Fiber & Materials, Market Report 2021 (**2021**). TextileExchange. Available at: https://textileexchange.org/wp-content/uploads/2021/08/Textile-Exchange_Preferred-Fiber-and-Materials-Market-Report_2021.pdf.

Purolite Life Sciences Product: Lifetech™ CalB immo Plus - Immobilized Lipase - Purolite (**2021**) *Purolite Life Sciences*. Available at: http://www.purolite.com/ls-product/calb-immo-plus (Accessed: 8 September 2021).

Rabnawaz, M., Wyman, I., Auras, R. and Cheng, S. (**2017**) 'A roadmap towards green packaging: the current status and future outlook for polyesters in the packaging industry', *Green Chem.*, 19(20), pp. 4737–4753.

Rafiqah, S. A., Khalina, A., Harmaen, A. S., Tawakkal, I. A., Zaman, K., Asim, M., Nurrazi, M. N. and Lee, C. H. (**2021**) 'A Review on Properties and Application of Bio-Based Poly(Butylene Succinate)', *Polymers*, 13(9), p. 1436.

Rajesh, R. O., Godan, T. K., Sindhu, R., Pandey, A. and Binod, P. (**2020**) 'Bioengineering advancements, innovations and challenges on green synthesis of 2, 5-furan dicarboxylic acid', *Bioengineered*, 11(1), pp. 19–38.

Ravindranath, K. and Mashelkar, R. A. (**1984**) 'Polyethylene terephthalate-I. Chemistry, thermodynamics and transport properties', *Chemical Engineering Science*, 41(9), pp. 2197–2214.

Sajid, M., Zhao, X. and Liu, D. (**2018**) 'Production of 2,5-furandicarboxylic acid (FDCA) from 5-hydroxymethylfurfural (HMF): recent progress focusing on the chemical-catalytic routes', *Green Chemistry*, 20(24), pp. 5427–5453.

Santos, Y. L. de los, Chew-Fajardo, Y. L., Brault, G. and Doucet, N. (**2019**) 'Dissecting the evolvability landscape of the CalB active site toward aromatic substrates', *Scientific Reports*, 9(1).

Schyns, Z. O. G. and Shaver, M. P. (**2021**) 'Mechanical Recycling of Packaging Plastics: A Review', *Macromolecular Rapid Communications*, 42(3), p. 2000415.

Shoda, S., Uyama, H., Kadokawa, J., Kimura, S. and Kobayashi, S. (**2016**) 'Enzymes as Green Catalysts for Precision Macromolecular Synthesis', *Chemical Reviews*, 116(4), pp. 2307–2413.

Silvestrini, L. and Cianci, M. (**2020**) 'Principles of lipid–enzyme interactions in the limbus region of the catalytic site of Candida antarctica Lipase B', *International Journal of Biological Macromolecules*, 158, pp. 358–363.

Siracusa, V. and Blanco, I. (**2020**) 'Bio-Polyethylene (Bio-PE), Bio-Polypropylene (Bio-PP) and Bio-Poly(ethylene terephthalate) (Bio-PET): Recent Developments in Bio-Based Polymers Analogous to Petroleum-Derived Ones for Packaging and Engineering Applications', *Polymers*, 12(8), p. 1641.

Skoczinski, P., Espinoza Cangahuala, M. K., Maniar, D., Albach, R. W., Bittner, N. and Loos, K. (**2020**) 'Biocatalytic Synthesis of Furan-Based Oligomer Diols with Enhanced End-Group Fidelity', *ACS Sustainable Chemistry & Engineering*, 8(2), pp. 1068–1086.

Sonseca, A. and El Fray, M. (**2017**) 'Enzymatic synthesis of an electrospinnable poly(butylene succinate-co-dilinoleic succinate) thermoplastic elastomer', *RSC Advances*, 7(34), pp. 21258–21267.

Stergiou, P.-Y., Foukis, A., Filippou, M., Koukouritaki, M., Parapouli, M., Theodorou, L. G., Hatziloukas, E., Afendra, A., Pandey, A. and Papamichael, E. M. (**2013**) 'Advances in lipase-catalyzed esterification reactions', *Biotechnology Advances*, 31(8), pp. 1846–1859.

Takamoto, T., Kerep, P., Uyama, H. and Kobayashi, S. (**2001**) 'Lipase-Catalyzed Transesterification of Polyesters to Ester Copolymers', *Macromolecular Bioscience*, 1(6), pp. 223–227.

Taresco, V., Creasey, R. G., Kennon, J., Mantovani, G., Alexander, C., Burley, J. C. and Garnett, M. C. (**2016**) 'Variation in structure and properties of poly(glycerol adipate) via control of chain branching during enzymatic synthesis', *Polymer*, 89, pp. 41–49.

Terzopoulou, Z., Karakatsianopoulou, E., Kasmi, N., Tsanaktsis, V., Nikolaidis, N., Kostoglou, M., Papageorgiou, G. Z., Lambropoulou, D. A. and Bikiaris, D. N. (**2017**) 'Effect of catalyst type on molecular weight increase and coloration of poly(ethylene furanoate) biobased polyester during melt polycondensation', *Polymer Chemistry*, 8(44), pp. 6895–6908.

Terzopoulou, Z., Papadopoulos, L., Zamboulis, A., Papageorgiou, D. G., Papageorgiou, G. Z. and Bikiaris, D. N. (**2020**) 'Tuning the Properties of Furandicarboxylic Acid-Based Polyesters with Copolymerization: A Review', *Polymers*, 12(6), p. 1209.

Tomás, R. A. F., Bordado, J. C. M. and Gomes, J. F. P. (**2013**) '*p* -Xylene Oxidation to Terephthalic Acid: A Literature Review Oriented toward Process Optimization and Development', *Chemical Reviews*, 113(10), pp. 7421–7469.

Tournier, V., Topham, C. M., Gilles, A., David, B., Folgoas, C., Moya-Leclair, E., Kamionka, E., Desrousseaux, M.-L., Texier, H., Gavalda, S., Cot, M., Guémard, E., Dalibey, M., Nomme, J., Cioci, G., Barbe, S., Chateau, M., André, I., Duquesne, S. and Marty, A. (**2020**) 'An engineered PET depolymerase to break down and recycle plastic bottles', *Nature*, 580(7802), pp. 216–219.

Tserki, V., Matzinos, P., Pavlidou, E., Vachliotis, D. and Panayiotou, C. (**2006**) 'Biodegradable aliphatic polyesters. Part I. Properties and biodegradation of poly(butylene succinate-co-butylene adipate)', *Polymer Degradation and Stability*, 91(2), pp. 367–376.

Tümer, E. H. and Erbil, H. Y. (**2021**) 'Extrusion-Based 3D Printing Applications of PLA Composites: A Review', *Coatings*, 11(4), p. 390.

Varma, I. K., Albertsson, A.-C., Rajkhowa, R. and Srivastava, R. K. (**2005**) 'Enzyme catalyzed synthesis of polyesters', *Progress in Polymer Science*, 30(10), pp. 949–981.

Volanti, M., Cespi, D., Passarini, F., Neri, E., Cavani, F., Mizsey, P. and Fozer, D. (**2019**) 'Terephthalic acid from renewable sources: early-stage sustainability analysis of a bio-PET precursor', *Green Chemistry*, 21(4), pp. 885–896.

Vouyiouka, S. N., Topakas, E., Katsini, A., Papaspyrides, C. D. and Christakopoulos, P. (**2013**) 'A Green Route for the Preparation of Aliphatic Polyesters via Lipase-catalyzed Prepolymerization and Low-temperature Postpolymerization', *Macromolecular Materials and Engineering*, 298(6), pp. 679–689.

Xanthopoulou, E., Zamboulis, A., Terzopoulou, Z., Kostoglou, M., Bikiaris, D. N. and Papageorgiou, G. Z. (**2021**) 'Effectiveness of Esterification Catalysts in the Synthesis of Poly(Ethylene Vanillate)', *Catalysts*, 11(7), p. 822.

Yagi, Y., Kimura, T., Kamezawa, M. and Naoshima, Y. (**2018**) 'Biomolecular Chemical Simulations toward Elucidation of the Enantioselectivity and Reactivity of Lipases in Organic Synthesis', *Chem-Bio Informatics Journal*, 18(0), pp. 21–31.

Yang, Q., Zhu, S., Yang, Q., Huang, W., Yu, P., Zhang, D. and Wang, Z. (**2019**) 'Comparative techno-economic analysis of oil-based and coal-based ethylene glycol processes', *Energy Conversion and Management*, 198, p. 111814.

'YXY® Technology' (**2021**) *Avantium*. Available at: https://www.avantium.com/technologies/yxy/ (Accessed: 14 September 2021).

Sous-chapitre 1.2. Enzymatic esterification, transesterification and polyesterification of aromatic acids from lignocellulosic biomass, a review

*Alfred Bazin, Luc Avérous, Eric Pollet**

Soon submitted for publication

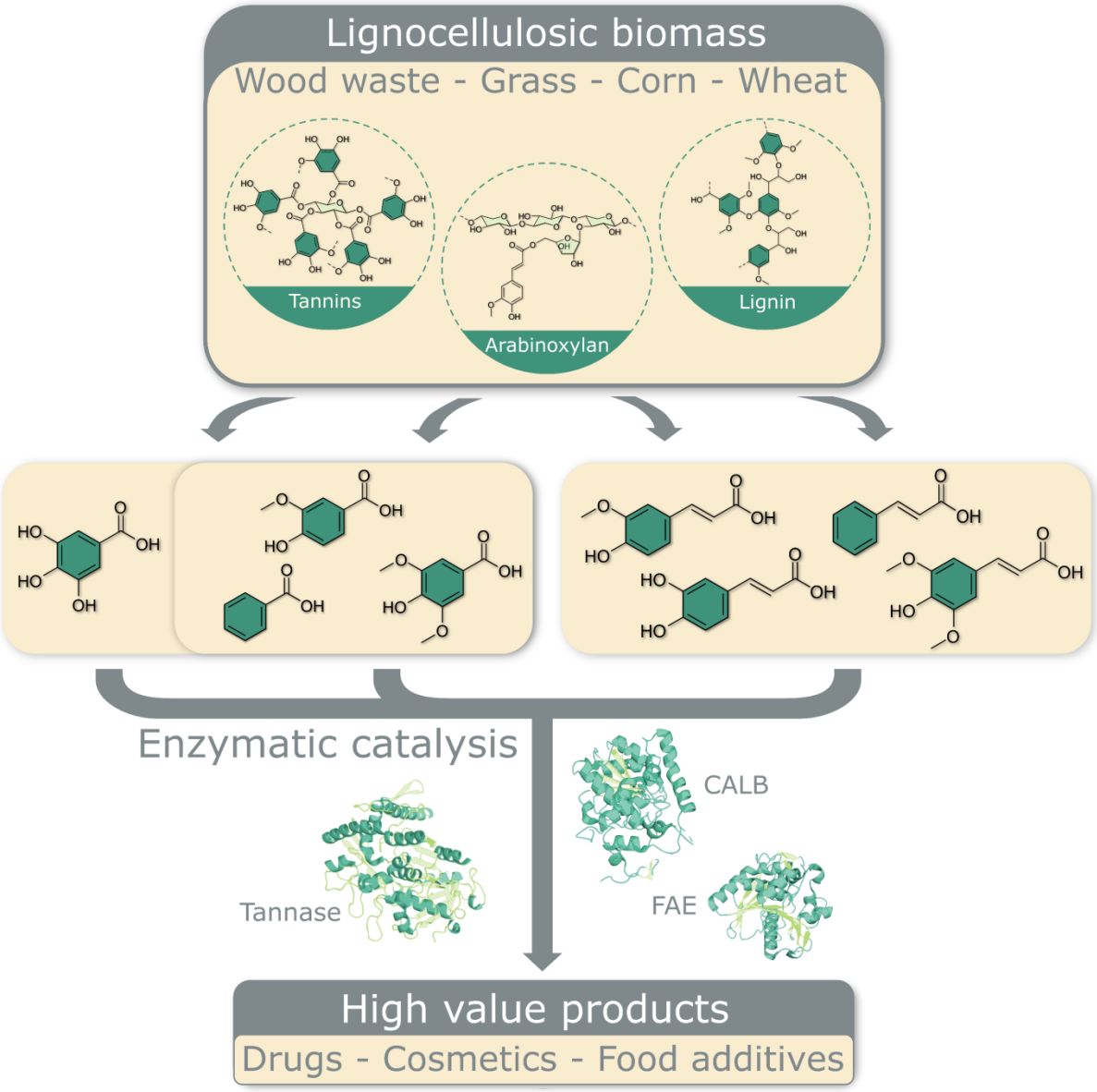

1. Introduction

The pressure of human activities on ecosystems is growing and so is the awareness of the scientific community. In particular, this leads nowadays the research in chemistry to be more focused on environmental impact, thanks to the establishment of fundamentals principles called “green chemistry” (Anastas *et al.*, 2010). Thus, in accordance with these principles and to reduce the impact of the chemical industry on the environment, the use of natural biobased compounds has gained a lot of interest. This is illustrated by the increasing number of studies dedicated to phenolic compounds such as ferulic acid (Figure 1.2.1).

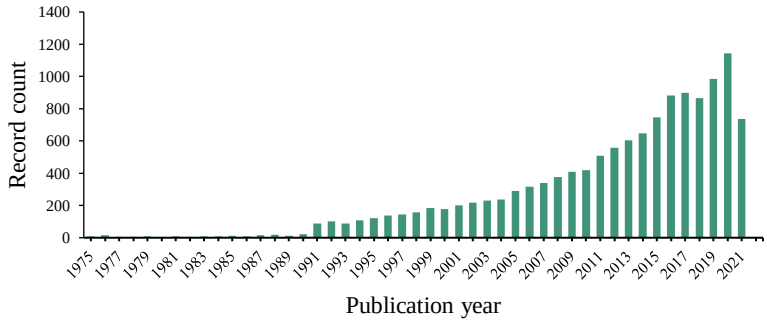

Figure 1.2.1: Count over the years of publications containing the word “ferulic acid”. From Web of Science, 2021.

Natural phenolic compounds have now been studied for a long time because of their potential use as additives, as drugs or in material science. Indeed, these compounds have been found in significant quantities in the plants composing traditional medicines (Cai *et al.*, 2004; Spiridon *et al.*, 2011). These compounds have beneficial health effects that could help to the treatment of several diseases such as cardiovascular disorder or cancers and they also show promising anti-inflammatory and anti-microbial effects (Srinivasulu *et al.*, 2018; Kahkeshani *et al.*, 2019; Kumar *et al.*, 2019; Khan *et al.*, 2021; Rychlicka *et al.*, 2021). Besides their positive health effects, phenolic compounds also display remarkable antioxidant and anti-UV properties (Natella *et al.*, 1999; Svobodova *et al.*, 2003; Genaro-Mattos *et al.*, 2015). This makes them suitable to replace potentially hazardous oil-based additives commonly employed in cosmetics (Gunia-Krzyżak *et al.*, 2018). Their use as natural preservatives in food is also largely investigated (Ou *et al.*, 2004). Finally, these compounds represent an alternative to the petroleum based BTX (Benzene, Toluene, Xylene) used as platform chemicals for the synthesis of many common compounds (Sun *et al.*, 2018b). As an example, natural phenolic compounds are being studied for the elaboration of rigid polymeric materials (Llevot *et al.*, 2016; Fonseca *et al.*, 2019). Due to the growing interest in phenolic compounds, multiple ways of extraction or production of these compounds from the biomass have been developed and are still being investigated (Valanciene *et al.*, 2020; Flourat *et al.*, 2021).

However, cinnamic and benzoic derivatives present a poor solubility in various nonpolar or aqueous media (Tsuchiyama *et al.*, 2006; Figueroa-Espinoza *et al.*, 2013). This poor solubility hinders the bioavailability of such compounds in pharmaceutical applications and their use in cosmetics or in food applications, as an example. In order to address this issue, the chemical modification of natural phenolic compounds has been studied (Figueroa-Espinoza *et al.*, 2005). Lipophilization of phenolic compounds is generally performed by esterification with a fatty molecule. On the contrary, the solubility of phenolic compounds in aqueous media can be improved by esterification with sugars or natural polyols such as glycerol (Villeneuve, 2007; Compton *et al.*, 2012; Laguerre *et al.*, 2013). Due to the general concern about the environmental impact of such modification and in accordance with the principles of green chemistry mentioned earlier, safe and environmentally friendly synthesis methods have been investigated.

Enzymes are considered to be non-polluting and non-toxic protein-based catalysts. They are classified depending on their substrate specificity, structure, and origin. As an example, proteases are enzymes that catalyze the cleavage of peptide bonds of proteins. They are the most commonly employed enzymes in industrial applications, especially in detergents (Kirk *et al.*, 2002). Moreover, because of their high specificity, catalytic activity and their low environmental impact, processes based on enzymatic catalysis have been developed in multiple industrial fields. Enzymes have been identified or engineered in a wide variety of sizes, properties and substrate specificities. These processes includes food processing, synthesis of fine chemicals or antimicrobial treatments (Kirk *et al.*, 2002; Chapman *et al.*, 2018). Among these reactions, the enzymatic esterification and transesterification of natural phenolic compounds have been thoroughly studied in the past twenty years. Indeed, enzymes as hydrolases allow to perform esterification or transesterification under mild conditions that are compatible with the frequent sensitivity of natural compounds to harsh conditions. In this field, the most studied enzyme is the lipase B from *Candida antarctica* (CALB). It is commercially available immobilized on beads under the brand name Novozym 435 (N435) (Heldt-Hansen *et al.*, 1989; Nielsen *et al.*, 1999; Compton *et al.*, 2000; Ortiz *et al.*, 2019). Other enzymes have also been screened for their activity such as the lipase from *Rhizomucor miehei* (RML) or highly specific enzymes as tannases (Stamatis *et al.*, 1999; Aharwar *et al.*, 2018). However, several studies have demonstrated that the reactivity of natural phenolic compounds, as those represented in Figure 1.2.2, with enzymes is hardly predictable and has mostly been assessed empirically (Stamatis *et al.*, 1999; Villeneuve, 2007). Efforts have also been devoted to determine the optimal conditions for the enzyme-catalyzed modification of phenolic-based substrates (Figueroa-Espinoza *et al.*, 2013; Suárez-Escobedo *et al.*, 2021).

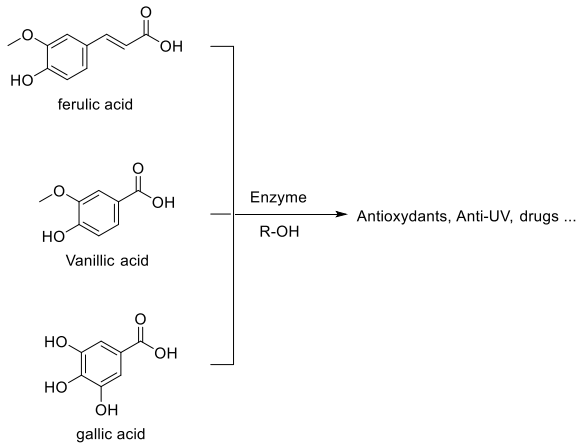

Figure 1.2.2: Examples of natural phenolics compounds investigated for the synthesis of high value-added products by enzyme-catalyzed esterification.

The use of biocatalysts in order to fulfill the requirements of green chemistry principles is currently a hot research topic both in academic research and for industrial purposes. Indeed, the use of enzyme is considered and perceived as a natural process which can be a strong marketing argument (Søndergaard *et al.*, 2005). In addition to their use as preservatives, natural phenolic compounds and their modification have recently been studied for a variety of innovative application such as therapeutic molecules (Rychlicka *et al.*, 2021) as well as in material science (Fodor *et al.*, 2017). Due to the high interest of this research, the enzymatic esterification of natural phenolic compounds has already been reviewed in the literature in the past (Villeneuve, 2007; Figueroa-Espinoza *et al.*, 2005; Antonopoulou *et al.*, 2016). The aim of this review is therefore to provide an updated and broader overview of the literature on the hydrolase-catalyzed esterification and transesterification of natural aromatic compounds from lignocellulosic biomass and tannins as these resources represent the largest natural source of biobased aromatics (Crozier *et al.*, 2006). This overview tends to be as broad as possible by including for example tannase which is often treated in separate studies. Innovative types of enzymes and reactive media are also discussed.

2. Cinnamic and hydroxycinnamic derivatives

Cinnamic acid derivatives are α,β-unsaturated aromatic acids present mostly in plants cell wall and produced through the Shikimate pathway (Crozier *et al.*, 2006). The cinnamic derivatives can present hydroxyl or methoxy groups in *meta* or *para* of the aromatic ring. The structure of the most common cinnamic derivatives associated with their name is presented in Figure 1.2.3.

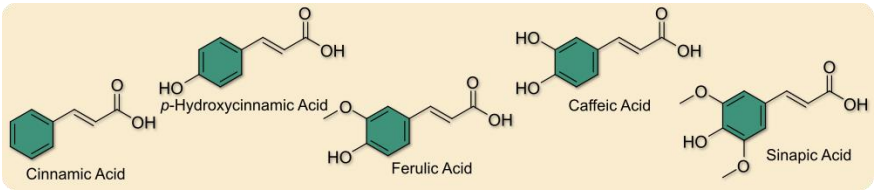

Figure 1.2.3: Schematic representation of the most common natural cinnamic derivatives.

Cinnamic derivatives are found in a wide variety of natural sources, often in an esterified form. The most common cinnamic derivative is caffeic acid or 3,4-dihydroxycinnamic acid (Clifford, 2000). As its name suggests, it is found in significant amounts in coffee beans. It is generally found esterified with quinic acid. This ester, often referred as chlorogenic acid, corresponds to the 5-caffeoylquinic acid and is found in common dietary products as blueberries or ciders (Clifford, 2000). Other cinnamic derivatives can be found in high quantities in plants. As an example, ferulic acid (FA) can act as a crosslinker of arabinoxylan in the plant cell wall (Figure 1.2.4). It has also been found to participate to the linkage between lignin and hemicellulose (Mathew *et al.*, 2004; Ralph, 2010; Hatfield *et al.*, 2017; Terrett *et al.*, 2019). Ferulic acid can be extracted from grains as corn bran, wheat bran or in fruits as grapefruits and is therefore part of our diet (Zhao *et al.*, 2008; Flourat *et al.*, 2021).

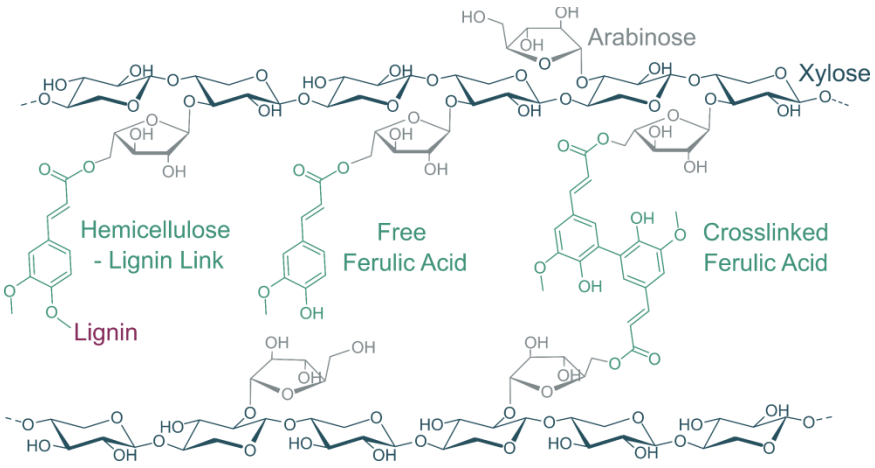

Figure 1.2.4: Schematic representation of ferulic acid in its free, lignin-bound and crosslinked forms in hemicellulose. Adapted from (Oliveira et al., 2019; Terrett et al., 2019).

Multiple techniques of extraction of cinnamic derivatives from biomass have been developed (Ferri *et al.*, 2020; Valanciene *et al.*, 2020; Flourat *et al.*, 2021). The enzymatic modification of cinnamic derivatives is mainly motivated by the excellent therapeutic (Paiva *et al.*, 2013; Kumar *et al.*, 2019; Rychlicka *et al.*, 2021), antioxidant and anti-UV (Natella *et al.*, 1999; Svobodova *et al.*, 2003; Genaro-Mattos *et al.*, 2015) properties of the obtained products.

2.1. Impact of the substrate substitution and unsaturation

As mentioned before, natural cinnamic and *p*-hydroxycinnamic derivatives have various structures with different hydroxy and methoxy substituents borne by the aromatic ring. The reactivity of these natural compounds toward enzymes has been investigated for more than twenty years. It started, to our knowledge, with the study from Guyot *et al.* (B. Guyot *et al.*, 1997) in which the authors assessed the reactivity of cinnamic, ferulic and caffeic acid toward CALB. The esterification activity of the enzyme with alcohols of different lengths was assessed. The reactivity of dihydrocaffeic acid was investigated as well. Compounds with hydroxy or methoxy substituents as ferulic and caffeic acid systematically resulted in low esterification yields, even after 40 days of reaction. On the contrary, cinnamic acid and hydrogenated caffeic acid resulted in yields up to 97 % in eight days, and 90% in

fifteen days, respectively. These results indicate that the presence of substituents on the cinnamic acid aromatic ring has a significant impact on the lipase esterification activity. However, once hydrogenated the reactivity of substituted acid was similar to that of the non-hydrogenated unsubstituted cinnamic acid.

Such substituent and double bound correlated differences in the lipase catalytic activity was later investigated by Stamatis *et al.* (Stamatis *et al.*, 1999). The authors also observed a strong inequality of reactivity between cinnamic acid derivatives directly related to their aromatic ring substitution. Cinnamic derivatives with different substitution were assessed in esterification with octanol catalyzed by CALB as well as with RML. The results are presented in Table 1.2.. The higher yields were obtained with unsubstituted cinnamic acid for both enzymes. Equivalently for both lipases, the ring substitutions with hydroxyl groups in *ortho* and *para* positions were found to be the most unfavorable substitutions for the reactivity of the cinnamic derivatives. On the other hand, the *meta*-substitution of the aromatic ring had a much lesser impact. Thus, due to its structure, caffeic acid was converted only in traces amounts with both enzymes. However, the activity of CALB and RML differed regarding the conversion of ferulic acid. Most probably because of the presence of a methoxy group, CALB converted ferulic acid with low esterification yield where the RML was less impacted by the *meta*-methoxy substitution and converted ferulic acid with a yield comparable to that of m-hydroxycinnamic acid.

Table 1.2.1: Effect of cinnamic derivative structure on the reaction rate and conversion yields for esterification in octanol catalyzed by the lipase from *Candida Antarctica* (CALB) and *Rhizomucor miehei* (RML)for 12 days. Adapted from (Stamatis *et al.*, 1999)

Acid	CALB		RML	
	Reaction rate (mM h^{-1})	Conversion after 12 days (%)	Reaction rate (mM h^{-1})	Conversion after 12 days (%)
Cinnamic	0.57	82	0.32	59
o-hydroxycinnamic	0.18	21	0.20	18
m- hydroxycinnamic	0.27	38	0.25	32
p- hydroxycinnamic	0.18	25	0.18	22
Ferulic	ND[a]	11	0.10	30
Caffeic	ND[a]	Traces	ND[a]	Traces

[a]ND, not determined.

This difference in selectivity and activity of the RML was recently confirmed by Schär *et al.* (Schär *et al.*, 2017) in esterification of cinnamic derivatives with ethanol. In this study, higher yields of ethyl ferulate (76.2% ± 2.0) compared to ethyl m-hydroxycinnamate (69.0% ± 1.7) were obtained in 72h. Another interesting result was the important yield of sinapic acid (66.7%±1.4) compared to caffeic acid (16.1%±1.2). This confirms that in the case of the RML, hydroxyl groups in *meta* position decrease the reactivity more significantly that their methoxy counterparts.

Weitkamp *et al.* (Weitkamp *et al.*, 2006) obtained similar results to those of Stamatis *et al.* (Stamatis *et al.*, 1999) with CALB when comparing the reactivity of cinnamate ethyl and methyl esters

with substituent on different positions in transesterification with long chain alcohols such as oleyl alcohol. The impact of the hydroxyl substituent position on the conversion of the substrate by the lipase is presented in Figure 1.2.5.b. The influence of the hydroxyl groups on the CALB activity was ranked in the order *ortho* > *para* > *meta*. Again, the introduction of supplementary hydroxyl or methoxy group, as in caffeic and ferulic acid, reduced even more the reactivity of these derivatives and/or the CALB activity. Methoxy groups were found to be less detrimental than hydroxyl groups. The same authors showed that a similar trend was observed in direct esterification of cinnamic derivatives (Vosmann *et al.*, 2006). Importantly, the reactivity in esterification and transesterification of hydrogenated cinnamic derivatives was also assessed. The time-course conversion in transesterification of hydrogenated cinnamate and caffeate esters in comparison to unsaturated ones are given in Figure 1.2.5a and c. It can be drawn from these results that the presence of the double bound greatly reduces the reactivity of the cinnamate derivatives toward the enzyme for compounds containing hydroxyl groups. As an example, the CALB enzymatic activity with methyl dihydrocaffeate was 20 folds higher than with methyl caffeate, its unsaturated precursor. This observation is in agreement with previous results from Stamatis *et al*. (Stamatis *et al.*, 2001) showing a similar trend for cinnamic acid. The authors showed that five hydrolases including CALB presented a much higher reaction rate when used for the esterification of hydrogenated *p*-hydroxycinnamic acid with octanol when compared with unsaturated *p*-hydroxycinnamic acid.

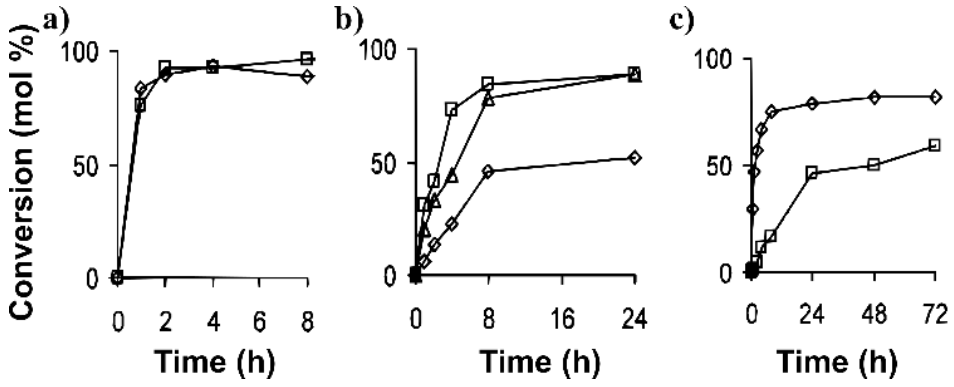

Figure 1.2.5: Conversion of the CALB-catalyzed transesterification of cinnamic methyl and ethyl ester derivatives with oleyl alcohol: a) ◇hydrogenated oleyl cinnamate, □ oleyl cinnamate; b) oleyl ◇ortho-hydroxycinnamate, □ meta-hydroxycinnamate and △ para-hydroxycinnamate; c) ◇hydrogenated oleyl caffeate, □ oleyl caffeate. Reproduced from (Weitkamp *et al.*, 2006).

Stevenson *et al.* (Stevenson *et al.*, 2007) investigated the activity of CALB for the esterification of cinnamic derivatives with aromatic alcohols. The reactivity of the phenylethanol, methoxy-phenylethanol and tyrosol as aromatic alcohols were studied, as represented in Scheme 1.2.1. The reaction rates were substrate dependent with the following order: cinnamic acid > *p*-methoxycinnamic acid > dimethoxy-cinnamic acid > ferulic acid > *o*-hydroxycinnamic acid > caffeic acid. Again, as in the previous studies, hydroxyl groups had a greater impact on the reactivity than methoxy ones.

Interestingly, sinapic acid, methoxy- and dimethoxy-cinnamic acids led to unidentified side-products. This is rather unexpected as enzymatic catalysis allows mild reaction conditions and usually shows a high specificity which are factors limiting the likelihood of side-products occurrence.

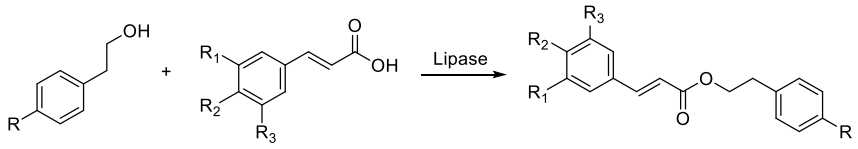

Alcohol	R
Phenyl-ethanol	H
Methoxy phenyl-ethanol	OH
Tyrosol	OMe

Acid	R_1	R_2	R_3
Cinnamic	H	H	H
Methyl cinnamic	H	OMe	H
Dimethyl cinnamic	OMe	OMe	H
Sinapic	OMe	OH	OMe
Ferulic	OMe	OH	H
p-hydroxycinnamic	H	OH	H
Caffeic	OH	OH	H

Scheme 1.2.1: Aromatic acids and alcohols tested in the CALB-catalyzed esterification for the synthesis of biobased antimicrobial compounds. Adapted from (Stevenson et al., 2007).

Cassani *et al.* (Cassani *et al.*, 2007) studied more specifically the impact of the presence of a double bound on cinnamic derivatives reactivity in esterification with alcohols of different length. CALB-catalyzed conversion of *p*-hydroxycinnamic and ferulic acid could not reach more than 55% in 360h. Once hydrogenated the substrates were both converted at yields higher than 90% in a timeframe between 48 and 360h. This result was also supported by M. Zoumpanioti *et al.* (Zoumpanioti *et al.*, 2010) whose observations suggest that the negative impact of hydroxyl substituent on cinnamic derivatives aromatic ring could be mostly attributed to electronic effects. Indeed, hydrogenating the double bound of cinnamic derivatives breaks the conjugation between the acid function and the aromatic ring. Moreover, the hydroxyl substituents have an important mesomeric electronic effect. The rigidity of the double bound could also be incriminated in the low reactivity of these compounds. The lipase-catalyzed esterification of the hydrogenated versions of the cinnamic derivatives has been studied (Priya *et al.*, 2002, 2003; Yang *et al.*, 2012; Buzatu *et al.*, 2020; Zieniuk *et al.*, 2020) because of the high yields usually observed with these derivatives and the fact that they may also have pharmaceutical applications. However, these compounds have not been considered into the focus of this review and their reactivity will not be fully covered.

Thus, enzymes such as the CALB and RML were proven to have a different selectivity. Interchanging these enzymes could in some cases improve the esterification of specific compounds such as ferulic acid.

2.2. The screening of enzymes:

Because of their high substrate-related specificity, screening the activity of new enzymes is a way to unlock the hydrolase-catalyzed esterification of specific substrates. Therefore, enzymes from various sources have been screened for their ability to synthesize cinnamic derivatives esters.

As described earlier, CALB is the most described hydrolase because of its commercial availability and good reactivity (Buisman *et al.*, 1998; Compton *et al.*, 2000). Still, H. Stamatis *et al.* (Stamatis *et al.*, 2001) investigated the reactivity of three other hydrolases and compared it with that of CALB and the previously mentioned RML. The authors studied the lipase from *Candida rugosa* (CRL), the esterase from *Fusarium oxysporum* (FOE) and the cutinase from *Fusarium solani* (FSC). These enzymes were essayed for the esterification of cinnamic, p-hydroxycinnamic and ferulic acids with octanol in solvent free conditions. Within 12 days, all the cinnamic derivates were successfully esterified by the selected enzymes. However, inequal yields were obtained. The reactivities of the enzymes toward the cinnamic and p-hydroxycinnamic acid were in the following order: CALB > RML > FSC > FOE. For all enzymes, the reaction rates were higher for the conversion of cinnamic acid when compared to p-hydroxycinnamic and ferulic acids. However, the RML converted ferulic acid in higher yields when compared to p-hydroxycinnamic acid. Moreover, the obtained yields of octyl ferulate were the highest (30%) when compared with the other enzymes yields (up to 11%). This shows the important selectivity of the RML for m-methoxy substituents. Unfortunately, the poor solubility and low reaction rate of ferulic acid did not allow a deeper investigation of the reaction kinetics.

More recently, Schär *et al.* (Schär *et al.*, 2015) employed the RML for the direct esterification of ferulic acid with alcohols of different lengths. The parameters of the reactions were optimized by 3-level-5-factor design. The obtained reaction yields were slightly lower than those predicted by the model. However, yields up to 76% and 92% of ethyl ferulate and hexyl ferulate, respectively, were obtained after only 72h. This study also indicated that short primary alcohols are preferred, and that the activity of the enzyme increases with the alcohol length until C6. After this limit, longer alcohols presented a lower reactivity. Secondary alcohols were the least reactive species.

Immobilized RML is available under the brand name Novozym 40086. Sun *et al.* (Sun *et al.*, 2018a) studied the esterification of cinnamic acid with benzyl alcohol with Novozym 40086 as catalyst. The activity of the enzyme was compared with that of commercially available immobilized CALB (N435) and lipase from *Thermomyces linuginosous* (Lipozyme TLIM) as well as the free enzymes. As represented in the Figure 1.2.6, the Novozym 40086 showed the highest final conversion (92.3 %) when compared to TLIM (55.1 %) and N435 (51.3 %). Possibly due to aggregation, the free enzymes systematically resulted in lower yields. Through extensive optimization, a yield of 96.2 % of benzyl cinnamate was obtained with Novozym 40086 in only 11.3 hours of reaction. Moreover, this catalyst showed no significant loss of activity after 9 cycles of reuse, demonstrating its high reusability. In this

context, the immobilized form of RML is therefore an interesting competitor to the classically used N435.

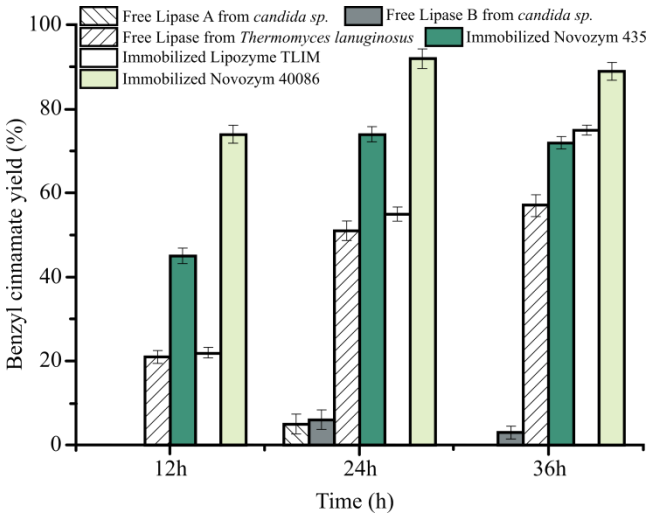

Figure 1.2.6: Comparison of the conversion of benzyl cinnamate obtained by esterification of cinnamic acid with benzyl alcohol with different biocatalysts. Adapted from (Sun *et al.*, 2018a).

Mastihubova *et al.* (Mastihubová *et al.*, 2006) screened the activity of several enzymes for the transesterification of activated ferulic esters as vinyl ferulate with different glucosides. The transesterification of vinyl esters leads to the production of vinyl alcohol as a byproduct. This vinyl alcohol is then transformed into volatile acetaldehyde by keto-enol tautomerism. The latter can be easily eliminated, thus shifting the reaction equilibrium. The lipases from *Aspergilus niger* (Lipase A, Amano) and *Thermomyces lanuginosus* (Lipolase 100L and Lipolase 100T, Novozymes), the xylanase from *Thermomyces lanuginosus* (Pentopan 500 BG, Novozymes) and the hemicellulase from *Humicola insolens* (Ultraflo L, Novozymes) were assessed. The Lipolase 100T was found to have the highest enzymatic activity. Interestingly, this enzyme was able to work in highly polar solvent as acetonitrile or methyl isobutyl ketone, facilitating the solubility of the substrate. High yields of feruloylated glycosides were obtained (up to 90% in 65 hours).

The authors later reported the use of the same enzyme for the transesterification of methyl α-D-glucopyranoside with cinnamic and benzoic derivatives vinyl esters (Mastihubová *et al.*, 2013). This study also highlighted the Lipolase 100T substrate specificity. As for the CALB, the presence of the double bound of cinnamic derivatives was deleterious to the activity of the enzyme. Hydroxyl substituents presented a negative effect as well. Methoxy substituents were found to be less detrimental, and their presence could even result in high conversion. As an example, vinyl ferulate was converted in higher yield than vinyl *p*-hydroxycinnamate (68% in 64 hours and 56% in 78 hours, respectively). Vinyl caffeate, because of its two phenols, presented an even lower conversion (16% in 96 hours). However, other authors assayed the same enzyme but immobilized on silica gel (TLIM) and obtained total conversion of vinyl caffeate when transesterified with β-glucopyranoside (Chyba *et al.*, 2016). The

reaction was performed in *tert*-butanol at 40°C. The immobilization of the enzyme thus seems to play an important role in its selectivity.

Similarly, Wang *et al*. (Wang *et al.*, 2016a) employed TLIM for the esterification of cinnamic acid with ethanol. After an extensive optimization of reaction conditions (solvent, enzyme loading, temperature, water activity, substrate ratio, shaking rate) a conversion of 99 % in ethyl cinnamate was obtained in 24 hours in isooctane. This yield is much higher than previous results obtained for example with CALB. Interestingly, non-null water activity was in favor of the lipase activity. Water in the reaction medium could allow a good balance between the absorbance of the support and the structural water required by the enzyme. However, too high water activity promoted hydrolysis, reducing the reaction yield. Indeed, it is a well-known phenomenon in the lipase-catalyzed synthesis of esters and polyesters (Compton *et al.*, 2000; Giuliani *et al.*, 2001; Mahapatro *et al.*, 2003; Ülger *et al.*, 2017).

Recently, the same enzyme was employed by Gherbovet *et al*. (Gherbovet *et al.*, 2020) for the esterification of vinyl ferulate with chromogenic aromatic substrates in acetonitrile as represented in Scheme 1.2.2. The reaction was performed overnight at 37 °C and allowed to obtain high yield (up to 97%). The yields obtained as a function of the alcohol structure are given in Table 1.2.2. Interestingly, the enzyme activity was hindered by electron withdrawing groups in *ortho* position of the alcohol used in the transesterification. Moreover, transesterification of the vinyl ferulate with a compound presenting a primary and secondary alcohol as well as with a phenol demonstrated the high selectivity of the enzyme toward primary alcohol. Thus, the product containing a free secondary alcohol was produced with a yield of 94 %, as represented in Scheme 1.2.2b.

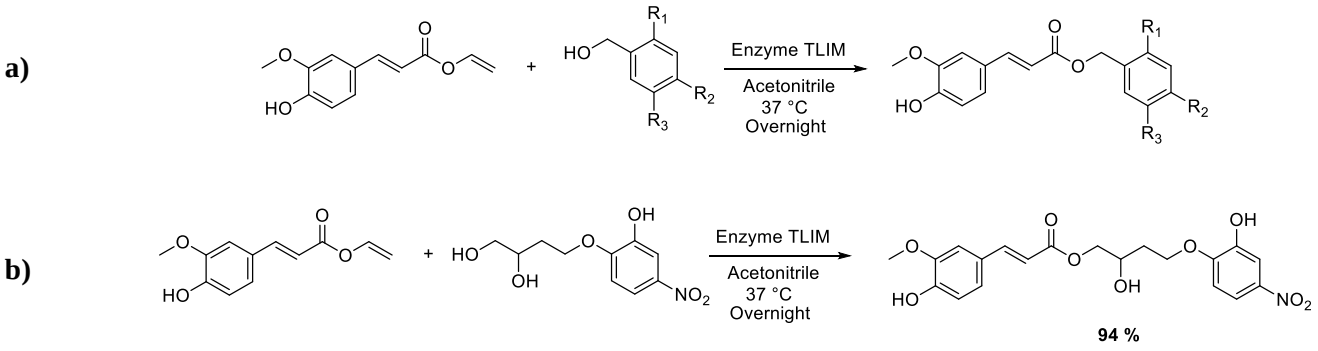

Scheme 1.2.2: Synthesis of feruloylated chromogenic compounds by TLIM-catalyzed transesterification: a) study of the impact of the alcohol structure on the enzyme reactivity; b) Selective synthesis of a chromogenic compound from a diol. Adapted from (Gherbovet *et al.*, 2020).

Table 1.2.2: study of the impact of the alcohol structure on the reaction yield in the synthesis of feruloylated chromogenic compounds by TLIM-catalyzed transesterification. Reproduced from (Gherbovet *et al.*, 2020).

R_1	R_2	R_3	Yield (%)
H	H	NO_2	79
OH	H	NO_2	76
Cl	H	NO_2	44
F	H	NO_2	46
H	NO_2	H	97

Another type of enzymes that brought much attention in this domain is the ferulic acid esterase (FAE) family. First purified in 1991 (Faulds *et al.*), FAE (E.C. 3.1.1.73) is a subclass of carboxylic esterases that are specific to the hydrolysis of ferulic and sometimes caffeic or p-hydroxycinnamic ester moieties in plants cell wall (Crepin *et al.*, 2004). Originally, FAEs were classified in four classes (A, B, C and D) according to their substrate specificity (toward methyl ester of cinnamic derivatives) and sequence resemblance. Today, other classification systems exist based again on the substrate specificity but also on phylogenic analysis. More than 80 types of microbial FAEs have already been identified. Their origin, activity and biotechnological application have been reviewed by Topakas *et al*. (Topakas *et al.*, 2007), Dilokpimol (Dilokpimol *et al.*, 2016) and more recently by Oliveira *et al*. (Oliveira *et al.*, 2019).

Because of the FAE specificity toward natural cinnamic derivatives, Giuliani *et al*. (Giuliani *et al.*, 2001) tested the activity of an FAE from *Aspergillus niger* (AnFaeA) for the esterification of ferulic acid. The esterification of ferulic acid with pentanol in a water-in-oil microemulsion was performed. The solvent was composed of a mix of cetyltrimethylammoniumbromide (CTAB), hexane and pentanol. A yield of 60% could be obtained after 8 hours of reaction. This high conversion was attributed to the enzyme high activity associated with the use of an emulsion as reactive medium. Indeed, the authors explained that such an emulsion allowed a high concentration and a convenient orientation of the alcohol, favoring the enzyme activity.

Topakas *et al*. (Topakas *et al.*, 2003b) extracted and purified a FAE (FoFAE-II) from *Fusarium oxysporum* F3 from cumin. The activity of the FAE-II was assessed with cinnamic derivatives. The esterifications were again performed with propanol in an emulsion but this time without surfactant. The solvent consisted of an emulsion of hexane, propanol and MES-NaOH buffer pH 6.6. The conversion of cinnamic acid into its propyl ester only resulted in trace amounts after 224 h of reaction. However, p-hydroxycinnamic and ferulic acid were converted with a yield of 13 and 16%, respectively, in the same period of time.

The same research group later assessed the esterase activity of another FAE (FoFAE-I from *Fusarium oxysporum* F3) (Topakas *et al.*, 2003c). Its activity was tested this time for the transesterification of methyl p-hydroxycinnamate, methyl ferulate, methyl caffeate and methyl sinapate with butanol in the same system of surfactant free microemulsion. This time the selectivity was different

than with the previous enzyme. After 140h of reaction, methyl p-hydroxycinnamate gave the highest yield (71%). It was followed by methyl caffeate (22%), methyl ferulate (13%) and methyl sinapate (1%). This study demonstrates the great difference in selectivity between the different FAEs and thus the importance of their source.

Topakas *et al.* (Topakas *et al.*, 2005) also reported for the first time the use of FAE from *Sporotrichum thermophile* (StFaeC) for the transesterification of methyl ferulate with L-arabinose. As mentioned before, the coupling of ferulic acid with sugars and polyols interestingly increases the substrate solubility in aqueous medium (for cosmetic or medical applications, as an example). Yields up to 39% were obtained after more than 160 h of reaction. It is worth mentioning that the authors assessed the specificity of the enzyme in transesterification toward several ferulate esters (Vafiadi *et al.*, 2005). The enzyme showed a higher conversion with short ferulate esters such as the methyl ferulate.

To date, FAEs are not yet commercially available. However, FAE can be found mixed with other enzymes in commercial preparations. Thus, Tsuchiyama *et al*. (Tsuchiyama *et al.*, 2006) screened several enzymatic preparation from Amano and Novozymes. These preparations were known to contain other enzymes as contaminants. Some of them were hemicellulase, cellulase and pectinase, which are enzymes that are produced by microorganisms to metabolize components of the plant cell wall, so does FAE. There is therefore a high probability that these microorganisms also produced FAE as contaminant in the preparation. Among the fifteen enzymatic preparations tested, only one showed FAE activity: the pectinase PL from Amano. The FAE present in the preparation was then purified. Finally, it was assessed for the esterification and transesterification of several phenolic acids and esters with glycerol. Again, as described before, glycolyzed phenolic acids are more hydrophilic and therefore easier to utilize in medical application or in beverage. The highest catalytic activity was observed for the conversion of sinapic acid. Ferulic acid showed medium activity while little to no activity was detected with caffeic and p-hydroxycinnamic acids. It is worth mentioning that no activity was either detected with natural hydroxybenzoic acids as vanillic acid which will be presented later. Higher activities were measured in transesterification but without differences in selectivity. Interestingly, ethyl ferulate presented a higher conversion than methyl ferulate. Nevertheless, the reactions were performed in an aqueous buffer-dimethyl sulfoxide-glycerol mixture and significant hydrolysis was reported. The same team later obtained higher yields for the esterification of p-hydroxycinnamic acid with glycerol (up to 60 % in 72h) in a similar buffer-dimethyl sulfoxide-glycerol mixture with 80% of glycerol (Tsuchiyama *et al.*, 2007). To summarize, FAE with interesting activity toward natural cinnamic derivatives can be extracted from commercially available preparation, making it easier to source for laboratories that are not well-equipped for enzymes biosynthesis.

Vafiadi *et al*. (Vafiadi *et al.*, 2008) assessed the activity of the AnFaeA in n-hexane:butanol:water microemulsion for the transesterification of various cinnamic derivatives with butanol. The pure enzyme was employed as crosslinked enzyme aggregates (CLEA). Its activity toward

methyl ferulate, methyl p-hydroxycinnamate, methyl caffeate and methyl sinapate was compared. The highest transesterification activity was obtained for methyl sinapate with a conversion up to 78% after 120 h. It was followed by methyl ferulate and methyl p-hydroxycinnamate with a conversion of 42 and 2%, respectively. No enzymatic activity was detected with methyl caffeate as reactant. According to the authors, these results show the specificity of AnFaeA for methoxy-substituted substrates. The effect of the solvent on the conversion of methyl sinapate was studied with various amounts of n-hexane versus water and butanol. The ternary system with the highest amount of n-hexane (i.e. with n-hexane:butanol:water ratio of 47.2:50.8:2.0 in volume) was proven to be the one promoting the highest enzymatic reactivity.

Such ternary solvent mixtures have recently been used by Antonopoulou *et al*. (Antonopoulou *et al.*, 2017) for the transesterification of vinyl ferulate with prenol (3-methylbut-2-en-ol, a biobased unsaturated alcohol), as represented in Scheme 1.2.3. The activity of five FAEs: FaeA1, FaeA2, FaeB1 and FaeB2 from *Myceliophthora thermophila* C1 as well as MtFae1a from *Myceliophthora thermophila* ATCC 42464 were assessed. The optimal reactive conditions such as the solvent composition, reactants nature, pH and temperature were specific to each enzyme. The enzyme offering the highest yield was the FaeB2. It converted vinyl ferulate to prenyl ferulate (PFA) with a yield of 72 % in only 24h. As a comparison, in the same reaction conditions, the conversion of methyl ferulate to prenyl ferulate only reached 26 % of yield in 72h. The direct esterification of ferulic acid only resulted in a yield of 1 % in 96h. The time-course of the yield in PFA obtained from the various ferulic derivatives are shown in Figure 1.2.7. This confirms the shifting effect of vinyl esters. Indeed, as depicted earlier, the transesterification of vinyl ester leads to the production of a vinyl alcohol adduct that gets transformed into acetaldehyde by tautomerism. This acetaldehyde can easily be eliminated from the medium, shifting the reaction equilibrium.

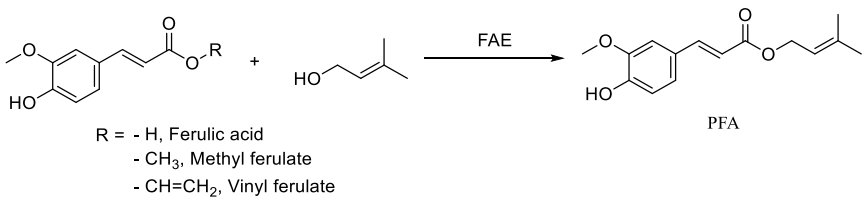

Scheme 1.2.3: FAE catalyzed esterification and transesterification of ferulic moieties with prenol. Adapted from (Antonopoulou et al., 2017).

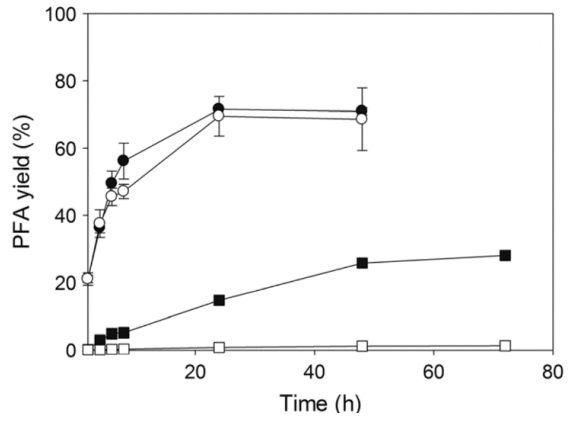

Figure 1.2.7: Evolution over time of the yield in PFA obtained by FAE-catalyzed esterification of prenol with various ferulic moieties: ● Vinyl ferulate, ○ Vinyl ferulate and stirring, ■ Methyl ferulate and □ Ferulic acid. Reproduced from (Antonopoulou et al., 2017).

The same protocol was used to assess the activity of the previously cited enzymes for the transesterification of vinyl ferulate toward L-arabinose (Antonopoulou *et al.*, 2018)(Scheme 1.2.4). In these conditions FaeA1 offered the highest yield (52.2% in L-arabinose ferulate in 8h). After a longer period of time, the selectivity of the enzymes decreased, and the hydrolysis resulted in the decrease of the reaction yield until 24h. A similar phenomenon was observed for all enzymes, as shown in Figure 1.2.8. According to the authors, this could be explained by the hydrophilicity of the L-arabinose ferulate which could stay in the aqueous phase in relatively large amounts, leading to a significant hydrolysis.

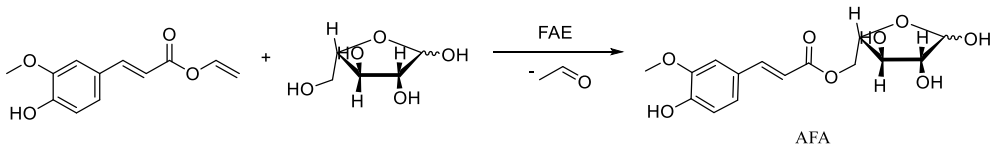

Scheme 1.2.4: FAE catalyzed esterification and transesterification of vinyl ferulate with L-arabinose. Adapted from (Antonopoulou *et al.*, 2018).

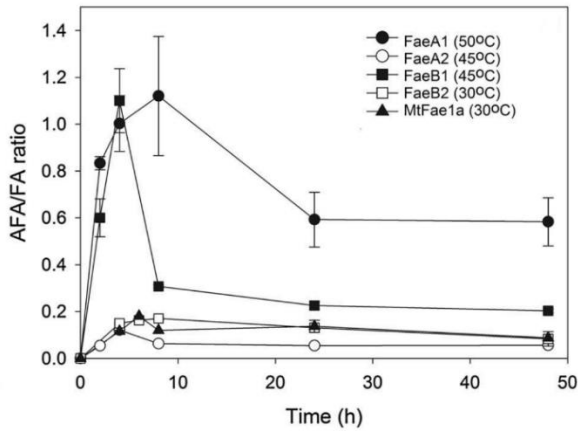

Figure 1.2.8: Ratio of arabinose ferulate (AFA) and ferulic acid (FA) in the reaction medium for the transesterification of arabinose with vinyl ferulate catalyzed with different enzymes. Reproduced from (Antonopoulou *et al.*, 2018).

Later on, Antonopoulou *et al*. (Antonopoulou *et al.*, 2019) published a study on three FAEs from *Talaromyces wortmannii*: Fae125, Fae7262, Fae68. The conversion of vinyl ferulate with prenol and L-arabinose was evaluated in various polar and nonpolar solvents and even in ionic liquids. The solvents consisted of a mix 96.8:3.2 solvent:buffer pH 6. In 8h, Fae125 allowed to obtain the highest yields both in the synthesis of prenyl ferulate and L-arabinose ferulate (50.2% and 25%, respectively). Interestingly, the optimal solvent was different depending on the chosen enzyme and on substrate. As an example, for the synthesis of prenyl ferulate, Fae125 and Fae68 gave higher yields in nonpolar solvents while with Fae7262 the highest conversion was obtained using a hexane:butanol mixture. Likewise, the maximum conversion of vinyl ferulate to L-arabinose ferulate with Fae125 and Fae7262 was maximal in the same hexane:butanol mixture. Finally, Fae68 produced L-arabinose ferulate at its highest yield in hexane. Adding small amounts of DMSO to hexane facilitated the solubilization of the substrate and its mass transfer. Adding 5% (in volume) of DMSO improved the synthesis of prenyl ferulate to a yield up to 92.8% (after 24h). For the synthesis of L-arabinose ferulate, adding DMSO allowed to reach a yield of 67.1% in 6h. However, for DMSO content higher than 20% in volume, the enzyme appeared to be deactivated. The reusability of the enzyme was possible after up to 5 cycles without major decrease of the yield. On the sixth cycle, the obtained yield decreased to 66.6%. According to the authors, these results highlighted the possibility to use FAE in a continuous process for the production in large scale of prenyl and L-arabinose ferulate.

A different ternary system was used by Romero-Borbón *et al.* (Romero-Borbón *et al.*, 2018) that used a microemulsion composed of isooctane:butanol:water with 73:25:2 (in volume) to determine the reactivity of a FAE from *Aspergillus ochraceus* (AocFaeC). It was compared with AnFaeA and FAE B from *Aspergillus niger* (AnFaeB). First, methyl ferulate was transesterified with alcohols of different length (from C2 to C12). AocFaeC was highly specific and could nearly only synthesize butyl ferulate. AnFaeA showed a higher activity with C3 alcohols and AnFaeB was the least active and could not synthesize any alkyl ferulate. Finally, the selectivity of the enzymes toward different methyl hydroxy-cinnamate in transesterification with butanol was assessed. Methyl p-coumarate, methyl ferulate, methyl caffeate and methyl sinapate were tested. AocFaeC showed a higher selectivity for the conversion of methyl caffeate. AnFaeA showed a higher activity toward methyl sinapate when AnAFeaB showed a better activity with methyl p-coumarate. In these conditions, for a same substrate, AocFaeC showed a 2.5 to 5 times higher activity. Its activity was also 16 and 35 times higher than those of StFaeC and FoFae-I, other type C FAEs.

It has been pointed that the classification of FAE into types A to D is mostly based on the activity of the enzyme toward short alcohol moieties. In plants, FAE converts cinnamic derivatives linked to pentose monosaccharides as in arabinose. Thus, Hunt *et al*. (Hunt *et al.*, 2017) investigated the activity of AnFaeA with ferulate and caffeate methyl- or arabinose-esters. The docking of the substrates with FAE has been studied through computational modelling. In agreement with the A-D classification of the

enzyme, ferulate methyl esters were more rapidly converted than the caffeic methyl esters. Esters based on arabinose moieties led to higher activity when compared to methyl ester. However, the kinetics of conversion of ferulate and caffeate arabinose esters showed comparable affinity toward the enzyme, proving the complexity of classifying the FAEs. Modelling of the docking of caffeic derivatives revealed favorable non-catalytic binding orientation, as represented in the Figure 1.2.9. This docking simulation could explain the difference in AnFaeA activity between ferulic and caffeic esters. Indeed, small esters of caffeic derivatives can occupy a small hydrophobic pocket. This tends to move the ester function away from the catalytic site. When esterified with a bulky arabinose, the sugar cannot enter the small hydrophobic pocket. As a result, the catalytic binding is favorized.

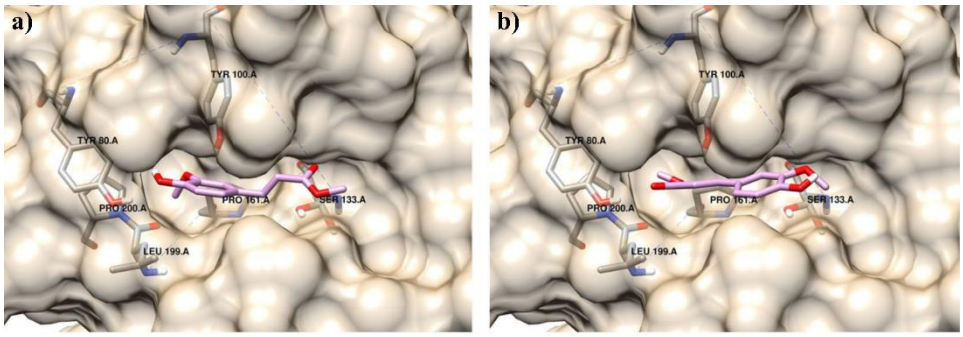

Figure 1.2.9: Binding of the methyl caffeate with the AnFaeA active site: a) catalytic energetically favorable orientation; b) non-catalytic also energetically favorable orientation. Reproduced from (Hunt *et al.*, 2017).

Immobilization of the FAE also plays an important role in its activity and selectivity. Recently Grajales- Hernández *et al.* (Grajales-Hernández *et al.*, 2020) studied in detail the immobilization of AnFaeA for the esterification of cinnamic derivatives. A wide variety of immobilization methods were assayed (i.e. covalent linking, adsorption, ionic linking). Carrier-bound immobilization was also compared to carrier-free immobilization methods (i.e. CLEA). With FAE immobilized as CLEA, ferulic and sinapic acids were fully converted to their butyl esters after 48 and 24 hours, respectively. Moreover, the reaction could be performed in solvent free conditions. Interestingly, the caffeic and p-hydroxycinnamic acids were not converted by the immobilized FAE, again confirming its high selectivity. The enzyme immobilization allowed high reusability (up to 10 times) of the enzyme while maintaining maximum activity. However, carrier-bounded and carrier-free immobilized enzymes did not show improved thermal stability.

These experiments confirmed that the activity and selectivity of enzymes are very different depending on the enzyme source and structure. Many sources of lipases and esterases have been screened in order to characterize their affinity and selectivity. Even more complex, enzymes mixture has also been investigated and could maximize yield while reducing the important cost of enzymatic catalysis (Rahman *et al.*). New enzymes can also be carefully engineered through various processes such as structure-based engineering or through directed evolution (Zhang *et al.*, 2012; Cao *et al.*, 2015; Varriale *et al.*, 2018; Cerullo *et al.*, 2019; Santos *et al.*, 2019).

As an example, Lopez de los Santos *et al.* (Santos *et al.*, 2019) employed directed evolution for optimizing the activity of CALB-based enzymes toward the esterification of cinnamic and salicylic acids through iterative semi-rational design. *In silico* modelling of substrate docking and residue interaction network were combined with experimental measurement of mutant enzyme catalytic activity. 14 variants were identified with higher activity than the CALB wild type for the production of methyl cinnamate. Widening of the enzyme docking site without disrupting the enzyme integrity was identified as a critical step toward the improvement of CALB activity for the conversion of bulky aromatic compounds.

2.3. Impact of the solvent

As mentioned previously, solvents can have a strong impact on enzymes activity. Again, the activity of a given enzyme with cinnamic derivatives in a given solvent is difficult to predict and has mostly been investigated empirically. As an example, hydrophobic solvents can block water from accessing the substrate, limiting hydrolysis. However, enzymes such as FAE are deactivated by highly hydrophobic solvents. As we saw earlier, several FAE catalyzed reactions have been performed in binary or ternary microemulsion systems containing a mix of aqueous and organic solvents (Giuliani *et al.*, 2001; Topakas *et al.*, 2003b, 2003c, 2005; Tsuchiyama *et al.*, 2006, 2007; Vafiadi *et al.*, 2008; Antonopoulou *et al.*, 2017, 2018, 2019; Romero-Borbón *et al.*, 2018). In this way, the enzyme can remain in the aqueous phase and the presence of an organic solvent facilitates the solubilization of the substrate and its transesterification.

CALB is known to be soluble and stable in organic solvents such as cyclohexane or toluene. Therefore, transesterification and esterification of hydroxy-cinnamic compounds have been studied in such hydrophobic solvents. Buisman *et al.* (Buisman *et al.*, 1998) investigated the CALB catalyzed esterification of cinnamic acid with 1-butanol in several organic solvents. The yields obtained after 5 days of reaction in diethyl ether, t-butylmethyl ether, 1-butanol, cyclohexane and n-pentane were compared. The highest yield (85%) was obtained in n-pentane followed by cyclohexane (68%). All other studied solvents gave negligible yields.

This was confirmed by several studies. Lee *et al.* (Lee *et al.*, 2006) performed the CALB-catalyzed esterification of cinnamic derivatives with 2-ethyl hexanol and showed that solvents with an octanol water partition coefficient (logP) > 3.5 offered the higher conversion. Isooctane (logP = 4.5) was identified as a good solvent for the esterification of ferulic acid offering a conversion of the substrate above 90 % in 48 h. From their side, Jakovetic *et al.* (Jakovetić *et al.*, 2013) determined the activity of CALB for the esterification of cinnamic acid with butanol in different solvents. Isooctane offered the higher yield in butyl cinnamate (45 %) when compared with solvent of lower logP as chloroform (logP = 2, 9 %) or tert-butanol (logP = 0.35, 28 %). Interestingly hexadecane (logP = 8.8) led to lower

conversion than isooctane (16 %), showing that the relation between the solvent polarity and the conversion follows a bell shape with an optimum. Finally, this was also confirmed by Lue *et al.* (Lue *et al.*, 2005) for the CALB-catalyzed esterification of cinnamic acid with oleyl alcohol. The highest yield of 78 % was obtained when hexane was employed as solvent (logP = 3.5) while isooctane and heptane (logP = 4.0) resulted in a lower yield (71 %). More polar solvents as octanone and butanone resulted in even lower yields (1.6 and 0.5 %, respectively). It is worth pointing out that these results are different from those obtained by Lee *et al.* (Lee *et al.*, 2006) and by Jakovetic *et al.* (Jakovetić *et al.*, 2013). The optimal polarity of the solvent therefore tends to be specific to the substrate studied.

Recently, Suárez-Escobedo *et al.* (Suárez-Escobedo *et al.*, 2021) studied in detail the impact of solvent on the lipase-catalyzed esterification of cinnamic derivatives. The authors underlined that previous studies generally required high temperatures and that the nonpolar solvents used were potentially hazardous and/or polluting. They therefore focused on the possibility of using mild conditions and if possible green alternative solvents. However, the highest conversion was still obtained with hexane (92 % in 72 hours). Unfortunately, greener alternative solvents as 2-methyl tetrahydrofuran, Cyrene, or deep eutectic solvents (that will be developed later) systematically resulted in lower conversions.

Schär *et al.* (Schär *et al.*, 2016) studied the conversion of ferulic derivatives and β-sitosterol with the lipase from *Candida rugosa* in hexane. Direct esterification and transesterification resulted in yields up to 35 and 55%, respectively, in 5 days. However, when the parameters of the reaction were mathematically optimized, the low solubility of ferulic acid in the medium was pointed out. Thus, the concentration of ferulic acid could not be increased beyond a certain point, possibly impacting the reaction yield. Because of this lack of solubility, many authors chose to perform the esterification of cinnamic derivatives with co-solvents such as butanone (Karboune *et al.*, 2008; Sorour *et al.*, 2012; Yang *et al.*, 2012).

Indeed, the mixture of a nonpolar solvent ensuring a good reactivity of the enzyme and a polar solvent improving the solubility of the substrate is an interesting alternative. As an example, Yang *et al.* (Yang *et al.*, 2013) studied the CALB-catalyzed transesterification of ethyl ferulate with phosphatidylcholine, as represented in Scheme 1.2.5, and found that mixture of toluene with polar solvent such as butanol or chloroform offered higher yield when compared to common solvent as hexane. After optimization, a mixture of toluene and chloroform (9:1 v/v) was found to be the optimal composition, allowing to reach yields up to 40%. The esterification and transesterification of ferulic moieties with phosphatidylcholine from egg-yolk was recently studied in details by Rychlicka *et al.* (Rychlicka *et al.*, 2020). Similarly, and as presented in Figure 1.2.10, the authors also obtained the higher yields of feruloylated phosphatidylcholine in a mixture of toluene and chloroform with a yield up to 62 % after reaction optimization.

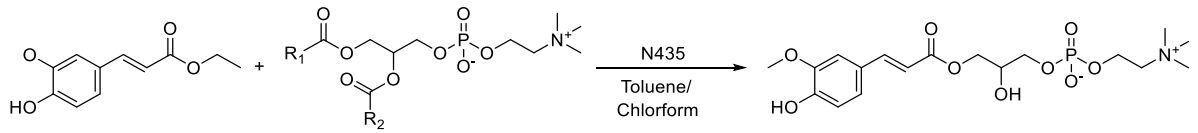

Scheme 1.2.5: Transesterification of ethyl ferulate with phosphatidylcholine (Yang *et al.*, 2013; Rychlicka *et al.*, 2020).

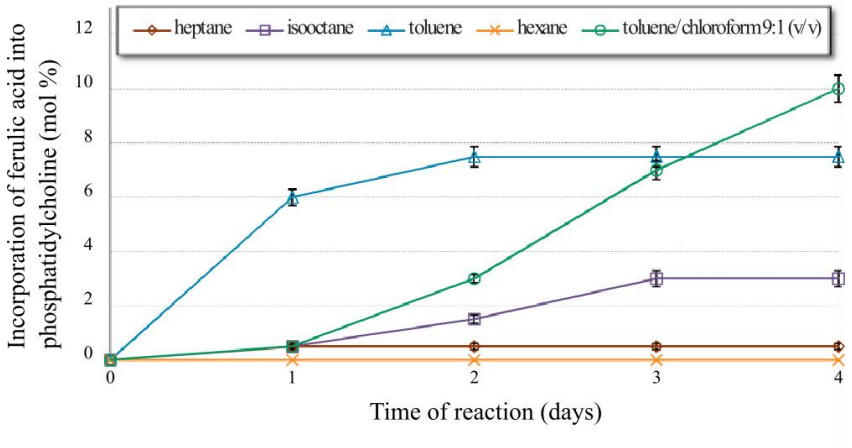

Figure 1.2.10: Effect of the solvent on the transesterification of ferulic acid with phosphatidylcholine. Reproduced from (Rychlicka *et al.*, 2020).

Highly polar solvents are generally considered not suitable because they could denaturate the enzyme through hydrogen bonding or by withdrawing structural water from the enzyme. However, polar solvents such as alcohols or ketones have been proven to be suitable for lipase-catalyzed processes. Back in 2000, Guyot *et al*. (B. Guyot *et al.*, 2000) studied the CALB-catalyzed transesterification of 5-caffeoyl quinic acid ester with fatty alcohols in 2-methyl-2-butanol. This solvent was employed because it allows a higher solubility of the substrates compared to the solvent-free reaction. Moreover, secondary alcohols being weakly reactive toward lipase, they have often been used as solvents (Compton *et al.*, 2000, 2012). Enzymes mentioned in studies cited earlier, like the lipase from *Thermomyces lanuginosus*, allow to perform reactions in highly polar solvents such as acetonitrile (Mastihubová *et al.*, 2006, 2013; Chyba *et al.*, 2016; Gherbovet *et al.*, 2020). The high solubilizing power of these solvents is particularly necessary for esterification of sugars derivatives as they are poorly soluble in non-polar solvents.

Several studies among those discussed above have performed the esterification or transesterification of cinnamic derivatives under solvent-free conditions (B. Guyot *et al.*, 1997; Stamatis *et al.*, 1999, 2001; Weitkamp *et al.*, 2006). This method presents three major advantages. First, the employed alcohols can often solubilize the cinnamic derivatives, which improves the contact between substrates and enzyme. Moreover, the excess of alcohol shifts the equilibrium of the reaction toward the esterification or transesterification. Finally, it allows to replace the hazardous nonpolar solvent (such as hexane or toluene) by an often less hazardous substrate. This method is popular for the conversion of cinnamic derivatives with glycerol.

Sun *et al*. (Sun *et al.*, 2007) performed the synthesis of glyceryl ferulate thanks to immobilized CALB in solvent free conditions. In direct esterification, ferulic acid was weakly soluble in glycerol, reducing its reactivity. Thus, the glyceryl ferulate was produced by transesterification of ethyl ferulate and 96 % conversion was obtained in only 10 hours of reaction. The same authors converted ethyl caffeate to glyceryl monocaffeate with a good selectivity thanks to CALB catalysis (Sun *et al.*, 2017a). The reaction was performed in solvent-free conditions. Through optimization, yields in glyceryl monocaffeate above 95 % were obtained after 10.5 hours. This is an interesting result considering the aforementioned low activity of CALB toward caffeic acid.

The same authors obtained similar results but this time with monoacyl glycerol as substrate (Sun *et al.*, 2017b). Recently, Yao *et al*. (Yao *et al.*, 2020) used a similar method to produce glyceryl ferulate but using free CALB instead of the immobilized one. This study pointed out the importance of good substrate solubility and mass transfer to maximize its reactivity toward the enzyme.

Always with the idea of performing solvent-free reactions, Yang *et al*. (Yang *et al.*, 2012) studied the transesterification of ethyl ferulate directly in fish oil. The aim was to synthesize feruloylated fish oil, a powerful additive to protect fish oil against oxidation. A mixture of feruloylated glycerides was obtained. Full conversion of ethyl ferulate was observed with a yield of feruloylated fish oil higher than 92%. Interestingly, the addition of glycerol to the mixture improved the reaction yield.

Recently, Abdelgawad *et al*. (Abdelgawad *et al.*, 2021) performed solvent-free transesterification of palm stearin with ferulic acid. The authors assessed the selectivity of three enzymes: the lipase from *Thermomyces lanuginosus* (Lipozyme 100L, Novozymes), the CALB as well as the Lipase A from *Candida antarctica*. The reactions were performed directly in the oil with, evaluating the impact of adding glycerol to the mixture. Addition of free glycerol was shown to improve the reaction yield. Moreover, a synergistic effect of the lipase from *Thermomyces lanuginosus* was observed with either CALB or the lipase A from *Candida antarctica* allowing to produce the feruloylated oil in higher yields. According to the authors, employing the Lipozyme 100L in mixture with either the lipase A or B from *Candida antarctica* allows to obtain high yield while reducing the reaction costs.

A new type of solvent that brings much attention today is the use of ionic liquids (IL). IL are able to solubilize a large diversity of substrates and are compatible with enzymatic catalysis (Elgharbawy *et al*., 2018, 2020, 2021). They are considered as a green alternative to classical solvents because of their negligible vapor pressure, non-flammability and high stability.

Katsoura *et al*. (Katsoura *et al.*, 2009) compared the activity of CALB and RML in an IL medium constituted of [BMIM]PF_6 (represented in Figure 1.2.12). The esterification of several cinnamic derivatives with octanol gave results comparable to those of conventional organic solvents. The esterification of ferulic acid was specifically studied with both enzymes. The esterification of ferulic

acid with alcohols of different lengths in IL demonstrated that the enzymes presented the same selectivity than in conventional organic solvents, offering yields up to 53 % (for the esterification with butanol catalyzed by RML in 72 h). The esterification of ferulic acid with butanol in conventional solvents and several IL types (shown in Figure 1.2.12) was also studied. Among all the solvents, [BMIM]PF_6 was found to give the higher yields for both enzymes. As for the conventional solvents, no correlation between the IL polarity and the obtained yield was found. The results obtained by the authors are presented in Figure 1.2.11 where the yields obtained in different solvents are compared with their ability to solubilize the substrate. Finally, the use of IL did not improve the reusability of CALB. On the contrary, RML was found to be more fragile, and its activity decreased after each reuse.

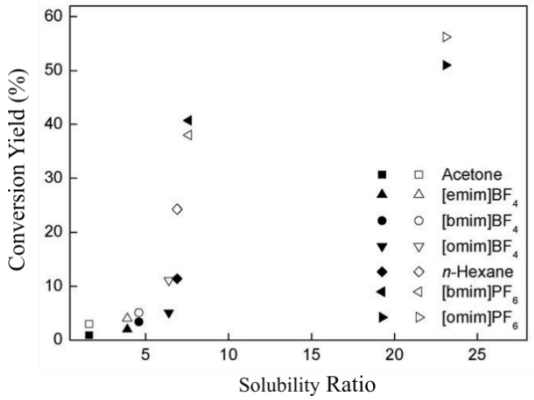

Figure 1.2.11: Yield of the lipase-catalyzed esterification of ferulic acid with butanol in common organic solvents and ionic liquids. The reaction was catalyzed by CALB (black symbols) or RML (white symbols). Reproduced from (Katsoura *et al.*, 2009).

FAE has also been tested in IL. Vafiadi *et al*. (Vafiadi *et al.*, 2009) converted sinapic acid into glyceryl sinapate in [C_5O_2mim][PF6] (Figure 1.2.12) with AnFaeA reaching high yields (76.7±1.8%). Adding water (up to 15%) improved the activity which can be explained by the fact that the activity of FAE requires a rather large amount of water compared to lipases.

The transesterification of ethyl ferulate with fatty oils in IL was also investigated. Sun *et al*. (Sun *et al.*, 2015) studied the CALB-catalyzed transesterification of ethyl ferulate with castor oil in [EMIM]PF_6 (Figure 1.2.12). A high conversion of ethyl ferulate to feruloylated glyceryls was obtained. According to the authors, the use of an IL favored the production of feruloylated glyceryls, brought a protection to the enzymatic catalyst, promoted mass transfer and reduced the coloration of the solution when compared to solvent-free reactions. Both media (solvent-free and IL) allowed to reach full conversion of ethyl ferulate in approximatively the same timeframe. The same team later screened several IL and employed [BMIM]PF_6 for the transesterification of ethyl caffeate with castor oil in high yields (72.48% ± 2.67) (Sun *et al.*, 2019).

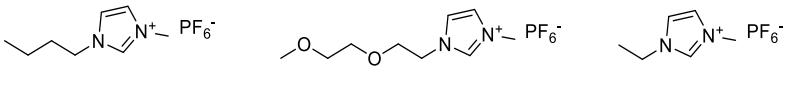

[BMIM]PF_6 [C_5O_2MIM]PF_6 [EMIM]PF_6

Figure 1.2.12: Structures of the various IL employed for enzyme-catalyzed esterification and transesterification reactions.

One important drawback of IL is their high viscosity. In order to address this problematics, Shi *et al*. (Shi *et al*., 2017) used a mixture of IL/hexane for the CALB-catalyzed esterification of ferulic acid with lauryl alcohol. Adding hexane to IL (with a ratio 1/1) allowed to decrease the viscosity of the medium, thus increasing the reaction rate. Thanks to this method a high yield up to 90.1% in lauryl ferulate was obtained.

Another drawback of IL is their cost and in some cases their potential toxicity (Bubalo *et al.*, 2017). A new type of solvent with properties comparable to IL but a much lower price has emerged with deep eutectic solvents (DES). DES are a mixture of compounds that once mixed together have a lower melting point than the compounds taken separately. As IL, they have very low vapor pressure and good solubilizing properties. Moreover, there are often constituted of non-toxic moieties and are considered therefore less toxic than IL. Finally, the good activity of enzymes such as lipases in DES has already been demonstrated (Durand *et al.*, 2012).

Durand *et al*. (Durand *et al.*, 2013a) evaluated the use of DES for the CALB catalyzed transesterification of methyl *p*-hydroxycinnamate and methyl ferulate with octanol. A choline-chloride/urea mixture allowed to obtain the highest conversion for both methyl esters with yields above 98%. It is worth mentioning that the equilibrium was reached with methyl p-hydroxycinnamate in 72 h while it was reached for methyl ferulate in 168 h. Surprisingly, adding water to the mixture was necessary in order to maximize the enzyme activity and such addition of water (below a certain amount) did not promote hydrolysis. These results were confirmed by an extensive study of the influence of each component of the medium on the reactivity (Durand *et al.*, 2014). The same team investigated much further the use of DES for the successful lipophilization of phenolic acids reported in several review articles (Durand *et al.*, 2013b, 2015).

Shi *et al*. (Shi *et al.*, 2019) also employed DES for the CALB-catalyzed transesterification of methyl ferulate with alcohols of different lengths with the aid of ultra-sonication. In agreement with previous studies discussed above, the highest yield was obtained with the C6 alcohol, allowing a yield of 94 % within 3 days of reaction.

Finally, among the various media used and reported for hydrolase-catalyzed cinnamic derivatives esterification, one must mention the use of supercritical CO_2 ($ScCO_2$). $ScCO_2$ as IL and DES presents good solubilizing properties and is considered as green and less hazardous solvent in comparison to conventional organic solvents. $ScCO_2$ has already been successfully employed for lipase-catalyzed transesterification of cinnamic derivatives (Compton *et al*., 2001; Ciftci *et al*., 2012). However, the practical application of ScCO2 is limited by the need for very specific equipment supporting the high pressure required by the supercritical fluid.

Other parameters have been investigated in order to increase the kinetics and the yield of enzymatic esterification of cinnamic derivatives. One example is the use of reduced pressure. Partial vacuum allows the evaporation of small adducts of esterification or transesterification, shifting the equilibrium of reaction. As an example, Sun *et al*. (Sun *et al.*, 2015) (cited above) assessed the use of reduced pressure during the transesterification of ethyl ferulate with castor oil in IL with CALB. As shown in Figure 1.2.13, reducing the pressure from atmospheric pressure to 10 mmHg increased the yield from 60 % to 89 %. In a similar way, Huang *et al*. (Huang *et al*., 2015) performed the esterification of ferulic acid with 2-ethyl hexanol in solvent free conditions under reduced pressure (560 mmHg) with CALB. In order to maximize the medium agitation and to reduce the pressure, the reaction was performed directly in a rotary evaporator. This method allowed to obtain yield of esterified ferulic acid up to 99.5 %. Beside improving reaction yields, reduced pressure can also avoid side reactions such as hydrolysis, thus improving the selectivity of lipase-catalyzed transesterification (Sun *et al.*, 2017a).

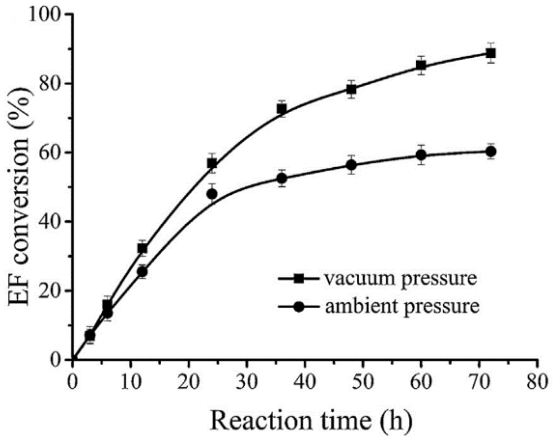

Figure 1.2.13: Effect of vacuum on the CALB-catalyzed transesterification of ferulic acid with castor oil (EF: Ethyl ferulate). Reproduced from (Sun *et al.*, 2015).

Finally, a popular method to improve enzymes stability and reusability is their immobilization, which has been briefly mentioned earlier. The most common support for CALB immobilization is Lewatit acrylic resin beads (corresponding to N435). However, other methods of immobilization have been investigated in the literature for the conversion of cinnamic derivatives. As an example, Hüttner *et al*. (Hüttner *et al.*, 2017) employed mesoporous silica with various architecture to support FAE. These supported enzymes allowed the transesterification of methyl ferulate with butanol and showed a good reusability with a high productivity up to 9 cycles of reuse.

Grajales-Hernández *et al.* (Grajales-Hernández *et al.*, 2020) also investigated methods for convenient immobilization of the AnFaeA. The authors studied both supports (covalent and non-covalent) and support-free immobilization methods (as CLEA). CLEA realized by crosslinking with glutaraldehyde showed promising results. Surprisingly, the enzyme immobilization did not improve its thermal stability. The enzyme showed however an important activity and selectivity for the esterification of multiple cinnamic derivatives with butanol reaching conversion up to 98 % in 24 hours in solvent

free conditions. The crosslinked enzyme conserved its selectivity toward methoxylated substrates as shown in Figure 1.2.14. Moreover, the immobilized enzyme showed an important reusability with no significant loss of activity after 10 reuse cycles.

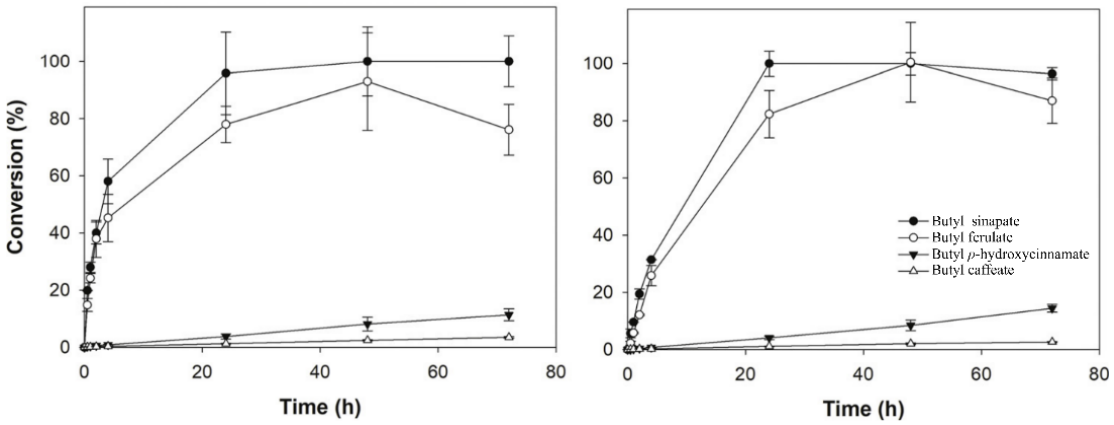

Figure 1.2.14: AnFaeA-catalyzed transesterification of cinnamic derivatives with butanol: a) Free enzyme; b) Enzyme immobilized as CLEA. Reproduced from (Grajales-Hernández et al., 2020).

More unexpectedly, Sankar *et al.* (Sankar *et al.*, 2017) employed cuttle bone powder to immobilize a lipase from *Bacillus subtilis* and assessed this catalyst for the esterification of ferulic acid with ethanol. Cuttle bone powder is a biobased high surface support. This support enhanced the thermal stability of the enzyme allowing the esterification of ferulic acid with ethanol in high yields (above 85 % in 24 hours). Many more examples of enzymes supports can be found in the literature (Chandel *et al.*, 2011; Kumar *et al.*, 2011).

3. Benzoic and hydroxybenzoic derivatives:

As described earlier, cinnamic derivatives are not the only aromatic compounds extracted from biomass. Benzoic and hydroxybenzoic acids are also produced in the plant through the Shikimate pathway (Valanciene *et al.*, 2020) and can also be extracted in significant amounts from various plant sources. The most common natural phenolic acid is gallic acid as it is present in high quantities in tannins, a constituent of plants cell wall (Crozier *et al.*, 2006). However, since gallic acid esterification presents its own specificities, it will be described later in a separated part. Benzoic, vanillic and syringic acid (see Figure 1.2.15) can be found in various plant sources such as blueberries or breadnut (Valanciene *et al.*, 2020). These aromatic platform chemicals can be directly extracted from biomass (Dandekar *et al.*, 2020) or produced from lignin depolymerization (Li *et al.*, 2021; Poveda-Giraldo *et al.*, 2021). Moreover, the synthesis of vanillic acid from vanillin or from the previously mentioned ferulic acid (Topakas *et al.*, 2003a) have been described. Hydroxybenzoic derivatives are found in plants from traditional medicines (Cai *et al.*, 2004) and have been shown to possess beneficial actions on the treatment of cardiovascular disorders or cancers (Srinivasulu *et al.*, 2018; Kumar *et al.*, 2019; Ingole *et al.*, 2021). Moreover, they present interesting antioxidant properties (Srinivasulu *et al.*, 2018; Kumar *et*

al., 2019). However, as for cinnamic derivatives, they are poorly soluble in organic solvents and oils as well as in aqueous solutions. Therefore, the enzymatic esterification of these adducts with solubilizing moieties has been investigated.

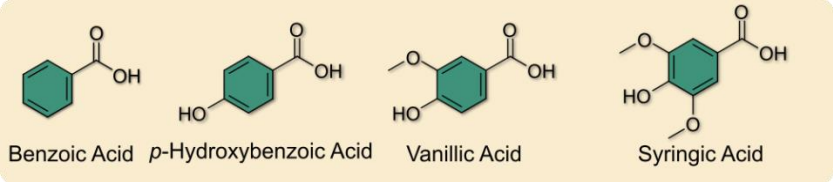

Figure 1.2.15: Schematic representation of the more common natural benzoic derivatives.

As for cinnamic derivatives, the substitution of the aromatic ring with hydroxyl and methoxy groups highly influences the reactivity of the hydroxybenzoic derivatives. Guyot *et al.* (B. Guyot *et al.*, 1997) studied the CALB-catalyzed esterification of hydroxybenzoic derivatives. The impact of the position of hydroxy substituent was determined by assessing the reactivity of *ortho*, *meta* and *para*-hydroxybenzoic acid in esterification with octanol. After 30 days of reaction, the *m*-hydroxybenzoic acid was obtained with a yield of 14%. The *ortho* and *para*-hydroxybenzoic acid both resulted in a lower yield of 4%. Dihydroxyl benzoic acid even gave lower yields, even after 50 days. Thus, among the hydroxyl substituents, the meta position seems the less impacting one. Moreover, lower yields were obtained with hydroxybenzoic acids when compared with hydroxycinnamic acids. This was confirmed by Buisman *et al.* (Buisman *et al.*, 1998) who compared the esterification of benzoic derivatives as the *p*-hydroxybenzoic, *m*-hydroxybenzoic, vanillic, syringic and gallic acid with the esterification of cinnamic acid butanol catalyzed by the CALB. Only trace amounts of the benzoic derivatives were obtained. The same result was obtained from Stamatis *et al.* (Stamatis *et al.*, 1999) when comparing the reactivity in CALB and RML-catalyzed esterification with octanol of *p*-benzoic acid with cinnamic derivatives. It is worth mentioning that the *p*-hydroxyphenyl acetic acid, a compound presenting an acid function spaced from the aromatic ring, presented a reactivity comparable to cinnamic acid.

Thus, this low reactivity of benzoic derivatives compared to cinnamic derivatives could be explained by both electronic and steric effects as the carboxylic acid is directly linked to the aromatic ring. Otto *et al.* (Otto *et al.*, 2000) studied via computer modelling the interactions of benzoic derivatives with CALB during esterification with glucose and compared them to those of cinnamic derivatives. Because of its rigidity and non-polarity, the bulky aromatic ring led to unfavorable interaction of the substrate with the enzyme binding site. It was also stated that spacing carbons from the aromatic rings (as in cinnamic derivatives) could reduce the impact of the aromatic ring on the substrate binding. However *meta* and *para* hydroxyl substitution of the aromatic ring of hydroxybenzoic derivatives were found to have a limited steric effect thanks to the wide hydrophobic pocket of CALB, confirming the dominance of electronic inhibitory effects. These observations were correlated to the experimental yields obtained for the esterification of the benzoic and cinnamic derivatives with glucose through

CALB-catalyzed reaction. The yield associated to the different substrates studied are given in the Figure 1.2.16 (the reactions were performed for 48 h in t-butanol).

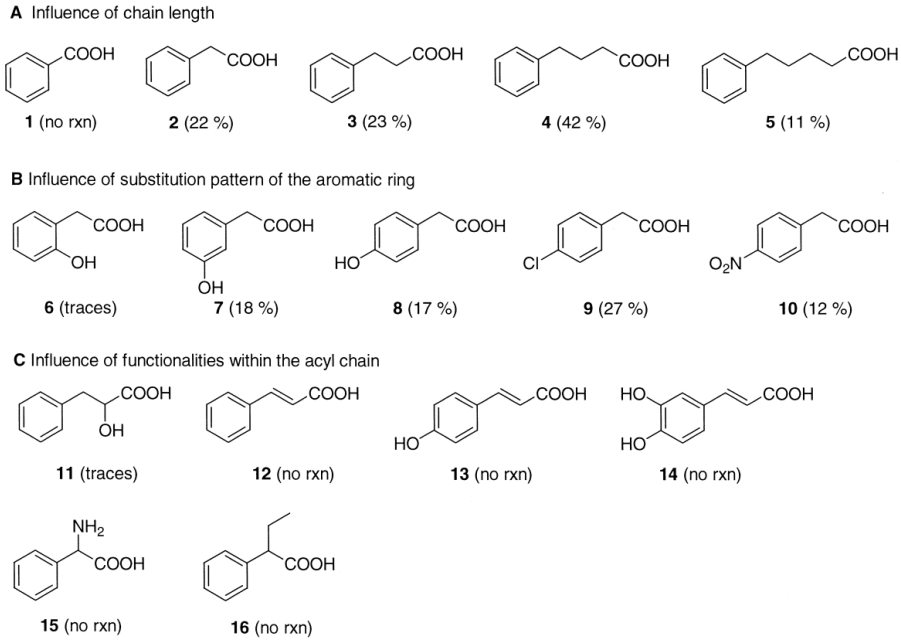

Figure 1.2.16: Yield of the CALB-catalyzed esterification of cinnamic and benzoic derivatives with glucose; Influence of the chain length, substitution of the aromatic ring and functionality of the acyl chain. "no rxn" stands for no product detected. Reproduced from (Otto *et al.*, 2000).

This substitution-related reactivity was investigated in details by Vosmann *et al*. (Vosmann *et al.*, 2008). The reactivity of methyl hydroxybenzoate with oleyl alcohol was assessed with CALB. The transesterification of methyl *meta* and *para*-hydroxybenzoate resulted for both in high yields (around 90%) after 72h. The methyl *ortho*-hydroxybenzoate was less reactive and reached 78% of conversion after 72h. According to Otto *et al*. (Otto *et al.*, 2000) this could be caused by *ortho*-hydroxyl groups giving hydrogen to the oxyanion in the reactive pocket of the enzyme. This is in adequation with the fact that the CALB activity was enhanced when the hydroxyl groups were replaced with methoxy groups. Both methyl *ortho, meta* and *para*-methoxylbenzoate reached 90% conversion with oleyl alcohol in 72h. It is worth mentioning that the authors also assessed the reactivity of the methyl vanillate in the same conditions which resulted in 89% conversion after 48h.

As enounced earlier, CALB has been described as less reactive toward hydroxybenzoic derivatives than cinnamic derivatives in similar reaction conditions (B. Guyot *et al.*, 1997; Buisman *et al.*, 1998; Stamatis *et al.*, 1999; Vosmann *et al.*, 2008). As for the cinnamic derivatives presented above, the ability of other enzymes to convert benzoic acid derivatives into esters has been investigated. Yiang *et al*. (Yang *et al.*, 2010) performed the transesterification of benzoic and cinnamic vinyl esters with arbutin and the lipase from *Penicillium expansum* as represented in the Scheme 1.2.6. As for the CALB, the negative impact of the electronic delocalization of the carbonyl with the aromatic ring as well as the steric hindrance were pointed out. Interestingly, cinnamic derivatives were not converted much faster

than benzoic derivatives as in previous studies. The presence of hydroxyl et methoxy substituents on the aromatic ring was deleterious to the enzyme activity. As an example, vinyl vanillate conversion only reached 30% in 96 h in comparison to vinyl benzoate that was converted at 97 % in 72 h. According to the authors, these observations could reinforce the hypothesis that electronic delocalization and steric hindrance play a crucial role in the lack of reactivity of these compounds toward enzymes.

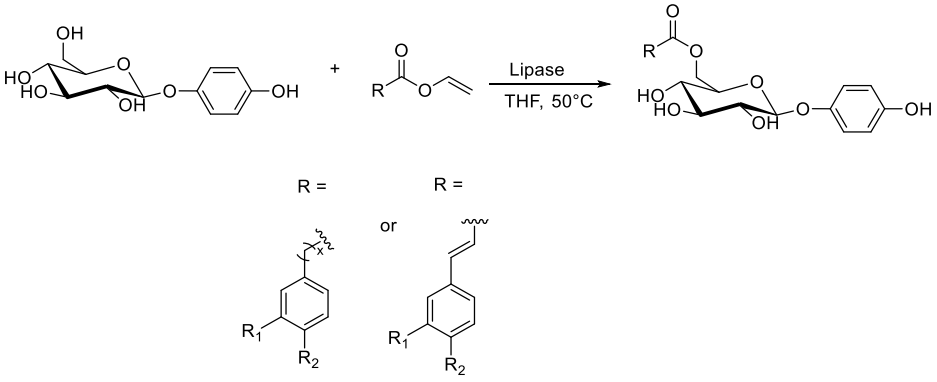

a, x = 0, $R_1 = R_2 = H$
b, x = 1, $R_1 = R_2 = H$
c, x = 2, $R_1 = R_2 = H$
d, x = 3, $R1 = R_2 = H$
e, x = 4, $R_1 = R_2 = H$
f, x = 0, $R_1 = OCH_3$; $R_2 = OH$
g, $R_1 = R_2 = H$
h, $R_1 = H$; $R_2 = OH$
i, $R_1 = H$; $R_2 = OCH_3$
j, $R_1 = R_2 = OCH_3$

Scheme 1.2.6: Comparison of the transesterification of cinnamic and benzoic vinyl esters with arbutin catalyzed by the lipase from *Penicillium expansum*. Adapted from (Yang et al., 2010).

The activity of ten enzymes was screened by Tan *et al.* (Tan *et al.*, 2013) for the synthesis of phytosteryl phenolates, compounds with promising health benefits. Among these enzymes were the previously cited RML and CALB. The lipase from *Candida rugosa* type VII was the only one to enable the transesterification of vinyl vanillate with a mixture of phytosterols which main constituents are represented in Figure 1.2.17. The reaction was performed in a binary solvent because of the weak solubility of vinyl vanillate in non-polar solvents. The solvent was composed of a mixture of hexane and 2-butanone (85:15 in volume). After ten days of reaction, the vinyl vanillate conversion was up to 88%.

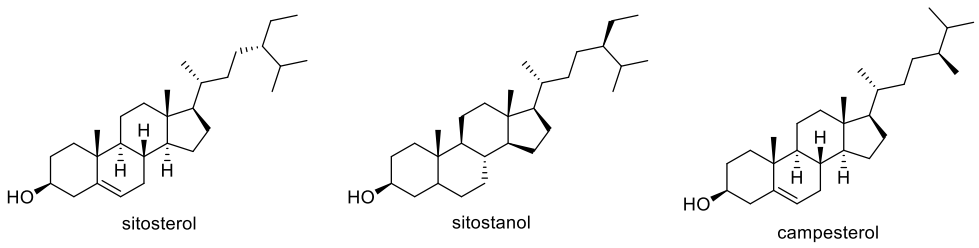

Figure 1.2.17: Structure of the main phytosterols present in the mixture employed by Tan *et al.* (Tan *et al.*, 2013).

Wang *et al*. (Wang *et al.*, 2015b) also studied the transesterification of vinyl vanillate with phytosterols (composed in majority of sitosterol) and the lipase from *Candida rugosa*. The reactions were also performed in a mixture of hexane and 2-butanone (80:20 in volume). A yield of 23.6 % was obtained after 24h. As a comparison, in the same conditions, vinyl ferulate and 4-hydroxybenzoate were converted with 45.4 and 17.3% yield, respectively. The same team employed a similar protocol for the CALB catalyzed transesterification of policosanols (long C_{24} to C_{34} aliphatic primary alcohols obtained from the biomass) with vinyl vanillate (Wang *et al.*, 2016b). This time, the yield of vinyl vanillate was only 8.6% after 4 days. The yield in vinyl *p*-hydroxybenzoate was even lower (1.8%).

The previously mentioned lipase from *Thermomyces lanuginosus* was assayed for the transesterification of benzoic vinyl esters with methyl α-D-glucopyranoside (Mastihubová *et al.*, 2013). Vinyl benzoate, *p*-hydroxybenzoate, *o*-hydroxybenzoate, vanillate, syringate, gallate and 3,4,5-trimethoxybenzoate were studied. Consistent with previously reported results, hydroxyl substituents generally showed a stronger negative effect on the reactivity that methoxy substituents. Thus, the attribution of this detrimental effect on the enzyme activity would be in favor of an electronic or a hydrogen donating effect in opposition to steric hindrance. Again, the *o*-hydroxyl substituent had a stronger negative effect on the enzymatic activity than the *p*-substituents.

As for cinnamic derivatives, the solvent employed in the reaction was identified as a critical parameter. Reactions performed in various media have been investigated such as in non-polar solvents (Buisman *et al.*, 1998), a mixture of polar and non-polar (Tan *et al.*, 2013; Wang *et al.*, 2015b, 2016b), highly polar solvents (Otto *et al.*, 2000; Yang *et al.*, 2010) or in solvent free conditions (B. Guyot *et al.*, 1997; Stamatis *et al.*, 1999; Vosmann *et al.*, 2008; de Meneses *et al.*, 2020). The use of polar solvent seems preferable because of the high solubility of benzoic derivatives in these solvents compared to non-polar solvents. DES have also been employed with benzoic derivatives. Guajardo *et al*. (Guajardo *et al.*, 2017) used deep eutectic solvent for the CALB-catalyzed esterification of benzoic acid with glycerol. DES composed of choline chloride or methylammonium chloride associated with urea, glycerol and ethylene glycol as hydrogen bond donor were assessed (1:2 molar ratio). Among them, the DES composed of choline chloride and glycerol generated the highest yields, glycerol acting here both as a solvent and as a reactant. Full conversion was obtained in 24h when between 8 and 20% of water was added to the mixture. Indeed, the addition of water decreased the viscosity of the medium, improving the mass transfer of the reactants. Below 20%, the water was somehow stabilized by the solvent and could not participate to hydrolysis. The same team later used a similar protocol for the continuous production of glycerol benzyl ester in packed-bed reactor [10]. These studies demonstrates that DES are also applicable to benzoic derivatives, opening the field toward new processes for their hydrolase-catalyzed esterification.

Recently, de Meneses *et al*. (de Meneses *et al.*, 2020) studied the lipase-catalyzed production of benzyl benzoate, a common pharmaceutical compound. Instead of employing carboxylic acid or esters

as carbonyl sources, the authors used benzoic anhydride. Indeed, when reacted with an alcohol, anhydride can be converted to an ester by lipase catalysis. This avoids the production of a small alcohol or water adduct along the reaction and therefore shifts the reaction equilibrium. Three commercial immobilized enzymes were assessed: CALB, RML and the lipase from *Thermomyces lanuginosus*. The use of the lipase from *Thermomyces lanuginosus* in solvent-free conditions was identified as the optimal reaction conditions. High conversion yields were obtained (up to 90%) in batch as well as in fed-batch process. It is worth pointing that ultrasonic activation of the reaction was assessed and led to high reaction rates. However, the catalyst solid carriers did not tolerate ultrasonication, hindering the reusability of the support.

As shown in the previous examples, hydroxybenzoic derivatives are often esterified in order to produce antioxidants or bioactive molecules. However, material science applications have also been investigated. Fordor *et al*. (Fodor *et al.*, 2017) investigated the enzymatic polymerization of methyl *p*-hydroxyethoxybenzoate derivatives with CALB. The transesterification of methyl *p*-hydroxyethoxybenzoic derivatives issued from benzoate, vanillate and syringate methyl ester was assessed in homopolymerisation as represented in the Scheme 1.2.7. Hydroxyethoxybenzoic derivatives have been employed preferably to hydroxybenzoic derivatives because of the poor reactivity of phenols toward CALB. The presence of methoxy groups on the aromatic ring was proven to reduce the activity of CALB. Indeed, the conversion of syringic derivative was below 3% and negligible amounts of oligomers were obtained. Vanillic derivatives resulted in oligomers with molar mass between 1070 and 1210 g.mol^{-1}. Finally, after optimization, methyl p-hydroxyethoxybenzoate allowed to produce polyesters with an average molar mass between 1060 and 2340 g. mol^{-1}.

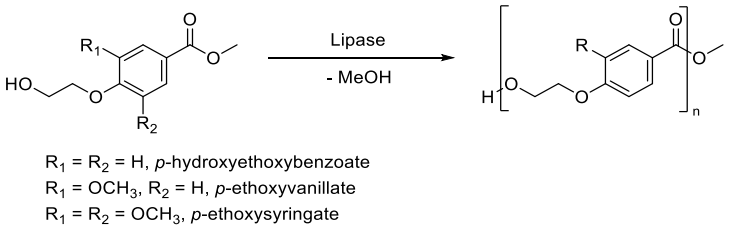

Scheme 1.2.7: CALB-catalyzed polymerization of a benzoic acid derivative. Adapted from (Fodor *et al.*, 2017).

4. Gallic acid

Tannins are natural polyphenols found in almost all parts of vascular plants. They are especially present in certain species such as oaks, black mimosa, chestnut, and green tea (de Hoyos-Martínez *et al.*, 2019). Plants present high concentration of tannins in specific locations such as the bark, leaves, seeds, and roots. Tannins have several roles in the plant and among them the protection against bacteria, fungi, and insects. As cinnamic derivatives, tannins have been identified in various food sources and could have a beneficial impact on health (Sharma *et al.*, 2019). Since the 18th century, gallic acid (Figure 1.2.18) has been identified as a major component of tannins (Pizzi, 2019). Tannins have a structure that

can vary depending on its source but also on the season, temperature, quality of the soil… (de Hoyos-Martínez *et al.*, 2019).

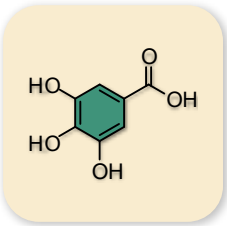

Figure 1.2.18: Structure of the gallic acid.

Tannins are divided into two classes: hydrolysable and condensed tannins, themselves composed of subclasses. Hydrolysable tannins are composed of gallo-tannins and ellagi-tannins. Most gallo-tannins are constituted of a central polyol (most of the time glucose) surrounded by units of gallic and digallic acids (see Figure 1.2.19). Ellagi-tannins have a more complex structure since they are also constituted of a central polyol but surrounded by gallic and hexahydroxydiphenic acids units (Figure 1.2.19). The hexahydroxydiphenic acid is a dimer of gallic acid produced by oxidoreduction (de Hoyos-Martínez *et al.*, 2019). Condensed tannins are defined as polymers or oligomers of flavonoids (see Figure 1.2.19). They can be found with various degrees of polymerization. Flavonoids, as phenolic acid derivatives, have been studied for their lipase-catalyzed modification to facilitate their use in therapeutic applications. This topic has been reviewed by several authors (Chebil *et al.*, 2006; de Araújo *et al.*, 2016). Finally, other less common classifications of tannins exist such as complex tannins and phlorotannins (de Hoyos-Martínez *et al.*, 2019).

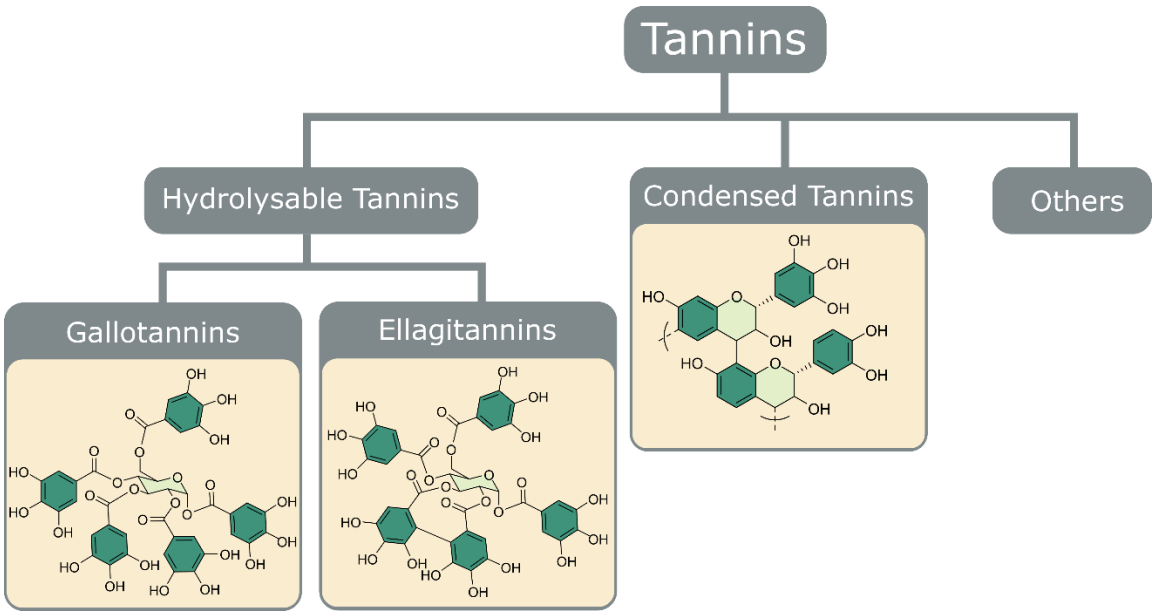

Figure 1.2.19: Schematic structure of classified tannins (Sharma *et al.*, 2019) (de Hoyos-Martínez *et al.*, 2019).

Tannins have been employed for centuries in the tanning of leather. Today, tannins are used in numerous industrial application such as wood adhesives, medical applications or as antioxidants in food and beverages. The extraction of tannins from natural sources can be performed through various processes (water, ILs, microwave…) and is still an important topic for research (de Hoyos-Martínez *et al.*, 2019).

Due to their availability, tannins are a natural source of choice for aromatic compounds. From tannins, the main aromatic compound extracted is gallic acid. Gallic acid is already broadly used in industry for its properties. Antioxidant properties of gallic acid are known for a long time. Already in the forties, gallic esters were presented as powerful food antioxidants (Higgins *et al.*, 1944). However, as for cinnamic derivatives presented previously, its poor solubility in hydrophobic products (as in natural oils) oriented the research toward its ester derivatives (Higgins *et al.*, 1944). Several gallate esters are currently employed as food additives, in Europe under the code E310, 311 and 312 for the propyl, octyl and dodecyl gallate, respectively. Today, their use in food can be controversial because of potential effects on reproduction (Ham *et al.*, 2019) and allergies (Gamboni *et al.*, 2013). However, properly used, gallate esters could have potential beneficial features as anti-fungal or anti-cancerous properties (Locatelli *et al.*, 2013; Ito *et al.*, 2014).

The esterification of gallic acid is generally performed by Fischer esterification with strong acid catalyst as sulfuric acid or *p*-toluenesulfonic acid (EFSA, 2014, 2015). Replacing this process by enzymatic esterification would represent a greener alternative and a more compatible with food applications. Therefore, enzymatic esterification of gallic acid has been investigated by many authors since Toth *et al*. in 1952 (Toth *et al.*, 1952) and is still an ongoing research topic.

4.1. Tannase

As depicted previously, gallic acid can be extracted from tannins. Tannase is a specific enzyme for the hydrolysis of ester bonds in tannins. Tannase has been known for a long time and is widely used in the pharmaceutical and food industry. As an example, in teas, tannase degrades tannins avoiding them from precipitating and blurring the beverage (Aharwar *et al.*, 2018). It is also employed in the extraction of gallic acid from tannins. Tannases are commercially available from several companies as Sigma-Aldrich or Kikkoman. A wide variety of tannases are expressed in microbial, animal, or vegetal sources (Chávez-González *et al.*, 2012; Aharwar *et al.*, 2018; de las Rivas *et al.*, 2019). The properties of the tannase greatly vary depending on its sources. Their molecular weight can vary from 50 to 320 kDa but all have in common the same serine-based active site (Chávez-González *et al.*, 2012). Tannases were classically produced in submerged liquid fermentation systems. However solid-state fermentation proved to be a promising alternative way presenting several advantages as higher efficiency and compacity of the installations (Chávez-González *et al.*, 2012). Tannases, like FAEs, are classified into several sub-classes, depending on their molecular structure and properties. Many sources of tannases are yet to be discovered. It has even been shown that other enzymes such as some specific FAEs present

a tannase activity (de las Rivas *et al.*, 2019). Tannases have been largely employed, at industrial scale, for the hydrolysis of tannins. However, they are also able to esterify and transesterify gallic acid. Therefore, they have largely been investigated for the production of valuable gallate esters.

In 1985, Weetal (Weetal, 1985) reported the esterification of gallic acid by tannase with propanol and pentanol. Free form of tannase as well as immobilized form on alkylaminosilanized porous silica were assessed. The enzyme was pre-soaked in buffer and a pH of 6 was found to be optimal for the enzyme activity. First the syntheses were performed in solvent-free conditions with a large excess of alcohol. Interestingly, the optimal temperature for the conversion of propyl gallate was 35°C and was only of 4°C for pentyl gallate. When gallic acid was substituted with various hydroxybenzoic or benzoic acids no conversion was observed. This proves the high specificity of tannase for gallic acid. While the free enzyme promoted the synthesis of methyl and ethyl alcohol, the immobilized enzyme promoted the conversion of propyl and pentyl gallate. Finally, the yields of esterification were generally improved when hexane was employed as solvent. This could be explained by the low concentration of water in hexane compared to alcohols, avoiding hydrolysis and shifting the reaction equilibrium.

Yu *et al*. (Yu *et al.*, 2004b) studied the conversion of gallic acid by the tannase from A*spergillus niger*, encapsulated in chitosan-alginate beads. In a first study, the reactions were performed in a biphasic medium of buffer, hexane and propanol. The enzyme allowed the synthesis of propyl gallate but in low yields. Later, the same authors investigated the impact of the solvent on the reaction (Yu *et al.*, 2004a). The yield of propyl gallate was found to be maximal when the reaction was performed in a mixture of hexane and propanol without added water. Even more, when drying salts (as $MgSO_4$) or molecular sieve were added to the reaction medium, the yield was improved by nearly 10%. Among the solvents tested, the polar solvents (with logP < 1) resulted in low conversion of gallic acid. The best results were obtained in benzene (44.3% in 12h), followed by hexane (35.7%). More hydrophobic solvents (logP > 4) also resulted in low yields, maybe due to the low solubility of the substrate. The corresponding results of the study are represented in Figure 1.2.20. Finally, primary and secondary alcohols of various lengths were assessed for the esterification of gallic acid. The higher reactivity was observed with propanol (yield of 44.3% in 12h), followed by butanol (37.5%) and pentanol (33.8%). Other primary alcohols, such as ethanol or octanol, and secondary alcohols resulted in low conversion. Interestingly, the authors studied in similar conditions, the tannase from *Aspergillus oryzae* and obtained this time a higher yield of propyl gallate (53%) (Yu *et al.*, 2008). The same authors studied the kinetic and thermodynamic parameters of the conversion of gallic acid with propanol by the tannase from *Aspergillus niger* (Yu *et al.*, 2006). The reactions were performed in benzene with an excess of propanol. It has been shown that the esterification reaction followed a Ping–Pong Bi–Bi kinetic, a kinetic model that has as an example been fitted to the behaviors of other hydrolases as lipases (Chulalaksananukul *et al.*, 1990).

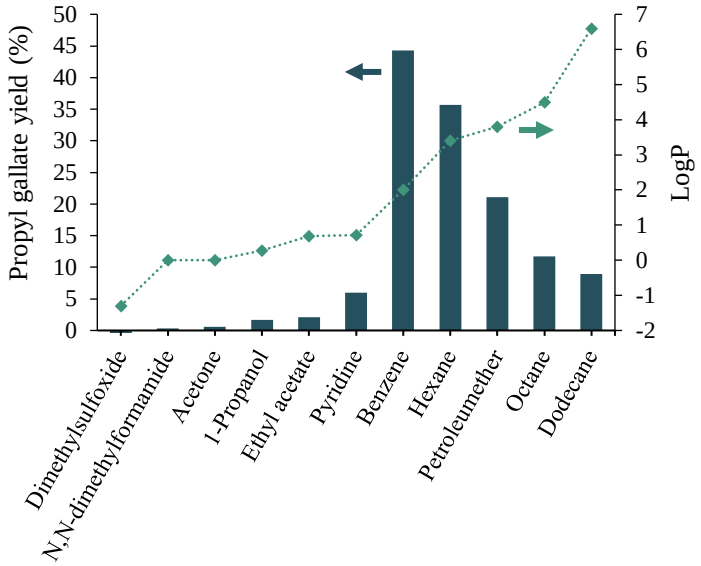

Figure 1.2.20: Yield of propyl gallate obtained through the tannase-catalyzed esterification of gallic acid with propanol in solvents with different logP for 12 h. Data from (Yu *et al.*, 2004a).

Meanwhile, Raab *et al*. (Raab *et al.*, 2007) assessed the activity of tannase in ionic liquids. As depicted previously, ILs are generally considered as green alternative to conventional organic solvents. Performing the enzymatic esterification of gallic acid in an IL, because of its low water activity, could favorably shift the reaction equilibrium. The authors performed the tannase-catalyzed esterification of gallic acid with (-)-epicatechin. Among seven ILs, [BMIM][MEESO4] offered the highest yield of reaction (3.5%). In this medium, free tannase was less reactive than tannase immobilized with Eupergit C as carrier. A water content of 20% was found to be optimal for the reaction. Indeed, lower water amounts resulted in the loss of enzymatic activity, probably due to the lack of essential hydration water. Higher water amounts likely promoted the hydrolysis reaction, thus opposing the esterification. The reaction tends to reach equilibrium after only 5h and always resulted in low yields (below 4%). Finally, tannase proved again to be highly specific, even in ILs, towards gallic acid compared to 14 other benzoic and cinnamic derivatives. Propyl and butyl gallate could also be synthesized but the authors did not give the yield of reaction.

ILs seem a greener alternative to conventional organic solvents, however as depicted earlier, they are still much more expensive than these last and are potentially toxic (Bubalo *et al.*, 2017) which reduces their potential for industrial scale applications.

Because of the high specificity of tannases, another method for producing gallate esters is to directly transesterify tannins instead of starting from gallic acid. This reduces the number of steps for the preparation of the derivatives. Gaathon *et al*. (Gaathon *et al.*, 1989) enzymatically synthesized propyl gallate by transesterification of tannic acid with propanol. A reverse micelle emulsion composed of buffer and hexane was used as solvent for the reaction. This way, tannase was encapsulated in micro-droplets of buffer solution while propyl gallate could be solubilized in the organic phase. This system

allowed to shift the equilibrium of the reaction toward the transesterification by disadvantaging the hydrolysis. Important yields in propyl gallate (up to 51% after 72 h) were obtained with this method. Moreover, it was observed that the optimal pH for the enzymatic transesterification (4.5) was lower than the hydrolysis optimal pH (5.5).

Aithal *et al*. (Aithal *et al.*, 2013a). compared the production of propyl gallate starting either from gallic acid or from tannins, the second being the more economical alternative. The authors studied the cell-associated tannase from *Bacillus massiliensis*, studied for the production of propyl gallate by the same authors (Aithal *et al.*, 2013b). The reactions were performed in benzene, with an excess of propanol and with a controlled water activity (a_w = 0.33). When gallic acid was substituted by tannic acid, the yield of reaction decreased from 25% to 10.4% showing a weaker activity of the immobilized tannase. However, bio-imprinting of the enzyme with tannic acid improved the yield of reaction by 50%.

The bio-imprinting consist of putting an enzyme in an aqueous solution with a stimulus affecting its conformation (a substrate, surfactants, pH …). This conformation is then fixed by transferring the enzyme from the aqueous solution to an organic medium, as an example by lyophilization (Rich *et al.*, 2002). As the catalytic activity of an enzyme is directly linked to its conformation, it can thus be improved by bio-imprinting. The principle of bio-imprinting is described in the Figure 1.2.21.

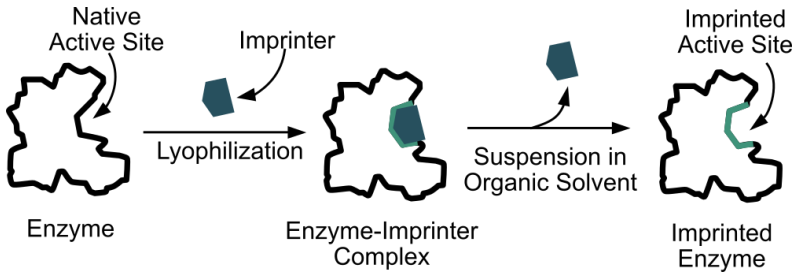

Figure 1.2.21: Principle of the bio-imprinting. Adapted from (Rich et al., 2002).

The bio-imprinting of tannase with tannic acid was studied earlier by Nie *et al* (Nie *et al.*, 2012b). The authors assessed the bio-imprinting of tannase with tannic acid in function of pH, temperature, and surfactants addition. All the methods influenced the activity of the enzyme for the transesterification of tannic acid with propanol. The enzyme once bio-imprinted with Triton X-100 and tannic acid and further immobilized on celite was 100-fold more active than the non-imprinted control enzyme. Once this bio-imprinted enzyme was used for the transesterification of tannic acid with propanol high yields up to 75% were obtained (Nie *et al.*, 2012a).

A year later, the authors further improved the preparation of tannase for the synthesis of propyl gallate. First, because tannase is heat-sensitive, cryo-protectant were investigated (Nie *et al.*, 2013) in order to avoid a loss in activity due to the lyophilization step (necessary to the bio-imprinting). Surfactants, sugars and metals were assessed as cryoprotectant and the best candidates were estimated to be Triton X-100, mannose and magnesium, respectively. Finally, a mutant cell-associated tannase

from *Aspergillus niger* was assayed (Nie *et al.*, 2014). The enzyme was again optimized through bio-imprinting and gave yields close to those of the free tannase. The authors pointed out that the use of a cell-associated enzyme could be a more ecological and economical approach to classical biocatalyst. Indeed, with this method the enzyme purification and immobilization steps are no longer required.

4.2. Other enzymes

Tannase present a high specificity for gallic derivatives, however other hydrolases as lipases have been shown to produce gallate esters through esterification or transesterification. Bouaziz *et al*. (Bouaziz *et al.*, 2010) studied the catalytic activity of the lipase from *Staphylococcus xylosus* immobilized on $CaCO_3$. The reactions were performed in hexane. The lipase-catalyzed synthesis of propyl gallate from gallic acid was computationally optimized. After optimization with a well-fitting model, the yield of propyl gallate was maximized to 90 ± 3.5 % in only 4 hours. As an example, the free enzyme only reached around 55% of conversion in the same time frame, showing the interest of the enzyme immobilization.

Sharma *et al*. (Sharma *et al.*, 2015) performed the lipase-catalyzed esterification of gallic acid in solvent-free conditions. The authors studied the esterification of gallic acid with alcohols of different lengths with the lipase from *Bacillus licheniformis* immobilized on celite. The water amount in the reaction medium was reduced by employing molecular sieves. The gallic acid:alcohol ratio 1:1 gave the highest yield for methyl gallate while for ethyl, propyl, and butyl gallate, a ratio of 1:2 was more advantageous. After 10 hours of reaction, the highest yield was obtained with propyl gallate (72.1%). The yields of the ethyl, butyl and methyl gallate then followed (with 66.8, 63.8 and 58.2%, respectively).

The same authors later reported the use of lipase from *Bacillus thermoamylovorans* for the esterification of gallic acid (Sharma *et al.*, 2017). The enzyme was immobilized on $MgFe_2O_4$ based magnetic nanoparticles. Magnetic nanoparticles present high surface specific area and can be removed with a magnet at the end of the reaction, simplifying the purification and reuse of the catalyst. Yields of propyl gallate up to 82% could be obtained within 12 h at 55°C, in solvent-free conditions.

As depicted earlier, gallic acid is hardly soluble in oily products. However, it is also difficult to solubilize in aqueous media. This limits its use as antioxidant in aqueous food, cosmetic and pharmaceutical products. As for cinnamic acid, the glycolysis of gallic acid improves its solubility in water (Nam *et al.*, 2017). Otherwise, gallic acid can be reacted with glycerol. This strategy was employed by Zhang *et al*. (Zhang *et al.*, 2019). The transesterification was performed with immobilized CALB (Lipozyme 435, Novozymes) in solvent-free conditions. After optimization of the reaction parameters, the yield of glyceryl gallate was 67.1 ± 1.9 % in 120 h. The glycerol:gallic acid ratio was found to be optimal at 25:1 with a load of enzyme of 23.8% and a reaction temperature of 50°C. In the same conditions, the commercial enzyme N435 allowed to reach an even higher yield of 75.0 ± 2.5%. Finally, in an organic solvent (t-butanol) the reaction yield remained below 1% even after 120 h. This

is particularly interesting results as previous studies on the CALB-catalyzed esterification of gallic acid with hexanol in an nonpolar solvent resulted in no yield (Buisman *et al.*, 1998).

Recently, the same authors optimized the enzymatic production of glyceryl gallate on a larger scale (Zhang *et al.*, 2020b). Because of lower temperature homogeneity when scaling-up, the optimal temperature was found to be 55°C. Lipozyme 435©, because of its food-compatible grade, was employed as catalyst. The yield of glyceryl gallate after 120 h was higher than previously with approximatively 78%. The author attributes this higher yield to the better mass transfer induced by the mechanical stirring. The authors then proved the good antioxidant capacity of glyceryl gallate (Zhang *et al.*, 2020a).

5. Conclusion:

A large variety of cinnamic and benzoic derivatives can be extracted from biomass. These derivatives have promising antioxidant and medical applications. However, their lack of solubility in aqueous and hydrophobic media limits their potential applications. A common method to overcome the lack of solubility of cinnamic derivatives is to esterify them with solubilizing moieties. Various solubilizing entities have been used depending on the targeted application. Fatty alcohols are employed for lipophilization and sugars polyols for hydrophilization. However, natural cinnamic and benzoic derivatives are often heat sensitive and must be transformed under mild conditions. For this reason, and to promote green processes, enzymatic esterification and transesterification of these compounds have been extensively investigated in the past 20 years.

It has been proven that esterification and transesterification of cinnamic and benzoic derivatives can be performed enzymatically and with high yields despite their aromaticity (Wang *et al.*, 2015a). However, many parameters must be considered. The architecture of the employed substrate directly impacts its reactivity toward enzymes. As an example, the conversion of benzoic derivatives was systematically lower than their cinnamic equivalents. This phenomenon might be due to a combination of steric hindrance and electronic effects. Indeed, the carboxylic acid in benzoic derivatives is located directly on the aromatic ring and is therefore conjugated with it. This loss of reactivity could explain why *p*-hydroxybenzoic, vanillic and syringic acid are less represented in literature compared to cinnamic derivatives as far as enzyme-catalyzed esterification is concerned. Because of steric and most likely electronic effects, substituents on the aromatic ring highly affect the substrate reactivity toward most enzymes in esterification and transesterification reactions. Generally, the *ortho* substituents have as stronger negative impact on the reactivity followed in that order by *para* and *meta* substituents. Moreover, hydroxyl substituents were shown to be more detrimental than methoxy substituents. This loss of reactivity is not observed in hydrogenated cinnamic derivatives (Pion *et al.*, 2014; Reano *et al.*, 2015). However, this specificity is enzyme dependent. As an example, the RML presents a high affinity toward *m*-methoxylated substrate as ferulic acid. Also, one must mention the possible inhibitory effect of phenolic compounds observed on the pancreatic lipase (Buchholz *et al*., 2015). For these reasons,

several lipases from various sources have been screened for their activity toward natural cinnamic derivatives.

Several studies focused on the FAEs which are specific to ferulic and cinnamic moieties. They can be expressed in many organisms and allow the conversion of cinnamic derivatives in significant yields. However, this enzyme is not yet commercially available and must be extracted from biological medium or from commercial preparations of enzymes mixtures. The reaction conditions, especially the solvent nature, are crucial for an optimal activity. Enzymatic esterification and transesterification with lipase are classically performed in non-polar organic solvents. However, many other solvent systems such as solvent free reaction, microemulsions, polar solvents or ionic liquids have emerged and are still investigated. Several other parameters have been investigated such as enzyme immobilization on various supports or the use of vacuum or ultrasonic activation (Sun *et al.*, 2020).

This review work also concerned gallic acid, a natural benzoic acid derivative which can be extracted from tannins, and which has many applications in industry, notably due to its good antioxidant properties. However, the solubility of gallic acid must be improved in oil or in aqueous solution to fully satisfy the targeted applications. The afore presented studies showed the potential of enzymatic catalyst in the production of oil- or water-soluble gallate esters. Since it is commonly used to transform tannins, tannase is an enzyme of choice to produce gallate esters. Tannins, which are far less costly than gallic acid, can directly and efficiently be transesterified by tannase to produce gallate esters. Other enzymes as lipases have also been proven to be efficient in the production of gallate esters. As for every enzymatic process, the impact of several parameters such as the solvent, temperature and reaction time have been investigated and optimized.

Nowadays, studies are increasingly directed towards continuous synthesis (Yoshida *et al*., 2006) and pilot scale production (Compton *et al*., 2009) of this type of compounds. This would allow the production of biobased phenolic antioxidant and medicines under more environmentally friendly conditions and would enhance the use of enzymatic industrial processes.

6. References

Abdelgawad, A., Eid, M., Abou-Elmagd, W. and Abou-Elregal, M. (**2021**) 'Lipase catalysed transesterification of palm stearin with ferulic acid in solvent-free media', *Biocatalysis and Biotransformation*, pp. 1–8.

Aharwar, A. and Parihar, D. K. (**2018**) 'Tannases: Production, properties, applications', *Biocatalysis and Agricultural Biotechnology*, 15, pp. 322–334.

Aithal, M. and Belur, P. D. (**2013**)**a** 'Enhancement of propyl gallate yield in nonaqueous medium using novel cell-associated tannase of *Bacillus massiliensis*', *Preparative Biochemistry and Biotechnology*, 43(5), pp. 445–455.

Aithal, M. and Belur, P. D. (**2013**)**b** 'Production of propyl gallate in nonaqueous medium using cell-associated tannase of *Bacillus massiliensis* : Effect of various parameters and statistical optimization: Production of Propyl Gallate in Nonaqueous Medium', *Biotechnology and Applied Biochemistry*, 60(2), pp. 210–218.

Anastas, P. and Eghbali, N. (**2010**) 'Green Chemistry: Principles and Practice', *Chem. Soc. Rev.*, 39(1), pp. 301–312.

Antonopoulou, I., Iancu, L., Jütten, P., Piechot, A., Rova, U. and Christakopoulos, P. (**2019**) 'Screening of novel feruloyl esterases from Talaromyces wortmannii for the development of efficient and sustainable syntheses of feruloyl derivatives', *Enzyme and Microbial Technology*, 120, pp. 124–135.

Antonopoulou, I., Leonov, L., Jütten, P., Cerullo, G., Faraco, V., Papadopoulou, A., Kletsas, D., Ralli, M., Rova, U. and Christakopoulos, P. (**2017**) 'Optimized synthesis of novel prenyl ferulate performed by feruloyl esterases from Myceliophthora thermophila in microemulsions', *Applied Microbiology and Biotechnology*, 101(8), pp. 3213–3226.

Antonopoulou, I., Papadopoulou, A., Iancu, L., Cerullo, G., Ralli, M., Jütten, P., Piechot, A., Faraco, V., Kletsas, D., Rova, U. and Christakopoulos, P. (**2018**) 'Optimization of enzymatic synthesis of l-arabinose ferulate catalyzed by feruloyl esterases from Myceliophthora thermophila in detergentless microemulsions and assessment of its antioxidant and cytotoxicity activities', *Process Biochemistry*, 65, pp. 100–108.

Antonopoulou, I., Varriale, S., Topakas, E., Rova, U., Christakopoulos, P. and Faraco, V. (**2016**) 'Enzymatic synthesis of bioactive compounds with high potential for cosmeceutical application', *Applied Microbiology and Biotechnology*, 100(15), pp. 6519–6543.

de Araújo, M., Franco, Y., Messias, M., Longato, G., Pamphile, J. and Carvalho, P. (**2016**) 'Biocatalytic Synthesis of Flavonoid Esters by Lipases and Their Biological Benefits', *Planta Medica*, 83(01/02), pp. 7–22.

B. Guyot, B. Bosquette, M. Pina, and J. Graille (**1997**) 'Esterification of phenolic acids from green coffee with an immobilized lipase from Candida antarctica in solvent-free medium', *Biotechnology Letters*, 19(6), p. 4.

B. Guyot, D.Gueule, M. Pina, J. Graille, V.Farines, and M.Farines (**2000**) 'Enzymatic synthesis of fatty esters in 5-caffeoyl quinic acid', *Eur. J. Lipid Sci. Technol.*, p. 4.

Bouaziz, A., Horchani, H., Salem, N. B., Chaari, A., Chaabouni, M., Gargouri, Y. and Sayari, A. (**2010**) 'Enzymatic propyl gallate synthesis in solvent-free system: Optimization by response surface methodology', *Journal of Molecular Catalysis B: Enzymatic*, 67(3–4), pp. 242–250.

Bubalo, M. C., Radošević, K., Redovniković, I. R., Slivac, I. and Srček, V. G. (**2017**) 'Toxicity mechanisms of ionic liquids', *Archives of Industrial Hygiene and Toxicology*, 68(3), pp. 171–179.

Buchholz, T. and Melzig, M. (**2015**) 'Polyphenolic Compounds as Pancreatic Lipase Inhibitors', *Planta Medica*, 81(10), pp. 771–783.

Buisman, G. J. H. and Cuperus, F. P. (**1998**) 'Enzymatic esterifications of functionalized phenols for the synthesis of lipophilic antioxidants', *Biotechnology Letters*, 20(2), p. 6.

Buzatu, A. R., Frissen, A. E., van den Broek, L. A. M., Todea, A., Motoc, M. and Boeriu, C. G. (**2020**) 'Chemoenzymatic Synthesis of New Aromatic Esters of Mono- and Oligosaccharides', *Processes*, 8(12), p. 1638.

Cai, Y., Luo, Q., Sun, M. and Corke, H. (**2004**) 'Antioxidant activity and phenolic compounds of 112 traditional Chinese medicinal plants associated with anticancer', *Life Sciences*, 74(17), pp. 2157–2184.

Cao, L., Chen, R., Xie, W. and Liu, Y. (**2015**) 'Enhancing the Thermostability of Feruloyl Esterase EstF27 by Directed Evolution and the Underlying Structural Basis', *Journal of Agricultural and Food Chemistry*, 63(37), pp. 8225–8233.

Cassani, J., Luna, H., Navarro, A. and Castillo, E. (**2007**) 'Comparative esterification of phenylpropanoids versus hydrophenylpropanoids acids catalyzed by lipase in organic solvent media', *Electronic Journal of Biotechnology*, 10(4), pp. 508–513.

Cerullo, G., Varriale, S., Bozonnet, S., Antonopoulou, I., Christakopoulos, P., Rova, U., Gherbovet, O., Fauré, R., Piechot, A., Jütten, P., Brás, J. L. A., Fontes, C. M. G. A. and Faraco, V. (**2019**) 'Directed evolution of the type C feruloyl esterase from Fusarium oxysporum FoFaeC and molecular docking analysis of its improved variants', *New Biotechnology*, 51, pp. 14–20.

Chandel, C., Kumar, A. and Kanwar, S. S. (**2011**) 'Enzymatic Synthesis of Butyl Ferulate by Silica-Immobilized Lipase in a Non-Aqueous Medium', *Journal of Biomaterials and Nanobiotechnology*, 02(04), pp. 400–408.

Chapman, J., Ismail, A. and Dinu, C. (**2018**) 'Industrial Applications of Enzymes: Recent Advances, Techniques, and Outlooks', *Catalysts*, 8(6), p. 238.

Chávez-González, M., Rodríguez-Durán, L. V., Balagurusamy, N., Prado-Barragán, A., Rodríguez, R., Contreras, J. C. and Aguilar, C. N. (**2012**) 'Biotechnological Advances and Challenges of Tannase: An Overview', *Food and Bioprocess Technology*, 5(2), pp. 445–459.

Chebil, L., Humeau, C., Falcimaigne, A., Engasser, J.-M. and Ghoul, M. (**2006**) 'Enzymatic acylation of flavonoids', *Process Biochemistry*, 41(11), pp. 2237–2251.

Chulalaksananukul, W., Condoret, J. S., Delorme, P. and Willemot, R. M. (**1990**) 'Kinetic study of esterification by immobilized lipase in *n* -hexane', *FEBS Letters*, 276(1–2), pp. 181–184.

Chyba, A., Mastihuba, V. and Mastihubová, M. (**2016**) 'Effective enzymatic caffeoylation of natural glucopyranosides', *Bioorganic & Medicinal Chemistry Letters*, 26(6), pp. 1567–1570.

Ciftci, D. and Saldaña, M. D. A. (**2012**) 'Enzymatic synthesis of phenolic lipids using flaxseed oil and ferulic acid in supercritical carbon dioxide media', *The Journal of Supercritical Fluids*, 72, pp. 255–262.

Clifford, M. N. (**2000**) 'Chlorogenic acids and other cinnamates – nature, occurrence, dietary burden, absorption and metabolism', *J Sci Food Agric*, p. 11.

Compton, D. L. and King, J. W. (**2001**) 'Lipase-catalyzed synthesis of triolein-based sunscreens in supercritical CO $_2$', *Journal of the American Oil Chemists' Society*, 78(1), pp. 43–47.

Compton, D. L. and Laszlo, J. A. (**2009**) '1,3-Diferuloyl-sn-glycerol from the biocatalytic transesterification of ethyl 4-hydroxy-3-methoxy cinnamic acid (ethyl ferulate) and soybean oil', *Biotechnology Letters*, 31(6), pp. 889–896.

Compton, D. L., Laszlo, J. A. and Berhow, M. A. (**2000**) 'Lipase-catalyzed synthesis of ferulate esters', *Journal of the American Oil Chemists' Society*, 77(5), pp. 513–519.

Compton, D. L., Laszlo, J. A. and Evans, K. O. (**2012**) 'Antioxidant properties of feruloyl glycerol derivatives', *Industrial Crops and Products*, 36(1), pp. 217–221.

Crepin, V. F., Faulds, C. B. and Connerton, I. F. (**2004**) 'Functional classification of the microbial feruloyl esterases', *Applied Microbiology and Biotechnology*, 63(6), pp. 647–652.

Crozier, A., Jaganath, I. B. and Clifford, M. N. (**2006**) 'Phenols, Polyphenols and Tannins: An Overview', in Crozier, A., Clifford, M. N., and Ashihara, H. (eds) *Plant Secondary Metabolites*. Oxford, UK: Blackwell Publishing Ltd, pp. 1–24.

Dandekar, P. and Wasewar, K. L. (**2020**) 'Experimental investigation on extractive separation of vanillic acid', *Chemical Data Collections*, 30, p. 100564.

Dilokpimol, A., Mäkelä, M. R., Aguilar-Pontes, M. V., Benoit-Gelber, I., Hildén, K. S. and de Vries, R. P. (**2016**) 'Diversity of fungal feruloyl esterases: updated phylogenetic classification, properties, and industrial applications', *Biotechnology for Biofuels*, 9(1), p. 231.

Durand, E., Lecomte, J., Baréa, B., Dubreucq, E., Lortie, R. and Villeneuve, P. (**2013**)**a** 'Evaluation of deep eutectic solvent–water binary mixtures for lipase-catalyzed lipophilization of phenolic acids', *Green Chemistry*, 15(8), p. 2275.

Durand, E., Lecomte, J., Baréa, B., Piombo, G., Dubreucq, É. and Villeneuve, P. (**2012**) 'Evaluation of deep eutectic solvents as new media for Candida antarctica B lipase catalyzed reactions', *Process Biochemistry*, 47(12), pp. 2081–2089.

Durand, E., Lecomte, J., Baréa, B. and Villeneuve, P. (**2014**) 'Towards a better understanding of how to improve lipase-catalyzed reactions using deep eutectic solvents based on choline chloride: Towards a better understanding of how to improve lipase-catalyzed …', *European Journal of Lipid Science and Technology*, 116(1), pp. 16–23.

Durand, E., Lecomte, J. and Villeneuve, P. (**2013**)**b** 'Deep eutectic solvents: Synthesis, application, and focus on lipase-catalyzed reactions', *European Journal of Lipid Science and Technology*, 115(4), pp. 379–385.

Durand, E., Lecomte, J. and Villeneuve, P. (**2015**) 'Are emerging deep eutectic solvents (DES) relevant for lipase-catalyzed lipophilizations?', *OCL*, 22(4), p. D408.

EFSA (**2014**) 'Scientific Opinion on the re-evaluation of propyl gallate (E 310) as a food additive', *EFSA Journal*, 12(4), p. 3642.

EFSA (**2015**) 'Scientific Opinion on the re-evaluation of octyl gallate (E 311) as a food additive: Re-evaluation of octyl gallate (E 311) as a food additive', *EFSA Journal*, 13(10), p. 4248.

Elgharbawy, A. A. M., Moniruzzaman, M. and Goto, M. (**2020**) 'Recent advances of enzymatic reactions in ionic liquids: Part II', *Biochemical Engineering Journal*, 154, p. 107426.

Elgharbawy, A. A. M., Moniruzzaman, M. and Goto, M. (**2021**) 'Facilitating enzymatic reactions by using ionic liquids: A mini review', *Current Opinion in Green and Sustainable Chemistry*, 27, p. 100406.

Elgharbawy, A. A., Riyadi, F. A., Alam, Md. Z. and Moniruzzaman, M. (**2018**) 'Ionic liquids as a potential solvent for lipase-catalysed reactions: A review', *Journal of Molecular Liquids*, 251, pp. 150–166.

Faulds, C. B. and Williamson, G. , 'The purification and characterization of 4-hydroxy-3-methoxycinnamic (ferulic) acid esterase from Streptomyces olitrochromogenes', p. 7.

Ferri, M., Happel, A., Zanaroli, G., Bertolini, M., Chiesa, S., Commisso, M., Guzzo, F. and Tassoni, A. (**2020**) 'Advances in combined enzymatic extraction of ferulic acid from wheat bran', *New Biotechnology*, 56, pp. 38–45.

Figueroa-Espinoza, M. C., Laguerre, M., Villeneuve, P. and Lecomte, J. (**2013**) 'From phenolics to phenolipids: Optimizing antioxidants in lipid dispersions', *Lipid Technology*, 25(6), pp. 131–134.

Figueroa-Espinoza, M.-C. and Villeneuve, P. (**2005**) 'Phenolic Acids Enzymatic Lipophilization', *Journal of Agricultural and Food Chemistry*, 53(8), pp. 2779–2787.

Flourat, A. L., Combes, J., Bailly-Maitre-Grand, C., Magnien, K., Haudrechy, A., Renault, J. and Allais, F. (**2021**) 'Accessing *p*-Hydroxycinnamic Acids: Chemical Synthesis, Biomass Recovery, or Engineered Microbial Production?', *ChemSusChem*, 14(1), pp. 118–129.

Fodor, C., Golkaram, M., Woortman, A. J. J., van Dijken, J. and Loos, K. (**2017**) 'Enzymatic approach for the synthesis of biobased aromatic–aliphatic oligo-/polyesters', *Polymer Chemistry*, 8(44), pp. 6795–6805.

Fonseca, A. C., Lima, M. S., Sousa, A. F., Silvestre, A. J., Coelho, J. F. J. and Serra, A. C. (**2019**) 'Cinnamic acid derivatives as promising building blocks for advanced polymers: synthesis, properties and applications', *Polymer Chemistry*, 10(14), pp. 1696–1723.

Gaathon, A., Gross, Z. and Rozhanski, M. (**1989**) 'Propyl gailate: enzymatic synthesis in a reverse micelle system', *Enzyme and Microbial Technology*, 11, p. 6.

Gamboni, S. E., Palmer, A. M. and Nixon, R. L. (**2013**) 'Allergic contact stomatitis to dodecyl gallate? A review of the relevance of positive patch test results to gallates: Allergic contact stomatitis to gallates', *Australasian Journal of Dermatology*, 54(3), pp. 213–217.

Genaro-Mattos, T. C., Maurício, Â. Q., Rettori, D., Alonso, A. and Hermes-Lima, M. (**2015**) 'Antioxidant Activity of Caffeic Acid against Iron-Induced Free Radical Generation—A Chemical Approach', *PLOS ONE*. Edited by G. P. Tochtrop, 10(6), p. e0129963.

Gherbovet, O., Ferreira, F., Clément, A., Ragon, M., Durand, J., Bozonnet, S., O'Donohue, M. J. and Fauré, R. (**2020**) *Regioselective chemo-enzymatic syntheses of ferulate conjugates as chromogenic substrates for feruloyl esterases*. preprint. organic chemistry. Available at: https://www.beilstein-archives.org/xiv/preprints/2020107 (Accessed: 23 August 2021).

Giuliani, S., Piana, C., Setti, L., Hochkoeppler, A., Pifferi, P. G. and Williamson, G. (**2001**) 'Synthesis of pentylferulate by a feruloyl esterase from Aspergillus niger using water-in-oil microemulsions', p. 6.

Grajales-Hernández, D. A., Velasco-Lozano, S., Armendáriz-Ruiz, M. A., Rodríguez-González, J. A., Camacho-Ruíz, R. M., Asaff-Torres, A., López-Gallego, F. and Mateos-Díaz, J. C. (**2020**) 'Carrier-bound and carrier-free immobilization of type A feruloyl esterase from Aspergillus niger: Searching for an operationally stable heterogeneous biocatalyst for the synthesis of butyl hydroxycinnamates', *Journal of Biotechnology*, 316, pp. 6–16.

Guajardo, N., Domínguez de María, P., Ahumada, K., Schrebler, R. A., Ramírez-Tagle, R., Crespo, F. A. and Carlesi, C. (**2017**) 'Water as Cosolvent: Nonviscous Deep Eutectic Solvents for Efficient Lipase-Catalyzed Esterifications', *ChemCatChem*, 9(8), pp. 1393–1396.

Guajardo, N., Schrebler, R. A. and Domínguez de María, P. (**2019**) 'From batch to fed-batch and to continuous packed-bed reactors: Lipase-catalyzed esterifications in low viscous deep-eutectic-solvents with buffer as cosolvent', *Bioresource Technology*, 273, pp. 320–325.

Gunia-Krzyżak, A., Słoczyńska, K., Popiół, J., Koczurkiewicz, P., Marona, H. and Pękala, E. (**2018**) 'Cinnamic acid derivatives in cosmetics: current use and future prospects', *International Journal of Cosmetic Science*, 40(4), pp. 356–366.

Ham, J., Lim, W., Park, S., Bae, H., You, S. and Song, G. (**2019**) 'Synthetic phenolic antioxidant propyl gallate induces male infertility through disruption of calcium homeostasis and mitochondrial function', *Environmental Pollution*, 248, pp. 845–856.

Hatfield, R. D., Rancour, D. M. and Marita, J. M. (**2017**) 'Grass Cell Walls: A Story of Cross-Linking', *Frontiers in Plant Science*, 7.

Heldt-Hansen, H. P., Ishii, M., Patkar, S. A., Hansen, T. T. and Eigtved, P. (**1989**) 'A New Immobilized Positional Nonspecific Lipase for Fat Modification and Ester Synthesis', in Whitaker, J. R. and Sonnet, P. E. (eds) *Biocatalysis in Agricultural Biotechnology*. Washington, DC: American Chemical Society, pp. 158–172.

Higgins, J. W. and Black, H. C. (**1944**) 'A preliminary comparison of the stabilizing effect of several recently proposed antioxidants for edible fats and oils', *Oil & Soap*, 21(9), pp. 277–279.

de Hoyos-Martínez, P. L., Merle, J., Labidi, J. and Charrier – El Bouhtoury, F. (**2019**) 'Tannins extraction: A key point for their valorization and cleaner production', *Journal of Cleaner Production*, 206, pp. 1138–1155.

Huang, K.-C., Li, Y., Twu, Y.-K. and Shieh, C.-J. (**2015**) 'High Efficient Synthesis of Enzymatic 2-Ethylhexyl Ferulate at Solvent-Free and Reduced Pressure Evaporation System', *Journal of Materials Science and Chemical Engineering*, 03(06), pp. 33–40.

Hunt, C. J., Antonopoulou, I., Tanksale, A., Rova, U., Christakopoulos, P. and Haritos, V. S. (**2017**) 'Insights into substrate binding of ferulic acid esterases by arabinose and methyl hydroxycinnamate esters and molecular docking', *Scientific Reports*, 7(1), p. 17315.

Hüttner, S., Zezzi Do Valle Gomes, M., Iancu, L., Palmqvist, A. and Olsson, L. (**2017**) 'Immobilisation on mesoporous silica and solvent rinsing improve the transesterification abilities of feruloyl esterases from Myceliophthora thermophila', *Bioresource Technology*, 239, pp. 57–65.

Ingole, A., Kadam, M. P., Dalu, A. P., Kute, S. M., Mange, P. R., Theng, V. D., Lahane, O. R., Nikas, A. P., Kawal, Y. V., Nagrik, S. U. and Patil, P. A. (**2021**) 'A Review of the Pharmacological Characteristics of Vanillic Acid', *Journal of Drug Delivery and Therapeutics*, 11(2-S), pp. 200–204.

Ito, S., Nakagawa, Y., Yazawa, S., Sasaki, Y. and Yajima, S. (**2014**) 'Antifungal activity of alkyl gallates against plant pathogenic fungi', *Bioorganic & Medicinal Chemistry Letters*, 24(7), pp. 1812–1814.

Jakovetić, S. M., Jugović, B. Z., Gvozdenović, M. M., Bezbradica, D. I., Antov, M. G., Mijin, D. Ž. and Knežević-Jugović, Z. D. (**2013**) 'Synthesis of Aliphatic Esters of Cinnamic Acid as Potential Lipophilic Antioxidants Catalyzed by Lipase B from Candida antarctica', *Applied Biochemistry and Biotechnology*, 170(7), pp. 1560–1573.

Kahkeshani, N., Farzaei, F., Fotouhi, M., Alavi, S. S., Bahramsoltani, R., Naseri, R., Momtaz, S., Abbasabadi, Z., Rahimi, R., Farzaei, M. H. and Bishayee, A. (**2019**) 'Pharmacological effects of gallic acid in health and disease: A mechanistic review', *Iranian Journal of Basic Medical Sciences*, 22(3).

Karboune, S., St-Louis, R. and Kermasha, S. (**2008**) 'Enzymatic synthesis of structured phenolic lipids by acidolysis of flaxseed oil with selected phenolic acids', *Journal of Molecular Catalysis B: Enzymatic*, 52–53, pp. 96–105.

Katsoura, M. H., Polydera, A. C., Tsironis, L. D., Petraki, M. P., Rajačić, S. K., Tselepis, A. D. and Stamatis, H. (**2009**) 'Efficient enzymatic preparation of hydroxycinnamates in ionic liquids enhances their antioxidant effect on lipoproteins oxidative modification', *New Biotechnology*, 26(1–2), pp. 83–91.

Khan, F., Bamunuarachchi, N. I., Tabassum, N. and Kim, Y.-M. (**2021**) 'Caffeic Acid and Its Derivatives: Antimicrobial Drugs toward Microbial Pathogens', *Journal of Agricultural and Food Chemistry*, 69(10), pp. 2979–3004.

Kirk, O., Borchert, T. V. and Fuglsang, C. C. (**2002**) 'Industrial enzyme applications', *Current Opinion in Biotechnology*, 13(4), pp. 345–351.

Kumar, A. and Kanwar, S. S. (**2011**) 'Synthesis of ethyl ferulate in organic medium using celite-immobilized lipase', *Bioresource Technology*, 102(3), pp. 2162–2167.

Kumar, N. and Goel, N. (**2019**) 'Phenolic acids: Natural versatile molecules with promising therapeutic applications', *Biotechnology Reports*, 24, p. e00370.

Laguerre, M., Bayrasy, C., Lecomte, J., Chabi, B., Decker, E. A., Wrutniak-Cabello, C., Cabello, G. and Villeneuve, P. (**2013**) 'How to boost antioxidants by lipophilization?', *Biochimie*, 95(1), pp. 20–26.

Lee, G.-S., Widjaja, A. and Ju, Y.-H. (**2006**) 'Enzymatic Synthesis of Cinnamic Acid Derivatives', *Biotechnology Letters*, 28(8), pp. 581–585.

Li, M. and Wilkins, M. (**2021**) 'Lignin bioconversion into valuable products: fractionation, depolymerization, aromatic compound conversion, and bioproduct formation', *Systems Microbiology and Biomanufacturing*, 1(2), pp. 166–185.

Llevot, A., Grau, E., Carlotti, S., Grelier, S. and Cramail, H. (**2016**) 'From Lignin-derived Aromatic Compounds to Novel Biobased Polymers', *Macromolecular Rapid Communications*, 37(1), pp. 9–28.

Locatelli, C., Filippin-Monteiro, F. B. and Creczynski-Pasa, T. B. (**2013**) 'Alkyl esters of gallic acid as anticancer agents: A review', *European Journal of Medicinal Chemistry*, 60, pp. 233–239.

Lue, B.-M., Karboune, S., Yeboah, F. K. and Kermasha, S. (**2005**) 'Lipase-catalyzed esterification of cinnamic acid and oleyl alcohol in organic solvent media', *Journal of Chemical Technology & Biotechnology*, 80(4), pp. 462–468.

Mahapatro, A., Kalra, B., Kumar, A. and Gross, R. A. (**2003**) 'Lipase-Catalyzed Polycondensations: Effect of Substrates and Solvent on Chain Formation, Dispersity, and End-Group Structure', *Biomacromolecules*, 4(3), pp. 544–551.

Mastihubová, M. and Mastihuba, V. (**2013**) 'Donor specificity and regioselectivity in Lipolase mediated acylations of methyl α-d-glucopyranoside by vinyl esters of phenolic acids and their analogues', *Bioorganic & Medicinal Chemistry Letters*, 23(19), pp. 5389–5392.

Mastihubová, M., Mastihuba, V., Bilaničová, D. and Boreková, M. (**2006**) 'Commercial enzyme preparations catalyse feruloylation of glycosides', *Journal of Molecular Catalysis B: Enzymatic*, 38(1), pp. 54–57.

Mathew, S. and Abraham, T. E. (**2004**) 'Ferulic Acid: An Antioxidant Found Naturally in Plant Cell Walls and Feruloyl Esterases Involved in its Release and Their Applications', *Critical Reviews in Biotechnology*, 24(2–3), pp. 59–83.

de Meneses, A. C., Balen, M., de Andrade Jasper, E., Korte, I., de Araújo, P. H. H., Sayer, C. and de Oliveira, D. (**2020**) 'Enzymatic synthesis of benzyl benzoate using different acyl donors: Comparison of solvent-free reaction techniques', *Process Biochemistry*, 92, pp. 261–268.

Nam, S.-H., Park, J., Jun, W., Kim, D., Ko, J.-A., Abd El-Aty, A. M., Choi, J. Y., Kim, D.-I. and Yang, K.-Y. (**2017**) 'Transglycosylation of gallic acid by using Leuconostoc glucansucrase and its characterization as a functional cosmetic agent', *AMB Express*, 7(1), p. 224.

Natella, F., Nardini, M., Di Felice, M. and Scaccini, C. (**1999**) 'Benzoic and Cinnamic Acid Derivatives as Antioxidants: Structure−Activity Relation', *Journal of Agricultural and Food Chemistry*, 47(4), pp. 1453–1459.

Nie, G., Chen, Z., Zheng, Z., Jin, W., Gong, G., Wang, L. and Yue, W. (**2013**) 'Enhancement of transesterification-catalyzing capability of bio-imprinted tannase in organic solvents by cryogenic protection and immobilization', *Journal of Molecular Catalysis B: Enzymatic*, 94, pp. 1–6.

Nie, G., Liu, H., Chen, Z., Wang, P., Zhao, G. and Zheng, Z. (**2012**)**a** 'Synthesis of propyl gallate from tannic acid catalyzed by tannase from Aspergillus oryzae: Process optimization of transesterification in anhydrous media', *Journal of Molecular Catalysis B: Enzymatic*, 82, pp. 102–108.

Nie, G., Zheng, Z., Jin, W., Gong, G. and Wang, L. (**2012**)**b** 'Development of a tannase biocatalyst based on bio-imprinting for the production of propyl gallate by transesterification in organic media', *Journal of Molecular Catalysis B: Enzymatic*, 78, pp. 32–37.

Nie, G., Zheng, Z., Yue, W., Liu, Y., Liu, H., Wang, P., Zhao, G., Cai, W. and Xue, Z. (**2014**) 'One-pot bio-synthesis of propyl gallate by a novel whole-cell biocatalyst', *Process Biochemistry*, 49(2), pp. 277–282.

Nielsen, T. B., Ishii, M. and Kirk, O. (**1999**) 'Lipases A and B from the yeast Candida antarctica', in *Biotechnological Application of Cold-Adapted Organisms*. Springer Berlin Heidelberg, pp. 49–61.

Oliveira, D. M., Mota, T. R., Oliva, B., Segato, F., Marchiosi, R., Ferrarese-Filho, O., Faulds, C. B. and dos Santos, W. D. (**2019**) 'Feruloyl esterases: Biocatalysts to overcome biomass recalcitrance and for the production of bioactive compounds', *Bioresource Technology*, 278, pp. 408–423.

Ortiz, C., Ferreira, M. L., Barbosa, O., dos Santos, J. C. S., Rodrigues, R. C., Berenguer-Murcia, Á., Briand, L. E. and Fernandez-Lafuente, R. (**2019**) 'Novozym 435: the "perfect" lipase immobilized biocatalyst?', *Catalysis Science & Technology*, 9(10), pp. 2380–2420.

Otto, R. T., Scheib, H., Bornscheuer, U. T., Pleiss, J., Syldatk, C. and Schmid, R. D. (**2000**) 'Substrate specificity of lipase B from Candida antarctica in the synthesis of arylaliphatic glycolipids', *Journal of Molecular Catalysis B: Enzymatic*, 8(4–6), pp. 201–211.

Ou, S. and Kwok, K.-C. (**2004**) 'Ferulic acid: pharmaceutical functions, preparation and applications in foods', *Journal of the Science of Food and Agriculture*, 84(11), pp. 1261–1269.

Paiva, L. B. de, Goldbeck, R., Santos, W. D. dos and Squina, F. M. (**2013**) 'Ferulic acid and derivatives: molecules with potential application in the pharmaceutical field', *Brazilian Journal of Pharmaceutical Sciences*, 49(3), pp. 395–411.

Pion, F., Ducrot, P.-H. and Allais, F. (**2014**) 'Renewable Alternating Aliphatic-Aromatic Copolyesters Derived from Biobased Ferulic Acid, Diols, and Diacids: Sustainable Polymers with Tunable Thermal Properties', *Macromolecular Chemistry and Physics*, 215(5), pp. 431–439.

Pizzi (**2019**) 'Tannins: Prospectives and Actual Industrial Applications', *Biomolecules*, 9(8), p. 344.

Poveda-Giraldo, J. A., Solarte-Toro, J. C. and Cardona Alzate, C. A. (**2021**) 'The potential use of lignin as a platform product in biorefineries: A review', *Renewable and Sustainable Energy Reviews*, 138, p. 110688.

Priya, K. and Chadha, A. (**2003**) 'Synthesis of hydrocinnamic esters by Pseudomonas cepacia lipase', *Enzyme and Microbial Technology*, 32(3–4), pp. 485–490.

Priya, K., Venugopal, T. and Chadha, A. (**2002**) 'Pseudomonas cepacia lipase-mediated transesterification reactions of hydrocinnamates', *Indian Journal of Biochemistry & Biophysics*, 39, pp. 259–263.

Raab, T., Bel-Rhlid, R., Williamson, G., Hansen, C.-E. and Chaillot, D. (**2007**) 'Enzymatic galloylation of catechins in room temperature ionic liquids', *Journal of Molecular Catalysis B: Enzymatic*, 44(2), pp. 60–65.

Rahman, N. J. A., Radzi, S. M. and Noor, H. M. , 'Dual Lipases System in Transesterification of Ethyl Ferulate with Olive Oil: Optimization by Response Surface Methodology', p. 7.

Ralph, J. (**2010**) 'Hydroxycinnamates in lignification', *Phytochemistry Reviews*, 9(1), pp. 65–83.

Reano, A. F., Chérubin, J., Peru, A. M. M., Wang, Q., Clément, T., Domenek, S. and Allais, F. (**2015**) 'Structure–Activity Relationships and Structural Design Optimization of a Series of *p* - Hydroxycinnamic Acids-Based Bis- and Trisphenols as Novel Sustainable Antiradical/Antioxidant Additives', *ACS Sustainable Chemistry & Engineering*, 3(12), pp. 3486–3496.

Rich, J. O., Mozhaev, V. V., Dordick, J. S., Clark, D. S. and Khmelnitsky, Y. L. (**2002**) 'Molecular Imprinting of Enzymes with Water-Insoluble Ligands for Nonaqueous Biocatalysis', *Journal of the American Chemical Society*, 124(19), pp. 5254–5255.

de las Rivas, B., Rodríguez, H., Anguita, J. and Muñoz, R. (**2019**) 'Bacterial tannases: classification and biochemical properties', *Applied Microbiology and Biotechnology*, 103(2), pp. 603–623.

Romero-Borbón, E., Grajales-Hernández, D., Armendáriz-Ruiz, M., Ramírez-Velasco, L., Rodríguez-González, J. A., Cira-Chávez, L. A., Estrada-Alvarado, M. I. and Mateos-Díaz, J. C. (**2018**) 'Type C feruloyl esterase from Aspergillus ochraceus: A butanol specific biocatalyst for the synthesis of hydroxycinnamates in a ternary solvent system', *Electronic Journal of Biotechnology*, 35, pp. 1–9.

Rychlicka, M., Maciejewska, G., Niezgoda, N. and Gliszczyńska, A. (**2020**) 'Production of feruloylated lysophospholipids via a one-step enzymatic interesterification', *Food Chemistry*, 323, p. 126802.

Rychlicka, M., Rot, A. and Gliszczyńska, A. (**2021**) 'Biological Properties, Health Benefits and Enzymatic Modifications of Dietary Methoxylated Derivatives of Cinnamic Acid', *Foods*, 10(6), p. 1417.

Sankar, K., Achary, A., Mehala, N. and Rajendran, L. (**2017**) 'Empirical and Analytical Correlation of the Reaction Kinetics Parameters of Cuttle Bone Powder Immobilized Lipase Catalyzed Ethyl Ferulate Synthesis', *Catalysis Letters*, 147(8), pp. 2232–2245.

Santos, Y. L. de los, Chew-Fajardo, Y. L., Brault, G. and Doucet, N. (**2019**) 'Dissecting the evolvability landscape of the CalB active site toward aromatic substrates', *Scientific Reports*, 9(1), p. 15588.

Schär, A., Liphardt, S. and Nyström, L. (**2017**) 'Enzymatic synthesis of steryl hydroxycinnamates and their antioxidant activity', *European Journal of Lipid Science and Technology*, 119(5), p. 1600267.

Schär, A. and Nyström, L. (**2015**) 'High yielding and direct enzymatic lipophilization of ferulic acid using lipase from Rhizomucor miehei', *Journal of Molecular Catalysis B: Enzymatic*, 118, pp. 29–35.

Schär, A. and Nyström, L. (**2016**) 'Enzymatic synthesis of steryl ferulates: Enzymatic synthesis of steryl ferulates', *European Journal of Lipid Science and Technology*, 118(10), pp. 1557–1565.

Sharma, A., Kumar, A., Meena, K. R., Rana, S., Singh, M. and Kanwar, S. S. (**2017**) 'Fabrication and functionalization of magnesium nanoparticle for lipase immobilization in n -propyl gallate synthesis', *Journal of King Saud University - Science*, 29(4), pp. 536–546.

Sharma, K., Kumar, V., Kaur, J., Tanwar, B., Goyal, A., Sharma, R., Gat, Y. and Kumar, A. (**2019**) 'Health effects, sources, utilization and safety of tannins: a critical review', *Toxin Reviews*, pp. 1–13.

Sharma, S., Kanwar, S. S., Dogra, P. and Chauhan, G. S. (**2015**) 'Gallic acid-based alkyl esters synthesis in a water-free system by celite-bound lipase of *B acillus licheniformis* SCD11501', *Biotechnology Progress*, 31(3), pp. 715–723.

Shi, Y., Bian, L., Zhu, Y., Zhang, R., Shao, S., Wu, Y., Chen, Y., Dang, Y., Ding, Y. and Sun, H. (**2019**) 'Multifunctional alkyl ferulate esters as potential food additives: Antibacterial activity and mode of action against Listeria monocytogenes and its application on American sturgeon caviar preservation', *Food Control*, 96, pp. 390–402.

Shi, Y., Wu, Y., Lu, X., Ren, Y., Wang, Q., Zhu, C., Yu, D. and Wang, H. (**2017**) 'Lipase-catalyzed esterification of ferulic acid with lauryl alcohol in ionic liquids and antibacterial properties in vitro against three food-related bacteria', *Food Chemistry*, 220, pp. 249–256.

Søndergaard, H. A., Grunert, K. G. and Scholderer, J. (**2005**) 'Consumer attitudes to enzymes in food production', *Trends in Food Science & Technology*, 16(10), pp. 466–474.

Sorour, N., Karboune, S., Saint-Louis, R. and Kermasha, S. (**2012**) 'Lipase-catalyzed synthesis of structured phenolic lipids in solvent-free system using flaxseed oil and selected phenolic acids as substrates', *Journal of Biotechnology*, 158(3), pp. 128–136.

Spiridon, I., Bodirlau, R. and Teaca, C.-A. (**2011**) 'Total phenolic content and antioxidant activity of plants used in traditional Romanian herbal medicine', *Open Life Sciences*, 6(3), pp. 388–396.

Srinivasulu, C., Ramgopal, M., Ramanjaneyulu, G., Anuradha, C. M. and Suresh Kumar, C. (**2018**) 'Syringic acid (SA) – A Review of Its Occurrence, Biosynthesis, Pharmacological and Industrial Importance', *Biomedicine & Pharmacotherapy*, 108, pp. 547–557.

Stamatis, H., Sereti, V. and Kolisis, F. N. (**1999**) 'Studies on the enzymatic synthesis of lipophilic derivatives of natural antioxidants', *Journal of the American Oil Chemists' Society*, 76(12), p. 1505.

Stamatis, H., Sereti, V. and Kolisis, F. N. (**2001**) 'Enzymatic synthesis of hydrophilic and hydrophobic derivatives of natural phenolic acids in organic media', *Journal of Molecular Catalysis B: Enzymatic*, 11(4–6), pp. 323–328.

Stevenson, D. E., Parkar, S. G., Zhang, J., Stanley, R. A., Jensen, D. J. and Cooney, J. M. (**2007**) 'Combinatorial enzymic synthesis for functional testing of phenolic acid esters catalysed by Candida antarctica lipase B (Novozym 435®)', *Enzyme and Microbial Technology*, 40(5), pp. 1078–1086.

Suárez-Escobedo, L. and Gotor-Fernández, V. (**2021**) 'Solvent role in the lipase-catalysed esterification of cinnamic acid and derivatives. Optimisation of the biotransformation conditions', *Tetrahedron*, 81, p. 131873.

Sun, S. and Hu, B. (**2017**)**a** 'A novel method for the synthesis of glyceryl monocaffeate by the enzymatic transesterification and kinetic analysis', *Food Chemistry*, 214, pp. 192–198.
Sun, S. and Hu, B. (**2017**)**b** 'Enzymatic preparation of novel caffeoyl structured lipids using monoacylglycerols as caffeoyl acceptor and transesterification mechanism', *Biochemical Engineering Journal*, 124, pp. 78–87.
Sun, S., Lv, Y. and Zhu, S. (**2019**) 'Influence of ionic liquid on Novozym 435-catalyzed the transesterification of castor oil and ethyl caffeate', *3 Biotech*, 9(1), p. 34.
Sun, S., Shan, L., Jin, Q., Liu, Y. and Wang, X. (**2007**) 'Solvent-free synthesis of glyceryl ferulate using a commercial microbial lipase', *Biotechnology Letters*, 29(6), pp. 945–949.
Sun, S. and Tian, L. (**2018**)**a** 'Novozym 40086 as a novel biocatalyst to improve benzyl cinnamate synthesis', *RSC Advances*, 8(65), pp. 37184–37192.
Sun, S. and Zhu, S. (**2015**) 'Enzymatic preparation of castor oil-based feruloylated lipids using ionic liquids as reaction medium and kinetic model', *Industrial Crops and Products*, 73, pp. 127–133.
Sun, T., Zhang, H., Dong, Z., Liu, Z. and Zheng, M. (**2020**) 'Ultrasonic-promoted enzymatic preparation, identification and multi-active studies of nature-identical phenolic acid glycerol derivatives', *RSC Advances*, 10(19), pp. 11139–11147.
Sun, Z., Fridrich, B., de Santi, A., Elangovan, S. and Barta, K. (**2018**)**b** 'Bright Side of Lignin Depolymerization: Toward New Platform Chemicals', *Chemical Reviews*, 118(2), pp. 614–678.
Svobodova, A., Psotova, J. and Walterova, D. (**2003**) 'Natural phenolics in the prevention of UV-induced skin damage. A review', *Biomedical Papers*, 147(2), pp. 137–145.
Tan, Z. and Shahidi, F. (**2013**) 'Phytosteryl sinapates and vanillates: Chemoenzymatic synthesis and antioxidant capacity assessment', *Food Chemistry*, 138(2–3), pp. 1438–1447.
Terrett, O. M. and Dupree, P. (**2019**) 'Covalent interactions between lignin and hemicelluloses in plant secondary cell walls', *Current Opinion in Biotechnology*, 56, pp. 97–104.
Topakas, E., Kalogeris, E., Kekos, D., Macris, B. J. and Christakopoulos, P. (**2003**)**a** 'Bioconversion of ferulic acid into vanillic acid by the thermophilic fungus Sporotrichum thermophile', *LWT - Food Science and Technology*, 36(6), pp. 561–565.
Topakas, E., Stamatis, H., Biely, P., Kekos, D., Macris, B. J. and Christakopoulos, P. (**2003**)**b** 'Purification and characterization of a feruloyl esterase from Fusarium oxysporum catalyzing esterification of phenolic acids in ternary water–organic solvent mixtures', *Journal of Biotechnology*, 102(1), pp. 33–44.
Topakas, E., Stamatis, H., Mastihubova, M., Biely, P., Kekos, D., Macris, B. J. and Christakopoulos, P. (**2003**)**c** 'Purification and characterization of a Fusarium oxysporum feruloyl esterase (FoFAE-I) catalysing transesterification of phenolic acid esters', *Enzyme and Microbial Technology*, 33(5), pp. 729–737.
Topakas, E., Vafiadi, C. and Christakopoulos, P. (**2007**) 'Microbial production, characterization and applications of feruloyl esterases', *Process Biochemistry*, 42(4), pp. 497–509.
Topakas, E., Vafiadi, C., Stamatis, H. and Christakopoulos, P. (**2005**) 'Sporotrichum thermophile type C feruloyl esterase (StFaeC): purification, characterization, and its use for phenolic acid (sugar) ester synthesis', *Enzyme and Microbial Technology*, 36(5–6), pp. 729–736.
Toth, G. and Hensler, D. (**1952**) 'Über die enzymatische synthese der gallussäure-derivaten', *Acta chimica Hungarica*, 2, pp. 209–210.
Tsuchiyama, M., Sakamoto, T., Fujita, T., Murata, S. and Kawasaki, H. (**2006**) 'Esterification of ferulic acid with polyols using a ferulic acid esterase from Aspergillus niger', *Biochimica et Biophysica Acta (BBA) - General Subjects*, 1760(7), pp. 1071–1079.
Tsuchiyama, M., Sakamoto, T., Tanimori, S., Murata, S. and Kawasaki, H. (**2007**) 'Enzymatic Synthesis of Hydroxycinnamic Acid Glycerol Esters Using Type A Feruloyl Esterase from *Aspergillus niger*', *Bioscience, Biotechnology, and Biochemistry*, 71(10), pp. 2606–2609.
Ülger, C. and Takaç, S. (**2017**) 'Kinetics of lipase-catalysed methyl gallate production in the presence of deep eutectic solvent', *Biocatalysis and Biotransformation*, 35(6), pp. 407–416.
Vafiadi, C., Topakas, E., Alissandratos, A., Faulds, C. B. and Christakopoulos, P. (**2008**) 'Enzymatic synthesis of butyl hydroxycinnamates and their inhibitory effects on LDL-oxidation', *Journal of Biotechnology*, 133(4), pp. 497–504.

Vafiadi, C., Topakas, E., Nahmias, V. R., Faulds, C. B. and Christakopoulos, P. (**2009**) 'Feruloyl esterase-catalysed synthesis of glycerol sinapate using ionic liquids mixtures', *Journal of Biotechnology*, 139(1), pp. 124–129.

Vafiadi, C., Topakas, E., Wong, K. K. Y., Suckling, I. D. and Christakopoulos, P. (**2005**) 'Mapping the hydrolytic and synthetic selectivity of a type C feruloyl esterase (StFaeC) from Sporotrichum thermophile using alkyl ferulates', *Tetrahedron: Asymmetry*, 16(2), pp. 373–379.

Valanciene, E., Jonuskiene, I., Syrpas, M., Augustiniene, E., Matulis, P., Simonavicius, A. and Malys, N. (**2020**) 'Advances and Prospects of Phenolic Acids Production, Biorefinery and Analysis', *Biomolecules*, 10(6), p. 874.

Varriale, S., Cerullo, G., Antonopoulou, I., Christakopoulos, P., Rova, U., Tron, T., Fauré, R., Jütten, P., Piechot, A., Brás, J. L. A., Fontes, C. M. G. A. and Faraco, V. (**2018**) 'Evolution of the feruloyl esterase MtFae1a from Myceliophthora thermophila towards improved catalysts for antioxidants synthesis', *Applied Microbiology and Biotechnology*, 102(12), pp. 5185–5196.

Villeneuve, P. (**2007**) 'Lipases in lipophilization reactions', *Biotechnology Advances*, 25(6), pp. 515–536.

Vosmann, K., Weitkamp, P. and Weber, N. (**2006**) 'Solvent-free Lipase-Catalyzed Preparation of Long-Chain Alkyl Phenylpropanoates and Phenylpropyl Alkanoates', *Journal of Agricultural and Food Chemistry*, 54(8), pp. 2969–2976.

Vosmann, K., Wiege, B., Weitkamp, P. and Weber, N. (**2008**) 'Preparation of lipophilic alkyl (hydroxy)benzoates by solvent-free lipase-catalyzed esterification and transesterification', *Applied Microbiology and Biotechnology*, 80(1), pp. 29–36.

Wang, Y., Zhang, D.-H., Chen, N. and Zhi, G.-Y. (**2015**)**a** 'Synthesis of benzyl cinnamate by enzymatic esterification of cinnamic acid', *Bioresource Technology*, 198, pp. 256–261.

Wang, Y., Zhang, D.-H., Zhang, J.-Y., Chen, N. and Zhi, G.-Y. (**2016**)**a** 'High-yield synthesis of bioactive ethyl cinnamate by enzymatic esterification of cinnamic acid', *Food Chemistry*, 190, pp. 629–633.

Wang, Z., Hwang, S. H. and Lim, S. S. (**2015**)**b** 'Lipophilization of phenolic acids with phytosterols by a chemoenzymatic method to improve their antioxidant activities: Lipophilization of phenolic acids with phytosterols', *European Journal of Lipid Science and Technology*, 117(7), pp. 1037–1048.

Wang, Z., Hwang, S. H. and Lim, S. S. (**2016**)**b** 'Effect of Novel Synthesised Policosanyl Phenolates on Lipid Oxidation', *Czech Journal of Food Sciences*, 34(No. 5), pp. 414–421.

Weetal, H. H. (**1985**) 'Enzymatic gallic acid esterification', *Biotechnology and Bioengineering*, 27(2), pp. 124–127.

Weetall, H. H. (**1985**) 'Enzymatic synthesis of gallic acid esters', *Applied Biochemistry and Biotechnology*, 11(1), pp. 25–28.

Weitkamp, P., Vosmann, K. and Weber, N. (**2006**) 'Highly Efficient Preparation of Lipophilic Hydroxycinnamates by Solvent-free Lipase-Catalyzed Transesterification', *Journal of Agricultural and Food Chemistry*, 54(19), pp. 7062–7068.

Yang, H., Mu, Y., Chen, H., Xiu, Z. and Yang, T. (**2013**) 'Enzymatic synthesis of feruloylated lysophospholipid in a selected organic solvent medium', *Food Chemistry*, 141(4), pp. 3317–3322.

Yang, R.-L., Li, N., Ye, M. and Zong, M.-H. (**2010**) 'Highly regioselective synthesis of novel aromatic esters of arbutin catalyzed by immobilized lipase from Penicillium expansum', *Journal of Molecular Catalysis B: Enzymatic*, 67(1–2), pp. 41–44.

Yang, Z., Glasius, M. and Xu, X. (**2012**)**a** 'Enzymatic Transesterification of Ethyl Ferulate with Fish Oil and Reaction Optimization by Response Surface Methodology', p. 10.

Yang, Z., Guo, Z. and Xu, X. (**2012**)**b** 'Enzymatic lipophilisation of phenolic acids through esterification with fatty alcohols in organic solvents', *Food Chemistry*, 132(3), pp. 1311–1315.

Yao, N. and Sun, S. (**2020**) 'Hydrophilic Glyceryl Ferulates Preparation Catalyzed by Free Lipase B from *Candida antartica*', *Journal of Oleo Science*, 69(1), pp. 43–53.

Yoshida, Y., Kimura, Y., Kadota, M., Tsuno, T. and Adachi, S. (**2006**) 'Continuous synthesis of alkyl ferulate by immobilized Candida antarctica lipase at high temperature', *Biotechnology Letters*, 28(18), pp. 1471–1474.

Yu, X., Li, Y. and Wu, D. (**2004**)**a** 'Enzymatic synthesis of gallic acid esters using microencapsulated tannase: effect of organic solvents and enzyme specificity', *Journal of Molecular Catalysis B: Enzymatic*, 30(2), pp. 69–73.

Yu, X., Li, Y. and Wu, D. (**2004**)**b** 'Microencapsulation of tannase by chitosan–alginate complex coacervate membrane: synthesis of antioxidant propyl gallate in biphasic media', *Journal of Chemical Technology & Biotechnology*, 79(5), pp. 475–479.

Yu, X.-W. and Li, Y.-Q. (**2006**) 'Kinetics and thermodynamics of synthesis of propyl gallate by mycelium-bound tannase from Aspergillus niger in organic solvent', *Journal of Molecular Catalysis B: Enzymatic*, 40(1–2), pp. 44–50.

Yu, X.-W. and Li, Y.-Q. (**2008**) 'Expression of Aspergillus oryzae Tannase in Pichia pastoris and Its Application in the Synthesis of Propyl Gallate in Organic Solvent', p. 6.

Zhang, S. and Akoh, C. C. (**2019**) 'Solvent-Free Enzymatic Synthesis of 1-*o*-Galloylglycerol Optimized by the Taguchi Method', *Journal of the American Oil Chemists' Society*, 96(8), pp. 877–889.

Zhang, S. and Akoh, C. C. (**2020**)**a** 'Antioxidant property and characterization data of 1-o-galloylglycerol synthesized via enzymatic glycerolysis', *Data in Brief*, 29, p. 105110.

Zhang, S. and Akoh, C. C. (**2020**)**b** 'Enzymatic synthesis of 1-o-galloylglycerol: Characterization and determination of its antioxidant properties', *Food Chemistry*, 305, p. 125479.

Zhang, S.-B., Pei, X.-Q. and Wu, Z.-L. (**2012**) 'Multiple amino acid substitutions significantly improve the thermostability of feruloyl esterase A from Aspergillus niger', *Bioresource Technology*, 117, pp. 140–147.

Zhao, Z. and Moghadasian, M. H. (**2008**) 'Chemistry, natural sources, dietary intake and pharmacokinetic properties of ferulic acid: A review', *Food Chemistry*, 109(4), pp. 691–702.

Zieniuk, B., Wołoszynowska, M., Białecka-Florjańczyk, E. and Fabiszewska, A. (**2020**) 'Synthesis of Industrially Useful Phenolic Compounds Esters by Means of Biocatalysts Obtained Along with Waste Fish Oil Utilization', p. 18.

Zoumpanioti, M., Merianou, E., Karandreas, T., Stamatis, H. and Xenakis, A. (**2010**) 'Esterification of phenolic acids catalyzed by lipases immobilized in organogels', *Biotechnology Letters*, 32(10), pp. 1457–1462.

Conclusion chapitre 1

La première partie de ce chapitre a introduit les notions clefs de cette thèse. Après une rapide introduction sur la synthèse de polyesters, il a été mis en avant que le PET, toujours majoritairement pétrosourcé aujourd'hui, est le polyester de référence de par ses excellentes propriétés mécaniques, thermiques et barrières. De leur côté, les polyesters issus de ressources renouvelables tels que le PLA, le PBS et les PHA ont été présentés comme des alternatives intéressantes et prometteuses. Cependant, ces polyesters sont aliphatiques et présentent donc des valeurs de module et des températures de transitions faibles en comparaison du PET. Une autre solution développée ces dernières années repose sur les polyesters partiellement biosourcés comme le bio-PET, le PBT et le PTT. Grâce à leur aromaticité, ceux-ci présentent des propriétés voisines ou identiques à celles du PET.

Dans ce contexte, les études récentes sur la synthèse de polymères aromatiques entièrement issus de ressources renouvelables sont présentées et discutées. Ces études reposent notamment sur l'utilisation de synthons tels que le FDCA ou encore de phénols naturels issus de biomasses lignocellulosiques. Ces polyesters aromatiques biosourcés partagent cependant comme point commun avec le PET le fait d'être généralement synthétisés à haute température à l'aide de catalyseurs métalliques potentiellement toxiques ou polluants.

La catalyse enzymatique a été présentée comme une alternative intéressante pour la synthèse de polyesters et notamment de polyesters biosourcés. La CALB est une enzyme qui, de par sa réactivité et sa stabilité, s'avère particulièrement adaptée à la synthèse de polyesters. L'utilisation de cette lipase a ainsi été largement décrite dans la littérature pour la synthèse de polyesters aliphatiques biosourcés. Toutefois, la synthèse de polyesters aromatiques catalysés par la CALB n'a été que très peu étudiée et ne concerne qu'un nombre restreint d'études récentes. Des matériaux présentant des températures de transitions relativement élevées peuvent ainsi être obtenus à partir de monomères aromatiques. Les masses molaires de ces polyesters ont cependant systématiquement été limitées à des valeurs faibles et bien inférieures à celles des polymères aliphatiques obtenus par synthèse enzymatique.

De nombreux dérivés phénoliques naturels pourraient être de bons candidats pour la synthèse enzymatique de polyesters aromatiques. Le chapitre s'est donc poursuivi par une étude bibliographique portant plus spécifiquement sur la réactivité en estérification et transestérification enzymatique des dérivés phénoliques biosourcés. Il ressort notamment de cet état de l'art que la réactivité très variable, et parfois limitée, de ces synthons peut être attribuée à des effets stériques et électroniques propres au substrat et à l'enzyme utilisée. De nombreuses enzymes et conditions réactionnelles différentes ont ainsi été étudiées. Parmi ces études, la CALB s'est encore une fois démarquée par sa réactivité ainsi que sa résistance et stabilité dans différents milieux (apolaires, polaire, liquides ioniques …).

La première partie de ce travail de thèse, présentée au chapitre suivant, s'intéressera donc dans un premier temps à la synthèse de polyesters catalysée par la CALB à partir d'un composé furanique, le

DMFDC, un diester dérivé du FDCA, un synthon biosourcé déjà largement étudié pour la synthèse de polyesters aromatiques. Cette première partie de l'étude vise à mieux comprendre l'origine des faibles masses molaires généralement obtenues pour les polyesters aromatiques en catalyse enzymatique afin de trouver une solution pour contourner cette limitation. La suite de nos investigations, présentée dans les chapitres ultérieurs, portera sur l'étude d'autres synthons aromatiques biosourcés, notamment les composés phénoliques que sont les dérivés des acides féruliques et caféiques.

Chapitre 2. Synthèse de polyesters aromatiques à base de furane par catalyse enzymatique.

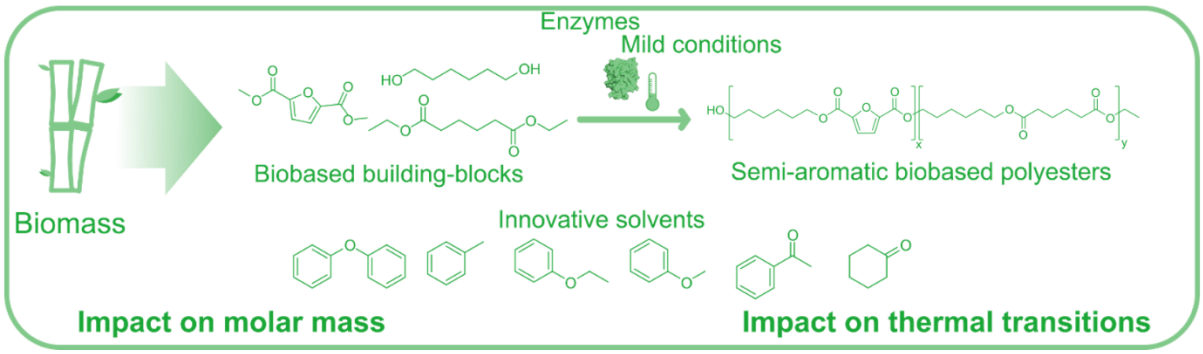

Introduction chapitre 2

Comme nous l'avons mentionné dans l'Introduction et au chapitre précédent, la synthèse de polyesters biosourcés est un levier important dans la transition vers une production de matériaux polymères plus durable et plus respectueuse de l'environnement. Dans ce contexte, la catalyse enzymatique et notamment l'utilisation de lipases telles que la CALB constitue une voie de synthèse plus douce et durable que les méthodes reposant sur la catalyse organométallique classiquement employées.

Il existe une très grande variété de composés issus de la biomasse permettant la synthèse de polyesters. La polymérisation catalysée par la CALB d'un grand nombre de ces synthons a déjà été étudiée dans la littérature. Les monomères les plus couramment étudiés et qui ont montré une bonne compatibilité vis-à-vis de la polymérisation enzymatique sont essentiellement des substrats aliphatiques tels que le 1,6-hexanediol ou l'acide adipique. La polymérisation enzymatique de ces composés mène cependant à des polyesters aliphatiques aux propriétés mécaniques et thermiques plus faibles que celles du PET, qui bien qu'étant aromatique et pétrosourcé reste le polyester le plus courant et donc la référence pour ce type de polymères.

Afin de remédier à cette problématique, l'intérêt s'est naturellement porté vers la polymérisation de molécules plateforme aromatiques par catalyse enzymatique. Ces molécules aromatiques, plus volumineuses et fortement insaturées, sont cependant très différentes des substrats naturels de la CALB que sont les triglycérides. De ce fait, la structure de ces synthons aromatiques peut avoir une influence non négligeable sur l'activité catalytique de l'enzyme. Le FDCA est un substrat aromatique biosourcé qui se démarque par sa disponibilité et ses propriétés proches de l'acide téréphtalique. Son utilisation en polymérisation enzymatique a déjà été rapportée dans la littérature mais elle conduit cependant à des polyesters de faibles masses molaires présentant donc des propriétés thermiques et mécaniques limitées. Ainsi, une meilleure compréhension et une amélioration de la réactivité du FDCA ou de ses dérivés vis-à-vis de CALB s'avèrent aujourd'hui nécessaires.

Le chapitre 2 de ce manuscrit repose donc sur un article intitulé 'Lipase-catalyzed synthesis of furan-based aliphatic-aromatic biobased copolyesters: Impact of the solvent' publié dans *European Polymer Journal*. Celui-ci porte notamment sur l'étude de l'influence de différents solvants de réaction pour la copolymérisation enzymatique du DMFDC, un dérivé du FDCA, avec le 1,6-HDO ou le 1,4-BDO comme diol. Le diéthyle adipate a également été utilisé et ajouté comme co-diester afin d'étudier en détail l'impact de la proportion de monomères aromatiques sur l'activité de la CALB et sur la structure et les propriétés des polymères ainsi formés.

Chapitre 2 Lipase-catalyzed synthesis of furan-based aliphatic-aromatic biobased copolyesters: Impact of the solvent

*Alfred Bazin, Luc Avérous, Eric Pollet**

*Publié par European polymer journal (**2021**, volume 159, p. 110717).*

1. Abstract

Enzymatic polymerization is a promising route for a greener synthesis of biobased polyesters. However, this approach is still often limited to aliphatic polyesters, which present limited properties such as low thermal resistance. In this context and till now, introduction of aromatic monomers into polyesters very often resulted in low molar mass chains. Herein, aliphatic-aromatic copolyesters based on dimethyl-2,5-furandicarboxylate were enzymatically synthesized using immobilized *Candida antarctica* lipase B with a particular focus on the influence of the solvent used. Two series of poly(hexylene adipate)-co-(hexylene furanoate) and poly(butylene adipate)-co-(butylene furanoate) copolyesters were successfully synthesized in diphenyl ether, displaying high molar masses (M_n up to 19 000 $g.mol^{-1}$) for aromatic monomer contents up to 70 and 50%, respectively. High aromatic content resulted in reduced molar masses due to a loss of solubility of the growing aromatic chains. Replacing diphenyl ether by acetophenone, which had never been used before as solvent for enzymatic synthesis of polyesters, led to significantly enhanced solubility and thus an increase in the average molar masses of poly(hexylene furanoate) and poly(butylene furanoate). The resulting polyesters showed greater thermal stability and higher T_g, offering new perspectives for expanding the potential applications of such enzymatically-produced biobased aromatic copolyesters.

2. Introduction

Due to the current environmental context and the global perspectives, polymer science research is now increasingly oriented towards higher sustainability, notably by following the principles of green chemistry. Thus, the synthesis of bio-based polyesters has aroused strong interest in recent decades (Vilela *et al.*, 2014; Rebouillat *et al.*, 2016; Zia *et al.*, 2016), to replace fossil-based polyesters and to develop new macromolecular architectures. Numerous compounds produced from biomass, such as building blocks or monomers, have been used for the elaboration of these polyesters (Becker *et al.*, 2015; Kristufek *et al.*, 2017). For example, the conversion of biobased succinic and adipic acids with butane- and propanediol into polymeric material has been studied (Debuissy *et al.*, 2017c, 2017d). It is thus possible to obtain a wide range of aliphatic copolyesters but their behaviors, such as thermal and mechanical properties, are often limited. As an example, biobased poly(butylene succinate) presents a glass transition temperature (T_g) of -37°C and a Young's modulus of approximately 368 MPa (Jin *et*

al.). These values are far below the most common fossil-based polyester, namely polyethylene terephthalate (PET) with a T_g of 76°C (Nguyen *et al.*, 2018) and Young's modulus above 2 600 MPa (Bedoui *et al.*, 2006). In order to improve these properties, aromatic and semi-aromatic bio-based polyesters are now gaining a lot of attention since the aromaticity brings higher thermal resistance and rigidity linked to higher transition temperatures. Several sources of aromatic building blocks have been considered. As an example, lignocellulosic biomass is an important source of aromatic building blocks such as vanillic and ferulic acids (Llevot *et al.*, 2016; Nguyen *et al.*, 2018). For instance, derivatives of ferulic acid have been copolymerized to produce high thermal transition polyesters with T_g ranging from 32 to 113 °C (Figure 2.1, a) (Nguyen *et al.*, 2015). Recently, vanillic-based polyesters have been studied and showed thermal transitions comparable to PET with a T_g up to 77°C (Figure 2.1, b) (Xanthopoulou *et al.*, 2021).

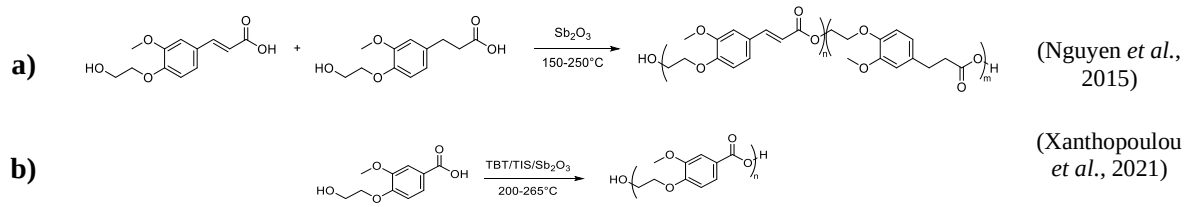

Figure 2.1: Examples of polyesters synthesis from biobased aromatic building blocks.

Among the aromatic monomers or building blocks that are attracting a lot of interest today, furan derivatives occupy an important place (Poulopoulou *et al.*, 2019). These compounds, often synthesized from fructose, can be used in various polymeric materials such as polyamides, polyethers or polyesters (Sousa *et al.*, 2015). For instance, polyesters based on furan derivatives such as dimethyl 2,5-furandicarboxylate (DMFDC) have been extensively studied (Papageorgiou *et al.*, 2016; Terzopoulou *et al.*, 2020). The aim of these studies is often to develop biobased polymers that mimic the structures and the properties of PET. Recently, it has been shown that furan-based polyesters, such as polyethylene furanoate (PEF), have properties comparable or even higher than those of PET and therefore represent a very promising alternative (Gandini *et al.*, 2009; Loos *et al.*, 2020). It was also claimed that PEF presented good enzymatic degradability (Weinberger *et al.*, 2017). However, the synthesis of such polyesters requires high temperatures as well as potentially toxic metal-based catalysts (Nguyen *et al.*, 2015; Terzopoulou *et al.*, 2017; Xanthopoulou *et al.*, 2021) (such as antimony (*Diantimony trioxide*, 2021) and tin oxides (*Dibutyltin oxide*, 2021)), which are not in line with a green chemistry approach.

In order to address these problems, enzyme-catalyzed synthesis of polyesters represents a very promising alternative and has been largely investigated (Douka *et al.*, 2018; Kobayashi *et al.*, 2019; Pellis *et al.*, 2016a; Jiang *et al.*, 2016). Enzymatic polymerization was also studied by our group to develop biobased aliphatic polyesters (Debuissy *et al.*, 2017b, 2017a). Enzymes are environmentally friendly and non-toxic catalysts that have demonstrated their efficiency in a large number of reactions and that can be immobilized on solid supports to improve their stability and to be reused (Poojari *et al.*,

2013; Öztürk *et al.*, 2016). The most commonly used enzymes for polyester synthesis are the esterases, such as the immobilized form of *Candida antarctica* Lipase B (CALB) (Ortiz *et al.*, 2019). Immobilization of the enzyme allows greater stability and reusability (Mateo *et al.*, 2007). CALB-catalyzed polymerization can be performed in solution or in bulk (Douka *et al.*, 2018). Bulk polymerization is more relevant for industrial large scale processes but high viscosity and infusibility issues linked to the mild temperatures imposed by enzymatic catalysis severely limit this route.

Enzymatic syntheses of furan-based oligomers or polyesters catalyzed by CALB have already been performed but always resulted in polymers with lower molar masses than their aliphatic counterparts (Jiang *et al.*, 2015; Morales-Huerta *et al.*, 2018; Flores *et al.*, 2019; Comerford *et al.*, 2020). In this case, the impact of the structure and aromaticity of the monomers on the activity of CALB is not well understood, till now.

Thus, this study aimed at investigating the (bio)synthesis of biobased aromatic copolyesters by enzymatic catalysis. The influence of furan-based aromatic monomers on the activity of CALB in the synthesis of several semi-aromatic copolyesters has been particularly examined. The reactivity of DMFDC combined with diethyl adipate (DEA), 1,6-hexanediol (HDO) and 1,4-butanediol (BDO) in different ratio was assessed (Figure 2.2). These esters were chosen to allow easier comparison with results from the literature (Jiang *et al.*, 2015; Debuissy *et al.*, 2017b; Flores *et al.*, 2019). For that, the polymerization kinetics as well as the molar masses, compositions and chemical architectures of the synthesized copolyesters were determined by SEC and NMR analyses. Different solvents were screened in order to enhance the enzymatic synthesis of poly(hexylene furanoate) (PHF) and poly(butylene furanoate) (PBF). Finally, the influence of the aromatic monomer content on the thermal properties of the synthesized copolyesters was particularly studied and discussed.

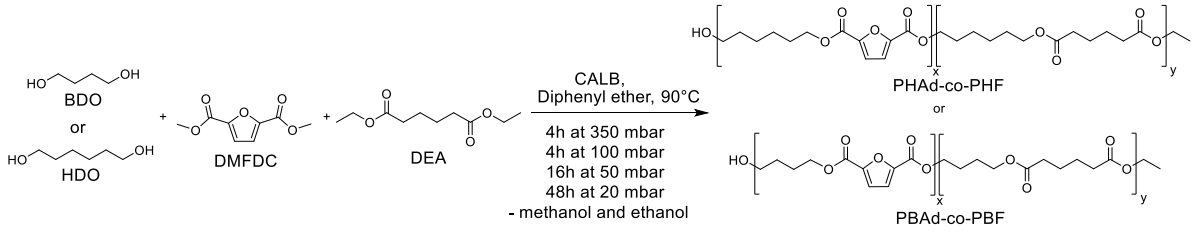

Figure 2.2: CALB-catalyzed synthesis of poly(hexylene adipate)-co-(hexylene furanoate) and poly(butylene adipate)-co-(butylene furanoate)

3. Experimental part

3.1. Materials

DEA (99% purity), and diphenyl ether were supplied by Acros Organics. HDO (97% purity), Lipase from *Candida antarctica* immobilized on acrylic resin (activity >5,000 U/g) (CALB) and deuterated chloroform ($CDCl_3$) were purchased from Sigma-Aldrich. BDO (99% purity) was supplied by Alfa Aesar. Methanol was supplied by Fisher scientific. DMFDC (97% purity) was supplied by

Fluorochem. Chloroform was purchased from Carlo Erba. CALB was dried at 25° C for 24 h under vacuum before use. All other reactants were used without further purification. All solvents used for the analytical methods were of analytical grade.

3.2. Synthesis of the aliphatic-aromatic copolyesters

Two series of copolyesters were synthesized, one for each diol, with different ratios in the furan-based aromatic monomer. Both the Poly(hexylene adipate-co-furanoate) (PHAd-co-PHF) and Poly(butylene adipate-co-furanoate) (PBAd-co-PBF) series were synthesized using an equimolar proportion of ester and alcohol groups.

For that, the diol (HDO or BDO) was added to a mixture of DMFDC and DEA in various ratio (given in Table 2.1 and Table 2.2, respectively) in a 10 mL Schlenk reactor. Then, 2 ml of dry diphenyl ether (150 wt.% in comparison to the total mass of monomers) and 144 mg of pre-dried CALB (10 wt.% in comparison to the total mass of monomers) were added.

The solution was magnetically stirred and heated at 90° C under partial vacuum. The pressure was set to 350 mbar and was then decreased to 100, 50 and 20 mbar after 4, 8 and 24 hours of reaction, respectively.

After 72h, or at precipitation of the sample, the reaction was quenched by adding 5 ml of chloroform. The mixture was filtered to remove the CALB and the excess of chloroform in the filtrate was eliminated by rotary evaporator. The obtained polyester was precipitated in a large volume of ice-cold methanol and centrifuged at 8 000 g for 1 minute. The supernatant was eliminated. Finally, the polymer was dried in a vacuum oven at 40°C for 24h before analysis.

Poly(hexylene adipate-co-furanoate) (PHAd-co-PHF): ^{1}H NMR ($CDCl_3$, 400 MHz): δ_H 1.25 ppm (3H, -O-CH_2-C**H**$_3$ of the terminal esters of DEA), 1.33-1.53 ppm (2H, -C**H**$_2$-CH_2-CH_2-O of the HDO units), 1.54-1.87 ppm (C**H**$_2$-CH_2-O of the HDO units superimposed with signals of C**H**$_2$-CH_2-COO of the DEA units), 2.32 ppm (2H, C**H**$_2$-COO of the DEA groups), 3.63-3.67 ppm (2H, C**H**$_2$-OH of the end BDO groups), 3.87-3.95 ppm (3H, O-C**H**$_3$ of the furan terminal ester), 4.00-4.38 ppm (C**H**$_2$-O of the HDO core units superimposed with signals of O-C**H**$_2$-CH_3 of the DEA terminal units), δ = 7.19 ppm (2H, C**H**-C**H** of the aromatic furan units).

Poly(butylene adipate-co-furanoate) (PBAd-co-PBF): ^{1}H NMR ($CDCl_3$, 400 MHz): δ_H 1.25 ppm (3H, -O-CH_2-C**H**$_3$ of the terminal esters of DEA), 1.59-1.91 ppm (C**H**$_2$-CH_2-O of the BDO units superimposed with signals of C**H**$_2$-CH_2-COO of the DEA units), 2.32 ppm (2H, C**H**$_2$-COO of the DEA groups), 3.67-3.71 ppm (2H, C**H**$_2$-OH of the end BDO groups), 3.87-3.95 ppm (3H, O-C**H**$_3$ of the furan terminal ester), 4.00-4.38 ppm (C**H**$_2$-O of the BDO core units superimposed with signals of O-C**H**$_2$-CH_3 of the DEA terminal units), δ = 7.20 ppm (2H, C**H**-C**H** of the aromatic furan units).

3.3. Influence of the solvent on the synthesis of PHF and PBF

For the synthesis of PHF and PBF in different solvents, the previous protocol was slightly modified. The proportions of diol and DMFDC were kept constant while the solvent and CALB were doubled in order to avoid early polymer precipitation. The solution was magnetically stirred and heated at 90° C. The pressure was reduced, when possible, depending on the solvent, to values indicated in Table 2.3. After 72h, or at precipitation of the sample, the reaction was quenched by adding 5 ml of chloroform. The polymer was then precipitated and recovered with the same method afore described.

3.4. Kinetics monitoring

The enzymatic polymerizations were monitored by NMR spectroscopy. Aliquots of solution were withdrawn at 24, 48 and 72h from the medium. These samples were dissolved in chloroform and filtered. They were then precipitated in a large volume of ice-cold methanol. The solution was centrifuged at 8 000 g for 1 minute, the supernatant was discarded, and the polyester was dried in a vacuum oven at 40°C for 24h before analysis.

3.5. Enzymatic activity assay

Samples of 14 mg of CALB beads were added into 5 mL vials. Before the vial sealing, 200 µl of 1-butanol, 69 µl of diethyl adipate and 380 µl of the desired solvent were added. The solution was placed at 50°C under mild magnetic agitation (100 rpm) to avoid deterioration of the fragile catalyst support. Aliquots of 10 µl were withdrawn at different times and rapidly analyzed by NMR spectroscopy to quantify the transesterification activity. In order to assess the leaching of the enzyme, samples of CALB were incubated at 90°C for 24h in 380 µl of a given solvent. At the end of the incubation, the solvent was carefully pipetted out of the vial. 5 mL vials were filled with the solvent of incubation, 200 µl of 1-butanol and 69 µl of diethyl adipate. The vials were placed at 50°C and aliquots were withdrawn at given times and analyzed by NMR spectroscopy.

3.6. Characterizations

^{1}H NMR spectra were obtained on a Bruker 400 MHz spectrometer. 2D and ^{13}C NMR spectra were obtained on a Bruker 500 MHz spectrometer. $CDCl_3$ was used as a solvent. For the polymers hardly soluble in $CDCl_3$, few microliters of trifluoroacetic acid (TFA) were added to achieve proper dissolution. Calibration of the spectra was performed using the $CDCl_3$ peak (δH = 7.26 ppm, δC = 77.16 ppm).

Size Exclusion Chromatography (SEC) was used to estimate the number average molar mass (M_n), weight average molar mass (M_w) and dispersity (Đ). The analyses were performed on a Shimadzu liquid chromatograph in chloroform at a flow rate of 0.8 mL/min. The apparatus was equipped with a PLGel Mixed-C and PLGeL 100 Å columns. A calibration curve using polystyrene (PS) standards was built for molar mass determination.

Differential scanning calorimetry (DSC) analyses have been performed on the samples to estimate their glass transition temperature (T_g), melting temperature (T_m), and crystallization

temperature (T_c), if applicable. The analyses were performed using a Q2000 DSC apparatus from TA instrument (TA instrument, New Castle, Delaware, USA). Typically, a 1 mg sample in sealed aluminum pan was fast heated to 170°C. The sample was kept 5 minutes at such high temperature to erase all thermal history. The sample was then cooled a 5°C/min to -80°C followed by an isotherm of 5 minutes. Finally, a second heating was performed at 10°C/min to 170°C. Modulated DSC (MDSC) was also performed. For that, the samples were heated 10°C above T_m, then rapidly quenched in liquid nitrogen. Samples were then analyzed by MDSC at a rate of 2°C/min, an amplitude of ± 1.2°C and a frequency of 60s.

Thermogravimetric analysis (TGA) was performed to determine the polymers thermal stability. The measurements were conducted on a High-Res TGA Q5000 from TA instrument. Samples between 1 and 2 mg were heated at 10°C/min from room temperature to 600°C under air.

Mass measurements were carried out on an AutoflexTM MALDI-TOF mass spectrometer (Bruker Daltonics GmbH, Bremen, Germany) used at a maximum accelerating potential of 20 kV in positive mode and operated in linear mode. The delay extraction was fixed at 560 ns and the frequency of the laser (nitrogen 337 nm) was set at 5 Hz. The acquisition mass range was set to 1500-10000 m/z with a matrix suppression deflection (cut off) set to 1500 m/z. The equipment was calibrated with ACTH 1-17 ($[M+H]^+$ 2094.42), insulin ($[M+H]^+$ 5732.52), ubiquitin I ($[M+H]^+$ 8565.76) and myoglobin ($[M+H]^+$ 16952.31). Spectra were processed with flexAnalysis software (Bruker Daltonics). Sample preparation was performed with the dried droplet method using a mixture of 0.5 µl of sample with 0.5 µl of matrix solution dried at room temperature. The 2-[(2E)-3-(4-tert-butylphenyl)-2-methylprop-2-enylidene]malononitrile (DCTB) matrix was prepared at 20 mg/ml in dichloromethane.

4. Results and discussions

4.1. Polyesters synthesis

Semi-aromatic furan-based polyesters of different composition were synthesized by enzymatic polymerization. A first series of experiments was conducted by reacting HDO with different ratios of DMFDC and DEA.

The chemical structure of each polymer has been determined by ^{1}H NMR spectroscopy. The spectra of the obtained polyesters are shown in Figure 2.3, and also Figure S2.1 to Figure S2.7 in Annexes. The structure and the attribution of the peaks were confirmed by COSY, HMBC and HSQC 2D NMR spectroscopy (Figure S2.8 to Figure S2.10 in Annexes).

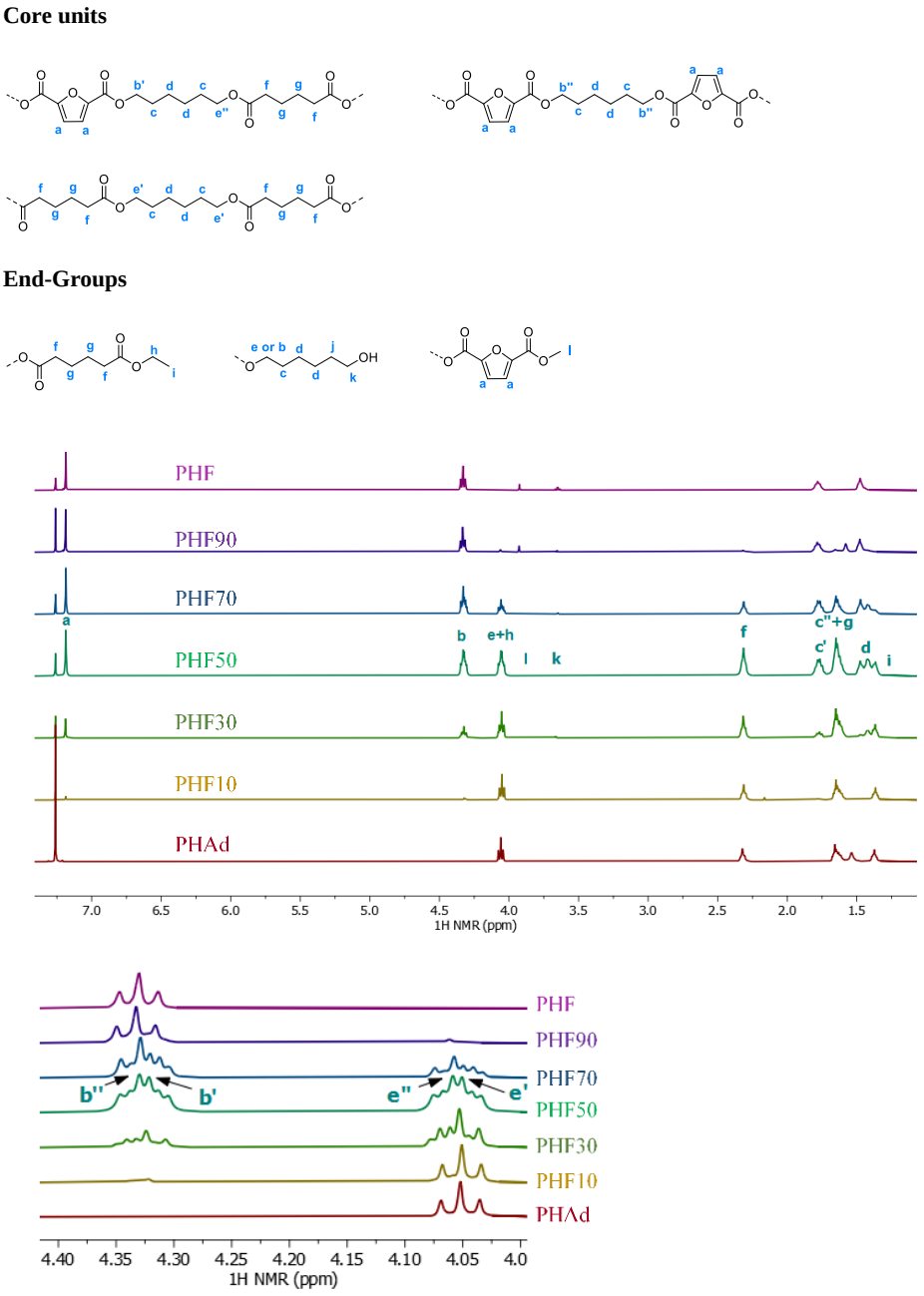

Figure 2.3: ^{1}H NMR spectra of the enzymatically synthesized PHAd-co-PHF with various ratio of furan (from 0% (PHAd), to 100 % (PHF) in $CDCl_3$.

The signals of the protons of the (C**H**$_2$-O) at the end of the diol units included in the polymeric chain are shifted differently depending on the nature of the esters surrounding them. This phenomenon has already been observed by Wu *et al.* (Wu *et al.*, 2014) with BDO. In our case, the protons (C**H**$_2$-O) of the diol surrounded by two adipate units form the less shifted triplet (4.05 ppm, e'). Then the (C**H**$_2$-O) protons of the diol next to an adipate unit when this diol is surrounded by both an adipate and a furan unit are shifted to 4.06 ppm (e''). The (C**H**$_2$-O) protons of the diol also between an adipate and a furan group but linked to a furan unit are shifted to 4.32 ppm (b'). Finally, the more shifted (C**H**$_2$-O) protons are the ones of the diol surrounded by two furan units at 4.33 ppm (b'').

These attributions allow to formulate several assumptions about the structure of the copolymers. First, the M_n of the polyesters can be estimated thanks to the intensities of the signals corresponding to the end-groups compared to the ones of the core-units. Eq. 1 is inspired by the method given by Izunobi *et al.* (Izunobi *et al.*, 2011). It is comparable to the equation given by Jiang *et al.* (Jiang *et al.*, 2015) but also takes into account the adipic units as well as the ends group as part of the polymeric chain as did Debuissy *et al.* (Debuissy *et al.*, 2017b). It is a quick method to compare polyesters chain-lengths with each other, but long polymeric chains show low intensity (I) end-groups signals, which consequently decrease the accuracy of the calculated molar masses (Eq. 1).

$$Mn_{NMR} = \frac{\left(\frac{(I_b + I_e) - I_k - \frac{2 * I_i}{3}}{4}\right) * 116.16 + \frac{I_f}{4} * 112.13 + \frac{I_k}{2} * 117.17 + \frac{I_i}{3} * 45.06 + \frac{I_l}{3} * 31.03 + \frac{I_a}{2} * 122.08}{\frac{1}{2} * (\frac{I_i}{3} + \frac{I_k}{2} + \frac{I_l}{3})} \quad (1)$$

Also, characteristics signals corresponding to each monomeric unit are present and confirm the synthesis of semi-aromatic polyesters. Characteristic signals of the furan and adipate moieties, the two diesters employed, can be distinguished at 7.15 and 2.32 ppm, respectively. It is clearly noticeable that the furan's signal intensity is lower when the amount of DMFDC in the feed is low and that the signal corresponding to the adipate moieties is inversely affected. The ratio of each diester inserted in the polymeric chain can therefore be estimated by calculating the intensity ratio between the furan and adipate signals (Eq. 2).

$$\%\ of\ furan\ moeties\ in\ the\ chain = \frac{I_a}{I_a + \frac{I_f}{2}} \quad (2)$$

Table 2.1 gives the M_n values determined from NMR spectra compared to M_n, M_w and Đ obtained from SEC analyses (Figure S2.18 and Table S2.1 in Annexes) of the synthesized polyesters.

Table 2.1: Compositions and molar masses values of the PHAd-co-PHF, as determined by NMR spectroscopy and SEC.

Sample name	Ratio of DMFDC (%)	Ratio of DEA (%)	Yield (%) [a]	NMR		SEC		
				Measured ratio of aromatic moieties (%)	M_n (g.mol^{-1})	M_n (g.mol^{-1})	M_w (g.mol^{-1})	Đ
PHAd	0	100	98	--	6 300	19 000	33 500	1.76
PHF10	10	90	98	9.1	5 300	18 600	28 500	1.53
PHF30	30	70	97	31.4	5 400	18 300	38 800	2.11
PHF50	50	50	97	47.8	6 100	18 000	29 800	1.65
PHF70	70	30	97	65.6	6 600	19 400	34 400	1.77
PHF90	90	10	91	88.5	2 500	6 100	8 700	1.42
PHF	100	0	89	--	2 100	4 100	5 200	1.29

a Calculated from NMR spectra data.

The obtained PHAd and PHF have $M_{n(NMR)}$ of 6 300 and 2 100 g.mol^{-1}, respectively. These values are rather low but they are in accordance with those reported in the literature. For instance, Nasr *et al.* (Nasr *et al.*, 2020) obtained, after an extensive optimization of the reaction parameters, PHAd with an average molar mass (M_n determined by SEC) of 18 500 g.mol^{-1} in 48h. Concerning PHF, with a protocol similar to ours but at a temperature of 95°C, Jiang *et al.* (Jiang *et al.*, 2015) obtained $M_{n(NMR)}$ of 3 500 g.mol^{-1}. The values determined by NMR spectroscopy and SEC are different since SEC values are given as polystyrene-equivalent molar masses (polystyrene standards were used for the calibration) which are thus overestimated compared to the true molar masses. One can also note that in all the cases, the molar masses of PHAd and PHF obtained by CALB-catalyzed polymerization are very different. However, increasing the amount of aromatic moieties surprisingly did not induce a linear decrease in the molar mass of the obtained copolyesters. Indeed, polyesters with a ratio of aromatic diester up to 70% have an identical average molar mass. Dispersity (Đ) values are quite high (from 1.5 to 2.1) but consistent with the transesterification activity of the lipase. The slightly lower molar mass calculated from NMR analyses for the PHAd-co-PHF containing 10 and 30% of DMFDC could be explained by remaining traces of unreacted HDO in the final polymer. This increases the intensity of end groups in comparison to the core units, thus lowering the calculated molar mass. Indeed, these copolyesters being highly amorphous it was difficult to eliminate all traces of residual oligomers.

The progress of the reaction has been monitored by NMR spectroscopy. Thanks to Eq. 1, the molar masses of the copolyesters could be calculated and plotted versus the reaction time (Figure 2.4).

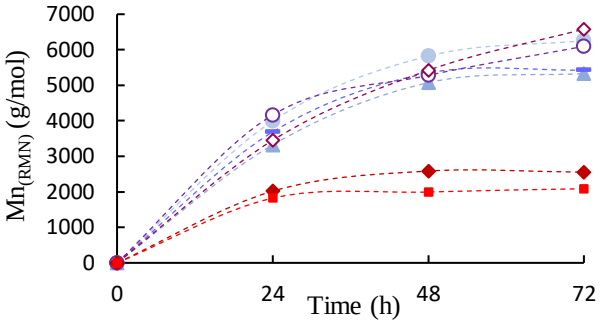

Figure 2.4: Time evolution of the M_n values determined by NMR spectroscopy of the PHAd-co-PHF. ● PHAd, ▲ 10% of DMFDC, ▬ 30% of DMFDC, ○ 50% of DMFDC, ◊ 70% of DMFDC, ♦ 90% of DMFDC, ■ PHF

When the aromatic diester (DMFDC) content is lower than 70%, the kinetics of the enzymatic polymerization is not affected. However, the polyesters containing 90 % of aromatic diesters and the PHF both precipitated before 24 h of reaction, which could explain the constant and low molar mass obtained after 24 h of reaction. The solubility of the polymer in the medium would therefore be a critical parameter influencing its final molar mass. In order to confirm these results, a similar study has been conducted replacing HDO by a shorter diol, BDO. If the precipitation of the polymer in the medium is the key parameter, a shorter diol should amplify the phenomenon at stake by inducing higher rigidity of the polymer chain backbone and thus lower solubility. The molar mass of the polymers synthesized with BDO evaluated by SEC and NMR spectroscopy are shown in Table 2.2 and Figure 2.5. The NMR spectra of the resulting polymers are given in Annexes Figure S2.11 to Figure S2.17 while the SEC traces and results are given in Annexes Figure S2.19 and Table S2.2 The average molar masses were evaluated by NMR spectroscopy using an equation similar to equation 1 but using the molar mass of the corresponding constituting moieties as coefficients.

Table 2.2: Compositions and molar masses values of the PBAd-co-PBF as determined by NMR spectroscopy and SEC

Sample name	Ratio of DMFDC (%)	Ratio of DEA (%)	Yield (%) [a]	NMR		SEC		
				Measured ratio of aromatic moieties (%)	M_n (g.mol^{-1})	M_n (g.mol^{-1})	M_w (g.mol^{-1})	Đ
PBAd	0	100	98	--	5 100	16 600	34 700	2.08
PBF10	10	90	98	9.1	4 700	16 800	33 100	1.96
PBF30	30	70	97	30.2	4 500	11 100	19 500	1.73
PBF50	50	50	97	48.3	4 300	10 200	17 500	1.71
PBF70	70	30	94	68.3	2 800	6 200	10 400	1.68
PBF90	90	10	88	85.5	1 500	2 800	4 300	1.50
PBF	100	0	85	--	1 400	2 000	2400	1.20

[a] Calculated from NMR spectra data.

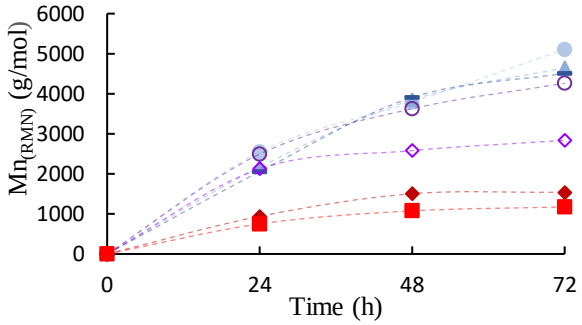

Figure 2.5: Time evolution of the M_n values determined by NMR spectroscopy of the PBAd-co-PBF. ● PBAd, ▲ 10% of DMFDC, ▬ 30% of DMFDC, ○ 50% of DMFDC, ◊ 70% of DMFDC, ♦ 90% of DMFDC, ■ PBF

PBAd and PBF with $M_{n(NMR)}$ of respectively 5 100 and 1 200 g.mol^{-1} were synthesized. Again, these results are comparable with values reported in the literature. Pellis *et al.* (Pellis *et al.*, 2018) obtained, with both enzymatic synthesis and a thermal post processing, PBF with M_n of approximatively 1 000 g.mol^{-1}. While Jiang *et al.* obtained PBF with a $M_{n(NMR)}$ of 1 500 g.mol^{-1} (Jiang *et al.*, 2015). In a previous study, our group obtained PBAd with a comparable $M_{n(NMR)}$ of 5 600 g.mol^{-1} (Debuissy *et al.*, 2017b). Here again, the difference between M_n values determined from NMR analyses and by SEC comes from the fact that the latter are given as polystyrene-equivalent. In comparison with the aforementioned results, the average molar mass of the synthesized PBAd is significantly lower than PHAd. This phenomenon was described in several previous studies (Mahapatro *et al.*, 2003; Cruz-Izquierdo *et al.*, 2015; Jiang *et al.*, 2015; Debuissy *et al.*, 2017b; Pellis *et al.*, 2018). In connection with its natural hydrolytic activity, CALB has a better affinity for longer monomers, especially C6 monomers, resulting in higher molar masses for the obtained polymers. Therefore, the decrease of average molar mass between PHAd and PBAd is effective and not only due to the different molar mass of the diol. Indeed, from the NMR analysis, the DPn values of PHAd and PHF (27 and 8, respectively) are also higher than those of PBAd and PBF (25 and 5, respectively).

PBAd-co-PBF copolyesters with a ratio up to 50% of DMFDC could be obtained with high molar masses. However, a slight decrease in the average molar mass with the DMFDC content is noticeable. Dispersity values around 2 are obtained which is in agreement with the literature and the transesterification activity of the enzyme (Mahapatro *et al.*, 2003; Debuissy *et al.*, 2017b). The molar mass distribution observed on SEC elution profiles (Annexes Figure S2.19) revealed shouldered peaks for PBAd-co-PBF containing between 10 and 50% DMFDC. This could indicate a bimodal distribution and therefore the presence of less reactive growing chains during the polymerization, resulting from a high aromatic content. The PBAd-co-PBF containing 70% of DMFDC precipitated in the medium after 30 hours of reaction resulting in low molar mass polymers. The copolyester containing 90% of DMFDC and the PBF also precipitated, and it occurred even earlier, after approximatively 8 hours. Therefore, reducing the diol length leads to the precipitation of the polymer in the medium for a lower ratio in

aromatic diester. It also seems to reduce the reactivity of CALB towards highly aromatic polymeric chains.

The ratio of aromatic moieties in the polyesters depending on time could be calculated thanks to Eq. 2. These results for PHAd-co-PHF and PBAd-co-PBF, respectively plotted in Figure 2.6 and Figure 2.7, show similar behavior. The ratio of aromatic moieties inserted in the polymer remains equal to the feed ratio in DMFDC all along the reaction, indicating no specific preference of the enzyme toward one or another diester.

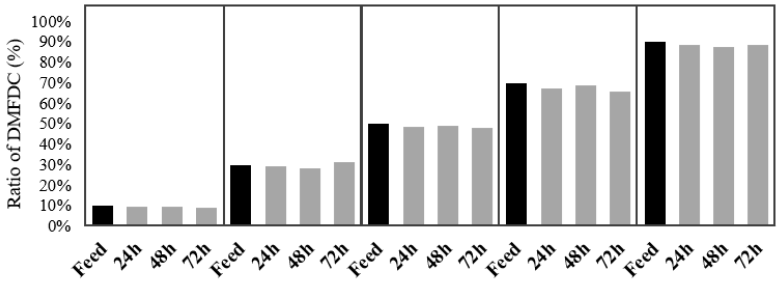

Figure 2.6: Determined ratios of aromatic moieties in the PHAd-co-PHF depending on time for different ratio of DMFDC

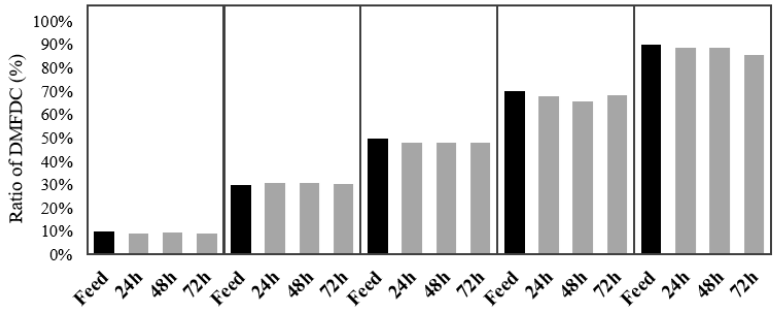

Figure 2.7: Determined ratios of aromatic moieties in the PBAd-co-PBF depending on time for different ratio of DMFDC

These results led us to consider that the activity of the enzyme was only slightly impacted by the amount of aromatic diesters in the medium but that the solubility of the synthesized polymer chains in the medium was the main parameter responsible for the low molar masses obtained. Maniar *et al.* (Maniar *et al.*, 2019) reported that for the CALB-catalyzed synthesis of polyester an increase in aromaticity leads to a decrease in DPn. This behavior was attributed to side reactions with the aromatic diol and to potential substrate specificity of the enzyme with intermediate structures inhibiting the polymerization. In our study, we observed that the copolyesters with a high content in aromatic monomer display a chain growth with a kinetics that does not depend on the aromatic content until they are no longer soluble in the reaction medium. At this point, the polymer precipitates and is no longer available for the enzyme, completely stopping the chain growth (see Figure S2.44 in Annexes). Low molar masses polymers have a direct impact on the thermal properties of the corresponding material. It

particularly leads to low T_g when the main goal of introducing aromatic moieties, when producing furan-based polymers, is to obtain high T_g materials.

In order to facilitate the solubility of the copolyester in the medium and thus avoid precipitation, different options can be considered. First, the temperature of reaction could be raised. Indeed, it has been shown that CALB can be used at temperatures higher than 90°C, without denaturation (Poojari *et al.*, 2013; Jiang *et al.*, 2015; Frampton *et al.*, 2013; Lozano *et al.*, 2003). However, such high temperatures increase the risk of denaturation with a rapid loss of activity of the enzyme. Besides, higher temperature conditions are against the main advantage of using enzymes, which allow polymerization under mild conditions. The second option is to find the appropriate solvent which is (i) able to support the reaction conditions (especially with a high boiling point, since the reaction is performed under partial vacuum), (ii) compatible with the enzyme and (iii) solubilizing the final polyester. Debuissy *et al.* (Debuissy *et al.*, 2016, 2017a) have already screened different solvents for CALB catalyzed polymerization and reported anisole and phenetole as potential candidates. To complement these previous works, other solvents have been investigated based on their partition coefficient (log P) and their boiling points. The log P is the logarithm of the studied product concentration in octanol divided by its concentration in water. It is an empirical method for the estimation of the lipophilicity of a given solvent. A high log P value corresponds to a highly lipophilic solvent and vice versa. Other parameters could be considered such as the dielectric properties of the solvent or the interaction of the substrates with the solvents with computational tools as did Pellis *et al.* (Pellis *et al.*, 2019a). However, the log P has been used as a reference as it has already been employed in previous studies (Kobayashi *et al.*, 1998; Dong *et al.*, 1999; Kumar *et al.*, 2000; Juais *et al.*, 2010).

The study of the solvents influence was focused on the synthesis of PHF and PBF, which are the polymers with the highest backbone rigidity and therefore the most difficult to get dissolved. Solvents with a variety of log P have been investigated, taking diphenyl ether and toluene as references. Toluene having a boiling point of 111°C, the reaction has been performed at atmospheric pressure. Phenetole, anisole, acetophenone and cyclohexanone have been used at a minimal pressure of 250 mbar. Diphenyl ether having a high boiling point, it has been used as described before through a four steps method to reach 20 mbar. Early precipitation of the polymer was sometimes observed due to evaporation of the solvent. Thus, the volume of solvent was doubled to avoid such issue but the amount of enzyme was also multiplied by 2 in order to keep a constant enzyme concentration. Kinetics of the reaction was proven to be similar to previous reaction conditions. The resulting polymers were analyzed by NMR spectroscopy (Figure S2.32 to Figure S2.37 in Annexes) and MALDI-TOF MS (Figure S2.45 to Figure S2.48 in Annexes) analyses. As MALDI-TOF-MS analysis of polydisperse polymers are not quantitative (McEwen *et al.*, 1997; Rashidzadeh *et al.*, 1998), only rough estimates of M_n values were given in order to compare polymers with each other but they should not be taken as absolute values. The characteristics of the solvents and molar masses of the obtained polyesters are shown in Table 2.3.

Table 2.3: Influence of solvents on molar masses of PHF and PBF (CALB 20 wt.%, solvent 300 wt.%, 90°C 72 h)

Solvent	Log P	Boiling point (°C)	PHF		PBF	
			M_{nNMR} (g.mol^{-1})	$M_{nMALDI-TOF}$ (g.mol^{-1})	M_{nNMR} (g.mol^{-1})	$M_{nMALDI-TOF}$ (g.mol^{-1})
Diphenyl ether	4.2	258	2 100[a]	2 800 [a]	1 400 [a]	2 300 [a]
Toluene	2.7	111	2 300[b]	n.a.	1 200 [b]	n.a.
Phenetole	2.5	168	2 700[c]	n.a.	1 200 [c]	n.a.
Anisole	2.1	154	6 700 [c]	3 300 [c]	1 200 [c]	2 600 [c]
Acetophenone	1.6	202	7 600 [c]	3 500 [c]	2 000 [c]	2 700 [c]
Cyclohexanone	0.8	155	1 500 [c]	n.a.	1 500 [c]	n.a.

[a] Program of pressure: 4 h at 350mbar, 4 h at 200 mbar, 16 h at 50 mbar, 48 h at 20 mbar.
[b] Ambient pressure.
[c] Program of pressure: 4 h at 350mbar, 68 h at 250 mbar.
n.a.: not available (these polymers have not been analyzed by MALDI-TOF MS).

A strong influence of the solvent on the resulting molar masses can be observed, especially for PHF. Acetophenone and anisole, solvents with log P lower than 2.5 but higher than 0.8, gave the higher molar masses for both PHF and PBF (Table 2.3). In these solvents, the reaction could be carried out for a longer time before observing the precipitation of the synthesized polymer. Acetophenone was the solvent allowing the longer reaction time before precipitation (around 24 hours for PHF) and thus allowed to synthesize a semi-aromatic copolyester whose molar mass determined from NMR analyses is nearly four times greater than that obtained in diphenyl ether. Anisole also allowed the synthesis of more than three-fold higher molar mass PHF, as calculated from NMR spectra, when compared to diphenyl ether. However, anisole has no effect on the final molar mass of PBF. One may note from the experimental part that, when synthesized in anisole and phenetole, PHF needed the addition of 5 µl of anhydrous TFA for complete solubilization before NMR analysis. This method has already been described and proved not to alter the polymer structure (Hariharan *et al.*, 1993).

In the literature, Dong *et al*. (Dong *et al.*, 1999) studied the impact of solvent log P on the enzymatic ring opening polymerization of lactones. They reported that solvents with log P value higher than 4 were preferable whereas solvents with log P values between 4 and 2 gave unpredictable results. Finally, solvents with log P lower than 2 resulted in low enzymatic activity. However, in their study 1,2-dichloroethane (log P = 1.52) was an exception and led to higher molar masses than expected. Kumar *et al.* (Kumar *et al.*, 2000) also observed inconsistencies in the relationship between log P and CALB enzymatic activity. Our results also demonstrated that the log P value alone does not allow to predict the CALB activity. Because of precipitation issue, the solubility of the polymer in the medium is also a critical parameter to be considered. Unfortunately, this solubility in a given solvent cannot simply be predicted by log P. As depicted before, research with computational tools also showed that monomers stability in a given solvent greatly impacted the CALB reactivity and the obtained molar mass (Pellis *et al.*, 2019a). Nevertheless, acetophenone and anisole were clearly identified here as new promising solvents for the enzymatic synthesis of PHF and PBF.

MALDI-TOF-MS analysis also allows to determine the molar mass distribution and to estimate the average molar masses of the polyesters. The obtained spectra confirm an increase in molar mass when PHF and PBF are synthesized in acetophenone or anisole in comparison to diphenyl ether. However, the average values are significantly lower than those determined from NMR analyses. Two phenomena can explain this difference. First, MALDI-TOF-MS analysis of polydisperse polymer samples is not quantitative and the largest polymer chains are underrepresented, which results in an underestimation of the average molar masses. On the other hand, the determination of molar masses by NMR spectroscopy is based on the measurement of the intensity of chain ends compared to that of the core repeating units. If the end groups are consumed by a side reaction, their intensity decreases, resulting in an overestimation of the molar masses.

However, this last hypothesis can be verified since MALDI-TOF-MS allows of the analysis of polymer chain ends. The end groups of PHF and PBF synthesized in the different solvents have been analyzed (Figure 8 and Figure S2.45 to Figure S2.48 in Annexes). When synthesized in diphenyl ether, the PHF is mostly ended by both an ester and a hydroxyl or by two hydroxyl groups. A minority of chains with an ester group at both ends can be observed (Figure 2.8.a). When synthesized in anisole, the PHF was mostly ended by hydroxyl groups (Figure S2.45). When PHF was synthesized in acetophenone, chains were ended by hydroxyl groups or by a carboxylic acid and hydroxyl group (Figure 2.8.b). This carboxylic acid could be produced by hydrolysis in the reaction medium even though the acetophenone used for the reaction was anhydrous. Indeed, as previously mentioned, acetophenone allows to prolong the reaction time thus leaving more time for an eventual hydrolysis of the polyester. Moreover, acetophenone is much more polar than the other solvents. This could facilitate the hydration of the solvent under partial vacuum. Such hydrolysis of the polyester chains could be responsible for the apparent increase in molar mass calculated by NMR spectroscopy through the phenomenon impacting the chain ends depicted earlier. End groups analysis was also performed on PBF (Figure S2.46-Figure S2.48). Interestingly, no hydrolysis was observed this time for the PBF chains synthesized in acetophenone. Acetophenone had already been studied as solvent or as co-solvent for the synthesis of aromatic polyesters (Imai *et al.*, 1984; Akutsu *et al.*, 1996) but had never been used in enzymatic polymerizations.

a)

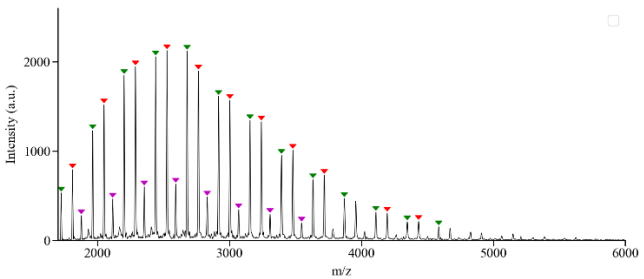

b)

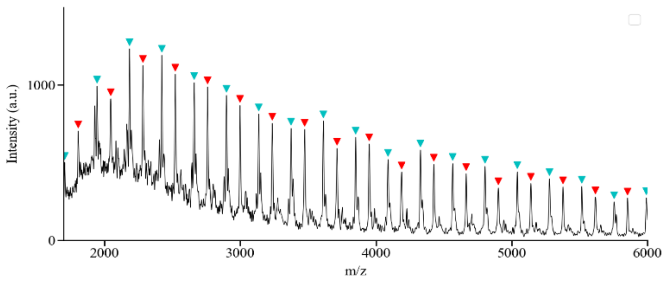

c)

Polymer structures and end-groups	Residual mass	Symbol
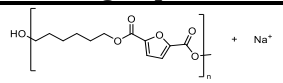	55.04	▼
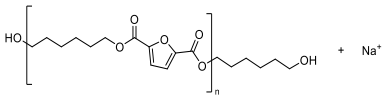	140.17	▼
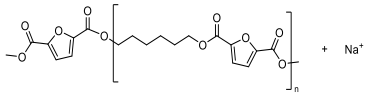	207.14	▼
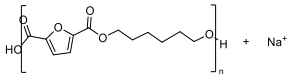	41.01	▼

Figure 2.8: MALDI-TOF-MS spectra of PHF synthesized in a) diphenyl ether and b) acetophenone with c) corresponding end-groups identification.

The catalytic activity of CALB was measured in the newly selected solvents, acetophenone and anisole, and compared to the one in diphenyl ether. For that, and in order to avoid the problem of polymer solubility, a simpler reaction of transesterification on model substrates was considered. The enzymatic activity has thus been assayed by studying the transesterification of diethyl adipate with 1-butanol at 50°C and atmospheric pressure (Figure 2.9). The reaction being reversible, an excess of 1-butanol was used to displace the reaction equilibrium.

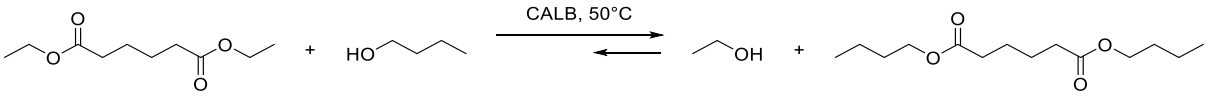

Figure 2.9: Assessment of the activity of CALB with diethyl adipate and 1-butanol

Moreover, it has been reported that in certain solvents, part of the enzyme can leak from the supporting beads (José *et al.*, 2011; Ortiz *et al.*, 2019). Presence of free enzyme could promote the reaction of polymerization. However, this enzyme leaching reduces the reusability of the beads. The impact of the selected solvents on the CALB activity and leaching has therefore been evaluated. After incubation of the beads at 90°C in a given solvent, the catalytic activity of the solvent was determined (after removal of the immobilized enzyme) in order to detect the possible presence of free enzymes that would have leached from the support.

The progress of reaction was determined from the conversion of ester groups (Figure 2.10).

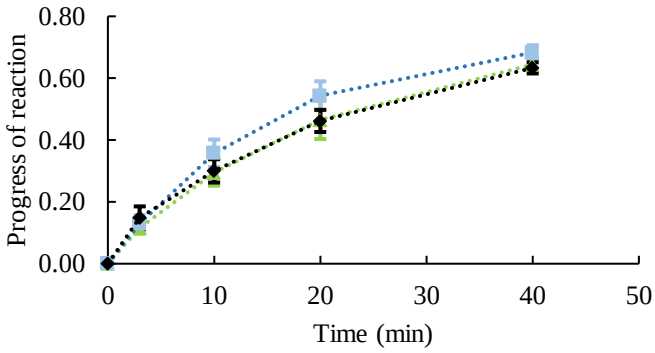

Figure 2.10: CALB catalyzed conversion of diethyl adipate with 1-butanol in various solvents: ▲ Diphenyl ether, ■ Acetophenone, ♦ Anisole.

The catalytic activity of CALB was found to be similar in all solvents. Only a slightly higher activity was observed in acetophenone. These results tend to imply that the higher molar masses obtained for the polyesters in acetophenone, and anisole are not due to a higher specific activity of the enzyme in such solvents. Moreover, no activity was detected in the solvent alone after incubation with the CALB. This indicates that among these solvents, none was found to cause significant leaching of the enzyme from the support to the medium. Therefore, no free enzyme participated to the improvement of the molar mass of PHF and PBF. The high potential of solubilization of these solvents, delaying the precipitation of the polymer in the medium, leads to longer time of reaction with a higher accessibility of the substrate to the enzyme and therefore allows to obtain higher molar masses.

4.2. Polyesters thermal properties

As depicted before, one of the main goals of increasing the aromatic content of polyesters is to improve their behaviors such as their thermal properties. Moreover, the molar masses and thus the synthesis method can also affect these properties. Consequently, the thermal behavior of the synthesized polymers has been determined to evaluate the impact of the aromatic content and synthesis method.

4.2.1. Thermal properties of PHAd-co-PHF and PBAd-co-PBF copolyesters

The thermal properties of PHAd-co-PHF and PBAd-co-PBF synthesized in diphenyl ether with different ratio of DMFDC have been studied by DSC, MDSC and TGA (Table 2. And Figure S2.20, Figure S2.21, Figure S2.24 and Figure S2.25 in Annexes).

Table 2.4: Thermal properties of PHAd-co-PHF and PBAd-co-PBF

Polyester	T_g [b] (°C)	T_m [c] (°C)	$T_{d5\%}$ (°C)	T_{dmax} (°C)
PHAd	--[a]	58	270	374
PHF10	-52	51	305	390
PHF30	-40	32	329	387
PHF50	-32	83	336	384
PHF70	-19	107	347	387
PHF90	-6	135	334	379
PHF	-1	140	332	381

PBAd	-- [a]	60	283	387
PBF10	-58	41	302	389
PBF30	-39	--	345	386
PBF50	-25	102	327	387
PBF70	-8	141	340	383
PBF90	-3	148	307	381
PBF	15	153	264	375

[a] T_g gap was too weak and in the limit of the apparatus to be precisely measured.
[b] from Modulated DSC analyses
[c] from classical DSC analyses

For a given aromatic content, the T_g values of the hexanediol-based polyesters were systematically lower than those of the butanediol-based ones. In polyesters, the thermal properties are highly dependent on the length of the monomers. These results are in agreement with previous observations on aliphatic polyesters (Debuissy *et al.*, 2017b). Indeed, hexanediol brings more flexibility to the polymeric chains compared to a shorter diol, lowering the T_g.

The impact of the aromatic content on the T_g values of the PHAd-co-PHF and PBAd-co-PBF copolyesters have been evaluated (Figure 2.11 and Figure 2.12). As expected, an increase in the aromatic content leads to an overall increase in the Tg value. The experimental T_g values of the copolyesters have been compared to the values calculated with the Fox law. For both polyesters, samples with an aromatic content below 70% generally followed the Fox law. However, PHAd-co-PHF with an aromatic ratio above 90% and PBAd-co-PBF with an aromatic ratio above 70% have T_g below the values predicted by the Fox law. The values are also lower than those found in the literature. For instance, T_g of PBF90 and PBF have been measured at 23 and 36 °C, respectively, by Wu *et al.* (Wu *et al.*, 2014) who synthesized high molar mass PBAd-co-PBF with an organometallic catalyst. As described by Fox-Flory equation (Fox *et al.*, 1950), molar mass and T_g are directly linked. The low molar mass of PBF, PBF90 and PHF obtained by CALB-catalyzed polymerization thus explain the low T_g values. This has been confirmed by Little *et al.* (Little *et al.*, 2020) who synthesized by organometallic catalysis PBF and PHF chains, with molar masses similar to ours, displaying T_g values of 15 and 4 °C, respectively.

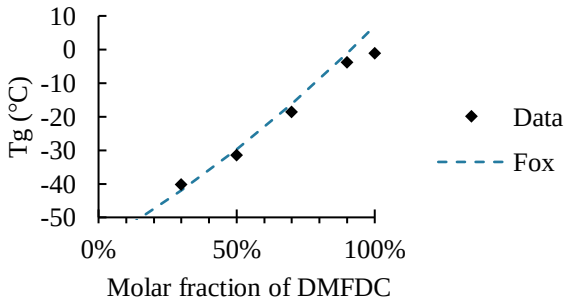

Figure 2.11: Evolution of Tg of the PHAd-co-PHF with different proportions of DMFDC (experimental data compared to the theoretical ones from Fox equation)

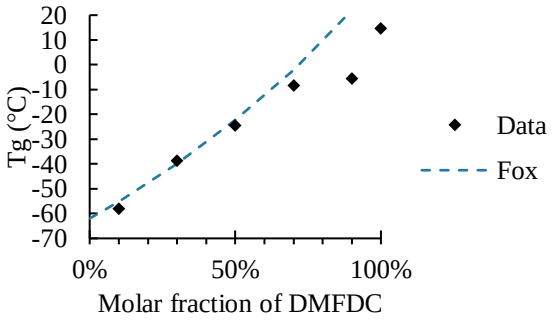

Figure 2.12: Evolution of Tg of the PBAd-co-PBF with different proportions of DMFDC (experimental data compared to the theoretical ones from Fox equation)

DSC analysis also showed a variation in T_m of the copolyesters (Table 2.4). The incorporation of 10 to 30% DMFDC decreased the T_m of the polyesters with even a fully amorphous material for PBF30. Then for higher DMFDC contents, T_m values increased again even if the melting endotherms of PBF50, PHF50 and PHF70 were hardly discernible. Polyesters with a DMFDC content higher than 70% showed relatively high melting temperature (above 100°C) and higher crystallinity. This is in perfect agreement with results reported in the literature (Yu *et al.*, 2013; Zhou *et al.*, 2013; Wu *et al.*, 2014; Papadopoulos *et al.*, 2018).

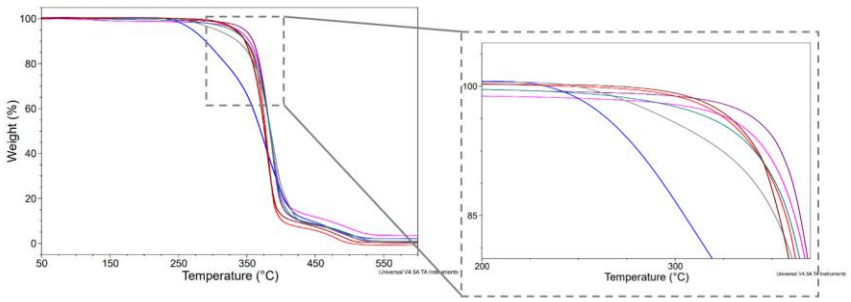

Figure 2.13: TGA measurements of PHAd-co-PHF with different ration of DMFDC — PHAd, — 10% of DMFDC, — 30% of DMFCD, — 50% of DMFDC, — 70% of DMFDC, — 90% of DMFDC, — PHF

Polyesters properties have been also evaluated by TGA. For both series of polyesters, increased thermal stability, measured as $Td_{5\%}$, is observed when the aromatic content increases, up to 70% of DMFDC (Figure 2.13). Then, $Td_{5\%}$ is dramatically reduced for higher aromatic content. This evolution is less marked on Td_{max}, especially for the PBAd-co-PBF series. A similar but less pronounced phenomenon has been reported in the literature with a decrease of $Td_{5\%}$ above 80% of aromatic content (Wu *et al.*, 2014). The decrease in $Td_{5\%}$ is intensified by the low molar masses of the co-polyesters (Chrissafis *et al.*, 2006). Increasing the aromatic content of these polyesters was therefore an efficient way to increase their thermal resistance until their molar masses were negatively impacted and thus led to a decrease in the thermal stability.

According to these results, reaching sufficiently high molar masses seems essential to produce polyesters with high thermal properties. Indeed, the low molar masses of the polyesters containing high aromatic contents are responsible for the decrease of the T_d and T_g of the polymers.

4.2.2. Thermal properties of the PHF and PBF synthesized in different solvents

PHF and PBF synthesized in acetophenone and in anisole were also analyzed and compared to the polyesters synthesized in diphenyl ether to determine the impact of the higher molar masses on the thermal properties (Table 2.5 and Figure S2.28 to Figure S2.31 in Annexes).

Table 2.5: Thermal properties of the PHF and PBF synthesized in different solvents

Polymer	Solvent	T_g (°C)	T_m (°C)	$T_{d5\%}$ (°C)	T_{dmax} (°C)
PHF	Diphenyl ether	-1	140	331	381
	Anisole	11	145	338	374
	Acetophenone	10	146	351	385
PBF	Diphenyl ether	15	153	264	375
	Anisole	16	159	307	386
	Acetophenone	17	163	288	384

As expected, for PHF a significant increase of at least 10°C in the T_g was observed when the polymer was synthesized in acetophenone or in anisole due to the higher molar masses evaluated from NMR analyses of 7 600 g.mol^{-1} and 6 700 g.mol^{-1}, respectively, compared to diphenyl ether (which resulted in PHF with a molar mass of 2 100 g.mol^{-1}). In the case of PBF, no significant change was observed due to the lower impact of these solvents on the obtained molar masses. For both PHF and PBF, the melting temperature slightly increased for the polymers synthesized in acetophenone and anisole when compared to diphenyl ether. The thermal resistance (measured as $Td_{5\%}$) was improved for both polymers. PHF showed a $Td_{5\%}$ value 6°C higher when synthesized in acetophenone. For PBF, the $Td_{5\%}$ was increased by 23°C when synthesized in acetophenone. For both polyesters, the improvement in thermal resistance could be linked to the higher molar masses obtained when using acetophenone. However, we do not explain the significant improvement observed for PBF synthesized in anisole since the Mn value (1 200 g.mol^{-1}) was not found to be higher than the one obtained in diphenyl ether (1 400 g.mol^{-1}).

5. Conclusion

In this work, PHAd-co-PHF and PBAd-co-PBF biobased aliphatic-aromatic copolyesters were synthesized in various solvents via the green route of enzyme-catalyzed transesterification reactions using immobilized *Candida antarctica* lipase B as biocatalyst.

For reactions carried out in diphenyl ether the highest molar masses were obtained for the PHAd-co-PHF series. M_w values above 30 000 g.mol^{-1} were obtained for aromatic diester contents

ranging from 0 to 70 %. Replacing HDO with BDO as a shorter diol resulted in copolyesters with slightly lower molar masses at up to 50% aromatic monomer content. In this composition range, an increase in the furan-based monomer content resulted in improved thermal properties (higher T_g and degradation temperature) for both copolyesters series. The obtained molar masses are similar or even slightly higher than those reported so far in the literature for equivalent systems (Jiang *et al.*, 2015; Comerford *et al.*, 2020).

As in previous published studies, the molar masses remain low and reach a plateau at high aromatic monomer content (Jiang *et al.*, 2015). However, our results then showed that CALB was able to insert the furan-based aromatic monomer into the macromolecular architectures of different copolyesters chains in proportions equal to those of the feed without negative impact on the reaction kinetics or on the obtained molar masses.

In contrast, this study highlighted that it is the loss of solubility observed for polyesters with high aromatic content (above 50% and 70% in DMFDC with butanediol and hexanediol, respectively) that is stopping the polyester chain growth thus leading to lower molar masses and consequently lower thermal properties.

The screening of various alternative solvents showed that replacing diphenyl ether with acetophenone or anisole resulted in significantly improved solubility for both the highly aromatic PHF and PBF polyesters. The best results were obtained with acetophenone, which had never been reported so far as a solvent for the enzymatic synthesis of polyesters, resulting in a significant increase in molar masses for PHF up to 7 600 $g.mol^{-1}$ as measured from NMR analysis and 3 500 $g.mol^{-1}$ as estimated from MALDI-TOF MS. Consequently, the polymer presented a greater thermal stability and a T_g increased by 11 °C. However, a possible hydrolysis of the polyester in the reaction medium was highlighted and will be further investigated.

This study clearly demonstrated the impact of the solvent in such enzymatic systems to obtain high molar mass copolyesters based on elevated aromatic content with improved thermal behavior. To complete this study, additional investigations should be carried out (mechanical properties, biodegradation...) in connection with the potential uses of these biobased aliphatic-aromatic copolyesters such as packaging or biomedical applications.

6. References

Akutsu, F., Inoki, M., Takahashi, K., Yonemura, T., Kasashima, Y. and Naruchi, K. (**1996**) 'Synthesis and Properties of Polyarylates Derived from 4,4″-Dihydroxy-o-terphenyl', *Polymer Journal*, 28(12), pp. 1107–1109.

Becker, J., Lange, A., Fabarius, J. and Wittmann, C. (**2015**) 'Top value platform chemicals: bio-based production of organic acids', *Current Opinion in Biotechnology*, 36, pp. 168–175.

Bedoui, F., Diani, J., Regnier, G. and Seiler, W. (**2006**) 'Micromechanical modeling of isotropic elastic behavior of semicrystalline polymers', *Acta Materialia*, 54(6), pp. 1513–1523.

Chrissafis, K., Paraskevopoulos, K. M. and Bikiaris, D. N. (**2006**) 'Effect of molecular weight on thermal degradation mechanism of the biodegradable polyester poly(ethylene succinate)', *Thermochimica Acta*, 440(2), pp. 166–175.

Comerford, J. W., Byrne, F. P., Weinberger, S., Farmer, T. J., Guebitz, G. M., Gardossi, L. and Pellis, A. (**2020**) 'Thermal Upgrade of Enzymatically Synthesized Aliphatic and Aromatic Oligoesters', *Materials*, 13(2), p. 368.

Cruz-Izquierdo, Á., van den Broek, L. A. M., Serra, J. L., Llama, M. J. and Boeriu, C. G. (**2015**) 'Lipase-catalyzed synthesis of oligoesters of 2,5-furandicarboxylic acid with aliphatic diols', *Pure and Applied Chemistry*, 87(1), pp. 59–69.

Debuissy, T., Pollet, E. and Avérous, L. (**2016**) 'Enzymatic Synthesis of a Bio-Based Copolyester from Poly(butylene succinate) and Poly((*R*)-3-hydroxybutyrate): Study of Reaction Parameters on the Transesterification Rate', *Biomacromolecules*, 17(12), pp. 4054–4063.

Debuissy, T., Pollet, E. and Avérous, L. (**2017**)**a** 'Enzymatic synthesis of biobased poly(1,4-butylene succinate- ran -2,3-butylene succinate) copolyesters and characterization. Influence of 1,4- and 2,3-butanediol contents', *European Polymer Journal*, 93, pp. 103–115.

Debuissy, T., Pollet, E. and Avérous, L. (**2017**)**b** 'Lipase-catalyzed synthesis of biobased and biodegradable aliphatic copolyesters from short building blocks. Effect of the monomer length', *European Polymer Journal*, 97, pp. 328–337.

Debuissy, T., Pollet, E. and Avérous, L. (**2017**)**c** 'Synthesis and characterization of biobased poly(butylene succinate- ran -butylene adipate). Analysis of the composition-dependent physicochemical properties', *European Polymer Journal*, 87, pp. 84–98.

Debuissy, T., Sangwan, P., Pollet, E. and Avérous, L. (**2017**)**d** 'Study on the structure-properties relationship of biodegradable and biobased aliphatic copolyesters based on 1,3-propanediol, 1,4-butanediol, succinic and adipic acids', *Polymer*, 122, pp. 105–116.

Diantimony trioxide (**2021**) *European Chemical Agency*. Available at: https://echa.europa.eu/substance-information/-/substanceinfo/100.013.796 (Accessed: 10 August 2021).

Dibutyltin oxide (**2021**) *European Chemical Agency*. Available at: https://echa.europa.eu/substance-information/-/substanceinfo/100.011.317 (Accessed: 12 August 2021).

Dong, H., Cao, S.-G., Li, Z.-Q., Han, S.-P., You, D.-L. and Shen, J.-C. (**1999**) 'Study on the enzymatic polymerization mechanism of lactone and the strategy for improving the degree of polymerization', *Journal of Polymer Science Part A: Polymer Chemistry*, 37(9), pp. 1265–1275.

Douka, A., Vouyiouka, S., Papaspyridi, L.-M. and Papaspyrides, C. D. (**2018**) 'A review on enzymatic polymerization to produce polycondensation polymers: The case of aliphatic polyesters, polyamides and polyesteramides', *Progress in Polymer Science*, 79, pp. 1–25.

Flores, I., Martínez de Ilarduya, A., Sardon, H., Müller, A. J. and Muñoz-Guerra, S. (**2019**) 'Synthesis of Aromatic–Aliphatic Polyesters by Enzymatic Ring Opening Polymerization of Cyclic Oligoesters and their Cyclodepolymerization for a Circular Economy', *ACS Applied Polymer Materials*, 1(3), pp. 321–325.

Fox, T. G. and Flory, P. J. (**1950**) 'Second-Order Transition Temperatures and Related Properties of Polystyrene. I. Influence of Molecular Weight', *Journal of Applied Physics*, 21(6), pp. 581–591.

Frampton, M. B. and Zelisko, P. M. (**2013**) 'Synthesis of lipase-catalysed silicone-polyesters and silicone-polyamides at elevated temperatures', *Chemical Communications*, 49(81), p. 9269.

Gandini, A., Silvestre, A. J. D., Neto, C. P., Sousa, A. F. and Gomes, M. (**2009**) 'The furan counterpart of poly(ethylene terephthalate): An alternative material based on renewable resources', *Journal of Polymer Science Part A: Polymer Chemistry*, 47(1), pp. 295–298.

Hariharan, R. and Pinkus, A. G. (**1993**) 'Useful NMR solvent mixture for polyesters: Trifluoroacetic acid-d/chloroform-d', *Polymer Bulletin*, 30(1), pp. 91–95.

Imai, Y. and Tassavori, S. (**1984**) 'Preparation and properties of aromatic polyesters and copolyesters containing phenylindane unit', *Journal of Polymer Science: Polymer Chemistry Edition*, 22(6), pp. 1319–1325.

Izunobi, J. U. and Higginbotham, C. L. (**2011**) 'Polymer Molecular Weight Analysis by 1 H NMR Spectroscopy', *Journal of Chemical Education*, 88(8), pp. 1098–1104.

Jiang, Y. and Loos, K. (**2016**) 'Enzymatic Synthesis of Biobased Polyesters and Polyamides', *Polymers*, 8(7), p. 243.

Jiang, Y., Woortman, A. J. J., Alberda van Ekenstein, G. O. R. and Loos, K. (**2015**) 'A biocatalytic approach towards sustainable furanic–aliphatic polyesters', *Polymer Chemistry*, 6(29), pp. 5198–5211.

Jin, H.-J., Lee, B.-Y., Kim, M.-N. and Yoon, J.-S. , 'Thermal and mechanical properties of mandelic acid-copolymerized poly(butylene succinate) and poly(ethylene adipate)', p. 8.

José, C., Bonetto, R. D., Gambaro, L. A., Torres, M. del P. G., Foresti, M. L., Ferreira, M. L. and Briand, L. E. (**2011**) 'Investigation of the causes of deactivation–degradation of the commercial biocatalyst Novozym® 435 in ethanol and ethanol–aqueous media', *Journal of Molecular Catalysis B: Enzymatic*, 71(3–4), pp. 95–107.

Juais, D., Naves, A. F., Li, C., Gross, R. A. and Catalani, L. H. (**2010**) 'Isosorbide Polyesters from Enzymatic Catalysis', *Macromolecules*, 43(24), pp. 10315–10319.

Kobayashi, S., Takeya, K., Suda, S. and Uyama, H. (**1998**) 'Lipase-catalyzed ring-opening polymerization of medium-size lactones to polyesters', *Macromolecular Chemistry and Physics*, 199(8), pp. 1729–1736.

Kobayashi, S. and Uyama, H. (**2019**) 'Synthesis of Polyesters I: Hydrolase as Catalyst for Polycondensation (Condensation Polymerization)', in Kobayashi, S., Uyama, H., and Kadokawa, J. (eds) *Enzymatic Polymerization towards Green Polymer Chemistry*. Singapore: Springer Singapore (Green Chemistry and Sustainable Technology), pp. 105–163.

Kristufek, S. L., Wacker, K. T., Tsao, Y.-Y. T., Su, L. and Wooley, K. L. (**2017**) 'Monomer design strategies to create natural product-based polymer materials', *Natural Product Reports*, 34(4), pp. 433–459.

Kumar, A. and Gross, R. A. (**2000**) '*Candida a ntartica* Lipase B Catalyzed Polycaprolactone Synthesis: Effects of Organic Media and Temperature', *Biomacromolecules*, 1(1), pp. 133–138.

Little, A., Pellis, A., Comerford, J. W., Naranjo-Valles, E., Hafezi, N., Mascal, M. and Farmer, T. J. (**2020**) 'Effects of Methyl Branching on the Properties and Performance of Furandioate-Adipate Copolyesters of Bio-Based Secondary Diols', *ACS Sustainable Chemistry & Engineering*.

Llevot, A., Grau, E., Carlotti, S., Grelier, S. and Cramail, H. (**2016**) 'From Lignin-derived Aromatic Compounds to Novel Biobased Polymers', *Macromolecular Rapid Communications*, 37(1), pp. 9–28.

Loos, K., Zhang, R., Pereira, I., Agostinho, B., Hu, H., Maniar, D., Sbirrazzuoli, N., Silvestre, A. J. D., Guigo, N. and Sousa, A. F. (**2020**) 'A Perspective on PEF Synthesis, Properties, and End-Life', *Frontiers in Chemistry*, 8, p. 585.

Lozano, P., De Diego, T., Carrie, D., Vaultier, M. and Iborra, J. L. (**2003**) 'Lipase Catalysis in Ionic Liquids and Supercritical Carbon Dioxide at 150 °C', *Biotechnology Progress*, 19(2), pp. 380–382.

Mahapatro, A., Kalra, B., Kumar, A. and Gross, R. A. (**2003**) 'Lipase-Catalyzed Polycondensations: Effect of Substrates and Solvent on Chain Formation, Dispersity, and End-Group Structure', *Biomacromolecules*, 4(3), pp. 544–551.

Maniar, D., Jiang, Y., Woortman, A. J. J., van Dijken, J. and Loos, K. (**2019**) 'Furan-Based Copolyesters from Renewable Resources: Enzymatic Synthesis and Properties', *ChemSusChem*, 12(5), pp. 990–999.

Mateo, C., Palomo, J. M., Fernandez-Lorente, G., Guisan, J. M. and Fernandez-Lafuente, R. (**2007**) 'Improvement of enzyme activity, stability and selectivity via immobilization techniques', *Enzyme and Microbial Technology*, 40(6), pp. 1451–1463.

McEwen, C. N., Jackson, C. and Larsen, B. S. (**1997**) 'Instrumental effects in the analysis of polymers of wide polydispersity by MALDI mass spectrometry', *International Journal of Mass Spectrometry and Ion Processes*, 160(1–3), pp. 387–394.

Morales-Huerta, J. C., Martínez de Ilarduya, A. and Muñoz-Guerra, S. (**2018**) 'Blocky poly(ε-caprolactone- *co* -butylene 2,5-furandicarboxylate) copolyesters via enzymatic ring opening polymerization', *Journal of Polymer Science Part A: Polymer Chemistry*, 56(3), pp. 290–299.

Nasr, K., Meimoun, J., Favrelle-Huret, A., Winter, J. D., Raquez, J.-M. and Zinck, P. (**2020**) 'Enzymatic Polycondensation of 1,6-Hexanediol and Diethyl Adipate: A Statistical Approach Predicting the Key-Parameters in Solution and in Bulk', *Polymers*, 12(9), p. 1907.

Nguyen, H. T. H., Qi, P., Rostagno, M., Feteha, A. and Miller, S. A. (**2018**) 'The quest for high glass transition temperature bioplastics', *Journal of Materials Chemistry A*, 6(20), pp. 9298–9331.

Nguyen, H. T. H., Reis, M. H., Qi, P. and Miller, S. A. (**2015**) 'Polyethylene ferulate (PEF) and congeners: polystyrene mimics derived from biorenewable aromatics', *Green Chemistry*, 17(9), pp. 4512–4517.

Ortiz, C., Ferreira, M. L., Barbosa, O., dos Santos, J. C. S., Rodrigues, R. C., Berenguer-Murcia, Á., Briand, L. E. and Fernandez-Lafuente, R. (**2019**) 'Novozym 435: the "perfect" lipase immobilized biocatalyst?', *Catalysis Science & Technology*, 9(10), pp. 2380–2420.

Öztürk, H., Pollet, E., Phalip, V., Güvenilir, Y. and Avérous, L. (**2016**) 'Nanoclays for Lipase Immobilization: Biocatalyst Characterization and Activity in Polyester Synthesis', *Polymers*, 8(12), p. 416.

Papadopoulos, L., Magaziotis, A., Nerantzaki, M., Terzopoulou, Z., Papageorgiou, G. Z. and Bikiaris, D. N. (**2018**) 'Synthesis and characterization of novel poly(ethylene furanoate-co-adipate) random copolyesters with enhanced biodegradability', *Polymer Degradation and Stability*, 156, pp. 32–42.

Papageorgiou, G. Z., Papageorgiou, D. G., Terzopoulou, Z. and Bikiaris, D. N. (**2016**) 'Production of bio-based 2,5-furan dicarboxylate polyesters: Recent progress and critical aspects in their synthesis and thermal properties', *European Polymer Journal*, 83, pp. 202–229.

Pellis, A., Byrne, F. P., Sherwood, J., Vastano, M., Comerford, J. W. and Farmer, T. J. (**2019**)**a** 'Safer bio-based solvents to replace toluene and tetrahydrofuran for the biocatalyzed synthesis of polyesters', *Green Chemistry*, 21(7), pp. 1686–1694.

Pellis, A., Comerford, J. W., Maneffa, A. J., Sipponen, M. H., Clark, J. H. and Farmer, T. J. (**2018**) 'Elucidating enzymatic polymerisations: Chain-length selectivity of Candida antarctica lipase B towards various aliphatic diols and dicarboxylic acid diesters', *European Polymer Journal*, 106, pp. 79–84.

Pellis, A., Herrero Acero, E., Ferrario, V., Ribitsch, D., Guebitz, G. M. and Gardossi, L. (**2016**)**a** 'The Closure of the Cycle: Enzymatic Synthesis and Functionalization of Bio-Based Polyesters', *Trends in Biotechnology*, 34(4), pp. 316–328.

Poojari, Y. and Clarson, S. J. (**2013**) 'Thermal stability of Candida antarctica lipase B immobilized on macroporous acrylic resin particles in organic media', *Biocatalysis and Agricultural Biotechnology*, 2(1), pp. 7–11.

Poulopoulou, N., Kantoutsis, G., Bikiaris, D. N., Achilias, D. S., Kapnisti, M. and Papageorgiou, G. Z. (**2019**) 'Biobased Engineering Thermoplastics: Poly(butylene 2,5-furandicarboxylate) Blends', *Polymers*, 11(6), p. 937.

Rashidzadeh, H. and Guo, B. (**1998**) 'Use of MALDI-TOF To Measure Molecular Weight Distributions of Polydisperse Poly(methyl methacrylate)', *Analytical Chemistry*, 70(1), pp. 131–135.

Rebouillat, S. and Pla, F. (**2016**) 'Recent Strategies for the Development of Biosourced-Monomers, Oligomers and Polymers-Based Materials: A Review with an Innovation and a Bigger Data Focus', *Journal of Biomaterials and Nanobiotechnology*, 07(04), pp. 167–213.

Sousa, A. F., Vilela, C., Fonseca, A. C., Matos, M., Freire, C. S. R., Gruter, G.-J. M., Coelho, J. F. J. and Silvestre, A. J. D. (**2015**) 'Biobased polyesters and other polymers from 2,5-furandicarboxylic acid: a tribute to furan excellency', *Polymer Chemistry*, 6(33), pp. 5961–5983.

Terzopoulou, Z., Karakatsianopoulou, E., Kasmi, N., Tsanaktsis, V., Nikolaidis, N., Kostoglou, M., Papageorgiou, G. Z., Lambropoulou, D. A. and Bikiaris, D. N. (**2017**) 'Effect of catalyst type on molecular weight increase and coloration of poly(ethylene furanoate) biobased polyester during melt polycondensation', *Polymer Chemistry*, 8(44), pp. 6895–6908.

Terzopoulou, Z., Papadopoulos, L., Zamboulis, A., Papageorgiou, D. G., Papageorgiou, G. Z. and Bikiaris, D. N. (**2020**) 'Tuning the Properties of Furandicarboxylic Acid-Based Polyesters with Copolymerization: A Review', *Polymers*, 12(6), p. 1209.

Vilela, C., Sousa, A. F., Fonseca, A. C., Serra, A. C., Coelho, J. F. J., Freire, C. S. R. and Silvestre, A. J. D. (**2014**) 'The quest for sustainable polyesters – insights into the future', *Polym. Chem.*, 5(9), pp. 3119–3141.

Weinberger, S., Haernvall, K., Scaini, D., Ghazaryan, G., Zumstein, M. T., Sander, M., Pellis, A. and Guebitz, G. M. (**2017**) 'Enzymatic surface hydrolysis of poly(ethylene furanoate) thin films of various crystallinities', *Green Chemistry*, 19(22), pp. 5381–5384.

Wu, B., Xu, Y., Bu, Z., Wu, L., Li, B.-G. and Dubois, P. (**2014**) 'Biobased poly(butylene 2,5-furandicarboxylate) and poly(butylene adipate-co-butylene 2,5-furandicarboxylate)s: From synthesis using highly purified 2,5-furandicarboxylic acid to thermo-mechanical properties', *Polymer*, 55(16), pp. 3648–3655.

Xanthopoulou, E., Zamboulis, A., Terzopoulou, Z., Kostoglou, M., Bikiaris, D. N. and Papageorgiou, G. Z. (**2021**) 'Effectiveness of Esterification Catalysts in the Synthesis of Poly(Ethylene Vanillate)', *Catalysts*, 11(7), p. 822.

Yu, Z., Zhou, J., Cao, F., Wen, B., Zhu, X. and Wei, P. (**2013**) 'Chemosynthesis and characterization of fully biomass-based copolymers of ethylene glycol, 2,5-furandicarboxylic acid, and succinic acid', *Journal of Applied Polymer Science*, 130(2), pp. 1415–1420.

Zhou, W., Wang, X., Yang, B., Xu, Y., Zhang, W., Zhang, Y. and Ji, J. (**2013**) 'Synthesis, physical properties and enzymatic degradation of bio-based poly(butylene adipate-co-butylene furandicarboxylate) copolyesters', *Polymer Degradation and Stability*, 98(11), pp. 2177–2183.

Zia, K. M., Noreen, A., Zuber, M., Tabasum, S. and Mujahid, M. (**2016**) 'Recent developments and future prospects on bio-based polyesters derived from renewable resources: A review', *International Journal of Biological Macromolecules*, 82, pp. 1028–1040.

Conclusion chapitre 2

Ce chapitre a montré et confirmé la capacité de la CALB à produire des copolyesters à partir d'un synthon aromatique biosourcé, le DMFDC associé au 1,6-HDO ou au 1,4-BDO en tant que diol et au diéthyle adipate comme co-diester. L'enzyme a ainsi montré une activité importante même à des taux élevés de DMFDC, écartant l'hypothèse d'une inhibition de son activité de la part du substrat. Des polyesters de masses molaires relativement élevées ont ainsi été obtenus. Les propriétés thermiques des matériaux se sont retrouvées améliorées par l'ajout d'aromaticité, prouvant la pertinence d'envisager et d'étudier la conversion par catalyse enzymatique de monomères aromatiques.

Toutefois, des polyesters de plus faibles masses molaires ont été obtenus pour des teneurs élevées en DMFDC. Il a été montré que ceci résulterait d'une précipitation des chaines polymères en croissance. Cette précipitation empêcherait ainsi la diffusion du substrat dans le milieu réactionnel. La solubilité des substrats (monomères et chaînes en croissance) dans le milieu réactionnel est donc un paramètre important à considérer dans ce type de polymérisation enzymatique. De nouveaux solvants tels que l'acétophénone ou l'anisole ont ainsi montré avoir un effet bénéfique sur la solubilisation du substrat et ont permis, *in fine*, d'augmenter les masses molaires des polyesters obtenus.

Ce premier chapitre a donc permis la mise en lumière de deux points importants. Premièrement, ce chapitre a mis en exergue la bonne réactivité d'un synthon aromatique biosourcé vis-à-vis de la CALB. Ensuite, cette étude a mis en évidence l'importance des conditions réactionnelles sur l'activité de l'enzyme et la structure du polymère ainsi formé. Ces observations ouvrent donc la voie vers une investigation plus large portant sur la réactivité de synthons aromatiques biosourcés plus atypiques ou nouveaux afin d'améliorer encore les propriétés des polyesters obtenus ou de développer de nouveaux matériaux aux propriétés spécifiques.

Chapitre 3. L'acide férulique comme molécule plateforme pour la synthèse enzymatique de polyesters aromatiques biosourcés.

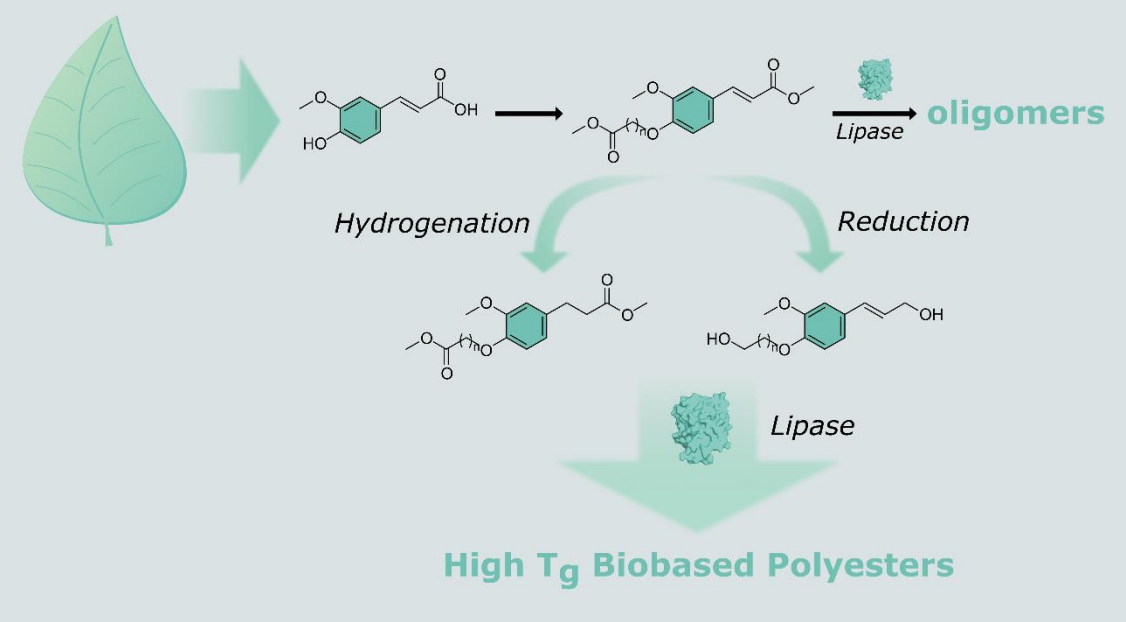

Introduction chapitre 3

Comme cela a été montré dans le chapitre précédent, l'insertion de monomères aromatiques est un moyen efficace pour améliorer les propriétés thermiques d'un polyester. Les dérivés de furanes, tels que ceux utilisés et étudiés dans le chapitre 2, sont ainsi les substrats les plus étudiés, et de loin, pour la synthèse de polyesters aromatiques aussi bien par catalyse organométallique qu'enzymatique. Il existe cependant une très grande variété de substrats aromatiques pouvant être directement extraits ou être produits à partir de la biomasse. C'est notamment le cas des dérivés phénoliques naturels.

Comme cela a été exposé au chapitre 1, les dérivés phénoliques biosourcés ont été largement étudiés pour leur réactivité en estérification et transestérification par catalyse enzymatique. Ces études se sont cependant concentrées sur la synthèse ou la modification enzymatique de petites molécules et synthons de faibles masses molaires. La synthèse par catalyse enzymatique de polyesters à partir de ces substrats reste donc un vaste champ qui reste à explorer.

Nous avons choisi dans ce chapitre d'étudier la réactivité de dérivés d'acide férulique en polymérisation par (trans)estérification catalysée par CALB. En effet, l'acide férulique peut directement être extrait d'une grande variété de sources naturelles et pourrait représenter à l'avenir une molécule plateforme importante pour la synthèse d'additifs et de matériaux. Ce chapitre repose donc sur le contenu d'un article intitulé 'Ferulic acid as building block for the lipase-catalyzed synthesis of biobased aromatic polyesters', publié dans *Polymers*. Plusieurs monomères ont été synthétisés à partir de l'acide férulique afin d'améliorer leur réactivité en polymérisation. L'influence de la structure de ces monomères sur leur réactivité vis-à-vis de l'enzyme et la structure des polymères obtenus ont ainsi été étudiées. En effet, la modification des monomères à base d'acide férulique permet également de moduler les propriétés du matériau obtenu. Le lien entre structure et propriété du matériau a donc également été analysé.

Ferulic acid as building-block for the lipase-catalyzed synthesis of biobased aromatic polyesters

*Alfred Bazin, Luc Avérous, Eric Pollet**

*Publié par Polymers (**2021**, volume 13, n°21, p. 3693)*

1. Abstract

Enzymatic synthesis of aromatic biobased polyesters is a recent and rapidly expanding research field. However, the direct lipase-catalyzed synthesis of polyesters from ferulic acid has not yet been reported. In this work, various ferulic-based monomers were considered for their capability to undergo CALB-catalyzed polymerization. After conversion into diesters of different lengths, the CALB-catalyzed polymerization of these monomers with 1,4-butanediol resulted in short oligomers with a DP_n up to 5. Hydrogenation of the double bond resulted in monomers allowing to obtain polyesters of higher molar masses, with DP_n up to 58 and M_w up to 33 100 $g.mol^{-1}$. These polyesters presented good thermal resistance up to 350°C and T_g up to 7°C. Reduction of the ferulic-based diesters into diols allowed to preserve the double bond and to synthesize polyesters with a DP_n up to 19 and, M_w up to 15 500 $g.mol^{-1}$ and higher T_g (up to 21°C). This study has thus shown that the monomer hydrogenation strategy proved to be the most promising route to achieve ferulic-based polyester chains of high DP_n. This study also demonstrates for the first time that ferulic-based diols allow the synthesis of high T_g polyesters. This is therefore an important first step towards the synthesis of competitive biobased aromatic polyesters by enzymatic catalysis.

2. Introduction

The current environmental issues are directing research towards the production of greener materials through more environmentally friendly processes. This trend is particularly important in the field of polyesters. Indeed, the vast majority of polyesters are fossil-based, often show poor biodegradability, and are synthesized through harsh reaction conditions (Mandal *et al.*, 2019).

For this reason, biobased polymers are gaining much attention. Indeed, such polymers are produced from a renewable feedstock (Delidovich *et al.*, 2016; John *et al.*, 2019) and can sometimes present good biodegradability (Satti *et al.*, 2020). However, like their oil-based counterparts, these biobased polymers are also generally synthesized at high temperatures by employing potentially hazardous organometallic catalysts (Li *et al.*, 2019).

The lipase B from *Candida antarctica* (CALB) is an enzyme capable, in specific conditions, to catalyze esterification and transesterification reactions. It is a versatile enzyme that accepts a wide

variety of substrates (Ortiz *et al.*, 2019). Thus, CALB can be employed as a biocatalyst for the synthesis of various polyesters, replacing the organometallic catalyst and allowing milder reaction conditions (Pellis *et al.*, 2019c; Todea *et al.*, 2021). As an example, our team studied the synthesis of various biobased aliphatic polyesters (Debuissy *et al.*, 2017b, 2017a; Duchiron *et al.*, 2017). However, because of the superior thermal and mechanical properties of aromatic and semi-aromatic polyesters, their enzymatic synthesis is gaining attention (Albanese *et al.*, 2016; Nguyen *et al.*, 2018). As an example, the enzymatic synthesis of semi-aromatic furan-based polyesters has been studied (Flores *et al.*, 2019; Comerford *et al.*, 2020; Skoczinski *et al.*, 2020; Bazin *et al.*, 2021b) as these polymers represent a promising alternative to common oil-based aromatic polyesters such as polyethylene terephthalate (Loos *et al.*, 2020). However, furans are a particular case of C5 aromatic molecules. We therefore directed our research towards more classical C6 aromatic compounds as is the case for terephthalic acid. Several biobased compounds with C6 aromatic rings can be extracted from biomass and are promising candidates for biobased polymers synthesis, one of them being ferulic acid (Crozier *et al.*, 2006; Tinikul *et al.*, 2018).

Ferulic acid can be extracted from various natural sources such as orange pulp, sugarcane bagasse, or corn and wheat bran (Flourat *et al.*, 2021). This compound is present in hemicellulose as a crosslinker of the polysaccharide chains (Terrett *et al.*, 2019) and can also be produced from lignin (Li *et al.*, 2021). Ferulic acid has been considered for potential uses as an additive in food and cosmetic products due to its interesting antioxidant and potential drug-like properties (Figueroa-Espinoza *et al.*, 2013; Mancuso *et al.*, 2014; Sandoval *et al.*, 2015). Because of its rigid structure and adequate functionality, ferulic acid has been investigated for the synthesis of various polyesters with advanced properties. As an example, Thi *et al*. investigated the homopolymerization of coumaric derivatives, such as ferulic acid, catalyzed by an anhydride at temperatures up to 200°C. The obtained polyesters showed interesting liquid-crystalline behavior but presented limited solubility in common organic solvents. Indeed, purely ferulic-based polymers result in very rigid materials with high glass transition and melting temperatures around 113 °C and 325 °C (Elias *et al.*, 1985), respectively. The processability of these materials ends up hindered and strategies of copolymerization as well as the modification of ferulic acid have been investigated to produce materials with more controlled and appropriate thermal properties (Llevot *et al.*, 2016). Nguyen *et al*. (Nguyen *et al.*, 2015) studied the polymerization of ferulic acid derivatives bearing hydroxyether moieties of various lengths, as represented in Scheme 3.1. Varying the length of the hydroxyether allowed to fine-tune the polymers thermal properties. The authors also showed the strong influence of the ferulic acid double bound on the polyester thermal properties by hydrogenating the ferulic derivatives. The same authors obtained interesting results on the copolymerization of these derivatives with cyclic monomers such as ε-caprolactone or L-lactide (Nguyen *et al.*, 2017).

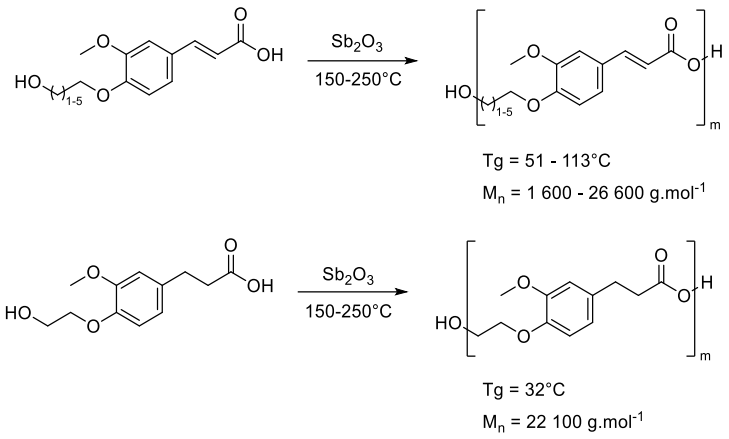

Scheme 3.1: Representation of the synthesis of polyesters from ferulic derivatives of different length as well as with and without hydrogenation. Adapted from (Nguyen *et al.*, 2015).

Recently, Kurt *et al.* (Kurt *et al.,* 2020) used hydrogenated derivatives of ferulic acid for the synthesis of aromatic polyesters catalyzed by zinc acetate and obtained M_n up to 8 000 g.mol^{-1}. Moreover, because of its therapeutic as well as anti-UV properties, native unmodified ferulic acid also allows the synthesis of material with innovative properties. As an example, Ouimet *et al.* produced a biobased copolyester from ferulic acid and diethyl adipate. Upon degradation, this polymer then allowed the controlled release of ferulic acid as an antibacterial and antioxidant agent (Ouimet *et al.,* 2013). Recently, Parthiban *et al.* used ferulic acid for the synthesis of UV absorbing polymers. Pospiech *et al.* (Pospiech *et al.,* 2021) showed that insertion of ferulic acid units in an aliphatic polyester significantly improved the material T_g.

Enzymes such as CALB have been investigated by Pion *et al.* in processes for the synthesis of ferulic-based monomers subsequently used for the elaboration of various materials (Pion *et al.,* 2013). This method allowed the production of various polymers such as isocyanate-free poly(hydroxy)urethanes (Ménard *et al.,* 2017a) and epoxy thermosets (Ménard *et al.,* 2017b). Polyesters were also synthesized with acyl chloride (Pion *et al.*, 2014) or by ADMET (Barbara *et al.*, 2015). These studies showed the great potential of ferulic acid for the synthesis of materials with tunable thermal and mechanical properties as well as antioxidant properties. However, the enzymatic catalysis was not used for the polymerization step. Besides, the polymerization of ferulic-based monomers is often performed under harsh thermal conditions that can be deleterious to the monomer integrity, leading to a coloration of the material. Moreover, the often-toxic metal-based catalyst can remain in the final material, leading to environmental and health issues (Rovira *et al.,* 2015).

CALB has already been used for the synthesis of aromatic polyesters (Pellis *et al.,* 2016b). However, lipase-catalyzed polymerization of aromatic monomers often results in low molar mass polyesters (Comerford *et al.,* 2020; Skoczinski *et al.,* 2020). Moreover, to the best of our knowledge, CALB and lipases in general have never been studied as biocatalysts for the polymerization of ferulic monomers.

In this study, ferulic acid was modified into new diesters of different lengths and polymerized with 1,4-butanediol using CALB as biocatalyst. Two strategies were then developed to enhance the reactivity of ferulic-based monomers in CALB-catalyzed polymerization and achieve higher molar masses: the hydrogenation and reduction of the monomer. The structure and the properties of the final materials were then investigated. The impact of the structure of the ferulic-based moieties first on the reactivity of the CALB and then on the thermal properties (glass transition, melting temperature, and degradation temperatures) of the final materials were assessed.

3. Materials and Methods

3.1. Materials

Lipase B from *Candida antarctica* immobilized on acrylic resin (activity measured to 11 000 PLU/g (propyl laurate units)) (CALB), deuterated chloroform ($CDCl_3$), dibutyl aluminum hydride (DIBAL-H) solution in toluene (25 wt%), and palladium on activated charcoal (Pd/C) were supplied by Sigma-Aldrich. Diethyl adipate (DEA), potassium iodine, methyl 4-chlorobutyrate, and diphenyl ether were purchased from Acros Organics. 1,4-butanediol (BDO), acetophenone, ferulic acid, and methyl chloroacetate were supplied by Alfa Aesar. Methanol and potassium carbonate were supplied by Fisher scientific. Chloroform was supplied by Carlo Erba. CALB was dried at 25° C for 24 h under vacuum before use. Other reactants were employed without further purification.

3.2. Characterization

A Bruker 400 MHz spectrometer was used for ^{1}H NMR analysis and a Bruker 500 MHz spectrometer was used for 2D and ^{13}C NMR analyses. The solvents employed were $CDCl_3$ and DMSO-d_6 depending on the solubility of the substrate. Calibration of the spectra was performed using the $CDCl_3$ peak (δH = 7.26 ppm, δC = 77.16 ppm) and DMSO-*d6* peak (δH = 2.50 ppm, δC = 39.52 ppm).

Size Exclusion Chromatography (SEC) was performed to estimate the number average molar mass (M_n), mass average molar mass (M_w), and dispersity (Đ). The analyses were performed in THF at 40 °C in an Acquity-APC (Waters) equipped with three columns (Acquity APC XT 450 Å 2.5 µm 4.6x150 mm, 200 and 45). 10 µL of dissolved polymer were injected and a flow of 0.6 mL/min was applied for the 11 minutes run. Refractive index (RI) detector and photodiode array (PDA) detector at 254 nm were used. A calibration curve with polystyrene (PS) standards was carried out for molar mass determination. The molar mass calculation was performed with data collected from the UV detector.

Differential scanning calorimetry (DSC) analyses were performed using a Q2000 DSC apparatus from TA Instrument (TA Instrument, New Castle, Delaware, USA) to estimate the polymers glass transition temperature (T_g) as well as their melting temperature (T_m) and crystallization temperature (T_c), if applicable. Typically, a 1 to 3 mg sample in a sealed aluminum pan was treated following a three-step method: (1) fast heating to 180 °C. The sample was kept for 3 minutes at this high

temperature to erase all thermal history, (2) cooling at 10 °C/min to -80 °C followed by an isotherm of 5 minutes and (3) second heating was performed at 10 °C/min to 180 °C. The characteristic temperatures were determined from this second heating scan. DSC was employed as well for the determination of the synthesized compounds melting points.

Thermogravimetric analysis (TGA) was performed to determine the thermal stability of the polymers. The measurements were conducted on a High-Res TGA Q5000 from TA Instrument. Samples between 1 and 2 mg were heated at 10 °C/min from room temperature to 600 °C.

Infrared spectroscopy (IR) was performed with a Nicolet 380 Fourier transformed infrared spectrometer (Thermo Electron Corporation) used in reflection mode and equipped with an ATR diamond module (ATR-FTIR). The spectra were collected at a resolution of 4 cm^{-1} and with 32 scans per run.

MALDI-TOF analyses were carried out on an AutoflexTM MALDI-TOF mass spectrometer (Bruker Daltonics GmbH, Bremen, Germany) used at a maximum accelerating potential of 20 kV in positive mode and operated in linear mode. The delay extraction was fixed at 560 ns and the frequency of the laser (nitrogen 337 nm) was set at 5 Hz. The acquisition mass range was set to 1500-10000 m/z with a matrix suppression deflection (cut off) set to 1500 m/z. The equipment was calibrated with ACTH 1-17 ($[M+H]^+$ 2094.42), insulin ($[M+H]^+$ 5732.52), ubiquitin I ($[M+H]^+$ 8565.76) and myoglobin ($[M+H]^+$ 16952.31). Spectra were processed with flexAnalysis software (Bruker Daltonics). Sample preparation was performed with the dried droplet method using a mixture of 0.5 µl of sample with 0.5 µl of matrix solution dried at room temperature. The 2-[(2E)-3-(4-tert-butylphenyl)-2-methylprop-2-enylidene]malononitrile (DCTB) matrix was prepared at 20 mg/ml in dichloromethane.

3.3. Synthesis of ferulic diesters

Ferulic acid was dissolved in a large volume of methanol. Few drops of sulfuric acid were added as catalyst. The solution was refluxed overnight. The solution was then neutralized by few drops of saturated sodium carbonate solution. The solvent was then evaporated, and the product was recovered in ethyl acetate and dried over $MgSO_4$. The salts were extracted by filtration, and the solvent was evaporated. Methyl ferulate (**MeFA**) was obtained as a clear yellow oil and used without further purification. (Yield: quantitative, IR: 3391 cm^{-1} (O-H), 2949 cm^{-1} (C-H), 1698 cm^{-1} (C=O ester), 1510 cm^{-1} (C=C Ar), 1262 cm^{-1} (C-O ester), ^1H NMR (400 MHz, $CDCl_3$) δ (in ppm): 7.62 (d, J = 15.9 Hz, 1H), 7.07 (dd, 1H), 7.03 (d, J = 1.9 Hz, 1H), 6.92 (d, J = 8.2 Hz, 1H), 6.29 (d, J = 15.9 Hz, 1H), 5.83 (brs, 1H), 3.93 (s, 3H), 3.80 (s, 3H)). ^{13}C NMR (126 MHz, $CDCl_3$) δ (in ppm): 167.81, 148.08, 146.87, 145.04, 126.93, 123.05, 115.12, 114.83, 109.47, 77.10, 55.95, 51.64, 30.93.

The methyl ferulate (**MeFA**) (4 g, 19.2 mmol, 1 eq.) was then dissolved in acetonitrile (95ml). Potassium carbonate (7.97 g, 57.63 mmol, 3 eq.) and potassium iodine (0.77g, 4.61 mmol, 0.24 eq.) were added as catalyst. The corresponding chloroester (methyl chloroacetate or methylchlorobutyrate)

was added (38.42 mmol, 2 eq.). The solution was then refluxed overnight. After cooling down, the solution was filtered to eliminate the undissolved catalyst. The solvent was evaporated under reduced pressure. The crude product was recovered in ethyl acetate and washed once with a saturated solution of sodium carbonate and twice with brine. The organic solution was dried over $MgSO_4$, and the solvent was evaporated. The product was then recrystallized in a mixture of ethanol and water.

The methyl 4-(methyl ethanoate-oxy)-ferulate (**DeFA^{I}**) was obtained as white crystals (yield: 80 %, melting point : 64 °C, IR (in cm^{-1}): 2952 (C-H), 1735 (C=O ester), 1709 (C=O ester), 1517 (C=C Ar), 1268 (C-O ester), ^{1}H NMR (400 MHz, $CDCl_3$) δ (in ppm): 7.62 (d, J = 16.0 Hz, 1H), 7.12 – 7.02 (m, 2H), 6.78 (d, J = 8.8 Hz, 1H), 6.32 (d, J = 16.0 Hz, 1H), 4.73 (s, 2H), 3.91 (s, 3H), 3.80 (s, 6H)). ^{13}C NMR (126 MHz, $CDCl_3$) δ (in ppm): 169.02, 167.56, 149.70, 149.14, 144.49, 128.90, 122.09, 116.31, 113.52, 110.59, 77.06, 66.10, 56.00, 52.38, 51.70.

The methyl 4-(methyl butanoate-oxy)-ferulate (**DeFA^{II}**) was obtained as off-white needles (yield: 80%, melting point : 83 °C, IR (in cm^{-1}): 2952 (C-H), 1699 (C=O ester), 1510 (C=C Ar), 1250 (C-O ester), ^{1}H NMR (400 MHz, $CDCl_3$) δ (in ppm) 7.62 (d, J = 15.9 Hz, 1H), 7.13 – 7.01 (m, 2H), 6.86 (d, J = 8.3 Hz, 1H), 6.30 (d, J = 16.0 Hz, 1H), 4.09 (t, J = 6.3 Hz, 2H), 3.88 (s, 3H), 3.79 (s, 3H), 3.68 (s, 3H), 2.54 (t, J = 7.2 Hz, 2H), 2.23 – 2.08 (m, 2H)). ^{13}C NMR (126 MHz, $CDCl_3$) δ (in ppm): 173.54, 167.69, 150.46, 149.60, 144.80, 127.54, 122.52, 115.53, 112.66, 110.22, 77.09, 67.79, 55.96, 51.68, 51.63, 30.41, 24.40.

3.4. Hydrogenation of the ferulic diesters

Pd/C (75 mg, 5 wt%) and the diester **DeFA^{I}** or **DeFA^{II}** (1,5 g, 5.1 mmol) were placed in a round bottom flask and sealed with a septum. The powders were placed under argon and ethanol (15ml) was carefully added with a syringe. Hydrogen was then bubbled for 15 minutes in the solution. Finally, the solution was stirred for 24 h with hydrogen overpressure. The solution was filtered through celite, and the solvent was evaporated under reduced pressure.

The methyl 3-(3-methoxy-4-(2-methoxy-2-oxoethoxy)phenyl)propanoate (**H-DeFA^{I}**) was obtained as a transparent oil (yield: 97%, IR (in cm^{-1}): 2952 (C-H), 1731 (C=O ester), 1512 (C=C Ar), 1258 (C-O ester), ^{1}H NMR (400 MHz, $CDCl_3$) δ (in ppm): 6.80 – 6.65 (m, 3H), 4.67 (s, 2H), 3.87 (s, 3H), 3.79 (s, 3H), 3.67 (s, 3H), 2.90 (t, J = 7.5 Hz, 2H), 2.61 (t, J = 7.5 Hz, 2H)). ^{13}C NMR (126 MHz, $CDCl_3$) δ (in ppm) 173.32, 169.61, 149.57, 145.69, 135.08, 120.11, 114.56, 112.38, 77.13, 66.62, 55.88, 52.18, 51.64, 35.84, 30.61.

The methyl 4-(2-methoxy-4-(3-methoxy-3-oxopropyl)phenoxy)butanoate (**H-DeFA^{II}**) was obtained as a yellow oil (yield: 99%, IR (in cm^{-1}): 2951 (C-H), 1731 (C=O ester), 1513 (C=C Ar), 1257 (C-O ester), ^{1}H NMR (400 MHz, $CDCl_3$) δ (in ppm): 6.80 (d, J = 7.9 Hz, 1H), 6.75 – 6.65 (m, 2H), 4.03 (t, J = 6.3 Hz, 2H), 3.84 (s, 3H), 3.67 (d, J = 3.6 Hz, 6H), 2.89 (t, J = 7.8 Hz, 2H), 2.61 (t, J = 7.5 Hz, 2H), 2.54 (t, J = 7.3 Hz, 2H), 2.13 (m, 2H). ^{13}C NMR (126 MHz, $CDCl_3$) δ (in ppm): 173.72, 173.42,

149.50, 146.75, 133.63, 120.19, 113.62, 112.25, 77.09, 68.03, 55.94, 51.64, 51.62, 35.99, 30.62, 30.54, 24.60.

3.5. Synthesis of the ferulic diols

Ferulic diester **DeFA^{I}** or **DeFA^{II}** (1.5g) was added to a three-neck flask equipped with a condenser and a dropping funnel. The flask was sealed with a septum and flushed with argon. Dry toluene (55 ml) was added. The solution was cooled at -78 °C and a solution of DIBAL-H in toluene (27.1 mmol, 5 eq.) was added dropwise over 20 minutes. The solution was then left for 2 hours at room temperature. The solution was then cooled down at 0 °C and ethyl acetate (20 ml) was carefully added. A saturated solution of Rochel salts was then added (30 ml) to complete the quenching of the reaction medium. The solution was left stirring overnight. The aqueous phase was washed 3 times with ethyl acetate. The organic phase was then washed once with brine and dried over $MgSO_4$. The solvent was then removed under reduced pressure.

The 4-(hydroxyethoxy)-coniferyl alcohol (**FAD^{I}**) was obtained as a white powder (yield: 94 %, melting point : 103 °C, IR (in cm^{-1}): 3448 (O-H), 2932 (C-H), 1511 (C=C Ar), ^{1}H NMR (400 MHz, DMSO-*d6*) δ (in ppm): 7.05 (s, 1H), 6.90 (s, 2H), 6.47 (d, J = 15.9 Hz, 1H), 6.26 (dt, J = 15.9, 5.3 Hz, 1H), 4.84 (t, J = 5.5 Hz, 1H), 4.81 (t, J = 5.4 Hz, 1H), 4.10 (t, J = 4.8 Hz, 2H), 3.96 (t, J = 5.1 Hz, 2H), 3.78 (s, 3H), 3.71 (q, J = 5.3 Hz, 2H). ^{13}C NMR (126 MHz, DMSO-*d6*) δ (in ppm): 149.51, 148.12, 130.43, 129.04, 129.00, 119.61, 113.49, 109.79, 70.63, 62.11, 60.06, 55.86, 39.98.

The 4-(hydroxybutoxy)-coniferyl alcohol (**FAD^{II}**) was obtained as an off-white powder (yield: 98 %, melting point : 87 °C, IR (in cm^{-1}): 3273 (O-H), 2923 (C-H), 1512 (C=C Ar), ^{1}H NMR (400 MHz, DMSO-*d6*) δ (in ppm): 7.04 (s, 1H), 6.88 (s, 2H), 6.46 (d, J = 15.9 Hz, 1H), 6.25 (dt, J = 15.9, 5.3 Hz, 1H), 4.80 (t, J = 5.4 Hz, 1H), 4.44 (t, J = 5.2 Hz, 1H), 4.10 (td, J = 5.3, 1.7 Hz, 2H), 3.94 (t, J = 6.5 Hz, 2H), 3.78 (s, 3H), 3.45 (q, J = 6.4 Hz, 2H), 1.85 – 1.67 (m, 2H), 1.64 – 1.50 (m, 2H). ^{13}C NMR (126 MHz, DMSO-*d6*) δ (in ppm): 149.54, 148.14, 130.30, 129.05, 128.94, 119.64, 113.42, 109.84, 68.59, 62.10, 60.90, 55.96, 39.99, 29.50, 26.02.

3.6. Enzymatic polymerization

Each polyester was synthesized according to a procedure adapted from a previous study (Bazin *et al.*, 2021b) (with optimal temperature, solvent and concentrations) but varying the nature of the solvent, reaction time and pressure when necessary or desired. The obtained polymers were then recovered with the same procedure as in the literature.

*3.6.1. From ferulic-based diesters (***PDeFA^{I-II}** *and* **PH-DeFA^{I-II}***):*

The ferulic-based diester (150 mg) and BDO were placed in a Schlenck reactor in equimolar proportions. Diphenyl ether (300 wt% *vs* the mass of the monomers) and supported CALB (20 wt% regarding the mass of the monomers) were then added. The solution was magnetically stirred and placed

at 90°C and 350 mbar. After 4 hours, the pressure was decreased to 100 mbar. After another 4 hours, the pressure was finally set to 20 mbar and was kept to this value until the end of the reaction.

*3.6.2. From ferulic-based diols (***PFAD^{I-II}***):*

The ferulic-based diol (150 mg) and diethyl adipate were placed in a Schlenck reactor in equimolar proportions. Acetophenone (300 wt% *vs* the mass of the monomers) and CALB (20 wt% regarding the mass of the monomers) were then added. The solution was magnetically stirred and placed at 90°C and 350 mbar. After 4 hours, the pressure was decreased to 250 mbar and was kept to this value until the end of the reaction.

3.6.3. Recovery of the polyesters:

The solution was diluted with chloroform (2 ml) and filtered through cotton wool to remove the catalyst. The polymer was then precipitated in a cold methanol bath under vigorous stirring. The solution was then centrifuged (8000 RCF, 10 min, 4 °C) and the supernatant was eliminated. Finally, the recovered polymer was dried for 24h in a vacuum oven at 40 °C before analysis.

4. Results and discussion

4.1. Polyesters based on ferulic diesters.

Various ferulic acid derivatives were synthesized and enzymatically polymerized. The first step has been to modify the ferulic acid to optimize its reactivity towards CALB. Indeed, CALB catalyzed polymerization results in faster kinetics and higher molar masses by transesterification with methyl or ethyl esters than by polycondensation (Vosmann *et al.*, 2008; Douka *et al.*, 2018; Kobayashi *et al.*, 2019). The small alcohol adduct in transesterification can easily be eliminated, compared to water, shifting the equilibrium of the reaction. Therefore, ferulic acid was first esterified to give methyl ferulate (**MeFA**) (confirmed by ^{1}H and ^{13}C NMR, see in Annexes Figure S.3.1 and Figure S.3.8). Ferulic acid is a bifunctional molecule able to undergo homopolymerization through polycondensation (Parthiban *et al.*, 2020). Homopolymers of ferulic acid give incredibly rigid polyesters with high T_g (Elias *et al.*, 1985) making them difficult to process because of their extreme melting temperature and difficulty to dissolve in common solvents. Besides, phenols, such as the one in methyl ferulate, have a lower reactivity compared to primary alcohols, especially in CALB-catalyzed transesterification (Christelle *et al.*, 2011; Sandoval *et al.*, 2015). For all these reasons, ferulic acid is often modified before polymerization (Kurt *et al.*, 2020; Llevot *et al.*, 2016; Nguyen *et al.*, 2015). This allows at the same time to fine-tune the properties of the monomer and those of the resulting polymer, especially of the chain rigidity. Methyl ferulate was thus modified through Williamson ether synthesis with chloroesters of different lengths (**DeFA^{I}** and **DeFA^{II}**) (Scheme 3.2). This process allowed to overcome the low reactivity of the methyl ferulate phenol group towards CALB. The structure of the obtained monomers was confirmed by ^{1}H and ^{13}C NMR (see in Annexes Figure S.3.2, Figure S.3.3, Figure S.3.9, and Figure S.3.10). The resulting products were diesters capable to undergo enzymatic transesterification with CALB.

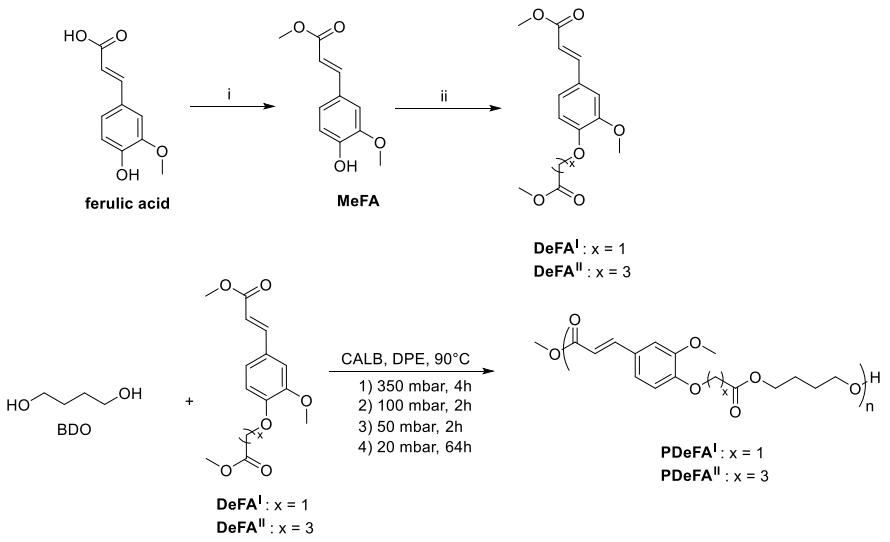

Scheme 3.2: Synthesis and polymerization of the ferulic diesters DeFA^{I} and DeFA^{II}, i: MeOH, H_2SO_4, 70 °C 16h. ii(a): Methyl chloroacetate, K_2CO_3, KI, acetonitrile, 85 °C 16h. ii(b): Methyl 4-chlorobutyrate, K_2CO_3, KI, acetonitrile, 85 °C 16h.

The obtained diesters were assayed for CALB-catalyzed polymerization with BDO in diphenyl ether under reduced pressure. The obtained products were then analyzed by ^{1}H NMR (Figure 3.1 and in Annexes Figure S.3.17 and Figure S.3.18).

The appearance of characteristic peaks (a-IV and b-IV on Figure 3.1) of the (C**H**$_2$-OC(O)) protons from esters between δ = 4.05 and 4.30 ppm confirms the transesterification of the methyl esters with BDO. For both monomers **DeFA^{I}** and **DeFA^{II}**, the intensity of the characteristic peaks of the methyl ester functions (respectively a-II, a-III on Figure 3.1 at δ = 3.72 ppm for **DeFA^{I}** and b-II at δ = 3.79 ppm and b-III at δ = 3.68 ppm on Figure 3.1 for **DeFA^{II}**) decreased after polymerization when compared with the starting material. This confirms that the methyl ester moieties were consumed during the reaction and therefore converted by CALB. However, the intensities of the end groups signals a-II, a-III, and b-II in the products are still important, indicating a low conversion of the monomer and consequently low molar mass chains. This was confirmed by SEC analysis (see Table 3.1 and in Annexes Figure S.3.23) that gave molar masses of 1 300 g.mol^{-1} and 2 000 g.mol^{-1} for **PDeFA^{I}** and **PDeFA^{II}**, respectively.

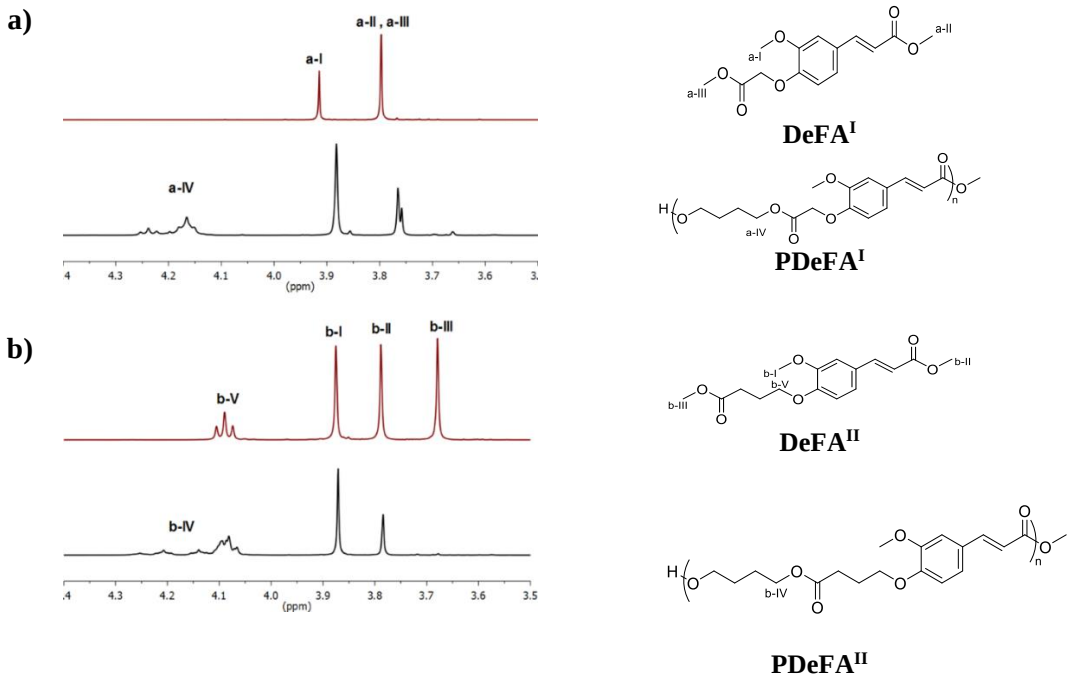

Figure 3.1: NMR spectra in $CDCl_3$ of the ferulic-based diesters and their corresponding polyesters: (a) $DeFA^I$ and $PDeFA^I$; (b) $DeFA^{II}$ and $PDeFA^{II}$.

The signals corresponding to the two esters of the ferulic diester **$DeFA^{II}$** can be distinguished and were unambiguously attributed thanks to 2D NMR (Figure 3.1 and in Annexes Figure S.3.15 and Figure S.3.16). The low intensity of the peak corresponding to the remaining terminal methyl of the methyl butyrate moiety (b-III) in the product suggests a quantitative conversion of this ester function. On the contrary, the intensity of the peak corresponding to the terminal protons of the ester neighboring the double bond (b-II) is only reduced by half after the reaction (Figure 3.1b and in Annexes Figure S.3.18). This suggests a lower conversion and thus a lower reactivity of this ester function towards CALB. This poorly reactive function could therefore rapidly become a terminal group at both ends of the growing chains and thus strongly limit their growth, leading to low molar masses.

The low reactivity of the ferulic acid and its corresponding ester towards CALB has already been described in the literature (Stamatis *et al.*, 1999; Cassani *et al.*, 2007; Zoumpanioti *et al.*, 2010) showing that *para* and *ortho* hydroxyl and methoxy substituents on the aromatic ring of coumaric derivatives had an inhibitory effect on the CALB activity in esterification and transesterification. Computational modeling performed by Otto et al. (Otto *et al.*, 2000) suggests that steric hindrance cannot explain this loss of reactivity towards specific substitutions and rather indicates that charge distribution could be the cause. We observe here that this lack of reactivity hindered the synthesis of high molar mass polyesters after 72 hours of reaction resulting in oligoesters with a DP_n up to 5.

4.2. Polyesters based on hydrogenated ferulic diesters.

The hydrogenation of the double bond has been shown to unlock the reactivity of ferulic acid (Cassani *et al.*, 2007; Zoumpanioti *et al.*, 2010). This method was previously used for the CALB-catalyzed synthesis of ferulic-based monomers (Pion *et al.*, 2013). It allowed a high conversion of the substrate in only 4 hours. We used a similar strategy to improve the reactivity of the studied monomers towards CALB but this time in a process of enzymatic polymerization.

The monomers **DeFA^{I}** and **DeFA^{II}** were hydrogenated using Pd/C as catalyst in ethanol to obtain **PH-DeFA^{I}** and **PH-DeFA^{II}**. The structure of the products was confirmed by ^{1}H and ^{13}C NMR (see in Annexes Figure S.3.4, Figure S.3.5, Figure S.3.11 and Figure S.3.12). They were then polymerized with BDO (Scheme 3.3). The reaction was monitored by SEC analysis of samples withdrawn at regular intervals (Figure 3.2).

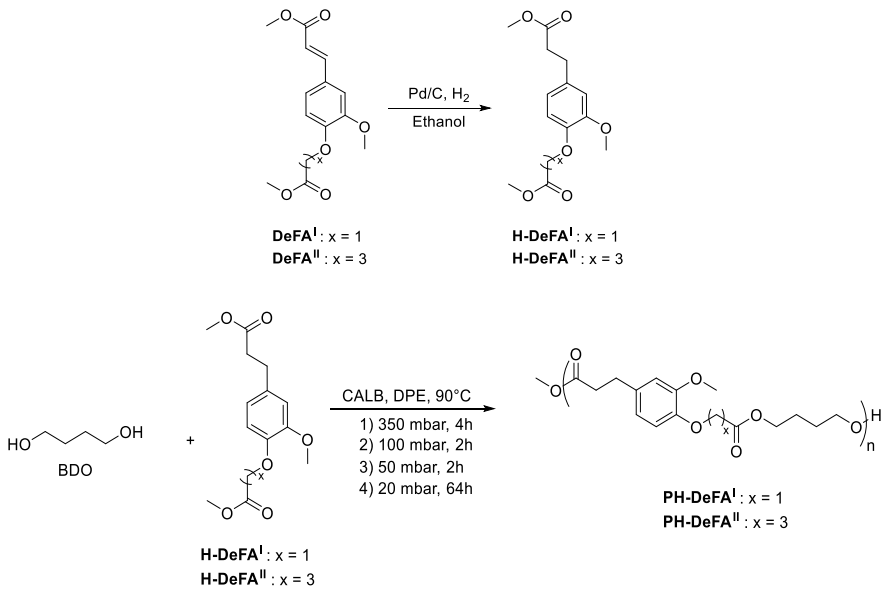

Scheme 3.3: Synthesis and polymerization of the hydrogenated ferulic diesters H-DeFA^{I} and H-DeFA^{II}.

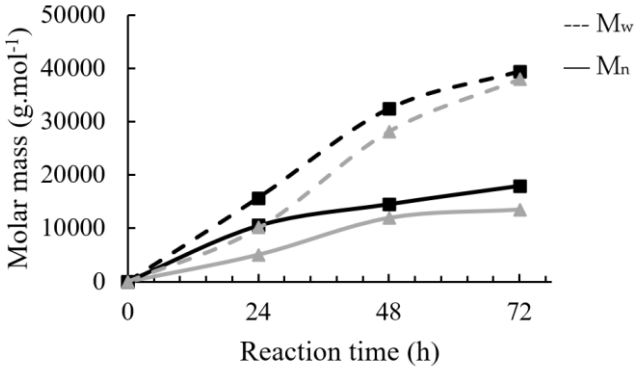

Figure 3.2: Molar mass of the polymers synthesized from the hydrogenated monomers. ■ PH-DeFA^{I}, ▲ PH-DeFA^{II}.

As expected, the reactivity of the ferulic moieties was greatly enhanced by hydrogenation. Quantitative conversion of the monomers 4a and 4b was observed from NMR analyses (in Annexes

Figure S.3.19 and Figure S.3.20). From NMR analysis of **PH-DeFA^{I}**, it is possible to distinguish the signal corresponding to the C**H**$_2$ of the diol linked to the ester vicinal to where was the double bond at δ = 4.19 ppm and the C**H**$_2$ of the diol linked to the ester coming from the Williamson ether synthesis at δ = 4.06 ppm. Both peaks have similar intensity, indicating that the diol has bound to both esters without distinction. This result would suggest that both esters have an equivalent reactivity towards CALB.

The polyesters **PH-DeFA^{I}** and **PH-DeFA^{II}** were obtained with high M_w of 39 400 g.mol^{-1} and 38 000 g.mol^{-1}, respectively, as measured by SEC (see in Annexes Figure S.3.24 and Table 3.1). It is interesting to notice that **PH-DeFA^{I}** systematically resulted in higher DP_n than **PH-DeFA^{II}** (58 for **PH-DeFA^{I}** compared to 37 for **PH-DeFA^{II}**). This result is counterintuitive and quite unexpected since previous studies showed that CALB presented a higher activity towards aliphatic monomers with a number of carbons higher than 4 (Mahapatro *et al.*, 2003; Debuissy *et al.*, 2017b; Pellis *et al.*, 2018). A higher reactivity of **H-DeFA^{II}** in comparison to **H-DeFA^{I}** would be expected as previous studies showed higher reactivity of the ester function with increasing distance from the bulky aromatic ring (Otto *et al.*, 2000). However, prediction of the enzyme activity cannot be only based on steric hindrance considerations because of the complex interactions with the substrate (Zoumpanioti *et al.*, 2010). The M_n of **PH-DeFA^{I}** (17 900 g.mol^{-1}) is comparable to values obtained for equivalent aliphatic polyesters enzymatically synthesized with HDO. However, the aromatic polyesters show lower DP_n compared to aliphatic ones because of the high molar mass of the ferulic-based diesters (58 for **H-DeFA^{I}** compared to 81-83 in the literature (Nasr *et al.*, 2020)).

Thus, the activity of CALB towards the ferulic-based diester was efficiently unlocked by hydrogenation of the double bond, leading to high molar mass polyesters. As depicted before, two main hypotheses could explain this result. First, the hydrogenation of the double bond lowers the rigidity of the molecule, facilitating its introduction and orientation in the active site of the enzyme. The second hypothesis is that the electronic conjugation between the ester and the aromatic ring is broken by the disappearance of the double bond. This conjugation could lower the reactivity of the ferulic esters (Otto *et al.*, 2000; Cassani *et al.*, 2007; Vosmann *et al.*, 2008). Indeed, because of its double bond, ferulic acid presents multiple resonance forms making it less prompt to nucleophilic attack from the serine amino acid of the CALB active site, hindering enzymatic activity.

The thermal properties of the obtained polyesters were assessed (Figure 3.3 and Table 3.1). Both polyesters **PH-DeFA^{I}** and **PH-DeFA^{II}** were fully amorphous with a T_g measured by DSC (Figure 3.3a) at 7 and - 9 °C, respectively. It is the first time these monomers are used for polymer synthesis and no similar structures, even synthesized by any other means than enzymatic catalysis, could be found in the literature for comparison. Polyesters **PH-DeFA^{I}** and **PH-DeFA^{II}** present low T_g in comparison to fully ferulic-based polyesters showing a T_g above 113 °C (Elias *et al.*, 1985). The hydrogenation of the monomer's double bond as well as the use of an aliphatic diol leads to a polymer structure with a lower T_g. However, when compared to fully aliphatic polyesters synthesized from BDO such as polybutylene

adipate (PBAd) or polybutylene succinate (PBS) (with a T_g of - 59 and -37 °C, respectively (Debuissy *et al.*, 2017b)), the use of the ferulic-based hydrogenated diester increased the T_g of the polyesters. These results are in agreement with previous studies showing that adding ferulic-based units to a polymeric structure leads to mostly amorphous materials with increased T_g (Kreye *et al.*, 2011; Barbara *et al.*, 2015). Finally, the polyester synthesized from methyl 4-chlorobutyrate-based diester (**PH-DeFA^{II}**) presents a lower T_g compared to the one based on methyl chloroacetate (**PH-DeFA^{I}**). Indeed, its longer aliphatic moiety induces more chain flexibility, reducing the T_g of the final polymer.

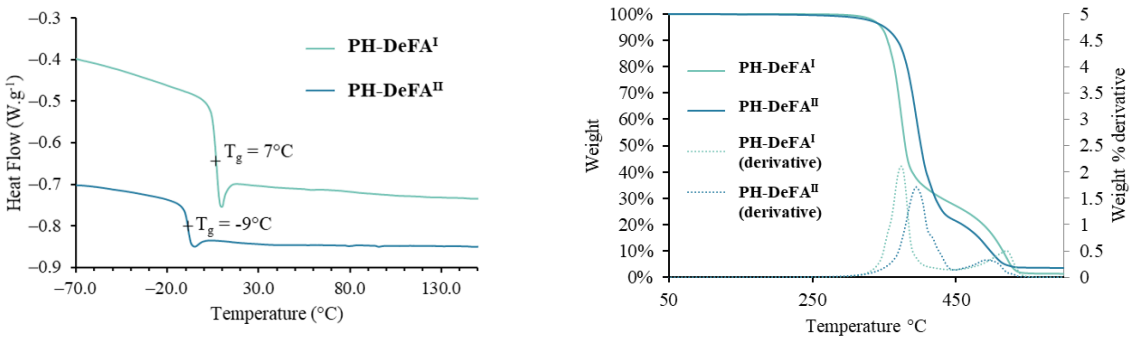

(a) **(b)**

Figure 3.3: Thermal analysis of PH-DeFA^{I} and PH-DeFA^{II}: (a) DSC measurement, heating rate 10 °C/min, data have been offset one from another by -0.5 W.g^{-1}; (b) TGA measurement, under air at a heating rate of 10 °C/min.

The polymers were also analyzed by TGA, and the weight loss curves are presented in Figure 3.3b. The temperature of degradation at the maximum rate (T_{dmax}) was measured at 373 °C and 394 °C for **PH-DeFA^{I}** and **PH-DeFA^{II}**, respectively. These values are within the range of those found for aliphatic polyesters such as PBAd and PBS (391 and 355 °C, respectively (Debuissy *et al.*, 2017b)). Interestingly, the degradation of both polyesters **PH-DeFA^{I}** and **PH-DeFA^{II}** occurred in two steps. This degradation pattern has already been observed in other aromatic polyesters such as PET (Oh *et al.*, 2006). The first step could correspond to the thermal degradation of the aliphatic parts of the polymer and correspond to the temperature of the ester bonds breaking. The aromatic parts get then reorganized into more thermally stable aromatic polycyclic ashes which get decomposed during the second step occurring at a much higher temperature.

4.3. Polyesters based on ferulic diols.

Another strategy of ferulic acid modification was evaluated. Reducing the methyl ferulate to its corresponding alcohol could offer a similar effect to hydrogenation. Indeed, after the reduction, the monomer gains a CH_2 and thus flexibility (Scheme 3.4), which could favor the accessibility of the molecule to the enzyme active site. Moreover, the alcohol resulting from the reduction would not be electronically conjugated to the aromatic ring. Additionally, along this synthesis path, the monomer

double bond is preserved, bringing rigidity to the chain backbone and allowing further modification of the polymer (Jawerth *et al.*, 2016; Parthiban *et al.*, 2020).

Both ferulic-based diesters previously synthesized (**DeFA^{I}** and **DeFA^{II}**) have been reduced to their corresponding diols by diisobutyl aluminum hydride (DIBAL-H). The structure of the monomers was confirmed by ^{1}H and ^{13}C NMR (see in Annexes Figure S.3.6, Figure S.3.7, Figure S.3.13 and Figure S.3.14). The monomers were then evaluated for the synthesis of polyesters via CALB-catalyzed polymerization as presented in Scheme 3.4. Diethyl adipate has been selected as a co-monomer since previous studies demonstrated its good reactivity with CALB, thus maximizing the chances of obtaining a high molar mass polyester (Mahapatro *et al.*, 2003; Debuissy *et al.*, 2017d).

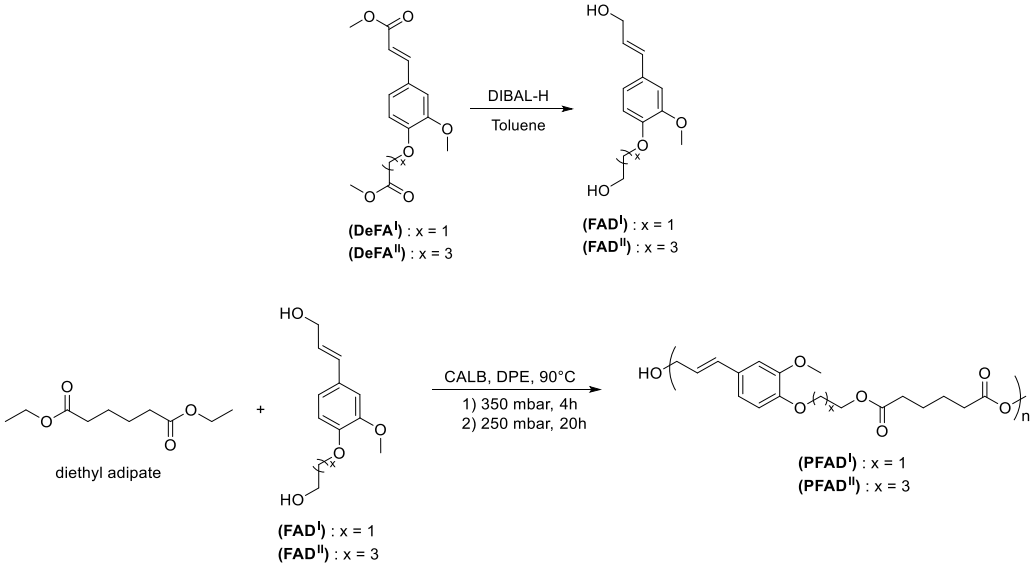

Scheme 3.4: Synthesis and polymerization of the ferulic-based diols FAD^{I} and FAD^{II}.

The obtained polyester **PFAD^{I}** and **PFAD^{II}** were analyzed by NMR (in Annexes Figure S.3.21 and Figure S.3.22) and SEC (in Annexes Figure S.3.25). The M_n of **PFAD^{I}** and **PFAD^{II}** determined by SEC after 24 hours were respectively of 6500 and 6300 g.mol^{-1} corresponding to a DP_n of 19 and 17. The two polyesters were obtained with similar molar masses and kinetics which is in agreement with the study by Pellis *et al.* (Pellis *et al.*, 2020) who showed that moving the hydroxyl group further away from the aromatic ring did not significantly alter the molar mass of the obtained polyesters. Longer times of polymerization did not increase the polymers molar masses. On the contrary, a decrease in M_n was even observed after 24h of reaction (Figure 3.4). Side reactions could be responsible for such a decrease in molar masses. To investigate this phenomenon and to understand more deeply the structure of the formed polymeric chains, the synthesized polyesters have been analyzed by MALDI-TOF MS.

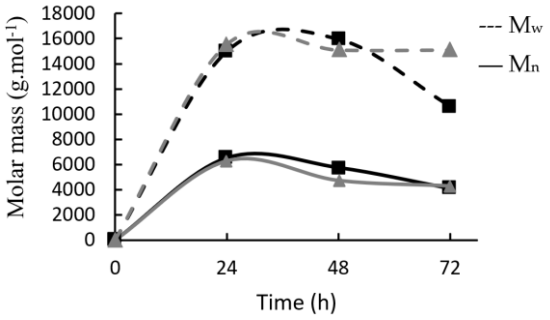

Figure 3.4: Molar masses of the polyesters synthesized from the ferulic-based diols. ■ PFAD^{I}, ▲ PFAD^{II}.

a)

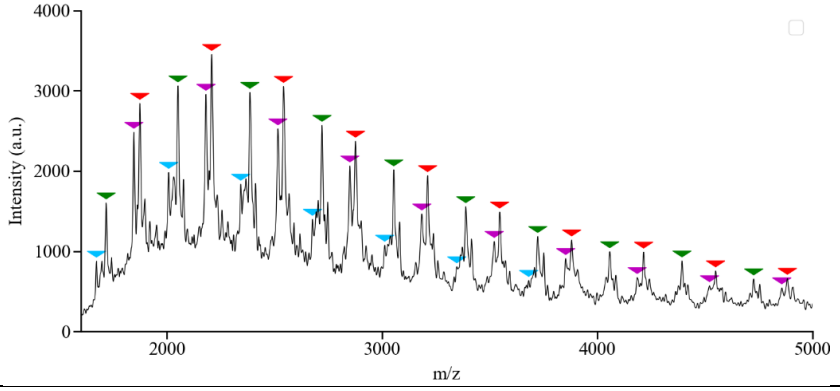

b)

Structure	End-group description	Residual mass (m/z)	Symbol
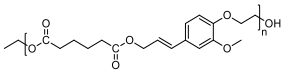	Ester and OH	46	▼
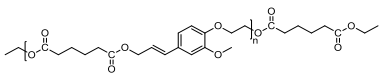	Both ester	202	▼
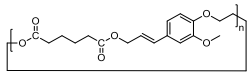	Macrocycles	0	▼
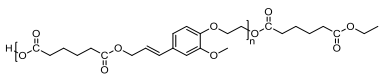	Hydrolysis	174	▼

Figure 3.5: (a) MALDI-TOF MS spectrum of PFAD^{I}; (b) corresponding identified polymer structures.

Although the large polydispersity of the polymer does not allow obtaining quantitative results from the MALDI-TOF MS (Rashidzadeh *et al.*, 1998), it is possible to qualitatively compare the end groups with each other. A large number of polymeric chains are ended with both an ester and a hydroxyl group (green triangles in Figure 3.5a). This is expected due to the one-to-one stoichiometry of the monomers. However, a significant proportion of polymeric chains are terminated on both ends by an ester group (red triangles in Figure 3.5a). This result indicates an unbalanced stoichiometry in the reaction medium with an excess of the diester. Side reactions involving one of the monomers could result in its deactivation or loss of reactivity and thus unbalance the stoichiometry of the reaction. However, no obvious traces of side products could be found on the NMR analyses. Moreover, reacting the diol alone with and without CALB in presence of ethanol did not allow to clearly identify any side product from **FAD^{I}**. Using an excess of diol resulted in polymers with a majority of chains terminated

with both an ester and a hydroxyl group (in Annexes Figure S.3.26). However, the polymer presented similar or lower molar masses (in Annexes Figure S.3.27) than for the synthesis with a stoichiometric ratio. The end group analysis also showed traces of hydrolysis with chains ended with both an acid and an ester, resulting in a residue m/z equal to 174 (purple triangles in Figure 3.5a). This phenomenon could also explain the end of chain growth followed by the slight decrease in molar masses (Figure 3.4). Finally, macrocycles were detected and although they were present in lower amount compared to other end groups, they could also contribute to lowering the apparent molar mass determined by SEC.

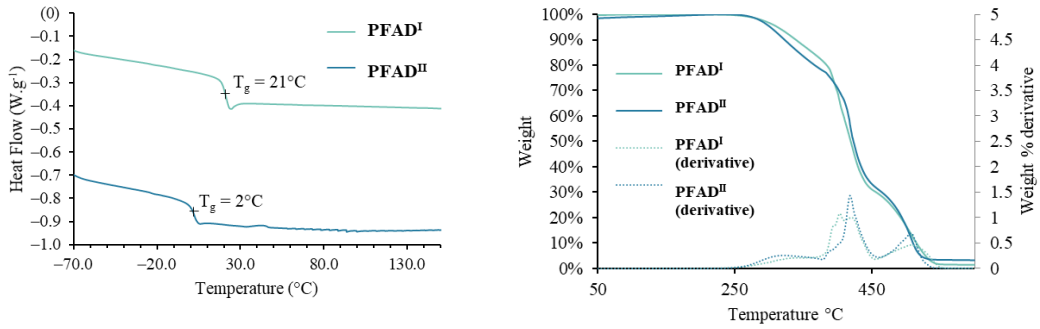

(a) **(b)**

Figure 3.6: Thermal analysis of PFAD^{I} and PFAD^{II}: (a) DSC measurement, heating rate 10 °C/min, data have been offset one from another by -0.5 W.g^{-1}; (b) TGA measurement, under air at a heating rate of 10 °C/min.

The thermal properties of the polyesters have then been assessed by DSC and TGA (Figure 3.6 and Table 3.1). The T_g of **PFAD^{I}** and **PFAD^{II}** were measured at 21 °C and 2 °C, respectively. Once again, the materials synthesized are fully amorphous and therefore present no melting or crystallization temperatures. However, despite a lower molar mass, polyester **PFAD^{I}** presents the highest T_g when compared with all other polymers from this study. As expected, the preservation of the double bond resulted in a more rigid polymeric backbone and therefore a higher T_g. This observation is in agreement with recent results from Prezzana *et al.* (Pezzana *et al.*, 2021). The diol originating from methyl 4-chlorobutyrate (**FAD^{II}**) gives a polyester with lower T_g compared to the diol obtained from methyl chloroacetate (**FAD^{I}**). Again, the longer aliphatic chain of monomer **FAD^{II}** decreases the T_g of the resulting polyester **PFAD^{II}**. The T_g of this polyester was even lower than the T_g measured for polyesters synthesized from the methyl 4-chlorobutyrate hydrogenated-based diester (**PH-DeFA^{II}**). However, these results are not fully comparable since in **PFAD^{II}** the aromaticity is brought by the diol when in **PH-DeFA^{II}** it comes from the diester. Thus, these polyesters present aliphatic comonomers (BDO and DEA) which are not directly comparable, and which could have an impact on the thermal transitions of the final material.

Table 3.1: Main properties of the enzymatically synthesized polyesters.

Ferulic-based monomer	Comonomer	Yield[a]	M_n (g.mol^{-1})	M_w (g.mol^{-1})	DP_n	T_g (°C)	T_{dmax} (°C)	$T_{d5\%}$ (°C)
(DeFA^{I}) 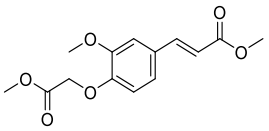	BDO	n.d.[b]	1 300	1 600	4	n.d.[b]	n.d.[b]	n.d.[b]
(DeFA^{II}) 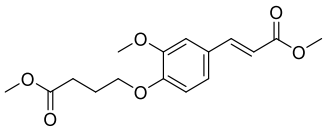	BDO	n.d.[b]	2 000	2 500	5	n.d.[b]	n.d.[b]	n.d.[b]
(H-DeFA^{I}) 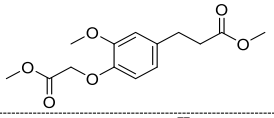	BDO	58 %	17 900	38 000	58	7	373	346
(H-DeFA^{II}) 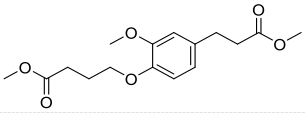	BDO	96 %	13 600	39 400	37	- 9	394	350
(FAD^{I}) 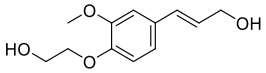	DEA	82 %	6 500	15 000	19	21	403	316
(FAD^{II}) 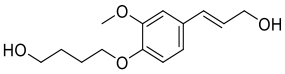	DEA	79 %	6 300	15 500	17	2	418	308

[a] Recovered mass yield taking into account the loss of methanol or ethanol during the reaction.
[b] Not determined as only low molar mass oligomers were obtained.

The thermal degradation of **PFAD^{I}** and **PFAD^{II}** was measured by TGA. A similar degradation behavior was observed for both polymers. When compared with **PH-DeFA^{I}** and **PH-DeFA^{II}**, the degradation begins at lower temperatures with a $T_{d5\%}$ of only 316 and 308 °C for **PFAD^{I}** and **PFAD^{II}**, respectively. This early degradation could be due to the presence of the double bond of the α,β-unsaturated alcohol (coniferyl). It is known to form by-products such as aldehydes through radical pathways during thermal degradation (Masuku, 1992). The degradation of the polymers appears as three steps with maximum rates of degradation at 343, 403, and 506 °C for **PFAD^{I}** and 321, 418, and 507 °C for **PFAD^{II}**. As depicted before, the first step of degradation could correspond to the degradation linked to the presence of coniferyl alcohol moieties. The second degradation step is the fastest and is in the temperature range of degradation of aliphatic polyesters. The final degradation step corresponds to the aromatic part of the polyesters that only get fully degraded above 530 °C, as observed for the previous polymers.

5. Conclusions

In this study, several various monomers derived from ferulic acid were synthesized and tested for CALB-catalyzed polymerization. First, ferulic acid was converted into a long and a short diester. With both substrates, only partial monomer conversion by CALB was observed, resulting in low molar mass oligomers. This observation was in good agreement with studies in the literature pointing the α,β-unsaturation as responsible for the lack of reactivity of ferulic compounds. Thus, α,β-unsaturation of the monomers was eliminated by hydrogenation prior to their assessment for CALB-catalyzed polymerization. The hydrogenation of the monomers allowed the synthesis of polyesters with the highest molar masses in this study, with M_w up to 33 100 g.mol^{-1} for the shorter diester (**H-DeFA^{I}**). The M_n of the polyester (17 900 g.mol^{-1}) is comparable to values obtained for equivalent fully aliphatic polyesters synthesized by CALB-catalyzed polymerization. However, lower DP_n (58 for **H-DeFA^{I}**) were obtained with aromatic monomers when compared to aliphatic ones (81-83 (Nasr *et al.*, 2020)) due to the high molar mass of the ferulic-based diester monomer. Moreover, hydrogenation of the ferulic-based monomers led to polymer T_g up to 7°C, below ambient temperature. Another strategy used in this study was the reduction of the ferulic diesters into their corresponding diols. The polyesters synthesized from the reduced monomers resulted in M_w up to 15 500 g.mol^{-1}. However, the presence of side reactions (hydrolysis, cyclization) was observed in the medium, explaining the lower molar mass obtained when compared to the hydrogenated monomers. However, in line with existing literature, it has been shown that preserving the monomer double bond, as in the reduction of the ferulic diesters, stiffens the polymer chain backbone, resulting in higher T_g (up to 21 °C). However, although the presence of the double bond increases the T_g of the polymer, it could constitute its weak point during thermal degradation, resulting in an early thermal degradation when compared with the other polyesters.

This study constitutes a first step in understanding the optimal condition for the CALB-catalyzed synthesis of ferulic-based aromatic polyesters. Other modifications of ferulic acid as well as the combination of the previously synthesized monomers with other comonomers will be investigated. Indeed, such monomers could give access to biobased polymers with innovative properties that could challenge conventional petroleum-based materials.

Moreover, the enzymatic degradation of the polymers produced in this study could be investigated in order to reduce their end-of-life environmental impact through recycling (Tournier *et al.*, 2020; Devi Salam *et al.*, 2021). Indeed, several studies focused on the CALB-catalyzed depolymerization of polyesters (Carniel *et al.*, 2017; Magnin *et al.*, 2021). This could allow both the synthesis and recycling of ferulic-based polyester using the same enzyme.

6. References

Albanese, M.; Boyenval, J.; Marchese, P.; Sullalti, S.; Celli, A. The Aliphatic Counterpart of PET, PPT and PBT Aromatic Polyesters: Effect of the Molecular Structure on Thermo-Mechanical Properties. *AIMS Mol. Sci.* **2016**, *3*, 32–51, doi:10.3934/molsci.2016.1.32.

Barbara, I., Flourat, A. L. and Allais, F. (**2015**) 'Renewable polymers derived from ferulic acid and biobased diols via ADMET', *European Polymer Journal*, 62, pp. 236–243.

Bazin, A., Avérous, L. and Pollet, E. (**2021**)**b** 'Lipase-catalyzed synthesis of furan-based aliphatic-aromatic biobased copolyesters: Impact of the solvent', *European Polymer Journal*, 159, p. 110717.

Carniel, A., Valoni, É., Nicomedes, J., Gomes, A. da C. and Castro, A. M. de (**2017**) 'Lipase from Candida antarctica (CALB) and cutinase from Humicola insolens act synergistically for PET hydrolysis to terephthalic acid', *Process Biochemistry*, 59, pp. 84–90.

Cassani, J.; Luna, H.; Navarro, A.; Castillo, E. Comparative Esterification of Phenylpropanoids versus Hydrophenylpropanoids Acids Catalyzed by Lipase in Organic Solvent Media. *Electron. J. Biotechnol.* **2007**, *10*, 508–513, doi:10.2225/vol10-issue4-fulltext-3.

Christelle, B., Eduardo, B. D. O., Latifa, C., Elaine-Rose, M., Bernard, M., Evelyne, R.-H., Mohamed, G., Jean-Marc, E. and Catherine, H. (**2011**) 'Combined docking and molecular dynamics simulations to enlighten the capacity of Pseudomonas cepacia and Candida antarctica lipases to catalyze quercetin acetylation', *Journal of Biotechnology*, 156(3), pp. 203–210.

Comerford, J. W., Byrne, F. P., Weinberger, S., Farmer, T. J., Guebitz, G. M., Gardossi, L. and Pellis, A. (**2020**) 'Thermal Upgrade of Enzymatically Synthesized Aliphatic and Aromatic Oligoesters', *Materials*, 13(2), p. 368.

Crozier, A., Jaganath, I. B. and Clifford, M. N. (**2006**) 'Phenols, Polyphenols and Tannins: An Overview', in Crozier, A., Clifford, M. N., and Ashihara, H. (eds) *Plant Secondary Metabolites*. Oxford, UK: Blackwell Publishing Ltd, pp. 1–24.

Debuissy, T., Pollet, E. and Avérous, L. (**2017**)**a** 'Enzymatic synthesis of biobased poly(1,4-butylene succinate- ran -2,3-butylene succinate) copolyesters and characterization. Influence of 1,4- and 2,3-butanediol contents', *European Polymer Journal*, 93, pp. 103–115.

Debuissy, T., Pollet, E. and Avérous, L. (**2017**)**b** 'Lipase-catalyzed synthesis of biobased and biodegradable aliphatic copolyesters from short building blocks. Effect of the monomer length', *European Polymer Journal*, 97, pp. 328–337.

Debuissy, T., Sangwan, P., Pollet, E. and Avérous, L. (**2017**)**d** 'Study on the structure-properties relationship of biodegradable and biobased aliphatic copolyesters based on 1,3-propanediol, 1,4-butanediol, succinic and adipic acids', *Polymer*, 122, pp. 105–116.

Delidovich, I., Hausoul, P. J. C., Deng, L., Pfützenreuter, R., Rose, M. and Palkovits, R. (**2016**) 'Alternative Monomers Based on Lignocellulose and Their Use for Polymer Production', *Chemical Reviews*, 116(3), pp. 1540–1599.

Devi Salam, M., Varma, A., Prashar, R. and Choudhary, D. (**2021**) 'Review on Efficacy of Microbial Degradation of Polyethylene Terephthalate and Bio-upcycling as a Part of Plastic Waste Management', *Applied Ecology and Environmental Sciences*, 9(7), pp. 695–703.

Douka, A., Vouyiouka, S., Papaspyridi, L.-M. and Papaspyrides, C. D. (**2018**) 'A review on enzymatic polymerization to produce polycondensation polymers: The case of aliphatic polyesters, polyamides and polyesteramides', *Progress in Polymer Science*, 79, pp. 1–25.

Duchiron, S. W., Pollet, E., Givry, S. and Avérous, L. (**2017**) 'Enzymatic synthesis of poly(ε-caprolactone- co -ε-thiocaprolactone)', *European Polymer Journal*, 87, pp. 147–158.

Elias, H.-G. and Palacios, J. A. (**1985**) 'Poly(ferulic acid) by Thionyl Chloride Activated Polycondensation', *Die Makromolekulare Chemie*, 186(5), pp. 1027–1045.

Figueroa-Espinoza, M. C., Laguerre, M., Villeneuve, P. and Lecomte, J. (**2013**) 'From phenolics to phenolipids: Optimizing antioxidants in lipid dispersions', *Lipid Technology*, 25(6), pp. 131–134.

Flores, I., Martínez de Ilarduya, A., Sardon, H., Müller, A. J. and Muñoz-Guerra, S. (**2019**) 'Synthesis of Aromatic–Aliphatic Polyesters by Enzymatic Ring Opening Polymerization of Cyclic Oligoesters and their Cyclodepolymerization for a Circular Economy', *ACS Applied Polymer Materials*, 1(3), pp. 321–325.

Flourat, A. L., Combes, J., Bailly-Maitre-Grand, C., Magnien, K., Haudrechy, A., Renault, J. and Allais, F. (**2021**) 'Accessing *p* -Hydroxycinnamic Acids: Chemical Synthesis, Biomass Recovery, or Engineered Microbial Production?', *ChemSusChem*, 14(1), pp. 118–129.

Jawerth, M., Lawoko, M., Lundmark, S., Perez-Berumen, C. and Johansson, M. (**2016**) 'Allylation of a lignin model phenol: a highly selective reaction under benign conditions towards a new thermoset resin platform', *RSC Advances*, 6(98), pp. 96281–96288.

John, G., Nagarajan, S., Vemula, P. K., Silverman, J. R. and Pillai, C. K. S. (**2019**) 'Natural monomers: A mine for functional and sustainable materials – Occurrence, chemical modification and polymerization', *Progress in Polymer Science*, 92, pp. 158–209.

Kobayashi, S. and Uyama, H. (**2019**) 'Synthesis of Polyesters I: Hydrolase as Catalyst for Polycondensation (Condensation Polymerization)', in Kobayashi, S., Uyama, H., and Kadokawa, J. (eds) *Enzymatic Polymerization towards Green Polymer Chemistry*. Singapore: Springer Singapore (Green Chemistry and Sustainable Technology), pp. 105–163.

Kreye, O., Tóth, T. and Meier, M. A. R. (**2011**) 'Copolymers derived from rapeseed derivatives via ADMET and thiol-ene addition', *European Polymer Journal*, 47(9), pp. 1804–1816.

Kurt, G. and Gokturk, E. (**2020**) 'Synthesis of polyesters mimicking polyethylene terephthalate and their thermal and mechanical properties', *Journal of Polymer Research*, 27(10), p. 314.

Li, M. and Wilkins, M. (**2021**) 'Lignin bioconversion into valuable products: fractionation, depolymerization, aromatic compound conversion, and bioproduct formation', *Systems Microbiology and Biomanufacturing*, 1(2), pp. 166–185.

Li, Q., Ma, S., Xu, X. and Zhu, J. (**2019**) 'Bio-based Unsaturated Polyesters', in *Unsaturated Polyester Resins*. Elsevier, pp. 515–555.

Llevot, A., Grau, E., Carlotti, S., Grelier, S. and Cramail, H. (**2016**) 'From Lignin-derived Aromatic Compounds to Novel Biobased Polymers', *Macromolecular Rapid Communications*, 37(1), pp. 9–28.

Loos, K., Zhang, R., Pereira, I., Agostinho, B., Hu, H., Maniar, D., Sbirrazzuoli, N., Silvestre, A. J. D., Guigo, N. and Sousa, A. F. (**2020**) 'A Perspective on PEF Synthesis, Properties, and End-Life', *Frontiers in Chemistry*, 8, p. 585.

Magnin, A., Entzmann, L., Bazin, A., Pollet, E. and Avérous, L. (**2021**) 'Green Recycling Process for Polyurethane Foams by a Chem-Biotech Approach', *ChemSusChem*, 14(19), pp. 4234–4241.

Mahapatro, A., Kalra, B., Kumar, A. and Gross, R. A. (**2003**) 'Lipase-Catalyzed Polycondensations: Effect of Substrates and Solvent on Chain Formation, Dispersity, and End-Group Structure', *Biomacromolecules*, 4(3), pp. 544–551.

Mancuso, C. and Santangelo, R. (**2014**) 'Ferulic acid: Pharmacological and toxicological aspects', *Food and Chemical Toxicology*, 65, pp. 185–195.

Mandal, S. and Dey, A. (**2019**) 'PET Chemistry', in *Recycling of Polyethylene Terephthalate Bottles*. Elsevier, pp. 1–22.

Masuku, C. P. (**1992**) 'Thermolytic decomposition of coniferyl alcohol', *Journal of Analytical and Applied Pyrolysis*, 23(2), pp. 195–208.

Ménard, R., Caillol, S. and Allais, F. (**2017**)**a** 'Chemo-Enzymatic Synthesis and Characterization of Renewable Thermoplastic and Thermoset Isocyanate-Free Poly(hydroxy)urethanes from Ferulic Acid Derivatives', *ACS Sustainable Chemistry & Engineering*, 5(2), pp. 1446–1456.

Ménard, R., Caillol, S. and Allais, F. **(2017)b** 'Ferulic acid-based renewable esters and amides-containing epoxy thermosets from wheat bran and beetroot pulp: Chemo-enzymatic synthesis and thermo-mechanical properties characterization', *Industrial Crops and Products*, 95, pp. 83–95.

Nasr, K., Meimoun, J., Favrelle-Huret, A., Winter, J. D., Raquez, J.-M. and Zinck, P. (**2020**) 'Enzymatic Polycondensation of 1,6-Hexanediol and Diethyl Adipate: A Statistical Approach Predicting the Key-Parameters in Solution and in Bulk', *Polymers*, 12(9), p. 1907.

Nguyen, H. T. H., Qi, P., Rostagno, M., Feteha, A. and Miller, S. A. (**2018**) 'The quest for high glass transition temperature bioplastics', *Journal of Materials Chemistry A*, 6(20), pp. 9298–9331.

Nguyen, H. T. H., Reis, M. H., Qi, P. and Miller, S. A. (**2015**) 'Polyethylene ferulate (PEF) and congeners: polystyrene mimics derived from biorenewable aromatics', *Green Chemistry*, 17(9), pp. 4512–4517.

Nguyen, H. T. H., Short, G. N., Qi, P. and Miller, S. A. (**2017**) 'Copolymerization of lactones and bioaromatics via concurrent ring-opening polymerization/polycondensation', *Green Chemistry*, 19(8), pp. 1877–1888.

Oh, S.-C.; Lee, D.-G.; Kwak, H.; Bae, S.-Y. Combustion Kinetics Of Polyethylene Terephthalate. *Environ. Eng. Res.* **2006**, *11*, 250–256, doi:10.4491/eer.2006.11.5.250.

Ortiz, C., Ferreira, M. L., Barbosa, O., dos Santos, J. C. S., Rodrigues, R. C., Berenguer-Murcia, Á., Briand, L. E. and Fernandez-Lafuente, R. (**2019**) 'Novozym 435: the "perfect" lipase immobilized biocatalyst?', *Catalysis Science & Technology*, 9(10), pp. 2380–2420.

Otto, R. T., Scheib, H., Bornscheuer, U. T., Pleiss, J., Syldatk, C. and Schmid, R. D. (**2000**) 'Substrate specificity of lipase B from Candida antarctica in the synthesis of arylaliphatic glycolipids', *Journal of Molecular Catalysis B: Enzymatic*, 8(4–6), pp. 201–211.

Ouimet, M. A., Griffin, J., Carbone-Howell, A. L., Wu, W.-H., Stebbins, N. D., Di, R. and Uhrich, K. E. (**2013**) 'Biodegradable Ferulic Acid-Containing Poly(anhydride-ester): Degradation Products with Controlled Release and Sustained Antioxidant Activity', *Biomacromolecules*, 14(3), pp. 854–861.

Parthiban, A. and Vasantha, V. A. (**2020**) 'Biorenewable functional oligomers and polymers – Direct copolymerization of ferulic acid to obtain polymeric UV absorbers and multifunctional materials', *Polymer*, 188, p. 122122.

Pellis, A., Comerford, J. W., Maneffa, A. J., Sipponen, M. H., Clark, J. H. and Farmer, T. J. (**2018**) 'Elucidating enzymatic polymerisations: Chain-length selectivity of Candida antarctica lipase B towards various aliphatic diols and dicarboxylic acid diesters', *European Polymer Journal*, 106, pp. 79–84.

Pellis, A., Herrero Acero, E., Gardossi, L., Ferrario, V. and Guebitz, G. M. (**2016**)**b** 'Renewable building blocks for sustainable polyesters: new biotechnological routes for greener plastics: Renewable building blocks for sustainable polyesters', *Polymer International*, 65(8), pp. 861–871.

Pellis, A., Nyanhongo, G. S. and Farmer, T. J. (**2019**)**c** 'Recent Advances on Enzymatic Catalysis as a Powerful Tool for the Sustainable Synthesis of Bio-Based Polyesters', in Bastidas-Oyanedel, J.-R. and Schmidt, J. E. (eds) *Biorefinery*. Cham: Springer International Publishing, pp. 555–570.

Pellis, A., Weinberger, S., Gigli, M., Guebitz, G. M. and Farmer, T. J. (**2020**) 'Enzymatic synthesis of biobased polyesters utilizing aromatic diols as the rigid component', *European Polymer Journal*, 130, p. 109680.

Pezzana, L., Mousa, M., Malmström, E., Johansson, M. and Sangermano, M. (**2021**) 'Bio-based monomers for UV-curable coatings: allylation of ferulic acid and investigation of photocured thiol-ene network', *Progress in Organic Coatings*, 150, p. 105986.

Pion, F., Ducrot, P.-H. and Allais, F. (**2014**) 'Renewable Alternating Aliphatic-Aromatic Copolyesters Derived from Biobased Ferulic Acid, Diols, and Diacids: Sustainable Polymers with Tunable Thermal Properties', *Macromolecular Chemistry and Physics*, 215(5), pp. 431–439.

Pion, F., Reano, A. F., Ducrot, P.-H. and Allais, F. (**2013**) 'Chemo-enzymatic preparation of new bio-based bis- and trisphenols: new versatile building blocks for polymer chemistry', *RSC Advances*, 3(23), p. 8988.

Pospiech, D., Korwitz, A., Komber, H., Jehnichen, D., Arnhold, K., Brünig, H., Scheibner, H., Müller, M. T. and Voit, B. (**2021**) 'Polyesters with bio-based ferulic acid units: crosslinking paves the way to property consolidation', *Polymer Chemistry*, 12(36), pp. 5139–5148.

Rashidzadeh, H. and Guo, B. (**1998**) 'Use of MALDI-TOF To Measure Molecular Weight Distributions of Polydisperse Poly(methyl methacrylate)', *Analytical Chemistry*, 70(1), pp. 131–135.

Rovira, J., Nadal, M., Schuhmacher, M. and Domingo, J. L. (**2015**) 'Human exposure to trace elements through the skin by direct contact with clothing: Risk assessment', *Environmental Research*, 140, pp. 308–316.

Sandoval, G., Quintana, P. G., Baldessari, A., Ballesteros, A. O. and Plou, F. J. (**2015**) 'Lipase-catalyzed preparation of mono- and diesters of ferulic acid', *Biocatalysis and Biotransformation*, 33(2), pp. 89–97.

Satti, S. M. and Shah, A. A. (**2020**) 'Polyester-Based Biodegradable Plastics: An Approach Towards Sustainable Development', *Letters in Applied Microbiology*.

Skoczinski, P., Espinoza Cangahuala, M. K., Maniar, D., Albach, R. W., Bittner, N. and Loos, K. (**2020**) 'Biocatalytic Synthesis of Furan-Based Oligomer Diols with Enhanced End-Group Fidelity', *ACS Sustainable Chemistry & Engineering*, 8(2), pp. 1068–1086.

Stamatis, H., Sereti, V. and Kolisis, F. N. (**1999**) 'Studies on the enzymatic synthesis of lipophilic derivatives of natural antioxidants', *Journal of the American Oil Chemists' Society*, 76(12), p. 1505.

Terrett, O. M. and Dupree, P. (**2019**) 'Covalent interactions between lignin and hemicelluloses in plant secondary cell walls', *Current Opinion in Biotechnology*, 56, pp. 97–104.

Tinikul, R., Chenprakhon, P., Maenpuen, S. and Chaiyen, P. (**2018**) 'Biotransformation of Plant-Derived Phenolic Acids', *Biotechnology Journal*, p. 1700632.

Todea, A., Dreavă, D. M., Benea, I. C., Bîtcan, I., Peter, F. and Boeriu, C. G. (**2021**) 'Achievements and Trends in Biocatalytic Synthesis of Specialty Polymers from Biomass-Derived Monomers Using Lipases', *Processes*, 9(4), p. 646.

Tournier, V., Topham, C. M., Gilles, A., David, B., Folgoas, C., Moya-Leclair, E., Kamionka, E., Desrousseaux, M.-L., Texier, H., Gavalda, S., Cot, M., Guémard, E., Dalibey, M., Nomme, J., Cioci, G., Barbe, S., Chateau, M., André, I., Duquesne, S. and Marty, A. (**2020**) 'An engineered PET depolymerase to break down and recycle plastic bottles', *Nature*, 580(7802), pp. 216–219.

Vosmann, K., Wiege, B., Weitkamp, P. and Weber, N. (**2008**) 'Preparation of lipophilic alkyl (hydroxy)benzoates by solvent-free lipase-catalyzed esterification and transesterification', *Applied Microbiology and Biotechnology*, 80(1), pp. 29–36.

Zoumpanioti, M., Merianou, E., Karandreas, T., Stamatis, H. and Xenakis, A. (**2010**) 'Esterification of phenolic acids catalyzed by lipases immobilized in organogels', *Biotechnology Letters*, 32(10), pp. 1457–1462.

Conclusion chapitre 3

Dans ce chapitre, l'utilisation de l'acide férulique a été étudiée pour la synthèse de polyesters aromatiques par catalyse enzymatique. Cette molécule plateforme biosourcée présente une fonctionnalité qui permet sa modification via des réactions rapides et quantitatives. Des diesters de plusieurs longueurs ont ainsi été synthétisés à partir d'acide férulique. Cette étude a mis en exergue la faible réactivité de l'ester vicinal de la double liaison des différents monomères féruliques. Celle-ci est en adéquation avec les observations rapportées dans la littérature et énoncées au chapitre 1. L'obtention d'oligomères de faibles masses molaires a ainsi été directement attribuée à ce manque de réactivité.

Afin de maximiser la réactivité des diesters d'acide férulique, deux stratégies ont été employées, à savoir l'hydrogénation et la réduction. Supprimer la double liaison des diesters par hydrogénation permet d'améliorer la réactivité des monomères vis-à-vis de l'enzyme. Encore une fois, cette observation est en adéquation avec les résultats de la littérature exposés au chapitre 1. La réduction des diesters d'acide férulique en leurs diols correspondant a également permis l'obtention de polymères de masses molaires élevés tout en conservant la double liaison de l'acide férulique. Nous avons ainsi pu montrer que la rigidité apportée par cette double liaison conduisait à des polyesters aux températures de transitions vitreuses supérieures à celles obtenues dans le cas des monomères hydrogénés.

Toutefois, les polyesters obtenus à partir des diols issus de la réduction des diesters féruliques ont montré une résistance thermique réduite. De plus, l'hydrogénation et la réduction des dérivés d'acide féruliques nécessitent l'utilisation de réactifs inflammables et ne répondent pas au principe d'économie d'atome. Le développement de stratégies faisant appel à des conditions de synthèses plus vertes pour la modification de ces dérivés d'acide férulique en vue de leur utilisation en polymérisation enzymatique constitue donc une voie d'amélioration intéressante à investiguer.

Chapitre 4. Dimères de dérivés d'acide férulique pour la synthèse enzymatique de polyesters aromatiques photo-dégradables.

- **Sous-Chapitre 4.1 : Etude sur la dimérisation par irradiation UV de dérivés d'acide férulique.**
- **Sous-Chapitre 4.2 : Photo-dimerization of ferulic derivatives for the CALB catalyzed synthesis of biobased cleavable polyesters.**

Introduction chapitre 4

Le chapitre précédent a permis de mettre en lumière le fait que la double liaison de l'acide férulique (FA) joue un rôle crucial dans sa réactivité vis-à-vis de la CALB dans les réactions de polymérisation par (trans)estérification. La délocalisation électronique du carbonyle avec le cycle aromatique via la double liaison serait responsable de cette faible réactivité. La rupture de cette délocalisation par hydrogénation ou réduction du carbonyle a permis d'améliorer la réactivité du monomère vis à vis de CALB. Cependant, l'hydrogénation du FA nécessite l'utilisation d'un catalyseur au palladium, un métal noble onéreux. La réduction du FA nécessite quant à elle des catalyseurs organométalliques comme l'hydrure de diisobutylaluminium qui sont facilement inflammables.

Ce chapitre s'intéresse donc à une modification de la double liaison du FA via une réaction plus « verte », la cycloaddition [2+2]. Cette réaction, en plus de se faire à température ambiante, ne nécessite pas de catalyseur et est initiée par irradiation UV. Celle-ci entraine la dimérisation de la molécule, remplaçant la double liaison par un cyclobutane. La dimérisation du FA par cycloaddition [2+2] permettrait d'éliminer la délocalisation électronique de son carbonyle avec le cycle aromatique. Cette réaction pourrait alors potentiellement améliorer la réactivité du carbonyle vis-à-vis de la CALB comme le permet l'hydrogénation de la double liaison. Le dimère résultant de la cycloaddition [2+2] du FA est à la fois un diacide et un diphénol. Comme décrit précédemment, les phénols sont très peu réactifs vis-à-vis de la CALB. Le dimère de FA pourrait alors être considéré comme étant difonctionnel en polymérisation catalysée par la CALB et permettrait donc la synthèse de polyesters linéaires.

De plus, cette réaction de cycloaddition est réversible. Dans le cas des dérivés cinnamiques, la cycloaddition a lieu à une longueur d'onde $\lambda > 350$ nm. La réaction inverse peut alors être initiée à une longueur d'onde de plus haute énergie $\lambda = 254$ nm. Cette dernière entraine alors la scission du cyclobutane et la reformation des doubles liaisons d'origine. La synthèse de polyesters à base de dimères de FA permettrait ainsi d'inclure dans la chaine polymère des motifs répétitifs présentant des liaisons covalentes dynamiques. La rétrocyclisation des entités cyclobutanes entrainerait alors la scission des chaines polymères et une diminution de leur masse molaire. Cette dépolymérisation par les UV pourrait alors être une première étape de recyclage chimique de ces polyesters aromatiques.

Ce chapitre est découpé en deux sous-chapitres avec le second qui est présenté sous forme d'une publication :

- Le sous-chapitre 4.1 présente l'étude de la réactivité de plusieurs dérivés cinnamiques. Certains de ces dérivés ont déjà été décrits dans la littérature et les autres ont été synthétisés dans le cadre de cette thèse. La capacité donner lieu à une cycloaddition ou une isomérisation a été étudiée pour ces différents composés.
- Le sous-chapitre 4.2 présente tout d'abord l'optimisation de la cycloaddition des composés réactifs identifiés dans le sous-chapitre précédent. Il s'intéresse ensuite à

la polymérisation enzymatique du dimère de diester de FA en combinaison avec des diols de différentes longueurs (1,3-propanediol, 1,4-butanediol, 1,6-hexanediol et 1,8-octanediol). Ce sous-chapitre est présenté sous la forme d'une publication intitulée 'Photo-dimerization of ferulic derivatives for the CALB catalyzed synthesis of biobased cleavable polyesters'.

Sous-chapitre 4.1. Etude sur la dimérisation par irradiation UV de dérivés d'acide férulique

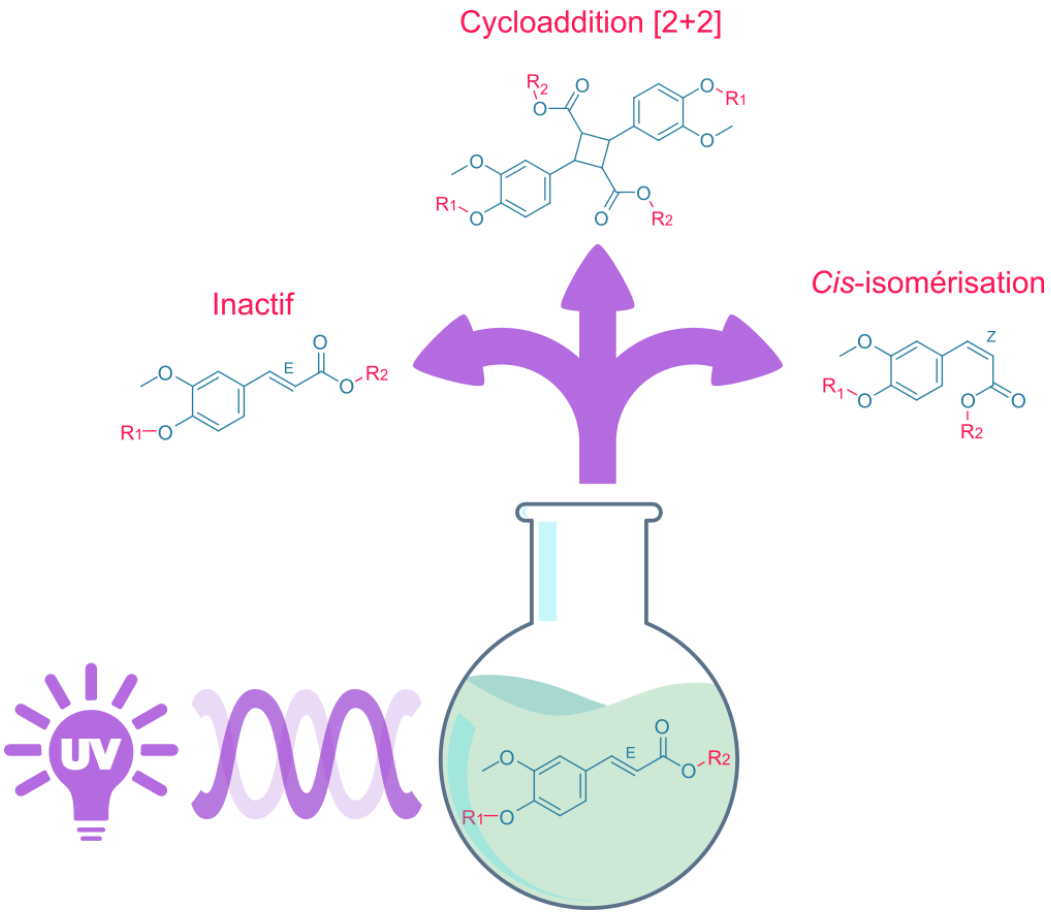

1. Introduction :

Comme exposé dans les chapitres 1 et 3, les dérivés cinnamiques sont présents dans la paroi cellulaire de nombreux végétaux. Ces dérivés, et notamment l'acide férulique (**FA**), participent au renforcement de l'hémicellulose en agissant comme point de réticulation entre les chaines polysaccharides (xylane et arabinoxylane) ou entre les chaines polysaccharides et la lignine (Grabber *et al.*, 2000; Hatfield *et al.*, 2017; Bento-Silva *et al.*, 2018; Terrett *et al.*, 2019). Ils protègent également la plante contre certains parasites (Santiago *et al.*, 2010). Ces nœuds de réticulation sont générés par des réactions radicalaires au sein de la plante. Cependant, des composés issus de la cycloaddition [2+2] de dérivés cinnamiques ont été identifiés dans la paroi cellulaire de plusieurs plantes (Hartley *et al.*, 1990; Morrison *et al.*, 1992). Ce type de réaction pourrait donc avoir lieu au sein de la plante. Les produits ainsi formés pourraient être des acteurs importants de la rigidité de la plante.

La réaction de cycloaddition entre dérivés cinnamiques est cependant connue depuis plus de cent ans (Stobbe, 1919). Il a été observé que l'organisation de la molécule à l'état cristallin, et notamment sa structure cristalline, avait un fort impact sur sa capacité ou non à dimériser par cycloaddition [2+2] (Cohen *et al.*, 1964; Schmidt, 1971; Ramamurthy *et al.*, 1987; Khan *et al.*, 2008). Les dérivés cinnamiques ont été classés en trois formes cristallines : α, β et γ (Schmidt, 1964; Ramamurthy *et al.*, 1987). La forme α correspond à des molécules orientées de manière dite « tête-queue » dans laquelle les molécules, dont les doubles liaisons sont les plus proches, sont tournées selon un axe de rotation normal au plan du cycle aromatique. Les doubles liaisons sont alors parallèles les unes aux autres avec une distance d'environ 4,2 Å, ce qui permet à la cycloaddition de se faire. Dans la forme β les molécules dont les doubles liaisons sont les plus proches sont alors symétriques selon un miroir dans le plan du cycle aromatique. On parle alors de forme « tête-tête ». Dans ce cas, la distance entre les doubles liaisons est comprise entre 3,8 et 4,2 Å et celles-ci sont parallèles ce qui permet également la cycloaddition. Enfin, dans la forme γ, les doubles liaisons des molécules ne se recouvrent pas et la distance entre celles-ci est supérieure à 4,8 Å, ce qui empêche la cycloaddition de se faire (Ramamurthy *et al.*, 1987). Les formes cristallines α, β et γ de l'acide cinnamique sont représentées schématiquement en Figure 4.1.1. La distance entre les doubles liaisons et leur orientation au sein de la maille cristalline permet donc de prévoir la capacité des dérivés cinnamiques à réagir par cycloaddition [2+2]. Cependant, il est également possible d'observer la cycloaddition de ces composés en solution (Shindo *et al.*, 1983).

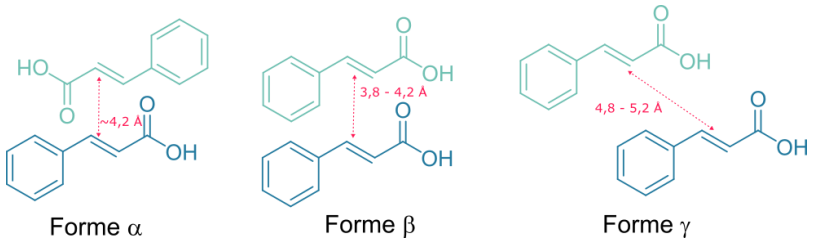

Figure 4.1.1: Représentation schématique de l'arrangement des molécules d'acide cinnamique dans les formes cristallines α, β et γ . Adapté de (Ramamurthy *et al.*, 1987).

La dimérisation de dérivés cinnamiques permet l'élaboration de molécules d'intérêt thérapeutique telles que des anti-inflammatoires, antidouleurs ou de potentiels anticancéreux (Chi *et al.*, 2005; Dembitsky, 2007; Priebe *et al.*, 2018; Yan *et al.*, 2018). Cette dimérisation a également été envisagée et investiguée pour l'élaboration de synthons pour la synthèse de nouveaux matériaux. Wang *et al.* (Wang *et al.*, 2017) ont utilisé l'acide truxillique, un dimère d'acide cinnamique (Figure 4.1.2), avec des diols de différentes longueurs pour la synthèse de polyesters. Ils ont ainsi obtenu des polyesters présentant une haute résistance chimique ainsi que des T_g allant jusqu'à 81°C. Ding *et al.* (Ding *et al.*, 2019) ont montré que l'ajout de motifs d'acide truxillique au sein d'une chaine de PET permet d'améliorer les propriétés de résistance aux UV du PET. La présence de dimères de dérivés cinnamiques au sein d'un matériau peut aussi induire des propriétés mécanochimiques innovantes. Par exemple, Zhang et *al.* (Zhang *et al.*, 2017) ont mis à profit l'utilisation de macrocycles à base d'acide truxinique, une autre forme de dimérisation de l'acide cinnamique (Figure 4.1.2), pour concevoir un matériau polymère contenant un cyclobutane pouvant être clivé via une contrainte mécanique, entrainant son allongement. Enfin, Castillo *et al.* (Castillo *et al.*, 2004) ont étudié des dimères de dérivés de **FA** pour la synthèse de polyesters et de polyamides à hautes propriétés thermiques. Après dimérisation de l'acide p-acétyle férulique (**AcFA)**, ils ont obtenu par chauffage à haute température un polyester tridimensionnel infusible et insoluble tel que représenté sur le Schéma 4.1.1.

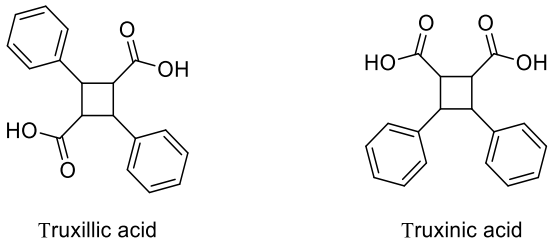

Figure 4.1.2: Représentation de la structure des acides truxillique et truxinique.

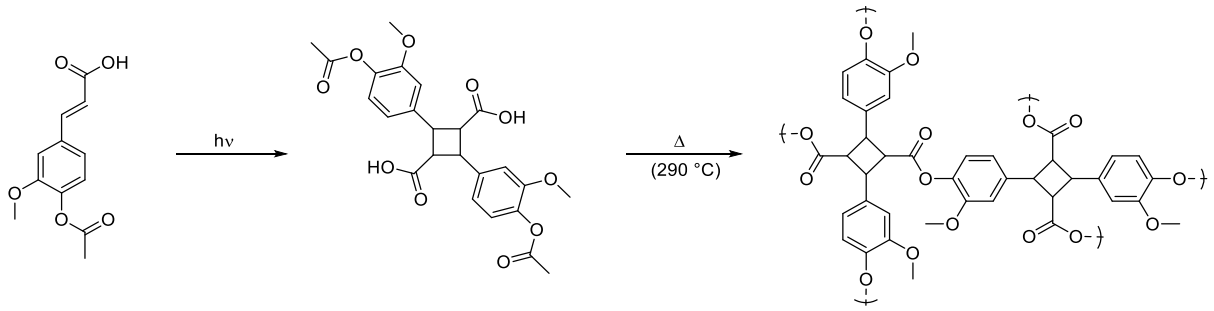

Schéma 4.1.1: Dimérisation et polymérisation de l'acide p-acétyle férulique. Adapté de (Castillo *et al.*, 2004).

Enfin, il convient de préciser que ces réactions de cycloadditions sont généralement faites à température ambiante, sans catalyseur et sont initiées par irradiation UV, ce qui les rend compatibles avec plusieurs principes de la chimie verte (Anastas *et al.*, 2010). Cependant, il est intéressant de noter qu'aucune des études menées jusqu'ici sur la synthèse de polymères à partir de ces dimères de dérivés cinnamiques n'emploie la catalyse enzymatique pour la conversion de ces composés en matériaux.

Ce sous-chapitre a pour but l'étude des propriétés de dimérisation par cycloaddition de plusieurs dérivés de **FA** que sont le méthyle férulate (**MeFA**), l'acide *p*-acétyle férulique (**AcFA**) et deux diesters présentés au chapitre précédent notés **DeFA^{I}** et **DeFA^{II}** et comparés au **FA** (Figure 4.1.3). La structure cristalline des composés en lien avec leur réactivité a ensuite été étudié à chaque fois que cela a été possible.

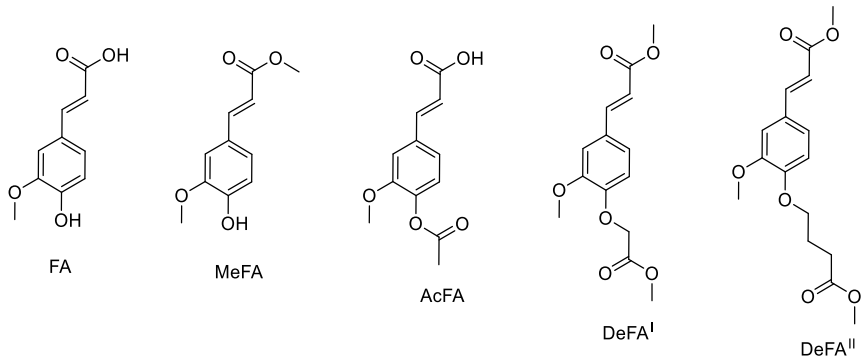

Figure 4.1.3 : Structure des dérivés de FA étudiés en photodimérisation.

2. Etude de la réactivité en cycloaddition [2+2] de dérivés féruliques

2.1. Synthèse et caractérisation des dérivés de FA :

Le **MeFA**, **DeFA^{I}** et **DeFA^{II}** ont été synthétisés et caractérisés selon les méthodes décrites dans le chapitre 3.

Le **AcFA** a été synthétisé de la manière suivante : 1g de **FA** a été dissout dans 2,2 ml d'un mélange d'anhydride acétique et de pyridine (3 équivalents molaires d'anhydride acétique pour 4 équivalents molaires de pyridine). La solution a été agitée pendant 3 heures à température ambiante. Le produit a ensuite été précipité dans un mélange d'eau et de glace. La solution a alors été centrifugée

(8000 g, 10 minutes) et le surnageant éliminé. Le produit a ainsi été lavé 3 fois à l'eau distillée et séché en étuve sous vide (40°C, 24h). Le produit obtenu est une poudre blanche et son point de fusion est de : 199 °C (lit. 195-201 °C (Castillo *et al.*, 2004; Allais *et al.*, 2009)). Le produit a été caractérisé par RMN ^{1}H à 400 MHz dans le DMSO-*d6* (Annexes Figure S4.1 et Figure S4.2). Le doublet à δ = 7,57 ppm (J = 16,0 Hz, 1H) a été attribué à l'hydrogène de la double liaison vicinale du carbonyle. Les doublets situés à δ = 7,47 ppm (J = 1,9 Hz, 1H) et 7,25 ppm (J = 1,8 Hz, 1H) ont été attribuées aux hydrogènes en position ortho du cycle aromatique. L'hydrogène situé du côté du groupement méthoxy est le plus déblindé des deux. L'hydrogène en position *méta* du cycle aromatique a été attribué au doublet situé à δ = 7,11 ppm (J = 8,2 Hz, 1H). Le doublet situé à δ = 6,28 ppm (J = 16,0 Hz, 1H) correspond à l'hydrogène de la double liaison vicinale du cycle aromatique. Enfin les singulets situés à δ = 3,82 (3H) et 2,26 ppm (3H) ont été attribués respectivement aux protons des groupements methoxy et acétate.

2.2. Essais de photo-dimérisation :

La dimérisation par cycloaddition [2+2] de dérivés cinnamiques est généralement faite dans des solvants apolaires tels que l'hexane ou le cyclohexane (Castillo *et al.*, 2004; Nguyen *et al.*, 2016). Le cyclohexane étant décrit comme moins toxique que l'hexane, c'est lui qui a été choisi comme solvant de réaction (Prat *et al.*, 2016; Tobiszewski *et al.*, 2017). Le **FA** ou ses dérivés (20 mg) ont été placés dans un flacon en verre et mis en suspension dans le cyclohexane (3 ml). Tous les dérivés se sont avérés être insolubles dans le cyclohexane à température ambiante. Les flacons ont alors été placés, sous agitation, dans un photoréacteur LZX-4X$_b$ (Luzchem Reasearch, Inc). Ce dernier est équipé de 14 lampes 8 Watts émettant des UV à une longueur d'onde de 350 nm et une puissance mesurée à 3,3 mW.cm^{-2}. Toutes les réactions ont été faites à température ambiante. Après 24h d'irradiation, les produits ont été solubilisés et extraits par ajout de 700 µl de DMSO-*d6*. La solution de DMSO-*d6* a ensuite été analysée par RMN. Les spectres des produits obtenus sont représentés en Figure 4.1.4.

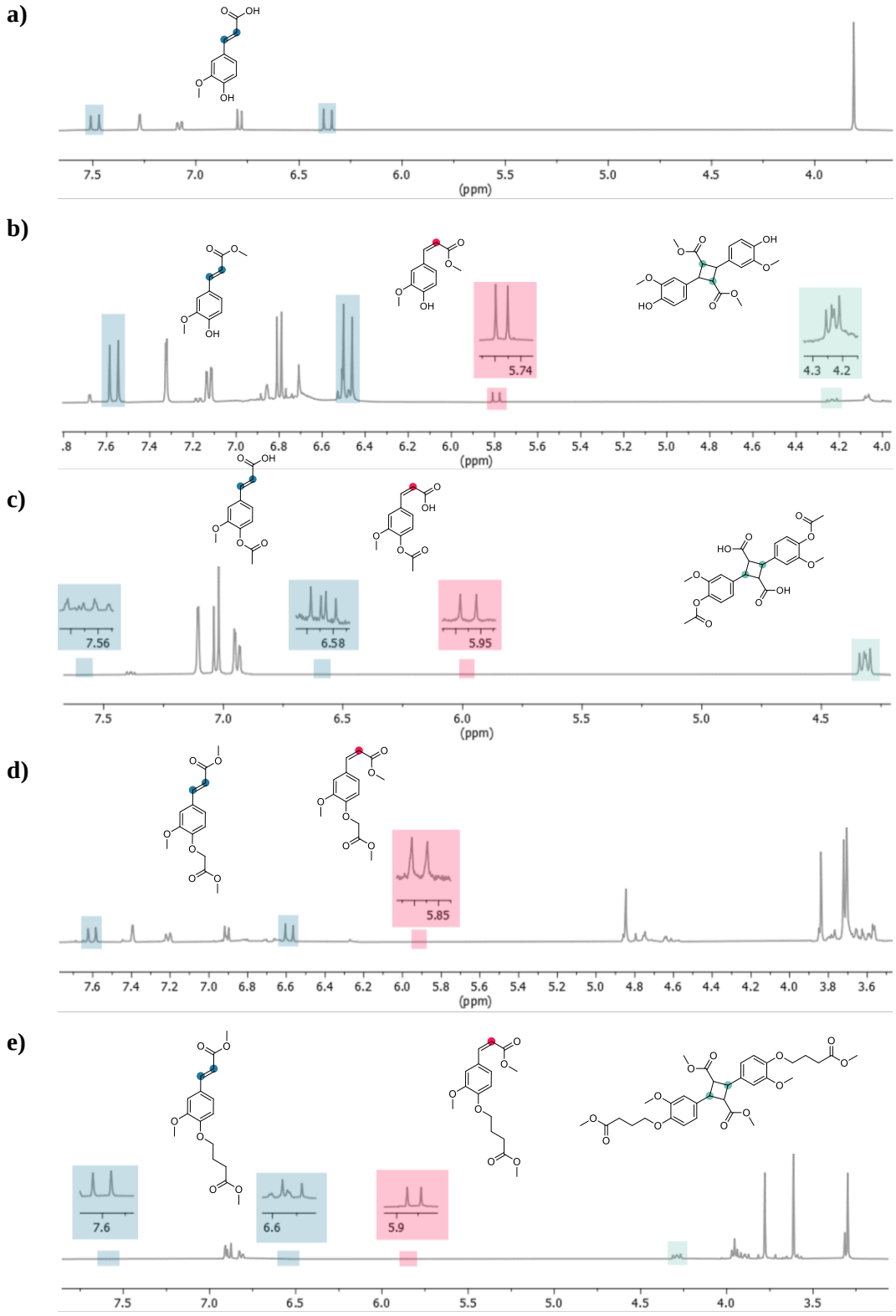

Figure 4.1.4 : Spectres de RMN ^{1}H des produits issus de l'irradiation à 350 nm dans le cyclohexane des dérivés de FA : a) FA ; b) MeFA ; c) AcFA ; d) DeFA^{I} et e) DeFA^{II}.

L'analyse de RMN du **FA** après irradiation par des UV-C à une longueur d'onde de 350 nm montre qu'aucun produit de dimérisation n'est obtenu. Des résultats similaires ont déjà été observés et

rapportés dans la littérature avec le **FA** (Ford *et al.*, 1989). Nethaji *et al.* (Nethaji *et al.*, 1988) ont étudié la structure cristallographique du **FA**. L'arrangement des molécules dont les doubles liaisons sont les plus proches est représenté en Figure 4.1.5. Sous cette forme les doubles liaisons les plus proches ne se recouvrent pas et sont séparées par une distance calculée à 4,64 Å. Le **FA** a donc une forme cristalline γ (Nethaji *et al.*, 1988). Cet arrangement des molécules et leur distance explique donc l'absence de réaction de cycloaddition sous irradiation UV observée expérimentalement.

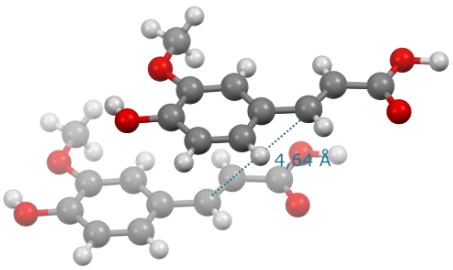

Figure 4.1.5 : Représentation de l'arrangement du FA sous forme cristalline. Adapté de (Nethaji *et al.*, 1988).

Le **MeFA**, après irradiation à 350 nm, semble converti en plusieurs sous-produits. Tout d'abord le doublet identifié δ = 5,79 ppm avec une constante de couplage égale à 12.89 Hz est attribuée à l'hydrogène de la double liaison vicinale du carbonyle du férulate de méthyle en configuration *cis*. En effet, le déplacement chimique et la constance de couplage des pics observés en RMN ^{1}H correspondent au *cis*-férulate de méthyle (Karakousi *et al.*, 2020). La *cis*-isomérisation de composés cinnamiques tels que le **FA** et ses dérivés sous irradiation UV a déjà été rapportée dans la littérature (Shindo *et al.*, 1984; Moni *et al.*, 2021). L'irradiation de la double liaison permet d'élever suffisamment son niveau d'énergie pour que la double liaison prenne la configuration électronique dite « anti-liante » (Horbury *et al.*, 2017). Dans cette configuration la molécule peut tourner selon l'axe de la liaison sigma et ainsi accéder à la forme *cis* de la double liaison. Le signal à δ = 4,23 ppm avec des constantes de couplage J = 10,5 et 7,2 Hz correspond à un doublet de doublets. Ce signal a été attribué à l'hydrogène vicinal du cycle aromatique et porté par le cyclobutane de la forme dimérisée de la molécule. La présence de ce signal atteste donc de la formation d'un dimère par cycloaddition [2+2] à partir de férulate de méthyle. Le rapport d'intensité de ces signaux rapporté au nombre d'hydrogènes qu'ils représentent permet d'estimer la conversion du férulate de méthyle. Le calcul du rendement de dimérisation est donné dans l'équation (1). Dans le cas présent, $I_{dimère}$ correspond à la valeur d'intégration du signal attribué au dimère de férulate de méthyle à δ = 4,23 ppm, I_{trans} correspond à la valeur d'intégration du signal attribué au trans-férulate de méthyle à δ = 6,48 ppm et I_{cis} correspond à la valeur d'intégration du signal attribué au *cis*-férulate de méthyle à δ = 5,79 ppm.

$$Rendement\ de\ dimerisation\ = \frac{I_{dimère}}{I_{trans} + I_{cis} + I_{dimère}} \quad (3)$$

Les proportions des produits issus de l'irradiation du férulate de méthyle sont données en Figure 4.1.6. On observe que la conversion en dimère est très faible (< 15%) et que s'ajoute à celle-ci environ 5% de cis-isomérisation. De plus, des traces de sous-produits de dégradation sont visibles entre δ = 3.50 et 3.80 ppm ainsi qu'à δ = 9,60 ppm. Ces observations sont confortées par un jaunissement de l'échantillon après irradiation. Le **MeFA** n'a pas pu être obtenu sous forme de monocristal de taille satisfaisante et n'a donc pas été analysé par diffraction des rayons X (DRX). Sa structure n'ayant pas été décrite dans la littérature, il n'est donc pas possible, pour le moment, d'expliquer la faible réactivité en dimérisation du **MeFA** par l'étude de sa structure cristalline. Cependant, la difficulté de cristallisation du **MeFA** peut être la raison de sa faible réactivité en dimérisation sous UV (Cohen *et al.*, 1964) même si des études ont montré que des esters cinnamiques amorphes pouvaient également dimériser par cycloaddition [2+2] (Shindo *et al.*, 1983).

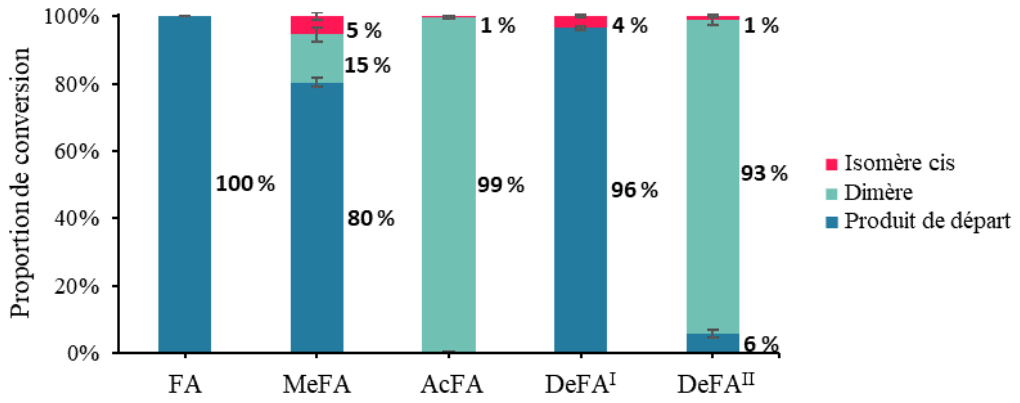

Figure 4.1.6 : Proportions en produit de départ, isomère *cis* et dimère obtenus après irradiation des dérivés de FA sous UV (λ = 350 nm) pendant 24 heures dans le cyclohexane.

Dans le cas du **AcFA**, les signaux correspondant aux hydrogènes de la double liaison à δ = 7,57 (J = 16 Hz) et 6,58 (J = 16 Hz) ppm sont quasi inexistants sur le spectre de RMN ^{1}H du produit. Le signal à δ = 5,98 ppm est un doublet de constante de couplage J = 12,7 Hz. Il correspond à l'hydrogène de la double liaison vicinal du carbonyle du *cis*-**FA** acétylé. Enfin le signal à δ = 4,32 ppm correspond à un doublet de doublets de constantes de couplage J = 10,5 et 7,2 Hz et est attribué à l'hydrogène vicinal du cycle aromatique et porté par le cyclobutane de la forme dimérisée du **AcFA**. Les proportions des différents produits obtenus par irradiation UV du **AcFA** ont été calculées grâce à l'équation 1 et sont données en Figure 4.1.6. On observe que **AcFA** est converti en dimère de manière quasi totale (99%) en seulement 24 heures. La structure cristalline du **AcFA** a été décrite dans la littérature et l'arrangement des molécules dont les doubles liaisons sont les plus proches est représenté en Figure 4.1.7 (Lee *et al.*, 1988). Ces molécules de **AcFA** sont ainsi organisées de manière « tête-queue » et la distance entre les doubles liaisons a été mesurée à 3,77 Å. Ce type de structure correspond donc à la forme cristalline α

qui est en adéquation avec une bonne réactivité par cycloaddition sous UV. Comme pour les autres dérivés cinnamiques, la cycloaddition du **AcFA** peut générer deux isomères de constitution dits « tête-tête » et « tête-queue » (Figure 4.1.8). À cause de leur symétrie, ces isomères sont difficilement différenciables par analyse de RMN. Ces isomères peuvent cependant être différenciés par spectrométrie de masse. En effet, le clivage du cyclobutane donne des fragments différents en fonction de l'isomère analysé. L'obtention d'isomères exclusivement « tête-queue » à partir du **AcFA** a ainsi été confirmée dans la littérature par Castillo *et al.* (Castillo *et al.*, 2004) et résulte de la structure cristalline « tête-queue » du **AcFA**. Cette observation est en adéquation avec la forme cristalline α du substrat sujet à dimérisation qui, d'après la littérature, induit la formation d'un produit « tête-queue » (Cohen *et al.*, 1964).

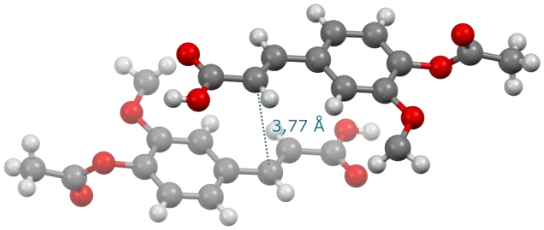

Figure 4.1.7 : Représentation de l'arrangement du AcFA sous forme cristalline. Adapté de (Lee *et al.*, 1988).

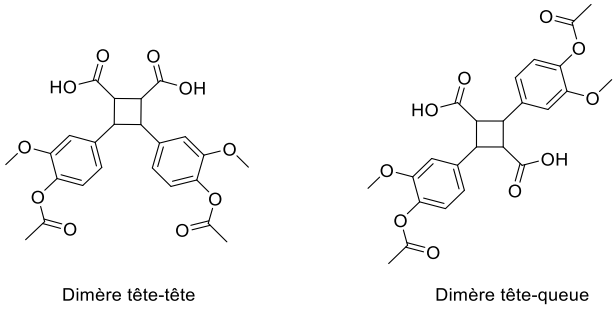

Figure 4.1.8 : Représentation des deux dimères possibles par cycloaddition du AcFA.

Le **DeFA^{I}** a également été étudié pour établir sa faculté à dimériser sous irradiation UV à 350 nm. Le pic correspondant à un doublet à δ = 7,57 et de constante de couplage J = 12,9 Hz a été attribué à l'hydrogène de la double liaison vicinale du carbonyle en conformation *cis* du **DeFA^{I}**. Comme pour les autres dérivés, une partie du **DeFA^{I}** est donc *cis*-isomérisée durant l'irradiation. Aucune trace de dimère n'a été observée sur le spectre de RMN ^{1}H. Le rendement de *cis*-isomérisation a été calculé grâce à l'équation 1 et n'est que de 4 % (Figure 4.1.6). Comme pour le **MeFA**, des signaux correspondant à des traces de sous-produits de dégradation sont observées entre δ = 4,50 et 4,90 ppm ainsi que dans la région dite des aromatiques autour de δ = 6,8 ppm. De plus, un jaunissement de l'échantillon a également été observé. Le **DeFA^{I}** n'a pas pu être obtenu sous la forme d'un monocristal de taille satisfaisante pour être étudié en DRX et sa structure n'a pas été décrite auparavant dans la littérature. Ici encore, comme pour le **MeFA**, la difficulté de cristallisation du **DeFA^{I}**, peut expliquer sa faible réactivité en dimérisation sous UV.

Enfin, les produits issus de l'irradiation du **DeFA^{II}** ont été étudiés. Comme pour le dérivé acétylé **AcFA**, les signaux correspondant à la double liaison du **DeFA^{II}** (à δ = 4,5 et 4,9 ppm) sont difficilement observables sur le spectre de RMN ^{1}H du produit. Comme pour les autres composés, un signal correspondant à l'isomère *cis* du **DeFA^{II}** est observable (δ = 5,86, J = 12,9 Hz). Enfin le doublet de doublets à δ = 4,29 ppm (J = 10,5 et 7,2 Hz) correspond à l'hydrogène vicinal du cycle aromatique et situé sur le cyclobutane de la forme dimérisée du **DeFA^{II}**. Le rendement des différents produits issus de l'irradiation a été calculé grâce à l'équation 1 et est donné dans la Figure 4.1.6. On observe que le produit de départ et l'isomère *cis* sont minoritaires et que le composé **DeFA^{II}** est converti de manière quasi totale (93%) en dimère, et cela en seulement 24h. La structure du **DeFA^{II}** n'a pas été décrite dans la littérature et a donc été analysée en DRX afin de mieux comprendre le lien entre structure cristalline et réactivité en cycloaddition (Figure 4.1.9). Comme pour le **AcFA**, les molécules de **DeFA^{II}** dont les doubles liaisons sont les plus proches s'avèrent être en position « tête-queue ». La distance entre les doubles liaisons a été mesurée à 3.59 Å. Cet arrangement correspond donc à une forme cristalline α qui vient corroborer la bonne réactivité du **DeFA^{II}** en cycloaddition (Schmidt, 1964; Ramamurthy *et al.*, 1987).

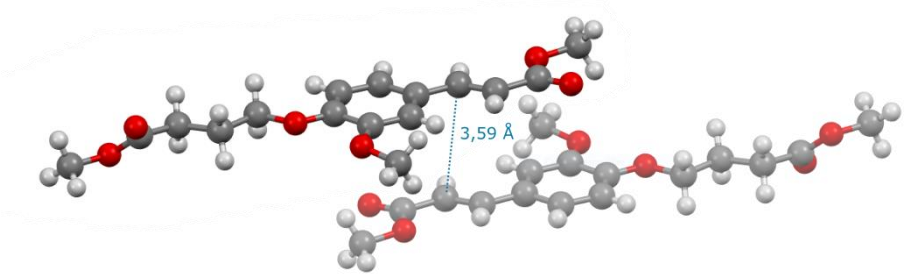

Figure 4.1.9 : Représentation de l'arrangement du DeFA^{II} sous forme cristalline tel que déterminé par DRX.

Comme indiqué précédemment, la dimérisation de dérivés cinnamiques peut conduire à la formation de deux isomères dits « tête-tête » et « tête-queue ». Ces deux formes sont difficilement discernables par RMN ^{1}H ou ^{13}C. Des analyses plus poussées par RMN à deux dimensions mesurant l'effet Overhauser nucléaire (permettant de déterminer le voisinage dans l'espace des atomes) n'ont pas permis de différencier les deux formes de dimères. Le dimère de **DeFA^{II}** n'est pas décrit dans la littérature et sa structure a donc également été déterminée par DRX (Figure 4.1.10). Cette analyse a confirmé l'obtention d'un dimère « tête-queue » dans lequel les fonctions acides carboxyliques sont en positions opposées sur le cyclobutane. Ce résultat correspond parfaitement à ce qui pouvait être attendu d'après la forme α du substrat **DeFA^{II}** sujet à dimérisation, lui aussi arrangé sous forme « tête-queue » (Cohen *et al.*, 1964).

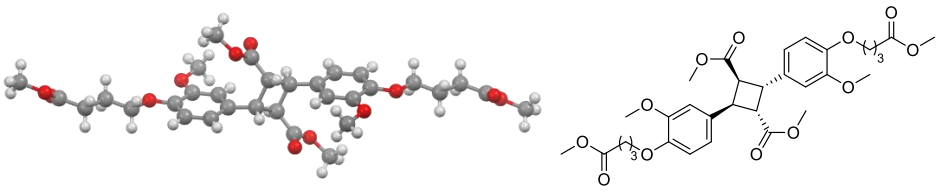

Figure 4.1.10: Représentation du dimère obtenu par cycloaddition du DeFA^{II} sous UV dans le cyclohexane. a) Représentation tridimensionnelle issu de l'analyse par DRX, b) Représentation schématique.

3. Conclusion :

Depuis de nombreuses années, la littérature dans le domaine fait état que l'obtention de dimères de dérivés cinnamiques tels que le **FA** permet d'envisager la synthèse de molécules à haute valeur ajoutée. Ces dimères peuvent notamment être directement utilisés à des fins thérapeutiques ou comme synthons pour la synthèse de matériaux innovants.

Plusieurs dérivés de **FA** ont ainsi été testés afin d'établir leur capacité à réagir par cycloaddition [2+2]. Conformément à ce qui a été rapporté jusqu'ici dans la littérature (Ford *et al.*, 1989), le **FA** s'est trouvé être inactif et n'a pas donné lieu à une isomérisation ou une dimérisation sous irradiation UV à 350 nm. Ce manque de réactivité est expliqué par la distance trop importante entre les doubles liaisons des molécules de **FA** dans la maille cristalline.

En revanche, tous les dérivés de **FA** testés ont donné lieu à une faible *cis*-isomérisation après exposition au rayonnement UV. Ce phénomène d'isomérisation des dérivés d'acide férulique a déjà été rapporté et étudié dans la littérature, notamment pour des applications pharmaceutiques ou cosmétiques (Horbury *et al.*, 2017; Moni *et al.*, 2021). Cependant la proportion en isomère *cis* est restée faible, inférieure ou égale à 5%, et ce produit est donc systématiquement largement minoritaire dans le milieu après 24 h de réaction. Les études présentées dans la littérature indiquent par ailleurs que les molécules en conformation *cis* ne peuvent pas donner lieu à une réaction de dimérisation (Schmidt, 1971; Ford *et al.*, 1989).

Seuls les **MeFA**, **AcFA** et **DeFA^{II}** ont pu être dimérisés sous irradiation UV. Le rendement le plus important en dimère a été obtenu pour le **AcFA** (99%) suivi du **DeFA^{II}** (93%) et du **MeFA** (14%). Il a été déterminé que le **AcFA** ainsi que le **DeFA^{II}** présentaient tous deux une structure cristalline de forme α. Cette structure particulière induit une forte proximité des doubles liaisons qui expliquerait leur bonne réactivité en cycloaddition [2+2]. Cette structure cristalline peut également justifier le fait que seul le produit de dimérisation « tête-queue » ait été obtenu. En effet, dans leur forme cristalline α, les molécules dont les doubles liaisons sont les plus proches présentent déjà un arrangement « tête-queue ».

Enfin, le **MeFA** ainsi que le **DeFA^{I}** ont montré des traces de dégradation après irradiation sous UV. Cette dégradation peut être liée à leur difficulté à cristalliser. A l'état amorphe les molécules

pourraient donner lieu à d'autres types de réactions sous irradiation UV, comme des réactions radicalaires, par exemple. Ainsi la structure de ces deux composés n'a pas pu être déterminée par DRX.

Les dérivés **AcFA** et **DeFA^{II}** sont donc deux candidats intéressants pour la synthèse de nouveaux matériaux à partir de leurs dimères respectifs. Leur fonctionnalité permet d'envisager leur utilisation pour la synthèse de polyesters où leurs cycles aromatiques et le cyclobutane formé permettraient l'obtention de matériaux particulièrement rigides avec des T_g élevées. La réactivité de la CALB, et celle des lipases en général, vis-à-vis de ce type de structure n'a pas encore été étudiée et pourrait être investiguée dans un objectif d'obtention de nouveaux matériaux biosourcés dans les conditions douces de la catalyse enzymatique.

4. Références

Allais, F., Martinet, S. and Ducrot, P.-H. (**2009**) 'Straightforward Total Synthesis of 2-O-Feruloyl-l-malate, 2-O-Sinapoyl-l-malate and 2-O-5-Hydroxyferuloyl-l-malate', *Synthesis*, 2009(21), pp. 3571–3578.

Anastas, P. and Eghbali, N. (**2010**) 'Green Chemistry: Principles and Practice', *Chem. Soc. Rev.*, 39(1), pp. 301–312.

Bento-Silva, A., Vaz Patto, M. C. and do Rosário Bronze, M. (**2018**) 'Relevance, structure and analysis of ferulic acid in maize cell walls', *Food Chemistry*, 246, pp. 360–378.

Castillo, E. A., Miura, H., Hasegawa, M. and Ogawa, T. (**2004**) 'Synthesis of novel polyamides starting from ferulic acid dimer derivative', *Designed Monomers and Polymers*, 7(6), pp. 711–725.

Chi, Y.-M., Nakamura, M., Yoshizawa, T., Zhao, X.-Y., Yan, W.-M., Hashimoto, F., Kinjo, J., Nohara, T. and Sakurada, S. (**2005**) 'Anti-inflammatory Activities of α-Truxillic Acid Derivatives and Their Monomer Components', 28(9), pp. 1776–1778.

Cohen, M. D. and Schmidt, G. M. J. (**1964**) '383. Topochemistry. Part I. A survey', *Journal of the Chemical Society (Resumed)*, p. 1996.

Dembitsky, V. M. (**2007**) 'Bioactive cyclobutane-containing alkaloids', *Journal of Natural Medicines*, 62(1), pp. 1–33.

Ding, L., Liu, L., Chen, Y., Du, Y., Guan, S., Bai, Y. and Huang, Y. (**2019**) 'Modification of poly(ethylene terephthalate) by copolymerization of plant-derived α-truxillic acid with excellent ultraviolet shielding and mechanical properties', *Chemical Engineering Journal*, 374, pp. 1317–1325.

Ford, C. W. and Hartley, R. D. (**1989**) 'GC/MS characterisation of cyclodimers fromp-coumaric and ferulic acids by photodimerisation—a possible factor influencing cell wall biodegradability', *Journal of the Science of Food and Agriculture*, 46(3), pp. 301–310.

Grabber, J. H., Ralph, J. and Hatfield, R. D. (**2000**) 'Cross-Linking of Maize Walls by Ferulate Dimerization and Incorporation into Lignin', *Journal of Agricultural and Food Chemistry*, 48(12), pp. 6106–6113.

Hartley, R. D., Morrison, W. H., Balza, F. and Towers, G. H. N. (**1990**) 'Substituted truxillic and truxinic acids in cell walls of Cynodon dactylon', *Phytochemistry*, 29(12), pp. 3699–3703.

Hatfield, R. D., Rancour, D. M. and Marita, J. M. (**2017**) 'Grass Cell Walls: A Story of Cross-Linking', *Frontiers in Plant Science*, 7, p 2056.

Horbury, M. D., Baker, L. A., Rodrigues, N. D. N., Quan, W.-D. and Stavros, V. G. (**2017**) 'Photoisomerization of ethyl ferulate: A solution phase transient absorption study', *Chemical Physics Letters*, 673, pp. 62–67.

Karakousi, C.-V., Gabrieli, C. and Kokkalou, E. (**2020**) 'Chemical composition and biological activities of *Indigofera hirsuta* aerial parts' methanol fractions', *Natural Product Research*, 34(4), pp. 558–562.

Khan, M., Brunklaus, G., Enkelmann, V. and Spiess, H.-W. (**2008**) 'Transient States in [2 + 2] Photodimerization of Cinnamic Acid: Correlation of Solid-State NMR and X-ray Analysis', *Journal of the American Chemical Society*, 130(5), pp. 1741–1748.

Lee, D. Y., Tachibana, S., Sumimoto, M. and Ohe, H. (**1988**) 'Structure of 4'-acetoxy-3'-methoxycinnamic acid', *Acta Crystallographica Section C Crystal Structure Communications*, 44(7), pp. 1240–1242.

Moni, L., Banfi, L., Basso, A., Mori, A., Risso, F., Riva, R. and Lambruschini, C. (**2021**) 'A Thorough Study on the Photoisomerization of Ferulic Acid Derivatives', *European Journal of Organic Chemistry*, 2021(11), pp. 1737–1749.

Morrison, W. Herbert., Hartley, R. D. and Himmelsbach, D. S. (**1992**) 'Synthesis of substituted truxillic acids from p-coumaric and ferulic acid: simulation of photodimerization in plant cell walls', *Journal of Agricultural and Food Chemistry*, 40(5), pp. 768–771.

Nethaji, M., Pattabhi, V. and Desiraju, G. R. (**1988**) 'Structure of 3-(4-hydroxy-3-methoxyphenyl)-2-propenoic acid (ferulic acid)', *Acta Crystallographica Section C Crystal Structure Communications*, 44(2), pp. 275–277.

Nguyen, T. B. and Al-Mourabit, A. (**2016**) 'Remarkably high homoselectivity in [2 + 2] photodimerization of trans-cinnamic acids in multicomponent systems', *Photochemical & Photobiological Sciences*, 15(9), pp. 1115–1119.

Prat, D., Wells, A., Hayler, J., Sneddon, H., McElroy, C. R., Abou-Shehada, S. and Dunn, P. J. (**2016**) 'CHEM21 selection guide of classical- and less classical-solvents', *Green Chemistry*, 18(1), pp. 288–296.

Priebe, A., Hunke, M., Tonello, R., Sonawane, Y., Berta, T., Natarajan, A., Bhuvanesh, N., Pattabiraman, M. and Chandra, S. (**2018**) 'Ferulic acid dimer as a non-opioid therapeutic for acute pain', *Journal of Pain Research*, Volume 11, pp. 1075–1085.

Ramamurthy, V. and Venkatesan, K. (**1987**) 'Photochemical reactions of organic crystals', *Chemical Reviews*, 87(2), pp. 433–481.

Santiago, R. and Malvar, R. (**2010**) 'Role of Dehydrodiferulates in Maize Resistance to Pests and Diseases', *International Journal of Molecular Sciences*, 11(2), pp. 691–703.

Schmidt, G. M. J. (**1964**) '385. Topochemistry. Part III. The crystal chemistry of some trans-cinnamic acids', *Journal of the Chemical Society (Resumed)*, p. 2014.

Schmidt, G. M. J. (**1971**) 'Photodimerization in the solid state', *Pure and Applied Chemistry*, 27(4), pp. 647–678.

Shindo, Y., Horie, K. and Mita, I. (**1983**) 'RATE FOR PHOTODIMERIZATION OF ETHYL CINNAMATE IN DILUTE SOLUTION', *Chemistry Letters*, 12(5), pp. 639–642.

Shindo, Y., Horie, K. and Mita, I. (**1984**) 'Photoisomerization of ethyl cinnamate in dilute solutions', *Journal of Photochemistry*, 26(2–3), pp. 185–192.

Stobbe, H. (**1919**) 'Lichtreaktionen der Allo- und Isozimtsäuren', *Berichte der deutschen chemischen Gesellschaft (A and B Series)*, 52(4), pp. 666–672.

Terrett, O. M. and Dupree, P. (**2019**) 'Covalent interactions between lignin and hemicelluloses in plant secondary cell walls', *Current Opinion in Biotechnology*, 56, pp. 97–104.

Tobiszewski, M., Namieśnik, J. and Pena-Pereira, F. (**2017**) 'Environmental risk-based ranking of solvents using the combination of a multimedia model and multi-criteria decision analysis', *Green Chemistry*, 19(4), pp. 1034–1042.

Wang, Z., Miller, B., Mabin, M., Shahni, R., Wang, Z. D., Ugrinov, A. and Chu, Q. R. (**2017**) 'Cyclobutane-1,3-Diacid (CBDA): A Semi-Rigid Building Block Prepared by [2+2] Photocyclization for Polymeric Materials', *Scientific Reports*, 7(1).

Yan, S., Elmes, M. W., Tong, S., Hu, K., Awwa, M., Teng, G. Y. H., Jing, Y., Freitag, M., Gan, Q., Clement, T., Wei, L., Sweeney, J. M., Joseph, O. M., Che, J., Carbonetti, G. S., Wang, L., Bogdan, D. M., Falcone, J., Smietalo, N., Zhou, Y., Ralph, B., Hsu, H.-C., Li, H., Rizzo, R. C., Deutsch, D. G., Kaczocha, M. and Ojima, I. (**2018**) 'SAR studies on truxillic acid mono esters as a new class of antinociceptive agents targeting fatty acid binding proteins', *European Journal of Medicinal Chemistry*, 154, pp. 233–252.

Zhang, H., Li, X., Lin, Y., Gao, F., Tang, Z., Su, P., Zhang, W., Xu, Y., Weng, W. and Boulatov, R. (**2017**) 'Multi-modal mechanophores based on cinnamate dimers', *Nature Communications*, 8(1), p. 1147.

Sous-chapitre 4.2. Photo-dimerization of ferulic derivatives for the CALB catalyzed synthesis of biobased cleavable polyesters

*Alfred Bazin, Matthieu Steuer, Luc Avérous, Eric Pollet**

Soon submitted for publication

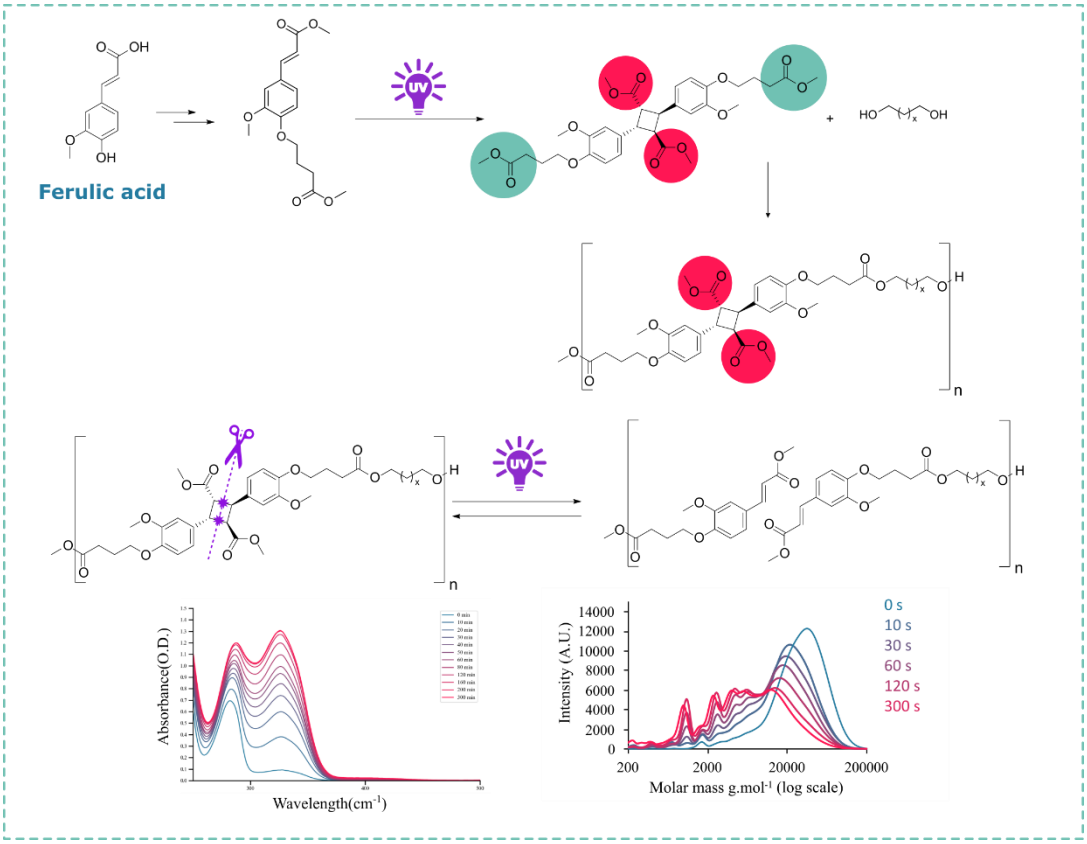

1. Abstract

Derivatives of ferulic acid were assayed for photo-dimerization through [2+2] cycloaddition. A clear link was established between the substrate crystalline arrangement and its ability to photo-dimerize and the resulting product structure. Interestingly, screening of greener alternative solvents showed that cyclohexane usually employed for the reaction could be advantageously substituted with water, offering the dimers in high yields. The obtained dimers were then tested for CALB catalyzed polymerization. Dimers from *p*-acetyl ferulic acid could not undergo polymerization, most likely due to steric hindrance. However, a dimer of a ferulic diester was successfully converted by CALB biocatalyst into aromatic biobased polyesters. In this case, the selectivity of CALB allowed the synthesis of peculiar polyester chains with pendant ester groups. Diols of different lengths (1,3-propanediol, 1,4-butanediol, 1,6-hexanediol and 1,8-octanediol) were used and allowed the synthesis of polyesters with high Mw up to 57 700 g.mol^{-1}. These polyesters also presented high T_g values measured within the range of 12 to 34 °C. The reversibility of the [2+2] cycloaddition used for the monomer synthesis was then demonstrated resulting in the controlled photo-depolymerization of the polyesters under UV-C with a drastic reduction in the chain length and production of oligomers with DP_n around 3. The combination of UV-induced photoreactions associated to enzymatic catalysis has thus allowed the synthesis as well as the controlled depolymerization of biosourced ferulic-based aromatic polyesters, thus placing these new materials within a circular economy model.

2. Introduction

The development of biobased building-blocks for the production of new materials is today being extensively studied (Becker *et al.*, 2015; Delidovich *et al.*, 2016; Sun *et al.*, 2018b; John *et al.*, 2019). These compounds represent an alternative to oil-based monomers employed for the synthesis of common polymers. These developments are motivated by the need to produce more environmentally friendly materials. Indeed, because of their sustainable nature, biobased polymers could present a lower impact on the environment than their oil-based equivalents (Hatti-Kaul *et al.*, 2019; Siracusa *et al.*, 2020). Such approaches are especially interesting for the replacement of the well-known oil-based BTX (benzene, toluene, xylene) building blocks. Therefore, various natural resources are investigated for the synthesis of alternative biobased building-block such as sugar canes, lignin from wood, or vegetal oils (Kristufek *et al.*, 2017; Stadler *et al.*, 2019; Siracusa *et al.*, 2020). Xylene is the principal raw material for the production of terephthalic acid, a constituent of the most widely used polyesters like polyethylene terephthalate (PET) (Mandal *et al.*, 2019). Thus, the replacement of oil-based monomers by biobased equivalents is currently a highly active research field (Pellis *et al.*, 2016b; Zia *et al.*, 2016).

Numerous biobased building-blocks have been identified for the synthesis of polyesters (Stadler *et al.*, 2019; Zhang *et al.*, 2021). As an example poly(butylene adipate) (PBAd) and poly(butylene succinate) (PBS) are produced from 1,4-butanediol, adipic acid and succinic acid (Debuissy *et al.*, 2016).

These building-blocks are produced from biorefining processes (Bozell *et al.*, 2010). However, these aliphatic polyesters such as PBS often present limited mechanical and thermal properties compared to PET which is the most widely used polyester, in particular because of the high properties brought by its aromaticity (Albanese *et al.*, 2016). For this reason, extensive research is being carried out on biobased aromatic building-blocks for the synthesis of polyesters (Nguyen *et al.*, 2018; Ali *et al.*, 2019). As an example, furan-based building-blocks, synthesized from sugars, represent a very promising alternative for the substitution of terephthalic acid (Nakajima *et al.*, 2017; Loos *et al.*, 2020). Among these biobased aromatic building blocks, cinnamic derivatives such as ferulic acid (FA) are gaining attention (Fonseca *et al.*, 2019).

FA is an alpha-beta unsaturated aromatic acid which presents a phenol in para and a methoxy group in meta position of the aromatic ring. It can be extracted from various natural sources such as wheat bran or corn stalk (Flourat *et al.*, 2021). Since FA presents good antioxidants, antifungal as well as drugs like properties (Mancuso *et al.*, 2014), the extraction of ferulic acid is largely investigated (Gopalan *et al.*, 2018; Ferri *et al.*, 2020). Thus, because of its availability and difunctionality, FA is a promising building-block for the synthesis of biobased aromatic polyesters. Ferulic-based polyesters have already been investigated (Nguyen *et al.*, 2015; Llevot *et al.*, 2016; Parthiban *et al.*, 2020). Polyesters only based on ferulic acid show extreme thermal transition temperature that could make them difficult to process (Elias *et al.*, 1985). When copolymerized, polyesters with tunable and high thermal properties could be obtained (Kreye *et al.*, 2013; Nguyen *et al.*, 2015; Kurt *et al.*, 2020). However, most of the syntheses were performed with organometallic catalysts. Such catalysts employed today present some disadvantages since they are often toxic, can lead to side reactions (Schoon *et al.*, 2017) and can remain trapped in the final material (Rovira *et al.*, 2015).

Lipases are enzymes that, in nature, catalyze hydrolysis of triglycerides during digestion. However, lipases have been employed for the catalysis of esterification and transesterification reactions (Shamim *et al.*, 2018). Because of its efficiency, versatility and resistance, the lipase B from *Candida antarctica* (CALB) is the most employed lipase (Ortiz *et al.*, 2019). CALB has thus been widely used for the synthesis of polyesters by esterification or transesterification, the later offering generally higher molar masses (Debuissy *et al.*, 2016, 2017b; Pellis *et al.*, 2019c). CALB has also been studied for the synthesis of aromatic biobased polyesters (Pellis *et al.*, 2019c). However, this is still a limited field of research when compared to aliphatic polyesters (Douka *et al.*, 2018). Our group assessed the reactivity of FA for the synthesis of aromatic polyesters (Bazin *et al.*, 2021a). However, the known low reactivity of FA towards CALB hindered the obtention of high molar mass polyesters (Stamatis *et al.*, 1999; Vosmann *et al.*, 2006). This lack of reactivity is attributed to the possible stabilization of the carbonyl due to the presence of electronic conjugation with the double bond and the aromatic ring. This electronic delocalization of the electrons is occurring along the FA double bond. Hydrogenation or breaking the conjugation improve the reactivity of the substrate towards CALB (Cassani *et al.*, 2007).

Cinnamic derivatives, of which ferulic acid is one, are known for their ability to undergo [2+2] cycloaddition under UV light (Curme *et al.*, 1967; Nguyen *et al.*, 2016). Such reaction leads to the dimerization of ferulic acid and thus transforms the double bond into a cyclobutane ring. Dimers of cinnamic derivatives are naturally found in plants (Morrison *et al.*, 1991, 1992). In such dimers, the carboxylic acid is no longer conjugated with the aromatic ring. The produced diacid could therefore potentially be more reactive towards CALB than the original monomer. Polymers based on cinnamic dimers have already been reported in the literature (Wang *et al.*, 2017; Zhang *et al.*, 2017). These polymers showed high thermal and mechanical properties. When blended with PET, the adduct allowed to obtain higher glass transition temperatures and better UV shielding (Ding *et al.*, 2019). Moreover, [2+2] cycloaddition is reversible under a specific wavelength (Marschner *et al.*, 2018). Thus, the use of cinnamic dimers as building-blocks allows the production of photocleavable polymers. Recycling of the polyesters is a major concern at present. In particular, innovative mechanical, chemical and biochemical processes for the recycling of the PET are currently being developed (Devi Salam *et al.*, 2021). Polymers displaying on purpose easy chemical degradation have also been developed to facilitate the material end of life management (Wang *et al.*, 2020a). The synthesis of photo-cleavable polyesters could benefit to the production of easily recyclable materials.

But, because of its crystalline structure, FA is known to react poorly by [2+2] cycloaddition (Ford *et al.*, 1989; Khan *et al.*, 2008). Thus, UV irradiation of FA leads to low yields of dimers. However, *p*-acetyl ferulic acid (**AcFA**), a derivative of FA, presents a high reactivity in [2+2] cycloaddition under UV light. This monomer was employed for the synthesis of polyesters and polyamides (Castillo *et al.*, 2004). Furthermore, we recently showed that a derivative of ferulic acid, the methyl 4-(methyl butanoate-oxy)-ferulate (**DeFA^{II}**), depicted in Scheme 4.2.1 (Bazin *et al.*, 2021a), presented an ester function with a high reactivity towards CALB-catalyzed transesterification with a diol. Dimerization of this substrate could result in a compound able to undergo CALB-catalyzed polymerization with potentially high conversion and therefore high molar mass. Thus, its ability to undergo [2+2] cycloaddition was also investigated.

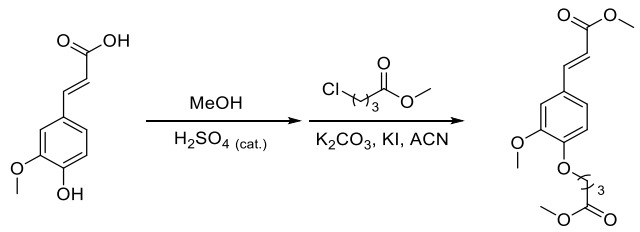

Scheme 4.2.1: Synthesis of the DeFA^{II} from ferulic acid (Bazin *et al.*, 2021a).

The two derivatives of FA, **AcFA** and **DeFA^{II}** were first dimerized through [2+2] cycloaddition under UV light. The solvent of reaction was optimized in order to obtain greener reaction conditions. The dimers of **AcFA** were assayed for polymerization with and without prior esterification. The lack of reactivity of these dimers oriented us towards the study of the polymerization of dimers of **DeFA^{II}**.

CALB-catalyzed polymerization of **DeFA^{II}** with diols of different lengths (1,3-propanediol (PDO), 1,4-butanediol (BDO), 1,6-hexanediol (HDO), 1,8-octanediol (ODO)) was performed. The polyesters structures, thermal properties as well as their photo-cleaving ability were investigated.

3. Experimental section

3.1. Materials

Ferulic acid, 1,3-propanediol (PDO), and pyridine were supplied by Alfa Aesar. Methyl 4-chlorobutyrate, potassium iodine, 1,4-butanediol (BDO) and diphenyl ether were supplied from Acros Organics. 1,6-hexanediol (HDO), acetic anhydride, Lipase from *Candida Antarctica* immobilized on acrylic resin (activity >5,000 U/g) (CALB) and deuterated chloroform ($CDCl_3$) were supplied by Sigma-Aldrich. 1,8-octanediol (ODO) was supplied from Fluka. Methanol, acetonitrile, cyclohexane and potassium carbonate were supplied by Fisher scientific. Ethanol, ethyl acetate and petroleum ether were purchased from VWR.

3.2. Characterization

The ^{1}H NMR spectra were collected on a Bruker 400 MHz spectrometer while ^{13}C NMR and 2D spectra were collected on a Bruker 500 MHz spectrometer. Typically, 10 mg of sample was dissolved in 600 µl of $CDCl_3$ before analysis. The spectra were calibrated using the $CDCl_3$ peak (δH = 7.26 ppm, δC = 77.16 ppm).

X-ray diffraction data collection was carried out on a Bruker PHOTON III DUO CPAD diffractometer equipped with an Oxford Cryosystem liquid N2 device, using Mo-Kα radiation (λ = 0.71073 Å). The crystal-detector distance was 37 mm. The cell parameters were determined (APEX3 software) from reflections taken from 1 set of 180 frames at 1s exposure. The structure was solved using the program SHELXT-2014. The refinement and all further calculations were carried out using SHELXL-2018. The other H-atoms were included in calculated positions and treated as riding atoms using SHELXL default parameters. The non-H atoms were refined anisotropically, using weighted full-matrix least-squares on F2. A semi-empirical absorption correction was applied using SADABS in APEX3; transmission factors: Tmin/Tmax = 0.6987/0.7456. The crystals were placed in oil, and a single crystal was selected, mounted on a glass fibre and placed in a low-temperature N2 stream.

HR-ESI-MS experiments were performed on a Bruker Daltonics microTOF spectrometer (Bruker Daltonik GmgH, Bremen, Germany) equipped with an orthogonal electrospray (ESI) interface. Calibration was performed using Tuning mix (Agilent Technologies). Sample solutions were introduced into the spectrometer source with a syringe pump (Harvard type 55 1111: Harvard Apparatus Inc., South Natick, MA, USA) with a flow rate of 4 µL.min^{-1}.

Number average molar mass (M_n), weight average molar mass (M_w), and dispersity (Đ) were measured by Size Exclusion Chromatography (SEC). The apparatus was a Shimadzu liquid

chromatograph equipped with a PLGel Mixed-C and PLGeL 100 Å columns and a refractive index (RI) detector. The analyses were performed in chloroform at a flow rate of 0.8 mL/min. Molar mass determination was performed via polystyrene calibration curves.

Differential scanning calorimetry (DSC) was employed to determine the samples glass transition temperature (T_g), melting temperature (T_m) and crystallization temperature (T_c), if applicable. The apparatus was a Q2000 DSC from TA instrument (TA instrument, New Castle, Delaware, USA). Samples of 1 to 3 mg were placed in sealed aluminum pan and fast heated to 160 °C to erase thermal history. The sample was then cooled to -80 °C at a cooling rate of 10 °C.min^{-1}. After an isotherm of 5 minutes, a second heating up to 160 °C was performed at a heating rate of 10 °C.min^{-1}.

Thermogravimetric analyses (TGA) were performed on a High-Res TGA Q5000 from TA instrument. Platinum pans containing between 1 and 2 mg of sample were heated at a heating rate of 10 °C.min^{-1} from room temperature to 600 °C.

Infrared spectroscopy (IR) at a resolution of 4 cm^{-1} and with 32 scans per run were performed on a Nicolet 380 Fourier transformed infrared spectrometer (Thermo Electron Corporation). The apparatus was used in reflection mode and equipped with an ATR diamond module (FTIR).

A Spectrometer UV-2600 (Shimadzu) was employed for UV-visible absorbance measurements. Liquid samples were analyzed in quartz cuvettes. Solid samples were analyzed after being cast on quartz plates as described later.

A photoreactor LZC-4X$_b$ (Luzchem Research, Inc) was employed for irradiation of the samples. The apparatus was equipped with 14 lamps emitting either UV-A (350 nm) or UV-C (254 nm). Solid samples were placed on a rotating plate for uniform irradiation.

3.3. Synthesis of the monomers

*3.3.1. Acetyl ferulic acid (**AcFA**)*

The synthesis of the acetyl ferulic acid was performed according to a protocol adapted from the literature (Allais *et al.*, 2009). Ferulic acid (1g, 5.15 mmol, 1 eq.) was dissolved in a mixture of acetic anhydride (1.5 ml, 15.5 mmol, 3 eq.) and pyridine (1.7 ml, 20.6 mmol, 4 eq.). The solution was stirred at room temperature. After 3 hours, the solution was poured into a large volume of ice and water and the product precipitated. The solution was centrifuged (8000 g, 10 minutes). The supernatant was eliminated and replaced with deionized water. This washing of the pellet was repeated 3 times and the product was dried 24 h in a vacuum oven at 40°C. The product was obtained as a white power with yield of 94 %. MP: 199 °C (lit. 195-201 °C(Castillo *et al.*, 2004; Allais *et al.*, 2009)), IR 1758, 1678, 1630 cm^{-1} (lit. 1762, 1689, 1632(Castillo *et al.*, 2004)). ^{1}H NMR (400 MHz, DMSO) δ (ppm) 7.57 (d, J = 16.0 Hz, 1H), 7.47 (d, J = 1.9 Hz, 1H), 7.25 (d, J = 1.8 Hz, 1H), 7.11 (d, J = 8.2 Hz, 1H), 6.58 (d, J = 16.0 Hz, 1H), 3.82 (s, 3H), 2.26 (s, 3H). ^{13}C NMR (126 MHz, DMSO) δ (ppm) 168.90, 168.07, 151.61, 143.82, 141.27, 133.72, 123.67, 121.79, 119.98, 112.30, 56.44, 20.85.

*3.3.2. Diester of ferulic acid (**DeFA^{II}**)*

The synthesis of the diester of ferulic acid was performed as depicted in a previous study (Bazin *et al.*, 2021a). Briefly, ferulic acid was first dissolved in an excess of methanol. A catalytic amount of H_2SO_4 was added and the solution was heated to reflux overnight. After neutralization with $NaHCO_3$, the solvent was evaporated under vacuum. The crude product was dissolved in ethyl acetate and the solution was dried over $MgSO_4$ and salts were eliminated by filtration. Evaporation of the solvent under vacuum yielded methyl ferulate as a yellow oil. Methyl ferulate was employed without further purification. The methyl ferulate (1g, 4.80 mmols, 1eq.) was dissolved in acetonitrile (24 ml). Potassium carbonate (1.99 g, 14.41 mmols, 3 eq.) and potassium iodine (0.19 g, 1.15 mmols, 0.24 eq.) were added as catalyst. Methyl chlorobutyrate (1.17 ml, 9.61 mmols, 2 eq.) was added to the solution. The solution was then vigorously stirred and heated to reflux overnight. The solution was then cooled down and the solid catalyst was eliminated by filtration. The solvent was eliminated by evaporation under vacuum and the crude product was dissolved in ethyl acetate. The organic solution was washed once with a saturated solution of sodium carbonate and twice with brine. The solution was recovered and dried over $MgSO_4$. The solvent was evaporated under vacuum and the product was recrystallized in a mixture of ethanol and water. The methyl 4-(methyl butanoate-oxy)-ferulate (2b) was obtained as off-white needles with a yield of 80%. MP: 83 °C, IR (in cm^{-1}): 2952 (C-H), 1699 (C=O ester), 1510 (C=C Ar), 1250 (C-O ester), ^{1}H NMR (400 MHz, $CDCl_3$) δ (in ppm) 7.62 (d, J = 15.9 Hz, 1H), 7.13 – 7.01 (m, 2H), 6.86 (d, J = 8.3 Hz, 1H), 6.30 (d, J = 16.0 Hz, 1H), 4.09 (t, J = 6.3 Hz, 2H), 3.88 (s, 3H), 3.79 (s, 3H), 3.68 (s, 3H), 2.54 (t, J = 7.2 Hz, 2H), 2.23 – 2.08 (m, 2H)). ^{13}C NMR (126 MHz, $CDCl_3$) δ (in ppm): 173.54, 167.69, 150.46, 149.60, 144.80, 127.54, 122.52, 115.53, 112.66, 110.22, 77.09, 67.79, 55.96, 51.68, 51.63, 30.41, 24.40.

3.3.3. UV dimerization

AcFA or the ferulic diester **DeFA^{II}**, (1g) was suspended in 500 ml of deionized water in an Erlenmeyer. The Erlenmeyer was plugged with a septum and placed in the photoreactor. The solution was magnetically stirred and irradiated under UV light (350 nm) for 48h. Progress of the reaction was controlled by NMR analyses. For that, aliquots were withdrawn at regular time intervals. The solvent was evaporated, and the product was dissolved in DMSO-*d6* before analysis. The final product was recovered by filtration (0.45 mm PVDF membranes, Merck Millipore) and dried under vacuum at 40°C.

Acetyl ferulic acid dimer (**DAcFA**): Yield: 90 %. MP: 274 °C (lit. 278 °C(Castillo *et al.*, 2004)), IR: 1754, 1692 cm^{-1} (lit. 1756, 1698(Castillo *et al.*, 2004)), ^{1}H NMR (400 MHz, DMSO-*d6*) δ (ppm) 12.24 (s, 2H), 7.09 (d, J = 2.0 Hz, 2H), 7.02 (d, J = 8.1 Hz, 2H), 6.93 (dd, J = 8.2, 1.9 Hz, 2H), 4.30 (dd, J = 10.5, 7.2 Hz, 2H), 3.82 (dd, J = 10.5, 7.3 Hz, 2H), 3.78 (s, 6H), 2.25 (s, 6H). ^{13}C NMR (126 MHz, DMSO-*d6*) δ (ppm) 172.99, 168.52, 150.36, 138.43, 138.04, 122.36, 119.42, 112.45, 55.71, 46.34, 40.86, 39.50, 20.41.

Ferulic diester dimer (**DDeFA^{II}**): Yield: 95 %. MP: 109 °C, IR: 2952, 1731, 1588 cm^{-1}, ^{1}H NMR (400 MHz, $CDCl_3$) δ (ppm) 6.85 – 6.78 (m, 6H), 4.36 (dd, J = 10.6, 7.2 Hz, 2H), 4.04 (t, J = 6.3 Hz, 4H), 3.94 – 3.86 (m, 2H), 3.87 (s, 6H), 3.68 (s, 6H), 3.36 (s, 6H), 2.54 (t, J = 7.3 Hz, 4H), 2.14 (d, J = 6.5 Hz, 4H). ^{13}C NMR (126 MHz, $CDCl_3$) δ (ppm) 103.77, 102.59, 79.41, 77.51, 61.84, 49.54, 43.26, 41.71, 7.16, -1.96, -13.85, -18.23, -18.25, -22.73, -28.69, -39.36, -45.32. HR-ESI-MS: *m/z* $[M + Na]^+$ calc = 639.242224, found = 639.241197.

*3.3.4. Diester of acetyl ferulic acid dimer (**DeDFA**):*

DAcFA (1g) was placed in a large volume of ethanol (100 ml). Few drops of H_2SO_4 were added as a catalyst. The solution was placed at reflux and the reaction progress was controlled by TLC (ethyl acetate). After 24 hours the reaction was stopped. The solution was neutralized with $NaHCO_3$, and the solvent was evaporated in rotary evaporator. The product was solubilized in ethyl acetate and the solution was dried over $MgSO_4$. The salts were filtered off and the solvent was evaporated. The product was recrystallized in a mixture of ethanol and water.

The product was recovered as orange needles: Yield: 99 %, MP: 149 °C, IR: 3418, 1709, 1610 cm^{-1}, ^{1}H NMR (400 MHz, $CDCl_3$) δ (ppm) 6.86 (d, J = 7.9 Hz, 2H), 6.85 – 6.77 (m, 4H), 5.53 (s, 2H), 4.36 (dd, J = 10.7, 7.2 Hz, 2H), 3.90 (s, 6H), 3.90 – 3.71 (m, 6H), 0.90 (t, J = 7.1 Hz, 6H). ^{13}C NMR (126 MHz, $CDCl_3$) δ (ppm) 172.06, 146.28, 144.73, 130.89, 120.36, 114.19, 110.52, 60.49, 56.00, 47.32, 41.21, 13.94. HR-ESI-MS: *m/z* $[M + Na]^+$ calc = 639.240787, found = 639.241197.

3.3.5. Enzymatic polymerization

Enzymatic polymerization conditions were identical for all substrates. As an example, **DDeFA^{II}** (100 mg, 0.16 mmol, 1 eq.) was placed in a Schlenk reactor. A diol was added in equimolar proportion (0.16 mmol, 1 eq.) or in excess when specified. Pre-dried CALB was added with a mass equivalent to 40 weight percent (wt.%) of the monomers or lower when specified. Finally, diphenyl ether was added (600 wt.% of the monomers). The solution was placed at 90 °C under a pressure of 350 mbar. After 4 hours of reaction, the pressure was reduced to 100 mbar. Finally, after 8 hours of reaction, the pressure was further reduced to 20 mbar and kept the same until the end of the reaction. At the end of the reaction, the solution was cooled down and diluted with chloroform. The catalyst was eliminated by filtration through cotton wool and the polymer was precipitated in petroleum ether cooled at -78 °C. The solution was then centrifuged, and the supernatant was eliminated. The polymer was dried for 24 h under vacuum at 40 °C prior to analysis.

3.3.6. Photo-depolymerization

For photo-depolymerization, the samples were irradiated in the photoreactor under UV-C lamps (λ = 254 nm) at a controlled distance of 4.5 cm.

For NMR analysis monitoring: polymer samples (10 mg) were dissolved in 500 µl of chloroform. The solution was poured on a watch glass and the solvent was first evaporated at ambient

temperature and pressure followed by drying 15 minutes at 40 °C under vacuum. The samples were then placed in the photoreactor on a rotating plate and irradiated for the corresponding amount of time. For UV absorption measurement, polymers were solvent cast on quartz plate before analysis. For that, 5 mg of sample was dissolved in 500 µl of chloroform. 20 µl of the solution was deposited on a quartz plate on a controlled area. The solvent was first evaporated at ambient followed by drying under vacuum at 40°C for 15 minutes prior to analysis.

4. Results and discussion

4.1. Synthesis of ferulic-based monomers for polymerization

As already mentioned in the introduction and reported in the literature, the carboxylic acid of FA presents a limited reactivity towards CALB. This phenomenon is most probably caused by electronic delocalization along the double bond stabilizing the ferulic acid. A previous study showed that preserving the double bond of the ferulic acid hindered the production of high molar mass polyesters (Bazin *et al.*, 2021a). On the contrary, hydrogenation of the double bond unlocked the reactivity of ferulic acid towards the enzyme and allowed to obtain high molar mass polyester. Similar unlocking of the reactivity by hydrogenation was also described in the literature (Cassani *et al.*, 2007). However, hydrogenation uses an excess of hydrogen which is a dangerous explosive gas. Therefore, we aimed at developing an alternative method to unlock the reactivity of ferulic based adducts towards CALB.

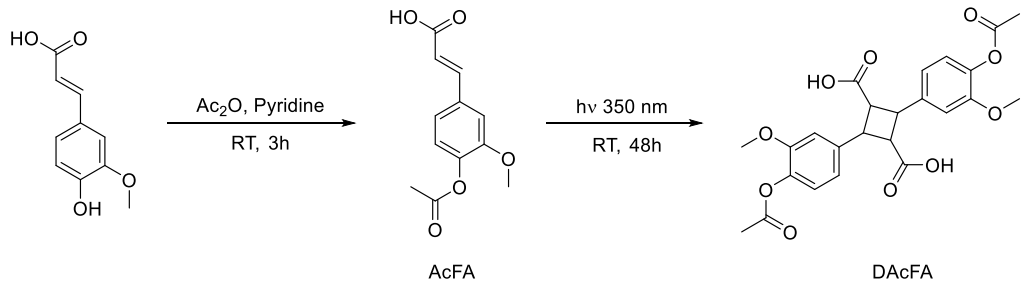

Scheme 4.2.2: Synthesis and dimerization of p-acetyl ferulic acid.

The [2+2] cycloaddition is a green method for reacting the double bond of cinnamic derivatives. By this method, a difunctional adduct is obtained. Moreover, the carboxylic acids in the dimer form are no longer conjugated with the aromatic ring, potentially unlocking their reactivity towards CALB. However, it has been shown in the literature that the UV dimerization of FA is difficult (Ford *et al.*, 1989). This is caused by the particular crystalline form of ferulic acid which leads to an excessive distance between the double bonds and an unfavorable alignment of the molecules one to another (Khan *et al.*, 2008).

Castillo *et al.* (Castillo *et al.*, 2004) discovered that once acetylated, the ferulic acid dimerized quantitatively through [2+2] cycloaddition (Scheme 4.2.2). Thus, ferulic acid was acetylated to give **AcFA**. Structure of the product was confirmed by IR and NMR. NMR spectra are available in Annexes

Figure S4.1 and Figure S4.2. Nonpolar solvents as hexane or cyclohexane are commonly employed for UV dimerization (Castillo *et al.*, 2004; Nguyen *et al.*, 2016; Horbury *et al.*, 2017). The **AcFA** was thus suspended in cyclohexane prior to exposition to UV light at a wavelength of 350 nm. After 24 hours of reaction, NMR analysis of the crude product obtained was performed (in Annexes Figure S4.3.a). The peaks attributed to the double bond of **AcFA** at δ = 6.58 and 7.57 ppm only remained as traces. Two new signals at δ = 3.80 and 4.30 ppm were attributed to the hydrogen of the cyclobutane resulting from the [2+2] cycloaddition. Quantitative conversion (99%) of **AcFA** into its dimer (**DAcFA**) was calculated. However, cyclohexane is a hazardous toxic and polluting solvent (*Cyclohexane*, 2021). Moreover, alternative less hazardous solvents have been shown to enable cycloaddition (Wang *et al.*, 2020b). Acetonitrile, ethyl acetate and water have therefore been tested for the cycloaddition of **AcFA**. These solvents are preferred to cyclohexane according to different rankings based on toxicity and environmental impact (Prat *et al.*, 2016; Tobiszewski *et al.*, 2017). After 24 h of irradiation, aliquots were analyzed by NMR (Figure 4.2.1 and in Annexes Figure S4.3.b-d).

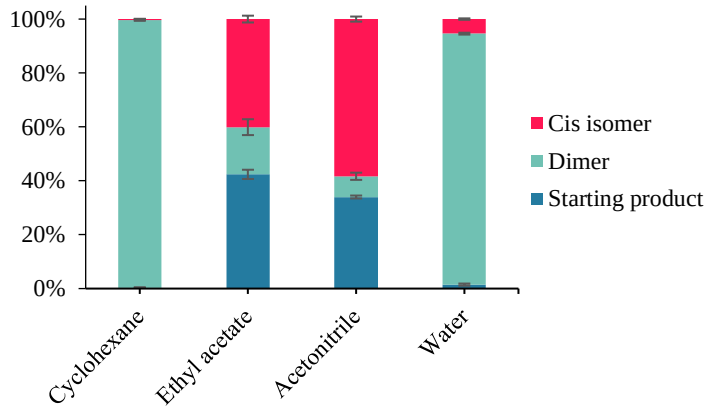

Figure 4.2.1: Yield of the dimer, *cis* isomer and starting product after exposition of AcFA to UV light (350 nm) for 24 hours in different solvents. All measurements were performed on triplicates.

The products of irradiation of **AcFA** were studied for all solvents. In addition to the product of dimerization, peaks at δ = 5.97 and 6.89 ppm with a coupling constant value of 12.8 Hz could be observed in all samples. These peaks were attributed to the hydrogens of the double bond of **AcFA** in *cis* conformation. Indeed, *cis* isomerization of ferulic acid and its derivatives can be induced by UV irradiation (Shindo *et al.*, 1984; Ramamurthy *et al.*, 1987; Salum *et al.*, 2015). The yield of dimerization and *cis* isomerization depended greatly on the solvent of reaction. In the case of ethyl acetate and acetonitrile, the product was mainly converted into its *cis* isomer. However, water allowed to obtain high yields of dimer similar to cyclohexane and is therefore a good substituent of this solvent as it is a safer alternative. Moreover, water could be easily reused in the process, making it even more environmentally friendly according to the principles of green chemistry.

The structure of the synthesized **DAcFA** was fully characterized by NMR (in Annexes Figure S4.4 and Figure S4.5) and the results were in agreement with those of the literature (Castillo *et al.*,

2004). **DAcFA** was then tested for CALB-catalyzed polymerization. However, the substrate was insoluble in diphenyl ether which is the common solvent for the enzymatic polymerization reaction, and it could not be melted at temperatures compatible with the enzyme catalytic activity. For these reasons, no conversion of **DAcFA** by the CALB was obtained (data not shown). However, esterification of a carboxylic acid is known to decrease its melting point and to greatly improve its solubility in organic solvents. For this purpose, **DAcFA** was esterified to produce **DeDFA** (see Scheme 4.2.3).

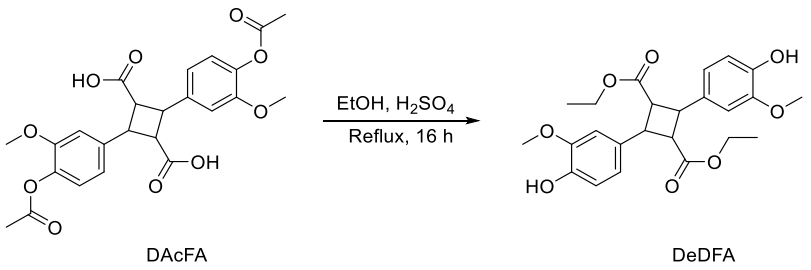

Scheme 4.2.3: Esterification of the DAcFA to produce DeDFA.

The structure of the **DeDFA** was confirmed by IR and NMR (in Annexes Figure S4.6 and Figure S4.7). The disappearance of the signal corresponding to the acetyl moieties at δ = 2.26 ppm indicates that the acetyl groups were removed by alcoholysis. This **DeDFA** dimer was soluble is diphenyl ether. Thus, its reactivity towards CALB was estimated in a model reaction with a monofunctional substrate. The **DeDFA** was reacted with an excess of butanol in diphenyl ether at 90 °C for 40 minutes in the presence of CALB. However, no conversion of the carbonyl was observed by NMR analysis. Polymerization tests with a diol (HDO) also did not result in polymer formation (data not shown).

The esters in **DeDFA** are close to each other and are surrounded by bulky phenolic groups. Steric hindrance can prevent the substrate from entering the reactive pocket of CALB (Otto *et al.*, 2000). In our case, the bulky groups surrounding the carbonyls could prevent them from reacting properly with CALB.

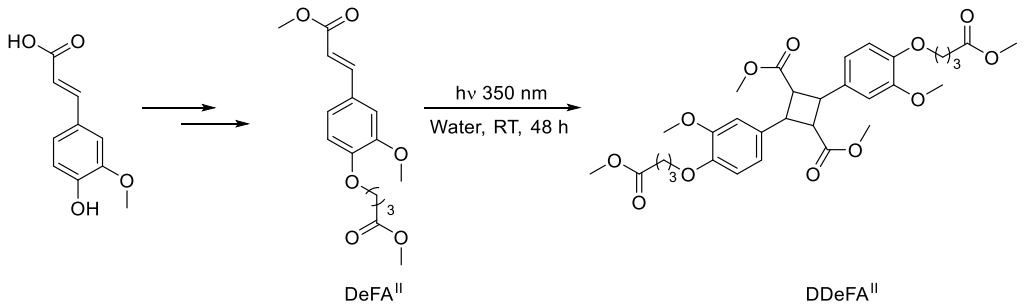

Scheme 4.2.4: Synthesis and dimerization of DeFA^{II} into DDeFA^{II}.

The ability of a diester of ferulic acid synthesized in a previous study (**DeFA^{II}**) to undergo [2+2] cycloaddition under UV light was assessed (Scheme 4.2.4). This reaction would lead to the formation of a tetra-ester (**DDeFA^{II}**) from which two esters are sterically hindered, like in **DeDFA**. However, the two other esters are distant from the bulky core of the molecule and could therefore be reactive towards

CALB. As for the dimerization of **AcFA**, different solvents were tested for the dimerization of **DeFA^{II}** under UV at 350 nm. The same solvent as before, namely cyclohexane, ethyl acetate, acetonitrile, and water were assayed. The resulting yields of dimerization and isomerization have been calculated from NMR analyses (Figure 4.2.2 and in Annexes Figure S4.8).

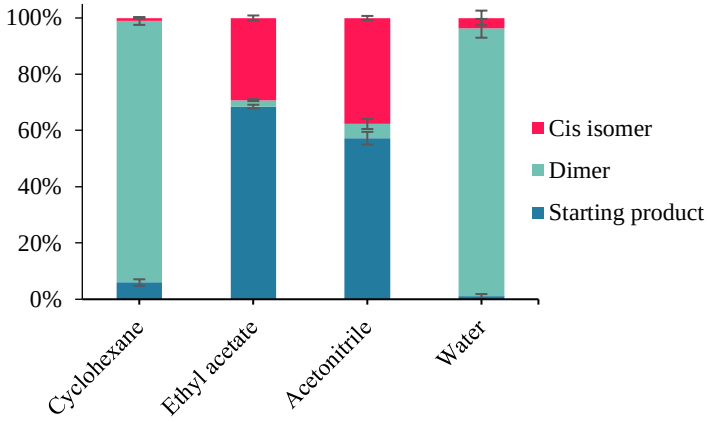

Figure 4.2.2: Yield of the dimer, *cis* isomer and starting product after exposition of DeFA^{II} to UV light (350 nm) for 24 hours in different solvents. All measurements were performed on triplicates.

As previously, a high conversion of **DeFA^{II}** into its dimer was obtained in cyclohexane (93%). Moreover, it was again found that water could also provide a high yield of the dimer (95%). Again, ethyl acetate and acetonitrile resulted in the production of a majority of *cis* isomer (identified at δ = 5.86 and 6.92 ppm with a coupling constant of 12.9 Hz). The ratio of *cis* isomerization was correlated to the solubility of **DeFA^{II}** in a given solvent. Indeed, **DeFA^{II}** was fully soluble in ethyl acetate and acetonitrile and insoluble in water and cyclohexane (determined qualitatively, in Annexes Figure S4.9). Similar observations have been reported in the literature (Ramamurthy *et al.*, 1987). When the substrate is solubilized, its mobility allows *cis* isomerization and the distance between the molecules does not favor cycloaddition. Inversely, when the substrate is suspended in its crystalline form it does not have the mobility to undergo the *cis* isomerization and the proximity of the double bonds promotes the cycloaddition. Therefore, as for the synthesis of **DAcFA**, cyclohexane was substituted with water in order to perform the reaction in safer and greener conditions.

The structure of DDeFa was fully characterized by NMR and IR spectroscopy (see Annexes Figure S4.10 and Figure S4.11). However, two forms of dimerization of **DDeFA^{II}** are possible (Figure 4.2.3). The compound can dimerize forming a cyclobutane with vicinal esters (head-to-head) or with esters opposite one to another (head-to-tail). As both compounds are fully symmetrical, it is difficult to distinguish them by NMR spectroscopy. Even by measuring nuclear Overhauser effect it was not possible to differentiate them. Moreover, no comparison could be found in the literature as DDeFa is a new compound. Thus, **DDeFA^{II}** was analyzed by X-ray diffraction measurement on a single crystal to

obtain the precise structure of the compound as well as its conformation in space (Figure 4.2.4 and in Annexes Figure S4.12).

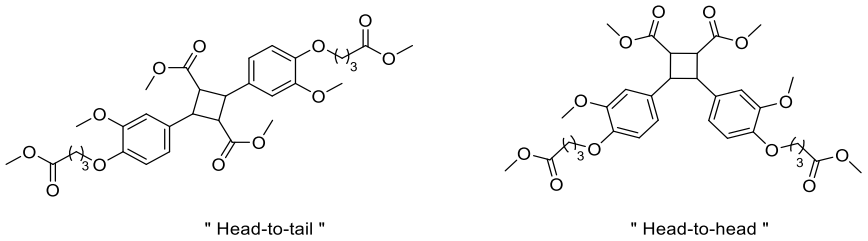

Figure 4.2.3: Schematic representation of the two possible isomers resulting from the [2+2] cycloaddition reaction of DeFA^{II}.

a)

b)

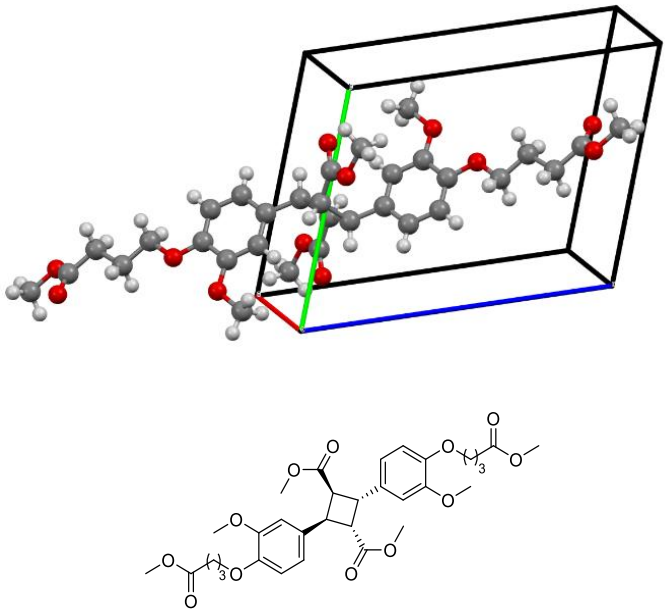

Figure 4.2.4: Head-to-tail structure of DDeFA^{II} determined by XRD analysis: a) Three-dimensional crystalline conformation; b) schematic representation.

X-ray diffraction confirmed that the obtained dimer corresponds to the head-to-tail one. This is in accordance with previous studies showing that the head-to-tail is the privileged form of dimerization (Khan *et al.*, 2008; Nguyen *et al.*, 2016). Moreover, the esters are in *trans* position with respect to the cyclobutane plane. The same is observed for the aromatic rings. As mentioned earlier, the packing arrangement of the molecules in the crystal governs their reactivity towards cycloaddition (Ramamurthy *et al.*, 1987). Three crystalline phases have been identified (α, β, and γ) but only the α and β crystalline forms are photoreactive because of convenient distance between the double bonds in the lattice (3.5 - 4.2 Å). The distance between the double bonds of **DeFA^{II}** was measured here as 3.59 Å by XRD analysis (in Annexes Figure S4.13). The structure of **DeFA^{II}** crystals corresponds to the α form which is in adequation with its ability to form head-to-tail dimers under UV light irradiation.

The reactivity of **DDeFA^{II}** towards CALB was assessed in transesterification with an excess of butanol. High conversion of the esters from the butyrate moieties was observed by NMR analysis (in Annexes Figure S4.14). However, the central ferulic esters were not converted, showing the high selectivity of CALB. This allowed to consider the **DDeFA^{II}** as a difunctional monomer which is thus suitable for the synthesis of linear polyesters by CALB-catalyzed polymerization.

4.2. Polymerization of ferulic-based dimers.

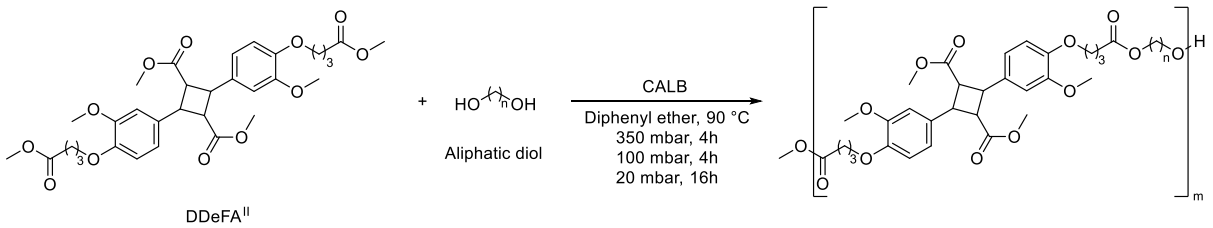

Scheme 4.2.5: CALB catalyzed polymerization of DDeFA^{II} with diols of different lengths.

DDeFA^{II} was used as diester for the synthesis of polyesters through CALB catalyzed polymerization. CALB has been described in the literature as highly selective (Mahapatro *et al.*, 2003; Douka *et al.*, 2018). This substrate specificity influences the molar mass of the obtained polyester as well as the kinetics of the reaction. Thus, in order to study the selectivity of CALB in such conditions, **DDeFA^{II}** was reacted with diols of different lengths (Scheme 4.2.5). This way, the influence of the diol length on the synthesis of the polyester by CALB was assessed. The structures of the polyesters were determined by NMR spectroscopy (in Annexes Figure S4.15). As an example, analysis of the polymer resulting from the CALB-catalyzed polymerization of **DDeFA^{II}** with HDO is presented and interpreted in Figure 4.2.5. The polymer NMR spectrum is compared with the one from the starting product.

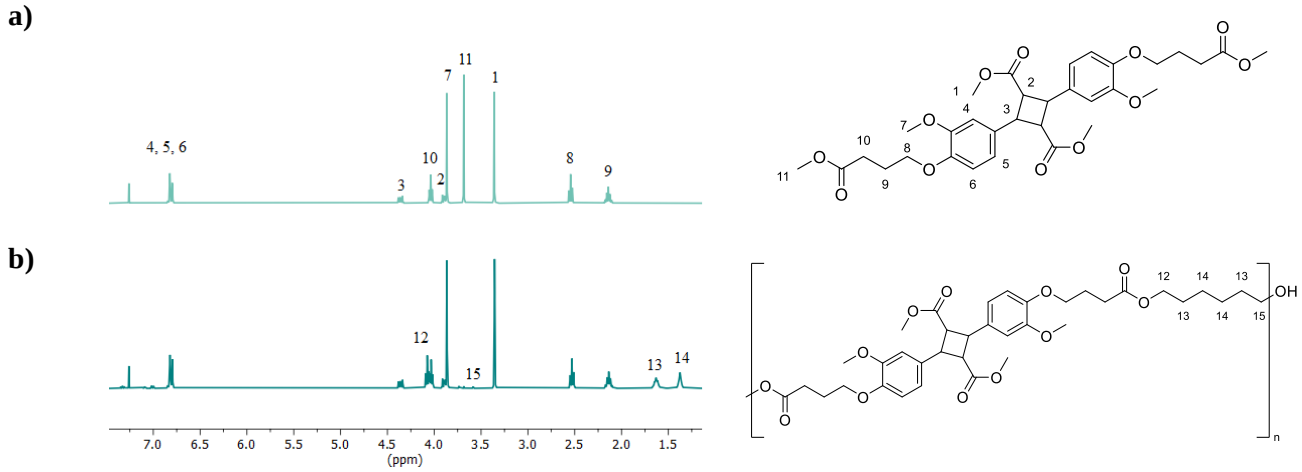

Figure 4.2.5: NMR spectra of: a) DDeFA^{II} and b) the polyester synthesized from DDeFA^{II} and HDO.

After the polymerization, a triplet in the range δ = 4.07-4.17 ppm (peak 12 on Figure 4.2.5) is observed. This peak has been attributed to the C**H**$_2$-O-C(O) of the reacted diol. This therefore confirms that HDO reacted with **DDeFA^{II}** by CALB-catalyzed transesterification reaction. The signal at δ = 3.68 ppm (peak 1 in Figure 4.2.5) corresponding to the esters situated the furthest from the aromatic rings is hardly discernable after polymerization. Therefore, one can conclude that this ester reacted with CALB and was consumed during the reaction, releasing methanol which was removed by reduced pressure. Moreover, the intensity (I) of the signal corresponding to the ester groups borne by the cyclobutane at δ = 3.35 ppm (peak 11 in Figure 4.2.5) remained identical before and after polymerization. This attests that the ester attached to the cyclobutane did not react and remain unchanged in the final polymer chain. Thus, **DDeFA^{II}** has successfully been converted to linear polyester chains with pendant ester groups whose peculiar structure results from the high selectivity of CALB.

NMR analysis can also be used to estimate the number average molar mass (M_n) of polymers (Izunobi *et al.*, 2011). Such estimation requires to identify isolated signals corresponding to the repeating unit as well as the polymer end-groups. This method has been described as an interesting tool for the

estimation of molar masses below 25 000 g.mol^{-1} (Izunobi *et al.*, 2011). Indeed, at higher molar masses the intensity of the signals corresponding to end-groups becomes hardly discernable from the background noise. In this study, the signal situated at δ = 4.36 ppm (peak 3 in Figure 4.2.5) is isolated from other signals and corresponds to a hydrogen from the repetitive unit. As mentioned before, the signal assigned to the esters situated the further from the aromatic rings at δ = 3.68 ppm (peak 1 in Figure 4.2.5) corresponds to the polymer ester end-group. The positions of the signal corresponding to the hydroxyl end-group varied depending on the employed diol and was attributed accordingly.

$$M_{n(NMR)} = \frac{I_{unit} * m_{unit} + \frac{I_{ester}}{3} * m_{ester} + \frac{I_{hydroxyl}}{2} * m_{hydroxyl}}{0.5 * (\frac{I_{ester}}{3} + \frac{I_{hydroxyl}}{2})} \quad (4)$$

Equation 4 was employed to calculate the average molar mass of the polyesters synthesized with CALB from **DDeFA^{II}** and the diols of different lengths. In this equation I_{unit} corresponds to the intensity of the signal situated at δ = 4.36 ppm (peak 3 in Figure 4.2.5), I_{ester} corresponds to the intensity of the signal at δ = 3.68 ppm (peak 1 in Figure 4.2.5) and $I_{hydroxyl}$ corresponds to the intensity of the C**H**$_2$-OH of the hydroxyl end-groups. The coefficients m_{unit}, m_{ester} and $m_{hydroxyl}$ correspond to the molar mass of the repetitive unit, the ester end-group, and the hydroxyl end-group, respectively. When PDO was employed as a diol, part of the signal corresponding to the hydroxyl end-group was shouldered by the signal of the methoxy at δ = 3.86 ppm. Furthermore, when BDO was employed as a diol, the signal corresponding to the hydroxyl end-group was shouldered by the ester end-group signal as δ = 4.36 ppm. In these two cases, the M_n was evaluated as well as possible, and the results should be considered cautiously. The molar masses calculated from NMR analyses of the polyesters synthesized with different diols along time are given in Figure 4.2.6 and Table 4.2.1.

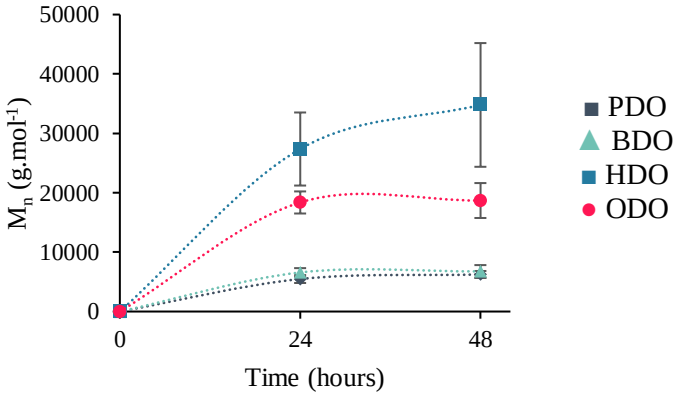

Figure 4.2.6: Time evolution of Mn values during the polymerization of DDeFA^{II} with diols of different length. Each measurement was performed in triplicates.

The higher molar masses were obtained with HDO as diol with a $M_{n(RMN)}$ up to 34 800 g.mol^{-1}. However, the estimated molar mass of the polymer is higher than 25 000 g.mol^{-1}. As mentioned earlier, in this case, the intensity of the signal corresponding to the polymer end-groups becomes difficult to

discern from the background noise. This could explain the higher variability of the values obtained with this diol. The polyester synthesized with ODO also resulted in high molar mass polyester with $M_{n(RMN)}$ up to 18 700 g.mol^{-1}. The polyester synthesized with BDO and PDO similarly resulted in much lower molar masses (up to 6 800 and 6 200 g.mol^{-1}, respectively). Previous studies from the group of Gross (Mahapatro *et al.*, 2003; Feder *et al.*, 2010) showed that the molar mass of aliphatic polyesters synthesized with CALB increased with the diol length. This is also supported by Pellis *et al*. (Pellis *et al.*, 2018) and Jiang *et al*. (Jiang *et al.*, 2015) who showed that the CALB-catalyzed synthesis of aromatic furan-based polyester followed the same trend. This is generally attributed to the higher affinity of CALB towards nonpolar substrates due to the hydrophobicity of the CALB docking pocket (Pleiss *et al.*, 1998). This would also explain that higher molar masses are obtained here with HDO and ODO as diols when compared to PDO and BDO. However, the fact that higher molar masses are obtained with HDO when compared with ODO is not in agreement with the previously cited literature. Uncertainty in the NMR molar mass estimation due to the signal to noise ratio or other phenomena (hydrolysis, macrocycles…) could explain this trend. Identification of the polymer end-groups on NMR spectra allows to calculate the ratio between the ester and hydroxyl end-groups. Thus, the percentage of ester end-groups is equal to $(I_{ester}/3)/(I_{hydroxyl}/2 + I_{ester}/3)$ and was calculated for each polymer after 24 and 48 hours of reaction (Figure 4.2.7).

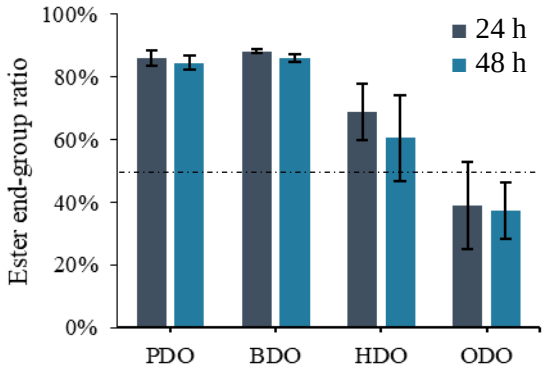

Figure 4.2.7: Calculated ratio of ester end-groups in the polyesters synthesized with diols of different lengths. Each measurement was performed in triplicates.

Polyesters synthesized with PDO and BDO presented a high ratio of esters end-groups (85-88 %). Similar results were obtained by our group for the CALB-catalyzed synthesis of aliphatic polyesters from BDO and PDO with diethyl adipate or succinate as diester (Debuissy *et al.*, 2017b). Loss of PDO and BDO during the reaction could explain the high ratio of ester end-groups. Indeed, PDO and BDO are the monomers with lower boiling temperature (211 and 235 °C at atmospheric pressure, respectively). Even if their boiling point at reduced pressure (estimated from a nomograph) was higher than the temperature of reaction, the non-null vapor pressure of these monomers combined with a partial vacuum can nevertheless lead to evaporation of the monomer. Evaporation of the diol during the reaction leads to an unbalanced stoichiometry that, according to Carothers' law, could explain the low molar

masses of the PDO and BDO-based polyesters. HDO, being less prone to evaporation, leads to lower ester to hydroxyl end-groups ratio (60 % after 48h). Finally, the polyester synthesized with ODO presents a ratio of ester to hydroxyl end-groups of 37 % after 48h. Such a ratio below 50 % indicates an excess of hydroxyl functions when compared to the ester end-groups. In this case, ester end-groups could be consumed by hydrolysis of the polymer during the reaction. This would result in a decrease of the ester signal intensity without impacting the hydroxyl signal intensity.

SEC was used as well to characterize the polymers molar mass distribution. The time evolution of the M_n values and the elution profiles of the different polyesters are given in Figure 4.2.8. The M_n, M_w as well as the dispersity (Đ) values of the polyesters synthesized from **DDeFA^{II}** and diols of different lengths are given in Table 4.2.1.

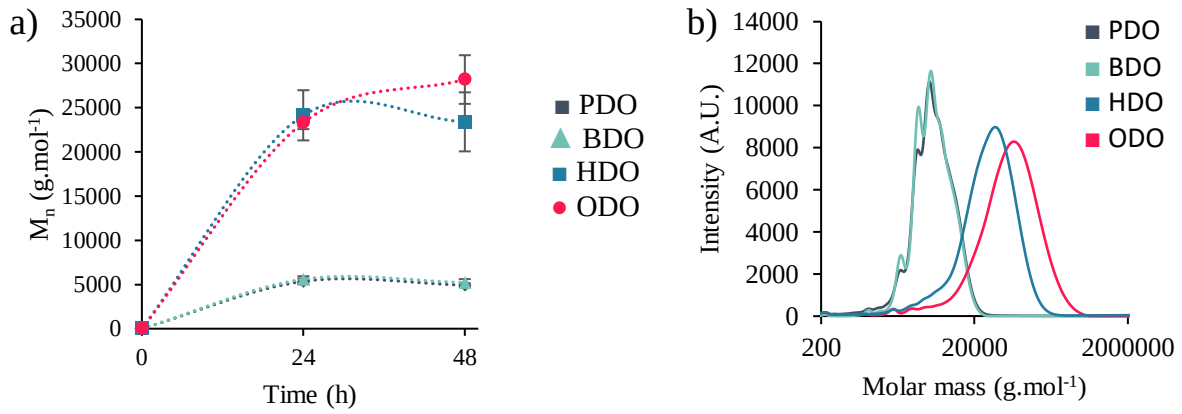

Figure 4.2.8: SEC analyses of the polyesters synthesized from DDeFA^{II} and diols of different lengths (diphenyl ether, 90°C, partial vacuum): a) Time evolution of M_n values; b) Chromatogram at 48 hours of reaction, values calculated from PS calibration curve and normalized on the area, logarithmic scale.

According to the SEC results, the polyester showing the highest molar mass was the one synthesized from ODO. M_n up to 28 200 g.mol^{-1} and Mw up to 57 700 g.mol^{-1} were reached in 48 hours. The polyester synthesized from HDO was obtained with M_n up to 24 100 g.mol^{-1}. Again, BDO and PDO led to polymers with the lowest M_n (5 200 and 4 900 g.mol^{-1}, respectively). Thus, from the SEC measurements, the longer diols allowed to produce polyester with higher molar mass which fully agrees with the literature (Mahapatro *et al.*, 2003; Feder *et al.*, 2010; Jiang *et al.*, 2015; Pellis *et al.*, 2018). For the sake of comparison, ferulic-based polyesters were synthesized with CALB by our group and M_n up to 17 900 g.mol^{-1} were obtained (Bazin *et al.*, 2021a). It is well known that CALB-catalyzed polymerization of aromatic monomers generally produces low molar mass polyesters (Fodor *et al.*, 2017; Comerford *et al.*, 2020). However, recent studies on furan-based polyesters (Flores *et al.*, 2019; Maniar *et al.*, 2019) allowed to obtain semi-aromatic polyesters with M_n up to 16 100 g.mol^{-1} and with higher DP_n values when compared to the current study. Thus, this demonstrates that with the appropriate optimization, CALB-catalysis can allow the synthesis of high molar mass aromatic polyesters.

We can also observe that M_n values are significatively different when estimated from NMR and SEC analyses. As depicted earlier, M_n estimation calculated from NMR analysis depends on the intensity of the signal corresponding to the polymer end-groups which leads to a low precision on the values for high molar mass polymers. Moreover, side reactions of the end-groups like hydrolysis can lead to overestimation of the molar mass. Indeed, if end-groups are consumed by another means that polymerization, M_n values estimated by NMR become biased. The same happens if macrocycles are formed in the medium. Finally, it is worth noting that SEC M_n values are given as PS standards equivalents and thus do not correspond to the true molar mass of the polyesters. The dispersity of the polymers was ranging from 1.4 to 2 which is in adequation with previous results reported in the literature for CALB-catalyzed (trans)esterification polymerization (Mahapatro *et al.*, 2003).

M_n values determined by NMR and SEC indicated that PDO and BDO-based polyesters were both obtained with low molar masses. As depicted earlier, evaporation of the diol along the reaction could cause an unbalanced stoichiometry and thus reduced molar masses. Thus, polymerization of **DDeFA^{II}** with PDO and BDO in excess (1.3 equivalent compared to the diester) were assayed. Other parameters were kept the same. The molar masses measured by SEC and by NMR as well as the SEC chromatogram of the polyesters synthesized with and without excess of diol are given in Figure 4.2.9, Table 4.2.1 and in Annexes Figure S4.16.

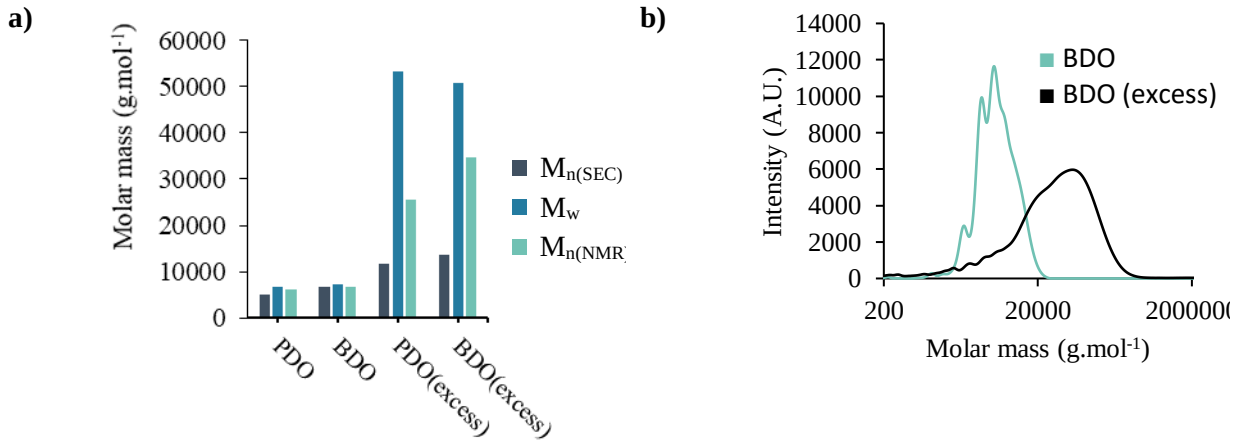

Figure 4.2.9: Molar masses of the PDO and BDO-based polyester synthesized with and without an excess of diol: a) M_n, M_w measured by SEC and M_n measured by NMR after 48h of reaction; b) SEC elution profile, values calculated from PS calibration curve and normalized by area, logarithmic scale.

Using an excess of diol allowed to significantly increase the molar mass of the PDO and BDO-based polyesters. The M_n estimated by SEC was multiplied by 2.4 and 2.6, respectively. However, the dispersity of the polyesters also increased drastically to value up to 4.5 and 3.7 when using PDO and BDO as diol in excess, respectively. SEC elution profiles clearly attest to the presence of a significant population of high molar mass chains. This greatly increases the M_w value that is multiplied by 7 and 8 when employing an excess of PDO and BDO, respectively. The obtained M_w are in the same range as the polyesters synthesized with HDO and ODO. The values of molar masses are high when compared

to PDO and BDO-based enzymatically synthesized aromatic polyesters (obtained from furan and pyridine dicarboxylates as diesters) (Jiang *et al.*, 2015; Comerford *et al.*, 2020). Aliphatic polyesters synthesized from PDO with diethyl adipate or succinate as diester through CALB-catalyzed polymerization present similar chain length (Debuissy *et al.*, 2017b). The ratio of ester to hydroxyl end-groups was measured to 26 and 25 % for the polyesters synthesized from PDO and BDO, respectively. This indicates that hydroxyl end-groups are predominant because of the excess of diol in the feed. It could suggest a too high excess of diol and further optimization of this ratio could be considered in the future. Overall, using an excess of diol allowed therefore to push further the reaction and to improve the polymer molar mass. Such improvement can directly impact the properties of the polymer as its thermal transition temperatures.

Table 4.2.1: Molecular parameters of the polyesters synthesized from DDeFA^{II} with diol of different lengths and different ratios.

		NMR		SEC		
Diol	Diester:diol feed ratio	Mn ($g.mol^{-1}$)	Ester end-groups ratio	Mn ($g.mol^{-1}$)	Mw ($g.mol^{-1}$)	Đ
PDO	1:1	6 200	85 %	4 900	6 700	1.4
PDO	1:1.3	25 600	26 %	11 800	53 300	4.5
BDO	1:1	6 800	86 %	5 200	7 300	1.4
BDO	1:1.3	34 700	25 %	13 700	50 900	3.7
HDO	1:1	34 800	60 %	24 100	42 700	2.0
ODO	1:1	18 700	37 %	28 200	57 700	2.0

4.3. Thermal properties of the polyesters

The thermal transition temperatures of the synthesized polyesters have been measured by DSC. First, the thermal transitions of the polyesters synthesized without any excess of diol were determined (Figure 4.2.10, Table 4.2.2). For all samples, no melting or crystallization phenomena were observed but glass transition temperatures were clearly noticeable. Thus, regardless of the diol nature, these materials are fully amorphous. This was confirmed by polarized light optical microscopy observations (data not shown). In the literature, polymers based on ferulic acid derivatives were often found to be amorphous (Barbara *et al.*, 2015; Nguyen *et al.*, 2015). Despite the possibility of π-π stacking of the aromatic rings, the bulkiness of the aromatic monomer and its structure highly different from the diol one makes difficult the crystallization. Amorphous materials are known to have lower mechanical modulus compared to their crystalline counterpart. However, such materials present a high transparency which is a desired property for multiple industrial applications such as packaging. All thermal transition temperatures were above 12 °C. However, the chosen diol strongly influenced the thermal properties of the polyesters. The polyester synthesized with HDO allowed to reach the highest T_g (up to 29°C). In this ranking by decreasing order of Tg values, it is then followed by the polyesters synthesized with PDO, ODO and finally BDO. It would be expected that shorter diols would produce the polyesters with higher T_g. Indeed, shorter monomers induce a higher rigidity of the chain backbone and thus higher T_g. Moreover, this trend has already been observed and reported several times in the literature (Jiang *et al.*, 2015). However, the polymer molar mass also strongly influences its thermal properties including the T_g. Thus, polyesters of equivalent molar mass only should be compared with each other. Therefore, the HDO-based polyester should only be compared with the ODO-based one. Likewise, the polyester synthesized from PDO should be compared to the one synthesized from 1,4-PDO, as they show similar molar mass. By doing so, one can clearly confirm that shorter diols induce a higher T_g in both cases. This trend is thus in perfect agreement with the results previously reported in the literature. Moreover, for the same polyester, an increase in the molar mass induced a higher T_g, which is also an expected trend according to the Flory-Fox equation.

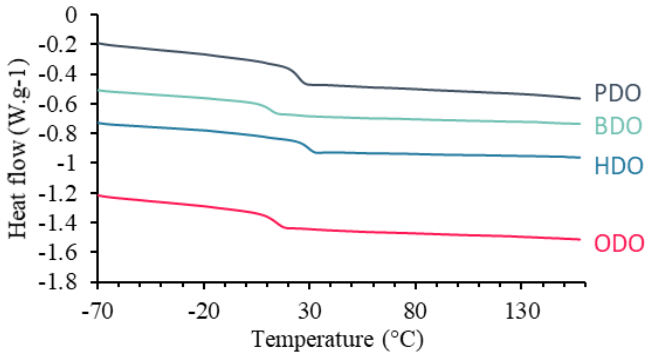

Figure 4.2.10: DSC second heating scans of polyesters synthesized from DDeFA^{II} with different diols. Heating rate = 10°C.min^{-1}. Curves are offset by 0.3 W.g^{-1} from each other (Exo Up).

Influence of the polyesters molar mass on T_g was further investigated. The thermal transition of the polyesters synthesized with excess of diol were also measured by DSC and compared to the previous values (Figure 4.2.11, Table 4.2.2). As depicted above, using an excess of diol leads to an increase in the polyesters molar masses. As it can be predicted from the Flory-Fox equation, such increase in molar mass induces higher T_g. The T_g values of the polyesters synthesized with PDO and BDO were increased by 9 and 19 °C, respectively. Again, the shorter the diol, the higher the T_g. The obtained T_g were comparable to those of enzymatically synthesized furan-based semi-aromatic polyesters reported in the literature (Jiang *et al.*, 2015).

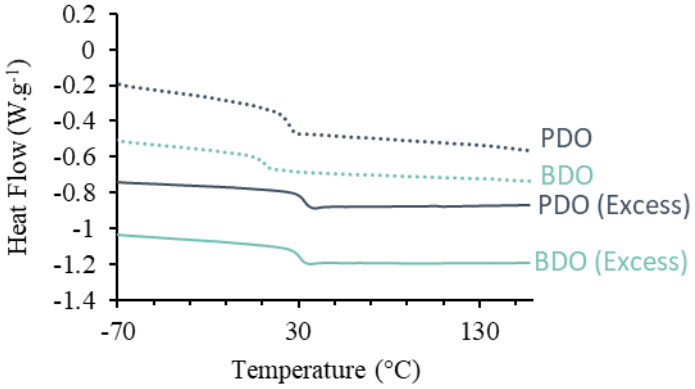

Figure 4.2.11: DSC second heating scans of polyesters synthesized from DDeFA^{II} with PDO and BDO in different ratio. Heating rate = 10°C.min^{-1}. Curves are offset by 0.3 W.g^{-1} from each other (Exo Up).

The thermal stability of the polyesters was evaluated by monitoring the temperature weight loss curves in TGA analysis (Figure 4.2.12, Table 4.2.2). A two steps weight loss was observed for all polyesters. This pattern of degradation has already been observed for aromatic polyesters based on ferulic acid (Bazin *et al.*, 2021a) and PET (Oh *et al.*, 2006). The first weight loss step (from which the temperature of maximal weight loss rate is defined as T_{dmax1}) corresponds to the thermal degradation involving the cleavage of ester and aliphatic bonds. The aromatics get rearranged and are later degraded by oxidation resulting in the second weight loss step (from which the temperature of maximal weight loss rate is defined as T_{dmax2}). The $T_{d5\%}$ values of the polyesters (corresponding to the temperature at 5%

of weight loss, associated to the degradation onset) are comparable to those obtained for polyethylene furanoate (PEF, 339 °C). However, the T_{dmax1} values, which correspond to the most important weight loss, are lower than those of PEF and PET (411 and 445 °C, respectively) (Thiyagarajan *et al.*, 2014).

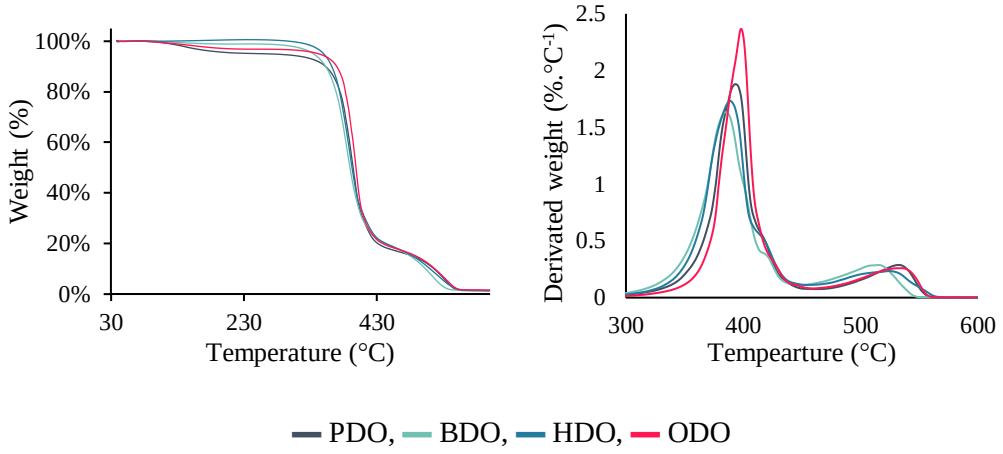

Figure 4.2.12: TGA thermal weight loss analysis of polyesters synthesized from DDeFA^{II} with different diols. Heating rate = 10°C.min^{-1}, under air.

The temperature corresponding to a 5% weight loss ($T_{d5\%}$) varied greatly depending on the molar mass range of the samples. The polyester presenting low molar masses, such as those synthesized from PDO or BDO, presented low $T_{d5\%}$ values in comparison to other samples. This difference could result from a facilitated alcoholysis of the polymer induced by the short polymer chains, leading to early degradation.

Table 4.2.2: Thermal properties of the polyesters synthesized from DDeFA^{II} with different diols (90°C, 24h, 40 % CALB).

Diol	Diester:diol feed ratio	Tg (°C)	Td5% (°C)	Tdmax1 (°C)	Tdmax2 (°C)
PDO	1:1	25	341 [a]	393	532
PDO	1:1.3	34	342[a]	397	545
BDO	1:1	12	338 [a]	385	515
BDO	1:1.3	31	318[a]	401	545
HDO	1:1	29	349	389	524
ODO	1:1	15	340	398	535

[a] Samples have been pre-heated to 150°C before measurement to eliminate water.

Overall, the polyesters synthesized from **DDeFA^{II}** with various diols presented high thermal properties. It is largely accepted that thermal [2+2] cycloaddition and retro-cycloaddition are not possible. However, in specific cases, the cyclobutane ring from such photo-dimerization has been shown to undergo thermal splitting at high temperature (Amjaour *et al.*, 2019). In the present study, no thermal splitting of **DDeFA^{II}** monomer or of the polymer was observed in DSC up to 300°C.

4.4. Photo-depolymerization of the polyester

As mentioned earlier, the [2+2] cycloaddition is a reversible reaction. The reverse reaction to the cycloaddition can be performed at λ = 254 nm. This photo-splitting of the cyclobutane ring leads to the recovery of the double bonds initially present in the ferulic acid derivatives (Scheme 4.2.6). The

reversibility of this reaction has already been employed and described in the literature for the synthesis of photo-reversible networks (Pilate *et al.*, 2018). Such materials are interesting for the synthesis of memory shape materials. In this study, the cyclobutane ring is included in the polymer chain backbone and therefore cannot participate in a reversible crosslinking process. However, splitting of the cyclobutane induces a direct cleavage of the polymer chain. The molar mass as well as the dispersity of the polymer should consequently be impacted. This could therefore represent a first step towards the recycling of the polyester into lower molar mass oligomers and subsequently into monomers.

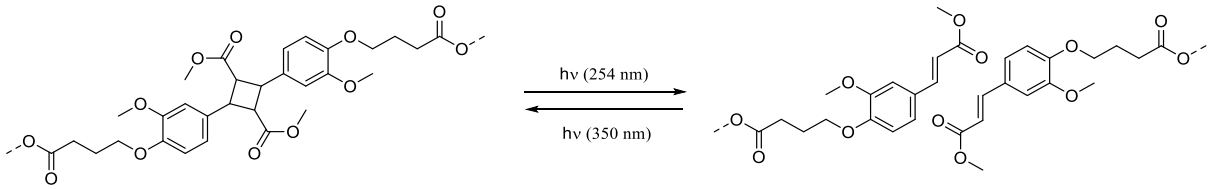

Scheme 4.2.6: Reversible reaction of [2+2] cycloaddition of the cyclobutane ring within the polymeric chain.

Electron delocalization between the double bond and the aromatic ring of cinnamic derivatives induces an absorbance around 300 nm. Thus, the UV-induced degradation of the polyesters synthesized from **DDeFA^{II}** was evaluated by measuring the absorbance of the samples to detect the emergence of the double bonds and thus the splitting of the cyclobutane ring (Curme *et al.*, 1967). Their absorbance was measured between 250 and 500 nm before and after several phases of UV-C irradiation. The curves obtained for the HDO-based polyester are given in Figure 4.2.13a. The maximal absorbance measured between 300 and 400 nm for the polyesters synthesized with different diols is presented in Figure 4.2.13b. The absorbance of the polymers increases rapidly in the early stage of photodegradation. As depicted earlier, this increase is attributed to the appearance of double bonds induced by cyclobutane splitting. All samples presented similar kinetics of photodegradation. The length of the diol has therefore no influence on the kinetics of photodegradation. All the maximum absorbance time evolution curves display an exponential asymptotic trend which reaches a plateau after 200 seconds of irradiation. The absorbance of the sample did not change after a longer time of irradiation.

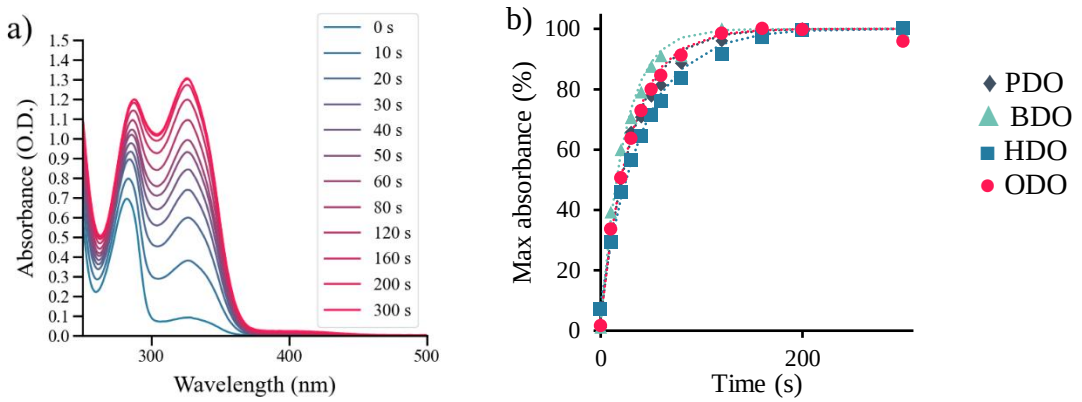

Figure 4.2.13: Absorbance of the polyesters after various times of UV-C irradiation: a) Absorbance spectra between 250 and 500 nm of the HDO-based polyester; b) maximum of absorbance between 300 and 400 nm for the polyesters synthesized from diols of different lengths with exponential model fitting.

NMR spectroscopy analyses have been performed to better understand the photodegradation mechanism of the polyesters. The photodegradation of the HDO-based polyester has been monitored by analyzing samples after different times of irradiation under UV-C (in Annexes Figure S4.17). For these irradiated samples, signals corresponding to protons of the double bond in *trans* configuration were observed at δ = 6.30 and 7.62 ppm. A signal at δ = 5.83 ppm was also attributed to a proton of the double bond in *cis* configuration. Indeed, at λ = 254 nm, ferulic acid derivatives can undergo a *cis-trans* isomerization. Other minor peaks observed on the NMR spectra could correspond to side-reaction products that could not be identified. This confirms that the increase in absorbance of the polymer under UV-C irradiation is induced by the appearance of double bonds. The conversion of sp^3 carbons from cyclobutane ring to sp^2 carbons of double bonds was calculated from the NMR data. This was done by comparing the ratio of the intensity of the peaks attributed to the double bonds to the intensity of the peaks attributed to the cyclobutane. This conversion was plotted as a function of the UV-C irradiation time (Figure 4.2.14). As for the absorbance, the double bond formation yield follows an exponential asymptotic trend. The plateau of photodegradation progress was reached between 300 and 600 seconds of irradiation in these conditions. The difference of thickness between the samples prepared for absorbance measurements and samples dedicated to NMR spectroscopy analysis could explain the discrepancy between the times of maximal degradation evaluated by UV and by NMR spectroscopy. Indeed, NMR measurements need higher amounts of material than absorbance measurements, leading to the preparation of larger and potentially thicker samples. It is also worth noticing that *cis* and *trans* isomers appear simultaneously in the samples. However, the proportion of *trans* isomers was systematically greater than the proportion of *cis* isomers. It has already been mentioned in the literature that only *trans*-isomers could undergo [2+2] cycloaddition (Schmidt, 1971; Ford *et al.*, 1989). It is thus reasonable to postulate that photo-splitting of the cyclobutane would mainly produce *trans*-isomers. These *trans*-double bonds can later be *cis* isomerized by UV-C irradiation. The maximum conversion

of cyclobutane rings into double bonds for the polyester synthesized with HDO as diol was evaluated to 29 %.

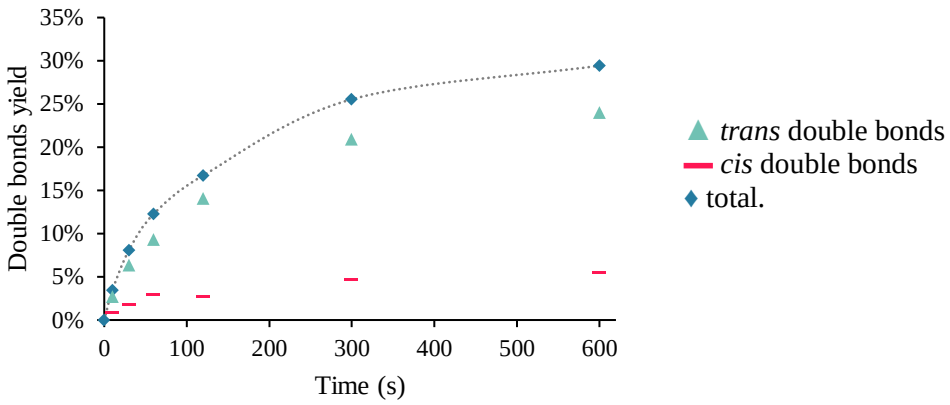

Figure 4.2.14: Yield in double bond formation measured from NMR analyses as a function of UV-C irradiation time for the polyester synthesized from DDeFA^{II} and HDO.

The polyesters synthesized from PDO, BDO and ODO were also subjected to UV-C irradiation for 600 seconds. The conversion of double bonds was calculated for each sample by NMR analysis (Figure 4.2.15 and in Annexes Figure S4.18). Interestingly, shorter diols resulted in lower yields of photodegradation. This is surprising since all samples showed similar photopolymerization kinetics as determined from UV absorption analysis. However, the greater mass concentration of **DDeFA^{II}** in samples with short diols could negatively impact the penetration of UV light in the material and could result in a lower overall conversion of the cyclobutane rings. Stiffness of the materials could also play a role in their ability to undergo retro-cycloaddition. The splitting of the cyclobutane rings requires a certain mobility of the involved moieties that might not be sufficient for stiff materials.

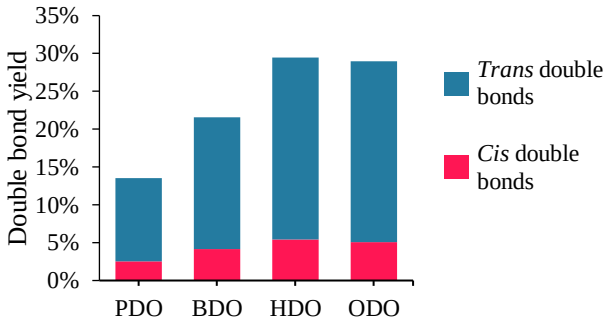

Figure 4.2.15: Yield in double bond formation measured from NMR analyses after UV-C irradiation (600s, RT) for the polyester synthesized from DDeFA^{II} and diols of different lengths.

The photo-depolymerization of the polyesters was also monitored by SEC. The polyester synthesized from **DDeFA^{II}** and HDO was analyzed by SEC after different times of irradiation under UV-C. The DP_n, and DP_w are given in the Figure 4.2.16. The corresponding chromatograms are shown in Figure 4.2.17 and Figure S4.19 in Annexes. Because these samples result from the upscaling of the

polymer synthesis, starting molar masses are lower than those reported above. As expected, the photodegradation leads to an overall reduction in the molar mass of the polymer. As already observed by UV absorption and NMR spectroscopy, the decrease in molar mass follows an exponential trend and reaches a plateau. The plateau value was evaluated at a DP_n of 3 and a DP_w of 13. Moreover, the resulting material presents an important dispersity of 3.5 thus indicating that the polymer tends to be randomly cleaved leading to oligomers with a large variety of sizes. Chains with a DPn down to 2 were clearly noticeable on SEC chromatograms (Figure 4.2.17). It is not clear why the photo-depolymerization reaches a plateau. Among the hypotheses, the existing literature mentions possible deactivation of the cyclobutane rings under UV light (Tanaka *et al.*, 1977). As mentioned above, the thickness of the material could also play an important role. In order to sort this issue, re-solubilization and recasting of the polymer into a thinner film could induce higher photo-depolymerization yields. As mentioned earlier, NMR analysis is also a tool that enables molar mass estimation. However, the photodepolymerization induces new end-groups and Equation 4 cannot be applied in this case. Indeed, the splitting of the cyclobutane rings produce two double bonds as end groups. Thus, the DP_n of the polyester at a given time was calculated according to Equation 5 (details on the calculation are given in Annexes Figure S4.20). The values calculated by NMR follow the same trend as those determined by SEC. This confirms than splitting of the cyclobutane is the main mechanism responsible for the reduction in molar masses. Moreover, a negative control performed on an aliphatic polyester (polyhexylene adipate) showed significantly lower photo-degradation under UV-C irradiation with a decrease in DP_n lower than 20 % of the initial value. The DP_n values estimated by NMR are systematically lower than those estimated by SEC. This could be caused by three phenomena; (i) as explained above, SEC results are given as PS equivalents. This could induce a shift in the true molar mass estimation of the polymer, (ii) molar mass determination from NMR spectra requires a good signal over noise ratio. This condition can be difficult to meet, especially at the beginning of the photodegradation since at this point the signals corresponding to the double bonds end-groups are weak compared to those of the polymer chain core. (iii) as UV-C are highly energetic rays, oxidative degradation side reactions could lead to the cleavage of the polymer chain in other positions. This would result in further diminution of the DP_n value and the corresponding adducts could correspond to the unidentified side products observed as traces in the NMR analyses, as mentioned before.

$$DP_{n(t)} = \frac{DP_{n(t=0)}}{0.5 * (2 + \alpha_{(t)} * DP_{n(t=0)})} \quad (5)$$

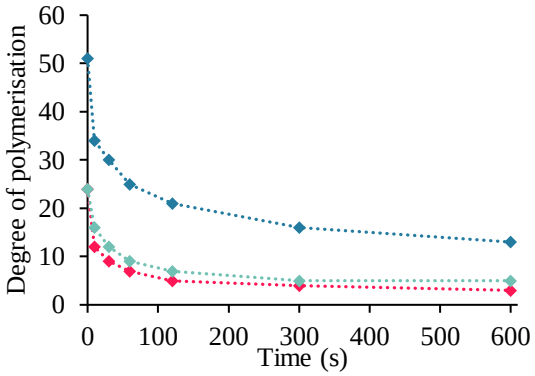

Figure 4.2.16: Degree of polymerization as a function of UV-C irradiation time for the polyester synthesized from DDeFA^{II} and HDO ♦ DP_w, ♦ $DP_{n(sec)}$, ♦ $DP_{n(NMR)}$.

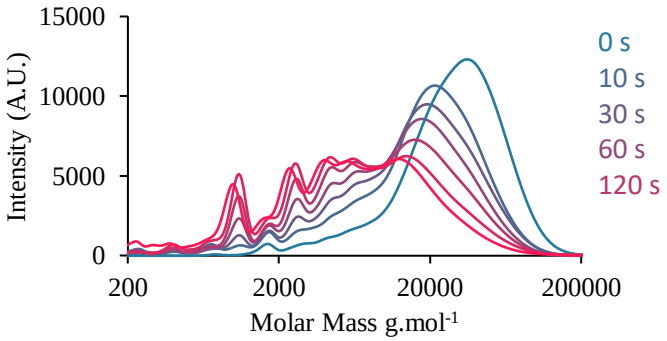

Figure 4.2.17: SEC molar mass distribution as a function of UV-C irradiation time for the polyester synthesized from DDeFA^{II} and HDO. Values given as PS equivalent and normalized by area, logarithmic scale.

The polyesters synthesized from other diols (PDO, BDO and ODO) were also analyzed by SEC after UV-C irradiation (Annexes Figure S4.19). The depolymerization followed the same trend and after 10 minutes of irradiation, all the polyesters presented DP_n between 6 and 4 as determined from NMR analysis and equal to 3 when calculated from SEC analysis. The final DP_n after photo-depolymerization seemed not to be affected by the initial molar mass of the polyester or by the length of the diols.

The reversibility of the depolymerization was finally studied on samples that were depolymerized through UV-C irradiation (at 254 nm for at least 600 seconds). The absorbance of these samples was then measured after different times of irradiation under UV-A (at 350 nm) to check the occurrence of a possible re-polymerization. The results obtained for the HDO-based polyester are presented in Figure 4.2.18.a. The absorbance at maximum value between 300 and 400 nm of the different polyesters are plotted in Figure 4.2.18.b. The absorbance of the samples decreased similarly for all the polyesters subjected to UV-A irradiation. After 120 minutes of UV-A irradiation the samples present an absorbance equivalent to that of the polymer before UV-C photodepolymerization. This indicates that the double bonds produced through photodegradation under UV-C are now being consumed, possibly through [2+2] cycloaddition, under the effect of UV-A. NMR analysis of the sample containing HDO as diol after 120 minutes of re-polymerization under UV-A showed complete conversion of the double bonds into cyclobutane moieties (Annexes Figure S4.21). However, some of the samples were hardly soluble

in chloroform and unidentified side products are visible on the NMR spectra. This could indicate that UV-A irradiation also induced side reactions during the process that could lead to undesired crosslinking of the polymer.

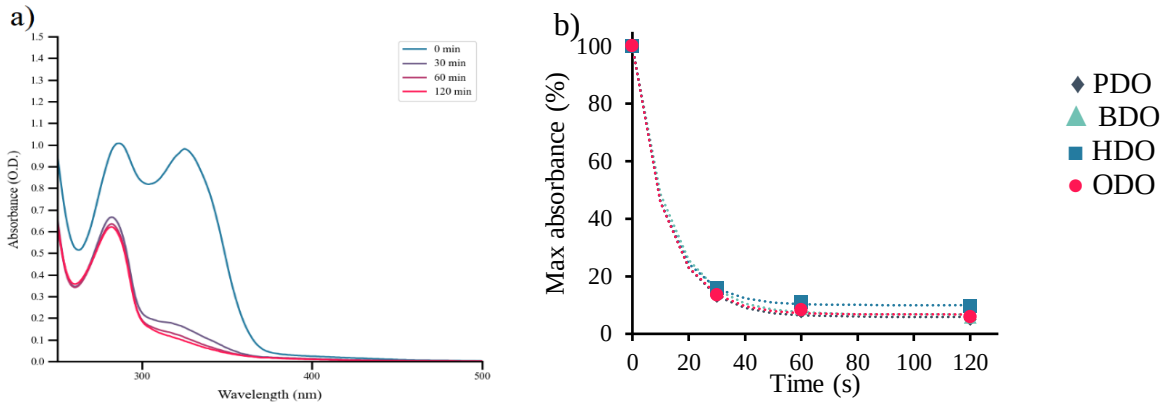

Figure 4.2.18: Absorbance of the polyester photodegraded under UV-C and subsequently irradiated under UV-A: a) Absorbance spectra between 250 and 500 nm of the HDO-based at different UV-A irradiation times; b) maximum of absorbance between 300 and 400 nm as a function of UV-A irradiation time for the polyester synthesized from diols of different lengths and exponential model fitting.

5. Conclusion:

FA is a promising building-block for the elaboration of new aromatic polyesters with advanced properties. Derivatives of FA can undergo [2+2] cycloaddition through a green, UV driven, process. **AcFA** and **DeFA^{II}** were quantitatively converted into dimers via a rapid UV irradiation. Greener solvents for the reaction were investigated. The toxic cyclohexane could be advantageously substituted by water, improving the environmental impact and safety of the photodimerization reaction. The synthesized dimers were then assessed for their reactivity through CALB-catalyzed polymerization.

The **AcFA** was rapidly identified as non-reactive towards CALB. The **DeFA^{II}** dimer was assessed for polymerization with diols of different lengths ($3 < n < 8$). **DeFA^{II}** was proven to have a high reactivity towards CALB allowing the production of polyester with high molar masses with M_w up to 57 700 g.mol^{-1}. The polyesters were shown to be fully linear as the ester groups attached to the cyclobutane ring remained untouched during the reaction. CALB was shown to have higher affinity for longer diols, leading to polyesters with higher DP_n. Besides, a probable evaporation of the short diols from the reactive medium unbalanced the stoichiometry of the reaction and thus limited the polymerization progress. Employing an excess of diol solved this issue and allowed to obtain high molar mass with M_w up to 53 300 and 50 900 g.mol^{-1} for polyesters synthesized from PDO and BDO, respectively. The molar masses of the obtained polyesters were superior to those of most of the enzymatically synthesized polyesters reported so far in the literature. Besides, these materials present higher thermal properties compared to enzymatically synthesized aliphatic polyesters. High T_g above 12 °C and up to 34°C were obtained. As expected, employing shorter diols led to polyesters with higher T_g.

The obtained polyesters were shown to undergo retro-cycloaddition under UV-C. This photodepolymerization of the polyester could be followed through UV absorption measurements. NMR and SEC analyses confirmed that the splitting of the cyclobutane ring under UV-C led to effective depolymerization of the polyesters chains leading to short oligomers. The chain scission was rapid and reached a maximum after only 200 seconds of irradiation. The UV-C-induced photodepolymerization was then shown to be reversible through UV-A irradiation. The cyclobutane could be restored, leading to the polyester chain reformation. The impact of multiple cycles of photo-depolymerization and re-polymerization on the polymer structure could be investigated in the future, as well as the influence on the mechanical and self-healing properties of the material.

The **DeFA^{II}** dimer allowed the synthesis of biobased aromatic polyesters with pendent esters. This atypical structure was obtained thanks to the specificity of the CALB. The development of such materials with advanced properties pushes further the competitiveness of biobased materials and enzymatically synthesized aromatic polyesters. Further modification of the pendent ester groups could even provide new properties and pave the way for the development of "smart materials."

6. References

Albanese, M., Boyenval, J., Marchese, P., Sullalti, S. and Celli, A. (**2016**) 'The aliphatic counterpart of PET, PPT and PBT aromatic polyesters: effect of the molecular structure on thermo-mechanical properties', *AIMS Molecular Science*, 3(1), pp. 32–51.

Ali, M. A. and Kaneko, T. (**2019**) 'Syntheses of Aromatic/Heterocyclic Derived Bioplastics with High Thermal/Mechanical Performance', *Industrial & Engineering Chemistry Research*, 58(35), pp. 15958–15974.

Allais, F., Martinet, S. and Ducrot, P.-H. (**2009**) 'Straightforward Total Synthesis of 2-O-Feruloyl-l-malate, 2-O-Sinapoyl-l-malate and 2-O-5-Hydroxyferuloyl-l-malate', *Synthesis*, 2009(21), pp. 3571–3578.

Amjaour, H., Wang, Z., Mabin, M., Puttkammer, J., Busch, S. and Chu, Q. R. (**2019**) 'Scalable preparation and property investigation of a *cis* -cyclobutane-1,2-dicarboxylic acid from β- *trans* -cinnamic acid', *Chemical Communications*, 55(2), pp. 214–217.

Barbara, I., Flourat, A. L. and Allais, F. (**2015**) 'Renewable polymers derived from ferulic acid and biobased diols via ADMET', *European Polymer Journal*, 62, pp. 236–243.

Becker, J., Lange, A., Fabarius, J. and Wittmann, C. (**2015**) 'Top value platform chemicals: bio-based production of organic acids', *Current Opinion in Biotechnology*, 36, pp. 168–175.

Bozell, J. J. and Petersen, G. R. (**2010**) 'Technology development for the production of biobased products from biorefinery carbohydrates—the US Department of Energy's "Top 10" revisited', *Green Chemistry*, 12(4), p. 539.

Cassani, J., Luna, H., Navarro, A. and Castillo, E. (**2007**) 'Comparative esterification of phenylpropanoids versus hydrophenylpropanoids acids catalyzed by lipase in organic solvent media', *Electronic Journal of Biotechnology*, 10(4), pp. 0–0.

Castillo, E. A., Miura, H., Hasegawa, M. and Ogawa, T. (**2004**) 'Synthesis of novel polyamides starting from ferulic acid dimer derivative', *Designed Monomers and Polymers*, 7(6), pp. 711–725.

Comerford, J. W., Byrne, F. P., Weinberger, S., Farmer, T. J., Guebitz, G. M., Gardossi, L. and Pellis, A. (**2020**) 'Thermal Upgrade of Enzymatically Synthesized Aliphatic and Aromatic Oligoesters', *Materials*, 13(2), p. 368.

Curme, H. G., Natale, C. C. and Kelley, D. J. (**1967**) 'Photosensitized reactions of cinnamate esters', *The Journal of Physical Chemistry*, 71(3), pp. 767-770.

Cyclohexane (**2021**) *ECHA*. Available at: https://echa.europa.eu/substance-information/-/substanceinfo/100.003.461 (Accessed: 17 August 2021).

Debuissy, T., Pollet, E. and Avérous, L. (**2016**) 'Enzymatic Synthesis of a Bio-Based Copolyester from Poly(butylene succinate) and Poly((*R*)-3-hydroxybutyrate): Study of Reaction Parameters on the Transesterification Rate', *Biomacromolecules*, 17(12), pp. 4054–4063.

Debuissy, T., Pollet, E. and Avérous, L. (**2017**)**b** 'Lipase-catalyzed synthesis of biobased and biodegradable aliphatic copolyesters from short building blocks. Effect of the monomer length', *European Polymer Journal*, 97, pp. 328–337.

Debuissy, T., Sangwan, P., Pollet, E. and Avérous, L. (**2017**)**d** 'Study on the structure-properties relationship of biodegradable and biobased aliphatic copolyesters based on 1,3-propanediol, 1,4-butanediol, succinic and adipic acids', *Polymer*, 122, pp. 105–116.

Delidovich, I., Hausoul, P. J. C., Deng, L., Pfützenreuter, R., Rose, M. and Palkovits, R. (**2016**) 'Alternative Monomers Based on Lignocellulose and Their Use for Polymer Production', *Chemical Reviews*, 116(3), pp. 1540–1599.

Devi Salam, M., Varma, A., Prashar, R. and Choudhary, D. (**2021**) 'Review on Efficacy of Microbial Degradation of Polyethylene Terephthalate and Bio-upcycling as a Part of Plastic Waste Management', *Applied Ecology and Environmental Sciences*, 9(7), pp. 695–703.

Ding, L., Liu, L., Chen, Y., Du, Y., Guan, S., Bai, Y. and Huang, Y. (**2019**) 'Modification of poly(ethylene terephthalate) by copolymerization of plant-derived α-truxillic acid with excellent ultraviolet shielding and mechanical properties', *Chemical Engineering Journal*, 374, pp. 1317–1325.

Douka, A., Vouyiouka, S., Papaspyridi, L.-M. and Papaspyrides, C. D. (**2018**) 'A review on enzymatic polymerization to produce polycondensation polymers: The case of aliphatic polyesters, polyamides and polyesteramides', *Progress in Polymer Science*, 79, pp. 1–25.

Elias, H.-G. and Palacios, J. A. (**1985**) 'Poly(ferulic acid) by Thionyl Chloride Activated Polycondensation', *Die Makromolekulare Chemie*, 186(5), pp. 1027–1045.

Feder, D. and Gross, R. A. (**2010**) 'Exploring Chain Length Selectivity in HIC-Catalyzed Polycondensation Reactions', *Biomacromolecules*, 11(3), pp. 690–697.

Ferri, M., Happel, A., Zanaroli, G., Bertolini, M., Chiesa, S., Commisso, M., Guzzo, F. and Tassoni, A. (**2020**) 'Advances in combined enzymatic extraction of ferulic acid from wheat bran', *New Biotechnology*, 56, pp. 38–45.

Flores, I., Martínez de Ilarduya, A., Sardon, H., Müller, A. J. and Muñoz-Guerra, S. (**2019**) 'Synthesis of Aromatic–Aliphatic Polyesters by Enzymatic Ring Opening Polymerization of Cyclic Oligoesters and their Cyclodepolymerization for a Circular Economy', *ACS Applied Polymer Materials*, 1(3), pp. 321–325.

Flourat, A. L., Combes, J., Bailly-Maitre-Grand, C., Magnien, K., Haudrechy, A., Renault, J. and Allais, F. (**2021**) 'Accessing *p*-Hydroxycinnamic Acids: Chemical Synthesis, Biomass Recovery, or Engineered Microbial Production?', *ChemSusChem*, 14(1), pp. 118–129.

Fodor, C., Golkaram, M., Woortman, A. J. J., van Dijken, J. and Loos, K. (**2017**) 'Enzymatic approach for the synthesis of biobased aromatic–aliphatic oligo-/polyesters', *Polymer Chemistry*, 8(44), pp. 6795–6805.

Fonseca, A. C., Lima, M. S., Sousa, A. F., Silvestre, A. J., Coelho, J. F. J. and Serra, A. C. (**2019**) 'Cinnamic acid derivatives as promising building blocks for advanced polymers: synthesis, properties and applications', *Polymer Chemistry*, 10(14), pp. 1696–1723.

Ford, C. W. and Hartley, R. D. (**1989**) 'GC/MS characterisation of cyclodimers fromp-coumaric and ferulic acids by photodimerisation—a possible factor influencing cell wall biodegradability', *Journal of the Science of Food and Agriculture*, 46(3), pp. 301–310.

Gopalan, N. and Nampoothiri, K. M. (**2018**) 'Biorefining of wheat bran for the purification of ferulic acid', *Biocatalysis and Agricultural Biotechnology*, 15, pp. 304–310.

Hatti-Kaul, R., Nilsson, L. J., Zhang, B., Rehnberg, N. and Lundmark, S. (**2019**) 'Designing Biobased Recyclable Polymers for Plastics', *Trends in Biotechnology*.

Horbury, M. D., Baker, L. A., Rodrigues, N. D. N., Quan, W.-D. and Stavros, V. G. (**2017**) 'Photoisomerization of ethyl ferulate: A solution phase transient absorption study', *Chemical Physics Letters*, 673, pp. 62–67.

Izunobi, J. U. and Higginbotham, C. L. (**2011**) 'Polymer Molecular Weight Analysis by 1 H NMR Spectroscopy', *Journal of Chemical Education*, 88(8), pp. 1098–1104.

Jiang, Y., Woortman, A. J. J., Alberda van Ekenstein, G. O. R. and Loos, K. (**2015**) 'A biocatalytic approach towards sustainable furanic–aliphatic polyesters', *Polymer Chemistry*, 6(29), pp. 5198–5211.

John, G., Nagarajan, S., Vemula, P. K., Silverman, J. R. and Pillai, C. K. S. (**2019**) 'Natural monomers: A mine for functional and sustainable materials – Occurrence, chemical modification and polymerization', *Progress in Polymer Science*, 92, pp. 158–209.

Khan, M., Brunklaus, G., Enkelmann, V. and Spiess, H.-W. (**2008**) 'Transient States in [2 + 2] Photodimerization of Cinnamic Acid: Correlation of Solid-State NMR and X-ray Analysis', *Journal of the American Chemical Society*, 130(5), pp. 1741–1748.

Kreye, O., Oelmann, S. and Meier, M. A. R. (**2013**) 'Renewable Aromatic-Aliphatic Copolyesters Derived from Rapeseed', *Macromolecular Chemistry and Physics*, 214(13), pp. 1452–1464.

Kristufek, S. L., Wacker, K. T., Tsao, Y.-Y. T., Su, L. and Wooley, K. L. (**2017**) 'Monomer design strategies to create natural product-based polymer materials', *Natural Product Reports*, 34(4), pp. 433–459.

Kurt, G. and Gokturk, E. (**2020**) 'Synthesis of polyesters mimicking polyethylene terephthalate and their thermal and mechanical properties', *Journal of Polymer Research*, 27(10), p. 314.

Llevot, A., Grau, E., Carlotti, S., Grelier, S. and Cramail, H. (**2016**) 'From Lignin-derived Aromatic Compounds to Novel Biobased Polymers', *Macromolecular Rapid Communications*, 37(1), pp. 9–28.

Loos, K., Zhang, R., Pereira, I., Agostinho, B., Hu, H., Maniar, D., Sbirrazzuoli, N., Silvestre, A. J. D., Guigo, N. and Sousa, A. F. (**2020**) 'A Perspective on PEF Synthesis, Properties, and End-Life', *Frontiers in Chemistry*, 8, p. 585.

Mahapatro, A., Kalra, B., Kumar, A. and Gross, R. A. (**2003**) 'Lipase-Catalyzed Polycondensations: Effect of Substrates and Solvent on Chain Formation, Dispersity, and End-Group Structure', *Biomacromolecules*, 4(3), pp. 544–551.

Mancuso, C. and Santangelo, R. (**2014**) 'Ferulic acid: Pharmacological and toxicological aspects', *Food and Chemical Toxicology*, 65, pp. 185–195.

Mandal, S. and Dey, A. (**2019**) 'PET Chemistry', in *Recycling of Polyethylene Terephthalate Bottles*. Elsevier, pp. 1–22.

Maniar, D., Jiang, Y., Woortman, A. J. J., van Dijken, J. and Loos, K. (**2019**) 'Furan-Based Copolyesters from Renewable Resources: Enzymatic Synthesis and Properties', *ChemSusChem*, 12(5), pp. 990–999.

Marschner, D. E., Frisch, H., Offenloch, J. T., Tuten, B. T., Becer, C. R., Walther, A., Goldmann, A. S., Tzvetkova, P. and Barner-Kowollik, C. (**2018**) 'Visible Light [2 + 2] Cycloadditions for Reversible Polymer Ligation', *Macromolecules*, 51(10), pp. 3802–3807.

Morrison, I. M., Robertson, G. W., Stewart, D. and Wightman, F. (**1991**) 'Determination and characterization of cyclodimers of naturally occurring phenolic acids', *Phytochemistry*, 30(6), pp. 2007–2011.

Morrison, W. Herbert., Hartley, R. D. and Himmelsbach, D. S. (**1992**) 'Synthesis of substituted truxillic acids from p-coumaric and ferulic acid: simulation of photodimerization in plant cell walls', *Journal of Agricultural and Food Chemistry*, 40(5), pp. 768–771.

Nakajima, H., Dijkstra, P. and Loos, K. (**2017**) 'The Recent Developments in Biobased Polymers toward General and Engineering Applications: Polymers that are Upgraded from Biodegradable Polymers, Analogous to Petroleum-Derived Polymers, and Newly Developed', *Polymers*, 9(12), p. 523.

Nguyen, H. T. H., Qi, P., Rostagno, M., Feteha, A. and Miller, S. A. (**2018**) 'The quest for high glass transition temperature bioplastics', *Journal of Materials Chemistry A*, 6(20), pp. 9298–9331.

Nguyen, H. T. H., Reis, M. H., Qi, P. and Miller, S. A. (**2015**) 'Polyethylene ferulate (PEF) and congeners: polystyrene mimics derived from biorenewable aromatics', *Green Chemistry*, 17(9), pp. 4512–4517.

Nguyen, T. B. and Al-Mourabit, A. (**2016**) 'Remarkably high homoselectivity in [2 + 2] photodimerization of trans-cinnamic acids in multicomponent systems', *Photochemical & Photobiological Sciences*, 15(9), pp. 1115–1119.

Oh, S.-C., Lee, D.-G., Kwak, H. and Bae, S.-Y. (**2006**) 'Combustion Kinetics Of Polyethylene Terephthalate', *Environmental Engineering Research*, 11(5), pp. 250–256.

Ortiz, C., Ferreira, M. L., Barbosa, O., dos Santos, J. C. S., Rodrigues, R. C., Berenguer-Murcia, Á., Briand, L. E. and Fernandez-Lafuente, R. (**2019**) 'Novozym 435: the "perfect" lipase immobilized biocatalyst?', *Catalysis Science & Technology*, 9(10), pp. 2380–2420.

Otto, R. T., Scheib, H., Bornscheuer, U. T., Pleiss, J., Syldatk, C. and Schmid, R. D. (**2000**) 'Substrate specificity of lipase B from Candida antarctica in the synthesis of arylaliphatic glycolipids', *Journal of Molecular Catalysis B: Enzymatic*, 8(4–6), pp. 201–211.

Parthiban, A. and Vasantha, V. A. (**2020**) 'Biorenewable functional oligomers and polymers – Direct copolymerization of ferulic acid to obtain polymeric UV absorbers and multifunctional materials', *Polymer*, 188, p. 122122.

Pellis, A., Comerford, J. W., Maneffa, A. J., Sipponen, M. H., Clark, J. H. and Farmer, T. J. (**2018**) 'Elucidating enzymatic polymerisations: Chain-length selectivity of Candida antarctica lipase B towards various aliphatic diols and dicarboxylic acid diesters', *European Polymer Journal*, 106, pp. 79–84.

Pellis, A., Herrero Acero, E., Gardossi, L., Ferrario, V. and Guebitz, G. M. (**2016**)**b** 'Renewable building blocks for sustainable polyesters: new biotechnological routes for greener plastics: Renewable building blocks for sustainable polyesters', *Polymer International*, 65(8), pp. 861–871.

Pellis, A., Nyanhongo, G. S. and Farmer, T. J. (**2019**)**c** 'Recent Advances on Enzymatic Catalysis as a Powerful Tool for the Sustainable Synthesis of Bio-Based Polyesters', in Bastidas-Oyanedel, J.-R. and Schmidt, J. E. (eds) *Biorefinery*. Cham: Springer International Publishing, pp. 555–570.

Pilate, F., Stoclet, G., Mincheva, R., Dubois, P. and Raquez, J.-M. (**2018**) 'Poly(ε-caprolactone) and Poly(ω-pentadecalactone)-Based Networks with Two-Way Shape-Memory Effect through [2+2] Cycloaddition Reactions', *Macromolecular Chemistry and Physics*, 219(4), p. 1700345.

Pleiss, J., Fischer, M. and Schmid, R. D. (**1998**) 'Anatomy of lipase binding sites: the scissile fatty acid binding site', *Chemistry and Physics of Lipids*, 93(1–2), pp. 67–80.

Prat, D., Wells, A., Hayler, J., Sneddon, H., McElroy, C. R., Abou-Shehada, S. and Dunn, P. J. (**2016**) 'CHEM21 selection guide of classical- and less classical-solvents', *Green Chemistry*, 18(1), pp. 288–296.

Ramamurthy, V. and Venkatesan, K. (**1987**) 'Photochemical reactions of organic crystals', *Chemical Reviews*, 87(2), pp. 433–481.

Rovira, J., Nadal, M., Schuhmacher, M. and Domingo, J. L. (**2015**) 'Human exposure to trace elements through the skin by direct contact with clothing: Risk assessment', *Environmental Research*, 140, pp. 308–316.

Salum, M. L., Arroyo Mañez, P., Luque, F. J. and Erra-Balsells, R. (**2015**) 'Combined experimental and computational investigation of the absorption spectra of E- and Z -cinnamic acids in solution: The peculiarity of Z -cinnamics', *Journal of Photochemistry and Photobiology B: Biology*, 148, pp. 128–135.

Schmidt, G. M. J. (**1971**) 'Photodimerization in the solid state', *Pure and Applied Chemistry*, 27(4), pp. 647–678.

Schoon, I., Kluge, M., Eschig, S. and Robert, T. (**2017**) 'Catalyst Influence on Undesired Side Reactions in the Polycondensation of Fully Bio-Based Polyester Itaconates', *Polymers*, 9(12), p. 693.

Shamim, S., Liaqat, U. and Rehman, A. (**2018**) 'Microbial lipases and their applications – a review', *Abasyn Journal Life Sciences*, pp. 54–76.

Shindo, Y., Horie, K. and Mita, I. (**1984**) 'Photoisomerization of ethyl cinnamate in dilute solutions', *Journal of Photochemistry*, 26(2–3), pp. 185–192.

Siracusa, V. and Blanco, I. (**2020**) 'Bio-Polyethylene (Bio-PE), Bio-Polypropylene (Bio-PP) and Bio-Poly(ethylene terephthalate) (Bio-PET): Recent Developments in Bio-Based Polymers Analogous to Petroleum-Derived Ones for Packaging and Engineering Applications', *Polymers*, 12(8), p. 1641.

Stadler, B. M., Wulf, C., Werner, T., Tin, S. and de Vries, J. G. (**2019**) 'Catalytic Approaches to Monomers for Polymers Based on Renewables', *ACS Catalysis*, 9(9), pp. 8012–8067.

Stamatis, H., Sereti, V. and Kolisis, F. N. (**1999**) 'Studies on the enzymatic synthesis of lipophilic derivatives of natural antioxidants', *Journal of the American Oil Chemists' Society*, 76(12), p. 1505.

Sun, Z., Fridrich, B., de Santi, A., Elangovan, S. and Barta, K. (**2018**)**b** 'Bright Side of Lignin Depolymerization: Toward New Platform Chemicals', *Chemical Reviews*, 118(2), pp. 614–678.

Tanaka, H. and Honda, K. (**1977**) 'Photoreversible reactions of polymers containing cinnamylideneacetate derivatives and the model compounds', *Journal of Polymer Science: Polymer Chemistry Edition*, 15(11), pp. 2685–2689.

Thiyagarajan, S., Vogelzang, W., J. I. Knoop, R., Frissen, A. E., van Haveren, J. and van Es, D. S. (**2014**) 'Biobased furandicarboxylic acids (FDCAs): effects of isomeric substitution on polyester synthesis and properties', *Green Chem.*, 16(4), pp. 1957–1966.

Tobiszewski, M., Namieśnik, J. and Pena-Pereira, F. (**2017**) 'Environmental risk-based ranking of solvents using the combination of a multimedia model and multi-criteria decision analysis', *Green Chemistry*, 19(4), pp. 1034–1042.

Vosmann, K., Weitkamp, P. and Weber, N. (**2006**) 'Solvent-free Lipase-Catalyzed Preparation of Long-Chain Alkyl Phenylpropanoates and Phenylpropyl Alkanoates', *Journal of Agricultural and Food Chemistry*, 54(8), pp. 2969–2976.

Wang, B., Ma, S., Li, Q., Zhang, H., Liu, J., Wang, R., Chen, Z., Xu, X., Wang, S., Lu, N., Liu, Y., Yan, S. and Zhu, J. (**2020**)**a** 'Facile synthesis of "digestible", rigid-and-flexible, bio-based building block for high-performance degradable thermosetting plastics', *Green Chemistry*, 22(4), pp. 1275–1290.

Wang, Z., Flores, Q., Guo, H., Trevizo, R., Zhang, X. and Wang, S. (**2020**)**b** 'Crystal engineering construction of caffeic acid derivatives with potential applications in pharmaceuticals and degradable polymeric materials', *CrystEngComm*, 22(45), pp. 7847–7857.

Wang, Z., Miller, B., Mabin, M., Shahni, R., Wang, Z. D., Ugrinov, A. and Chu, Q. R. (**2017**) 'Cyclobutane-1,3-Diacid (CBDA): A Semi-Rigid Building Block Prepared by [2+2] Photocyclization for Polymeric Materials', *Scientific Reports*, 7(1).

Zhang, H., Li, X., Lin, Y., Gao, F., Tang, Z., Su, P., Zhang, W., Xu, Y., Weng, W. and Boulatov, R. (**2017**) 'Multi-modal mechanophores based on cinnamate dimers', *Nature Communications*, 8(1), p. 1147.

Zhang, Q., Song, M., Xu, Y., Wang, W., Wang, Z. and Zhang, L. (**2021**) 'Bio-based polyesters: Recent progress and future prospects', *Progress in Polymer Science*, 120, p. 101430.

Zia, K. M., Noreen, A., Zuber, M., Tabasum, S. and Mujahid, M. (**2016**) 'Recent developments and future prospects on bio-based polyesters derived from renewable resources: A review', *International Journal of Biological Macromolecules*, 82, pp. 1028–1040.

Conclusion chapitre 4

Dans ce chapitre nous avons vu comment tirer profit de la capacité de dimérisation sous UV des dérivés cinnamiques. Une première étude a permis de déterminer les propriétés de dimérisation de dérivés cinnamiques nouvellement produits et étudiés au chapitre précédent ou ceux déjà décrits au préalable dans la littérature. Après avoir identifié les substrats les plus actifs en dimérisation, plusieurs solvants de réaction ont été étudiés afin de remplacer le cyclohexane. L'eau a ainsi été identifiée comme étant un excellent substitut au cyclohexane permettant de réaliser la dimérisation dans des conditions plus compatibles avec les principes de la chimie verte.

Les dimères obtenus par cette méthode ont ensuite été testés pour la synthèse enzymatique de polyesters. Comme cela avait été observé et présenté dans le chapitre 2, la solubilité du substrat est un paramètre important dont on peut supposer qu'il soit responsable de la non-réactivité du **DAcFA** avec la CALB. Cependant, même une fois estérifié et rendu entièrement soluble, celui-ci n'a montré aucune réactivité vis-à-vis de la CALB. Le fort encombrement stérique des acides carboxyliques des dimères d'acide férulique pourrait expliquer leur impossibilité à réagir dans les réactions de polycondensation catalysées par la CALB.

En tirant parti de la sélectivité de la CALB envers les esters peu encombrés du **DDeFA^{II}**, il a été possible de synthétiser des polyesters aromatiques présentant des groupements esters pendants. Ces polyesters présentent des T_g supérieures à l'ambiante et qui s'avèrent également être supérieures à celles de tous les autres polyesters synthétisés dans le cadre de cette thèse. De plus, la réversibilité de la cycloaddition employée pour la dimérisation du monomère permet la photo-dépolymérisation du polyester. Cette propriété particulièrement intéressante et innovante pour ce type de polymères pourrait être utilisée pour mieux gérer la fin de vie du matériau (par recyclage chimique, par exemple) ou pour des applications de relargage contrôlé de principes actifs.

Dans ce chapitre nous avons donc montré comment il est possible de tirer profit de la double liaison des dérivés cinnamiques ainsi que de la sélectivité de la CALB pour synthétiser des polyesters présentant des propriétés avancées et donc potentiellement à haute valeur ajoutée en utilisant des méthodes de synthèses (photo-dimérisation dans l'eau, catalyse enzymatique) qui peuvent être qualifiées de « vertes ».

Chapitre 5. Synthèse par catalyse enzymatique de polyesters biosourcés photo-réticulables à partir d'acide caféique.

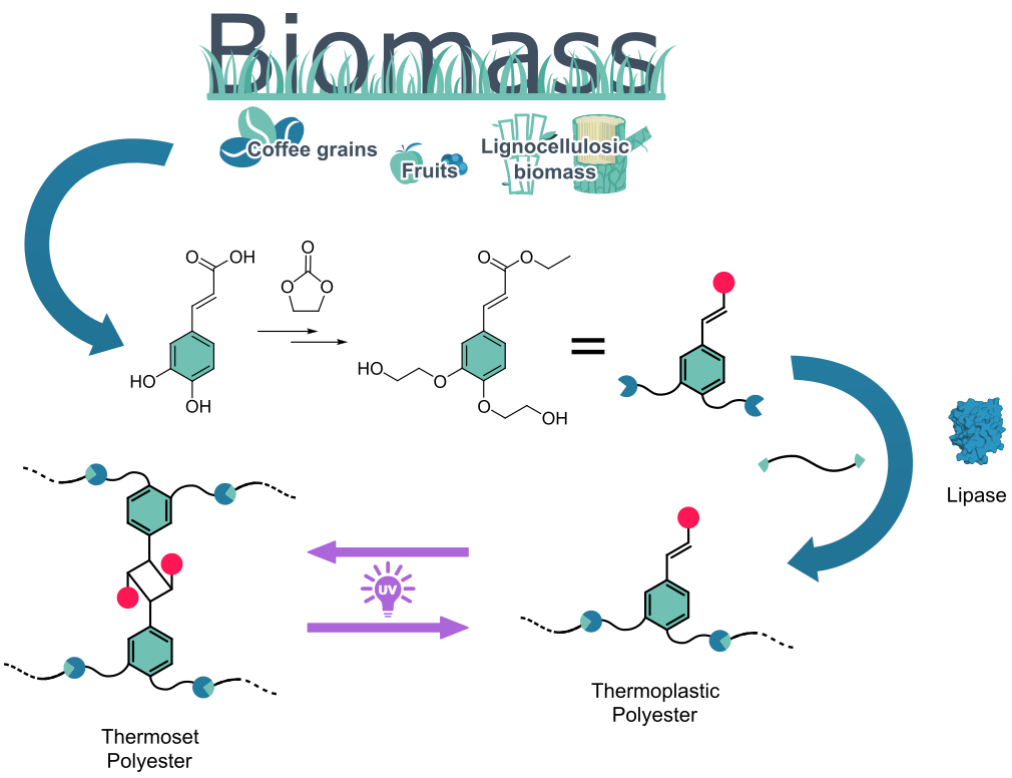

Introduction chapitre 5

Les chapitres précédents se sont intéressés à la capacité de la CALB à convertir des synthons issus de l'acide férulique en polyesters aromatiques de hautes masses molaires. Plusieurs stratégies ont été mises en place afin d'améliorer ou optimiser l'activité de la CALB vis-à-vis de ces substrats. Ces stratégies ont notamment mené à la synthèse de polyesters aromatiques aux propriétés améliorées ou innovantes comme par exemple la possibilité de réaliser sur ces matériaux des cycles de dépolymérisation/repolymérisation induits par irradiations UV.

Dans ce chapitre, nous allons étudier l'acide caféique, une molécule structurellement très proche de l'acide férulique et également issue de la biomasse. Dans un premier temps une nouvelle voie de synthèse entre un ester d'acide caféique et l'éthylène carbonate, un synthon également biosourcé, a été développée avec succès. Cette modification permet de convertir les deux phénols de l'acide caféique en alcools primaires. Le substrat résultant est un diol entièrement issu de carbone renouvelable et possédant un groupement ester α,β-insaturé. Cependant, on peut s'attendre à ce que cet ester soit très peu réactif au contact de la CALB comme l'indiquent les informations issues de la littérature présentées au chapitre 1 ainsi que nos observations décrites au chapitre 3. Ce substrat a donc été considéré comme un diol difonctionnel permettant la synthèse de polyesters aromatiques présentant des groupements ester α,β-insaturés pendants.

Ce type de structure est particulièrement recherché pour l'élaboration de matériaux photo-réticulable. En effet, comme l'ont montré les expériences menées dans le chapitre 4, les doubles liaisons de certains dérivés cinnamiques peuvent dimériser par cycloaddition [2+2] sous irradiation par les UV-A (e.g. λ = 350 nm). Si les chaînes polymères possèdent plusieurs de ces groupements, alors la dimérisation des doubles liaisons entraine la réticulation du matériau. La réaction de cycloaddition étant réversible sous les UV-C de longueur d'onde plus faible (e.g. λ = 254 nm), cette réticulation est alors théoriquement réversible. Ainsi, les polyesters formés à partir du diol caféique décrit ci-dessus pourraient permettre de telles réticulations réversibles grâce à leurs groupements esters α,β-insaturés pendants.

Ce chapitre se présente donc sous la forme d'une publication intitulée 'Synthesis of biobased photo-crosslinkable polyesters based on caffeic acid through selective lipase-catalyzed polymerization'. La première partie traite de la synthèse et de la caractérisation du diol obtenu via la modification de l'acide caféique par l'éthylène carbonate. La suite de l'article, et donc de ce chapitre, porte sur l'utilisation de ce diol caféique pour la synthèse, catalysée par la CALB, de polyesters aromatiques ainsi que de l'étude propriétés thermiques et photochimiques des matériaux ainsi obtenus.

Synthesis of biobased photo-crosslinkable polyesters based on caffeic acid through selective lipase-catalyzed polymerization

*Alfred Bazin, Matthieu Steuer, Luc Avérous, Eric Pollet**

Soon submitted for publication

1. Abstract

Caffeic acid was esterified and then successfully converted with ethylene carbonate into a new potentially fully biobased aromatic diol containing a pendant α,β-unsaturated ester. This diol was shown to undergo [2+2] cycloaddition under UV irradiation. The lipase B from *Candida antarctica* allowed the synthesis of polyesters from this caffeic based diol and diethyl adipate. 1,6-Hexanediol was also used as a second diol monomer to study the impact of the aromatic diol proportion on the enzymatic activity and final material properties. For a caffeic diol ratios of 10% and above, linear polyesters were obtained with M_w up to 28 000 g.mol^{-1}. Increasing the ratio of caffeic diol tend to reduce the polyester final molar masses, probably due to inhibition of the enzyme. However, increasing the proportion of caffeic diol in the polyester improved its thermal properties, reaching T_g up to 12°C. Finally, the pendant double bonds of the polyester were shown to undergo [2+2] cycloaddition under light irradiation, enabling its UV-A-activated crosslinking. This crosslinking was also shown to be partially reversible thanks to the UV-C-induced splitting of the cyclobutane rings in the network.

2. Introduction

Hindering climate change and environmental degradation is one of the main challenges in research for years to come. Reducing the impact of human activities on the environment is a key lever in this path. Plastics production and use represent a non-negligible part of the global environmental pollution (Chae *et al.*, 2018; Hohn *et al.*, 2020). Indeed, plastics are in vast majority based on non-degradable polymers produced from non-sustainable, petrol-based, sources. The production of biobased and therefore more environmentally friendly polymers seems clearly a very promising alternative (Siracusa *et al.*, 2020). For this mean, various natural sources of building blocks have been identified (Becker *et al.*, 2015; Delidovich *et al.*, 2016; Llevot *et al.*, 2016).

Caffeic acid (CA) is a cinnamic derivative present in various natural sources such as blueberries, apples or coffee beans and that is therefore part of our daily alimentation (Clifford, 2000). It can be directly extracted from plants as sunflower seed shell, coffee beans (Valanciene *et al.*, 2020; Flourat *et al.*, 2021) or produced from ferulic acid after extraction from natural sources such as wheat bran or

sugarcane bagasse (Sun *et al.*, 2018b; Flourat *et al.*, 2021). CA presents good antioxidants (Aytekin *et al.*, 2011; Genaro-Mattos *et al.*, 2015; Liu *et al.*, 2018) as well as antimicrobial (Khan *et al.*, 2021) and medicinal (Katayama *et al.*, 2013) properties. CA and cinnamic acid derivatives in general have already been studied for the production of polyesters (Nguyen *et al.*, 2018; Fonseca *et al.*, 2019). Indeed, their functionality as well as aromaticity allow the production of polyesters with high mechanical and thermal properties. As an example, Ishii *et al.* (Ishii *et al.*, 2013) synthesized poly(caffeic acid)s with glass transition temperatures higher than 100 °C.

Cinnamic derivatives such as CA have long been known to undergo a reversible [2+2] cycloaddition under UV light at a specific wavelength (Curme *et al.*, 1967; Tanaka *et al.*, 1977; Haddleton *et al.*, 1989). The reversibility of this cycloaddition makes cinnamic derivatives good candidates for the production of biobased photo-crosslinkable polymers and memory shape materials (MSM) (Li *et al.*, 2012). MSM are materials which shape can be programmed and modified by different stimuli (heat, light…). Cinnamic derivatives have already been employed in MSM as pendant groups (Lendlein *et al.*, 2005; Wu *et al.*, 2011; Rochette *et al.*, 2013; Pilate *et al.*, 2018) or directly included in the polymer chain (Nagata *et al.*, 2005, 2006). CA can advantageously replace toxic and non-sustainable adducts such as anthracene, thiols or azo compounds employed in photo-triggered MSM (Li *et al.*, 2012; Xie *et al.*, 2019). Since CA is potentially biobased, its use is therefore a greener path for the synthesis of photo-crosslinkable polymers.

CA-based or -grafted polymers have already been studied for the production of photo-crosslinkable polymers and MSM (Kaneko *et al.*, 2010). Thi *et al.* studied the properties of PLA (Hang Thi *et al.*, 2008; Thi *et al.*, 2009a), PCL and polyethylene glycol (PEG) (Thi *et al.*, 2011) grafted with CA. All polymers could undergo crosslinking under UV light. PLA modified with CA also allowed the synthesis of crosslinkable nanoparticles (Thi *et al.*, 2009b). Dong *et al.*(Dong *et al.*, 2012) studied caffeic acid copolymerized with 10-hydroxycaproic acid. The obtained polymer could be crosslinked under UV light, bringing higher tensile strength. Moreover, an increase in hydrolysis speed was observed, probably due to a reduced crystallinity of the material (Kaneko *et al.*, 2006). Li *et al.* (Li *et al.*, 2015) synthesized a crosslinkable polymer based on caffeic and 4-hydroxycinnamic acids. Once added to ethyl cellulose as microspheres, the UV crosslinking of the polymer allowed to reduce the permeability of the material. However, because of its carboxylic acid and the presence of two phenols on its aromatic ring, CA presents a functionality of three when involved in typical polymerization reactions. Such functionality leads to the production of polymers with hyperbranched or crosslinked structures with low or null solubility and extreme melting points (Thi *et al.*, 2008; Dong *et al.*, 2011), which complicates the material processability.

The lipase B from *Candida antarctica* (CALB) is an enzyme commonly used to catalyze transesterification reactions (Ortiz *et al.*, 2019). CALB has also been employed for the synthesis of various biobased polyesters, replacing the potentially toxic and pollutant metal-based catalysts (Shoda

et al., 2016; Debuissy *et al.*, 2017b; Duchiron *et al.*, 2017; Douka *et al.*, 2018). Recently, CALB was employed by our team for the synthesis of polyesters based on ferulic acid, another cinnamic derivative (Bazin *et al.*, 2021a). It was observed that the carbonyl of ferulic acid presented a poor reactivity towards CALB. Similarly, it has been shown that the carbonyl of CA also presents a poor to null reactivity towards CALB in esterification or transesterification (Stamatis *et al.*, 1999; Otto *et al.*, 2000; Yang *et al.*, 2012).

In this study, a caffeic diol (CD) was for the first time successfully obtained by modification of CA with ethylene carbonate. This CD presents 2 primaries OH and 1 ester group but can be considered as a difunctional monomer thanks to the selectivity of CALB, which is not active towards the carbonyl group. The CD was copolymerized with diethyl adipate and 1,6-hexanediol to obtain linear polymer chains with various ratios in caffeic moieties. The obtained biobased semi-aromatic polyesters present a peculiar structure with a pendant α,β-unsaturated ester, which was subsequently used to perform reversible photo-crosslinking.

3. Experimental section

3.1. Materials

Caffeic acid was supplied by Fluorochem. Lipase from *Candida antarctica* immobilized on acrylic resin (activity >5,000 U/g) (CALB), 1,6-hexanediol (HDO) and deuterated chloroform ($CDCl_3$) were purchased from Sigma-Aldrich. Ethanol was purchased from VWR. Potassium carbonate and methanol were supplied by Fisher Scientific. Chloroform was supplied by Carlo Erba. Diethyl adipate (DEA), ethylene carbonate and diphenyl ether were purchased from Acros Organics.

3.2. Characterization

^{1}H NMR, 2D and ^{13}C NMR analyses of the monomer were performed on a Bruker 500 MHz spectrometer. ^{1}H NMR analysis on the polymer were performed on a Bruker 400 MHz spectrometer. Analyses were performed in $CDCl_3$ or in DMSO-d_6 as a solvent. Calibration of the spectra was performed using the solvent peak ($CDCl_3$ δH = 7.26 ppm, δC = 77.16 ppm, DMSO-d_6 δH = 2.50 ppm, δC = 39.52 ppm).

Size Exclusion Chromatography (SEC) was used to determine the number average molar mass (M_n), weight average molar mass (M_w) and dispersity (Đ) of the polymers. The analyses were performed in THF at 40 °C in an Acquity-APC system (Waters) equipped with three columns (Acquity APC XT 450 Å 2.5 µm 4.6x150 mm, 200 and 45). The analyses were performed at a flow rate of 0.6 mL/min for 11 minutes run. Refractive index (RI) detector and photodiode array (PDA) detector at 254 nm were used. A calibration curve with polystyrene (PS) standards was carried out for molar mass determination. Molar mass calculation was performed with data collected from the RI detector.

Differential scanning calorimetry (DSC) analyses have been performed on the samples to determine their glass transition temperature (T_g) as well as their melting temperature (T_m) and crystallization temperature (T_c) if applicable. The analyses were done using a Q2000 DSC apparatus from TA instrument (TA instrument, New Castle, Delaware, USA). Typically, a 1 to 3 mg sample in sealed aluminium pan was rapidly heated to 140 °C. The sample was kept 3 minutes at such temperature to erase all thermal history. The sample was then cooled at 10 °C.min^{-1} to -80 °C followed by an isotherm of 5 minutes. Finally, a second heating was performed at 10 °C.min^{-1} to 140 °C.

Thermogravimetric analysis (TGA) was performed to determine the thermal stability of the polymers. The measurements were conducted on a High-Res TGA Q5000 from TA instrument. Samples between 1 and 2 mg were heated at 20 °C.min^{-1} from room temperature to 600 °C under air.

Infrared spectroscopy was performed with a Nicolet 380 Fourier transformed infrared spectrometer (Thermo Electron Corporation) used in reflection mode and equipped with an ATR diamond module (FTIR). The FTIR spectra were collected at a resolution of 4 cm^{-1} and with 32 scans per run.

UV-visible absorbance measurements were performed using a spectrometer UV-2600 (Shimadzu) in the 200-500 nm range. All measurements were performed on solid polymer cast on quartz microscope slides.

ESI-MS experiments were performed on a Bruker Daltonics microTOF spectrometer (Bruker Daltonics GmbH, Bremen, Germany) equipped with an orthogonal electrospray (ESI) interface. Calibration was performed using Tuning mix (Agilent Technologies). Sample solutions were introduced into the spectrometer source with a syringe pump (Harvard type 55 1111: Harvard Apparatus Inc., South Natick, MA, USA) with a flow rate of 4 µL.min^{-1}.

3.3. Ethyl caffeate

Caffeic acid (5g, 27.8 mmol) was dissolved in an excess of ethanol (250 ml). Few drops of sulfuric acid were added. The solution was refluxed 24h and progress was controlled by TLC (using ethyl acetate as eluent). The solution was neutralized with a saturated solution of Na_2CO_3 and the solvent was evaporated. The product was dissolved in ethyl acetate and washed once with a saturated solution of Na_2CO_3 and once with brine. The solution was dried over $MgSO_4$ and the solution was filtered. The solvent was evaporated, and the product was dried in a vacuum oven (40°C) over 16h. A beige to brown crystalline product was obtained (Yield : 85%, MP : 149 °C (148-149 °C lit. (Lamidey *et al.*, 2002)), FTIR (cm^{-1}): 3428.04, 3167.16 (O-H Phenols), 2982.96 (C-H), 1651.98 (C=O), 1530.84 (C-C Ar), ^{1}H NMR (500 MHz, DMSO-d_6) δ (ppm): 9.56 (s, 1H), 9.14 (s, 1H), 7.47 (d, J = 15.9 Hz, 1H), 7.04 (d, J = 2.1 Hz, 1H), 6.99 (s, 1H), 6.76 (d, J = 8.1 Hz, 3H), 6.25 (d, J = 15.9 Hz, 1H), 4.15 (q, J = 7.0 Hz, 6H), 1.24 (t, J = 7.1 Hz, 10H)., ^{13}C NMR (126 MHz, DMSO-d_6) δ (ppm): 166.55, 148.37, 145.56, 145.00,

125.51, 121.33, 115.72, 114.81, 114.05, 59.68, 14.27. NMR results were in accordance with the literature (Lamidey *et al.*, 2002).

3.4. Ethyl 3,4-bis(hydroxyethyl)caffeate (CD)

Ethyl caffeate (1g, 4.8 mmol, 1 eq.), ethylene carbonate (888 mg, 10.1 mmol, 2.1 eq.) and K_2CO_3 (133 mg, 1.0 mmol, 0.2 eq.) were placed in a round bottom flask. The flask was flushed with argon and 30 ml of anhydrous DMF was added to the medium. The reaction medium was heated at 130°C under a continuous flow of argon. The reaction progress was controlled by NMR spectroscopy. After 3 hours, the reaction was stopped. The reaction medium was diluted with ethyl acetate. The solution was then washed once with a saturated solution of Na_2CO_3 and twice with brine in order to eliminate the DMF as well as a major part of the by-products. The solvent was evaporated, and the product was purified by flash chromatography (gradient of ethyl acetate and methanol). The product was recovered as an off-white to beige solid (Yield: 58%, MP : 121 °C, FTIR (cm^{-1}): 3506.69 (O-H), 2944.68 (C-H), 1701.88 (C=O), 1596.98 (C-C Ar), ^{1}H NMR (500 MHz, DMSO-d_6) δ (ppm): 7.56 (d, J = 16.0 Hz, 1H), 7.37 (d, J = 2.1 Hz, 1H), 7.22 (dd, J = 8.4, 2.0 Hz, 1H), 7.00 (d, J = 8.4 Hz, 1H), 6.53 (d, J = 16.0 Hz, 1H), 4.84 (s, 2H), 4.17 (q, J = 7.1 Hz, 2H), 4.05 (dt, J = 10.1, 5.1 Hz, 4H), 3.72 (t, J = 5.1 Hz, 4H), 1.25 (t, J = 7.1 Hz, 3H), ^{13}C NMR (126 MHz, DMSO-d_6) δ (ppm): 166.99, 151.13, 149.01, 145.01, 127.44, 123.40, 116.13, 113.73, 112.89, 70.88, 70.79, 60.24, 60.00, 59.92, 14.71. ESI-MS: $[M + Na]^+$ (m/z) calc = 319.115209, found = 319.115193. Elemental analysis: Calc. for $C_{15}H_{20}O_6$: C, 60.81%; H, 6.76%. Found: C, 60.72%; H, 6.89%.

3.5. Enzymatic Polymerization

Diethyl adipate (600 mg, 2.97 mmol) was placed in a Schlenck reactor. HDO and CD were added (see Table 5.1 for the different ratios) while keeping an equimolar proportion of diol to diesters in the medium. Pre-dried CALB (20 wt% compared to the total mass of monomers) and diphenyl ether (300 wt% compared to the total mass of monomers) were added to the reaction medium. The reaction conditions were set at 90°C and 350 mbar. The pressure was then reduced to 100 mbar after 4h and further reduced to 20 mbar after another 4h. After 24h, the reaction was stopped by adding few mL of chloroform. The CALB was removed by filtration and the polymer was precipitated in a large volume of ice-cold methanol. When possible, the polymer was recovered by filtration. Otherwise, the polymer was recovered by centrifugation (8000 rcf, 10 minutes, 4°C). The recovered polymers were dried 24h in vacuum oven prior to analysis.

3.6. UV irradiation of the polymers

For spectrometric analysis: 10 mg of polymer was dissolved in 500 µL of acetone. 20 µL of the solution was spread on the quartz slide, and the solvent was evaporated in a vacuum oven at 40°C for 20 minutes. Irradiation of the polymer was performed in a photoreactor LZC-4X_b (Luzchem Research, Inc) equipped with 14 lamps. The solid samples were placed in the photoreactor on a rotating plate for uniform irradiation. Either UV-A (350 nm, 5.24 $mW.cm^{-2}$) or UV-C (254 nm) lamps were employed.

3.7. Measurement of Gel Content

The polymers were solvent cast from acetone solution in a glass vial. The solvent was evaporated in a vacuum oven at 40°C for 20 minutes. The polymers were placed on a rotating plate in the photoreactor then cured overnight using UV-A lamps (350 nm). After the photo-crosslinking, 3 mL of THF were then added to the vials and the solutions were continuously stirred for 48 h. The supernatant was then carefully recovered and placed in a round bottom flask before evaporation. Both the vials and the flask were then dried 24 h in a vacuum oven at 40°C. The soluble and insoluble fractions were then weighed before analysis.

4. Results and discussion

4.1. Synthesis of the caffeic diol monomer

CA is a natural polyphenol that has multiple interesting characteristics such as antioxidant properties or the capacity to undergo [2+2] cycloaddition. Caffeic acid by itself can be considered as a monofunctional monomer as phenols present a quasi-null reactivity towards CALB and the only reactive function is the carboxylic acid. However, as depicted in introduction, the carbonyl vicinal to the double bond of CA is known to present a limited reactivity towards CALB because of steric and most probably electronic effects (Stamatis *et al.*, 1999; Otto *et al.*, 2000; Yang *et al.*, 2012). In this way, it has been proven that hydrogenation of the double bond of caffeic acid unlocks its reactivity towards CALB, allowing the synthesis of various esters (Guyot *et al.*, 1997).

In this study, though, the double bond of caffeic acid was preserved in order to take advantage of the specificity of the enzyme as well as its properties to undergo [2+2] cycloaddition under UV light. Caffeic acid was first protected by a Fischer esterification with ethanol as reactive solvent (Scheme 5.1). The phenols were then converted into reactive primary alcohols. Such conversion of phenols is generally performed by using propylene oxide (Mialon *et al.*, 2011) or chloro-alcohols (Nguyen *et al.*, 2015). However, propylene oxide and chloro-alcohols are toxic. For this reason, we chose to use a cyclic carbonate which has already been described by our team for the modification of lignin (Duval *et al.*, 2016, 2017, 2021). Ethylene carbonate can react with a phenol in basic condition to yield a primary alcohol. However, the limited reactivity of coumaric derivatives towards ethylene carbonate has already been reported and systematically prevented the obtention of the desired product (Kreye *et al.*, 2013). It has only recently been used by Pospiech *et al.* (Pospiech *et al.*, 2021) for the modification of ferulic acid. In our study, CA was first esterified to give ethyl caffeate (structure confirmed by NMR, in Annexes Figure S5.1 and Figure S5.2). Then ethyl caffeate was reacted with ethylene carbonate. It is worth pointing out that when performed in bulk and at high temperature (above 130 °C) the reaction resulted in the polymerization of ethylene carbonate and transesterification with the caffeic ester, generating an insoluble product. Lower temperatures or lower reaction times gave no product at all in bulk conditions. However, the use of dimethyl formamide (DMF) as a solvent was found to allow the

production of the desired product (Scheme 5.1). The structure of the product was confirmed by FTIR, mass and NMR spectroscopies (Annexes Figure S5.3 and Figure S5.4). We suppose that the high solvating properties of DMF stabilize and dilute the ethylene carbonate, avoiding early polymerization of the substrate on itself.

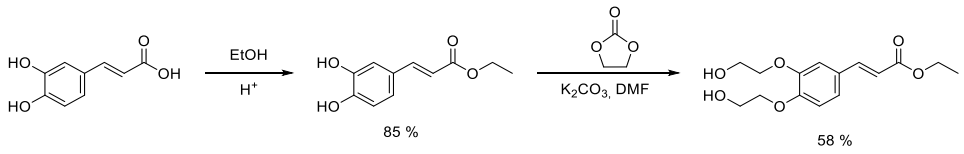

Scheme 5.1: Synthesis of the caffeic diol from caffeic acid

The resulting caffeic diol (CD) was then assayed for [2+2] cycloaddition under UV irradiation. The compound was suspended in cyclohexane and irradiated with UV at 350 nm. The obtained product was analyzed by NMR (Figure 5.1). The formation of the cycloaddition adduct was confirmed by the disappearance of the peaks attributed to the double bond at 6.53 and 7.56 ppm and the appearance of peaks corresponding to the cyclobutane at 4.27 and 3.83 ppm. The caffeic diol was found to rapidly dimerize by [2+2] cycloaddition with almost complete conversion in 24 h (93% yield).

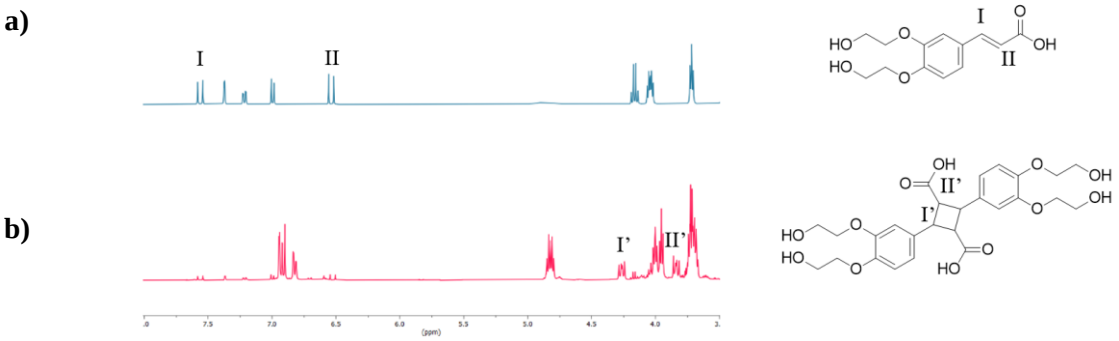

Figure 5.1: ^{1}H NMR analysis of the ethyl 3,4-bis(hydroxyethyl)caffeate (CD) a) before UV irradiation; b) after irradiation at 350 nm for 24h in cyclohexane.

4.2. Synthesis of the polymer

The CD was then tested in lipase-catalyzed polymerization. Diethyl adipate (DEA) was selected as diester since it has already been reported to be highly compatible with CALB in enzymatic polymerization processes, resulting in high molar masses polyesters (Mahapatro *et al.*, 2003; Debuissy *et al.*, 2017b). Moreover, DEA is produced from adipic acid which is an important platform chemical produced from biomass (Skoog *et al.*, 2018). An aliphatic diol, the 1,6-hexanediol (HDO), was also used as a co-monomer. All monomers were introduced in quantities that ensured equimolar proportions between the hydroxyl and ester functions (Scheme 5.2). The use of a co-diol allowed studying the influence of the CD on the reactivity by varying its proportion in the medium. Ratio of 0, 5, 10, 20, 50, 70 and 100% of CD were assessed in CALB-catalyzed polymerization.

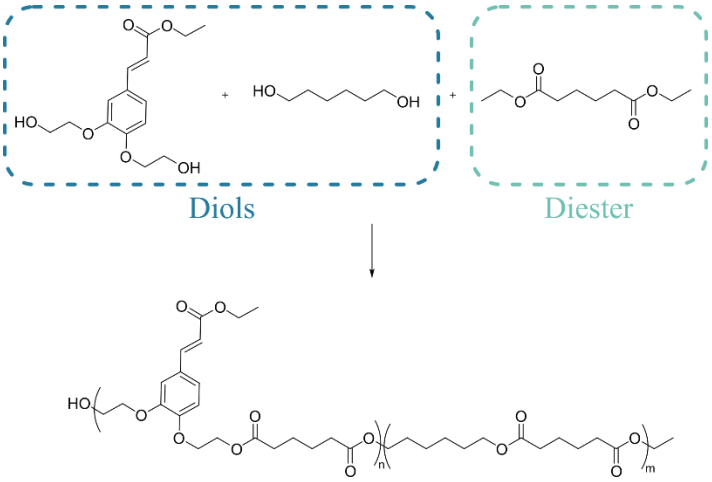

Scheme 5.2: Copolymerization of the CD with HDO and DEA as co-monomers.

The polyesters were synthesized over a period of 24 h. Longer reaction times did not increase further the final molar mass of the polyesters. The obtained polymers were soluble in $CDCl_3$ and in THF. The polyesters containing the CD were recovered in yields between 52 and 67%. The structures of the resulting polyesters were confirmed by NMR spectroscopy (Annexes Figure S5.5). The interpretation of a typical NMR spectrum is presented in Figure 5.2 for the polymer containing 50% of CD. The peak 9 (Figure 5.2) at δ = 4.41 ppm can be attributed to the CH_2 at the end of the CD included in the polymer. This signal can be observed in all polymers synthesized with CD, confirming that CD units were inserted in the polymer chain. The peak 13 (Figure 5.2) at δ = 4.05 was attributed to the HDO included in the polymer chain. Thus, the comparison of the intensities of these two characteristic peaks allows determining the proportions of the corresponding monomers. The proportion of CD included in the polymer chain was determined from the ratio = $I_9/(I_9 + I_{13})$ where I_9 and I_{13} are the intensity of the peaks 9 and 13, respectively. This calculated incorporated ratio of CD was then compared to the initial feed ratio in the reactive medium (Table 5.1).

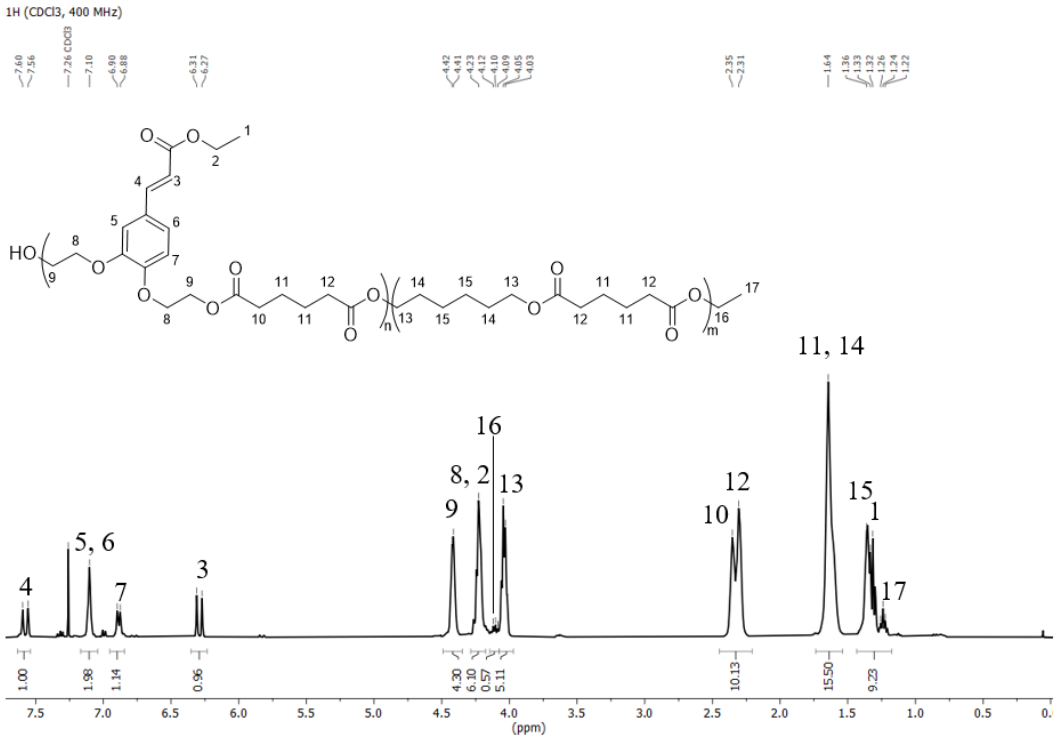

Figure 5.2: ^{1}H NMR analysis and interpretation of the polyester containing 50 % of CD (24 h, diphenyl ether, partial vacuum).

Table 5.1: Feed and incorporated ratio of CD in relation to HDO.

Feed ratio	Incorporated ratio
0,05	0,05
0,10	0,11
0,20	0,23
0,50	0,46
0,70	0,69

A ratio of incorporated diol similar to the feed ratio was found for all polyesters. Therefore, this demonstrates that CALB can insert these two diols into the polymer chain without distinction or preference. This also indicates that the final structure of the polyester can be fine-tuned by controlling the feed ratio of CD.

It is also interesting to note that as the ratio of CD increases, the signals corresponding to the end group of diethyl adipate at δ = 4.10 and 1.23 ppm (protons 16 and 17) get more and more pronounced. Therefore, an increase in CD ratio leads to an increase in end groups proportion and thus to shorter polymer chains. The signal corresponding to the protons next to the hydroxyl end groups should be found at δ = 3.95 ppm for the CD and δ = 3.63 for the HDO. These signals are difficult to discern on the NMR spectra, even for the polymers with high CD contents, and hence shorter chains. This observation suggests that the polyester chains are mostly ended by ester groups.

The peaks 1 and 2 (Figure 5.2) at δ = 1.32 and 4.23 ppm, respectively, were attributed to the ethyl ester of the CD. These peaks are well pronounced in polyesters containing ratio of CD above 10 %. This indicates that, even in presence of CALB, reactions on this ester of CD were marginal, avoiding crosslinking of the material. For ratio of CD of 10 % and below, the peaks are difficult to discern for multiple reasons. First, the ratio of CD in these compounds is particularly low, diminishing the intensity of all peaks attributed to the CD. Then, peaks 1 and 2 can be overlapped by peaks 13 and 15 at δ = 4.05 and 1.33 ppm, respectively. Finally, the absence of peaks 1 and 2 on the NMR spectra of the polyesters containing 10 % or less of CD could also indicate that, at these ratios, part of the ester is converted by CALB during the reaction.

FTIR analyses were performed on the polyesters (Figure 5.3 and in Annexes Figure S5.6). The band at 2937 cm^{-1} was attributed to the stretching of C-H from aromatics and aliphatics. The signals at 1598 and 1510 cm^{-1} were attributed to the C-C bond of the aromatic ring of the CD, confirming its incorporation in the polymer chain. The stretching of the CD double bond is responsible for the band at 1632 cm^{-1}. As FTIR is a quantitative method, the amount of CD included in the polymer chain can be measured by this means. The integration of the peaks at 1 632 and 1 598 cm^{-1} was found to be proportional to the feed ratio of CD (in Annexes Figure S5.7). Finally, the peak at 1727 cm^{-1} was attributed to the stretching of the C=O bond in the carbonyl of the esters. This peak appears shouldered in the polyesters having between 10 and 50 % of CD while a clear second peak appears at 1705 cm^{-1} for higher ratio. The first carbonyl corresponds to the ester resulting from the reaction between diethyl adipate and the diols. The second less intense peak can be attributed to the carbonyl of the ester from CD. This confirms again that the ester of the CD does not participate to the polymerization and is found as a pendant group in the final product.

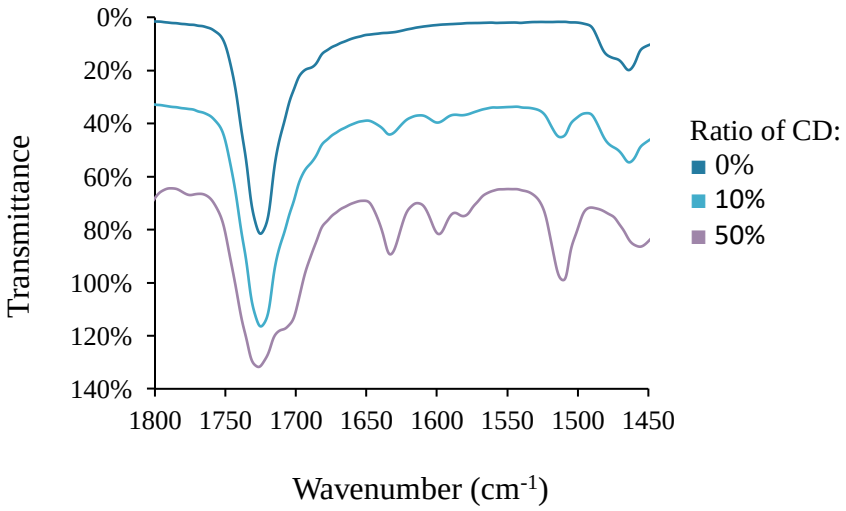

Figure 5.3: FTIR transmittance spectra of the polyesters containing 0, 10 and 50 of CD. Curves are offset by 30 % from each other.

The molar masses of the different polyesters were determined by SEC (Figure 5.4 and in Annexes Figure S5.8). The highest value of molar mass was obtained for a ratio of 5 % of CD, with a M_w up to 65 100 g.mol^{-1}. Slightly higher CD ratio of 10 and 20 % resulted in polymers with a M_w of 28 000 and 22 400 g.mol^{-1}, respectively. These values are very close to those of the purely aliphatic polyester (M_w = 23 900 g.mol^{-1}). Higher ratios of CD tend to further decrease the molar mass of the polyester. These results are in agreement with earlier observations on the NMR spectra. The M_n of the polyesters followed the same trend. This reversed proportionality between the CD and the polyester molar mass suggests that the CD could act as an inhibitor. One reason could be that CD inhibits the enzymatic activity. Inhibition of lipase activity caused by caffeic acid has already been reported in the literature (Karamać *et al.*, 1996). The authors observed the inhibition of pancreatic lipase towards cinnamic acid derivatives in the hydrolysis of *p*-nitrophenol acetate. Even though it was not measured in transesterification, a similar inhibition would explain why high contents in CD result in low enzymatic activity and therefore low molar masses. Another hypothesis would be that the CD can undergo side reactions that possibly consume the monomer. In this case, the higher the ratio of CD, the higher the possibility to alter the stoichiometry of the reaction. As described by Carothers equation, an unbalanced stoichiometry rapidly leads to lower molar mass polymers. This hypothesis would be in adequation with the earlier observation on the NMR spectra indicating that most of the polymer chains are ended with ester groups. Further experiments would be required in order to understand the phenomenon involved in the reduction of the molar mass with the ratio of CD.

Interestingly, a low ratio of 5% CD leads to extreme M_w as compared to other samples. This difference is much less marked for the M_n value, resulting in a high dispersity of 3.3. The M_w being highly impacted by the presence of few polymer chains with a very high molar mass, it thus suggests that some crosslinking could have occurred in this sample. This partial crosslinking could result from the reaction of some of the ester groups of CD, leading to the formation of polymer chains of high molar mass. The inhibitory effect of the CD described earlier might limit this phenomenon for higher CD contents, which correlates with the lower molar masses and dispersities observed for these samples. The crosslinking of the polymer chains seems to occur randomly and in a non-reproducible way, leading to high standard deviation in the average M_w values of the polyesters containing 5 % of CD.

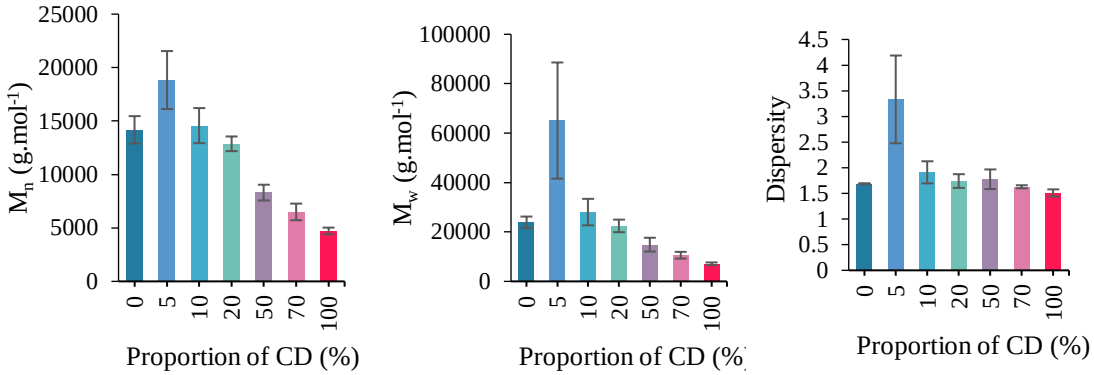

Figure 5.4: SEC analysis results of the polyesters synthesized with various ratios of CD (20 %wt CALB, 24 h, diphenyl ether, partial vacuum).

When considering the values given by the UV detector of the SEC, the intensity of detected polymer chains logically increased with the content in CD. Indeed, the aromatic ring of the CD absorbs UV light whereas the rest of the aliphatic chain does not generate a UV signal. The values of molar masses measured with the UV and in RI detectors were similar, indicating a statistical inclusion of the CD in the polymer chains.

A polymerization reaction was performed with a ratio of CD of 10 % in bulk with Zinc acetate ($Zn(OAc)_2$, 1.5 %wt) as catalyst, following a common protocol for organometallic synthesis of polyesters (190°C, under argon for 4 hours followed by vacuum of 20 mbar for 4 hours). The recovered product was a solid orange resin, insoluble in common organic solvents. In this case, the CD can be considered as a trifunctional monomer since $Zn(OAc)_2$ can easily convert the ester group. This leads to the production of an hyperbranched network, reducing the solubility of the obtained polymer (Flory, 1952; Dong *et al.*, 2011). Its analysis by FTIR showed that when synthesized by organometallic catalysis, the polyester presented a higher ratio of included CD compared to the polyester synthesized by CALB-catalyzed polymerization. This is in agreement with the fact that, in these conditions, the CD is considered as trifunctional and is therefore statistically more reactive than the other monomers. Thus, the selectivity of CALB is advantageous and essential for the production of thermoplastic polyesters from CD displaying a controlled structure, as depicted above.

4.3. Thermal properties:

The thermal transition temperatures of the polymers synthesized with different ratios of CD were analyzed by DSC (Table 5.2 and Figure 5.5).

Table 5.2: Thermal properties of the polyester synthesized with various ratios of CD as determined from TGA and DSC analyses.

CD ratio (%)	T_g (°C)	T_{m1} (°C)	T_{m2} (°C)	T_c (°C)	$T_{d5\%}$ (°C)	T_{dmax1} (°C)	T_{dmax2} (°C)
0	-56	57	n.a.	42	308	400	495
5	-50	51	n.a.	34	330	402	495
10	-43	43	48	27	341	403	496
20	-31	31	39	11	357	402	513
50	-23	n.a.	n.a.	n.a.	356	401	477
70	-13	n.a.	n.a.	n.a.	346	395	550
100	12	n.a.	n.a.	n.a.	354	401	542

n.a.: not available, no transition observed.

The polyesters with CD ratios between 0 and 20 % presented melting and crystallization temperatures that decreased with the increase in CD content. Samples with higher CD ratios were fully amorphous and thus presented no melting temperature. This behavior has already been encountered in a previous study on furan-based polyesters (Bazin *et al.*, 2021b). Increasing the amount of CD moieties enhances the degree of randomness of the copolyester and also increases the intrinsic rigidity of the chain backbone, hindering its potential organization in crystalline phase. Samples with 10 and 20 % of CD presented a double melting endotherm, suggesting the presence of two crystalline forms in the material. The T_g of the sample logically increased with the CD ratio since its aromatic ring brings rigidity to the polymer chain. Similar increase in polyesters T_g values due to the insertion of caffeic-based monomers or other aromatic monomers can be found in the literature (Thi *et al.*, 2009a; Dong *et al.*, 2012).

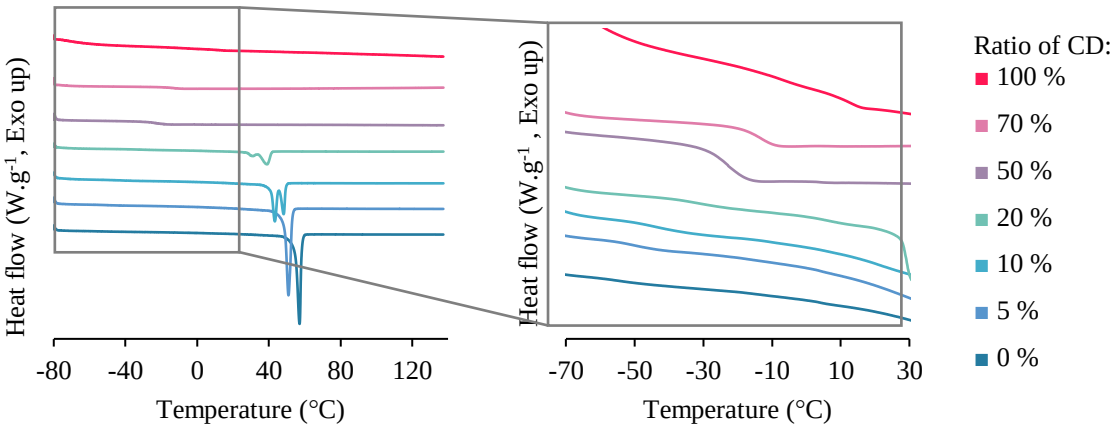

Figure 5.5: DSC analysis of the polyesters synthesized with various ratios of CD. Second heating scan, heating rate: 10 °C.min^{-1}.

The Fox law allows predicting the T_g of a copolymer based on the ratio of the monomers. The experimental data were plotted and compared to the theoretical data calculated from the Fox law (Figure 5.6). Experimental values for ratios of CD between 20 and 100 % do not tend to fit to the Fox law. However, this equation estimates the maximum T_g of the polymers. The SEC analysis showed that the polyesters containing more than 20 % of CD presented a reduced molar mass. According to the Flory-Fox equation, low molar mass negatively impacts the T_g. The experimental value of T_g measured for the

polymer containing more than 20 % of CD could therefore be lower than expected. Polyesters with a ratio of CD below 50 % presented high molar masses and are therefore expected to follow the Fox law. These points were fitted to a Fox law-like equation in order to give an estimation of the maximal T_g of the polymers that could present underestimated data due to low molar masses. After solving the equation, a model was constructed with a coefficient of determination R^2 of 0.998 calculated from the data of polyesters with a CD ratio below 50 % (Figure 5.6). The maximum T_g of the polyester containing 50, 70 and 100 % of CD were then estimated at -6, 7 and 21 °C, respectively. This model indicated that an optimization of the synthesis for polyesters with a ratio of CD above 20 % could increase their glass transition temperature up to 20 °C. This represents therefore an interesting way to improve the thermal properties and stiffness of the materials.

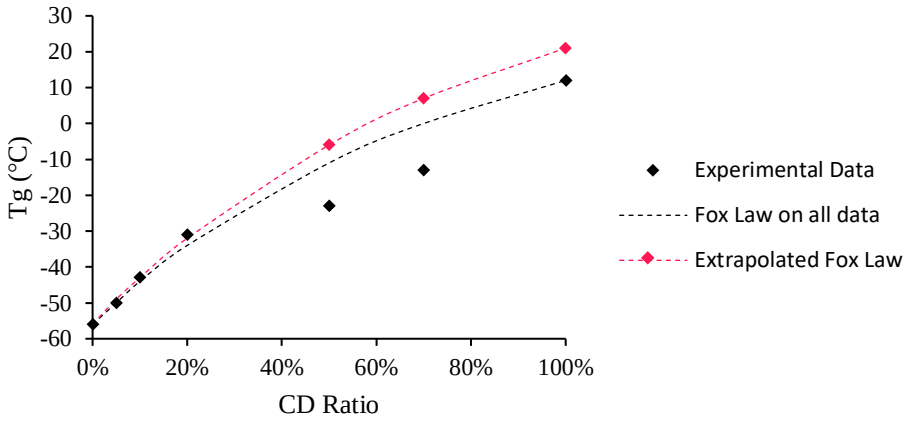

Figure 5.6: Glass transition temperature of the polyesters synthesized with various ratios of CD fitted with Fox laws calculated on all experimental data or extrapolated from first measurements.

The thermal weight loss of the polyesters with different ratios of CD was measured by TGA (Table 5.2 and Figure 5.7). All polyesters presented a two steps thermal degradation with a first step corresponding to the cleavage of the ester bonds and the degradation of the polymer into CO_2 with the formation of char. The second step corresponds to the oxidative degradation of this char. The amount of char and the steepness of the curve in the second step increased with the ratio of CD. Indeed, aromatic compounds produce more notably carbonaceous char which induces a more important second degradation step. This phenomenon has already been observed for common polyesters such as PET (Oh *et al.*, 2006) as well as in polyesters based on natural cinnamic derivatives (Bazin *et al.*, 2021a). The onset of the degradation (measured as $Td_{5\%}$) increased with the content in CD for ratios between 0 and 20 %. This increase in the thermal resistance is in agreement with the results from other studies (Thi *et al.*, 2009a, 2011; Dong *et al.*, 2011, 2012). At higher ratio of CD, the $Td_{5\%}$ does not follow a particular trend. Indeed, as depicted before, these polymers present low molar mass which can cause early degradation of the polymer. The temperature of the first degradation step is stable for all samples indicating a similar degradation pathway.

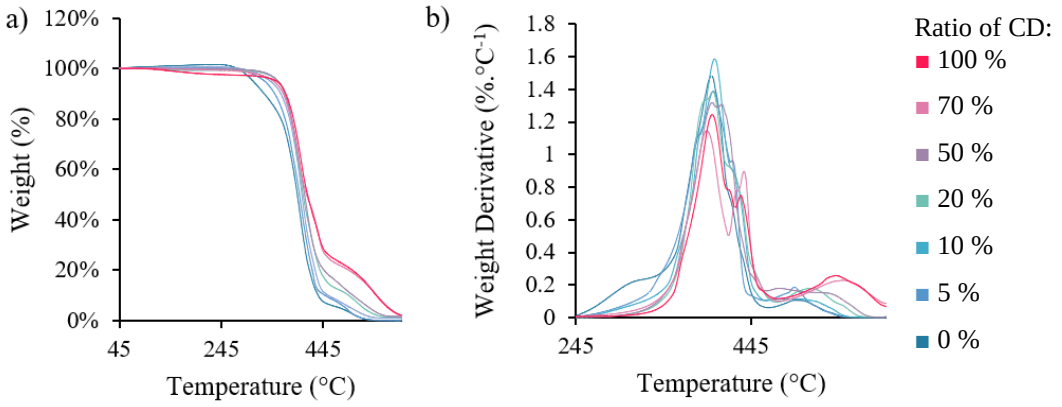

Figure 5.7: TGA analysis under air of the polyesters synthesized with various ratio of CD. Heating rate: 20 °C.min^{-1}.

4.4. Photo-crosslinking properties:

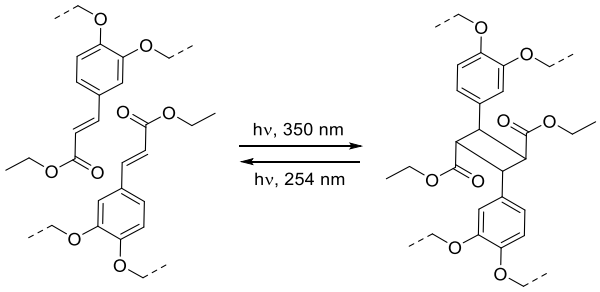

Scheme 5.3: Reversible photo-crosslinking of the CD-based polyesters under UV light.

As described earlier, CD was shown to undergo [2+2] cycloaddition under UV light at 350 nm. We then investigated if the reaction also occurred once the monomer was included in the polyester chain, leading to polymer crosslinking (Scheme 5.3). It was calculated from molar masses values that, for CD ratios above 5 %, the number of CD per chain was superior to 2. A cycloaddition of the caffeic moieties of these polymer chains would therefore lead to the formation of a three-dimensional network. A rapid experiment showed that after short exposition to UV light at 350 nm the obtained polymers were insoluble in common organic solvents such as THF and $CDCl_3$. The crosslinking of the polymer could therefore not be followed by NMR or SEC analyses. Measuring the absorbance of the sample in the UV range is a commonly used method to monitor cycloaddition reactions (Thi *et al.*, 2011; Dong *et al.*, 2012). The conjugated double bond of the cinnamic derivatives causes the sample to absorb light between 250 and 350 nm. The [2+2] cycloaddition consumes the double bond, thus diminishing the related absorbance. The polyester containing 10 % of CD was solvent cast on a quartz plate. The absorbance of the polyester was measured between 500 and 200 nm after different times of exposure to UV light at 350 nm (Figure 5.8a). The evolution of the maximum of absorbance between 250 and 400 nm was then plotted against the irradiation time (Figure 5.8b).

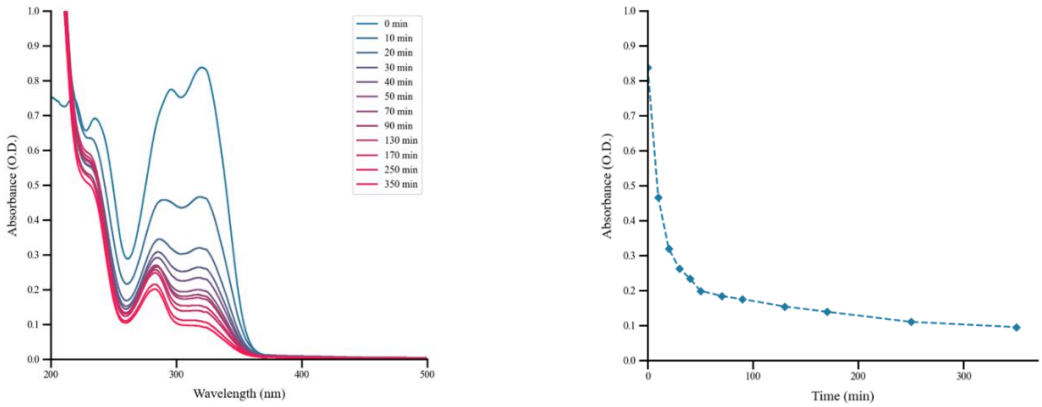

(a) **(b)**

Figure 5.8: Measurement of the absorbance of the polyester containing 10 % of CD. a) Absorption spectra between 500 and 200 nm for various times of UV-A irradiation and b) Evolution of the maximum of absorption against UV-A irradiation time.

The maximum of absorbance of the sample was measured at 320 nm. This value corresponds to the maximum of absorbance of the caffeic moieties (Cornard *et al.*, 2004) and can therefore be attributed to the presence of CD in the polymer. Exposure of the polymer to UV light rapidly decreased the absorbance of the sample until a plateau was reached at 250 min of irradiation. This decrease could be assimilated to an exponential decay. A similar trend was observed for the polymer containing 50 % of CD (Annexes Figure S5.9). These results are in agreement with previous experiments reported in the literature. Dong *et al.* (Dong *et al.*, 2011) obtained a full crosslinking after 230 min of irradiation for a copolymer of caffeic and lithocholic acid. In their study the decrease in absorbance, correlated to the yield of double bond conversion, was of 80 %. Similar conversion was obtained by Thi *et al.* (Hang Thi *et al.*, 2008; Thi *et al.*, 2009a) and a slightly lower conversion was obtained by Li *et al.* (Li *et al.*, 2015) (69.7%). In our case, the conversion yields were even higher with 87 and 96 % for the polyesters containing 10 and 50 % of CD, respectively.

Experiments were performed by exposing the polymer to natural sunlight. The sunlight is composed of visible as well as UV light that could trigger the crosslinking of the polymer. The absorbance of the polymer composed of 10 % of CD decreased by 69 % after 7h of exposition to natural sunlight (Annexes Figure S5.10). This clearly demonstrates that crosslinking of the polymer can therefore be triggered by both artificial and natural UV light.

The impact of the photo-crosslinking on the properties of the polymer was measured on the polymer containing 10, 20 and 50 % of CD. Each polymer was photo-crosslinked at 350 nm for 5 hours to ensure full crosslinking and then immersed in THF. THF is a solvent that, before curing, allows a complete solubilization of the polymers. After photo-curing the polymers appeared to be insoluble and swelled in THF (Annexes Figure S5.11). A measurement of gel content was performed on the crosslinked

polyesters (Figure 5.9). After curing, all the polyesters presented an insoluble fraction above 70 %. Thus, a majority of the material was fully crosslinked by UV irradiation. The polyesters with 20 and 50 % of CD presented similar results and the larger insoluble fraction (around 86 %). The polyester containing 10 % of CD presented a lower insoluble fraction. This result tends to indicate that the polymer containing 10 % of CD was less efficiently crosslinked that those having higher CD ratios. Indeed, among the considered polyesters, it is the one which contains the lowest theoretical amount of CD per chain which will thus induce a lower probability to obtain full crosslinking.

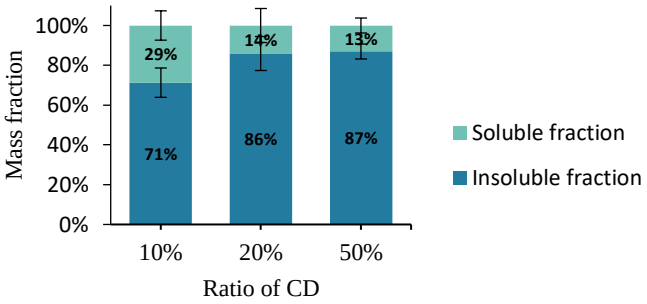

Figure 5.9: Soluble (in THF) and insoluble fractions of polyesters synthesized with various ratios of CD after crosslinking under UV light at 350 nm and swelling in THF for 48h.

The soluble fractions of the polymers containing 10 and 20 % of CD were large enough to be analyzed by NMR spectroscopy and SEC (Annexes Figure S5.12 and Figure S5.13). Interestingly, NMR analysis showed that the recovered soluble polymer exhibited only faint traces of CD with no signal corresponding to the double bonds of CD. Moreover, the molar mass of the recovered polymer was lower than the pre-cured polyesters (Mn = 10 200 and 7 600 $g.mol^{-1}$ compared to 14 600 and 12 600 $g.mol^{-1}$ for the polyesters containing 10 and 20 % of CD, respectively). The soluble fraction could therefore consist of low molar mass chains containing little or no CD and thus unable to participate in the photo-crosslinking. The probability to obtain such chains increases when the ratio of CD decreases in the feed. Moreover, this confirms that, as shown by UV absorption, the conversion of the caffeic moieties double bonds into cyclobutane rings seems complete in the material.

The insoluble fractions in THF of the polyesters were analyzed by FTIR spectroscopy (Annexes Figure S5.14). The bands at 2937, 1727, 1598 and 1510 cm^{-1}, corresponding to the stretching of C-H, the C-O in the carbonyl and the C-C of the aromatic, remained unchanged. The general structure of the polyester backbone thus seemed unaffected. However, the band at 1632 cm^{-1} corresponding to the stretching of the C=C of the CD double bond was no longer present. This confirms that the obtained crosslinking of the polyester is caused by the transformation of the CD double bond by [2+2] cycloaddition. These results are in perfect agreement with previous observation from the literature (Haddleton *et al.*, 1989).

The [2+2] cycloaddition has been described as a reversible reaction (Curme *et al.*, 1967). The bonds that are formed under irradiation at 350 nm can then be broken after irradiation at 254 nm. It is this

phenomenon that allows the production of MSM from polymer containing cinnamic derivatives. The reversibility of the crosslinking of the CD-based polyesters was therefore evaluated. A film of the polyester containing 10 % of CD was crosslinked under UV at 350 nm for 250 minutes. The film was then exposed to UV light at a wavelength of 254 nm (UV-C) for 5 minutes. The absorbance of the film was measured before and after each step of irradiation (Figure 5.10). The absorbance of the polymer film increased after being exposed to UV-C, suggesting that double bonds are generated from the splitting of cyclobutane ring. A maximum absorbance value of 47 % of the original one before photo-crosslinking was measured after only 5 minutes of UV-C irradiation. Longer times of irradiation did not increase further the absorbance of the polymer. Thus, the reverse reaction takes place faster than the direct cycloaddition reaction. This faster kinetics could be attributed to the higher energy of UV-C light when compared to UV-A. However, the reverse reaction seems incomplete as only part of the original absorbance is regained after UV-C irradiation. A similar trend was observed for the polymer containing 50 % of CD (Annexes Figure S5.15).

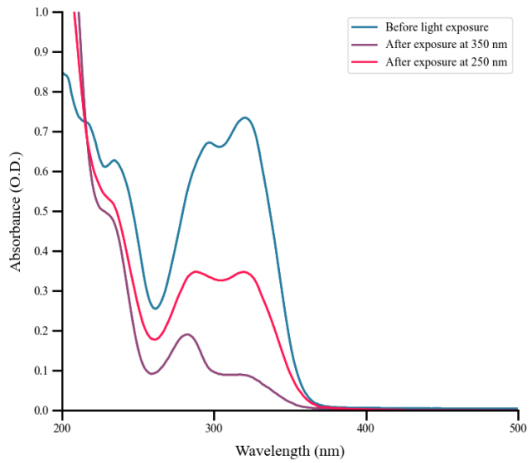

Figure 5.10: Absorption spectra of the polyester containing 10 % of CD before irradiation, after irradiation under UV-A (250 min at 350 nm) and after subsequent irradiation under UV-C (5 min at 254 nm).

The insoluble part (in THF) of the polymer containing 10, 20 and 50% of CD after irradiation by UV-A was exposed to UV-C light. FTIR analysis showed the reappearance of bands at 1632 cm^{-1} confirming the reversibility of the cycloaddition (Annexes Figure S5.16). However, only partial solubility of the sample was obtained. Incomplete reverse reactions has already been observed in the literature (Tanaka *et al.*, 1977) and could be caused by irreversible side reactions triggered by UV light. However, the ability of the light to penetrate the sample might also be an important parameter. Further investigation will be performed on the ability of the material to undergo several cycles of reversible photo-crosslinking and to behave as a memory-shape material.

5. Conclusion

Caffeic acid, a natural phenolic compound, was successfully converted with ethylene carbonate into a new caffeic diol (CD). This CD was then essayed for lipase-catalyzed polymerization with 1,6-hexanediol and diethyl adipate in different ratio using CALB as catalysts. FTIR and NMR analyses showed that for CD ratios above 10 %, the ester of the CD did not react, and no crosslinking was observed. Structural characterization of the obtained materials confirmed that linear polyesters of high molar masses (M_w up to 28 000 g.mol^{-1}) were obtained with statistical inclusion of CD within the polymer chains. The obtained biobased aromatic polyesters therefore present a peculiar structure, with a pendant α,β-unsaturated ester. Such structure could not be obtained through conventional organometallic catalysis and can only be achieved thanks to the selectivity of CALB towards the hydroxyl groups of the caffeic diol monomer. In accordance with the literature, determination of the polyesters thermal properties showed that inclusion of the CD in the polymeric structure improved its thermal resistance (with $T_{d5\%}$ above 350 °C) and glass transition temperature (with a T_g up to 12 °C). At low content of CD of 5%, a supposed minor crosslinking of the polyester resulted in higher molar masses, with M_w of 65 100 g.mol^{-1}. On the other hand, high CD ratios led to reduced molar masses (down to M_w = 7 100 g.mol^{-1}) due to a possible inhibitory effect of the caffeic diol.

After their irradiation under UV light at 350 nm, polyesters with CD ratios between 10 and 50 % became insoluble in THF, attesting for the crosslinking of the polymer. This crosslinking resulted from the [2+2] cycloaddition of the double bonds of the CD moieties. The UV-mediated crosslinking by cycloaddition was complete after 250 minutes of irradiation and reached up to 96 % of conversion. Swelling tests on the polyesters after irradiation showed that the polymers with a high CD ratio presented a higher content of insoluble fraction. On the contrary, polyesters with a low CD ratio presented soluble fraction in THF composed of low molar mass chains, with only traces amount of CD, which therefore were not crosslinked during irradiation.

Upon irradiation to a lower wavelength (254 nm), the reverse reaction to the cycloaddition occurs, leading to partial decrosslinking, as confirmed by UV absorbance measurement and FTIR analysis. However, under these conditions, the reverse reaction was shown to be incomplete probably due to the difficulty for light to penetrate the material. Further investigation will be conducted to assess the ability of the material to undergo multiple reversible photo-crosslinking cycles and to be used as memory-shape materials. Further modification of the CD (with different ester moieties) could also be investigated in order to bring new properties to the materials. Thus, this peculiar structure obtained thanks to the selectivity of CALB paves the way for the synthesis of biobased aromatic polyesters with advanced and innovative properties.

6. References

Aytekin, A. O., Morimura, S. and Kida, K. (**2011**) 'Synthesis of chitosan–caffeic acid derivatives and evaluation of their antioxidant activities', *Journal of Bioscience and Bioengineering*, 111(2), pp. 212–216.

Bazin, A., Avérous, L. and Pollet, E. (**2021**)**b** 'Lipase-catalyzed synthesis of furan-based aliphatic-aromatic biobased copolyesters: Impact of the solvent', *European Polymer Journal*, 159, p. 110717.

Becker, J., Lange, A., Fabarius, J. and Wittmann, C. (**2015**) 'Top value platform chemicals: bio-based production of organic acids', *Current Opinion in Biotechnology*, 36, pp. 168–175.

Chae, Y. and An, Y.-J. (**2018**) 'Current research trends on plastic pollution and ecological impacts on the soil ecosystem: A review', *Environmental Pollution*, 240, pp. 387–395.

Clifford, M. N. (**2000**) 'Chlorogenic acids and other cinnamates – nature, occurrence, dietary burden, absorption and metabolism', *J Sci Food Agric*, 80, pp. 1033–1043.

Cornard, J. P. and Lapouge, C. (**2004**) 'Theoretical and Spectroscopic Investigations of a Complex of Al(III) with Caffeic Acid', *The Journal of Physical Chemistry A*, 108(20), pp. 4470–4478.

Curme, H. G., Natale, C. C. and Kelley, D. J. (**1967**) 'Photosensitized reactions of cinnamate esters', *The Journal of Physical Chemistry*, 71(3), pp. 767–770.

Debuissy, T., Pollet, E. and Avérous, L. (**2017**)**b** 'Lipase-catalyzed synthesis of biobased and biodegradable aliphatic copolyesters from short building blocks. Effect of the monomer length', *European Polymer Journal*, 97, pp. 328–337.

Delidovich, I., Hausoul, P. J. C., Deng, L., Pfützenreuter, R., Rose, M. and Palkovits, R. (**2016**) 'Alternative Monomers Based on Lignocellulose and Their Use for Polymer Production', *Chemical Reviews*, 116(3), pp. 1540–1599.

Dong, W., Li, H., Chen, M., Ni, Z., Zhao, J., Yang, H. and Gijsman, P. (**2011**) 'Biodegradable bio-based polyesters with controllable photo-crosslinkability, thermal and hydrolytic stability', *Journal of Polymer Research*, 18(6), pp. 1239–1247.

Dong, W., Ren, J., Lin, L., Shi, D., Ni, Z. and Chen, M. (**2012**) 'Novel photocrosslinkable and biodegradable polyester from bio-renewable resource', *Polymer Degradation and Stability*, 97(4), pp. 578–583.

Douka, A., Vouyiouka, S., Papaspyridi, L.-M. and Papaspyrides, C. D. (**2018**) 'A review on enzymatic polymerization to produce polycondensation polymers: The case of aliphatic polyesters, polyamides and polyesteramides', *Progress in Polymer Science*, 79, pp. 1–25.

Duchiron, S. W., Pollet, E., Givry, S. and Avérous, L. (**2017**) 'Enzymatic synthesis of poly(ε-caprolactone- co -ε-thiocaprolactone)', *European Polymer Journal*, 87, pp. 147–158.

Duval, A. and Avérous, L. (**2016**) 'Oxyalkylation of Condensed Tannin with Propylene Carbonate as an Alternative to Propylene Oxide', *ACS Sustainable Chemistry & Engineering*, 4(6), pp. 3103–3112.

Duval, A. and Avérous, L. (**2017**) 'Cyclic Carbonates as Safe and Versatile Etherifying Reagents for the Functionalization of Lignins and Tannins', *ACS Sustainable Chemistry & Engineering*, 5(8), pp. 7334–7343.

Duval, A., Layrac, G., Zomeren, A., Smit, A. T., Pollet, E. and Avérous, L. (**2021**) 'Isolation of Low Dispersity Fractions of Acetone Organosolv Lignins to Understand their Reactivity: Towards Aromatic Building Blocks for Polymers Synthesis', *ChemSusChem*, 14(1), pp. 387–397.

Flory, P. J. (**1952**) 'Molecular Size Distribution in Three Dimensional Polymers. VI. Branched Polymers Containing A-R-B Type Units', 74, pp. 2718–2723.

Flourat, A. L., Combes, J., Bailly-Maitre-Grand, C., Magnien, K., Haudrechy, A., Renault, J. and Allais, F. (**2021**) 'Accessing *p*-Hydroxycinnamic Acids: Chemical Synthesis, Biomass Recovery, or Engineered Microbial Production?', *ChemSusChem*, 14(1), pp. 118–129.

Fonseca, A. C., Lima, M. S., Sousa, A. F., Silvestre, A. J., Coelho, J. F. J. and Serra, A. C. (**2019**) 'Cinnamic acid derivatives as promising building blocks for advanced polymers: synthesis, properties and applications', *Polymer Chemistry*, 10(14), pp. 1696–1723.

Genaro-Mattos, T. C., Maurício, Â. Q., Rettori, D., Alonso, A. and Hermes-Lima, M. (**2015**) 'Antioxidant Activity of Caffeic Acid against Iron-Induced Free Radical Generation—A Chemical Approach', *PLOS ONE*. Edited by G. P. Tochtrop, 10(6), p. e0129963.

Guyot, B., Bosquette, B., Pina, M. and Graille, J. (**1997**) 'Esterification of phenolic acids from green coffee with an immobilized lipase from Candida antarctica in solvent-free medium', *Biotechnology Letters*, 19(6), pp. 529–532.

Haddleton, D. M., Creed, D., Griffin, A. C., Hoyle, C. E. and Venkataram, K. (**1989**) 'Photochemical crosslinking of main-chain liquid-crystalline polymers containing cinnamoyl groups', *Die Makromolekulare Chemie, Rapid Communications*, 10(8), pp. 391–396.

Hang Thi, T., Matsusaki, M. and Akashi, M. (**2008**) 'Thermally stable and photoreactive polylactides by the terminal conjugation of bio-based caffeic acid', *Chemical Communications*, (33), p. 3918.

Hohn, S., Acevedo-Trejos, E., Abrams, J. F., Fulgencio de Moura, J., Spranz, R. and Merico, A. (**2020**) 'The long-term legacy of plastic mass production', *Science of The Total Environment*, 746, p. 141115.

Ishii, D., Maeda, H., Hayashi, H., Mitani, T., Shinohara, N., Yoshioka, K. and Watanabe, T. (**2013**) 'Effect of Polycondensation Conditions on Structure and Thermal Properties of Poly(caffeic acid)', in Cheng, H. N., Gross, R. A., and Smith, P. B. (eds) *Green Polymer Chemistry: Biocatalysis and Materials II*. Washington, DC: American Chemical Society, pp. 237–249.

Kaneko, T., Kaneko, D. and Wang, S. (**2010**) 'High-performance lignin-mimetic polyesters', *Plant Biotechnology*, 27(3), pp. 243–250.

Kaneko, T., Thi, T. H., Shi, D. J. and Akashi, M. (**2006**) 'Environmentally degradable, high-performance thermoplastics from phenolic phytomonomers', *Nature Materials*, 5(12), pp. 966–970.

Karamać, M. and Amarowicz, R. (**1996**) 'Inhibition of Pancreatic Lipase by Phenolic Acids - Examination in vitro', *Zeitschrift für Naturforschung C*, 51(11–12), pp. 903–906.

Katayama, S., Ohno, F., Yamauchi, Y., Kato, M., Makabe, H. and Nakamura, S. (**2013**) 'Enzymatic Synthesis of Novel Phenol Acid Rutinosides Using Rutinase and Their Antiviral Activity in Vitro', *Journal of Agricultural and Food Chemistry*, 61(40), pp. 9617–9622.

Khan, F., Bamunuarachchi, N. I., Tabassum, N. and Kim, Y.-M. (**2021**) 'Caffeic Acid and Its Derivatives: Antimicrobial Drugs toward Microbial Pathogens', *Journal of Agricultural and Food Chemistry*, 69(10), pp. 2979–3004.

Kreye, O., Oelmann, S. and Meier, M. A. R. (**2013**) 'Renewable Aromatic-Aliphatic Copolyesters Derived from Rapeseed', *Macromolecular Chemistry and Physics*, 214(13), pp. 1452–1464.

Lamidey, A., M., Fernon, L., Pouységu, L., Delattre, C. and Quideau, S. (**2002**) 'A Convenient Synthesis of the Echinacea-Derived Immunostimulator and HIV-1 Integrase Inhibitor (-)-(2R,3R)-Chicoric Acid', *Helvetica Chimica Acta*, 85, pp. 2328-2334.

Lendlein, A., Jiang, H., Jünger, O. and Langer, R. (**2005**) 'Light-induced shape-memory polymers', *Nature*, 434(7035), pp. 879–882.

Li, S., Li, W. and Khashab, N. M. (**2012**) 'Stimuli responsive nanomaterials for controlled release applications', *Nanotechnology Reviews*, 1(6), pp. 493–513.

Li, S., Moosa, B. A., Chen, Y., Li, W. and Khashab, N. M. (**2015**) 'A photo-tunable membrane based on inter-particle crosslinking for decreasing diffusion rates', *Journal of Materials Chemistry B*, 3(7), pp. 1208–1216.

Liu, J., Wang, X., Bai, R., Zhang, N., Kan, J. and Jin, C. (**2018**) 'Synthesis, characterization, and antioxidant activity of caffeic-acid-grafted corn starch: Characterization and antioxidant activity of caffeic-acid-grafted starch', *Starch - Stärke*, 70(1–2), p. 1700141.

Llevot, A., Grau, E., Carlotti, S., Grelier, S. and Cramail, H. (**2016**) 'From Lignin-derived Aromatic Compounds to Novel Biobased Polymers', *Macromolecular Rapid Communications*, 37(1), pp. 9–28.

Mahapatro, A., Kalra, B., Kumar, A. and Gross, R. A. (**2003**) 'Lipase-Catalyzed Polycondensations: Effect of Substrates and Solvent on Chain Formation, Dispersity, and End-Group Structure', *Biomacromolecules*, 4(3), pp. 544–551.

Mialon, L., Vanderhenst, R., Pemba, A. G. and Miller, S. A. (**2011**) 'Polyalkylenehydroxybenzoates (PAHBs): Biorenewable Aromatic/Aliphatic Polyesters from Lignin: Polyalkylenehydroxybenzoates (PAHBs) …', *Macromolecular Rapid Communications*, 32(17), pp. 1386–1392.

Nagata, M. and Kitazima, I. (**2006**) 'Photocurable biodegradable poly(ε-caprolactone)/poly(ethylene glycol) multiblock copolymers showing shape-memory properties', *Colloid and Polymer Science*, 284(4), pp. 380–386.

Nagata, M. and Sato, Y. (**2005**) 'Synthesis and properties of photocurable biodegradable multiblock copolymers based on poly(ε-caprolactone) and poly(L-lactide) segments', *Journal of Polymer Science Part A: Polymer Chemistry*, 43(11), pp. 2426–2439.

Nguyen, H. T. H., Qi, P., Rostagno, M., Feteha, A. and Miller, S. A. (**2018**) 'The quest for high glass transition temperature bioplastics', *Journal of Materials Chemistry A*, 6(20), pp. 9298–9331.

Nguyen, H. T. H., Reis, M. H., Qi, P. and Miller, S. A. (**2015**) 'Polyethylene ferulate (PEF) and congeners: polystyrene mimics derived from biorenewable aromatics', *Green Chemistry*, 17(9), pp. 4512–4517.

Oh, S.-C., Lee, D.-G., Kwak, H. and Bae, S.-Y. (**2006**) 'Combustion Kinetics Of Polyethylene Terephthalate', *Environmental Engineering Research*, 11(5), pp. 250–256.

Ortiz, C., Ferreira, M. L., Barbosa, O., dos Santos, J. C. S., Rodrigues, R. C., Berenguer-Murcia, Á., Briand, L. E. and Fernandez-Lafuente, R. (**2019**) 'Novozym 435: the "perfect" lipase immobilized biocatalyst?', *Catalysis Science & Technology*, 9(10), pp. 2380–2420.

Otto, R. T., Scheib, H., Bornscheuer, U. T., Pleiss, J., Syldatk, C. and Schmid, R. D. (**2000**) 'Substrate specificity of lipase B from Candida antarctica in the synthesis of arylaliphatic glycolipids', *Journal of Molecular Catalysis B: Enzymatic*, 8(4–6), pp. 201–211.

Pilate, F., Stoclet, G., Mincheva, R., Dubois, P. and Raquez, J.-M. (**2018**) 'Poly(ε-caprolactone) and Poly(ω-pentadecalactone)-Based Networks with Two-Way Shape-Memory Effect through [2+2] Cycloaddition Reactions', *Macromolecular Chemistry and Physics*, 219(4), p. 1700345.

Pospiech, D., Korwitz, A., Komber, H., Jehnichen, D., Arnhold, K., Brünig, H., Scheibner, H., Müller, M. T. and Voit, B. (**2021**) 'Polyesters with bio-based ferulic acid units: crosslinking paves the way to property consolidation', *Polymer Chemistry*, 12(36), pp. 5139–5148.

Rochette, J. M. and Ashby, V. S. (**2013**) 'Photoresponsive Polyesters for Tailorable Shape Memory Biomaterials', *Macromolecules*, 46(6), pp. 2134–2140.

Shoda, S., Uyama, H., Kadokawa, J., Kimura, S. and Kobayashi, S. (**2016**) 'Enzymes as Green Catalysts for Precision Macromolecular Synthesis', *Chemical Reviews*, 116(4), pp. 2307–2413.

Siracusa, V. and Blanco, I. (**2020**) 'Bio-Polyethylene (Bio-PE), Bio-Polypropylene (Bio-PP) and Bio-Poly(ethylene terephthalate) (Bio-PET): Recent Developments in Bio-Based Polymers Analogous to Petroleum-Derived Ones for Packaging and Engineering Applications', *Polymers*, 12(8), p. 1641.

Skoog, E., Shin, J. H., Saez-Jimenez, V., Mapelli, V. and Olsson, L. (**2018**) 'Biobased adipic acid – The challenge of developing the production host', *Biotechnology Advances*, 36(8), pp. 2248–2263.

Stamatis, H., Sereti, V. and Kolisis, F. N. (**1999**) 'Studies on the enzymatic synthesis of lipophilic derivatives of natural antioxidants', *Journal of the American Oil Chemists' Society*, 76(12), p. 1505.

Sun, Z., Fridrich, B., de Santi, A., Elangovan, S. and Barta, K. (**2018**)**b** 'Bright Side of Lignin Depolymerization: Toward New Platform Chemicals', *Chemical Reviews*, 118(2), pp. 614–678.

Tanaka, H. and Honda, K. (**1976**) 'Photoreversible reactions of polymers containing cinnamylideneacetate derivatives and the model compounds', *Journal of Polymer Science Part A-1: Polymer Chemistry*, 25, pp. 2685–2689.

Tanaka, H. and Honda, K. (**1977**) 'Photoreversible reactions of polymers containing cinnamylideneacetate derivatives and the model compounds', *Journal of Polymer Science: Polymer Chemistry Edition*, 15(11), pp. 2685–2689.

Thi, T. H., Matsusaki, M. and Akashi, M. (**2009**)**a** 'Development of Photoreactive Degradable Branched Polyesters with High Thermal and Mechanical Properties', *Biomacromolecules*, 10(4), pp. 766–772.

Thi, T. H., Matsusaki, M. and Akashi, M. (**2009**)**b** 'Photoreactive Polylactide Nanoparticles by the Terminal Conjugation of Biobased Caffeic Acid', *Langmuir*, 25(18), pp. 10567–10574.

Thi, T. H., Matsusaki, M., Hirano, H., Kawano, H., Agari, Y. and Akashi, M. (**2011**) 'Mechanism of high thermal stability of commercial polyesters and polyethers conjugated with bio-based caffeic acid', *Journal of Polymer Science Part A: Polymer Chemistry*, 49(14), pp. 3152–3162.

Thi, T. H., Matsusaki, M., Shi, D., Kaneko, T. and Akashi, M. (**2008**) 'Synthesis and properties of coumaric acid derivative homo-polymers', *Journal of Biomaterials Science, Polymer Edition*, 19(1), pp. 75–85.

Valanciene, E., Jonuskiene, I., Syrpas, M., Augustiniene, E., Matulis, P., Simonavicius, A. and Malys, N. (**2020**) 'Advances and Prospects of Phenolic Acids Production, Biorefinery and Analysis', *Biomolecules*, 10(6), p. 874.

Wu, L., Jin, C. and Sun, X. (**2011**) 'Synthesis, Properties, and Light-Induced Shape Memory Effect of Multiblock Polyesterurethanes Containing Biodegradable Segments and Pendant Cinnamamide Groups', *Biomacromolecules*, 12(1), pp. 235–241.

Xie, H., Yang, K.-K. and Wang, Y.-Z. (**2019**) 'Photo-cross-linking: A powerful and versatile strategy to develop shape-memory polymers', *Progress in Polymer Science*, 95, pp. 32–64.

Yang, Z., Guo, Z. and Xu, X. (**2012**) 'Enzymatic lipophilisation of phenolic acids through esterification with fatty alcohols in organic solvents', *Food Chemistry*, 132(3), pp. 1311–1315.

Conclusion chapitre 5

Ce dernier chapitre a porté sur l'étude de la réactivité des dérivés d'acide caféique en polymérisation enzymatique. L'acide caféique, qui possède une structure très proche de celle de l'acide férulique, doit lui aussi être modifié afin d'en faire un monomère difonctionnel réactif vis-à-vis de la CALB et ainsi permettre sa polymérisation.

Après estérification, l'acide caféique a été modifié avec succès par l'éthylène carbonate et converti en un diol entièrement biosourcé. Cette molécule n'avait, à notre connaissance, encore jamais été étudiée. Toutefois, la synthèse de ce diol caféique (CD) nécessite l'emploi de DMF, un solvant toxique. Aussi une optimisation de cette voie de synthèse vers des conditions plus vertes est une voie d'amélioration qu'il conviendrait d'envisager.

La capacité du CD ainsi formé à polymériser par catalyse enzymatique a ensuite été étudiée. Plusieurs copolyesters ont été obtenus en associant le CD au diéthyl adipate (DEA). L'ajout d'un second diol, tel que le 1,6-HDO, a permis de faire varier la proportion de CD afin d'étudier son influence sur l'activité en polymérisation de la CALB. Pour des teneurs en CD supérieures ou égales à 10%, des chaînes polyesters linéaires avec des groupements esters pendants insaturés ont été obtenues, confirmant le rôle de la sélectivité de la CALB dans le contrôle de la structure du polymère. Des polyesters possédant des masses molaires élevées et comparables à celles de leurs homologues aliphatiques ont été obtenus. Comme cela a été décrit dans les chapitres précédents, l'insertion d'unités aromatiques au sein des chaînes permet d'augmenter les propriétés thermiques du matériau.

De par leur double liaison pendante, les matériaux synthétisés ont montré des propriétés intéressantes de photo-réticulation sous irradiation par les UV-A. Cette propriété semble cependant dépendante du taux de CD dans le matériau et de l'épaisseur de ce dernier. Cette réticulation du matériau s'est trouvée être partiellement réversible sous l'effet d'un rayonnement UV-C. Les propriétés de ces systèmes devront être étudiées plus en détail, en lien avec de potentielles applications telles que l'élaboration de matériaux à mémoire de forme. La réversibilité de la réticulation sous rayonnement UV pourrait également permettre d'envisager l'élaboration de polymères pour la libération de substances actives de manière ciblée dans le corps. Une étude de la biocompatibilité de ces matériaux serait alors à considérer.

Conclusion générale et perspectives

Cette thèse, dirigée par le Dr Eric Pollet, a été financée par une bourse obtenue auprès de l'école doctorale de physique et chimie physique de Strasbourg (ED182). Le travail de recherche a été réalisé dans l'équipe BioTeam, dirigée par le Pr. Luc Avérous, au sein de l'Institut de Chimie et Procédés pour l'Énergie, l'Environnement et la Santé (ICPEES-UMR7515). Les perturbations engendrées par la crise sanitaire du COVID-19 ont entrainé une prolongation de deux mois de cette thèse. Le sujet de recherche alliant chimie de synthèse, biocatalyse et physico-chimie des polymères a pour but de fournir une meilleure compréhension des possibilités de la synthèse de polyesters aromatiques par catalyse enzymatique à partir de monomères issus de la biomasse.

Ce projet s'inscrit dans la continuité des recherches effectuées au sein de la BioTeam portant sur la synthèse de polymères par catalyse enzymatique. Plusieurs études avaient ainsi permis d'étudier en détail la réactivité en catalyse enzymatique de monomères aliphatiques tels que le 1,4-butanediol ou l'acide adipique par polycondensation ou encore celle de l'ε-caprolactone par polymérisation par ouverture de cycle. Ce travail de thèse a cependant été centré sur l'utilisation de nouveaux monomères aromatiques afin de produire des polyesters aux propriétés thermiques plus élevées. En pleine adéquation avec la thématique de recherche de l'équipe, l'utilisation de monomères contenant une large proportion de carbone renouvelable a naturellement été considérée. Cette démarche s'inscrit également dans une volonté de produire des matériaux s'inscrivant dans une logique d'économie circulaire.

Le premier chapitre de ce manuscrit, présentant l'état de l'art sur le sujet de recherche, est constitué d'un sous chapitre permettant d'introduire les nombreuses thématiques abordées dans ce projet. Cette première partie de chapitre met ainsi en lumière l'importance des matériaux polymères et plus précisément des polyesters dans notre quotidien. Elle souligne également l'importance actuelle des polyesters dans l'élaboration de matériaux biosourcés et biodégradables. En effet, les polyesters profitent tout d'abord d'une grande diversité de monomères pouvant être issus de la biomasse. Ensuite, leurs liaisons hydrolysables facilitent leur recyclage chimique ou leur biodégradation. Un grand nombre d'études portent sur le remplacement du PET, le polyester d'origine fossile le plus utilisé aujourd'hui, par des alternatives biosourcées. Cependant, comme souligné dans ce sous-chapitre 1.1, la synthèse des polyesters fait généralement appel à l'utilisation de hautes températures et de catalyseurs organométalliques qui peuvent avoir un fort impact environnemental ou sanitaire. La catalyse enzymatique représente donc comme une alternative plus douce et plus écologique. La remarquable activité catalytique des lipases et notamment de la CALB est ainsi soulignée. La popularité de cette enzyme repose notamment sur son importante résistance aux solvants organiques et à des températures supérieures à 100 °C ainsi qu'à un site actif permettant d'accueillir et de convertir un large éventail de substrats. De plus, sous sa forme immobilisée, la CALB est facile à manipuler et peut-être réutilisée dans un grand nombre de cycles réactionnels. Plusieurs études portant sur la synthèse de polyesters

biosourcés catalysée par la CALB sont ensuite présentées dans une partie du sous-chapitre 1.1. Cette partie évoque la grande diversité de substrats qui ont déjà été étudiés pour la synthèse enzymatique de polyesters. L'influence de la structure du substrat et des conditions réactionnelles sur l'activité de l'enzyme est discutée puisque cette dernière a une influence directe sur la masse molaire et donc sur les propriétés du polymère obtenu. Des monomères en grande majorité aliphatiques ont ainsi été étudiés dans la littérature, produisant des polyesters avec une T_g et un module très inférieur à ceux du PET. La littérature fait également état de polyesters aromatiques à base de furane synthétisés par catalyse enzymatique et qui présentent des T_g supérieures à la température ambiante. Toutefois, les travaux sur la polymérisation enzymatique de monomères aromatiques restent rares et seuls quelques dérivés aromatiques de la lignine ont été étudiés.

Il est pourtant possible d'extraire un grand nombre de molécules plateforme aromatiques de la biomasse lignocellulosique et notamment des composés phénoliques. Ces molécules pourraient ainsi être utilisées pour la production de polyesters aromatiques biosourcés par catalyse enzymatique. De ce fait, le sous-chapitre 1.2 présente une étude bibliographique qui porte sur la réactivité de divers composés aromatiques phénoliques issus de la biomasse lignocellulosique engagés de manière plus large dans des réactions d'estérification et de transestérification. Ces dérivés phénoliques ont été répartis en trois catégories distinctes : les dérivés cinnamiques, les composés benzoïques et les dérivés d'acide gallique. Ces composés sont largement étudiés en estérification et transestérification afin d'élaborer des molécules pouvant être utilisées comme antioxydant, anti-UV mais également à des fins thérapeutiques. La structure de ces composés et notamment la nature et la position des groupements situés sur leur cycle aromatique influencent grandement leur réactivité vis-à-vis de l'enzyme. À titre d'exemple, les groupements hydroxyles ont un effet plus délétère que les méthoxyles sur l'activité enzymatique. Cette sélectivité serait essentiellement imputable à des effets électroniques plutôt qu'à de la gêne stérique. La sélectivité d'une enzyme dépend cependant de sa nature, conditionnée par son origine. De ce fait, de nombreuses d'enzymes ont été étudiées pour leur activité d'estérification et de transestérification de composés phénoliques naturels. Si la CALB a été utilisée dans un très grand nombre d'études, d'autres enzymes comme les lipases de *Rhizomucor miehei* ou de *Thermomyces lanuginosus* ont montré une activité intéressante avec parfois des conversions supérieures à 90 %. Des hydrolases spécifiques aux dérivés cinnamiques (les acide férulique esterases, FAE) et spécifiques à l'acide gallique (les tannases) ont également été décrites. Les conditions réactionnelles jouent également un rôle très important sur l'activité de l'enzyme. C'est notamment le cas des propriétés du solvant (polarité, nature, activité en eau…) dont l'influence a été étudiée en détail. Cette étude bibliographique a également permis de déterminer que la réactivité des dérivés benzoïques était généralement plus faible que celle des dérivés cinnamiques dans ces estérifications et transestérifications enzymatiques. Si l'acide gallique est un dérivé d'acide benzoïque, il a été discuté dans une partie séparée du fait de l'originalité de sa source (les tannins) et de son utilisation spécifique avec les tannases.

Le chapitre 1.1 a mis en lumière la forte utilisation des furanes pour la synthèse de polyesters aromatiques biosourcés, mais également la problématique des faibles masses molaires obtenues par catalyse enzymatique. L'étude présentée au chapitre 2 s'attarde donc sur la compréhension de ce phénomène et la présentation d'une solution possible. Un diester de furane, le diméthyle furanedicarboxylate, a été co-polymérisé avec le 1,6-hexanediol et le diéthyle adipate en tant que second diester aliphatique. En faisant varier le ratio entre les deux diesters, il a été montré que des taux de monomère furanique aromatique jusqu'à 70 % n'entrainent pas de diminution significative des masses molaires. Des polyesters aromatiques possédant une M_n de 19 400 g.mol^{-1} ont ainsi été obtenus (en comparaison d'une M_n de 19 000 g.mol^{-1} pour le polymère aliphatique). Pour des taux de monomère aromatique supérieurs à 70 %, la précipitation du polymère dans le milieu réactionnel semble responsable de l'arrêt de la croissance des chaines polymères. Ce phénomène, exacerbé par la substitution du 1,6-hexanediol par le 1,4-butanediol, parait être en majorité responsable des faibles masses molaires obtenues par polymérisation enzymatique de dérivés de furane. De nouveaux solvants permettant de solubiliser les substrats aromatiques durant la polymérisation enzymatique ont donc été étudiés. Parmi plusieurs solvants de polarités variées, l'anisole et l'acétophénone se sont montrés particulièrement efficaces pour solubiliser ou tout du moins retarder la précipitation du polymère en croissance. Ces solvants alternatifs ont ainsi permis l'obtention de polyesters de masses molaires plus importantes et présentant des propriétés thermiques supérieures avec des T_g allant jusqu'à 17°C et donc proches de la température ambiante.

Le chapitre 2 montre donc que, malgré les limitations qui viennent d'être rappelées, la CALB présente une activité importante vis-à-vis des dérivés furanes et ceci malgré leur aromaticité et donc leur structure fortement éloignée de celle du substrat naturel des lipases (les triglycérides). Dans le chapitre 3, la réactivité d'un autre substrat aromatique biosourcé, l'acide férulique, est alors étudiée. Une fois convertis en diesters de longueurs variables, les dérivés d'acide férulique ont montré une faible réactivité au contact de la CALB et du 1,4-butanediol. Cette faible réactivité est cependant en accord avec les observations de la littérature décrites dans le chapitre 1.2 et serait intrinsèque à la structure de l'acide férulique. Dans ce cas, la conjugaison du cycle aromatique avec la double liaison et le carbonyle, stabilise ce dernier et rend la fonction acide ou ester correspondante très peu réactive. Ce phénomène s'est révélé être un frein à la production de polyesters de masses molaires importantes puisque des DP_n ne dépassant pas 5 ont été obtenus. Afin de résoudre ce défaut de réactivité, deux méthodes de modification de la structure des diesters féruliques ont été étudiées. La première, l'hydrogénation, permet l'obtention de polyesters aromatiques de masse molaire élevées avec des DP_n allant jusqu'à 58. Il est intéressant de noter que le monomère hydrogéné le plus court entraine les masses molaires les plus élevées. La réduction des diesters férulique conduit également à des polyesters aromatiques de masses molaires élevées (DP_n jusqu'à 19) et la rigidité apportée par la double liaison, qui est conservée dans ce cas, engendre des T_g proches de la température ambiante (jusqu'à 21 °C contre 7°C pour les monomères

hydrogénés). On peut également noter que l'acétophénone, dont les bonnes propriétés de solubilisation ont été décrites au chapitre 2, a été employée avec succès afin de solubiliser ces monomères.

Il a donc été montré que l'acide férulique est une molécule plateforme intéressante pour la synthèse enzymatique de polyesters aromatiques. Sa structure et notamment la délocalisation électronique au sein du monomère est cependant un frein à sa réactivité. Dans le quatrième chapitre de ce manuscrit, la cycloaddition [2+2] a été étudiée comme méthode alternative afin de transformer les dérivés d'acide féruliques en dimères polymérisables par la CALB. Cette voie de synthèse des dimères présente l'avantage d'être réalisée sous irradiation UV, donc dans des conditions relativement douces et respectant le principe d'économie d'atomes. Dans le sous-chapitre 4.1, il est ainsi montré que la structure cristalline des substrats utilisés a un impact important sur leur capacité à photo-dimériser. Deux dérivés d'acide férulique, l'acide *p*-acétylférulique et un diester d'acide férulique ($DeFA^{II}$), présentent des rendements de dimérisation quasi quantitatifs. Dans un second temps, la substitution du cyclohexane employé comme solvant par de l'eau a été menée avec succès et rend ainsi la réaction d'autant plus compatible avec les principes de la chimie verte. Pour des raisons d'encombrement stérique, seul le dimère de diester d'acide férulique ($DDeFA^{II}$) peut être converti en polyesters par la CALB au contact de diols. La présence de quatre fonctions ester sur le $DDeFA^{II}$ devrait mener à la synthèse de polymères réticulés. Cependant, grâce à la sélectivité de la CALB vis-à-vis des deux types de fonctions ester, ce dimère de diester d'acide férulique a été converti en polyesters linéaires porteurs de fonctions esters pendantes. Des polymères de M_n élevées (jusqu'à 28 200 $g.mol^{-1}$) ont été obtenus en 24 heures (contre 72 heures classiquement). Ces masses molaires sont comparables à celles obtenues dans le cas de la synthèse enzymatique des polyesters aliphatiques. Les polyesters ainsi formés présentent les T_g les plus élevées observées dans cette étude, dépassant même la température ambiante (jusqu'à 34°C). Enfin, grâce à la réversibilité de la cycloaddition [2+2], les polyesters ont pu être photo-dépolymérisés sous UV en oligomères. Les propriétés thermiques élevées ainsi que la photo-dépolymérisation aisée de ces polyesters en font des matériaux particulièrement innovants et prometteurs.

Comme dans le chapitre précédent, la sélectivité de la CALB est mise à profit dans le chapitre 5 pour la synthèse d'autres polyesters aromatiques biosourcés innovants. Grâce à une nouvelle voie de synthèse mise au point dans ce projet, l'acide caféique a été converti par le carbonate d'éthylène en un diol entièrement biosourcé. Ce diol présente une fonction ester α,β-insaturée pendante très peu réactive vis-à-vis de la CALB ce qui est en parfait accord avec les observations décrites au chapitre 1.1 et au chapitre 3. Grâce à la sélectivité de la CALB, ce diol peut donc être considéré comme un monomère difonctionnel et sa réactivité en polymérisation a été étudiée. Des polyesters de masse molaire équivalente à celle des polyesters aliphatiques correspondants ont là aussi été obtenus avec des M_n allant jusqu'à 19 000 $g.mol^{-1}$ en 24 h de réaction. Deux phénomènes concurrents peuvent cependant être remarqués. Premièrement, l'augmentation du ratio de diol caféique entraine une diminution de la masse molaire des polymères. Ce phénomène pourrait être engendré par une possible inhibition de l'enzyme

par ce monomère. Ensuite, pour des taux de diol caféique inférieurs à 10 %, une possible réactivité de l'ester pendant du diol pourrait entrainer une réticulation partielle du polymère et ainsi donner des polymères hyper-ramifiés. Ces polymères présentent alors des masses molaires et des polydispersités très élevées. Tous les polyesters obtenus sont cependant solubles dans les solvants organiques courants tels que le chloroforme ou le THF. L'ajout d'unités aromatiques dans la chaîne a permis une augmentation des propriétés thermiques du polymère. La T_g des matériaux (jusqu'à 12°C) ne dépasse cependant pas la température ambiante. Deux raisons peuvent expliquer ce phénomène : premièrement, la présence d'un groupe pendant diminue la T_g du polymère. Ensuite, les polymères avec le plus haut taux de monomère aromatique sont également ceux présentant la masse molaire la plus faible, abaissant leur T_g. Les matériaux obtenus ont cependant montré des propriétés intéressantes de photo-réticulation. En effet, l'irradiation des polyesters sous un rayonnement UV à une longueur d'onde de 350 nm entraine la cycloaddition des doubles liaisons pendantes issues du diol caféique. Les polyesters se retrouvent alors réticulés et ne sont en majeure partie plus solubles. Cette réticulation peut cependant être partiellement réversible par irradiation à une longueur d'onde plus faible. Ces polyesters synthétisés par catalyse enzymatique présentent donc des propriétés avancées de photo-réticulation réversible et pourraient être employés dans des procédés d'impression « 4D » ou pour du relargage ciblé de substances actives.

En résumé, les études présentées dans ce manuscrit mettent en avant la bonne réactivité de divers synthons aromatiques biosourcés vis-à-vis de la CALB. Cette importante réactivité peut être mise au profit de la synthèse de polyesters aromatiques afin de produire, de manière plus douce et plus sûre que par les méthodes classiques, des matériaux biosourcés présentant de hautes propriétés thermiques. La modification de molécules plateformes telles que l'acide férulique ou l'acide caféique s'est révélée être une stratégie pertinente pour l'obtention de polyesters aromatiques présentant des masses molaires équivalentes à celles de leurs homologues aliphatiques, mais avec des propriétés thermiques supérieures. De plus, l'importante sélectivité de la CALB permet la synthèse de polyesters à la structure atypique et présentant des propriétés particulières comme celle de photo-réticulation ou de photo-clivage des chaines. Ces propriétés en font des matériaux innovants et prometteurs qui pourraient justifier le coût actuellement encore supérieur de la catalyse enzymatique comparée à la catalyse organométallique.

L'ensemble des travaux de cette thèse a déjà donné lieu à la publication de deux articles dans les journaux *European Polymer Journal* et *Polymers*. Par ailleurs, trois articles seront prochainement soumis pour publication. Un article supplémentaire, publié dans *ChemSusChem*, a également été réalisé en collaboration avec la Dr Audrey Magnin et porte sur le recyclage, par polymérisation enzymatique, de monomères issus de la dégradation de polyuréthanes.

Perspectives à ce projet :

Ce travail de thèse constitue un premier pas vers l'élaboration de nouveaux matériaux polyesters biosourcés par une méthode de catalyse douce. Les résultats obtenus et décrits dans ce manuscrit ouvrent plusieurs perspectives quant à l'avenir de ces matériaux.

Dans un premier temps, il serait intéressant de caractériser les propriétés mécaniques des matériaux et notamment l'influence de la proportion et de la nature des unités aromatiques sur ces dernières. En effet, à titre d'exemple, le module d'Young d'un polyester est grandement affecté par son aromaticité. L'ajout de monomères aromatiques comme le FDCA, l'acide férulique ou l'acide caféique dans des structures polyesters aliphatiques devraient permettre une augmentation du module et plus globalement de la résistance mécanique de ces matériaux. Ceci permettrait ainsi d'élargir le domaine d'application des polyesters synthétisés par catalyse enzymatique. Les propriétés mécaniques des matériaux obtenus dans cette étude pourraient ainsi être comparées à celles des matériaux polymères employés aujourd'hui afin de cibler leurs domaines d'applications potentielles. Ainsi, viser un domaine d'application spécifique tel que l'emballage ou le textile permettrait de dresser un cahier des charges précis des propriétés attendues et vers lequel orienter les efforts de recherche.

Il serait également pertinent d'investiguer les propriétés de biodégradabilité des matériaux synthétisés et présentés dans ce manuscrit. En effet, il est important de considérer le bilan environnemental des matériaux dans l'ensemble de leur cycle de vie, « du berceau à la tombe ». De plus, les comonomères employés comme l'acide adipique ou le 1,6-hexanediol sont connus pour faciliter la biodégradabilité des matériaux polyesters. De bonnes propriétés de biodégradabilité inscriraient d'autant plus ces matériaux dans une logique d'économie circulaire et environnementale. D'autre part, les propriétés de biodégradabilité et de compostabilité des polyesters sont recherchées pour certains types d'applications et pourraient constituer des arguments supplémentaires pour la compétitivité des matériaux synthétisés.

Un paramètre crucial qui reste cependant à prendre en compte est la capacité de montée en échelle des procédés de synthèse de ces polyesters. En effet, l'ensemble des études de cette thèse s'est limité à des synthèses à l'échelle du gramme. Une étude de la littérature montre cependant la viabilité de la catalyse enzymatique pour la synthèse de polyesters à l'échelle de la tonne. Les nombreux procédés de synthèse de polyesters aromatique décrits dans ce manuscrit ainsi que dans la littérature forment déjà une base solide pour étudier leur montée en échelle. Parallèlement à ces travaux, une étude de la montée en échelle des méthodes d'extraction ou de production des monomères aromatiques biosourcés pourrait être menée. À titre d'exemple, de nombreuses études s'intéressent à la viabilité de la production de FDCA ou de l'extraction de l'acide férulique.

L'étude des enzymes employées pour la synthèse de polyesters aromatiques semble également une perspective intéressante et nécessaire à ce projet. En effet, les mécanismes régissant l'activité de

l'enzyme au contact de monomères aromatique ne sont pas entièrement compris et pourraient être éclairés, par exemple, au moyen de travaux de modélisation. Il serait ainsi possible d'étudier en détail la configuration des monomères dans le site actif de l'enzyme et éventuellement d'optimiser *in silico* leur structure pour optimiser l'activité enzymatique. L'investigation de nouvelles sources de d'enzymes pourrait également permettre de pousser plus loin la masse molaire des polyesters obtenus. Comme indiqué dans le chapitre 1, une grande variété d'enzymes capable de catalyser la synthèse de polyesters a été identifiée. À titre d'exemple, les cutinases attirent aujourd'hui beaucoup d'attention de par leur intéressante activité catalytique. Les lipases de *Rhizomucor miehei* ou de *Thermomyces lanuginosus* pourraient également être des enzymes de choix. L'ingénierie de protéines « sur mesure » par des méthodes telles que l'évolution dirigée pourrait également être appliquée à la synthèse enzymatique de polyesters afin d'améliorer les rendements et la résistance des enzymes. Enfin, le développement de méthodes d'immobilisation de l'enzyme est également une voie d'amélioration des rendements de réaction et pourrait également faciliter l'emploi des biocatalyseurs, favorisant la production à large échelle de ces polyesters.

Enfin, le champ d'application des stratégies de synthèses mises en place dans cette thèse pourrait être développé plus en détails. C'est le cas notamment de la synthèse de matériaux biosourcés UV-sensibles synthétisés grâce à la bonne réactivité en cycloaddition [2+2] des dérivés d'acide cinnamiques et à la sélectivité de la CALB. Au-delà de l'intérêt évident pour leur recyclage efficace, les matériaux pouvant être dépolymérisés à la demande, comme exposé au chapitre 4, ou pouvant être réticulés de manière réversible, comme démontré au chapitre 5, pourraient servir au relargage contrôlé de substances actives dans le domaine biomédical. Une étude de la biocompatibilité de ces matériaux serait alors nécessaire. De tels matériaux pourraient également être employés dans le domaine de l'impression 3D et 4D. En effet, les propriétés de photo-dépolymérisation ou de photo-réticulation alliées à la synthèse en conditions douces et à la nature majoritairement biosourcée de ces polyesters sont des atouts majeurs pour l'élaboration de structures complexes en impression 3D/4D par fusion de filament.

Liste complète des références bibliographiques

Abdelgawad, A., Eid, M., Abou-Elmagd, W. and Abou-Elregal, M. (**2021**) 'Lipase catalysed transesterification of palm stearin with ferulic acid in solvent-free media', *Biocatalysis and Biotransformation*, pp. 1–8.

Abdel-Rahman, M. A., Tashiro, Y. and Sonomoto, K. (**2013**) 'Recent advances in lactic acid production by microbial fermentation processes', *Biotechnology Advances*, 31(6), pp. 877–902.

Aharwar, A. and Parihar, D. K. (**2018**) 'Tannases: Production, properties, applications', *Biocatalysis and Agricultural Biotechnology*, 15, pp. 322–334.

Aithal, M. and Belur, P. D. (**2013**)**a** 'Enhancement of propyl gallate yield in nonaqueous medium using novel cell-associated tannase of *Bacillus massiliensis*', *Preparative Biochemistry and Biotechnology*, 43(5), pp. 445–455.

Aithal, M. and Belur, P. D. (**2013**)**b** 'Production of propyl gallate in nonaqueous medium using cell-associated tannase of *Bacillus massiliensis* : Effect of various parameters and statistical optimization: Production of Propyl Gallate in Nonaqueous Medium', *Biotechnology and Applied Biochemistry*, 60(2), pp. 210–218.

Akutsu, F., Inoki, M., Takahashi, K., Yonemura, T., Kasashima, Y. and Naruchi, K. (**1996**) 'Synthesis and Properties of Polyarylates Derived from 4,4″-Dihydroxy-o-terphenyl', *Polymer Journal*, 28(12), pp. 1107–1109.

Albanese, M., Boyenval, J., Marchese, P., Sullalti, S. and Celli, A. (**2016**) 'The aliphatic counterpart of PET, PPT and PBT aromatic polyesters: effect of the molecular structure on thermo-mechanical properties', *AIMS Molecular Science*, 3(1), pp. 32–51.

Ali, M. A. and Kaneko, T. (**2019**) 'Syntheses of Aromatic/Heterocyclic Derived Bioplastics with High Thermal/Mechanical Performance', *Industrial & Engineering Chemistry Research*, 58(35), pp. 15958–15974.

Allais, F., Martinet, S. and Ducrot, P.-H. (**2009**) 'Straightforward Total Synthesis of 2-O-Feruloyl-l-malate, 2-O-Sinapoyl-l-malate and 2-O-5-Hydroxyferuloyl-l-malate', *Synthesis*, 2009(21), pp. 3571–3578.

Amini, Z., Ilham, Z., Ong, H. C., Mazaheri, H. and Chen, W.-H. (**2017**) 'State of the art and prospective of lipase-catalyzed transesterification reaction for biodiesel production', *Energy Conversion and Management*, 141, pp. 339–353.

Amjaour, H., Wang, Z., Mabin, M., Puttkammer, J., Busch, S. and Chu, Q. R. (**2019**) 'Scalable preparation and property investigation of a *cis* -cyclobutane-1,2-dicarboxylic acid from β- *trans* -cinnamic acid', *Chemical Communications*, 55(2), pp. 214–217.

Anastas, P. and Eghbali, N. (**2010**) 'Green Chemistry: Principles and Practice', *Chem. Soc. Rev.*, 39(1), pp. 301–312.

Antonopoulou, I., Iancu, L., Jütten, P., Piechot, A., Rova, U. and Christakopoulos, P. (**2019**) 'Screening of novel feruloyl esterases from Talaromyces wortmannii for the development of efficient and sustainable syntheses of feruloyl derivatives', *Enzyme and Microbial Technology*, 120, pp. 124–135.

Antonopoulou, I., Leonov, L., Jütten, P., Cerullo, G., Faraco, V., Papadopoulou, A., Kletsas, D., Ralli, M., Rova, U. and Christakopoulos, P. (**2017**) 'Optimized synthesis of novel prenyl ferulate performed by feruloyl esterases from Myceliophthora thermophila in microemulsions', *Applied Microbiology and Biotechnology*, 101(8), pp. 3213–3226.

Antonopoulou, I., Papadopoulou, A., Iancu, L., Cerullo, G., Ralli, M., Jütten, P., Piechot, A., Faraco, V., Kletsas, D., Rova, U. and Christakopoulos, P. (**2018**) 'Optimization of enzymatic synthesis of l-arabinose ferulate catalyzed by feruloyl esterases from Myceliophthora thermophila in detergentless microemulsions and assessment of its antioxidant and cytotoxicity activities', *Process Biochemistry*, 65, pp. 100–108.

Antonopoulou, I., Varriale, S., Topakas, E., Rova, U., Christakopoulos, P. and Faraco, V. (**2016**) 'Enzymatic synthesis of bioactive compounds with high potential for cosmeceutical application', *Applied Microbiology and Biotechnology*, 100(15), pp. 6519–6543.

Aparaschivei, D., Todea, A., Frissen, A. E., Badea, V., Rusu, G., Sisu, E., Puiu, M., Boeriu, C. G. and Peter, F. (**2019**) 'Enzymatic synthesis and characterization of novel terpolymers from renewable sources', *Pure and Applied Chemistry*, 91(3), pp. 397–408.

de Araújo, M., Franco, Y., Messias, M., Longato, G., Pamphile, J. and Carvalho, P. (**2016**) 'Biocatalytic Synthesis of Flavonoid Esters by Lipases and Their Biological Benefits', *Planta Medica*, 83(01/02), pp. 7–22.

Arrakhiz, F. Z., Elachaby, M., Bouhfid, R., Vaudreuil, S., Essassi, M. and Qaiss, A. (**2012**) 'Mechanical and thermal properties of polypropylene reinforced with Alfa fiber under different chemical treatment', *Materials & Design*, 35, pp. 318–322.

Aytekin, A. O., Morimura, S. and Kida, K. (**2011**) 'Synthesis of chitosan–caffeic acid derivatives and evaluation of their antioxidant activities', *Journal of Bioscience and Bioengineering*, 111(2), pp. 212–216.

Azim, H., Dekhterman, A., Jiang, Z. and Gross, R. A. (**2006**) '*Candida antarctica* Lipase B-Catalyzed Synthesis of Poly(butylene succinate): Shorter Chain Building Blocks Also Work', *Biomacromolecules*, 7(11), pp. 3093–3097.

B. Guyot, B. Bosquette, M. Pina, and J. Graille (**1997**) 'Esterification of phenolic acids from green coffee with an immobilized lipase from Candida antarctica in solvent-free medium', *Biotechnology Letters*, 19(6), p. 4.

B. Guyot, D.Gueule, M. Pina, J. Graille, V.Farines, and M.Farines (**2000**) 'Enzymatic synthesis of fatty esters in 5-caffeoyl quinic acid', *Eur. J. Lipid Sci. Technol.*, p. 4.

Barbara, I., Flourat, A. L. and Allais, F. (**2015**) 'Renewable polymers derived from ferulic acid and biobased diols via ADMET', *European Polymer Journal*, 62, pp. 236–243.

Bazin, A., Avérous, L. and Pollet, E. (**2021**)**a** 'Ferulic Acid as Building Block for the Lipase-Catalyzed Synthesis of Biobased Aromatic Polyesters', *Polymers*, 13(21), p. 3693.

Bazin, A., Avérous, L. and Pollet, E. (**2021**)**b** 'Lipase-catalyzed synthesis of furan-based aliphatic-aromatic biobased copolyesters: Impact of the solvent', *European Polymer Journal*, 159, p. 110717.

Becker, J., Lange, A., Fabarius, J. and Wittmann, C. (**2015**) 'Top value platform chemicals: bio-based production of organic acids', *Current Opinion in Biotechnology*, 36, pp. 168–175.

Bedoui, F., Diani, J., Regnier, G. and Seiler, W. (**2006**) 'Micromechanical modeling of isotropic elastic behavior of semicrystalline polymers', *Acta Materialia*, 54(6), pp. 1513–1523.

Bento-Silva, A., Vaz Patto, M. C. and do Rosário Bronze, M. (**2018**) 'Relevance, structure and analysis of ferulic acid in maize cell walls', *Food Chemistry*, 246, pp. 360–378.

Binns, F., Harffey, P., Roberts, S. M. and Taylor, A. (**1999**) 'Studies leading to the large scale synthesis of polyesters using enzymes', *Journal of the Chemical Society, Perkin Transactions 1*, (19), pp. 2671–2676.

Bioplastics market data (**2020**) *European bioplastics*. Available at: https://www.european-bioplastics.org/market/ (Accessed: 2 September 2021).

Bouaziz, A., Horchani, H., Salem, N. B., Chaari, A., Chaabouni, M., Gargouri, Y. and Sayari, A. (**2010**) 'Enzymatic propyl gallate synthesis in solvent-free system: Optimization by response surface methodology', *Journal of Molecular Catalysis B: Enzymatic*, 67(3–4), pp. 242–250.

Bozell, J. J. and Petersen, G. R. (**2010**) 'Technology development for the production of biobased products from biorefinery carbohydrates—the US Department of Energy's "Top 10" revisited', *Green Chemistry*, 12(4), p. 539.

Brito e Cunha, D. A., Bartkevihi, L., Robert, J. M., Cipolatti, E. P., Ferreira, A. T. S., Oliveira, D. M. P., Gomes-Neto, F., Almeida, R. V., Fernandez-Lafuente, R., Freire, D. M. G. and Anobom, C. D. (**2019**) 'Structural differences of commercial and recombinant lipase B from Candida antarctica: An important implication on enzymes thermostability', *International Journal of Biological Macromolecules*, 140, pp. 761–770.

Bubalo, M. C., Radošević, K., Redovniković, I. R., Slivac, I. and Srček, V. G. (**2017**) 'Toxicity mechanisms of ionic liquids', *Archives of Industrial Hygiene and Toxicology*, 68(3), pp. 171–179.

Buchholz, T. and Melzig, M. (**2015**) 'Polyphenolic Compounds as Pancreatic Lipase Inhibitors', *Planta Medica*, 81(10), pp. 771–783.

Buisman, G. J. H. and Cuperus, F. P. (**1998**) 'Enzymatic esterifications of functionalized phenols for the synthesis of lipophilic antioxidants', *Biotechnology Letters*, 20(2), p. 6.

Buzatu, A. R., Frissen, A. E., van den Broek, L. A. M., Todea, A., Motoc, M. and Boeriu, C. G. (**2020**) 'Chemoenzymatic Synthesis of New Aromatic Esters of Mono- and Oligosaccharides', *Processes*, 8(12), p. 1638.

Cai, Y., Luo, Q., Sun, M. and Corke, H. (**2004**) 'Antioxidant activity and phenolic compounds of 112 traditional Chinese medicinal plants associated with anticancer', *Life Sciences*, 74(17), pp. 2157–2184.

Cao, L., Chen, R., Xie, W. and Liu, Y. (**2015**) 'Enhancing the Thermostability of Feruloyl Esterase EstF27 by Directed Evolution and the Underlying Structural Basis', *Journal of Agricultural and Food Chemistry*, 63(37), pp. 8225–8233.

Carniel, A., Valoni, É., Nicomedes, J., Gomes, A. da C. and Castro, A. M. de (**2017**) 'Lipase from Candida antarctica (CALB) and cutinase from Humicola insolens act synergistically for PET hydrolysis to terephthalic acid', *Process Biochemistry*, 59, pp. 84–90.

Cassani, J., Luna, H., Navarro, A. and Castillo, E. (**2007**) 'Comparative esterification of phenylpropanoids versus hydrophenylpropanoids acids catalyzed by lipase in organic solvent media', *Electronic Journal of Biotechnology*, 10(4), pp. 508–513.

Castillo, E. A., Miura, H., Hasegawa, M. and Ogawa, T. (**2004**) 'Synthesis of novel polyamides starting from ferulic acid dimer derivative', *Designed Monomers and Polymers*, 7(6), pp. 711–725.

Cerullo, G., Varriale, S., Bozonnet, S., Antonopoulou, I., Christakopoulos, P., Rova, U., Gherbovet, O., Fauré, R., Piechot, A., Jütten, P., Brás, J. L. A., Fontes, C. M. G. A. and Faraco, V. (**2019**) 'Directed evolution of the type C feruloyl esterase from Fusarium oxysporum FoFaeC and molecular docking analysis of its improved variants', *New Biotechnology*, 51, pp. 14–20.

Chae, Y. and An, Y.-J. (**2018**) 'Current research trends on plastic pollution and ecological impacts on the soil ecosystem: A review', *Environmental Pollution*, 240, pp. 387–395.

Chandel, C., Kumar, A. and Kanwar, S. S. (**2011**) 'Enzymatic Synthesis of Butyl Ferulate by Silica-Immobilized Lipase in a Non-Aqueous Medium', *Journal of Biomaterials and Nanobiotechnology*, 02(04), pp. 400–408.

Chapman, J., Ismail, A. and Dinu, C. (**2018**) 'Industrial Applications of Enzymes: Recent Advances, Techniques, and Outlooks', *Catalysts*, 8(6), p. 238.

Chávez-González, M., Rodríguez-Durán, L. V., Balagurusamy, N., Prado-Barragán, A., Rodríguez, R., Contreras, J. C. and Aguilar, C. N. (**2012**) 'Biotechnological Advances and Challenges of Tannase: An Overview', *Food and Bioprocess Technology*, 5(2), pp. 445–459.

Chebil, L., Humeau, C., Falcimaigne, A., Engasser, J.-M. and Ghoul, M. (**2006**) 'Enzymatic acylation of flavonoids', *Process Biochemistry*, 41(11), pp. 2237–2251.

Chen, G.-Q. (ed.) (**2010**) *Plastics from Bacteria*. Berlin, Heidelberg: Springer (Microbiology Monographs).

Chen, G.-Q. and Jiang, X.-R. (**2017**) 'Engineering bacteria for enhanced polyhydroxyalkanoates (PHA) biosynthesis', *Synthetic and Systems Biotechnology*, 2(3), pp. 192–197.

Chi, Y.-M., Nakamura, M., Yoshizawa, T., Zhao, X.-Y., Yan, W.-M., Hashimoto, F., Kinjo, J., Nohara, T. and Sakurada, S. (**2005**) 'Anti-inflammatory Activities of α-Truxillic Acid Derivatives and Their Monomer Components', 28(9), pp. 1776–1778.

Chrissafis, K., Paraskevopoulos, K. M. and Bikiaris, D. N. (**2006**) 'Effect of molecular weight on thermal degradation mechanism of the biodegradable polyester poly(ethylene succinate)', *Thermochimica Acta*, 440(2), pp. 166–175.

Christelle, B., Eduardo, B. D. O., Latifa, C., Elaine-Rose, M., Bernard, M., Evelyne, R.-H., Mohamed, G., Jean-Marc, E. and Catherine, H. (**2011**) 'Combined docking and molecular dynamics simulations to enlighten the capacity of Pseudomonas cepacia and Candida antarctica lipases to catalyze quercetin acetylation', *Journal of Biotechnology*, 156(3), pp. 203–210.

Chulalaksananukul, W., Condoret, J. S., Delorme, P. and Willemot, R. M. (**1990**) 'Kinetic study of esterification by immobilized lipase in *n* -hexane', *FEBS Letters*, 276(1–2), pp. 181–184.

Chyba, A., Mastihuba, V. and Mastihubová, M. (**2016**) 'Effective enzymatic caffeoylation of natural glucopyranosides', *Bioorganic & Medicinal Chemistry Letters*, 26(6), pp. 1567–1570.

Ciftci, D. and Saldaña, M. D. A. (**2012**) 'Enzymatic synthesis of phenolic lipids using flaxseed oil and ferulic acid in supercritical carbon dioxide media', *The Journal of Supercritical Fluids*, 72, pp. 255–262.

Clifford, M. N. (**2000**) 'Chlorogenic acids and other cinnamates – nature, occurrence, dietary burden, absorption and metabolism', *J Sci Food Agric*, 80, pp. 1033–1043.

Coca-Cola Expands Access to PlantBottle IP , *The Coca-Cola Company*. Available at: http://www.coca-colacompany.com/news/coca-cola-expands-access-to-plantbottle-ip (Accessed: 14 September 2021).

Cohen, M. D. and Schmidt, G. M. J. (**1964**) '383. Topochemistry. Part I. A survey', *Journal of the Chemical Society (Resumed)*, p. 1996.

Comerford, J. W., Byrne, F. P., Weinberger, S., Farmer, T. J., Guebitz, G. M., Gardossi, L. and Pellis, A. (**2020**) 'Thermal Upgrade of Enzymatically Synthesized Aliphatic and Aromatic Oligoesters', *Materials*, 13(2), p. 368.

Compton, D. L. and King, J. W. (**2001**) 'Lipase-catalyzed synthesis of triolein-based sunscreens in supercritical CO_2', *Journal of the American Oil Chemists' Society*, 78(1), pp. 43–47.

Compton, D. L. and Laszlo, J. A. (**2009**) '1,3-Diferuloyl-sn-glycerol from the biocatalytic transesterification of ethyl 4-hydroxy-3-methoxy cinnamic acid (ethyl ferulate) and soybean oil', *Biotechnology Letters*, 31(6), pp. 889–896.

Compton, D. L., Laszlo, J. A. and Berhow, M. A. (**2000**) 'Lipase-catalyzed synthesis of ferulate esters', *Journal of the American Oil Chemists' Society*, 77(5), pp. 513–519.

Compton, D. L., Laszlo, J. A. and Evans, K. O. (**2012**) 'Antioxidant properties of feruloyl glycerol derivatives', *Industrial Crops and Products*, 36(1), pp. 217–221.

Cornard, J. P. and Lapouge, C. (**2004**) 'Theoretical and Spectroscopic Investigations of a Complex of Al(III) with Caffeic Acid', *The Journal of Physical Chemistry A*, 108(20), pp. 4470–4478.

Crepin, V. F., Faulds, C. B. and Connerton, I. F. (**2004**) 'Functional classification of the microbial feruloyl esterases', *Applied Microbiology and Biotechnology*, 63(6), pp. 647–652.

Crozier, A., Jaganath, I. B. and Clifford, M. N. (**2006**) 'Phenols, Polyphenols and Tannins: An Overview', in Crozier, A., Clifford, M. N., and Ashihara, H. (eds) *Plant Secondary Metabolites*. Oxford, UK: Blackwell Publishing Ltd, pp. 1–24.

Cruz-Izquierdo, Á., van den Broek, L. A. M., Serra, J. L., Llama, M. J. and Boeriu, C. G. (**2015**) 'Lipase-catalyzed synthesis of oligoesters of 2,5-furandicarboxylic acid with aliphatic diols', *Pure and Applied Chemistry*, 87(1), pp. 59–69.

Curme, H. G., Natale, C. C. and Kelley, D. J. (**1967**) 'Photosensitized reactions of cinnamate esters', *The Journal of Physical Chemistry*, 71(3), pp. 767–770.

Cyclohexane (**2021**) *ECHA*. Available at: https://echa.europa.eu/substance-information/-/substanceinfo/100.003.461 (Accessed: 17 August 2021).

Dandekar, P. and Wasewar, K. L. (**2020**) 'Experimental investigation on extractive separation of vanillic acid', *Chemical Data Collections*, 30, p. 100564.

Debuissy, T., Pollet, E. and Avérous, L. (**2016**) 'Enzymatic Synthesis of a Bio-Based Copolyester from Poly(butylene succinate) and Poly((*R*)-3-hydroxybutyrate): Study of Reaction Parameters on the Transesterification Rate', *Biomacromolecules*, 17(12), pp. 4054–4063.

Debuissy, T., Pollet, E. and Avérous, L. (**2017**)**a** 'Enzymatic synthesis of biobased poly(1,4-butylene succinate- ran -2,3-butylene succinate) copolyesters and characterization. Influence of 1,4- and 2,3-butanediol contents', *European Polymer Journal*, 93, pp. 103–115.

Debuissy, T., Pollet, E. and Avérous, L. (**2017**)**b** 'Lipase-catalyzed synthesis of biobased and biodegradable aliphatic copolyesters from short building blocks. Effect of the monomer length', *European Polymer Journal*, 97, pp. 328–337.

Debuissy, T., Pollet, E. and Avérous, L. (**2017**)**c** 'Synthesis and characterization of biobased poly(butylene succinate- ran -butylene adipate). Analysis of the composition-dependent physicochemical properties', *European Polymer Journal*, 87, pp. 84–98.

Debuissy, T., Sangwan, P., Pollet, E. and Avérous, L. (**2017**)**d** 'Study on the structure-properties relationship of biodegradable and biobased aliphatic copolyesters based on 1,3-propanediol, 1,4-butanediol, succinic and adipic acids', *Polymer*, 122, pp. 105–116.

Delidovich, I., Hausoul, P. J. C., Deng, L., Pfützenreuter, R., Rose, M. and Palkovits, R. (**2016**) 'Alternative Monomers Based on Lignocellulose and Their Use for Polymer Production', *Chemical Reviews*, 116(3), pp. 1540–1599.

Dembitsky, V. M. (**2007**) 'Bioactive cyclobutane-containing alkaloids', *Journal of Natural Medicines*, 62(1), pp. 1–33.

Dettori, L., Jelsch, C., Guiavarc'h, Y., Delaunay, S., Framboisier, X., Chevalot, I. and Humeau, C. (**2018**) 'Molecular rules for selectivity in lipase-catalysed acylation of lysine', *Process Biochemistry*, 74, pp. 50–60.

Devi Salam, M., Varma, A., Prashar, R. and Choudhary, D. (**2021**) 'Review on Efficacy of Microbial Degradation of Polyethylene Terephthalate and Bio-upcycling as a Part of Plastic Waste Management', *Applied Ecology and Environmental Sciences*, 9(7), pp. 695–703.

Diantimony trioxide (**2021**) *European Chemical Agency*. Available at: https://echa.europa.eu/substance-information/-/substanceinfo/100.013.796 (Accessed: 10 August 2021).

Dibutyltin oxide (**2021**) *European Chemical Agency*. Available at: https://echa.europa.eu/substance-information/-/substanceinfo/100.011.317 (Accessed: 12 August 2021).

Dickson, J. T. and Whinfield, J. R. (**1946**) 'Improvements relating to the manufacture of highly polymeric substances', GB578079A.

Dilokpimol, A., Mäkelä, M. R., Aguilar-Pontes, M. V., Benoit-Gelber, I., Hildén, K. S. and de Vries, R. P. (**2016**) 'Diversity of fungal feruloyl esterases: updated phylogenetic classification, properties, and industrial applications', *Biotechnology for Biofuels*, 9(1), p. 231.

Ding, L., Liu, L., Chen, Y., Du, Y., Guan, S., Bai, Y. and Huang, Y. (**2019**) 'Modification of poly(ethylene terephthalate) by copolymerization of plant-derived α-truxillic acid with excellent ultraviolet shielding and mechanical properties', *Chemical Engineering Journal*, 374, pp. 1317–1325.

Dong, H., Cao, S.-G., Li, Z.-Q., Han, S.-P., You, D.-L. and Shen, J.-C. (**1999**) 'Study on the enzymatic polymerization mechanism of lactone and the strategy for improving the degree of polymerization', *Journal of Polymer Science Part A: Polymer Chemistry*, 37(9), pp. 1265–1275.

Dong, W., Li, H., Chen, M., Ni, Z., Zhao, J., Yang, H. and Gijsman, P. (**2011**) 'Biodegradable bio-based polyesters with controllable photo-crosslinkability, thermal and hydrolytic stability', *Journal of Polymer Research*, 18(6), pp. 1239–1247.

Dong, W., Ren, J., Lin, L., Shi, D., Ni, Z. and Chen, M. (**2012**) 'Novel photocrosslinkable and biodegradable polyester from bio-renewable resource', *Polymer Degradation and Stability*, 97(4), pp. 578–583.

Douka, A., Vouyiouka, S., Papaspyridi, L.-M. and Papaspyrides, C. D. (**2018**) 'A review on enzymatic polymerization to produce polycondensation polymers: The case of aliphatic polyesters, polyamides and polyesteramides', *Progress in Polymer Science*, 79, pp. 1–25.

Duchiron, S. W., Pollet, E., Givry, S. and Avérous, L. (**2015**) 'Mixed systems to assist enzymatic ring opening polymerization of lactide stereoisomers', *RSC Advances*, 5(103), pp. 84627–84635.

Duchiron, S. W., Pollet, E., Givry, S. and Avérous, L. (**2017**) 'Enzymatic synthesis of poly(ε-caprolactone- co -ε-thiocaprolactone)', *European Polymer Journal*, 87, pp. 147–158.

Durand, E., Lecomte, J., Baréa, B., Dubreucq, E., Lortie, R. and Villeneuve, P. (**2013**)**a** 'Evaluation of deep eutectic solvent–water binary mixtures for lipase-catalyzed lipophilization of phenolic acids', *Green Chemistry*, 15(8), p. 2275.

Durand, E., Lecomte, J., Baréa, B., Piombo, G., Dubreucq, É. and Villeneuve, P. (**2012**) 'Evaluation of deep eutectic solvents as new media for Candida antarctica B lipase catalyzed reactions', *Process Biochemistry*, 47(12), pp. 2081–2089.

Durand, E., Lecomte, J., Baréa, B. and Villeneuve, P. (**2014**) 'Towards a better understanding of how to improve lipase-catalyzed reactions using deep eutectic solvents based on choline chloride: Towards a better understanding of how to improve lipase-catalyzed …', *European Journal of Lipid Science and Technology*, 116(1), pp. 16–23.

Durand, E., Lecomte, J. and Villeneuve, P. (**2013**)**b** 'Deep eutectic solvents: Synthesis, application, and focus on lipase-catalyzed reactions', *European Journal of Lipid Science and Technology*, 115(4), pp. 379–385.

Durand, E., Lecomte, J. and Villeneuve, P. (**2015**) 'Are emerging deep eutectic solvents (DES) relevant for lipase-catalyzed lipophilizations?', *OCL*, 22(4), p. D408.

Duval, A. and Avérous, L. (**2016**) 'Oxyalkylation of Condensed Tannin with Propylene Carbonate as an Alternative to Propylene Oxide', *ACS Sustainable Chemistry & Engineering*, 4(6), pp. 3103–3112.

Duval, A. and Avérous, L. (**2017**) 'Cyclic Carbonates as Safe and Versatile Etherifying Reagents for the Functionalization of Lignins and Tannins', *ACS Sustainable Chemistry & Engineering*, 5(8), pp. 7334–7343.

Duval, A., Layrac, G., Zomeren, A., Smit, A. T., Pollet, E. and Avérous, L. (**2021**) 'Isolation of Low Dispersity Fractions of Acetone Organosolv Lignins to Understand their Reactivity: Towards Aromatic Building Blocks for Polymers Synthesis', *ChemSusChem*, 14(1), pp. 387–397.

EFSA (**2014**) 'Scientific Opinion on the re-evaluation of propyl gallate (E 310) as a food additive', *EFSA Journal*, 12(4), p. 3642.

EFSA (**2015**) 'Scientific Opinion on the re-evaluation of octyl gallate (E 311) as a food additive: Re-evaluation of octyl gallate (E 311) as a food additive', *EFSA Journal*, 13(10), p. 4248.

Elgharbawy, A. A. M., Moniruzzaman, M. and Goto, M. (**2020**) 'Recent advances of enzymatic reactions in ionic liquids: Part II', *Biochemical Engineering Journal*, 154, p. 107426.

Elgharbawy, A. A. M., Moniruzzaman, M. and Goto, M. (**2021**) 'Facilitating enzymatic reactions by using ionic liquids: A mini review', *Current Opinion in Green and Sustainable Chemistry*, 27, p. 100406.

Elgharbawy, A. A., Riyadi, F. A., Alam, Md. Z. and Moniruzzaman, M. (**2018**) 'Ionic liquids as a potential solvent for lipase-catalysed reactions: A review', *Journal of Molecular Liquids*, 251, pp. 150–166.

Elias, H.-G. and Palacios, J. A. (**1985**) 'Poly(ferulic acid) by Thionyl Chloride Activated Polycondensation', *Die Makromolekulare Chemie*, 186(5), pp. 1027–1045.

Engel, J., Cordellier, A., Huang, L. and Kara, S. (**2019**) 'Enzymatic Ring Opening Polymerization of Lactones: Traditional Approaches and Alternative Strategies', *ChemCatChem*, 11(20), pp. 4983–4997.

Fache, M., Boutevin, B. and Caillol, S. (**2015**) 'Vanillin, a key-intermediate of biobased polymers', *European Polymer Journal*, 68, pp. 488–502.

Faulds, C. B. and Williamson, G. , 'The purification and characterization of 4-hydroxy-3-methoxycinnamic (ferulic) acid esterase from Streptomyces olitrochromogenes', p. 7.

Feder, D. and Gross, R. A. (**2010**) 'Exploring Chain Length Selectivity in HIC-Catalyzed Polycondensation Reactions', *Biomacromolecules*, 11(3), pp. 690–697.

Feldman, D. (**2008**) 'Polymer History', *Designed Monomers and Polymers*, 11(1), pp. 1–15.

Ferri, M., Happel, A., Zanaroli, G., Bertolini, M., Chiesa, S., Commisso, M., Guzzo, F. and Tassoni, A. (**2020**) 'Advances in combined enzymatic extraction of ferulic acid from wheat bran', *New Biotechnology*, 56, pp. 38–45.

Figueroa-Espinoza, M. C., Laguerre, M., Villeneuve, P. and Lecomte, J. (**2013**) 'From phenolics to phenolipids: Optimizing antioxidants in lipid dispersions', *Lipid Technology*, 25(6), pp. 131–134.

Figueroa-Espinoza, M.-C. and Villeneuve, P. (**2005**) 'Phenolic Acids Enzymatic Lipophilization', *Journal of Agricultural and Food Chemistry*, 53(8), pp. 2779–2787.

Flores, I., Martínez de Ilarduya, A., Sardon, H., Müller, A. J. and Muñoz-Guerra, S. (**2019**) 'Synthesis of Aromatic–Aliphatic Polyesters by Enzymatic Ring Opening Polymerization of Cyclic Oligoesters and their Cyclodepolymerization for a Circular Economy', *ACS Applied Polymer Materials*, 1(3), pp. 321–325.

Flory, P. J. (**1952**) 'Molecular Size Distribution in Three Dimensional Polymers. VI. Branched Polymers Containing A-R-B Type Units', 74, pp. 2718–2723.

Flourat, A. L., Combes, J., Bailly-Maitre-Grand, C., Magnien, K., Haudrechy, A., Renault, J. and Allais, F. (**2021**) 'Accessing *p*-Hydroxycinnamic Acids: Chemical Synthesis, Biomass Recovery, or Engineered Microbial Production?', *ChemSusChem*, 14(1), pp. 118–129.

Fodor, C., Golkaram, M., Woortman, A. J. J., van Dijken, J. and Loos, K. (**2017**) 'Enzymatic approach for the synthesis of biobased aromatic–aliphatic oligo-/polyesters', *Polymer Chemistry*, 8(44), pp. 6795–6805.

Fonseca, A. C., Lima, M. S., Sousa, A. F., Silvestre, A. J., Coelho, J. F. J. and Serra, A. C. (**2019**) 'Cinnamic acid derivatives as promising building blocks for advanced polymers: synthesis, properties and applications', *Polymer Chemistry*, 10(14), pp. 1696–1723.

Ford, C. W. and Hartley, R. D. (**1989**) 'GC/MS characterisation of cyclodimers fromp-coumaric and ferulic acids by photodimerisation—a possible factor influencing cell wall biodegradability', *Journal of the Science of Food and Agriculture*, 46(3), pp. 301–310.

Fox, T. G. and Flory, P. J. (**1950**) 'Second-Order Transition Temperatures and Related Properties of Polystyrene. I. Influence of Molecular Weight', *Journal of Applied Physics*, 21(6), pp. 581–591.

Frampton, M. B. and Zelisko, P. M. (**2013**) 'Synthesis of lipase-catalysed silicone-polyesters and silicone-polyamides at elevated temperatures', *Chemical Communications*, 49(81), p. 9269.

Gaathon, A., Gross, Z. and Rozhanski, M. (**1989**) 'Propyl gailate: enzymatic synthesis in a reverse micelle system', *Enzyme and Microbial Technology*, 11, p. 6.

Gamboni, S. E., Palmer, A. M. and Nixon, R. L. (**2013**) 'Allergic contact stomatitis to dodecyl gallate? A review of the relevance of positive patch test results to gallates: Allergic contact stomatitis to gallates', *Australasian Journal of Dermatology*, 54(3), pp. 213–217.

Gandini, A., Silvestre, A. J. D., Neto, C. P., Sousa, A. F. and Gomes, M. (**2009**) 'The furan counterpart of poly(ethylene terephthalate): An alternative material based on renewable resources', *Journal of Polymer Science Part A: Polymer Chemistry*, 47(1), pp. 295–298.

Genaro-Mattos, T. C., Maurício, Â. Q., Rettori, D., Alonso, A. and Hermes-Lima, M. (**2015**) 'Antioxidant Activity of Caffeic Acid against Iron-Induced Free Radical Generation—A Chemical Approach', *PLOS ONE*. Edited by G. P. Tochtrop, 10(6), p. e0129963.

Gherbovet, O., Ferreira, F., Clément, A., Ragon, M., Durand, J., Bozonnet, S., O'Donohue, M. J. and Fauré, R. (**2020**) *Regioselective chemo-enzymatic syntheses of ferulate conjugates as chromogenic substrates for feruloyl esterases*. preprint. organic chemistry. Available at: https://www.beilstein-archives.org/xiv/preprints/2020107 (Accessed: 23 August 2021).

Gioia, C., Banella, M. B., Marchese, P., Vannini, M., Colonna, M. and Celli, A. (**2016**) 'Advances in the synthesis of bio-based aromatic polyesters: novel copolymers derived from vanillic acid and ε-caprolactone', *Polymer Chemistry*, 7(34), pp. 5396–5406.

Gioia, C., Banella, M. B., Totaro, G., Vannini, M., Marchese, P., Colonna, M., Sisti, L. and Celli, A. (**2018**) 'Biobased Vanillic Acid and Ricinoleic Acid: Building Blocks for Fully Renewable Copolyesters', *Journal of Renewable Materials*, 6(1), pp. 126–135.

Giuliani, S., Piana, C., Setti, L., Hochkoeppler, A., Pifferi, P. G. and Williamson, G. (**2001**) 'Synthesis of pentylferulate by a feruloyl esterase from Aspergillus niger using water-in-oil microemulsions', p. 6.

Gopalan, N. and Nampoothiri, K. M. (**2018**) 'Biorefining of wheat bran for the purification of ferulic acid', *Biocatalysis and Agricultural Biotechnology*, 15, pp. 304–310.

Grabber, J. H., Ralph, J. and Hatfield, R. D. (**2000**) 'Cross-Linking of Maize Walls by Ferulate Dimerization and Incorporation into Lignin', *Journal of Agricultural and Food Chemistry*, 48(12), pp. 6106–6113.

Grajales-Hernández, D. A., Velasco-Lozano, S., Armendáriz-Ruiz, M. A., Rodríguez-González, J. A., Camacho-Ruíz, R. M., Asaff-Torres, A., López-Gallego, F. and Mateos-Díaz, J. C. (**2020**) 'Carrier-bound and carrier-free immobilization of type A feruloyl esterase from Aspergillus niger: Searching for an operationally stable heterogeneous biocatalyst for the synthesis of butyl hydroxycinnamates', *Journal of Biotechnology*, 316, pp. 6–16.

Grebowicz, J., Lau, S.-F. and Wunderlich, B. (**2007**) 'The thermal properties of polypropylene', *Journal of Polymer Science: Polymer Symposia*, 71(1), pp. 19–37.

Guajardo, N., Domínguez de María, P., Ahumada, K., Schrebler, R. A., Ramírez-Tagle, R., Crespo, F. A. and Carlesi, C. (**2017**) 'Water as Cosolvent: Nonviscous Deep Eutectic Solvents for Efficient Lipase-Catalyzed Esterifications', *ChemCatChem*, 9(8), pp. 1393–1396.

Guajardo, N., Schrebler, R. A. and Domínguez de María, P. (**2019**) 'From batch to fed-batch and to continuous packed-bed reactors: Lipase-catalyzed esterifications in low viscous deep-eutectic-solvents with buffer as cosolvent', *Bioresource Technology*, 273, pp. 320–325.

Gunia-Krzyżak, A., Słoczyńska, K., Popiół, J., Koczurkiewicz, P., Marona, H. and Pękala, E. (**2018**) 'Cinnamic acid derivatives in cosmetics: current use and future prospects', *International Journal of Cosmetic Science*, 40(4), pp. 356–366.

Guyot, B., Bosquette, B., Pina, M. and Graille, J. (**1997**) 'Esterification of phenolic acids from green coffee with an immobilized lipase from Candida antarctica in solvent-free medium', *Biotechnology Letters*, 19(6), pp. 529–532.

Haddleton, D. M., Creed, D., Griffin, A. C., Hoyle, C. E. and Venkataram, K. (**1989**) 'Photochemical crosslinking of main-chain liquid-crystalline polymers containing cinnamoyl groups', *Die Makromolekulare Chemie, Rapid Communications*, 10(8), pp. 391–396.

Ham, J., Lim, W., Park, S., Bae, H., You, S. and Song, G. (**2019**) 'Synthetic phenolic antioxidant propyl gallate induces male infertility through disruption of calcium homeostasis and mitochondrial function', *Environmental Pollution*, 248, pp. 845–856.

Hang Thi, T., Matsusaki, M. and Akashi, M. (**2008**) 'Thermally stable and photoreactive polylactides by the terminal conjugation of bio-based caffeic acid', *Chemical Communications*, (33), p. 3918.

Hariharan, R. and Pinkus, A. G. (**1993**) 'Useful NMR solvent mixture for polyesters: Trifluoroacetic acid-d/chloroform-d', *Polymer Bulletin*, 30(1), pp. 91–95.

Hartley, R. D., Morrison, W. H., Balza, F. and Towers, G. H. N. (**1990**) 'Substituted truxillic and truxinic acids in cell walls of Cynodon dactylon', *Phytochemistry*, 29(12), pp. 3699–3703.

Hatfield, R. D., Rancour, D. M. and Marita, J. M. (**2017**) 'Grass Cell Walls: A Story of Cross-Linking', *Frontiers in Plant Science*, 7.

Hatti-Kaul, R., Nilsson, L. J., Zhang, B., Rehnberg, N. and Lundmark, S. (**2019**) 'Designing Biobased Recyclable Polymers for Plastics', *Trends in Biotechnology*.

Heldt-Hansen, H. P., Ishii, M., Patkar, S. A., Hansen, T. T. and Eigtved, P. (**1989**) 'A New Immobilized Positional Nonspecific Lipase for Fat Modification and Ester Synthesis', in Whitaker, J. R. and Sonnet, P. E. (eds) *Biocatalysis in Agricultural Biotechnology*. Washington, DC: American Chemical Society, pp. 158–172.

Heuss, R., Müller, N., Van Sintern, W., Starke, A. and Tschiesner, A. (**2012**) *Lightweight, heavy impact*. McKinsey & Comapny. Available at: https://www.mckinsey.com/~/media/mckinsey/dotcom/client_service/automotive%20and%20assembly/pdfs/lightweight_heavy_impact.ashx (Accessed: 1 September 2021).

Higgins, J. W. and Black, H. C. (**1944**) 'A preliminary comparison of the stabilizing effect of several recently proposed antioxidants for edible fats and oils', *Oil & Soap*, 21(9), pp. 277–279.

Hohn, S., Acevedo-Trejos, E., Abrams, J. F., Fulgencio de Moura, J., Spranz, R. and Merico, A. (**2020**) 'The long-term legacy of plastic mass production', *Science of The Total Environment*, 746, p. 141115.

Horbury, M. D., Baker, L. A., Rodrigues, N. D. N., Quan, W.-D. and Stavros, V. G. (**2017**) 'Photoisomerization of ethyl ferulate: A solution phase transient absorption study', *Chemical Physics Letters*, 673, pp. 62–67.

de Hoyos-Martínez, P. L., Merle, J., Labidi, J. and Charrier – El Bouhtoury, F. (**2019**) 'Tannins extraction: A key point for their valorization and cleaner production', *Journal of Cleaner Production*, 206, pp. 1138–1155.

Hu, H., Zhang, R., Wang, J., Ying, W. B. and Zhu, J. (**2018**) 'Fully bio-based poly(propylene succinate-co-propylene furandicarboxylate) copolyesters with proper mechanical, degradation and barrier properties for green packaging applications', *European Polymer Journal*, 102, pp. 101–110.

Huang, K.-C., Li, Y., Twu, Y.-K. and Shieh, C.-J. (**2015**) 'High Efficient Synthesis of Enzymatic 2-Ethylhexyl Ferulate at Solvent-Free and Reduced Pressure Evaporation System', *Journal of Materials Science and Chemical Engineering*, 03(06), pp. 33–40.

Hunt, C. J., Antonopoulou, I., Tanksale, A., Rova, U., Christakopoulos, P. and Haritos, V. S. (**2017**) 'Insights into substrate binding of ferulic acid esterases by arabinose and methyl hydroxycinnamate esters and molecular docking', *Scientific Reports*, 7(1), p. 17315.

Hüttner, S., Zezzi Do Valle Gomes, M., Iancu, L., Palmqvist, A. and Olsson, L. (**2017**) 'Immobilisation on mesoporous silica and solvent rinsing improve the transesterification abilities of feruloyl esterases from Myceliophthora thermophila', *Bioresource Technology*, 239, pp. 57–65.

Imai, Y. and Tassavori, S. (**1984**) 'Preparation and properties of aromatic polyesters and copolyesters containing phenylindane unit', *Journal of Polymer Science: Polymer Chemistry Edition*, 22(6), pp. 1319–1325.

Ingole, A., Kadam, M. P., Dalu, A. P., Kute, S. M., Mange, P. R., Theng, V. D., Lahane, O. R., Nikas, A. P., Kawal, Y. V., Nagrik, S. U. and Patil, P. A. (**2021**) 'A Review of the Pharmacological

Characteristics of Vanillic Acid', *Journal of Drug Delivery and Therapeutics*, 11(2-S), pp. 200–204.

Ishii, D., Maeda, H., Hayashi, H., Mitani, T., Shinohara, N., Yoshioka, K. and Watanabe, T. (**2013**) 'Effect of Polycondensation Conditions on Structure and Thermal Properties of Poly(caffeic acid)', in Cheng, H. N., Gross, R. A., and Smith, P. B. (eds) *Green Polymer Chemistry: Biocatalysis and Materials II*. Washington, DC: American Chemical Society, pp. 237–249.

Ito, S., Nakagawa, Y., Yazawa, S., Sasaki, Y. and Yajima, S. (**2014**) 'Antifungal activity of alkyl gallates against plant pathogenic fungi', *Bioorganic & Medicinal Chemistry Letters*, 24(7), pp. 1812–1814.

Izunobi, J. U. and Higginbotham, C. L. (**2011**) 'Polymer Molecular Weight Analysis by 1 H NMR Spectroscopy', *Journal of Chemical Education*, 88(8), pp. 1098–1104.

Jakovetić, S. M., Jugović, B. Z., Gvozdenović, M. M., Bezbradica, D. I., Antov, M. G., Mijin, D. Ž. and Knežević-Jugović, Z. D. (**2013**) 'Synthesis of Aliphatic Esters of Cinnamic Acid as Potential Lipophilic Antioxidants Catalyzed by Lipase B from Candida antarctica', *Applied Biochemistry and Biotechnology*, 170(7), pp. 1560–1573.

Jang, Y.-S., Kim, B., Shin, J. H., Choi, Y. J., Choi, S., Song, C. W., Lee, J., Park, H. G. and Lee, S. Y. (**2012**) 'Bio-based production of C2-C6 platform chemicals', *Biotechnology and Bioengineering*, 109(10), pp. 2437–2459.

Jawerth, M., Lawoko, M., Lundmark, S., Perez-Berumen, C. and Johansson, M. (**2016**) 'Allylation of a lignin model phenol: a highly selective reaction under benign conditions towards a new thermoset resin platform', *RSC Advances*, 6(98), pp. 96281–96288.

Jiang, Y. and Loos, K. (**2016**) 'Enzymatic Synthesis of Biobased Polyesters and Polyamides', *Polymers*, 8(7), p. 243.

Jiang, Y., Woortman, A. J. J., Alberda van Ekenstein, G. O. R. and Loos, K. (**2015**) 'A biocatalytic approach towards sustainable furanic–aliphatic polyesters', *Polymer Chemistry*, 6(29), pp. 5198–5211.

Jiang, Y., Woortman, A. J. J., Alberda van Ekenstein, G. O. R., Petrović, D. M. and Loos, K. (**2014**) 'Enzymatic Synthesis of Biobased Polyesters Using 2,5-Bis(hydroxymethyl)furan as the Building Block', *Biomacromolecules*, 15(7), pp. 2482–2493.

Jin, H.-J., Lee, B.-Y., Kim, M.-N. and Yoon, J.-S. , 'Thermal and mechanical properties of mandelic acid-copolymerized poly(butylene succinate) and poly(ethylene adipate)', p. 8.

John, G., Nagarajan, S., Vemula, P. K., Silverman, J. R. and Pillai, C. K. S. (**2019**) 'Natural monomers: A mine for functional and sustainable materials – Occurrence, chemical modification and polymerization', *Progress in Polymer Science*, 92, pp. 158–209.

José, C., Bonetto, R. D., Gambaro, L. A., Torres, M. del P. G., Foresti, M. L., Ferreira, M. L. and Briand, L. E. (**2011**) 'Investigation of the causes of deactivation–degradation of the commercial biocatalyst Novozym® 435 in ethanol and ethanol–aqueous media', *Journal of Molecular Catalysis B: Enzymatic*, 71(3–4), pp. 95–107.

Juais, D., Naves, A. F., Li, C., Gross, R. A. and Catalani, L. H. (**2010**) 'Isosorbide Polyesters from Enzymatic Catalysis', *Macromolecules*, 43(24), pp. 10315–10319.

Kahkeshani, N., Farzaei, F., Fotouhi, M., Alavi, S. S., Bahramsoltani, R., Naseri, R., Momtaz, S., Abbasabadi, Z., Rahimi, R., Farzaei, M. H. and Bishayee, A. (**2019**) 'Pharmacological effects of gallic acid in health and disease: A mechanistic review', *Iranian Journal of Basic Medical Sciences*, 22(3).

Kakadellis, S. and Rosetto, G. (**2021**) 'Achieving a circular bioeconomy for plastics', *Science*, 373(6550), pp. 49–50.

Kalia, V. C., Singh Patel, S. K., Shanmugam, R. and Lee, J.-K. (**2021**) 'Polyhydroxyalkanoates: Trends and advances toward biotechnological applications', *Bioresource Technology*, 326, p. 124737.

Kaneko, T., Kaneko, D. and Wang, S. (**2010**) 'High-performance lignin-mimetic polyesters', *Plant Biotechnology*, 27(3), pp. 243–250.

Kaneko, T., Thi, T. H., Shi, D. J. and Akashi, M. (**2006**) 'Environmentally degradable, high-performance thermoplastics from phenolic phytomonomers', *Nature Materials*, 5(12), pp. 966–970.

Karakousi, C.-V., Gabrieli, C. and Kokkalou, E. (**2020**) 'Chemical composition and biological activities of *Indigofera hirsuta* aerial parts' methanol fractions', *Natural Product Research*, 34(4), pp. 558–562.

Karamać, M. and Amarowicz, R. (**1996**) 'Inhibition of Pancreatic Lipase by Phenolic Acids - Examination in vitro', *Zeitschrift für Naturforschung C*, 51(11–12), pp. 903–906.

Karboune, S., St-Louis, R. and Kermasha, S. (**2008**) 'Enzymatic synthesis of structured phenolic lipids by acidolysis of flaxseed oil with selected phenolic acids', *Journal of Molecular Catalysis B: Enzymatic*, 52–53, pp. 96–105.

Katayama, S., Ohno, F., Yamauchi, Y., Kato, M., Makabe, H. and Nakamura, S. (**2013**) 'Enzymatic Synthesis of Novel Phenol Acid Rutinosides Using Rutinase and Their Antiviral Activity in Vitro', *Journal of Agricultural and Food Chemistry*, 61(40), pp. 9617–9622.

Katsoura, M. H., Polydera, A. C., Tsironis, L. D., Petraki, M. P., Rajačić, S. K., Tselepis, A. D. and Stamatis, H. (**2009**) 'Efficient enzymatic preparation of hydroxycinnamates in ionic liquids enhances their antioxidant effect on lipoproteins oxidative modification', *New Biotechnology*, 26(1–2), pp. 83–91.

Khan, F., Bamunuarachchi, N. I., Tabassum, N. and Kim, Y.-M. (**2021**) 'Caffeic Acid and Its Derivatives: Antimicrobial Drugs toward Microbial Pathogens', *Journal of Agricultural and Food Chemistry*, 69(10), pp. 2979–3004.

Khan, M., Brunklaus, G., Enkelmann, V. and Spiess, H.-W. (**2008**) 'Transient States in [2 + 2] Photodimerization of Cinnamic Acid: Correlation of Solid-State NMR and X-ray Analysis', *Journal of the American Chemical Society*, 130(5), pp. 1741–1748.

Kirk, O., Borchert, T. V. and Fuglsang, C. C. (**2002**) 'Industrial enzyme applications', *Current Opinion in Biotechnology*, 13(4), pp. 345–351.

Kobayashi, S., Takeya, K., Suda, S. and Uyama, H. (**1998**) 'Lipase-catalyzed ring-opening polymerization of medium-size lactones to polyesters', *Macromolecular Chemistry and Physics*, 199(8), pp. 1729–1736.

Kobayashi, S. and Uyama, H. (**2019**) 'Synthesis of Polyesters I: Hydrolase as Catalyst for Polycondensation (Condensation Polymerization)', in Kobayashi, S., Uyama, H., and Kadokawa, J. (eds) *Enzymatic Polymerization towards Green Polymer Chemistry*. Singapore: Springer Singapore (Green Chemistry and Sustainable Technology), pp. 105–163.

Korupp, C., Weberskirch, R., Müller, J. J., Liese, A. and Hilterhaus, L. (**2010**) 'Scaleup of Lipase-Catalyzed Polyester Synthesis', *Organic Process Research & Development*, 14(5), pp. 1118–1124.

Kreye, O., Oelmann, S. and Meier, M. A. R. (**2013**) 'Renewable Aromatic-Aliphatic Copolyesters Derived from Rapeseed', *Macromolecular Chemistry and Physics*, 214(13), pp. 1452–1464.

Kreye, O., Tóth, T. and Meier, M. A. R. (**2011**) 'Copolymers derived from rapeseed derivatives via ADMET and thiol-ene addition', *European Polymer Journal*, 47(9), pp. 1804–1816.

Kristufek, S. L., Wacker, K. T., Tsao, Y.-Y. T., Su, L. and Wooley, K. L. (**2017**) 'Monomer design strategies to create natural product-based polymer materials', *Natural Product Reports*, 34(4), pp. 433–459.

Kumar, A. and Gross, R. A. (**2000**) '*Candida a ntartica* Lipase B Catalyzed Polycaprolactone Synthesis: Effects of Organic Media and Temperature', *Biomacromolecules*, 1(1), pp. 133–138.

Kumar, A. and Kanwar, S. S. (**2011**) 'Synthesis of ethyl ferulate in organic medium using celite-immobilized lipase', *Bioresource Technology*, 102(3), pp. 2162–2167.

Kumar, N. and Goel, N. (**2019**) 'Phenolic acids: Natural versatile molecules with promising therapeutic applications', *Biotechnology Reports*, 24, p. e00370.

Kurt, G. and Gokturk, E. (**2020**) 'Synthesis of polyesters mimicking polyethylene terephthalate and their thermal and mechanical properties', *Journal of Polymer Research*, 27(10), p. 314.

Laane, C., Boeren, S., Vos, K. and Veeger, C. , 'Rules for optimization of biocatalysis in organic solvents', p. 8.

Laguerre, M., Bayrasy, C., Lecomte, J., Chabi, B., Decker, E. A., Wrutniak-Cabello, C., Cabello, G. and Villeneuve, P. (**2013**) 'How to boost antioxidants by lipophilization?', *Biochimie*, 95(1), pp. 20–26.

Lamidey, A.-M., Fernon, L., Pouységu, L., Delattre, C. and Quideau, S. (**2002**) 'A Convenient Synthesis of the Echinacea-Derived Immunostimulator and HIV-1 Integrase Inhibitor (−)-(2R,3R)-Chicoric Acid', *Helvetica Chimica Acta*, 85, p. 7.

Lassalle, V. L. and Ferreira, M. L. (**2008**) 'Lipase-catalyzed synthesis of polylactic acid: an overview of the experimental aspects', *Journal of Chemical Technology & Biotechnology*, 83(11), pp. 1493–1502.

Lee, D. Y., Tachibana, S., Sumimoto, M. and Ohe, H. (**1988**) 'Structure of 4'-acetoxy-3'-methoxycinnamic acid', *Acta Crystallographica Section C Crystal Structure Communications*, 44(7), pp. 1240–1242.

Lee, G.-S., Widjaja, A. and Ju, Y.-H. (**2006**) 'Enzymatic Synthesis of Cinnamic Acid Derivatives', *Biotechnology Letters*, 28(8), pp. 581–585.

Lendlein, A., Jiang, H., Jünger, O. and Langer, R. (**2005**) 'Light-induced shape-memory polymers', *Nature*, 434(7035), pp. 879–882.

Li, M. and Wilkins, M. (**2021**) 'Lignin bioconversion into valuable products: fractionation, depolymerization, aromatic compound conversion, and bioproduct formation', *Systems Microbiology and Biomanufacturing*, 1(2), pp. 166–185.

Li, Q., Ma, S., Xu, X. and Zhu, J. (**2019**) 'Bio-based Unsaturated Polyesters', in *Unsaturated Polyester Resins*. Elsevier, pp. 515–555.

Li, S., Li, W. and Khashab, N. M. (**2012**) 'Stimuli responsive nanomaterials for controlled release applications', *Nanotechnology Reviews*, 1(6), pp. 493–513.

Li, S., Moosa, B. A., Chen, Y., Li, W. and Khashab, N. M. (**2015**) 'A photo-tunable membrane based on inter-particle crosslinking for decreasing diffusion rates', *Journal of Materials Chemistry B*, 3(7), pp. 1208–1216.

Little, A., Pellis, A., Comerford, J. W., Naranjo-Valles, E., Hafezi, N., Mascal, M. and Farmer, T. J. (**2020**) 'Effects of Methyl Branching on the Properties and Performance of Furandioate-Adipate Copolyesters of Bio-Based Secondary Diols', *ACS Sustainable Chemistry & Engineering*.

Liu, J., Wang, X., Bai, R., Zhang, N., Kan, J. and Jin, C. (**2018**) 'Synthesis, characterization, and antioxidant activity of caffeic-acid-grafted corn starch: Characterization and antioxidant activity of caffeic-acid-grafted starch', *Starch - Stärke*, 70(1–2), p. 1700141.

Llevot, A., Grau, E., Carlotti, S., Grelier, S. and Cramail, H. (**2015**) 'Renewable (semi)aromatic polyesters from symmetrical vanillin-based dimers', *Polymer Chemistry*, 6(33), pp. 6058–6066.

Llevot, A., Grau, E., Carlotti, S., Grelier, S. and Cramail, H. (**2016**) 'From Lignin-derived Aromatic Compounds to Novel Biobased Polymers', *Macromolecular Rapid Communications*, 37(1), pp. 9–28.

Locatelli, C., Filippin-Monteiro, F. B. and Creczynski-Pasa, T. B. (**2013**) 'Alkyl esters of gallic acid as anticancer agents: A review', *European Journal of Medicinal Chemistry*, 60, pp. 233–239.

Loos, K., Zhang, R., Pereira, I., Agostinho, B., Hu, H., Maniar, D., Sbirrazzuoli, N., Silvestre, A. J. D., Guigo, N. and Sousa, A. F. (**2020**) 'A Perspective on PEF Synthesis, Properties, and End-Life', *Frontiers in Chemistry*, 8, p. 585.

Lozano, P., De Diego, T., Carrie, D., Vaultier, M. and Iborra, J. L. (**2003**) 'Lipase Catalysis in Ionic Liquids and Supercritical Carbon Dioxide at 150 °C', *Biotechnology Progress*, 19(2), pp. 380–382.

Lue, B.-M., Karboune, S., Yeboah, F. K. and Kermasha, S. (**2005**) 'Lipase-catalyzed esterification of cinnamic acid and oleyl alcohol in organic solvent media', *Journal of Chemical Technology & Biotechnology*, 80(4), pp. 462–468.

Magnin, A., Entzmann, L., Bazin, A., Pollet, E. and Avérous, L. (**2021**) 'Green Recycling Process for Polyurethane Foams by a Chem-Biotech Approach', *ChemSusChem*, 14(19), pp. 4234–4241.

Mahapatro, A., Kalra, B., Kumar, A. and Gross, R. A. (**2003**) 'Lipase-Catalyzed Polycondensations: Effect of Substrates and Solvent on Chain Formation, Dispersity, and End-Group Structure', *Biomacromolecules*, 4(3), pp. 544–551.

Mancuso, C. and Santangelo, R. (**2014**) 'Ferulic acid: Pharmacological and toxicological aspects', *Food and Chemical Toxicology*, 65, pp. 185–195.

Mandal, S. and Dey, A. (**2019**) 'PET Chemistry', in *Recycling of Polyethylene Terephthalate Bottles*. Elsevier, pp. 1–22.

Maniar, D., Jiang, Y., Woortman, A. J. J., van Dijken, J. and Loos, K. (**2019**) 'Furan-Based Copolyesters from Renewable Resources: Enzymatic Synthesis and Properties', *ChemSusChem*, 12(5), pp. 990–999.

Marschner, D. E., Frisch, H., Offenloch, J. T., Tuten, B. T., Becer, C. R., Walther, A., Goldmann, A. S., Tzvetkova, P. and Barner-Kowollik, C. (**2018**) 'Visible Light [2 + 2] Cycloadditions for Reversible Polymer Ligation', *Macromolecules*, 51(10), pp. 3802–3807.

Mastihubová, M. and Mastihuba, V. (**2013**) 'Donor specificity and regioselectivity in Lipolase mediated acylations of methyl α-d-glucopyranoside by vinyl esters of phenolic acids and their analogues', *Bioorganic & Medicinal Chemistry Letters*, 23(19), pp. 5389–5392.

Mastihubová, M., Mastihuba, V., Bilaničová, D. and Boreková, M. (**2006**) 'Commercial enzyme preparations catalyse feruloylation of glycosides', *Journal of Molecular Catalysis B: Enzymatic*, 38(1), pp. 54–57.

Masuku, C. P. (**1992**) 'Thermolytic decomposition of coniferyl alcohol', *Journal of Analytical and Applied Pyrolysis*, 23(2), pp. 195–208.

Mateo, C., Palomo, J. M., Fernandez-Lorente, G., Guisan, J. M. and Fernandez-Lafuente, R. (**2007**) 'Improvement of enzyme activity, stability and selectivity via immobilization techniques', *Enzyme and Microbial Technology*, 40(6), pp. 1451–1463.

Mathew, S. and Abraham, T. E. (**2004**) 'Ferulic Acid: An Antioxidant Found Naturally in Plant Cell Walls and Feruloyl Esterases Involved in its Release and Their Applications', *Critical Reviews in Biotechnology*, 24(2–3), pp. 59–83.

McEwen, C. N., Jackson, C. and Larsen, B. S. (**1997**) 'Instrumental effects in the analysis of polymers of wide polydispersity by MALDI mass spectrometry', *International Journal of Mass Spectrometry and Ion Processes*, 160(1–3), pp. 387–394.

McIntyre, J. E. (**2004**) 'The Historical Development of Polyesters', in Scheirs, J. and Long, T. E. (eds) *Wiley Series in Polymer Science*. Chichester, UK: John Wiley & Sons, Ltd, pp. 1–28.

Mei, Y., Kumar, A. and Gross, R. (**2003**)**a** 'Kinetics and Mechanism of *Candida a ntarctica* Lipase B Catalyzed Solution Polymerization of ε-Caprolactone', *Macromolecules*, 36(15), pp. 5530–5536.

Mei, Y., Miller, L., Gao, W. and Gross, R. A. (**2003**)**b** 'Imaging the Distribution and Secondary Structure of Immobilized Enzymes Using Infrared Microspectroscopy', *Biomacromolecules*, 4(1), pp. 70–74.

Ménard, R., Caillol, S. and Allais, F. (**2017**)**a** 'Chemo-Enzymatic Synthesis and Characterization of Renewable Thermoplastic and Thermoset Isocyanate-Free Poly(hydroxy)urethanes from Ferulic Acid Derivatives', *ACS Sustainable Chemistry & Engineering*, 5(2), pp. 1446–1456.

Ménard, R., Caillol, S. and Allais, F. (**2017**)**b** 'Ferulic acid-based renewable esters and amides-containing epoxy thermosets from wheat bran and beetroot pulp: Chemo-enzymatic synthesis and thermo-mechanical properties characterization', *Industrial Crops and Products*, 95, pp. 83–95.

de Meneses, A. C., Balen, M., de Andrade Jasper, E., Korte, I., de Araújo, P. H. H., Sayer, C. and de Oliveira, D. (**2020**) 'Enzymatic synthesis of benzyl benzoate using different acyl donors: Comparison of solvent-free reaction techniques', *Process Biochemistry*, 92, pp. 261–268.

Mialon, L., Vanderhenst, R., Pemba, A. G. and Miller, S. A. (**2011**) 'Polyalkylenehydroxybenzoates (PAHBs): Biorenewable Aromatic/Aliphatic Polyesters from Lignin: Polyalkylenehydroxybenzoates (PAHBs) …', *Macromolecular Rapid Communications*, 32(17), pp. 1386–1392.

Mochane, M. J., Magagula, S. I., Sefadi, J. S. and Mokhena, T. C. (**2021**) 'A Review on Green Composites Based on Natural Fiber-Reinforced Polybutylene Succinate (PBS)', *Polymers*, 13(8), p. 1200.

Moni, L., Banfi, L., Basso, A., Mori, A., Risso, F., Riva, R. and Lambruschini, C. (**2021**) 'A Thorough Study on the Photoisomerization of Ferulic Acid Derivatives', *European Journal of Organic Chemistry*, 2021(11), pp. 1737–1749.

Montanier, C. Y., Chabot, N., Emond, S., Guieysse, D., Remaud-Siméon, M., Peruch, F. and André, I. (**2017**) 'Engineering of Candida antarctica lipase B for poly(ε-caprolactone) synthesis', *European Polymer Journal*, 95, pp. 809–819.

Morales-Huerta, J. C., Ciulik, C. B., de Ilarduya, A. M. and Muñoz-Guerra, S. (**2017**) 'Fully bio-based aromatic–aliphatic copolyesters: poly(butylene furandicarboxylate-co-succinate)s obtained by ring opening polymerization', *Polymer Chemistry*, 8(4), pp. 748–760.

Morales-Huerta, J. C., Martínez de Ilarduya, A. and Muñoz-Guerra, S. (**2018**) 'Blocky poly(ε-caprolactone- *co* -butylene 2,5-furandicarboxylate) copolyesters via enzymatic ring opening polymerization', *Journal of Polymer Science Part A: Polymer Chemistry*, 56(3), pp. 290–299.

Morrison, I. M., Robertson, G. W., Stewart, D. and Wightman, F. (**1991**) 'Determination and characterization of cyclodimers of naturally occurring phenolic acids', *Phytochemistry*, 30(6), pp. 2007–2011.

Morrison, W. Herbert., Hartley, R. D. and Himmelsbach, D. S. (**1992**) 'Synthesis of substituted truxillic acids from p-coumaric and ferulic acid: simulation of photodimerization in plant cell walls', *Journal of Agricultural and Food Chemistry*, 40(5), pp. 768–771.

Muthusamy, K., Lalitha, K., Prasad, Y. S., Thamizhanban, A., Sridharan, V., Maheswari, C. U. and Nagarajan, S. (**2018**) 'Lipase-Catalyzed Synthesis of Furan-Based Oligoesters and their Self-Assembly-Assisted Polymerization', *ChemSusChem*, 11(14), pp. 2453–2463.

Nagata, M. and Kitazima, I. (**2006**) 'Photocurable biodegradable poly(ε-caprolactone)/poly(ethylene glycol) multiblock copolymers showing shape-memory properties', *Colloid and Polymer Science*, 284(4), pp. 380–386.

Nagata, M. and Sato, Y. (**2005**) 'Synthesis and properties of photocurable biodegradable multiblock copolymers based on poly(ε-caprolactone) and poly(L-lactide) segments', *Journal of Polymer Science Part A: Polymer Chemistry*, 43(11), pp. 2426–2439.

Nakajima, H., Dijkstra, P. and Loos, K. (**2017**) 'The Recent Developments in Biobased Polymers toward General and Engineering Applications: Polymers that are Upgraded from Biodegradable Polymers, Analogous to Petroleum-Derived Polymers, and Newly Developed', *Polymers*, 9(12), p. 523.

Nam, S.-H., Park, J., Jun, W., Kim, D., Ko, J.-A., Abd El-Aty, A. M., Choi, J. Y., Kim, D.-I. and Yang, K.-Y. (**2017**) 'Transglycosylation of gallic acid by using Leuconostoc glucansucrase and its characterization as a functional cosmetic agent', *AMB Express*, 7(1), p. 224.

Nasr, K., Meimoun, J., Favrelle-Huret, A., Winter, J. D., Raquez, J.-M. and Zinck, P. (**2020**) 'Enzymatic Polycondensation of 1,6-Hexanediol and Diethyl Adipate: A Statistical Approach Predicting the Key-Parameters in Solution and in Bulk', *Polymers*, 12(9), p. 1907.

Natella, F., Nardini, M., Di Felice, M. and Scaccini, C. (**1999**) 'Benzoic and Cinnamic Acid Derivatives as Antioxidants: Structure−Activity Relation', *Journal of Agricultural and Food Chemistry*, 47(4), pp. 1453–1459.

Nethaji, M., Pattabhi, V. and Desiraju, G. R. (**1988**) 'Structure of 3-(4-hydroxy-3-methoxyphenyl)-2-propenoic acid (ferulic acid)', *Acta Crystallographica Section C Crystal Structure Communications*, 44(2), pp. 275–277.

Nguyen, H. T. H., Qi, P., Rostagno, M., Feteha, A. and Miller, S. A. (**2018**) 'The quest for high glass transition temperature bioplastics', *Journal of Materials Chemistry A*, 6(20), pp. 9298–9331.

Nguyen, H. T. H., Reis, M. H., Qi, P. and Miller, S. A. (**2015**) 'Polyethylene ferulate (PEF) and congeners: polystyrene mimics derived from biorenewable aromatics', *Green Chemistry*, 17(9), pp. 4512–4517.

Nguyen, H. T. H., Short, G. N., Qi, P. and Miller, S. A. (**2017**) 'Copolymerization of lactones and bioaromatics via concurrent ring-opening polymerization/polycondensation', *Green Chemistry*, 19(8), pp. 1877–1888.

Nguyen, T. B. and Al-Mourabit, A. (**2016**) 'Remarkably high homoselectivity in [2 + 2] photodimerization of trans-cinnamic acids in multicomponent systems', *Photochemical & Photobiological Sciences*, 15(9), pp. 1115–1119.

Nie, G., Chen, Z., Zheng, Z., Jin, W., Gong, G., Wang, L. and Yue, W. (**2013**) 'Enhancement of transesterification-catalyzing capability of bio-imprinted tannase in organic solvents by cryogenic protection and immobilization', *Journal of Molecular Catalysis B: Enzymatic*, 94, pp. 1–6.

Nie, G., Liu, H., Chen, Z., Wang, P., Zhao, G. and Zheng, Z. (**2012**)**a** 'Synthesis of propyl gallate from tannic acid catalyzed by tannase from Aspergillus oryzae: Process optimization of transesterification in anhydrous media', *Journal of Molecular Catalysis B: Enzymatic*, 82, pp. 102–108.

Nie, G., Zheng, Z., Jin, W., Gong, G. and Wang, L. (**2012**)**b** 'Development of a tannase biocatalyst based on bio-imprinting for the production of propyl gallate by transesterification in organic media', *Journal of Molecular Catalysis B: Enzymatic*, 78, pp. 32–37.

Nie, G., Zheng, Z., Yue, W., Liu, Y., Liu, H., Wang, P., Zhao, G., Cai, W. and Xue, Z. (**2014**) 'One-pot bio-synthesis of propyl gallate by a novel whole-cell biocatalyst', *Process Biochemistry*, 49(2), pp. 277–282.

Nielsen, T. B., Ishii, M. and Kirk, O. (**1999**) 'Lipases A and B from the yeast Candida antarctica', in *Biotechnological Application of Cold-Adapted Organisms*. Springer Berlin Heidelberg, pp. 49–61.

Nikulin, M. and Švedas, V. (**2021**) 'Prospects of Using Biocatalysis for the Synthesis and Modification of Polymers', *Molecules*, 26(9), p. 2750.

Oh, S.-C., Lee, D.-G., Kwak, H. and Bae, S.-Y. (**2006**) 'Combustion Kinetics Of Polyethylene Terephthalate', *Environmental Engineering Research*, 11(5), pp. 250–256.

Oliveira, D. M., Mota, T. R., Oliva, B., Segato, F., Marchiosi, R., Ferrarese-Filho, O., Faulds, C. B. and dos Santos, W. D. (**2019**) 'Feruloyl esterases: Biocatalysts to overcome biomass recalcitrance and for the production of bioactive compounds', *Bioresource Technology*, 278, pp. 408–423.

Omay, D. and Guvenilir, Y. (**2013**) 'Synthesis and characterization of poly(d,l-lactic acid) via enzymatic ring opening polymerization by using free and immobilized lipase', *Biocatalysis and Biotransformation*, 31(3), pp. 132–140.

Ortiz, C., Ferreira, M. L., Barbosa, O., dos Santos, J. C. S., Rodrigues, R. C., Berenguer-Murcia, Á., Briand, L. E. and Fernandez-Lafuente, R. (**2019**) 'Novozym 435: the "perfect" lipase immobilized biocatalyst?', *Catalysis Science & Technology*, 9(10), pp. 2380–2420.

Otto, R. T., Scheib, H., Bornscheuer, U. T., Pleiss, J., Syldatk, C. and Schmid, R. D. (**2000**) 'Substrate specificity of lipase B from Candida antarctica in the synthesis of arylaliphatic glycolipids', *Journal of Molecular Catalysis B: Enzymatic*, 8(4–6), pp. 201–211.

Ou, S. and Kwok, K.-C. (**2004**) 'Ferulic acid: pharmaceutical functions, preparation and applications in foods', *Journal of the Science of Food and Agriculture*, 84(11), pp. 1261–1269.

Ouimet, M. A., Griffin, J., Carbone-Howell, A. L., Wu, W.-H., Stebbins, N. D., Di, R. and Uhrich, K. E. (**2013**) 'Biodegradable Ferulic Acid-Containing Poly(anhydride-ester): Degradation Products with Controlled Release and Sustained Antioxidant Activity', *Biomacromolecules*, 14(3), pp. 854–861.

Öztürk, H., Pollet, E., Phalip, V., Güvenilir, Y. and Avérous, L. (**2016**) 'Nanoclays for Lipase Immobilization: Biocatalyst Characterization and Activity in Polyester Synthesis', *Polymers*, 8(12), p. 416.

Paiva, L. B. de, Goldbeck, R., Santos, W. D. dos and Squina, F. M. (**2013**) 'Ferulic acid and derivatives: molecules with potential application in the pharmaceutical field', *Brazilian Journal of Pharmaceutical Sciences*, 49(3), pp. 395–411.

Pang, C., Zhang, J., Zhang, Q., Wu, G., Wang, Y. and Ma, J. (**2015**) 'Novel vanillic acid-based poly(ether–ester)s: from synthesis to properties', *Polymer Chemistry*, 6(5), pp. 797–804.

Papadopoulos, L., Magaziotis, A., Nerantzaki, M., Terzopoulou, Z., Papageorgiou, G. Z. and Bikiaris, D. N. (**2018**) 'Synthesis and characterization of novel poly(ethylene furanoate-co-adipate) random copolyesters with enhanced biodegradability', *Polymer Degradation and Stability*, 156, pp. 32–42.

Papageorgiou, G. Z., Papageorgiou, D. G., Terzopoulou, Z. and Bikiaris, D. N. (**2016**) 'Production of bio-based 2,5-furan dicarboxylate polyesters: Recent progress and critical aspects in their synthesis and thermal properties', *European Polymer Journal*, 83, pp. 202–229.

Parlement Européen (**2008**) *Concernant les enzymes alimentaires*, *Parlement Européen et du Conseil*. Available at: https://eur-lex.europa.eu/legal-content/FR/TXT/HTML/?uri=CELEX:32008R1332&from=EN.

Parthiban, A. and Vasantha, V. A. (**2020**) 'Biorenewable functional oligomers and polymers – Direct copolymerization of ferulic acid to obtain polymeric UV absorbers and multifunctional materials', *Polymer*, 188, p. 122122.

Pellis, A., Byrne, F. P., Sherwood, J., Vastano, M., Comerford, J. W. and Farmer, T. J. (**2019**)**a** 'Safer bio-based solvents to replace toluene and tetrahydrofuran for the biocatalyzed synthesis of polyesters', *Green Chemistry*, 21(7), pp. 1686–1694.

Pellis, A., Comerford, J. W., Maneffa, A. J., Sipponen, M. H., Clark, J. H. and Farmer, T. J. (**2018**) 'Elucidating enzymatic polymerisations: Chain-length selectivity of Candida antarctica lipase B towards various aliphatic diols and dicarboxylic acid diesters', *European Polymer Journal*, 106, pp. 79–84.

Pellis, A., Comerford, J. W., Weinberger, S., Guebitz, G. M., Clark, J. H. and Farmer, T. J. (**2019**)**b** 'Enzymatic synthesis of lignin derivable pyridine based polyesters for the substitution of petroleum derived plastics', *Nature Communications*, 10(1).

Pellis, A., Herrero Acero, E., Ferrario, V., Ribitsch, D., Guebitz, G. M. and Gardossi, L. (**2016**)**a** 'The Closure of the Cycle: Enzymatic Synthesis and Functionalization of Bio-Based Polyesters', *Trends in Biotechnology*, 34(4), pp. 316–328.

Pellis, A., Herrero Acero, E., Gardossi, L., Ferrario, V. and Guebitz, G. M. (**2016**)**b** 'Renewable building blocks for sustainable polyesters: new biotechnological routes for greener plastics: Renewable building blocks for sustainable polyesters', *Polymer International*, 65(8), pp. 861–871.

Pellis, A., Nyanhongo, G. S. and Farmer, T. J. (**2019**)**c** 'Recent Advances on Enzymatic Catalysis as a Powerful Tool for the Sustainable Synthesis of Bio-Based Polyesters', in Bastidas-Oyanedel, J.-R. and Schmidt, J. E. (eds) *Biorefinery*. Cham: Springer International Publishing, pp. 555–570.

Pellis, A., Weinberger, S., Gigli, M., Guebitz, G. M. and Farmer, T. J. (**2020**) 'Enzymatic synthesis of biobased polyesters utilizing aromatic diols as the rigid component', *European Polymer Journal*, 130, p. 109680.

Pezzana, L., Mousa, M., Malmström, E., Johansson, M. and Sangermano, M. (**2021**) 'Bio-based monomers for UV-curable coatings: allylation of ferulic acid and investigation of photocured thiol-ene network', *Progress in Organic Coatings*, 150, p. 105986.

Pilate, F., Stoclet, G., Mincheva, R., Dubois, P. and Raquez, J.-M. (**2018**) 'Poly(ε-caprolactone) and Poly(ω-pentadecalactone)-Based Networks with Two-Way Shape-Memory Effect through [2+2] Cycloaddition Reactions', *Macromolecular Chemistry and Physics*, 219(4), p. 1700345.

Pion, F., Ducrot, P.-H. and Allais, F. (**2014**) 'Renewable Alternating Aliphatic-Aromatic Copolyesters Derived from Biobased Ferulic Acid, Diols, and Diacids: Sustainable Polymers with Tunable Thermal Properties', *Macromolecular Chemistry and Physics*, 215(5), pp. 431–439.

Pion, F., Reano, A. F., Ducrot, P.-H. and Allais, F. (**2013**) 'Chemo-enzymatic preparation of new bio-based bis- and trisphenols: new versatile building blocks for polymer chemistry', *RSC Advances*, 3(23), p. 8988.

Pizzi (**2019**) 'Tannins: Prospectives and Actual Industrial Applications', *Biomolecules*, 9(8), p. 344.

Platics - the Facts 2020 (**2020**). Platics Europe. Available at: https://www.plasticseurope.org/application/files/5716/0752/4286/AF_Plastics_the_facts-WEB-2020-ING_FINAL.pdf.

Pleiss, J., Fischer, M. and Schmid, R. D. (**1998**) 'Anatomy of lipase binding sites: the scissile fatty acid binding site', *Chemistry and Physics of Lipids*, 93(1–2), pp. 67–80.

Poojari, Y. and Clarson, S. J. (**2013**) 'Thermal stability of Candida antarctica lipase B immobilized on macroporous acrylic resin particles in organic media', *Biocatalysis and Agricultural Biotechnology*, 2(1), pp. 7–11.

Pospiech, D., Korwitz, A., Komber, H., Jehnichen, D., Arnhold, K., Brünig, H., Scheibner, H., Müller, M. T. and Voit, B. (**2021**) 'Polyesters with bio-based ferulic acid units: crosslinking paves the way to property consolidation', *Polymer Chemistry*, 12(36), pp. 5139–5148.

Poulopoulou, N., Kantoutsis, G., Bikiaris, D. N., Achilias, D. S., Kapnisti, M. and Papageorgiou, G. Z. (**2019**) 'Biobased Engineering Thermoplastics: Poly(butylene 2,5-furandicarboxylate) Blends', *Polymers*, 11(6), p. 937.

Poveda-Giraldo, J. A., Solarte-Toro, J. C. and Cardona Alzate, C. A. (**2021**) 'The potential use of lignin as a platform product in biorefineries: A review', *Renewable and Sustainable Energy Reviews*, 138, p. 110688.

Prat, D., Wells, A., Hayler, J., Sneddon, H., McElroy, C. R., Abou-Shehada, S. and Dunn, P. J. (**2016**) 'CHEM21 selection guide of classical- and less classical-solvents', *Green Chemistry*, 18(1), pp. 288–296.

Preferred Fiber & Materials, Market Report 2021 (**2021**). TextileExchange. Available at: https://textileexchange.org/wp-content/uploads/2021/08/Textile-Exchange_Preferred-Fiber-and-Materials-Market-Report_2021.pdf.

Priebe, A., Hunke, M., Tonello, R., Sonawane, Y., Berta, T., Natarajan, A., Bhuvanesh, N., Pattabiraman, M. and Chandra, S. (**2018**) 'Ferulic acid dimer as a non-opioid therapeutic for acute pain', *Journal of Pain Research*, Volume 11, pp. 1075–1085.

Priya, K. and Chadha, A. (**2003**) 'Synthesis of hydrocinnamic esters by Pseudomonas cepacia lipase', *Enzyme and Microbial Technology*, 32(3–4), pp. 485–490.

Priya, K., Venugopal, T. and Chadha, A. (**2002**) 'Pseudomonas cepacia lipase-mediated transesterification reactions of hydrocinnamates', *Indian Journal of Biochemistry & Biophysics*, 39, pp. 259–263.

Purolite Life Sciences Product: Lifetech™ CalB immo Plus - Immobilized Lipase - Purolite (**2021**) *Purolite Life Sciences*. Available at: http://www.purolite.com/ls-product/calb-immo-plus (Accessed: 8 September 2021).

Raab, T., Bel-Rhlid, R., Williamson, G., Hansen, C.-E. and Chaillot, D. (**2007**) 'Enzymatic galloylation of catechins in room temperature ionic liquids', *Journal of Molecular Catalysis B: Enzymatic*, 44(2), pp. 60–65.

Rabnawaz, M., Wyman, I., Auras, R. and Cheng, S. (**2017**) 'A roadmap towards green packaging: the current status and future outlook for polyesters in the packaging industry', *Green Chem.*, 19(20), pp. 4737–4753.

Rafiqah, S. A., Khalina, A., Harmaen, A. S., Tawakkal, I. A., Zaman, K., Asim, M., Nurrazi, M. N. and Lee, C. H. (**2021**) 'A Review on Properties and Application of Bio-Based Poly(Butylene Succinate)', *Polymers*, 13(9), p. 1436.

Rahman, N. J. A., Radzi, S. M. and Noor, H. M. , 'Dual Lipases System in Transesterification of Ethyl Ferulate with Olive Oil: Optimization by Response Surface Methodology', p. 7.

Rajesh, R. O., Godan, T. K., Sindhu, R., Pandey, A. and Binod, P. (**2020**) 'Bioengineering advancements, innovations and challenges on green synthesis of 2, 5-furan dicarboxylic acid', *Bioengineered*, 11(1), pp. 19–38.

Ralph, J. (**2010**) 'Hydroxycinnamates in lignification', *Phytochemistry Reviews*, 9(1), pp. 65–83.

Ramamurthy, V. and Venkatesan, K. (**1987**) 'Photochemical reactions of organic crystals', *Chemical Reviews*, 87(2), pp. 433–481.

Rashidzadeh, H. and Guo, B. (**1998**) 'Use of MALDI-TOF To Measure Molecular Weight Distributions of Polydisperse Poly(methyl methacrylate)', *Analytical Chemistry*, 70(1), pp. 131–135.

Ravindranath, K. and Mashelkar, R. A. (**1984**) 'Polyethylene terephthalate-I. Chemistry, thermodynamics and transport properties', *Chemical Engineering Science*, 41(9), pp. 2197–2214.

Reano, A. F., Chérubin, J., Peru, A. M. M., Wang, Q., Clément, T., Domenek, S. and Allais, F. (**2015**) 'Structure–Activity Relationships and Structural Design Optimization of a Series of *p* - Hydroxycinnamic Acids-Based Bis- and Trisphenols as Novel Sustainable Antiradical/Antioxidant Additives', *ACS Sustainable Chemistry & Engineering*, 3(12), pp. 3486–3496.

Rebouillat, S. and Pla, F. (**2016**) 'Recent Strategies for the Development of Biosourced-Monomers, Oligomers and Polymers-Based Materials: A Review with an Innovation and a Bigger Data Focus', *Journal of Biomaterials and Nanobiotechnology*, 07(04), pp. 167–213.

Rich, J. O., Mozhaev, V. V., Dordick, J. S., Clark, D. S. and Khmelnitsky, Y. L. (**2002**) 'Molecular Imprinting of Enzymes with Water-Insoluble Ligands for Nonaqueous Biocatalysis', *Journal of the American Chemical Society*, 124(19), pp. 5254–5255.

de las Rivas, B., Rodríguez, H., Anguita, J. and Muñoz, R. (**2019**) 'Bacterial tannases: classification and biochemical properties', *Applied Microbiology and Biotechnology*, 103(2), pp. 603–623.

Rochette, J. M. and Ashby, V. S. (**2013**) 'Photoresponsive Polyesters for Tailorable Shape Memory Biomaterials', *Macromolecules*, 46(6), pp. 2134–2140.

Romero-Borbón, E., Grajales-Hernández, D., Armendáriz-Ruiz, M., Ramírez-Velasco, L., Rodríguez-González, J. A., Cira-Chávez, L. A., Estrada-Alvarado, M. I. and Mateos-Díaz, J. C. (**2018**) 'Type C feruloyl esterase from Aspergillus ochraceus: A butanol specific biocatalyst for the synthesis of hydroxycinnamates in a ternary solvent system', *Electronic Journal of Biotechnology*, 35, pp. 1–9.

Rovira, J., Nadal, M., Schuhmacher, M. and Domingo, J. L. (**2015**) 'Human exposure to trace elements through the skin by direct contact with clothing: Risk assessment', *Environmental Research*, 140, pp. 308–316.

Rychlicka, M., Maciejewska, G., Niezgoda, N. and Gliszczyńska, A. (**2020**) 'Production of feruloylated lysophospholipids via a one-step enzymatic interesterification', *Food Chemistry*, 323, p. 126802.

Rychlicka, M., Rot, A. and Gliszczyńska, A. (**2021**) 'Biological Properties, Health Benefits and Enzymatic Modifications of Dietary Methoxylated Derivatives of Cinnamic Acid', *Foods*, 10(6), p. 1417.

Sajid, M., Zhao, X. and Liu, D. (**2018**) 'Production of 2,5-furandicarboxylic acid (FDCA) from 5-hydroxymethylfurfural (HMF): recent progress focusing on the chemical-catalytic routes', *Green Chemistry*, 20(24), pp. 5427–5453.

Salum, M. L., Arroyo Mañez, P., Luque, F. J. and Erra-Balsells, R. (**2015**) 'Combined experimental and computational investigation of the absorption spectra of E- and Z -cinnamic acids in solution: The peculiarity of Z -cinnamics', *Journal of Photochemistry and Photobiology B: Biology*, 148, pp. 128–135.

Sandoval, G., Quintana, P. G., Baldessari, A., Ballesteros, A. O. and Plou, F. J. (**2015**) 'Lipase-catalyzed preparation of mono- and diesters of ferulic acid', *Biocatalysis and Biotransformation*, 33(2), pp. 89–97.

Sankar, K., Achary, A., Mehala, N. and Rajendran, L. (**2017**) 'Empirical and Analytical Correlation of the Reaction Kinetics Parameters of Cuttle Bone Powder Immobilized Lipase Catalyzed Ethyl Ferulate Synthesis', *Catalysis Letters*, 147(8), pp. 2232–2245.

Santiago, R. and Malvar, R. (**2010**) 'Role of Dehydrodiferulates in Maize Resistance to Pests and Diseases', *International Journal of Molecular Sciences*, 11(2), pp. 691–703.

Santos, Y. L. de los, Chew-Fajardo, Y. L., Brault, G. and Doucet, N. (**2019**) 'Dissecting the evolvability landscape of the CalB active site toward aromatic substrates', *Scientific Reports*, 9(1), p. 15588.

Satti, S. M. and Shah, A. A. (**2020**) 'Polyester-Based Biodegradable Plastics: An Approach Towards Sustainable Development', *Letters in Applied Microbiology*.

Schär, A., Liphardt, S. and Nyström, L. (**2017**) 'Enzymatic synthesis of steryl hydroxycinnamates and their antioxidant activity', *European Journal of Lipid Science and Technology*, 119(5), p. 1600267.

Schär, A. and Nyström, L. (**2015**) 'High yielding and direct enzymatic lipophilization of ferulic acid using lipase from Rhizomucor miehei', *Journal of Molecular Catalysis B: Enzymatic*, 118, pp. 29–35.

Schär, A. and Nyström, L. (**2016**) 'Enzymatic synthesis of steryl ferulates: Enzymatic synthesis of steryl ferulates', *European Journal of Lipid Science and Technology*, 118(10), pp. 1557–1565.

Schmidt, G. M. J. (**1964**) '385. Topochemistry. Part III. The crystal chemistry of some trans-cinnamic acids', *Journal of the Chemical Society (Resumed)*, p. 2014.

Schmidt, G. M. J. (**1971**) 'Photodimerization in the solid state', *Pure and Applied Chemistry*, 27(4), pp. 647–678.

Schoon, I., Kluge, M., Eschig, S. and Robert, T. (**2017**) 'Catalyst Influence on Undesired Side Reactions in the Polycondensation of Fully Bio-Based Polyester Itaconates', *Polymers*, 9(12), p. 693.

Schyns, Z. O. G. and Shaver, M. P. (**2021**) 'Mechanical Recycling of Packaging Plastics: A Review', *Macromolecular Rapid Communications*, 42(3), p. 2000415.

Shamim, S., Liaqat, U. and Rehman, A. (**2018**) 'Microbial lipases and their applications – a review', *Abasyn Journal Life Sciences*, pp. 54–76.

Sharma, A., Kumar, A., Meena, K. R., Rana, S., Singh, M. and Kanwar, S. S. (**2017**) 'Fabrication and functionalization of magnesium nanoparticle for lipase immobilization in n -propyl gallate synthesis', *Journal of King Saud University - Science*, 29(4), pp. 536–546.

Sharma, K., Kumar, V., Kaur, J., Tanwar, B., Goyal, A., Sharma, R., Gat, Y. and Kumar, A. (**2019**) 'Health effects, sources, utilization and safety of tannins: a critical review', *Toxin Reviews*, pp. 1–13.

Sharma, S., Kanwar, S. S., Dogra, P. and Chauhan, G. S. (**2015**) 'Gallic acid-based alkyl esters synthesis in a water-free system by celite-bound lipase of *B acillus licheniformis* SCD11501', *Biotechnology Progress*, 31(3), pp. 715–723.

Shi, Y., Bian, L., Zhu, Y., Zhang, R., Shao, S., Wu, Y., Chen, Y., Dang, Y., Ding, Y. and Sun, H. (**2019**) 'Multifunctional alkyl ferulate esters as potential food additives: Antibacterial activity and mode of action against Listeria monocytogenes and its application on American sturgeon caviar preservation', *Food Control*, 96, pp. 390–402.

Shi, Y., Wu, Y., Lu, X., Ren, Y., Wang, Q., Zhu, C., Yu, D. and Wang, H. (**2017**) 'Lipase-catalyzed esterification of ferulic acid with lauryl alcohol in ionic liquids and antibacterial properties in vitro against three food-related bacteria', *Food Chemistry*, 220, pp. 249–256.

Shindo, Y., Horie, K. and Mita, I. (**1983**) 'Rate for photodimerization of ethyl cinnamate in dilute solution', *Chemistry Letters*, 12(5), pp. 639–642.

Shindo, Y., Horie, K. and Mita, I. (**1984**) 'Photoisomerization of ethyl cinnamate in dilute solutions', *Journal of Photochemistry*, 26(2–3), pp. 185–192.

Shoda, S., Uyama, H., Kadokawa, J., Kimura, S. and Kobayashi, S. (**2016**) 'Enzymes as Green Catalysts for Precision Macromolecular Synthesis', *Chemical Reviews*, 116(4), pp. 2307–2413.

Silvestrini, L. and Cianci, M. (**2020**) 'Principles of lipid–enzyme interactions in the limbus region of the catalytic site of Candida antarctica Lipase B', *International Journal of Biological Macromolecules*, 158, pp. 358–363.

Singh, R. (**2020**) 'The New Normal for Bioplastics Amid the COVID-19 Pandemic', *Industrial Biotechnology*, 16(4), pp. 215–217.

Siracusa, V. and Blanco, I. (**2020**) 'Bio-Polyethylene (Bio-PE), Bio-Polypropylene (Bio-PP) and Bio-Poly(ethylene terephthalate) (Bio-PET): Recent Developments in Bio-Based Polymers Analogous to Petroleum-Derived Ones for Packaging and Engineering Applications', *Polymers*, 12(8), p. 1641.

Skoczinski, P., Espinoza Cangahuala, M. K., Maniar, D., Albach, R. W., Bittner, N. and Loos, K. (**2020**) 'Biocatalytic Synthesis of Furan-Based Oligomer Diols with Enhanced End-Group Fidelity', *ACS Sustainable Chemistry & Engineering*, 8(2), pp. 1068–1086.

Skoog, E., Shin, J. H., Saez-Jimenez, V., Mapelli, V. and Olsson, L. (**2018**) 'Biobased adipic acid – The challenge of developing the production host', *Biotechnology Advances*, 36(8), pp. 2248–2263.

Søndergaard, H. A., Grunert, K. G. and Scholderer, J. (**2005**) 'Consumer attitudes to enzymes in food production', *Trends in Food Science & Technology*, 16(10), pp. 466–474.

Sonseca, A. and El Fray, M. (**2017**) 'Enzymatic synthesis of an electrospinnable poly(butylene succinate-co-dilinoleic succinate) thermoplastic elastomer', *RSC Advances*, 7(34), pp. 21258–21267.

Sorour, N., Karboune, S., Saint-Louis, R. and Kermasha, S. (**2012**) 'Lipase-catalyzed synthesis of structured phenolic lipids in solvent-free system using flaxseed oil and selected phenolic acids as substrates', *Journal of Biotechnology*, 158(3), pp. 128–136.

Sousa, A. F., Vilela, C., Fonseca, A. C., Matos, M., Freire, C. S. R., Gruter, G.-J. M., Coelho, J. F. J. and Silvestre, A. J. D. (**2015**) 'Biobased polyesters and other polymers from 2,5-furandicarboxylic acid: a tribute to furan excellency', *Polymer Chemistry*, 6(33), pp. 5961–5983.

Spiridon, I., Bodirlau, R. and Teaca, C.-A. (**2011**) 'Total phenolic content and antioxidant activity of plants used in traditional Romanian herbal medicine', *Open Life Sciences*, 6(3), pp. 388–396.

Srinivasulu, C., Ramgopal, M., Ramanjaneyulu, G., Anuradha, C. M. and Suresh Kumar, C. (**2018**) 'Syringic acid (SA) – A Review of Its Occurrence, Biosynthesis, Pharmacological and Industrial Importance', *Biomedicine & Pharmacotherapy*, 108, pp. 547–557.

Stadler, B. M., Wulf, C., Werner, T., Tin, S. and de Vries, J. G. (**2019**) 'Catalytic Approaches to Monomers for Polymers Based on Renewables', *ACS Catalysis*, 9(9), pp. 8012–8067.

Stamatis, H., Sereti, V. and Kolisis, F. N. (**1999**) 'Studies on the enzymatic synthesis of lipophilic derivatives of natural antioxidants', *Journal of the American Oil Chemists' Society*, 76(12), p. 1505.

Stamatis, H., Sereti, V. and Kolisis, F. N. (**2001**) 'Enzymatic synthesis of hydrophilic and hydrophobic derivatives of natural phenolic acids in organic media', *Journal of Molecular Catalysis B: Enzymatic*, 11(4–6), pp. 323–328.

Stergiou, P.-Y., Foukis, A., Filippou, M., Koukouritaki, M., Parapouli, M., Theodorou, L. G., Hatziloukas, E., Afendra, A., Pandey, A. and Papamichael, E. M. (**2013**) 'Advances in lipase-catalyzed esterification reactions', *Biotechnology Advances*, 31(8), pp. 1846–1859.

Stevenson, D. E., Parkar, S. G., Zhang, J., Stanley, R. A., Jensen, D. J. and Cooney, J. M. (**2007**) 'Combinatorial enzymic synthesis for functional testing of phenolic acid esters catalysed by Candida antarctica lipase B (Novozym 435®)', *Enzyme and Microbial Technology*, 40(5), pp. 1078–1086.

Stobbe, H. (**1919**) 'Lichtreaktionen der Allo- und Isozimtsäuren', *Berichte der deutschen chemischen Gesellschaft (A and B Series)*, 52(4), pp. 666–672.

Suárez-Escobedo, L. and Gotor-Fernández, V. (**2021**) 'Solvent role in the lipase-catalysed esterification of cinnamic acid and derivatives. Optimisation of the biotransformation conditions', *Tetrahedron*, 81, p. 131873.

Sun, S. and Hu, B. (**2017**)**a** 'A novel method for the synthesis of glyceryl monocaffeate by the enzymatic transesterification and kinetic analysis', *Food Chemistry*, 214, pp. 192–198.

Sun, S. and Hu, B. (**2017**)**b** 'Enzymatic preparation of novel caffeoyl structured lipids using monoacylglycerols as caffeoyl acceptor and transesterification mechanism', *Biochemical Engineering Journal*, 124, pp. 78–87.

Sun, S., Lv, Y. and Zhu, S. (**2019**) 'Influence of ionic liquid on Novozym 435-catalyzed the transesterification of castor oil and ethyl caffeate', *3 Biotech*, 9(1), p. 34.

Sun, S., Shan, L., Jin, Q., Liu, Y. and Wang, X. (**2007**) 'Solvent-free synthesis of glyceryl ferulate using a commercial microbial lipase', *Biotechnology Letters*, 29(6), pp. 945–949.

Sun, S. and Tian, L. (**2018**)**a** 'Novozym 40086 as a novel biocatalyst to improve benzyl cinnamate synthesis', *RSC Advances*, 8(65), pp. 37184–37192.

Sun, S. and Zhu, S. (**2015**) 'Enzymatic preparation of castor oil-based feruloylated lipids using ionic liquids as reaction medium and kinetic model', *Industrial Crops and Products*, 73, pp. 127–133.

Sun, T., Zhang, H., Dong, Z., Liu, Z. and Zheng, M. (**2020**) 'Ultrasonic-promoted enzymatic preparation, identification and multi-active studies of nature-identical phenolic acid glycerol derivatives', *RSC Advances*, 10(19), pp. 11139–11147.

Sun, Z., Fridrich, B., de Santi, A., Elangovan, S. and Barta, K. (**2018**)**b** 'Bright Side of Lignin Depolymerization: Toward New Platform Chemicals', *Chemical Reviews*, 118(2), pp. 614–678.

Svobodova, A., Psotova, J. and Walterova, D. (**2003**) 'Natural phenolics in the prevention of UV-induced skin damage. A review', *Biomedical Papers*, 147(2), pp. 137–145.

Takamoto, T., Kerep, P., Uyama, H. and Kobayashi, S. (**2001**) 'Lipase-Catalyzed Transesterification of Polyesters to Ester Copolymers', *Macromolecular Bioscience*, 1(6), pp. 223–227.

Tan, Z. and Shahidi, F. (**2013**) 'Phytosteryl sinapates and vanillates: Chemoenzymatic synthesis and antioxidant capacity assessment', *Food Chemistry*, 138(2–3), pp. 1438–1447.

Tanaka, H. and Honda, K. (**1977**) 'Photoreversible reactions of polymers containing cinnamylideneacetate derivatives and the model compounds', *Journal of Polymer Science: Polymer Chemistry Edition*, 15(11), pp. 2685–2689.

Taresco, V., Creasey, R. G., Kennon, J., Mantovani, G., Alexander, C., Burley, J. C. and Garnett, M. C. (**2016**) 'Variation in structure and properties of poly(glycerol adipate) via control of chain branching during enzymatic synthesis', *Polymer*, 89, pp. 41–49.

Terrett, O. M. and Dupree, P. (**2019**) 'Covalent interactions between lignin and hemicelluloses in plant secondary cell walls', *Current Opinion in Biotechnology*, 56, pp. 97–104.

Terzopoulou, Z., Karakatsianopoulou, E., Kasmi, N., Tsanaktsis, V., Nikolaidis, N., Kostoglou, M., Papageorgiou, G. Z., Lambropoulou, D. A. and Bikiaris, D. N. (**2017**) 'Effect of catalyst type on molecular weight increase and coloration of poly(ethylene furanoate) biobased polyester during melt polycondensation', *Polymer Chemistry*, 8(44), pp. 6895–6908.

Terzopoulou, Z., Papadopoulos, L., Zamboulis, A., Papageorgiou, D. G., Papageorgiou, G. Z. and Bikiaris, D. N. (**2020**) 'Tuning the Properties of Furandicarboxylic Acid-Based Polyesters with Copolymerization: A Review', *Polymers*, 12(6), p. 1209.

Thi, T. H., Matsusaki, M. and Akashi, M. (**2009**)**a** 'Development of Photoreactive Degradable Branched Polyesters with High Thermal and Mechanical Properties', *Biomacromolecules*, 10(4), pp. 766–772.

Thi, T. H., Matsusaki, M. and Akashi, M. (**2009**)**b** 'Photoreactive Polylactide Nanoparticles by the Terminal Conjugation of Biobased Caffeic Acid', *Langmuir*, 25(18), pp. 10567–10574.

Thi, T. H., Matsusaki, M., Hirano, H., Kawano, H., Agari, Y. and Akashi, M. (**2011**) 'Mechanism of high thermal stability of commercial polyesters and polyethers conjugated with bio-based caffeic acid', *Journal of Polymer Science Part A: Polymer Chemistry*, 49(14), pp. 3152–3162.

Thi, T. H., Matsusaki, M., Shi, D., Kaneko, T. and Akashi, M. (**2008**) 'Synthesis and properties of coumaric acid derivative homo-polymers', *Journal of Biomaterials Science, Polymer Edition*, 19(1), pp. 75–85.

Thiyagarajan, S., Vogelzang, W., J. I. Knoop, R., Frissen, A. E., van Haveren, J. and van Es, D. S. (**2014**) 'Biobased furandicarboxylic acids (FDCAs): effects of isomeric substitution on polyester synthesis and properties', *Green Chem.*, 16(4), pp. 1957–1966.

Tinikul, R., Chenprakhon, P., Maenpuen, S. and Chaiyen, P. (**2018**) 'Biotransformation of Plant-Derived Phenolic Acids', *Biotechnology Journal*, p. 1700632.

Tobiszewski, M., Namieśnik, J. and Pena-Pereira, F. (**2017**) 'Environmental risk-based ranking of solvents using the combination of a multimedia model and multi-criteria decision analysis', *Green Chemistry*, 19(4), pp. 1034–1042.

Todea, A., Dreavă, D. M., Benea, I. C., Bîtcan, I., Peter, F. and Boeriu, C. G. (**2021**) 'Achievements and Trends in Biocatalytic Synthesis of Specialty Polymers from Biomass-Derived Monomers Using Lipases', *Processes*, 9(4), p. 646.

Tomás, R. A. F., Bordado, J. C. M. and Gomes, J. F. P. (**2013**) '*p* -Xylene Oxidation to Terephthalic Acid: A Literature Review Oriented toward Process Optimization and Development', *Chemical Reviews*, 113(10), pp. 7421–7469.

Topakas, E., Kalogeris, E., Kekos, D., Macris, B. J. and Christakopoulos, P. (**2003**)**a** 'Bioconversion of ferulic acid into vanillic acid by the thermophilic fungus Sporotrichum thermophile', *LWT - Food Science and Technology*, 36(6), pp. 561–565.

Topakas, E., Stamatis, H., Biely, P., Kekos, D., Macris, B. J. and Christakopoulos, P. (**2003**)**b** 'Purification and characterization of a feruloyl esterase from Fusarium oxysporum catalyzing esterification of phenolic acids in ternary water–organic solvent mixtures', *Journal of Biotechnology*, 102(1), pp. 33–44.

Topakas, E., Stamatis, H., Mastihubova, M., Biely, P., Kekos, D., Macris, B. J. and Christakopoulos, P. (**2003**)**c** 'Purification and characterization of a Fusarium oxysporum feruloyl esterase (FoFAE-I) catalysing transesterification of phenolic acid esters', *Enzyme and Microbial Technology*, 33(5), pp. 729–737.

Topakas, E., Vafiadi, C. and Christakopoulos, P. (**2007**) 'Microbial production, characterization and applications of feruloyl esterases', *Process Biochemistry*, 42(4), pp. 497–509.

Topakas, E., Vafiadi, C., Stamatis, H. and Christakopoulos, P. (**2005**) 'Sporotrichum thermophile type C feruloyl esterase (StFaeC): purification, characterization, and its use for phenolic acid (sugar) ester synthesis', *Enzyme and Microbial Technology*, 36(5–6), pp. 729–736.

Toth, G. and Hensler, D. (**1952**) 'Über die enzymatische synthese der gallussäure-derivaten', *Acta chimica Hungarica*, 2, pp. 209–210.

Tournier, V., Topham, C. M., Gilles, A., David, B., Folgoas, C., Moya-Leclair, E., Kamionka, E., Desrousseaux, M.-L., Texier, H., Gavalda, S., Cot, M., Guémard, E., Dalibey, M., Nomme, J., Cioci, G., Barbe, S., Chateau, M., André, I., Duquesne, S. and Marty, A. (**2020**) 'An engineered PET depolymerase to break down and recycle plastic bottles', *Nature*, 580(7802), pp. 216–219.

Tserki, V., Matzinos, P., Pavlidou, E., Vachliotis, D. and Panayiotou, C. (**2006**) 'Biodegradable aliphatic polyesters. Part I. Properties and biodegradation of poly(butylene succinate-co-butylene adipate)', *Polymer Degradation and Stability*, 91(2), pp. 367–376.

Tsuchiyama, M., Sakamoto, T., Fujita, T., Murata, S. and Kawasaki, H. (**2006**) 'Esterification of ferulic acid with polyols using a ferulic acid esterase from Aspergillus niger', *Biochimica et Biophysica Acta (BBA) - General Subjects*, 1760(7), pp. 1071–1079.

Tsuchiyama, M., Sakamoto, T., Tanimori, S., Murata, S. and Kawasaki, H. (**2007**) 'Enzymatic Synthesis of Hydroxycinnamic Acid Glycerol Esters Using Type A Feruloyl Esterase from *Aspergillus niger*', *Bioscience, Biotechnology, and Biochemistry*, 71(10), pp. 2606–2609.

Tümer, E. H. and Erbil, H. Y. (**2021**) 'Extrusion-Based 3D Printing Applications of PLA Composites: A Review', *Coatings*, 11(4), p. 390.

Ülger, C. and Takaç, S. (**2017**) 'Kinetics of lipase-catalysed methyl gallate production in the presence of deep eutectic solvent', *Biocatalysis and Biotransformation*, 35(6), pp. 407–416.

Vafiadi, C., Topakas, E., Alissandratos, A., Faulds, C. B. and Christakopoulos, P. (**2008**) 'Enzymatic synthesis of butyl hydroxycinnamates and their inhibitory effects on LDL-oxidation', *Journal of Biotechnology*, 133(4), pp. 497–504.

Vafiadi, C., Topakas, E., Nahmias, V. R., Faulds, C. B. and Christakopoulos, P. (**2009**) 'Feruloyl esterase-catalysed synthesis of glycerol sinapate using ionic liquids mixtures', *Journal of Biotechnology*, 139(1), pp. 124–129.

Vafiadi, C., Topakas, E., Wong, K. K. Y., Suckling, I. D. and Christakopoulos, P. (**2005**) 'Mapping the hydrolytic and synthetic selectivity of a type C feruloyl esterase (StFaeC) from Sporotrichum thermophile using alkyl ferulates', *Tetrahedron: Asymmetry*, 16(2), pp. 373–379.

Valanciene, E., Jonuskiene, I., Syrpas, M., Augustiniene, E., Matulis, P., Simonavicius, A. and Malys, N. (**2020**) 'Advances and Prospects of Phenolic Acids Production, Biorefinery and Analysis', *Biomolecules*, 10(6), p. 874.

Varma, I. K., Albertsson, A.-C., Rajkhowa, R. and Srivastava, R. K. (**2005**) 'Enzyme catalyzed synthesis of polyesters', *Progress in Polymer Science*, 30(10), pp. 949–981.

Varriale, S., Cerullo, G., Antonopoulou, I., Christakopoulos, P., Rova, U., Tron, T., Fauré, R., Jütten, P., Piechot, A., Brás, J. L. A., Fontes, C. M. G. A. and Faraco, V. (**2018**) 'Evolution of the feruloyl esterase MtFae1a from Myceliophthora thermophila towards improved catalysts for antioxidants synthesis', *Applied Microbiology and Biotechnology*, 102(12), pp. 5185–5196.

Vilela, C., Sousa, A. F., Fonseca, A. C., Serra, A. C., Coelho, J. F. J., Freire, C. S. R. and Silvestre, A. J. D. (**2014**) 'The quest for sustainable polyesters – insights into the future', *Polym. Chem.*, 5(9), pp. 3119–3141.

Villeneuve, P. (**2007**) 'Lipases in lipophilization reactions', *Biotechnology Advances*, 25(6), pp. 515–536.

Volanti, M., Cespi, D., Passarini, F., Neri, E., Cavani, F., Mizsey, P. and Fozer, D. (**2019**) 'Terephthalic acid from renewable sources: early-stage sustainability analysis of a bio-PET precursor', *Green Chemistry*, 21(4), pp. 885–896.

Vosmann, K., Weitkamp, P. and Weber, N. (**2006**) 'Solvent-free Lipase-Catalyzed Preparation of Long-Chain Alkyl Phenylpropanoates and Phenylpropyl Alkanoates', *Journal of Agricultural and Food Chemistry*, 54(8), pp. 2969–2976.

Vosmann, K., Wiege, B., Weitkamp, P. and Weber, N. (**2008**) 'Preparation of lipophilic alkyl (hydroxy)benzoates by solvent-free lipase-catalyzed esterification and transesterification', *Applied Microbiology and Biotechnology*, 80(1), pp. 29–36.

Vouyiouka, S. N., Topakas, E., Katsini, A., Papaspyrides, C. D. and Christakopoulos, P. (**2013**) 'A Green Route for the Preparation of Aliphatic Polyesters via Lipase-catalyzed Prepolymerization and Low-temperature Postpolymerization', *Macromolecular Materials and Engineering*, 298(6), pp. 679–689.

Wang, B., Ma, S., Li, Q., Zhang, H., Liu, J., Wang, R., Chen, Z., Xu, X., Wang, S., Lu, N., Liu, Y., Yan, S. and Zhu, J. (**2020**)**a** 'Facile synthesis of "digestible", rigid-and-flexible, bio-based building block for high-performance degradable thermosetting plastics', *Green Chemistry*, 22(4), pp. 1275–1290.

Wang, Y., Zhang, D.-H., Chen, N. and Zhi, G.-Y. (**2015**)**a** 'Synthesis of benzyl cinnamate by enzymatic esterification of cinnamic acid', *Bioresource Technology*, 198, pp. 256–261.

Wang, Y., Zhang, D.-H., Zhang, J.-Y., Chen, N. and Zhi, G.-Y. (**2016**)**a** 'High-yield synthesis of bioactive ethyl cinnamate by enzymatic esterification of cinnamic acid', *Food Chemistry*, 190, pp. 629–633.

Wang, Z., Flores, Q., Guo, H., Trevizo, R., Zhang, X. and Wang, S. (**2020**)**b** 'Crystal engineering construction of caffeic acid derivatives with potential applications in pharmaceuticals and degradable polymeric materials', *CrystEngComm*, 22(45), pp. 7847–7857.

Wang, Z., Hwang, S. H. and Lim, S. S. (**2015**)**b** 'Lipophilization of phenolic acids with phytosterols by a chemoenzymatic method to improve their antioxidant activities: Lipophilization of phenolic acids with phytosterols', *European Journal of Lipid Science and Technology*, 117(7), pp. 1037–1048.

Wang, Z., Hwang, S. H. and Lim, S. S. (**2016**)**b** 'Effect of Novel Synthesised Policosanyl Phenolates on Lipid Oxidation', *Czech Journal of Food Sciences*, 34(5), pp. 414–421.

Wang, Z., Miller, B., Mabin, M., Shahni, R., Wang, Z. D., Ugrinov, A. and Chu, Q. R. (**2017**) 'Cyclobutane-1,3-Diacid (CBDA): A Semi-Rigid Building Block Prepared by [2+2] Photocyclization for Polymeric Materials', *Scientific Reports*, 7(1).

Weetal, H. H. (**1985**) 'Enzymatic gallic acid esterification', *Biotechnology and Bioengineering*, 27(2), pp. 124–127.

Weinberger, S., Haernvall, K., Scaini, D., Ghazaryan, G., Zumstein, M. T., Sander, M., Pellis, A. and Guebitz, G. M. (**2017**) 'Enzymatic surface hydrolysis of poly(ethylene furanoate) thin films of various crystallinities', *Green Chemistry*, 19(22), pp. 5381–5384.

Weitkamp, P., Vosmann, K. and Weber, N. (**2006**) 'Highly Efficient Preparation of Lipophilic Hydroxycinnamates by Solvent-free Lipase-Catalyzed Transesterification', *Journal of Agricultural and Food Chemistry*, 54(19), pp. 7062–7068.

Wu, B., Xu, Y., Bu, Z., Wu, L., Li, B.-G. and Dubois, P. (**2014**) 'Biobased poly(butylene 2,5-furandicarboxylate) and poly(butylene adipate-co-butylene 2,5-furandicarboxylate)s: From synthesis using highly purified 2,5-furandicarboxylic acid to thermo-mechanical properties', *Polymer*, 55(16), pp. 3648–3655.

Wu, L., Jin, C. and Sun, X. (**2011**) 'Synthesis, Properties, and Light-Induced Shape Memory Effect of Multiblock Polyesterurethanes Containing Biodegradable Segments and Pendant Cinnamamide Groups', *Biomacromolecules*, 12(1), pp. 235–241.

Xanthopoulou, E., Zamboulis, A., Terzopoulou, Z., Kostoglou, M., Bikiaris, D. N. and Papageorgiou, G. Z. (**2021**) 'Effectiveness of Esterification Catalysts in the Synthesis of Poly(Ethylene Vanillate)', *Catalysts*, 11(7), p. 822.

Xie, H., Yang, K.-K. and Wang, Y.-Z. (**2019**) 'Photo-cross-linking: A powerful and versatile strategy to develop shape-memory polymers', *Progress in Polymer Science*, 95, pp. 32–64.

Yagi, Y., Kimura, T., Kamezawa, M. and Naoshima, Y. (**2018**) 'Biomolecular Chemical Simulations toward Elucidation of the Enantioselectivity and Reactivity of Lipases in Organic Synthesis', *Chem-Bio Informatics Journal*, 18(0), pp. 21–31.

Yan, S., Elmes, M. W., Tong, S., Hu, K., Awwa, M., Teng, G. Y. H., Jing, Y., Freitag, M., Gan, Q., Clement, T., Wei, L., Sweeney, J. M., Joseph, O. M., Che, J., Carbonetti, G. S., Wang, L., Bogdan, D. M., Falcone, J., Smietalo, N., Zhou, Y., Ralph, B., Hsu, H.-C., Li, H., Rizzo, R. C., Deutsch, D. G., Kaczocha, M. and Ojima, I. (**2018**) 'SAR studies on truxillic acid mono esters as a new class of antinociceptive agents targeting fatty acid binding proteins', *European Journal of Medicinal Chemistry*, 154, pp. 233–252.

Yang, H., Mu, Y., Chen, H., Xiu, Z. and Yang, T. (**2013**) 'Enzymatic synthesis of feruloylated lysophospholipid in a selected organic solvent medium', *Food Chemistry*, 141(4), pp. 3317–3322.

Yang, Q., Zhu, S., Yang, Q., Huang, W., Yu, P., Zhang, D. and Wang, Z. (**2019**) 'Comparative techno-economic analysis of oil-based and coal-based ethylene glycol processes', *Energy Conversion and Management*, 198, p. 111814.

Yang, R.-L., Li, N., Ye, M. and Zong, M.-H. (**2010**) 'Highly regioselective synthesis of novel aromatic esters of arbutin catalyzed by immobilized lipase from Penicillium expansum', *Journal of Molecular Catalysis B: Enzymatic*, 67(1–2), pp. 41–44.

Yang, Z., Guo, Z. and Xu, X. (**2012**) 'Enzymatic lipophilisation of phenolic acids through esterification with fatty alcohols in organic solvents', *Food Chemistry*, 132(3), pp. 1311–1315.

Yao, N. and Sun, S. (**2020**) 'Hydrophilic Glyceryl Ferulates Preparation Catalyzed by Free Lipase B from *Candida antartica*', *Journal of Oleo Science*, 69(1), pp. 43–53.

Yoshida, Y., Kimura, Y., Kadota, M., Tsuno, T. and Adachi, S. (**2006**) 'Continuous synthesis of alkyl ferulate by immobilized Candida antarctica lipase at high temperature', *Biotechnology Letters*, 28(18), pp. 1471–1474.

Yu, X., Li, Y. and Wu, D. (**2004**)**a** 'Enzymatic synthesis of gallic acid esters using microencapsulated tannase: effect of organic solvents and enzyme specificity', *Journal of Molecular Catalysis B: Enzymatic*, 30(2), pp. 69–73.

Yu, X., Li, Y. and Wu, D. (**2004**)**b** 'Microencapsulation of tannase by chitosan–alginate complex coacervate membrane: synthesis of antioxidant propyl gallate in biphasic media', *Journal of Chemical Technology & Biotechnology*, 79(5), pp. 475–479.

Yu, X.-W. and Li, Y.-Q. (**2006**) 'Kinetics and thermodynamics of synthesis of propyl gallate by mycelium-bound tannase from Aspergillus niger in organic solvent', *Journal of Molecular Catalysis B: Enzymatic*, 40(1–2), pp. 44–50.

Yu, X.-W. and Li, Y.-Q. (**2008**) 'Expression of Aspergillus oryzae Tannase in Pichia pastoris and Its Application in the Synthesis of Propyl Gallate in Organic Solvent', p. 6.

Yu, Z., Zhou, J., Cao, F., Wen, B., Zhu, X. and Wei, P. (**2013**) 'Chemosynthesis and characterization of fully biomass-based copolymers of ethylene glycol, 2,5-furandicarboxylic acid, and succinic acid', *Journal of Applied Polymer Science*, 130(2), pp. 1415–1420.

'YXY® Technology' (**2021**) *Avantium*. Available at: https://www.avantium.com/technologies/yxy/ (Accessed: 14 September 2021).

Zhang, H., Li, X., Lin, Y., Gao, F., Tang, Z., Su, P., Zhang, W., Xu, Y., Weng, W. and Boulatov, R. (**2017**) 'Multi-modal mechanophores based on cinnamate dimers', *Nature Communications*, 8(1), p. 1147.

Zhang, Q., Song, M., Xu, Y., Wang, W., Wang, Z. and Zhang, L. (**2021**) 'Bio-based polyesters: Recent progress and future prospects', *Progress in Polymer Science*, 120, p. 101430.

Zhang, S. and Akoh, C. C. (**2019**) 'Solvent-Free Enzymatic Synthesis of 1-*o*-Galloylglycerol Optimized by the Taguchi Method', *Journal of the American Oil Chemists' Society*, 96(8), pp. 877–889.

Zhang, S. and Akoh, C. C. (**2020**)**a** 'Antioxidant property and characterization data of 1-o-galloylglycerol synthesized via enzymatic glycerolysis', *Data in Brief*, 29, p. 105110.

Zhang, S. and Akoh, C. C. (**2020**)**b** 'Enzymatic synthesis of 1-o-galloylglycerol: Characterization and determination of its antioxidant properties', *Food Chemistry*, 305, p. 125479.

Zhang, S.-B., Pei, X.-Q. and Wu, Z.-L. (**2012**) 'Multiple amino acid substitutions significantly improve the thermostability of feruloyl esterase A from Aspergillus niger', *Bioresource Technology*, 117, pp. 140–147.

Zhao, Z. and Moghadasian, M. H. (**2008**) 'Chemistry, natural sources, dietary intake and pharmacokinetic properties of ferulic acid: A review', *Food Chemistry*, 109(4), pp. 691–702.

Zhou, W., Wang, X., Yang, B., Xu, Y., Zhang, W., Zhang, Y. and Ji, J. (**2013**) 'Synthesis, physical properties and enzymatic degradation of bio-based poly(butylene adipate-co-butylene furandicarboxylate) copolyesters', *Polymer Degradation and Stability*, 98(11), pp. 2177–2183.

Zia, K. M., Noreen, A., Zuber, M., Tabasum, S. and Mujahid, M. (**2016**) 'Recent developments and future prospects on bio-based polyesters derived from renewable resources: A review', *International Journal of Biological Macromolecules*, 82, pp. 1028–1040.

Zieniuk, B., Wołoszynowska, M., Białecka-Florjańczyk, E. and Fabiszewska, A. (**2020**) 'Synthesis of Industrially Useful Phenolic Compounds Esters by Means of Biocatalysts Obtained Along with Waste Fish Oil Utilization', p. 18.

Zoumpanioti, M., Merianou, E., Karandreas, T., Stamatis, H. and Xenakis, A. (**2010**) 'Esterification of phenolic acids catalyzed by lipases immobilized in organogels', *Biotechnology Letters*, 32(10), pp. 1457–1462.

Annexes

Annexes Chapitre 2 (supporting information) 267

Annexes Chapitre 3 (supporting information) 291

Annexes Chapitre 4 (supporting information) 305

Annexes Chapitre 5 (supporting information) 319

Annexes Chapitre 2 (supporting information)

NMR spectra of PHAd-co-PHF containing from 0 to 100 % of DMFDC

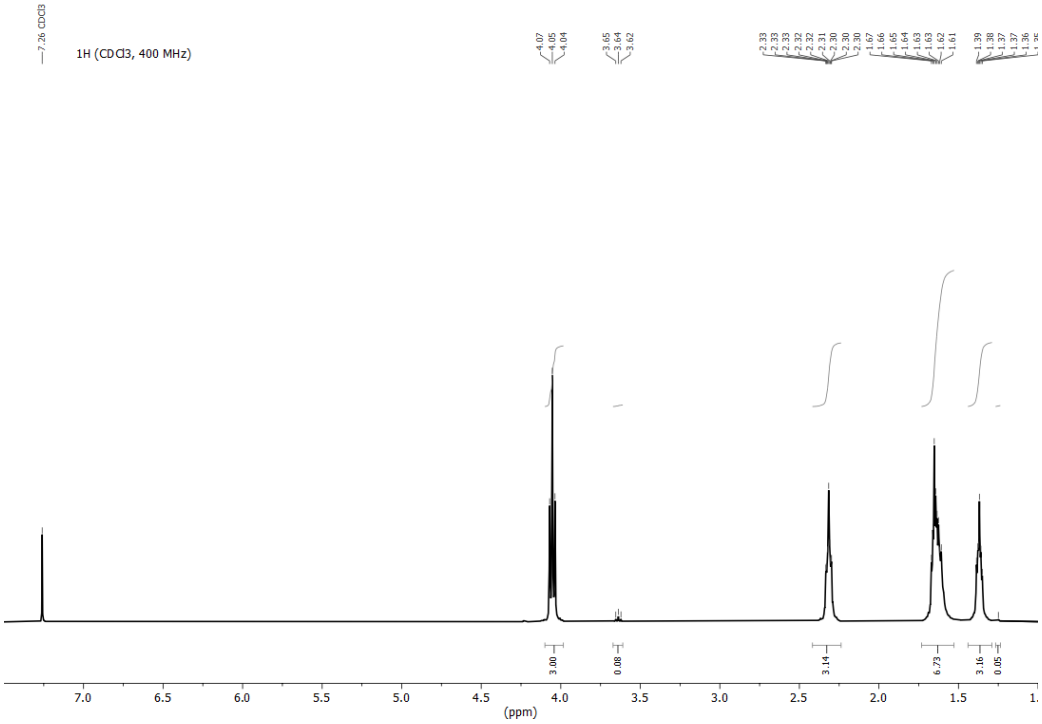

Figure S2.1: NMR spectrum of PHAd in $CDCl_3$

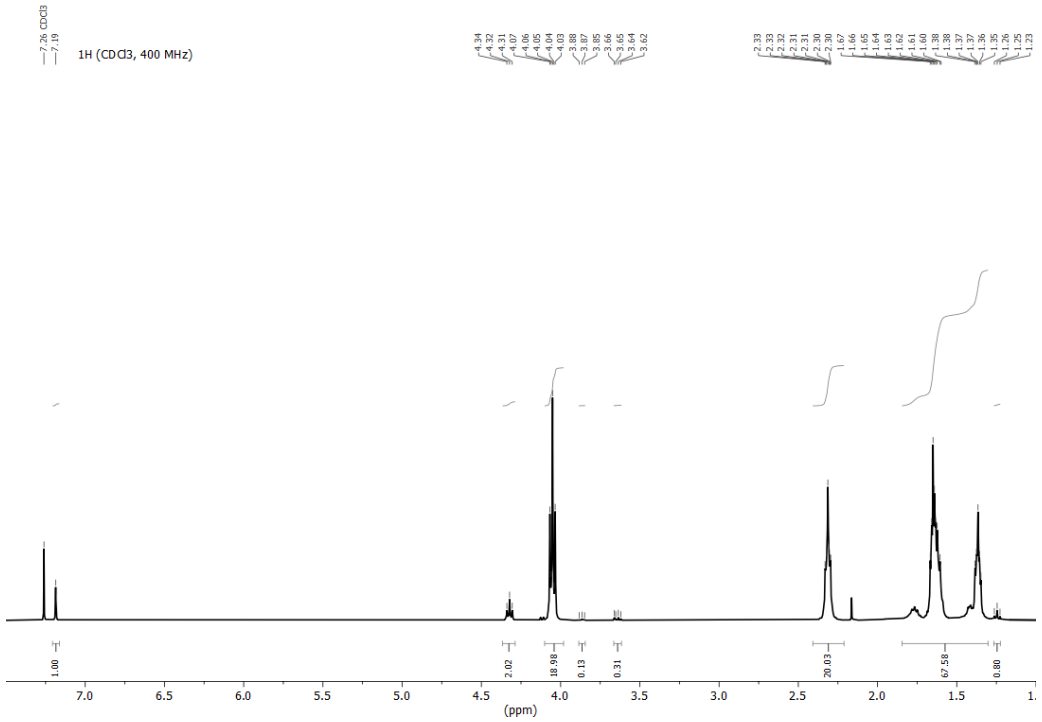

Figure S2.2: NMR spectrum of PHF10 in $CDCl_3$

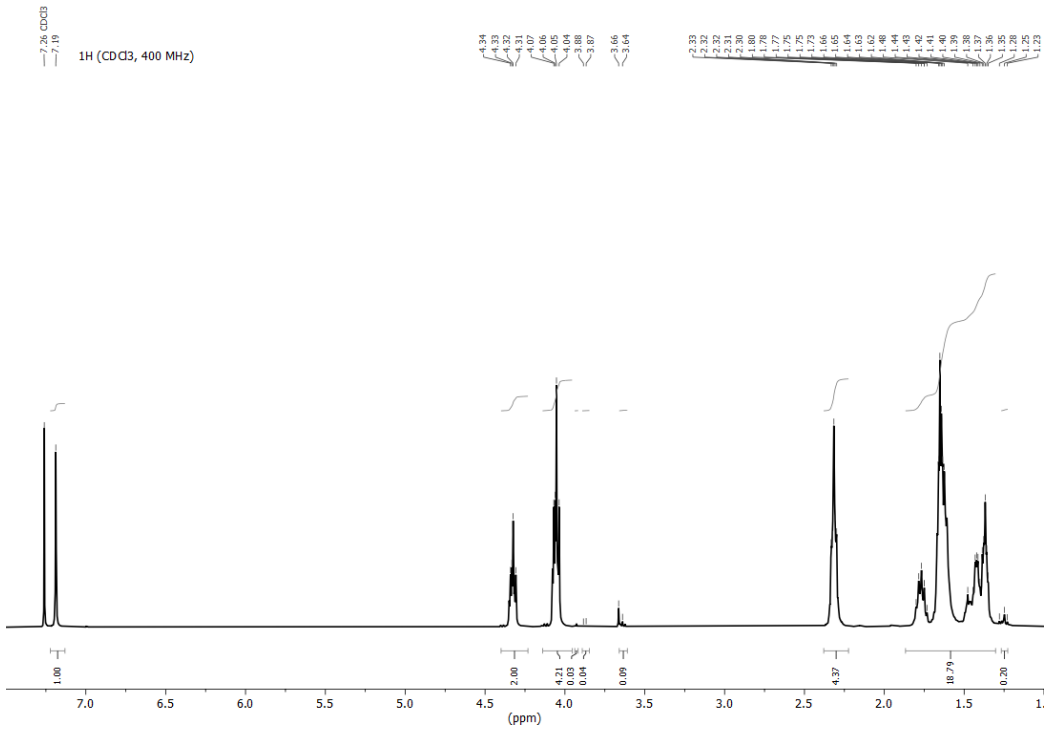

Figure S2.3: NMR spectrum of PHF30 in $CDCl_3$

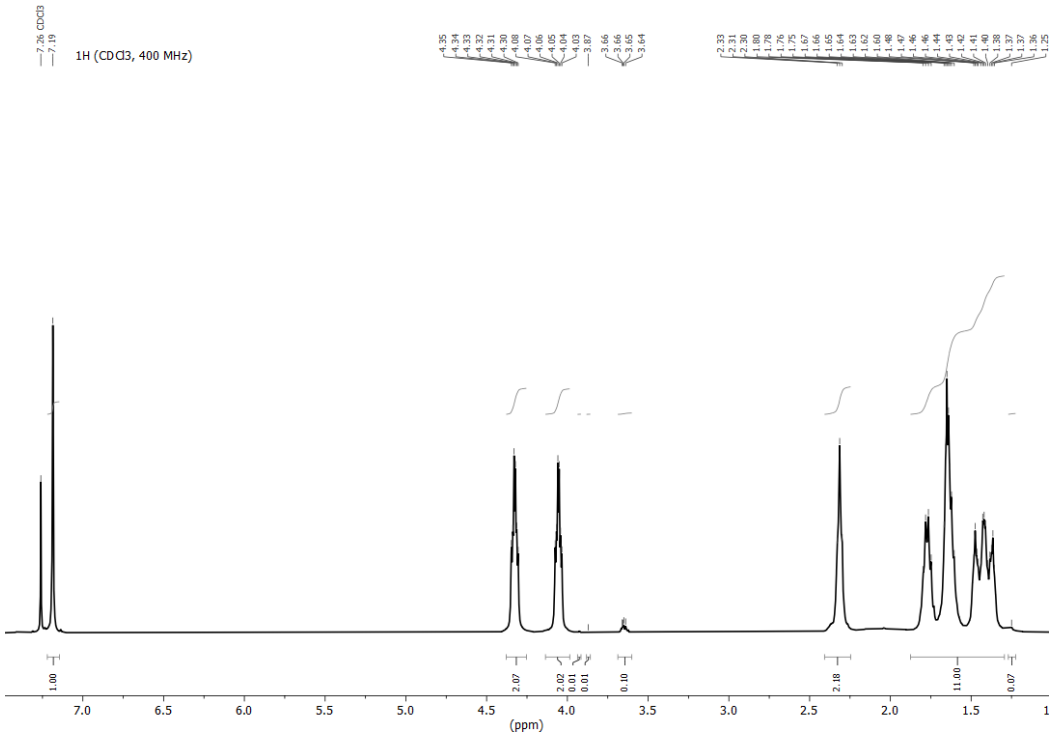

Figure S2.4: NMR spectrum of PHF50 in $CDCl_3$

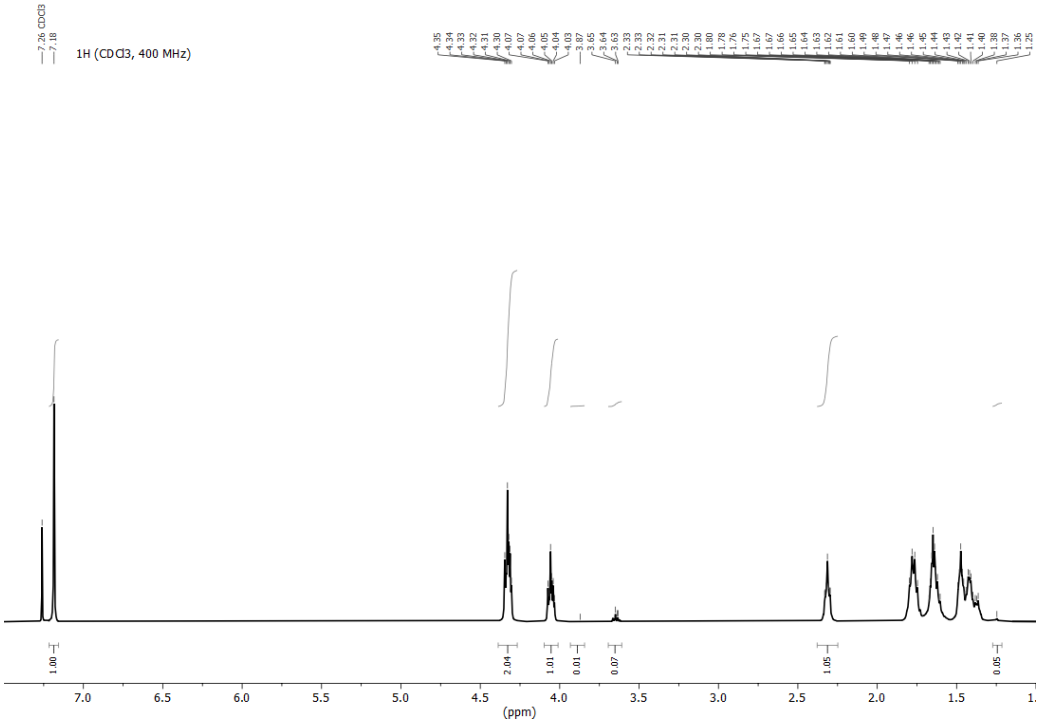

Figure S2.5: NMR spectrum of PHF70 in $CDCl_3$

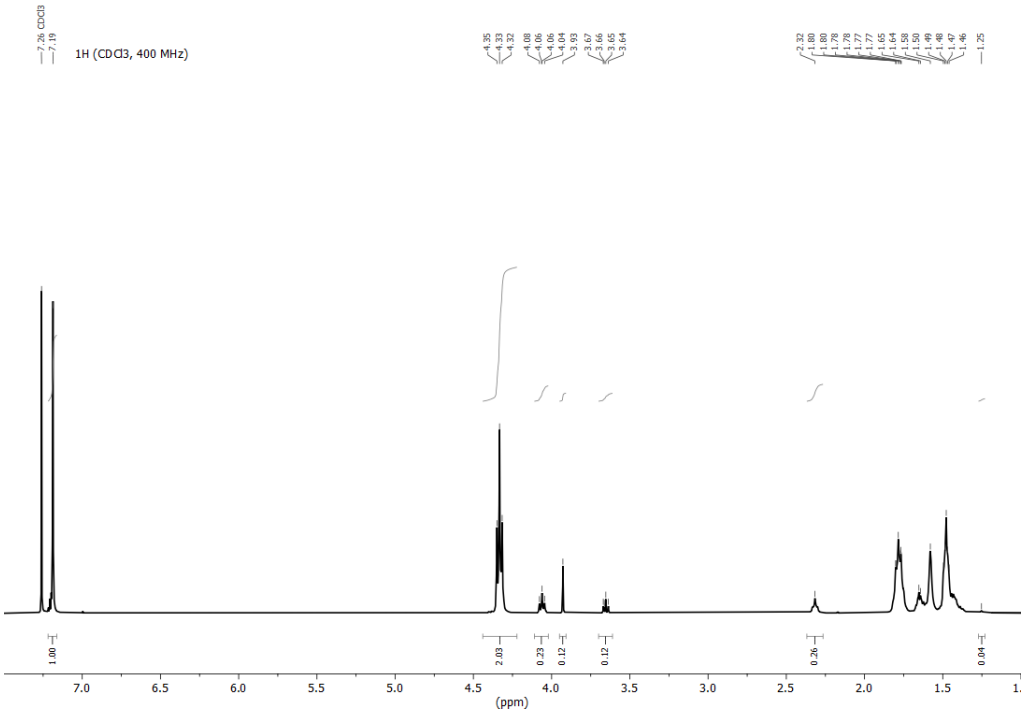

Figure S2.6: NMR spectrum of PHF90 in $CDCl_3$

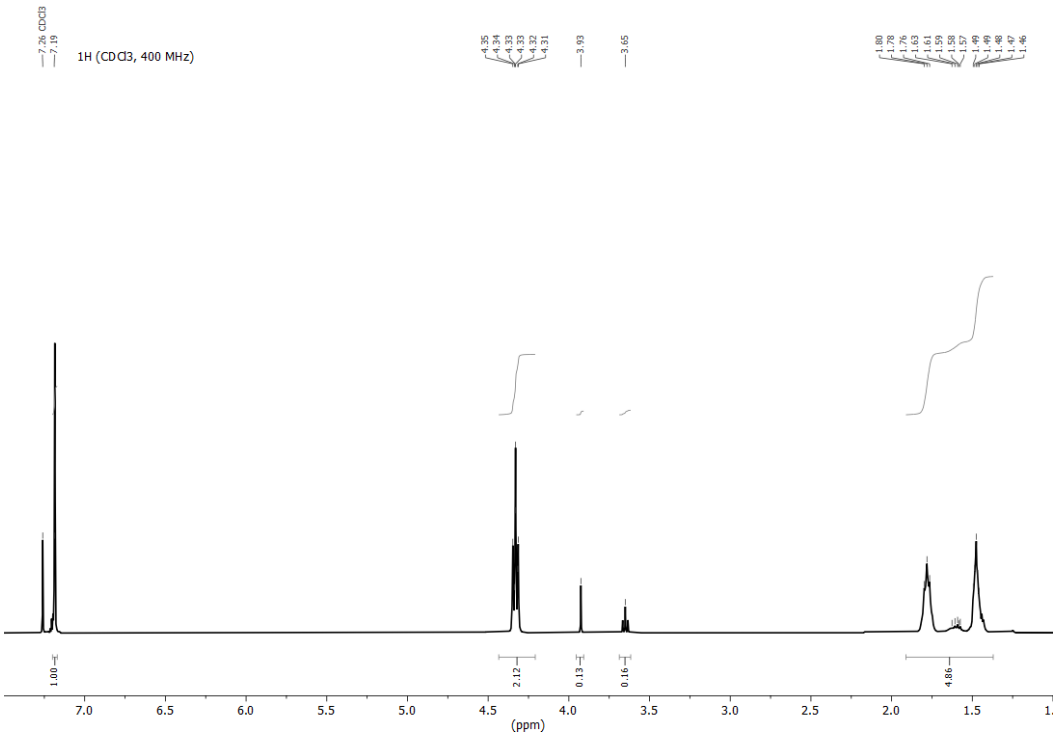

Figure S2.7: NMR spectrum of PHF in $CDCl_3$

2D NMR analyses of PHF50

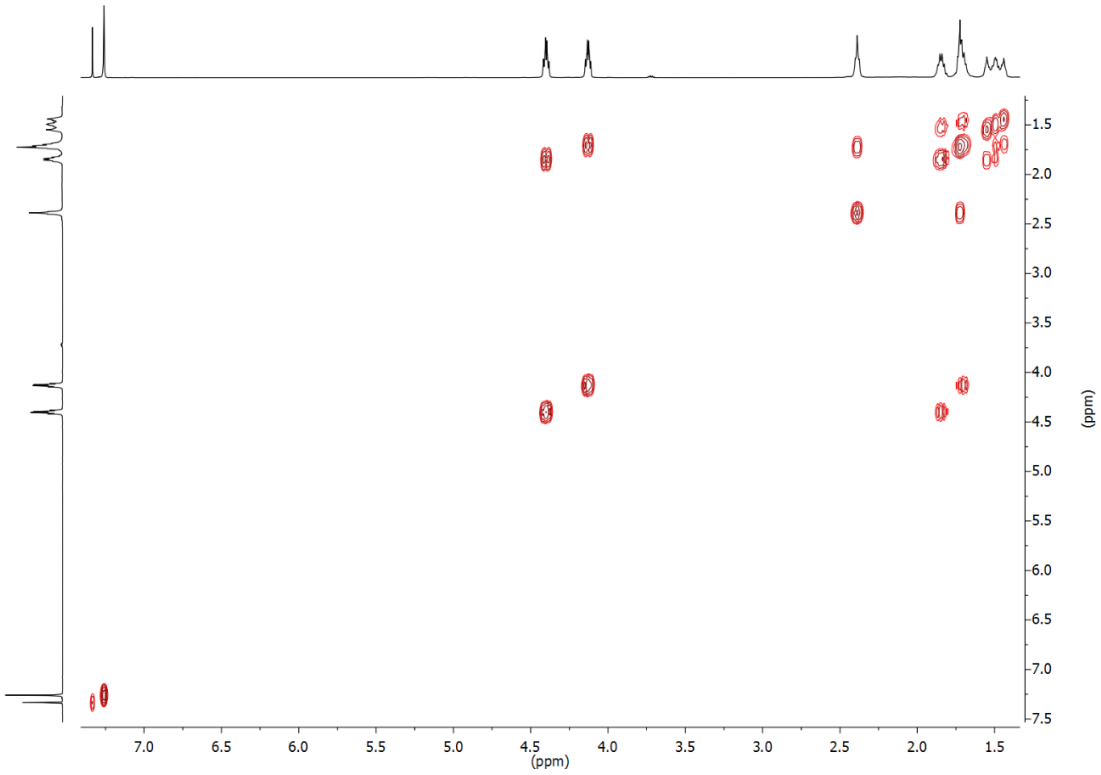

Figure S2.8: COSY NMR analysis of PHF50 in $CDCl_3$

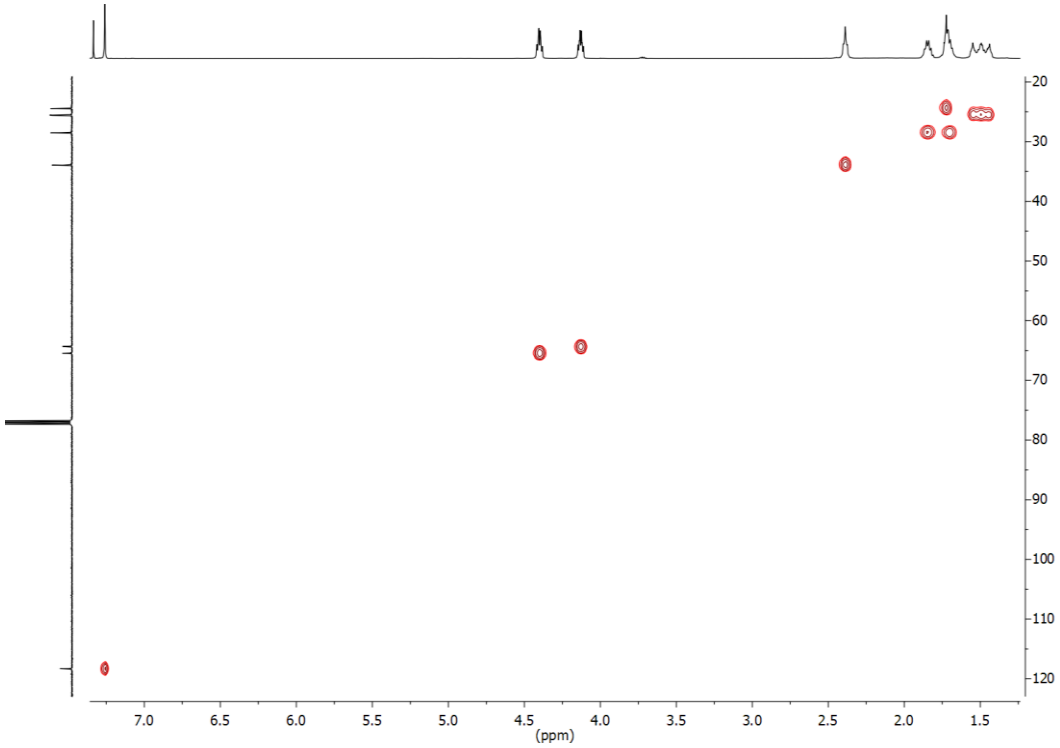

Figure S2.9: HSQC NMR analysis of PHF50 in $CDCl_3$

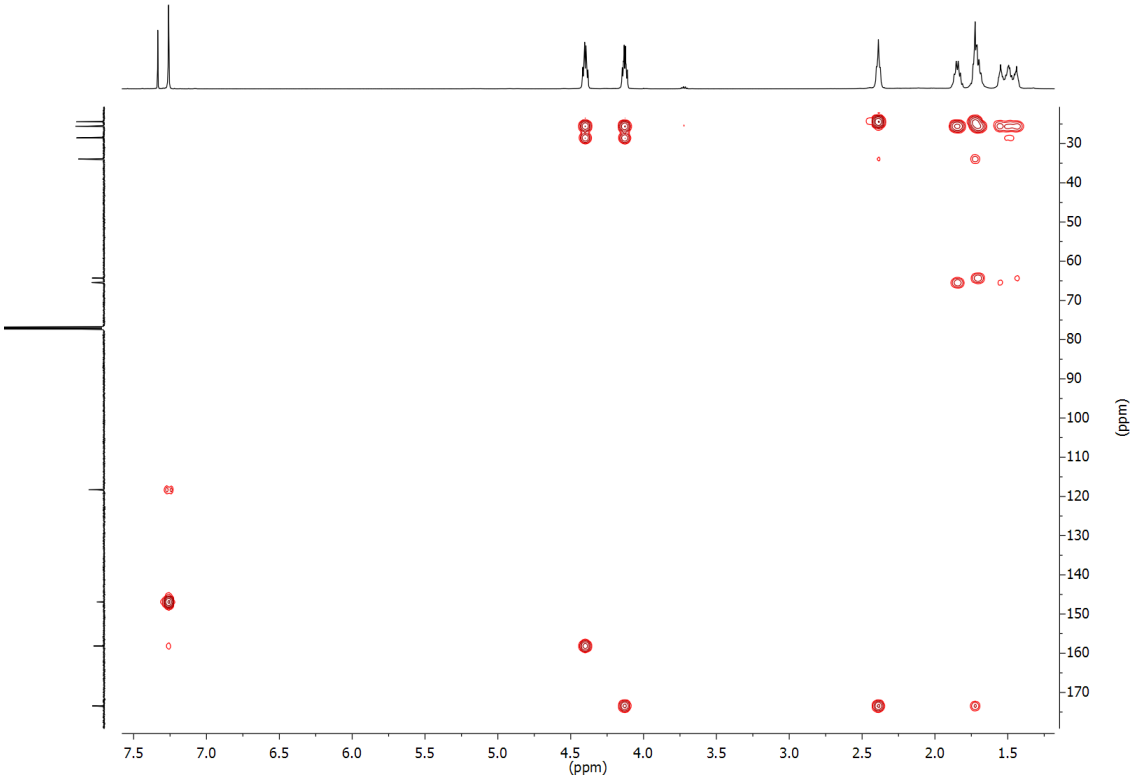

Figure S2.10: HMBC NMR analysis of PHF50 in $CDCl_3$

NMR spectra of PBAd-co-PBF containing from 0 to 100 % of DMFDC

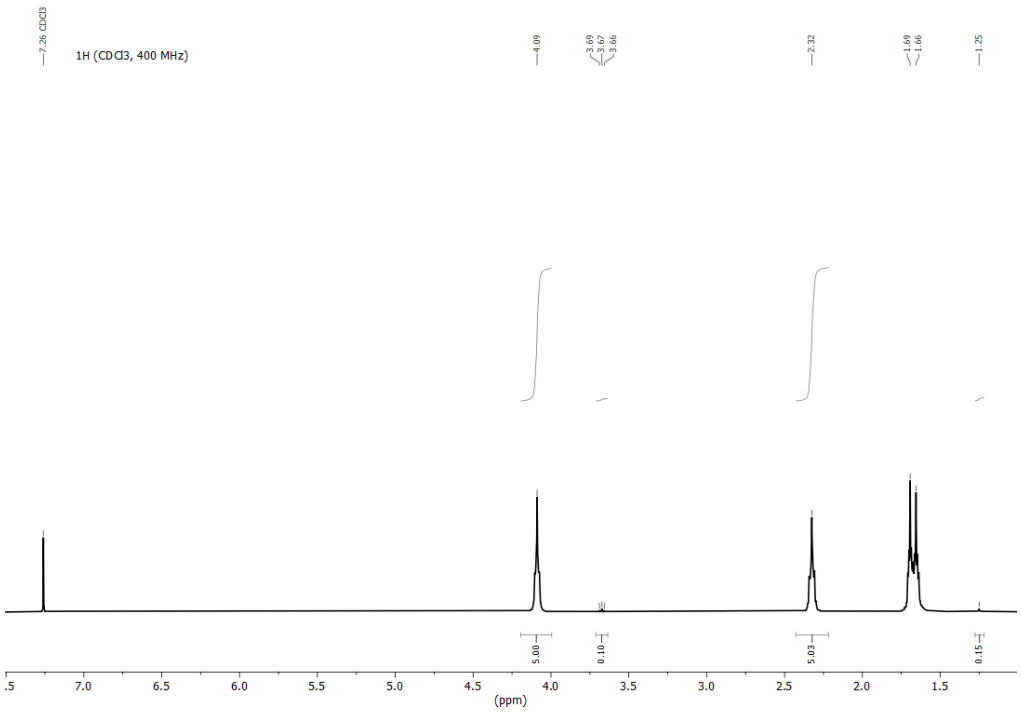

Figure S2.11: NMR spectrum of PBAd in $CDCl_3$

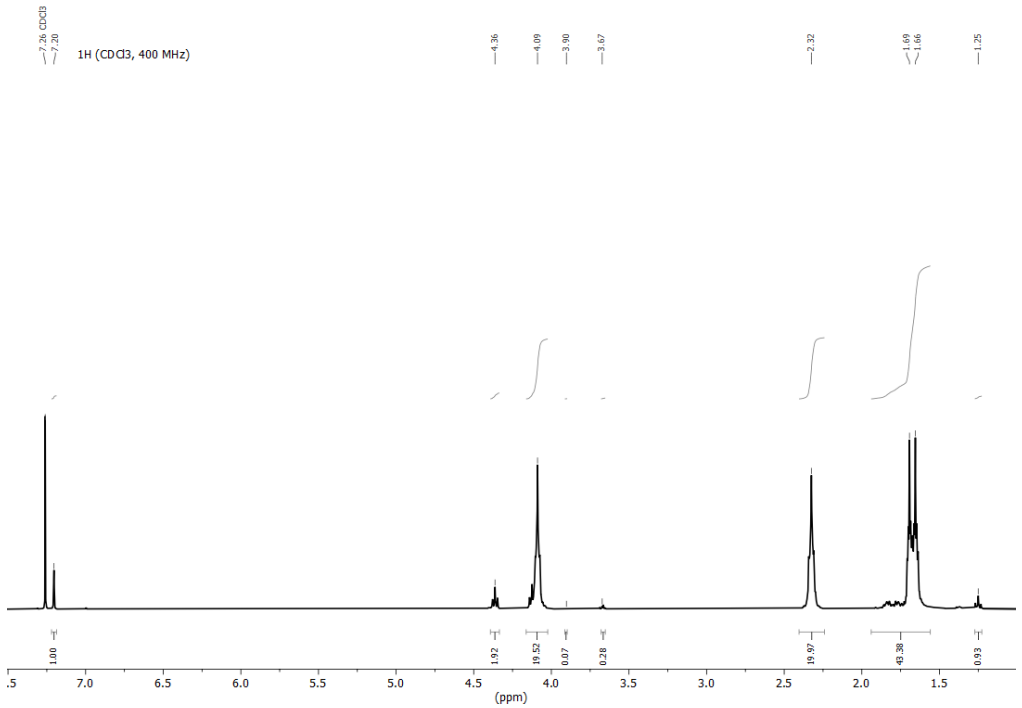

Figure S2.12: NMR spectrum of PBF10 in $CDCl_3$

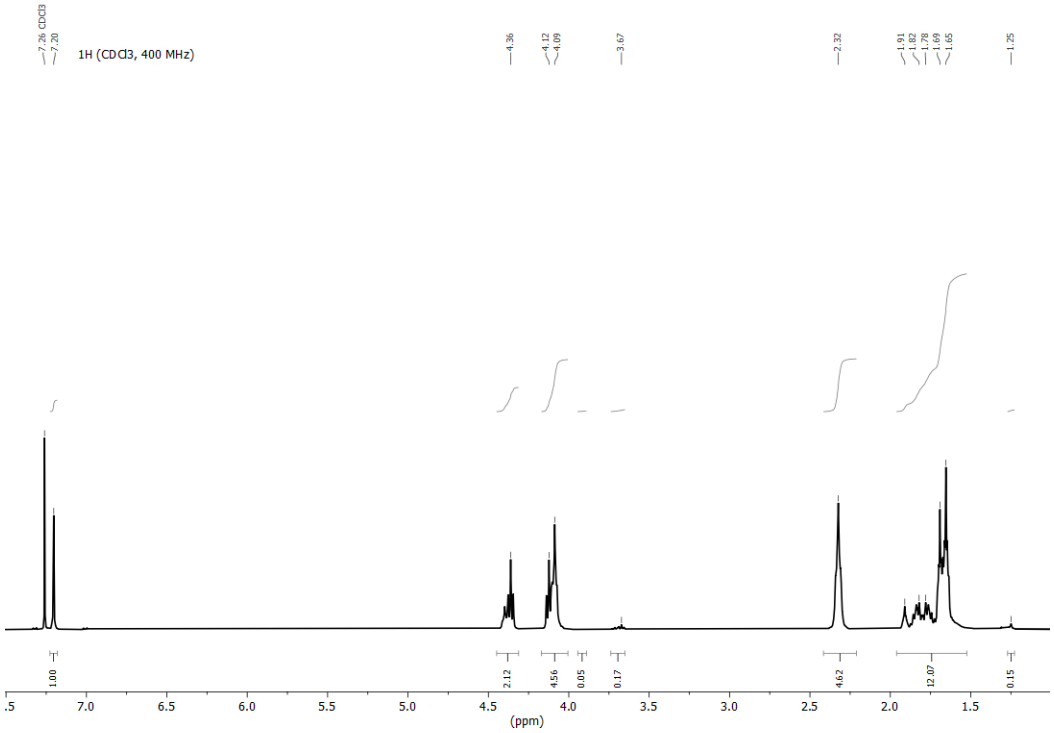

Figure S2.13: NMR spectrum of PBF30 in $CDCl_3$

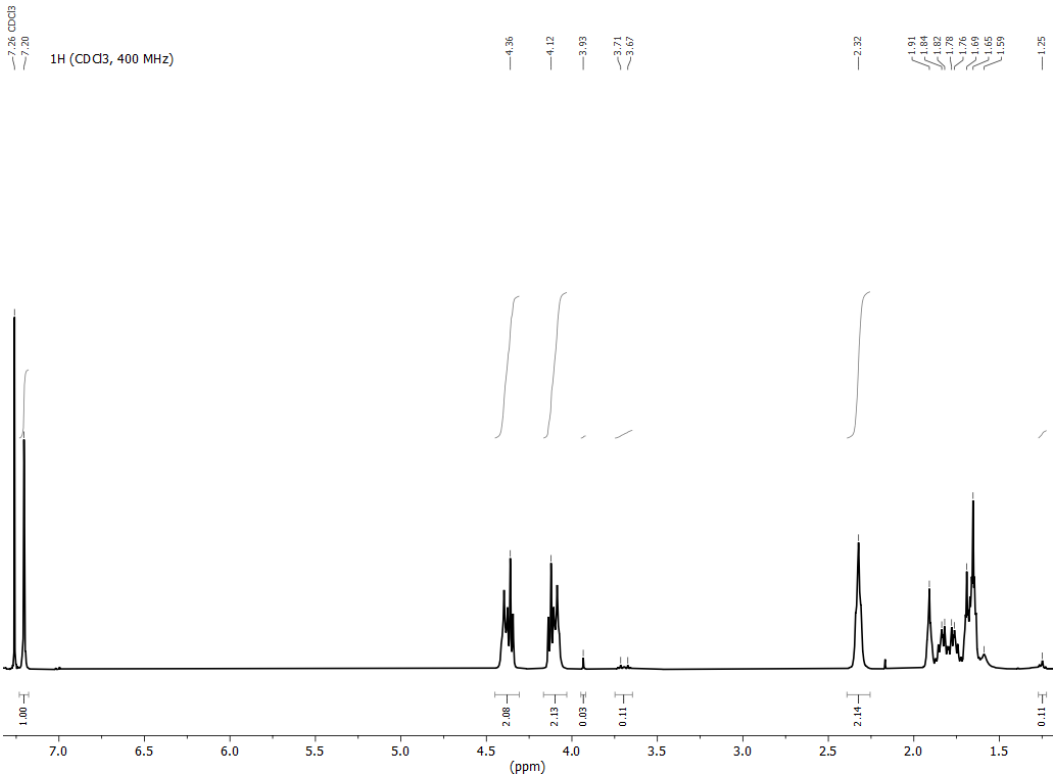

Figure S2.14: NMR spectrum of PBF50 in $CDCl_3$

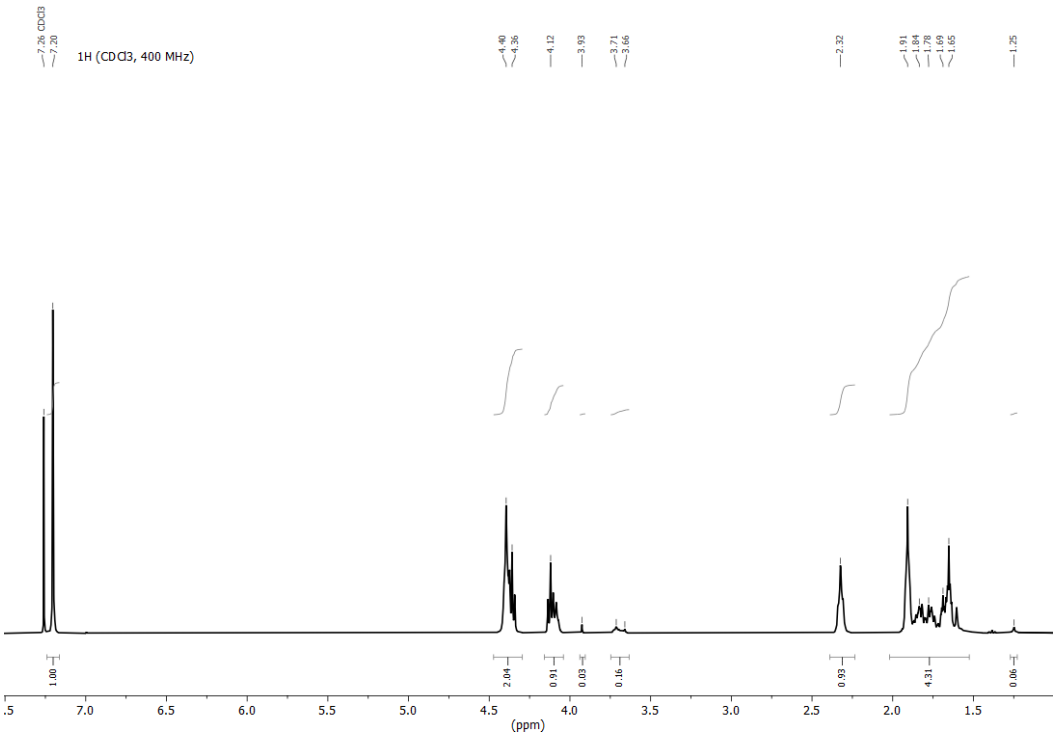

Figure S2.15: NMR spectrum of PBF70 in $CDCl_3$

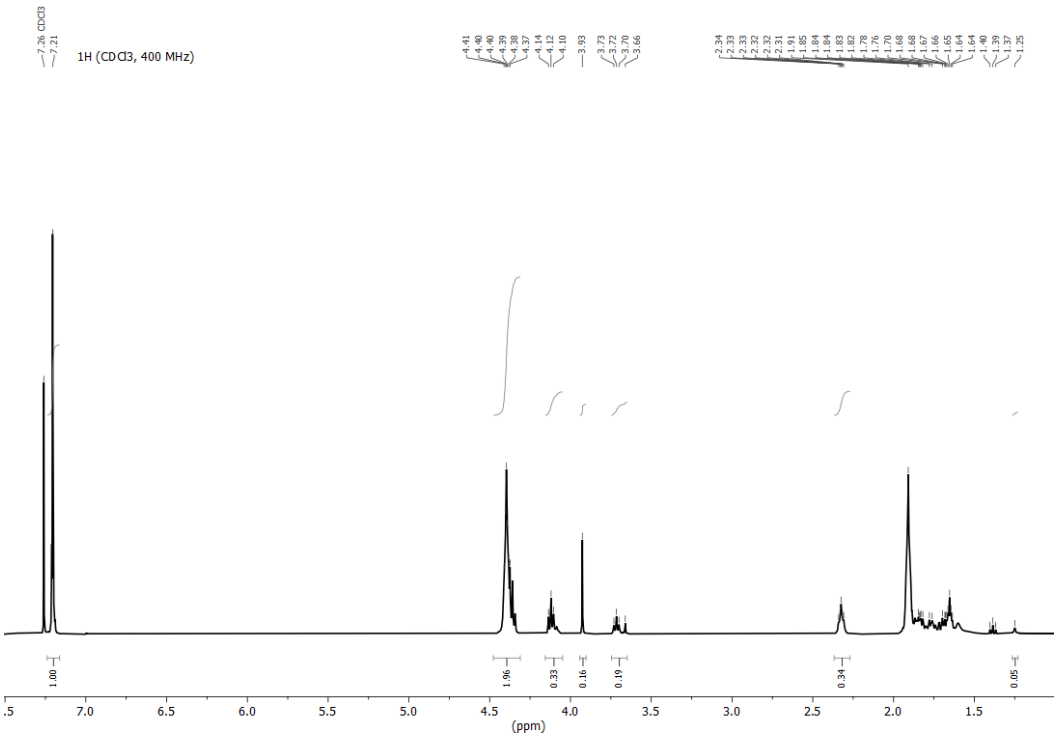

Figure S2.16: NMR spectrum of PBF90 in $CDCl_3$

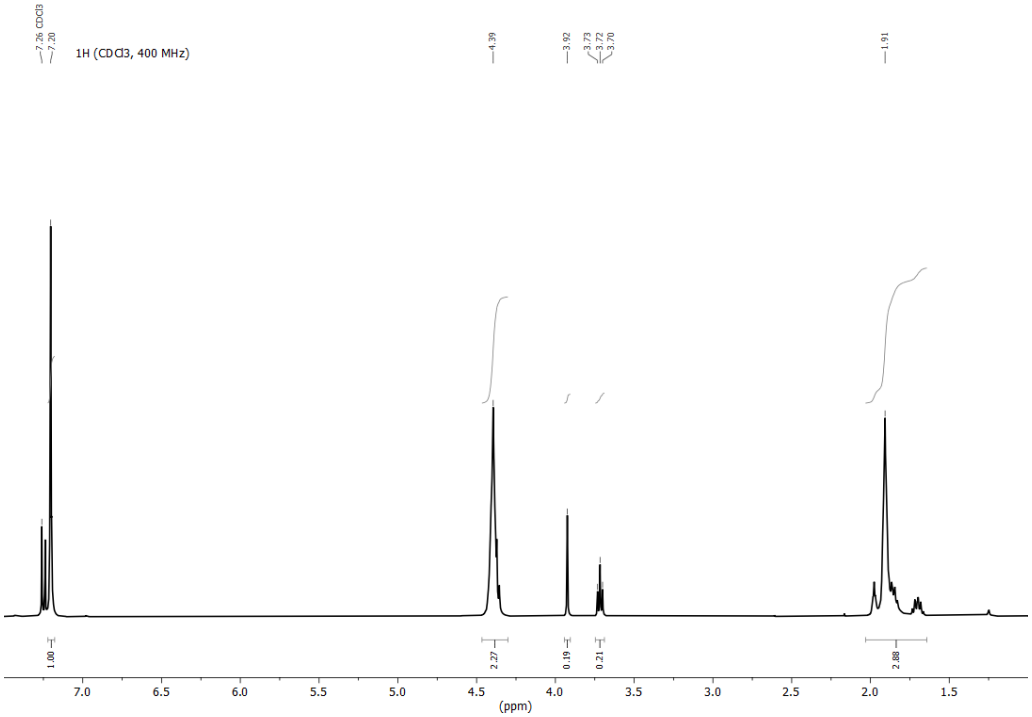

Figure S2.17: NMR spectrum of PBF in $CDCl_3$

SEC analyses of PHAd-co-PHF containing from 0 to 100 % of DMFDC

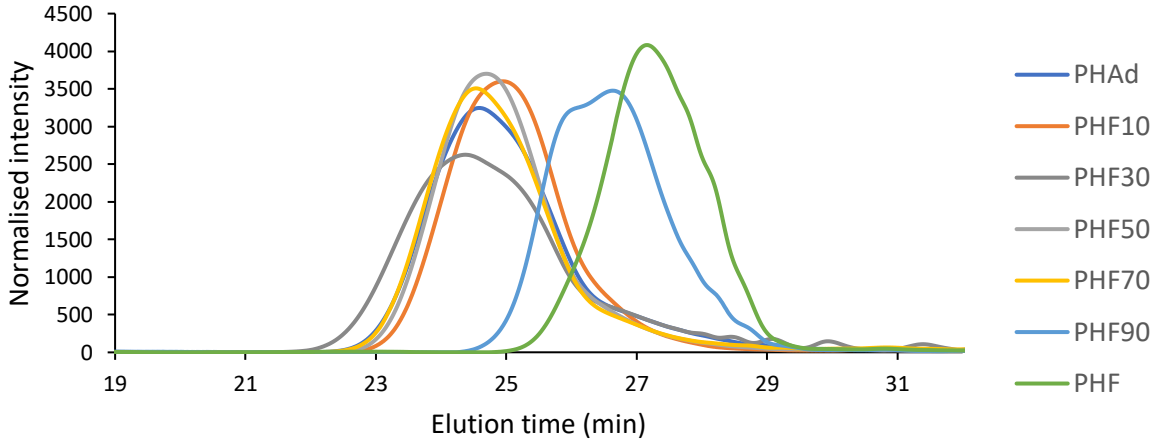

Figure S2.18: SEC elution curves of the PHAd-co-PHF. The intensities have been normalised by area.

Table S2.1: Results of SEC analysis for the PHAd-co-PHF containing from 0 to 100 % of DMFDC.

Sample name	*Ratio of DMFDC (%)*	*Ratio of DEA (%)*	*M_n (g.mol^{-1})*	*M_w (g.mol^{-1})*	*Đ*
PHAd	0	100	19 000	33 500	1.76
PHF10	10	90	18 600	28 500	1.53
PHF30	30	70	18 300	38 800	2.11
PHF50	50	50	18 000	29 804	1.65
PHF70	70	30	19 400	34 400	1.77
PHF90	90	10	6100	8700	1.42
PHF	100	0	4100	5200	1.29

SEC analyses of PBAd-co-PBF containing from 0 to 100 % of DMFDC

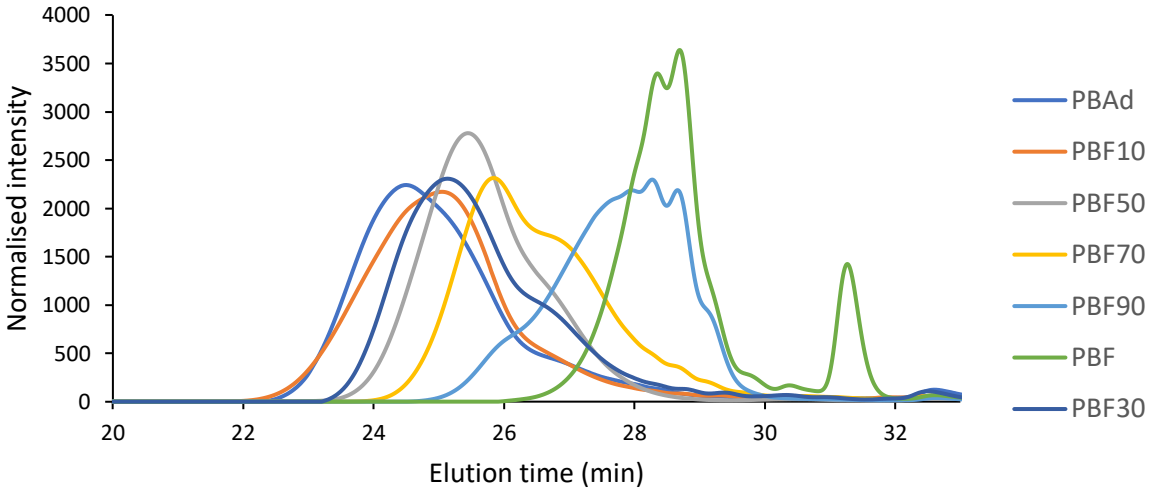

Figure S2.19: SEC elution curves of the PBAd-co-PBF. The intensities have been normalised by area.

Table S2.2: Results of SEC analysis for the PBAd-co-PBF containing from 0 to 100 % of DMFDC.

Sample name	*Ratio of DMFDC (%)*	*Ratio of DEA (%)*	*M_n (g.mol^{-1})*	*M_w (g.mol^{-1})*	*Đ*
PBAd	0	100	16 600	34 700	2.08
PBF10	10	90	16 800	33 100	1.96
PBF30	30	70	11 100	19 500	1.73
PBF50	50	50	10 200	17 500	1.71
PBF70	70	30	6 200	10 400	1.68
PBF90	90	10	2 800	4 300	1.50
PBF	100	0	2 000	2400	1.20

DSC analyses of PHAd-co-PHF containing from 0 to 100 % of DMFDC

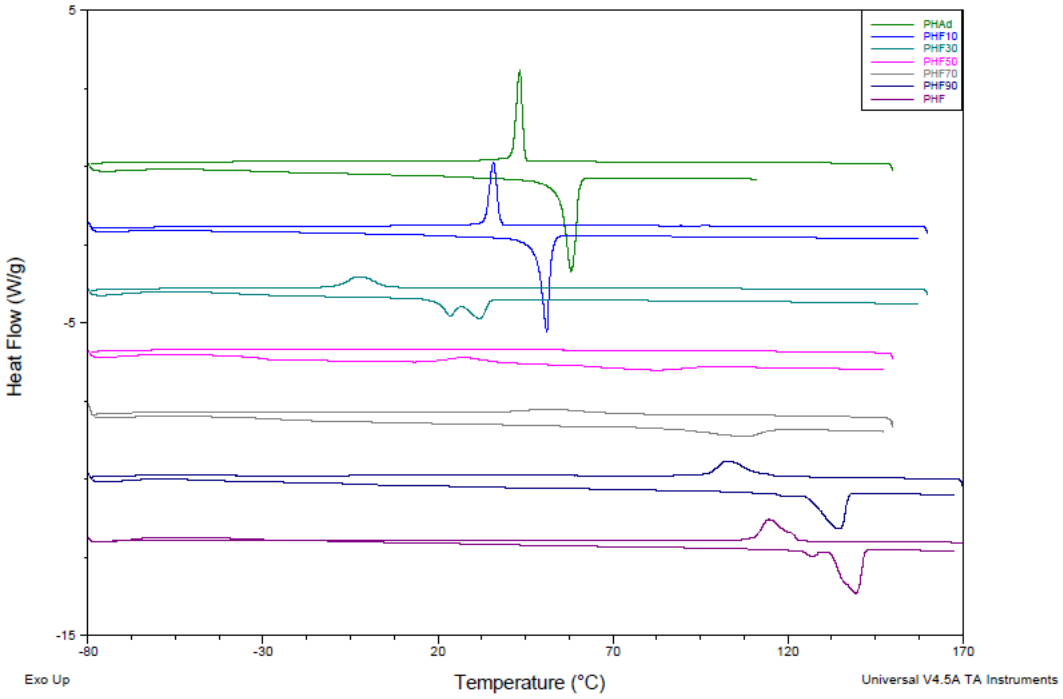

Figure S2.20: Stacked representation of the DSC analyses of the PHAd-co-PHF with various proportions of DMFDC. The heating was 10°C/min and the cooling rate 5°C/min.

MDSC analyses of PHAd-co-PHF containing from 0 to 100 % of DMFDC

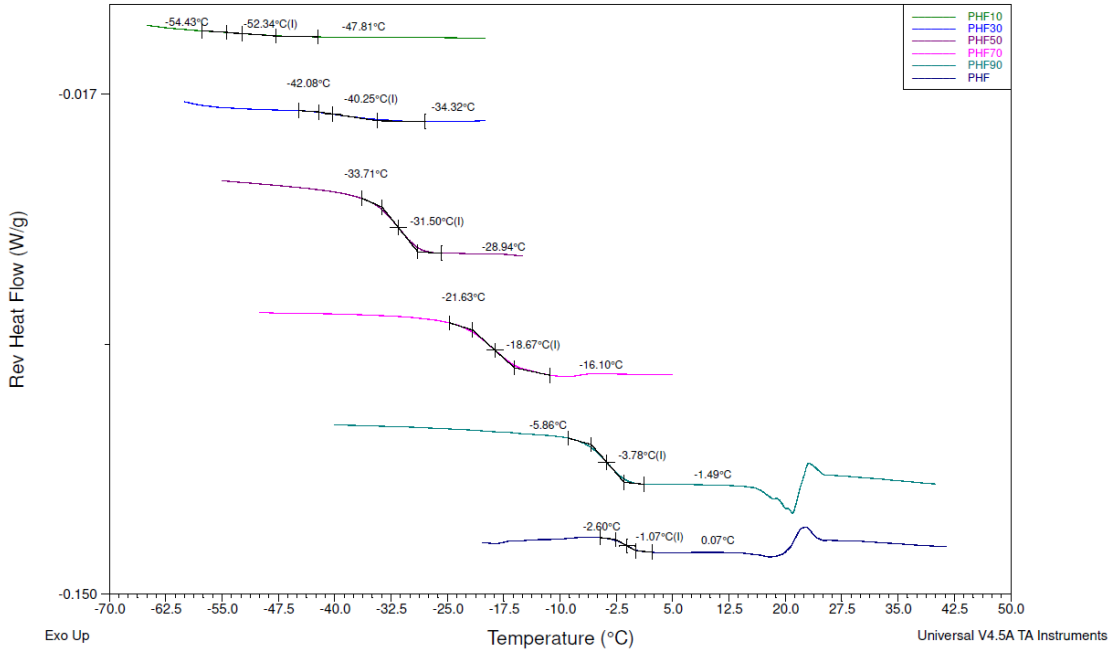

Figure S2.21: Stacked representation of the MDSC analyses of the PHAd-co-PHF with various proportions of DMFDC. The heating rate was 2°C/min modulated with an amplitude of 1.20°C every 60 seconds.

DSC analyses of PBAd-co-PBF containing from 0 to 100 % of DMFDC

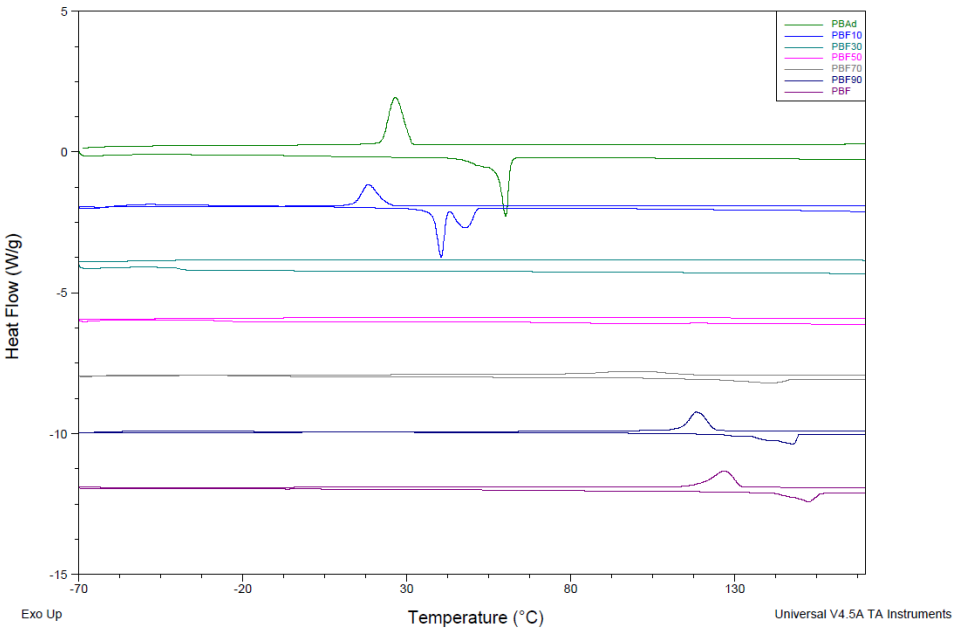

Figure S2.22: Stacked representation of the DSC analyses of the PBAd-co-PBF with various proportions of DMFDC. The heating was 10°C/min and the cooling rate 5°C/min.

MDSC analyses of PBAd-co-PBF containing from 0 to 100 % of DMFDC

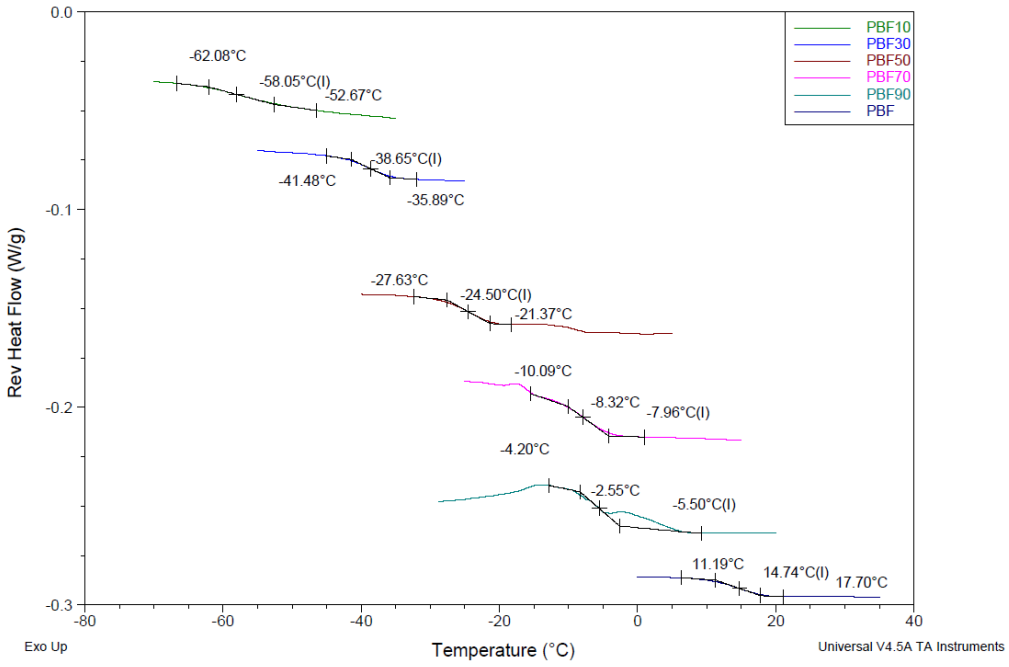

Figure S2.23: Stacked representation of the MDSC analyses of the PBAd-co-PBF with various proportions of DMFDC. The heating rate was 2°C/min modulated with an amplitude of 1.20°C every 60 seconds.

TGA of PHAd-co-PHF containing from 0 to 100 % of DMFDC

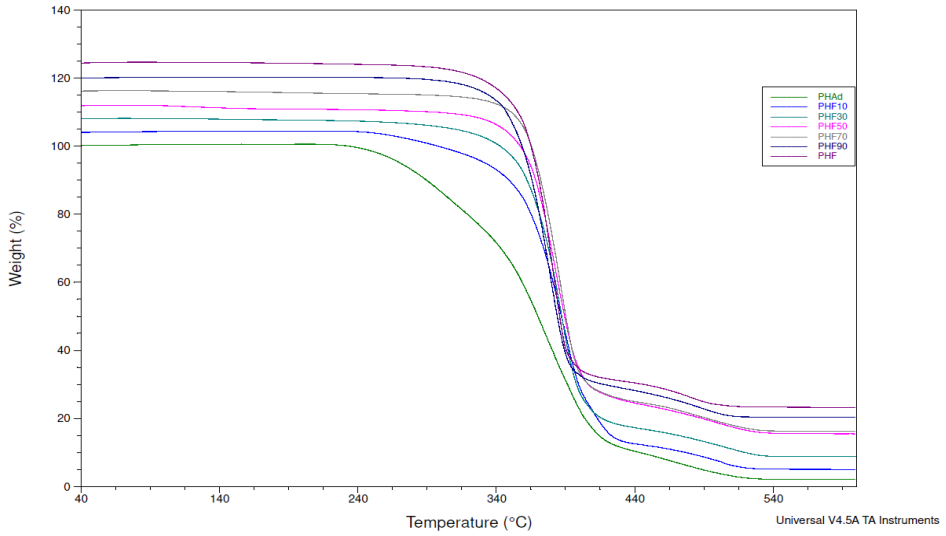

Figure S2.24: Weight loss curves of the PHAd-co-PHF with various proportions of DMFDC from TGA with a heating rate of 10°C/min. Each curve is offset by 4 wt.% from the previous one.

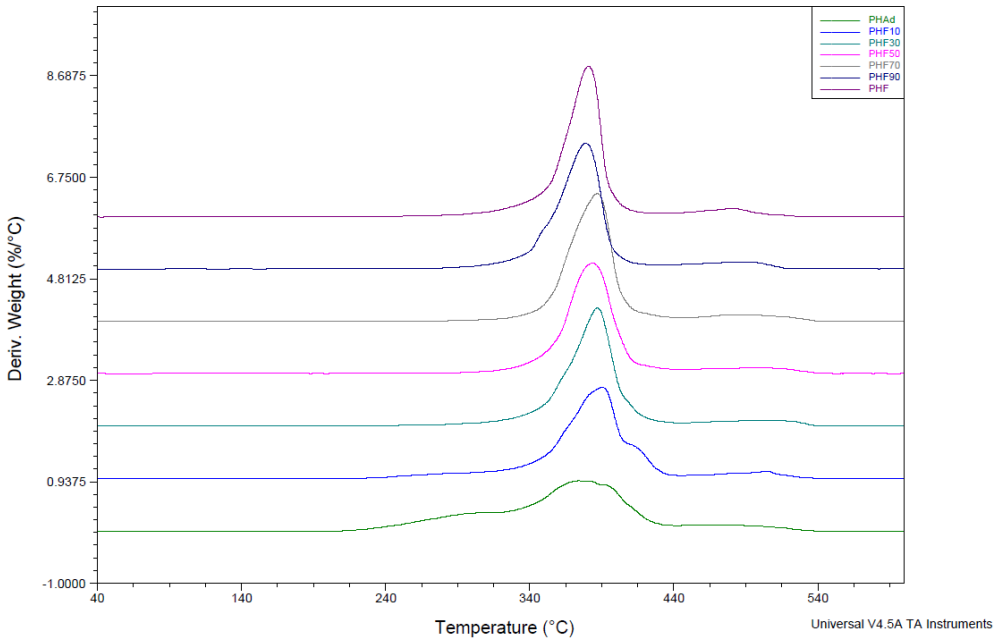

Figure S2.25: Derivative weight loss curves of the PHAd-co-PHF with various proportions of DMFDC from TGA with a heating rate of 10°C/min. Each curve is offset by 1 unit from the previous one.

TGA of PBAd-co-PHF containing from 0 to 100 % of DMFDC

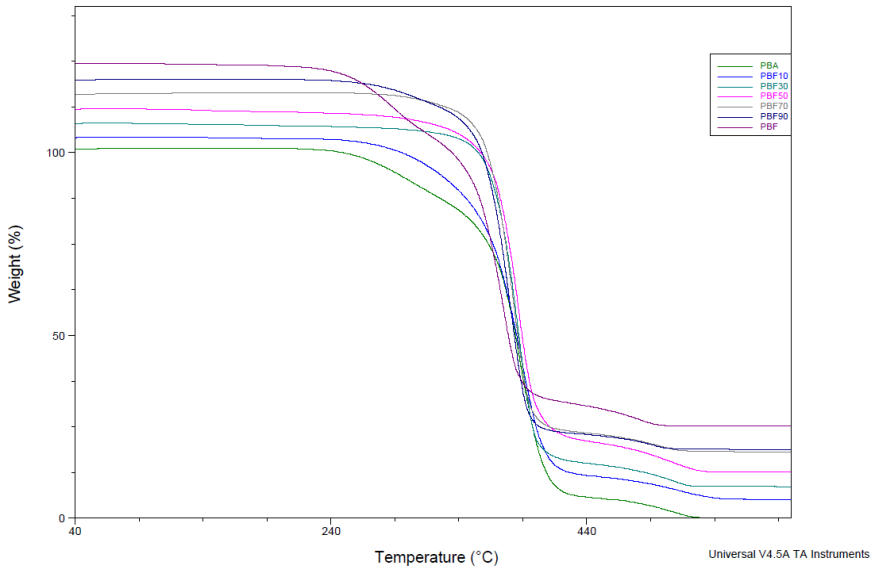

Figure S2.26: Weight loss curves of the PBAd-co-PBF with various proportions of DMFDC from TGA with a heating rate of 10°C/min. Each curve is offset by 4 wt.% from the previous one.

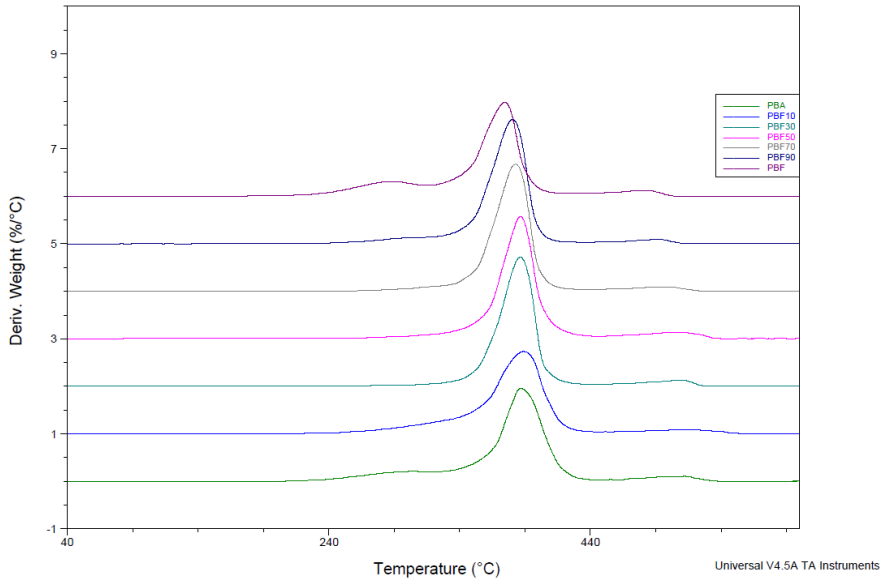

Figure S2.27: Derivative weight loss curves of the PHAd-co-PHF with various proportions of DMFDC from TGA with a heating rate of 10°C/min. Each curve is offset by 1 unit from the previous one.

MDSC analyses of PHF and PBF synthesized in different solvents

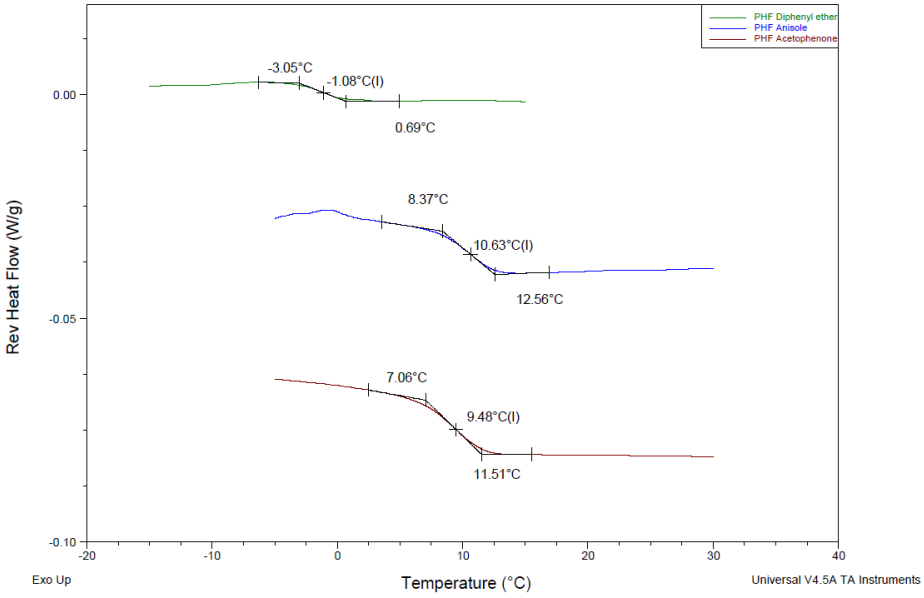

Figure S2.28: Stacked representation of the MDSC analyses of the PHF synthesized in different solvents. The heating rate was 2°C/min modulated with an amplitude of 1.20°C every 60 seconds.

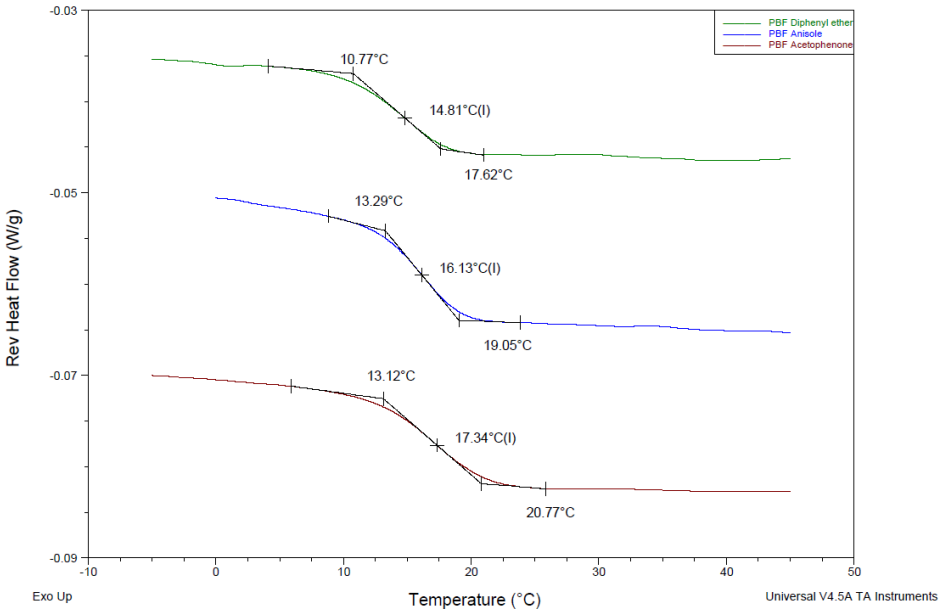

Figure S2.29: Stacked representation of the MDSC analyses of the PBF synthesized in different solvents. The heating rate was 2°C/min modulated with an amplitude of 1.20°C every 60 seconds.

DSC analyses of PHF and PBF synthesized in different solvents

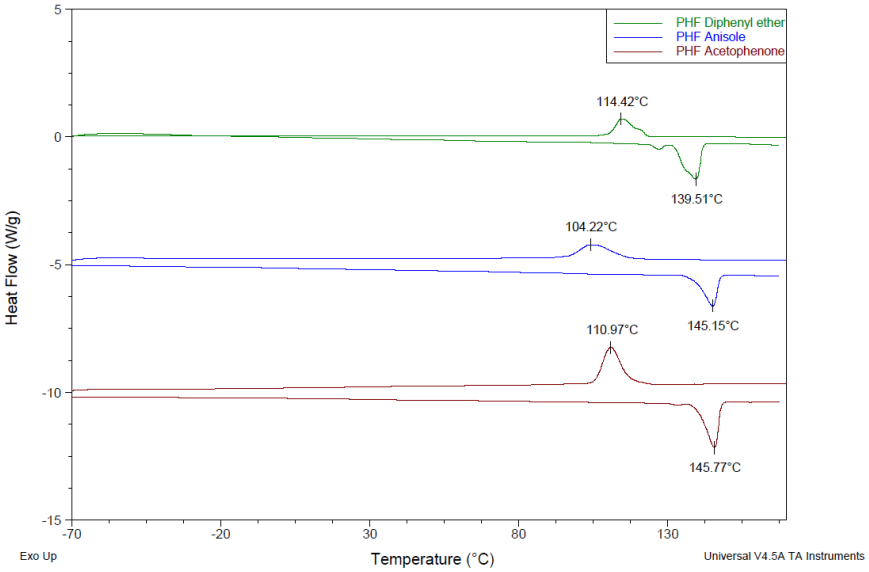

Figure S2.30: Stacked representation of the DSC analyses of the PHF synthesized in different. The heating was 10°C/min and the cooling rate 5°C/min.

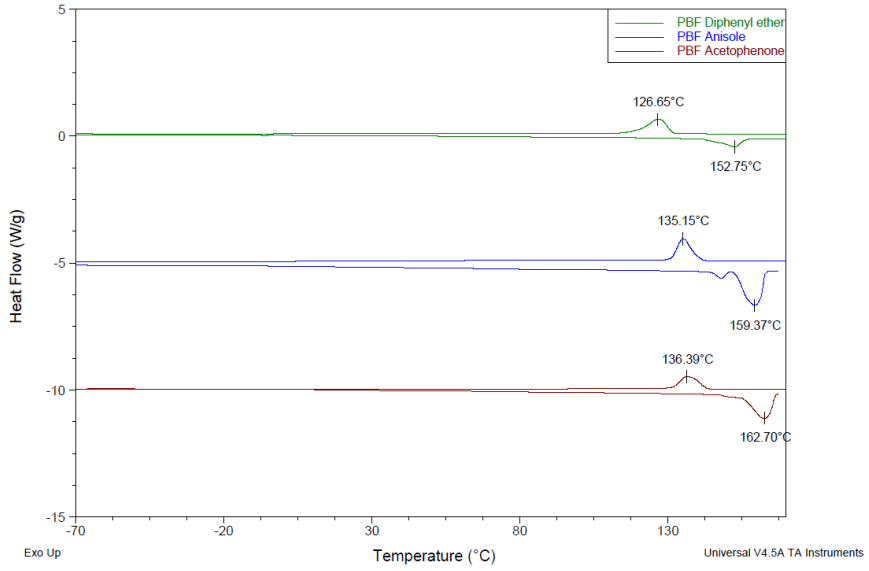

Figure S2.31: Stacked representation of the DSC analyses of the PBF synthesized in different. The heating was 10°C/min and the cooling rate 5°C/min.

NMR spectra of PHF synthesized in different solvents

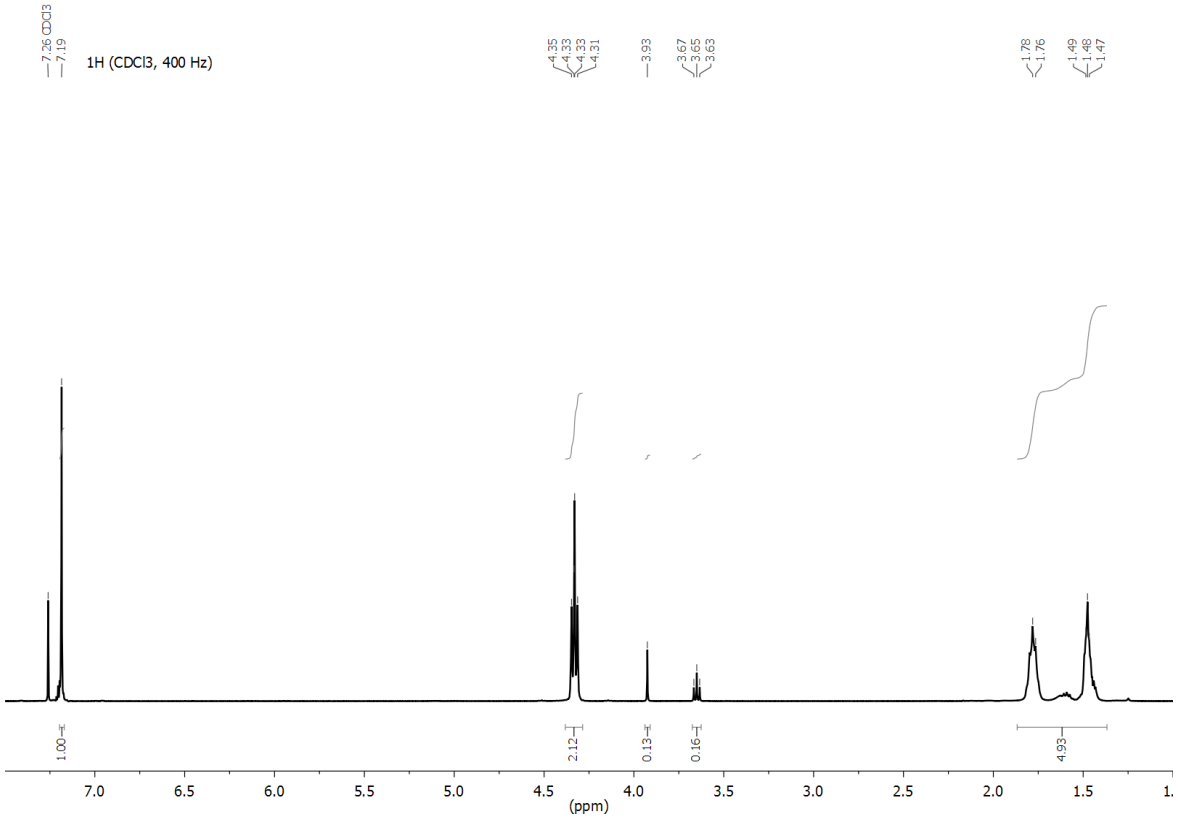

Figure S2.32: NMR spectrum of PHF synthesized in diphenyl ether in $CDCl_3$.

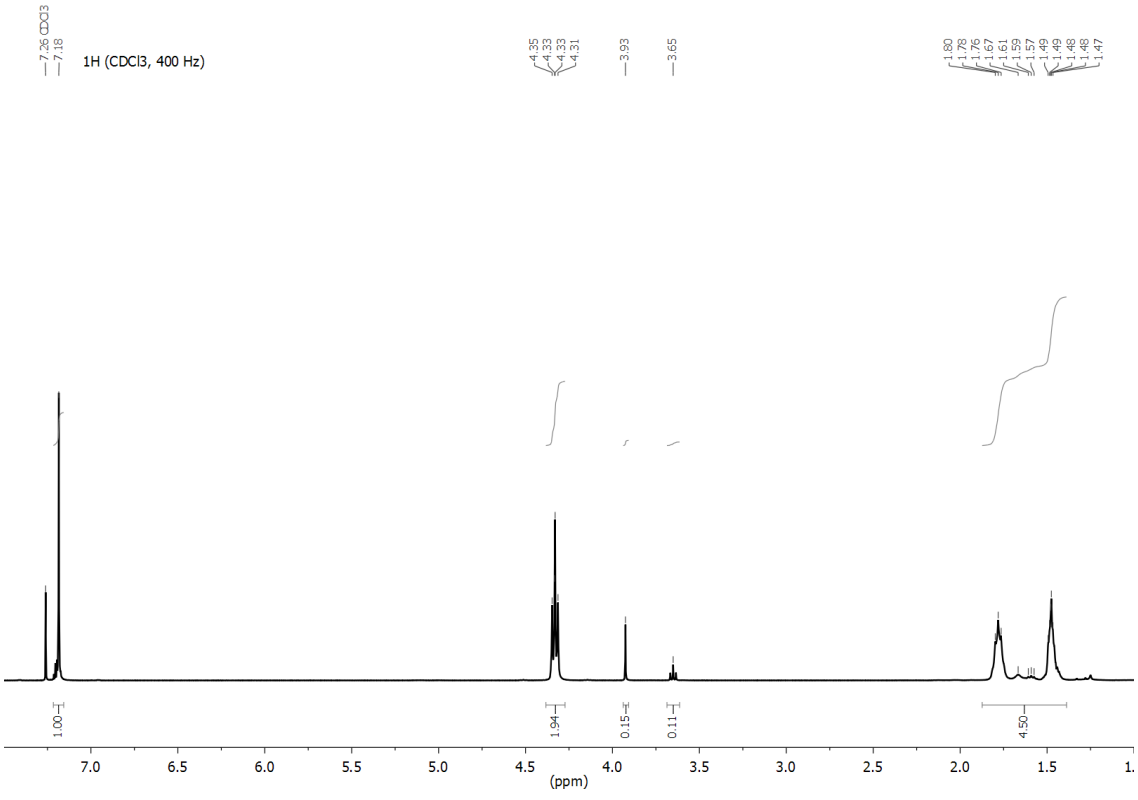

Figure S2.33: NMR spectrum of PHF synthesized in toluene in $CDCl_3$.

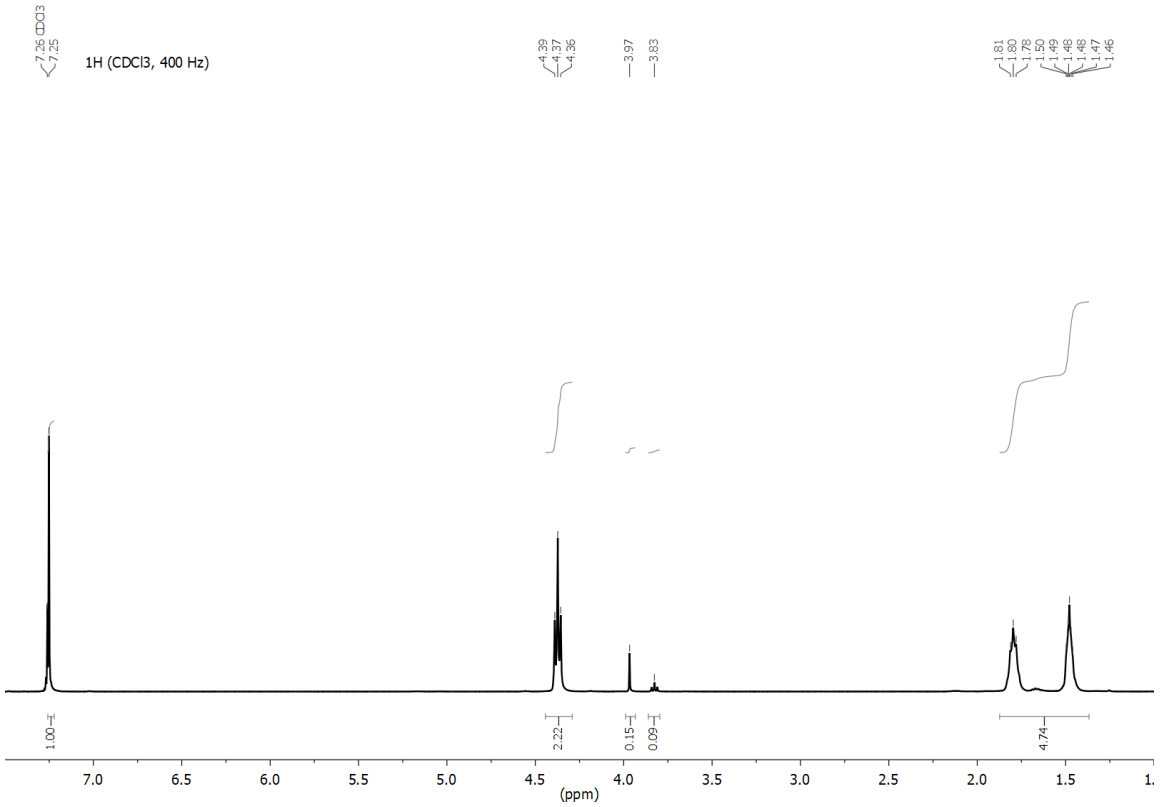

Figure S2.34: NMR spectrum of PHF synthesized in phenetole in $CDCl_3$.

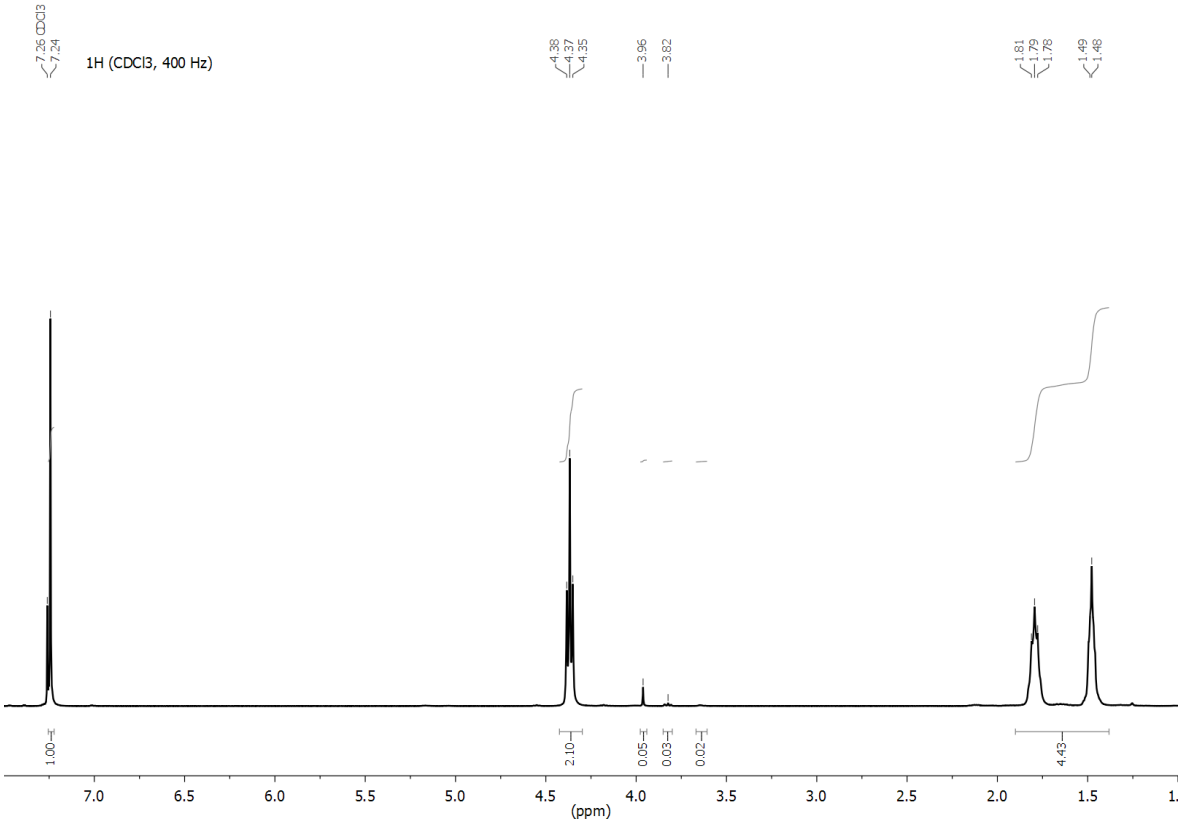

Figure S2.35: NMR spectrum of PHF synthesized in anisole in $CDCl_3$.

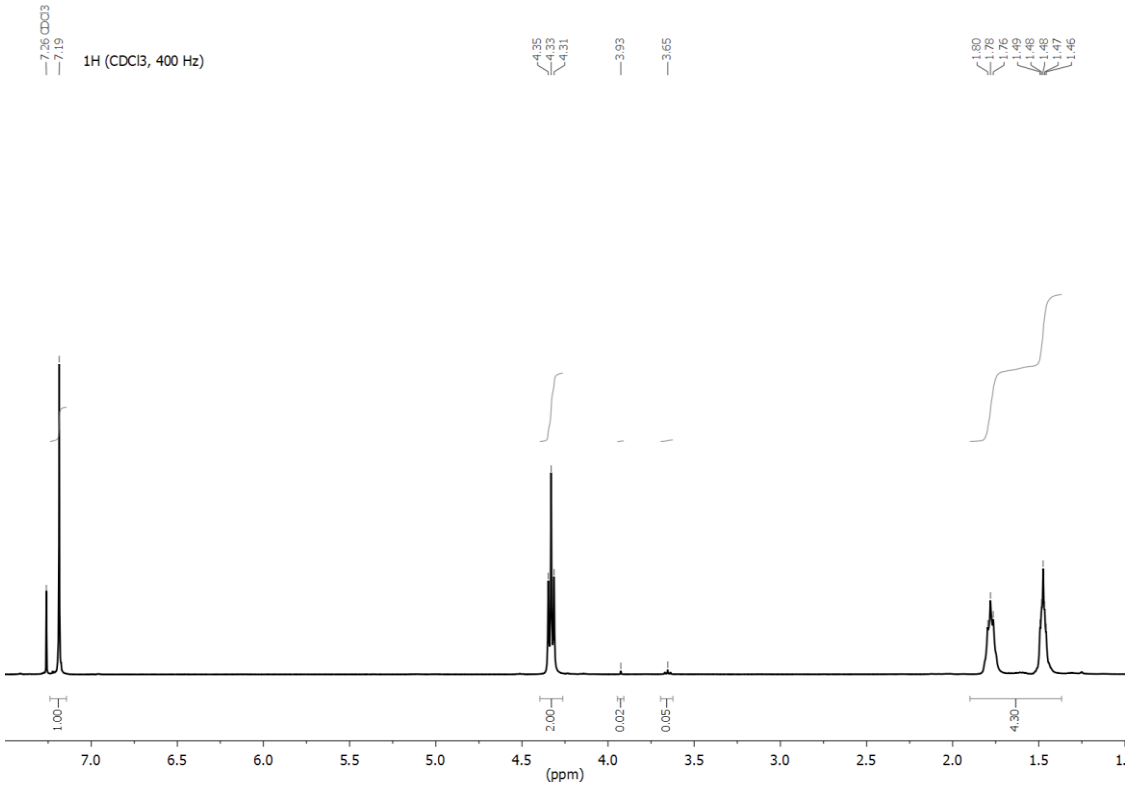

Figure S2.36: NMR spectrum of PHF synthesized in acetophenone in $CDCl_3$.

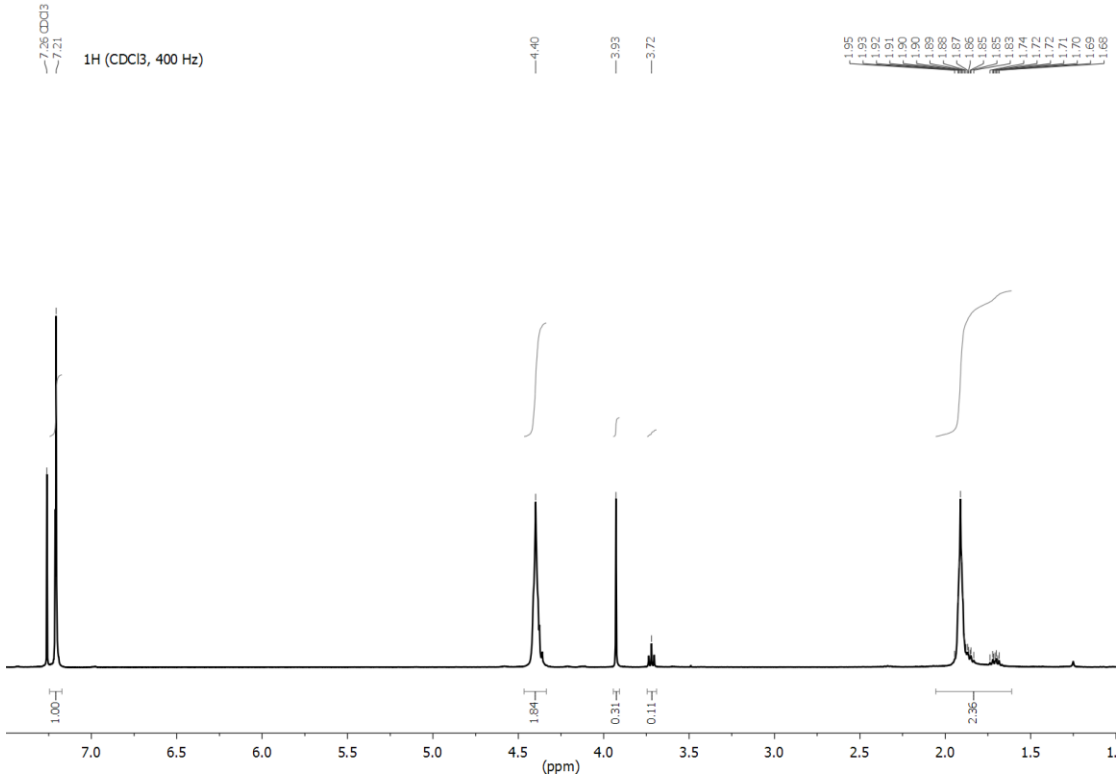

Figure S2.37: NMR spectrum of PHF synthesized in cyclohexanone in $CDCl_3$.

NMR spectra of PBF synthesized in different solvents

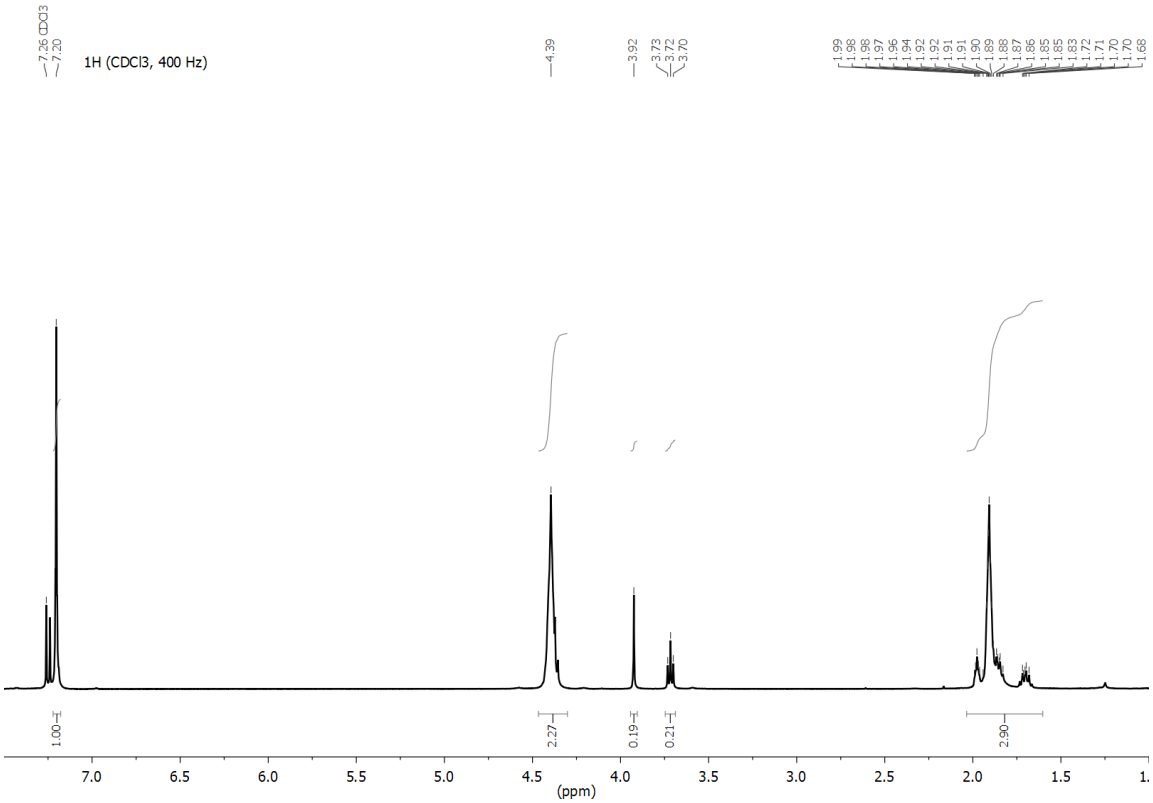

Figure S2.38: NMR spectrum of PBF synthesized in diphenyl ether in $CDCl_3$.

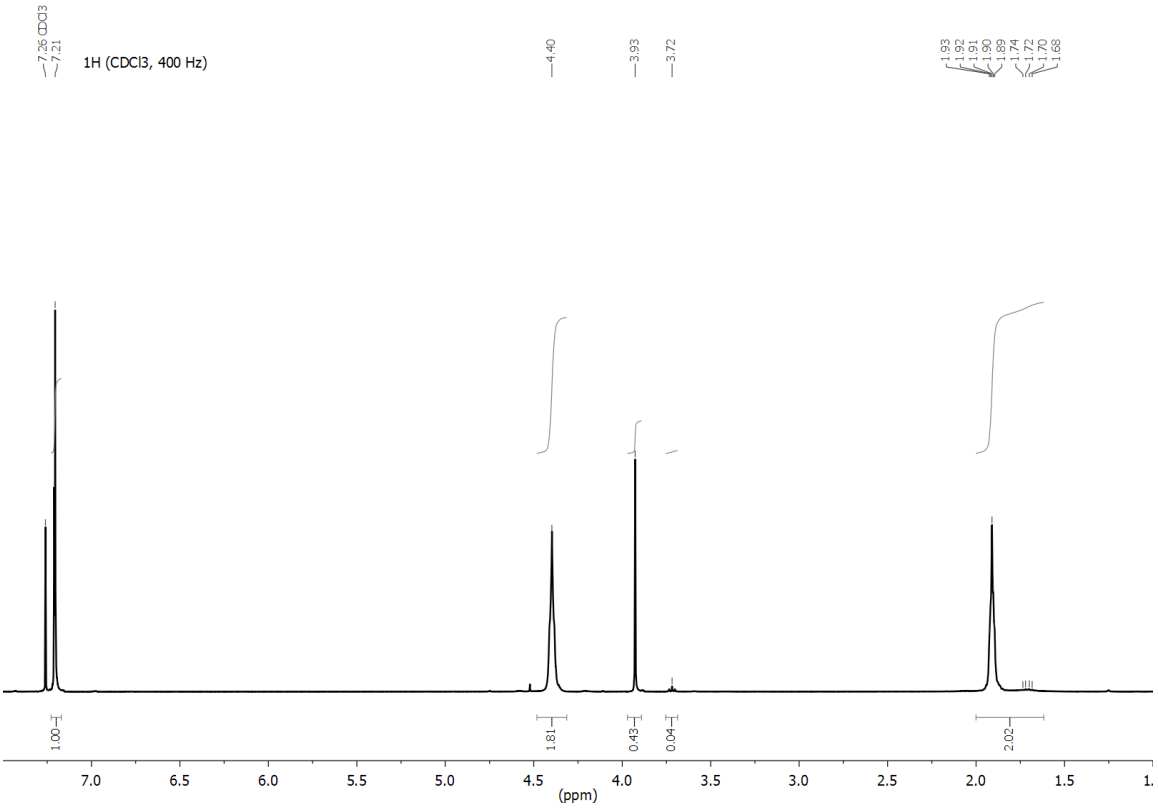

Figure S2.39: NMR spectrum of PBF synthesized in toluene in $CDCl_3$.

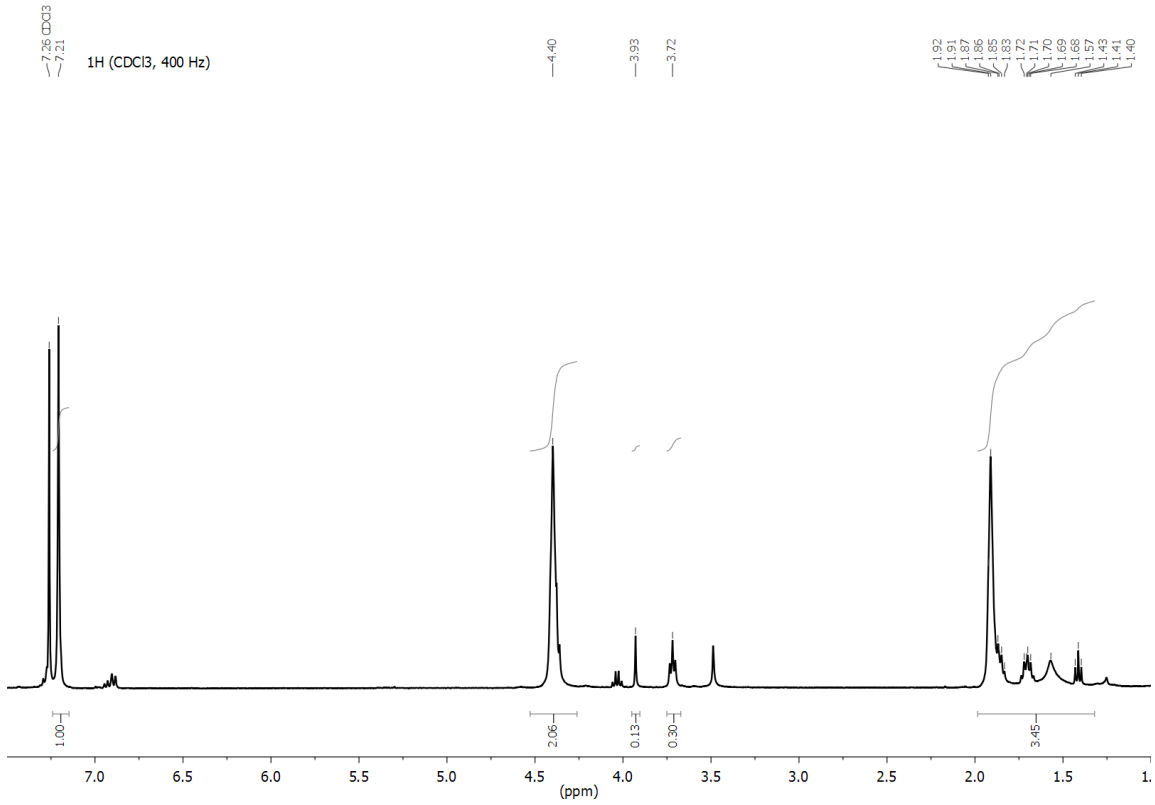

Figure S2.40: NMR spectrum of PBF synthesized in phenetole in $CDCl_3$.

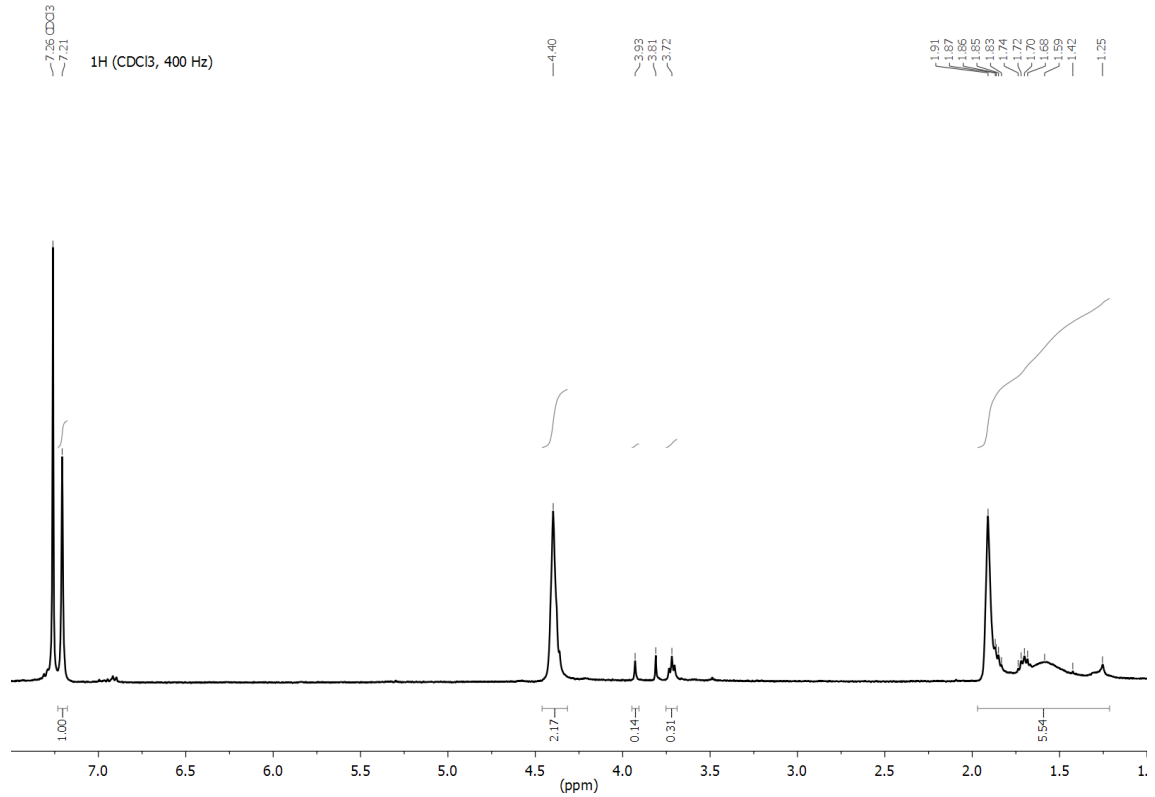

Figure S2.41: NMR spectrum of PBF synthesized in anisole in $CDCl_3$.

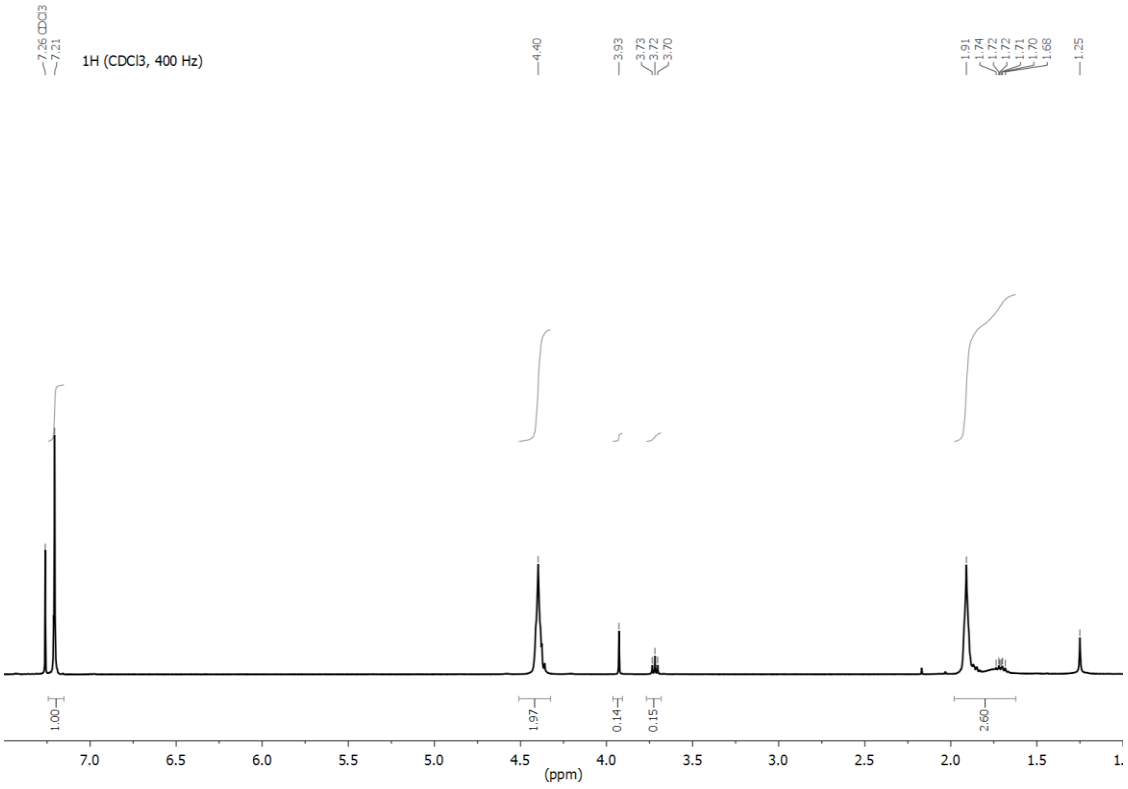

Figure S2.42: NMR spectrum of PBF synthesized in acetophenone in $CDCl_3$.

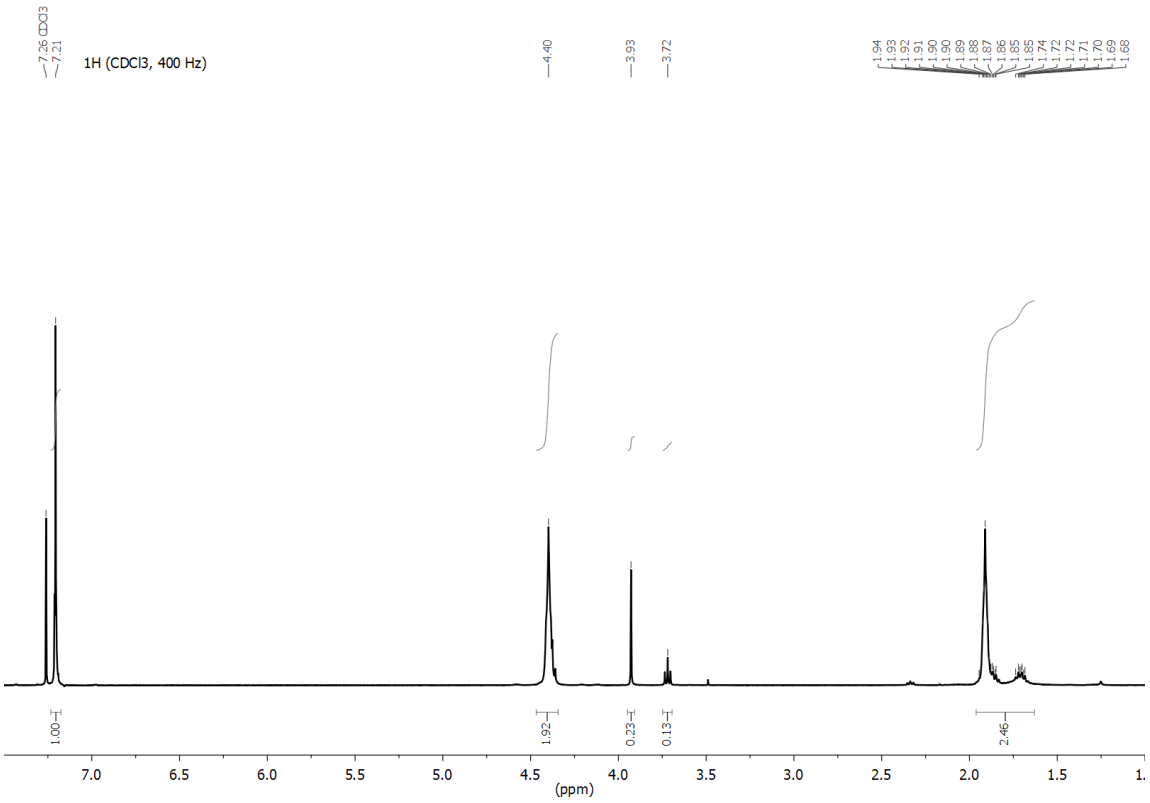

Figure S2.43: NMR spectrum of PBF synthesized in cyclohexanone in $CDCl_3$.

Picture of polymer precipitation

Figure S2.44: Reaction medium of the PHF synthesis in acetophenone after 24h of reaction.

MALDI-TOF MS analysis of PHF and PBF in different solvents

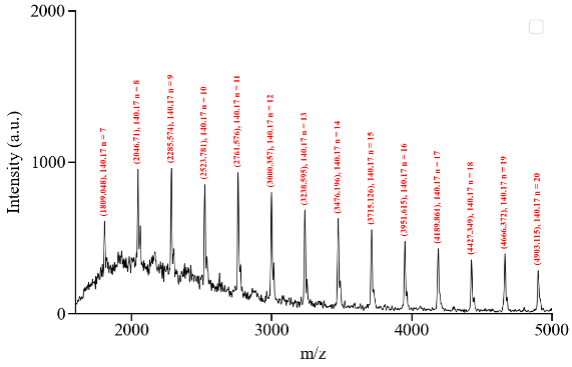

Figure S2.45: MALDI-TOF-MS analysis of PHF synthesized in anisole.

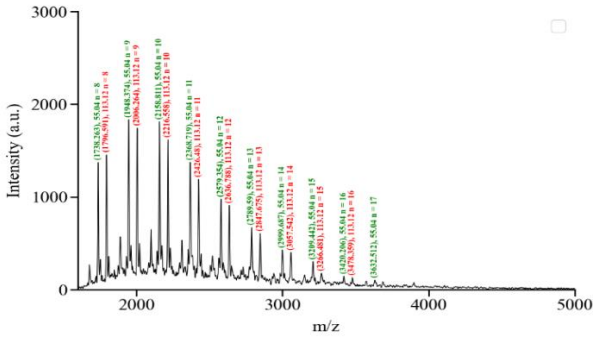

Figure S2.46: MALDI-TOF-MS analysis of PBF synthesized in diphenyl ether.

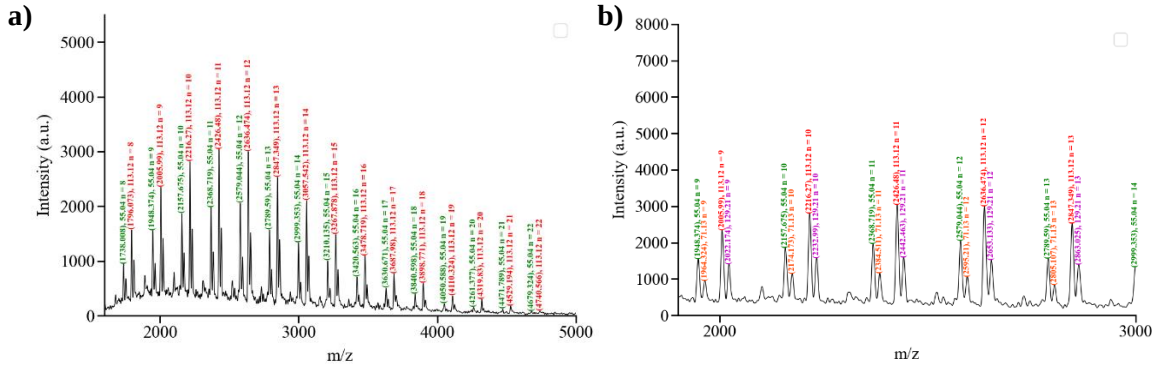

Figure S2.47: MALDI-TOF-MS analysis of PBF synthesized in anisole. a: full view, b: zoom.

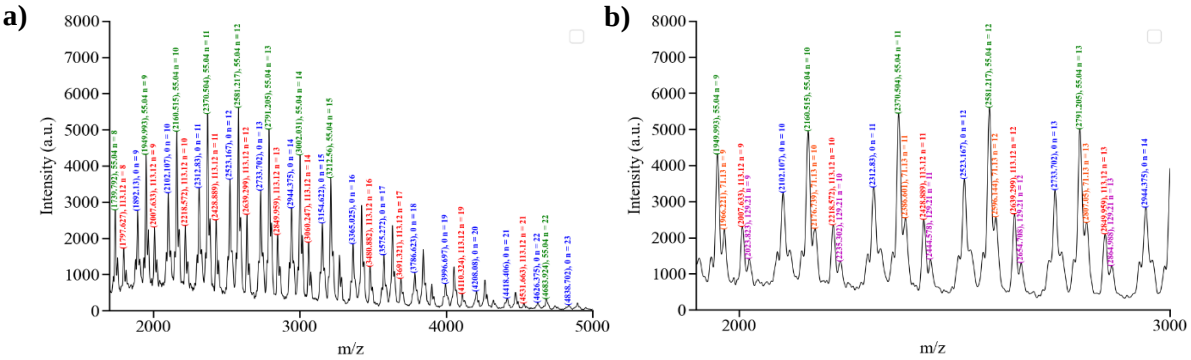

Figure S2.48: MALDI-TOF-MS analysis of PBF synthesized in acetophenone. a: full view, b: zoom.

Annexes Chapitre 3 (supporting information)

^{1}H NMR analyses of the monomers

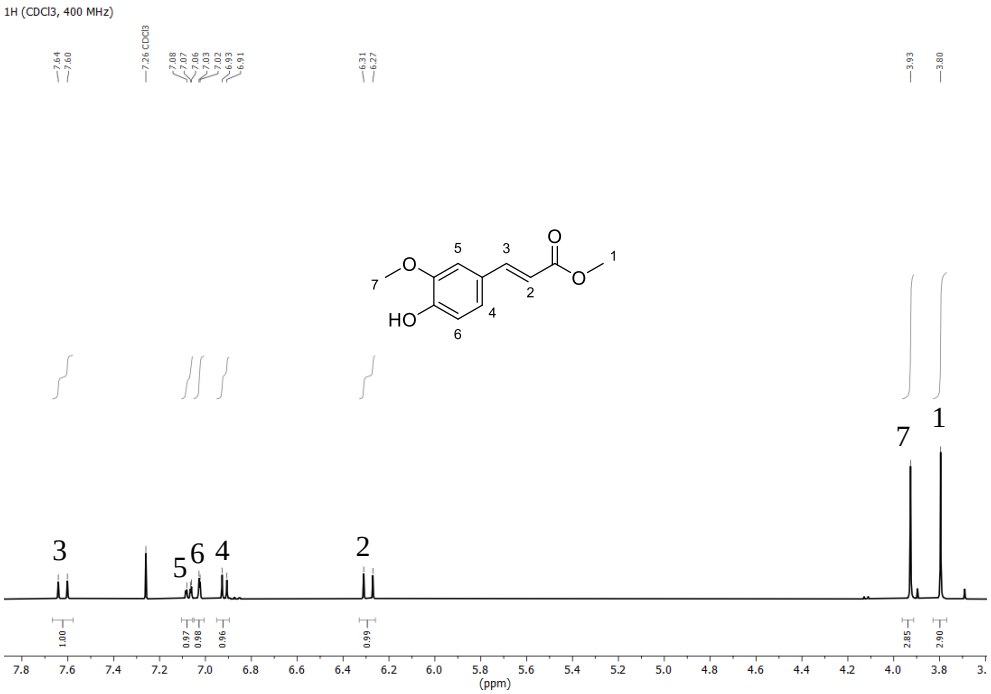

Figure S.3.1: ^{1}H NMR analysis of methyl ferulate (MeFA).

Figure S.3.2: ^{1}H NMR analysis of methyl 4-(methyl ethanoate-oxy)-ferulate (DeFA^{I}).

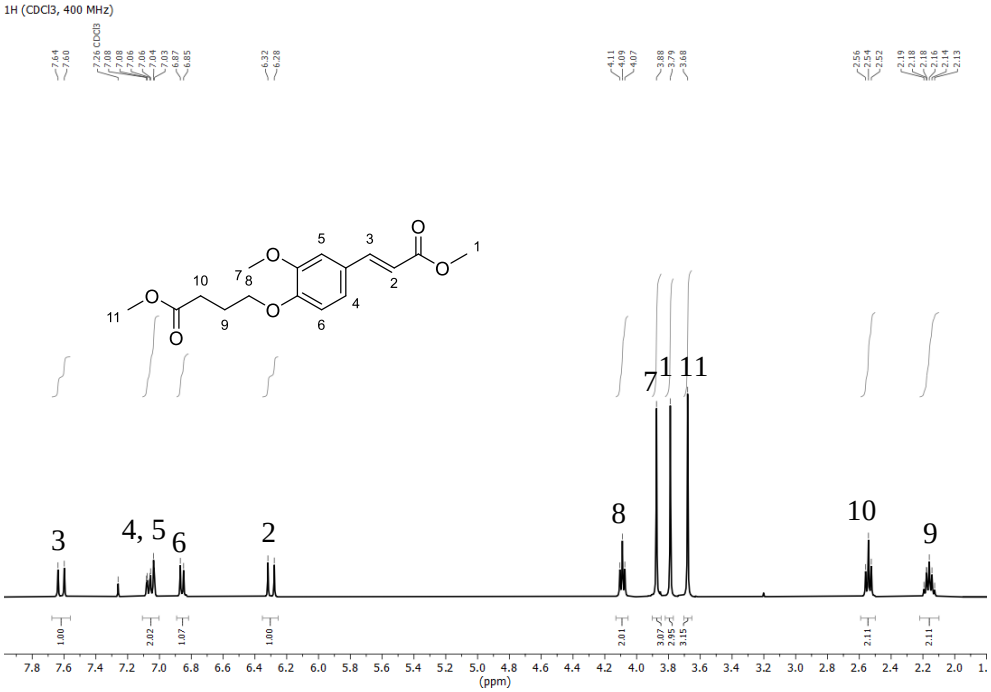

Figure S.3.3: ^{1}H NMR analysis of methyl 4-(methyl butanoate-oxy)-ferulate (DeFA^{II}).

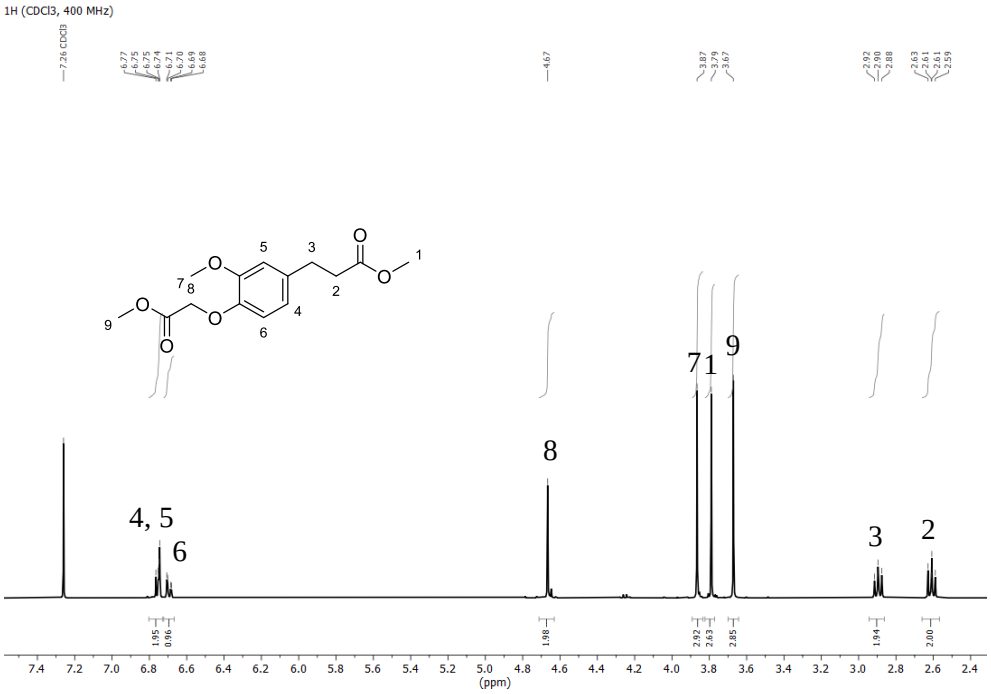

Figure S.3.4: ^{1}H NMR analysis of methyl 3-(3-methoxy-4-(2-methoxy-2-oxoethoxy)phenyl)propanoate (H-DeFA^{I}).

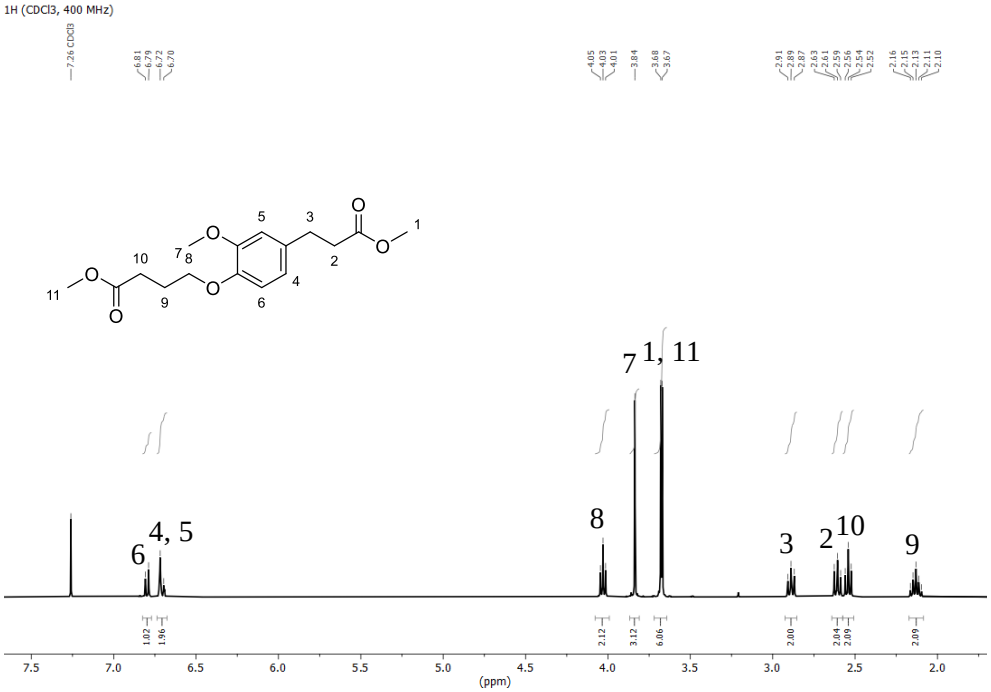

Figure S.3.5: ^{1}H NMR analysis of methyl 4-(2-methoxy-4-(3-methoxy-3-oxopropyl)phenoxy)butanoate (H-DeFA^{II}).

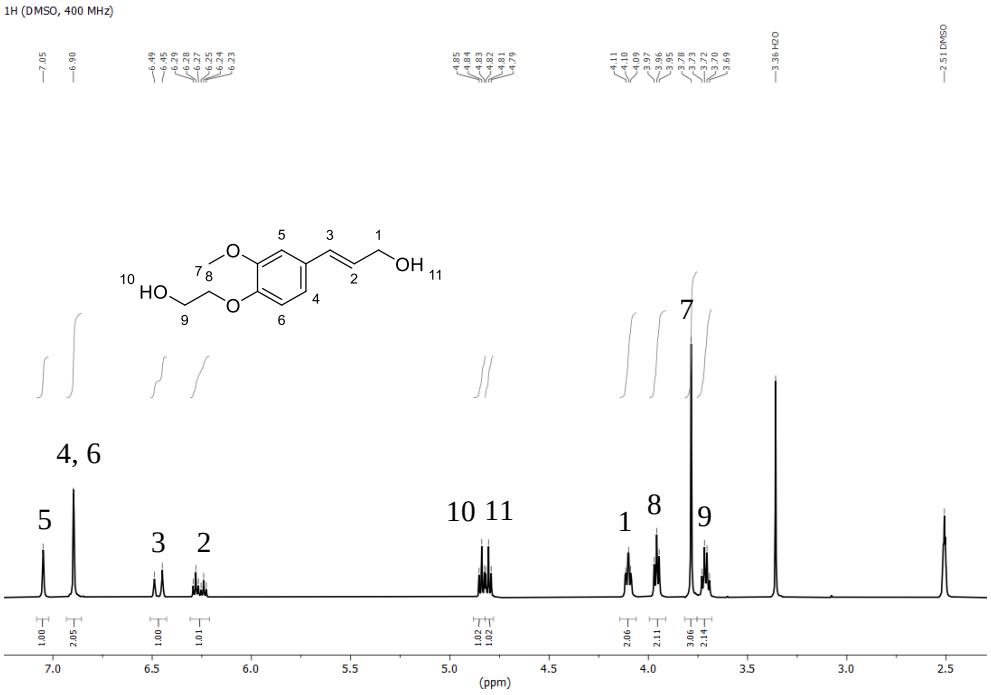

Figure S.3.6: ^{1}H NMR analysis of 4-(hydroxyethoxy)-coniferyl alcohol (FAD^{I}).

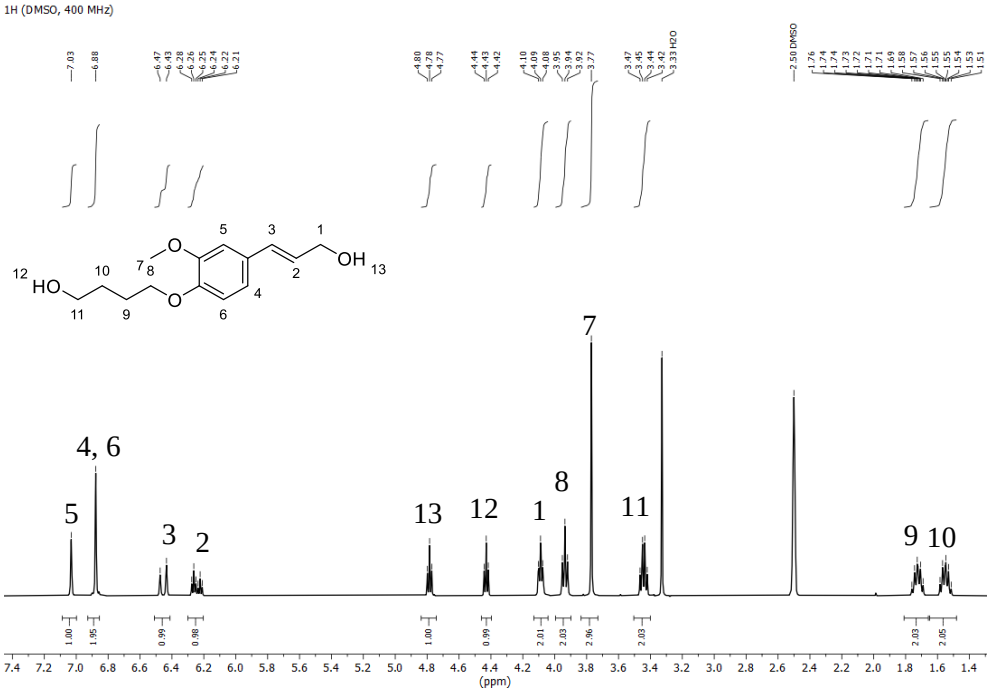

Figure S.3.7: ^{1}H NMR analysis of 4-(hydroxybutoxy)-coniferyl alcohol (FAD^{II}).

^{13}C NMR analysis of the monomers

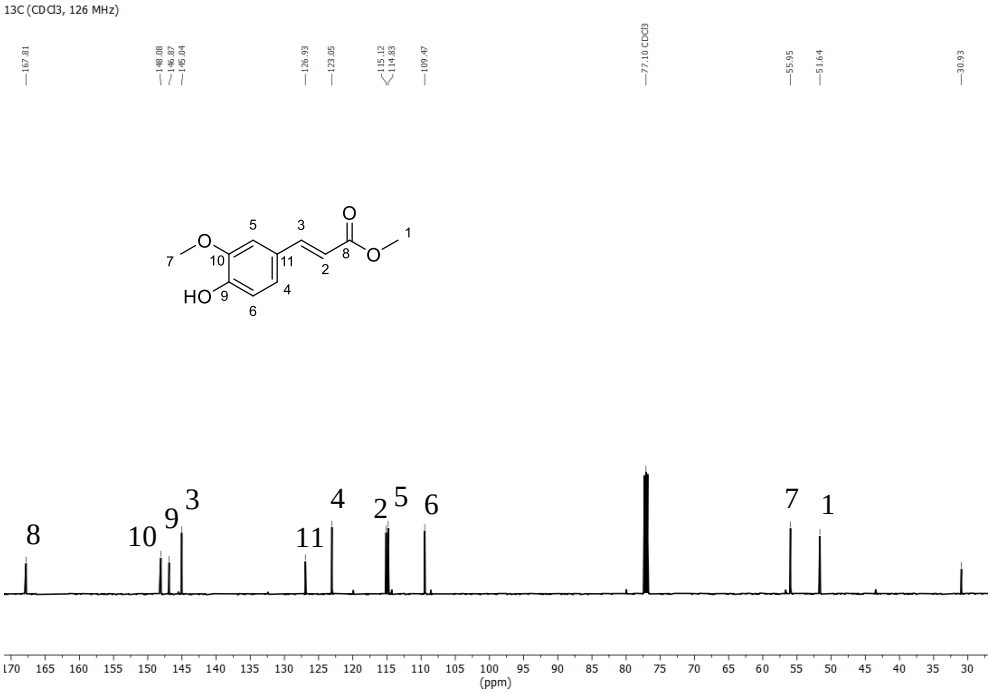

Figure S.3.8: ^{13}C NMR analysis of Methyl ferulate (MeFA)

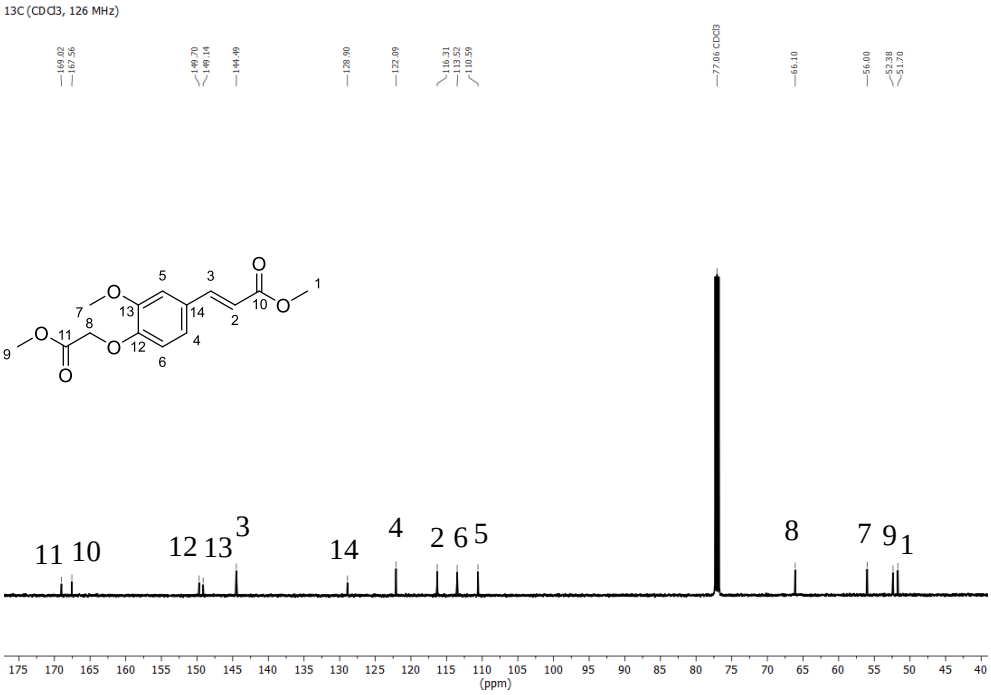

Figure S.3.9: ^{13}C NMR analysis of methyl 4-(methyl ethanoate-oxy)-ferulate (DeFA^{I}).

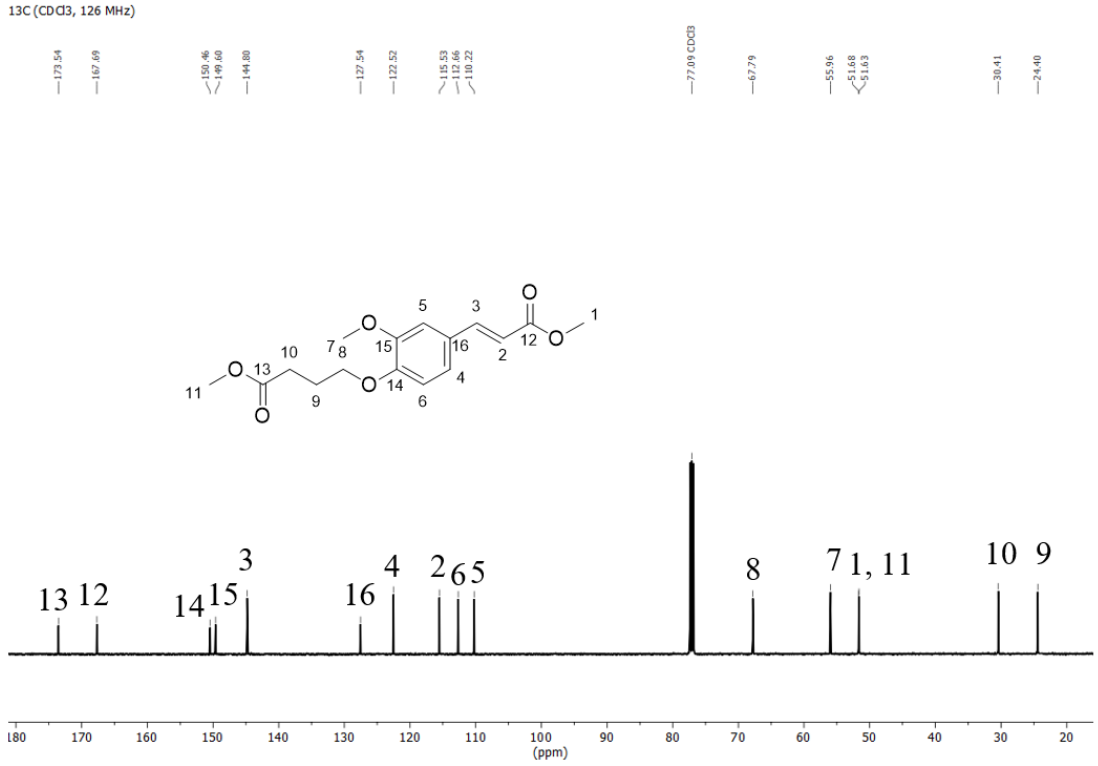

Figure S.3.10: ^{13}C NMR analysis of methyl 4-(methyl butanoate-oxy)-ferulate (DeFA^{II}).

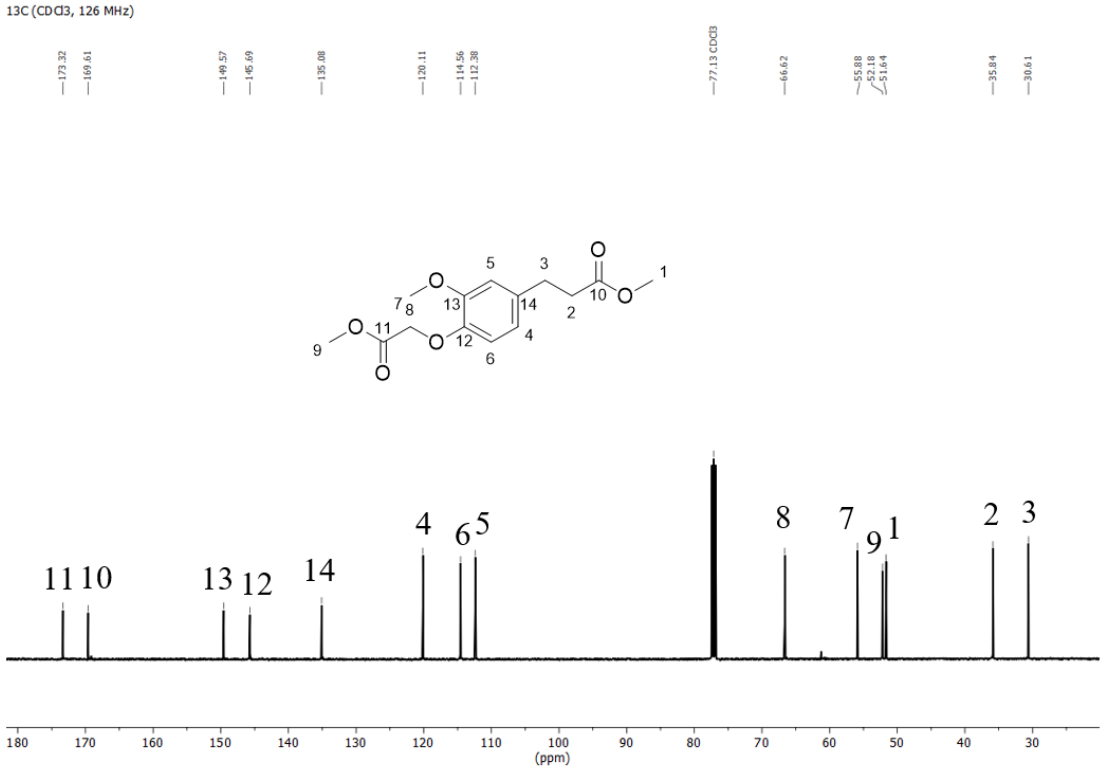

Figure S.3.11: ^{13}C NMR analysis of methyl 3-(3-methoxy-4-(2-methoxy-2-oxoethoxy)phenyl)propanoate (H-DeFA^{I}).

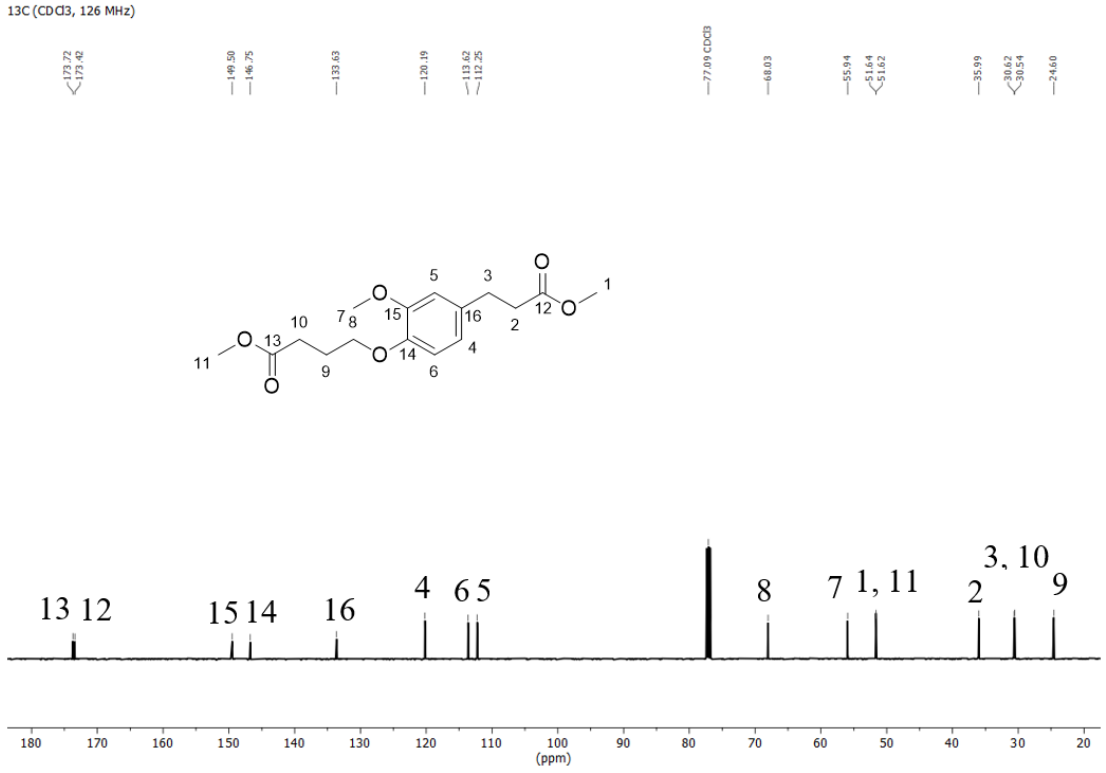

Figure S.3.12: ^{13}C NMR analysis of methyl 4-(2-methoxy-4-(3-methoxy-3-oxopropyl)phenoxy)butanoate (H-DeFA^{II}).

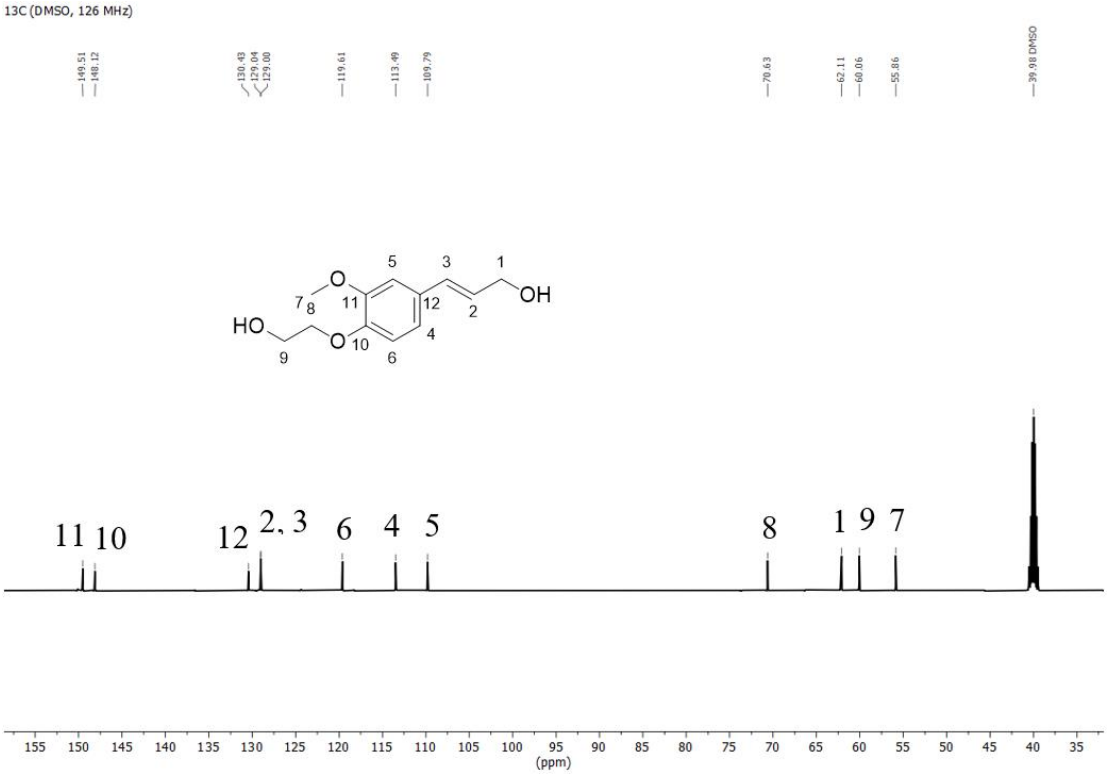

Figure S.3.13: ^{13}C NMR analysis of 4-(hydroxyethoxy)-coniferyl alcohol (FAD^{I}).

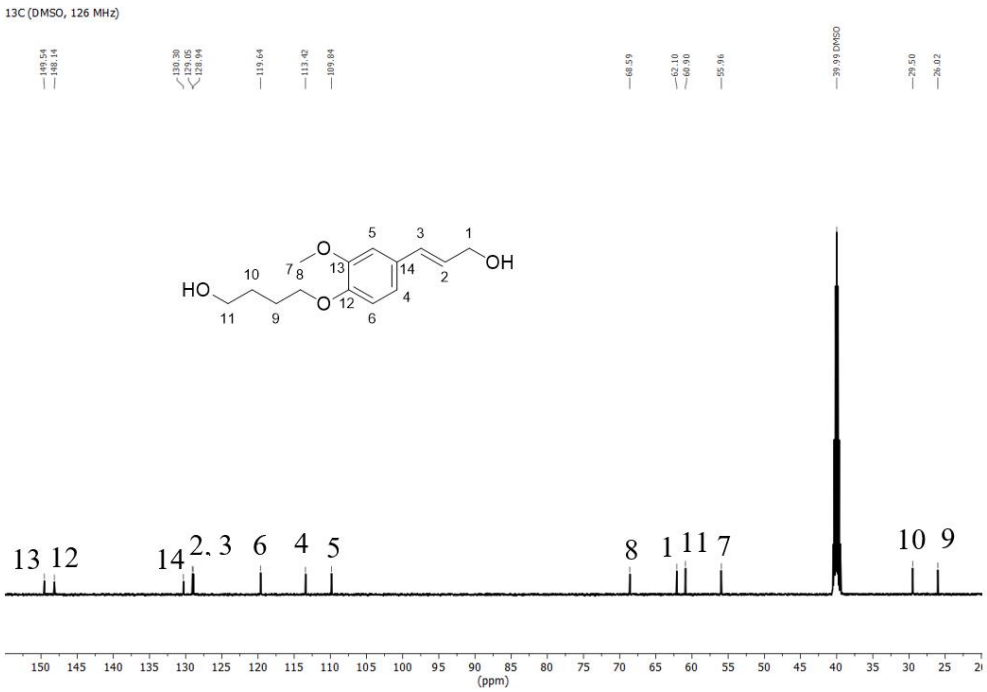

Figure S.3.14: ^{13}C NMR analysis of 4-(hydroxybutoxy)-coniferyl alcohol (FAD^{II}).

2D NMR analyses of 4-(methyl butanoate-oxy)-ferulate (DeFA^{II})

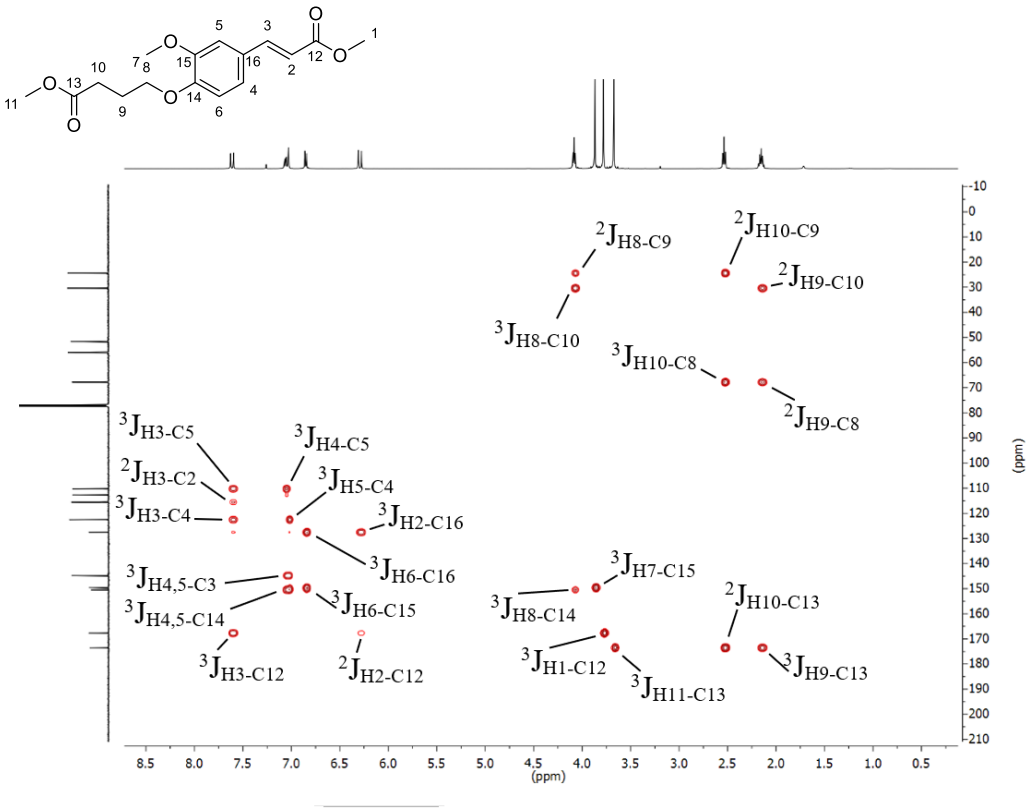

Figure S.3.15: HMBC NMR analysis of methyl 4-(methyl butanoate-oxy)-ferulate (DeFA^{II}) in $CDCl_3$

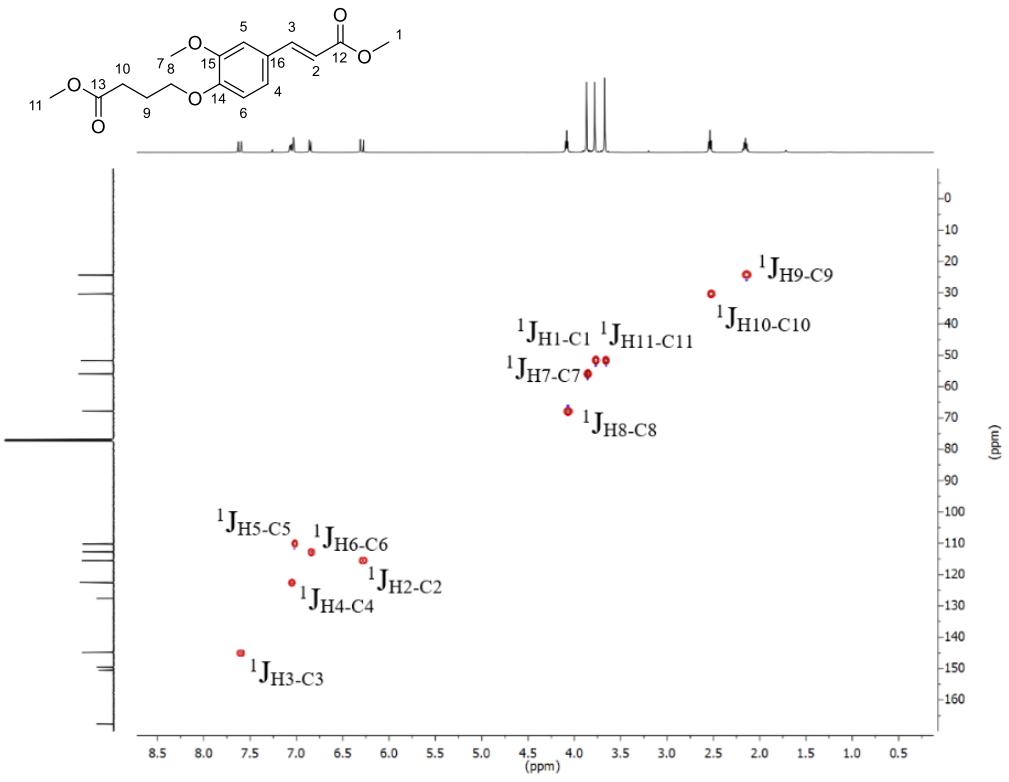

Figure S.3.16: HSQC NMR analysis of methyl 4-(methyl butanoate-oxy)-ferulate (DeFA^{II}) in $CDCl_3$

Polymers ^{1}H NMR analysis

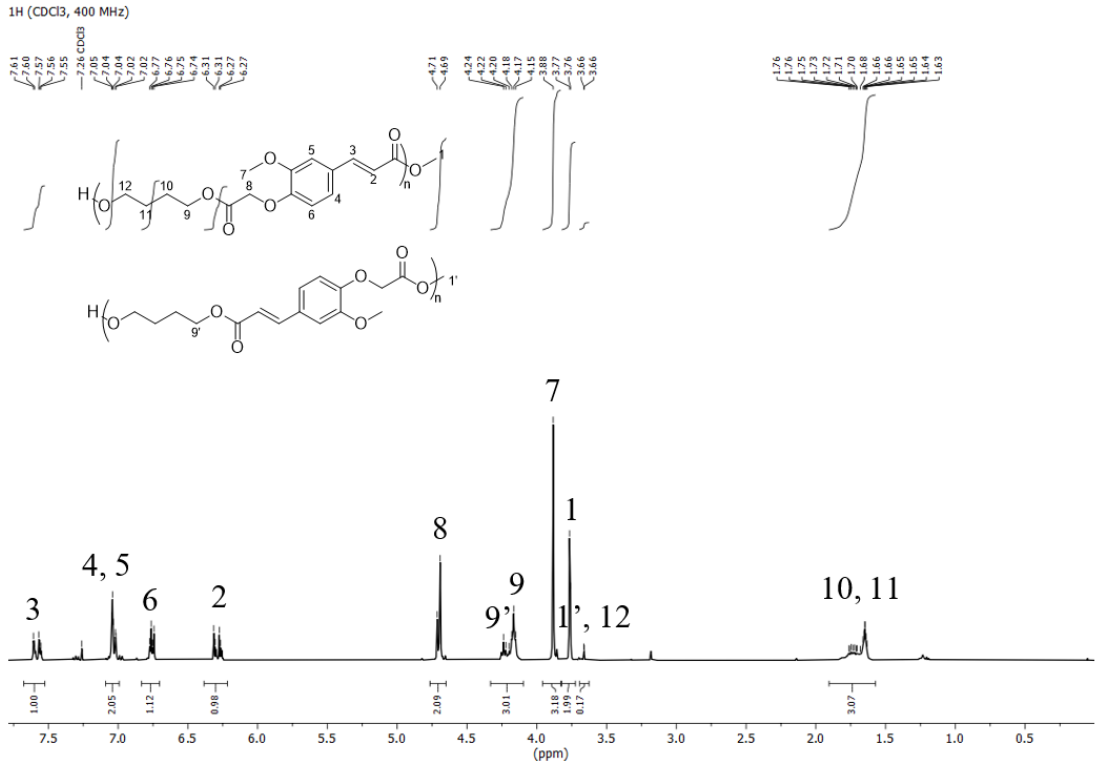

Figure S.3.17: ^{1}H NMR analysis of poly(butylene-co-4-(methyl ethanoate-oxy)-ferulate) (PDeFA^{I})

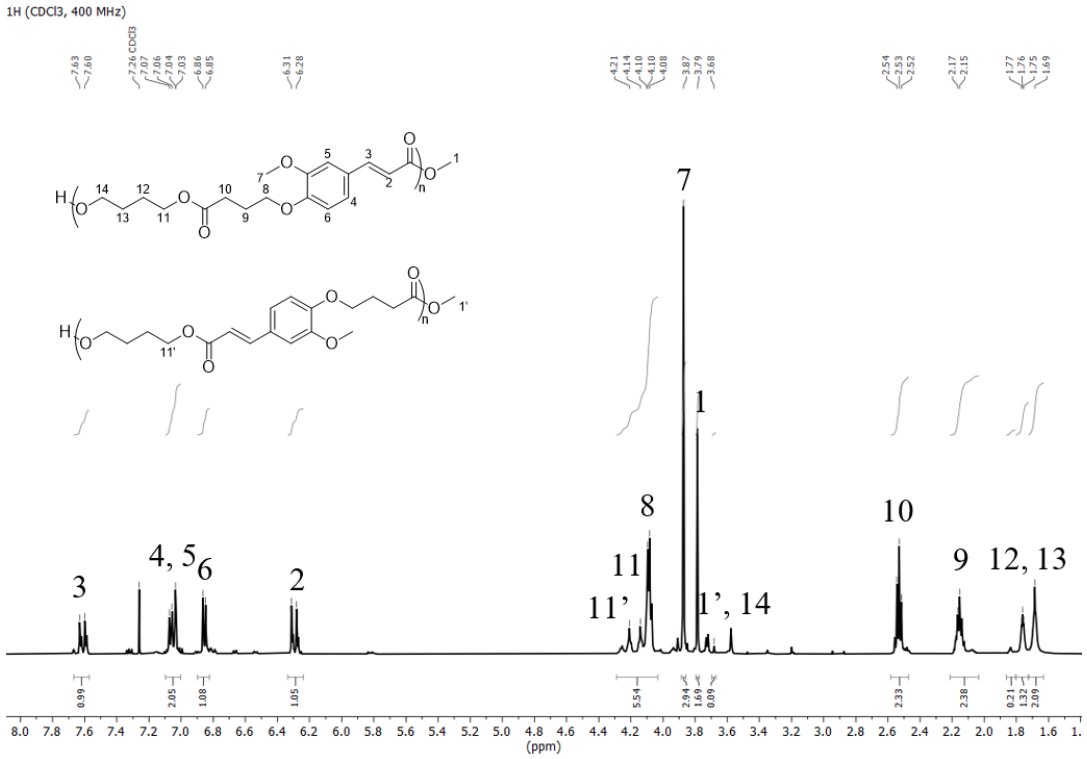

Figure S.3.18: ^{1}H NMR analysis of poly(butylene-co-4-(methyl butanoate-oxy)-ferulate) (PDeFA^{II})

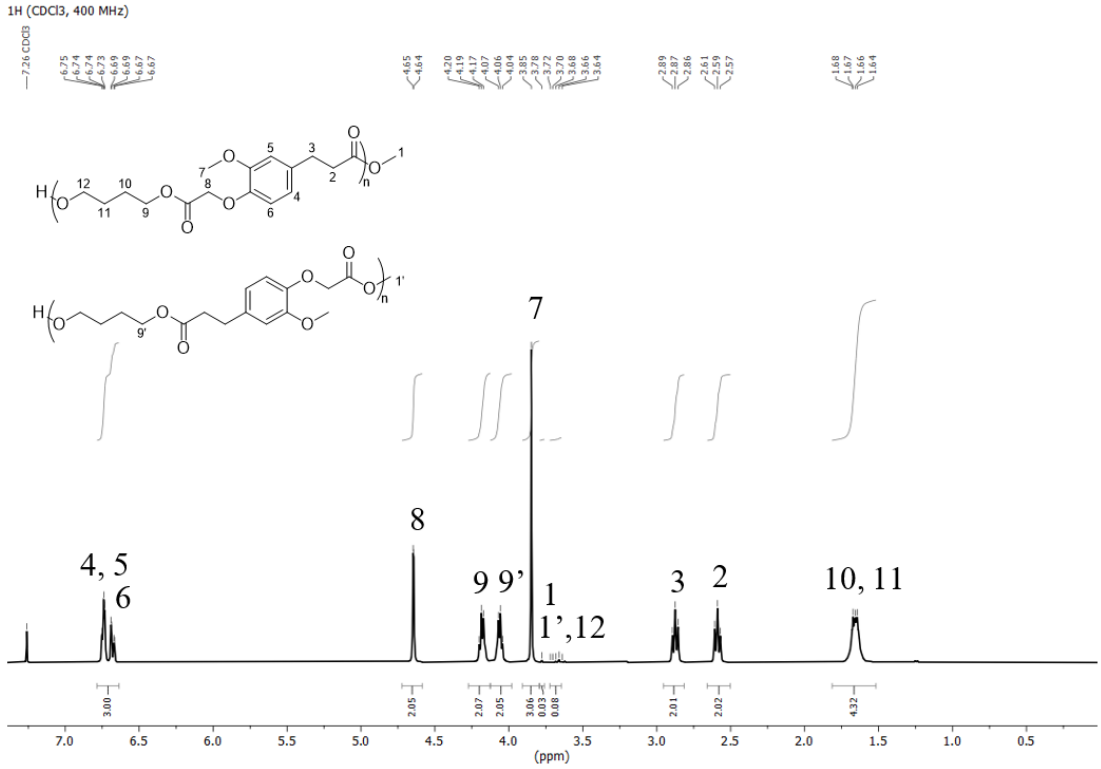

Figure S.3.19: ^{1}H NMR analysis of poly(butylene-co-3-(3-methoxy-4-(2-methoxy-2-oxoethoxy)phenyl)propanoate) (PH-DeFA^{I})

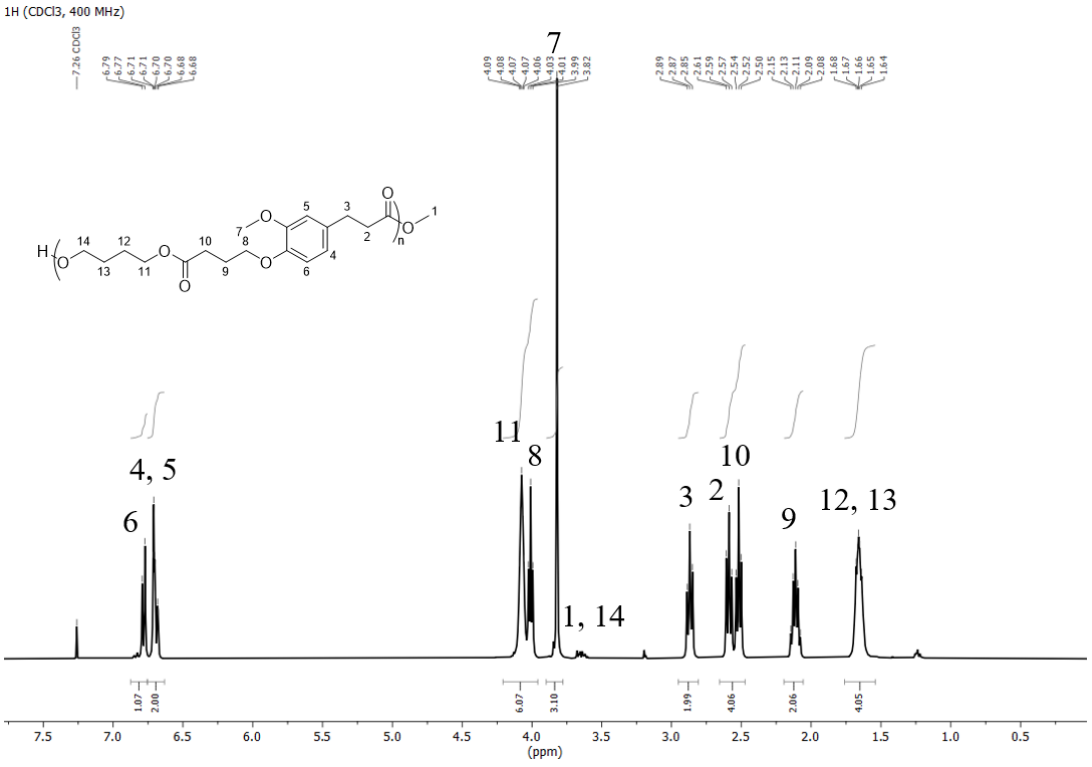

Figure S.3.20: ^{1}H NMR analysis of poly(butylene-co-4-(2-methoxy-4-(3-methoxy-3-oxopropyl)phenoxy)butanoate) (PH-DeFA^{II})

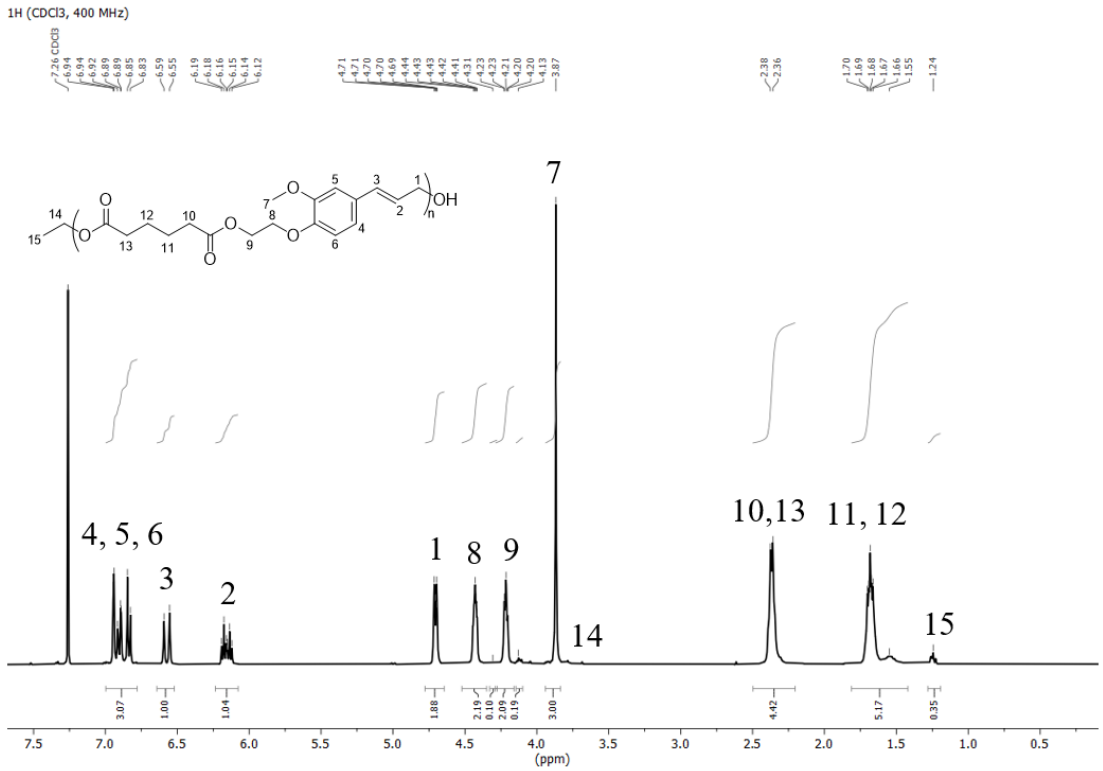

Figure S.3.21: ^{1}H NMR analysis of poly(4-(hydroxyethoxy)-coniferylene -co-adipate) (PFAD^{I})

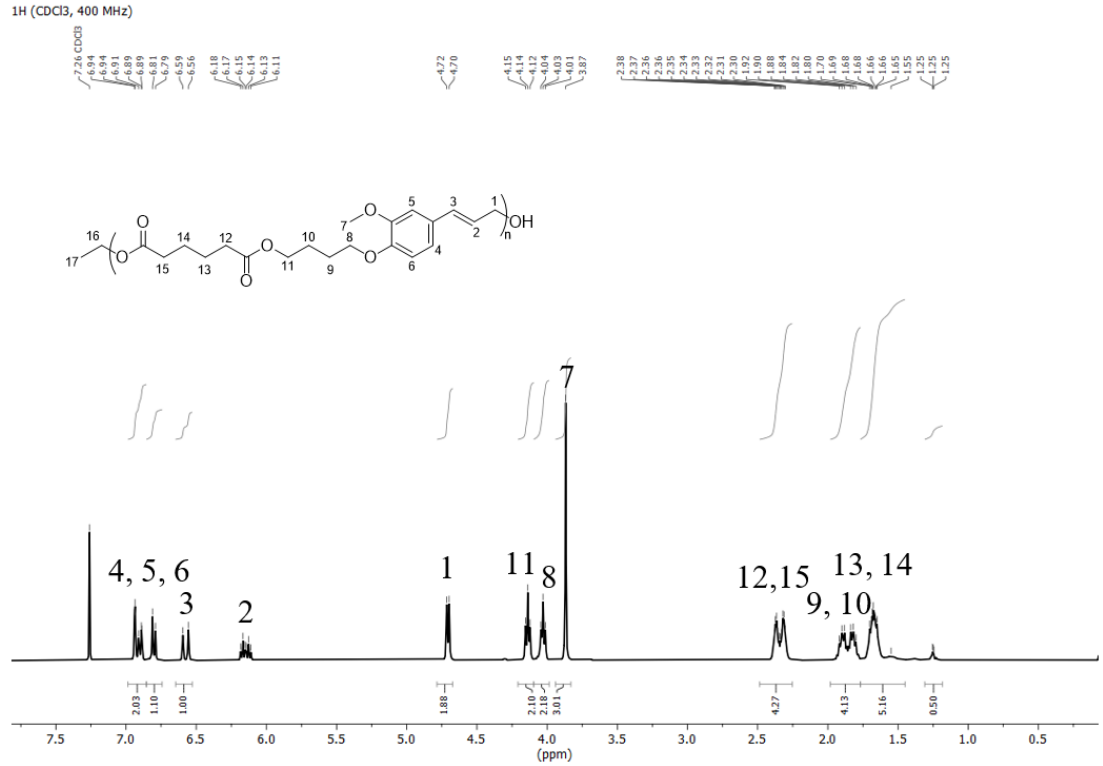

Figure S.3.22: ^{1}H NMR analysis of poly(4-(hydroxybutoxy)-coniferylene-co-adipate) (PFAD^{II})

SEC analyses of the polyesters

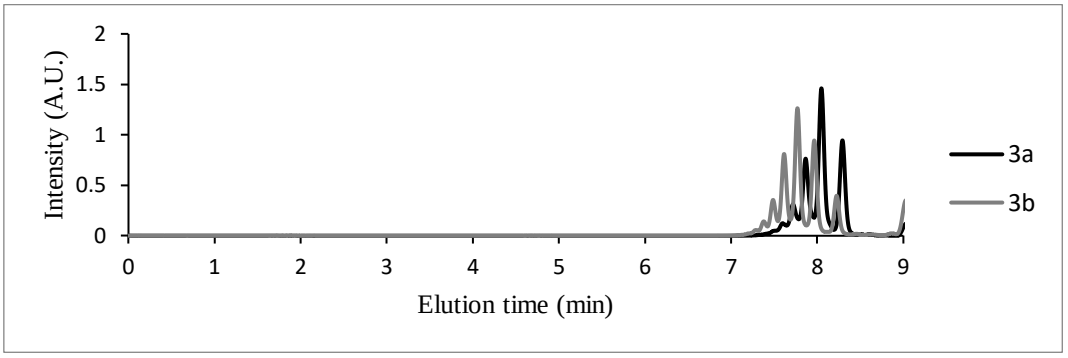

Figure S.3.23: SEC analyses in THF of the ferulic diester-based polyesters PDeFA^{I} and PDeFA^{II} (curves were normalised by their area).

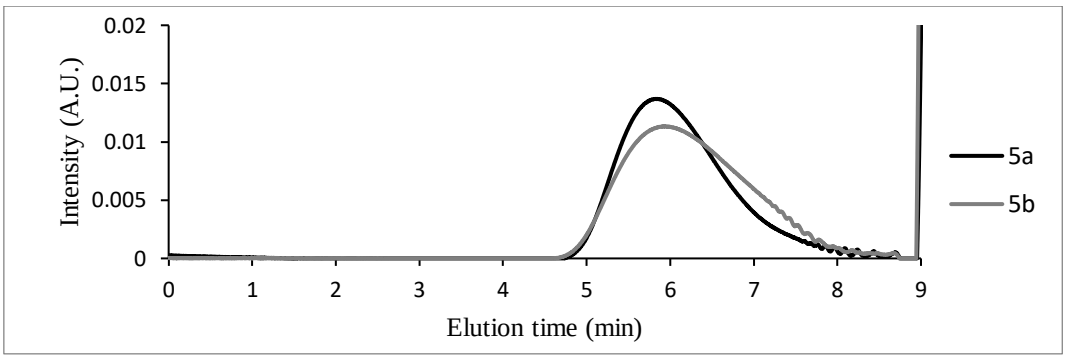

Figure S.3.24: SEC analyses in THF of the hydrogenated ferulic diester-based polyesters PH-DeFA^{I} and PH-DeFA^{II} (curves were normalised by their area).

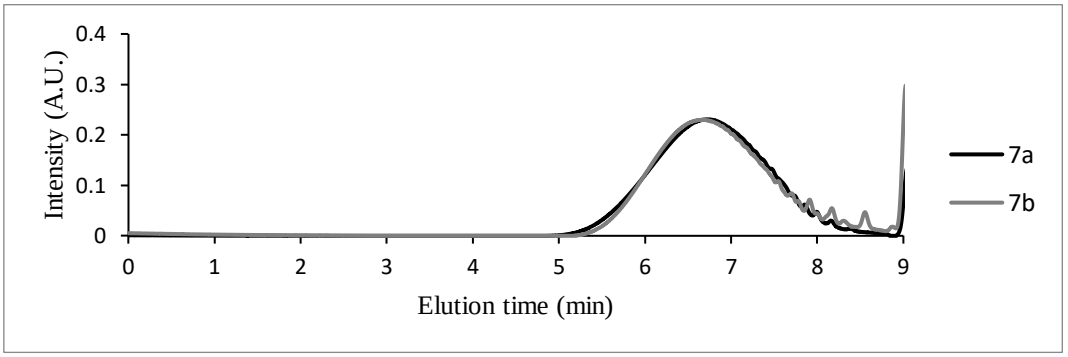

Figure S.3.25: SEC analyses in THF of ferulic diol-based polyesters PFAD^{I} and PFAD^{II} (curves were normalised by their area).

Polyesters synthesized from ferulic diol in excess

a)

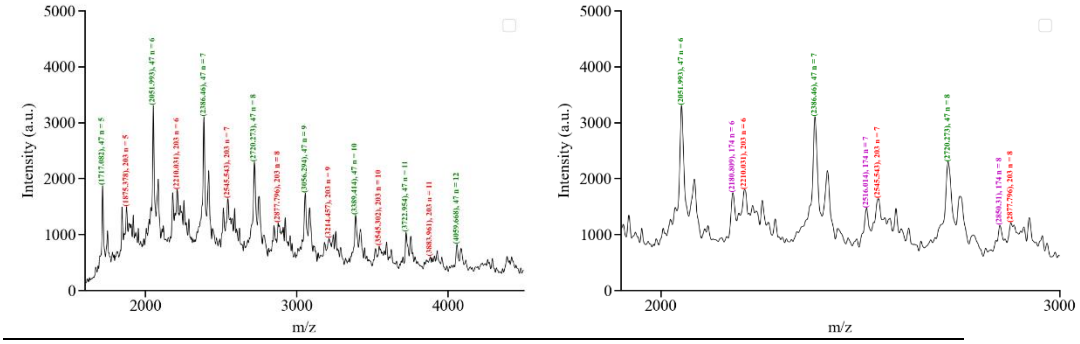

b)

Structure	End-group description	Residual mass (m/z)
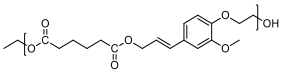	Ester and OH	46
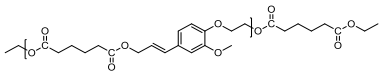	Both ester	202
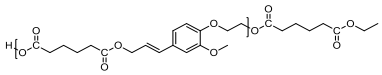	Hydrolysis	174

Figure S.3.26: MALDI-TOF MS analysis of PFAD^{I} obtained with 1.1 equivalent of diol in comparison to the diester after 24hours of synthesis in acetophenone at 90°C and under reduced pressure (a) MALD^{I}-TOF MS analysis, (b) mass of the corresponding end-groups.

a)

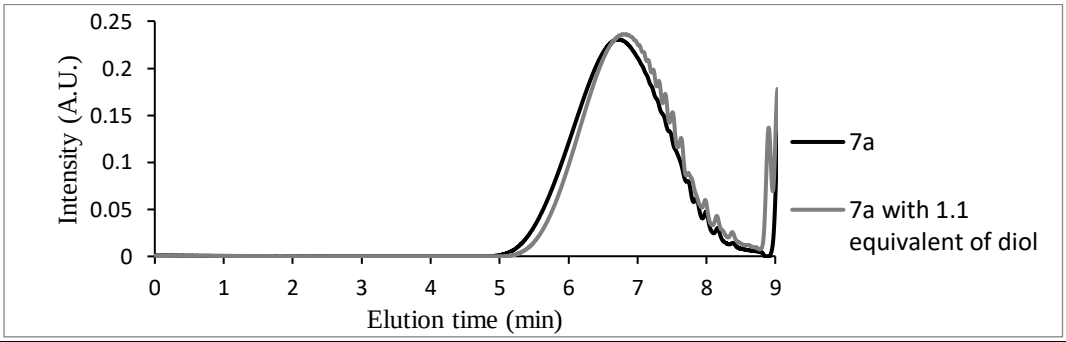

b)

Sample name	M_n (g.mol^{-1})	M_w (g.mol^{-1})	Đ
PFAD^{I}	6515	14970	2.298
PFAD^{I} with 1.1 equivalent of diol	5345	12528	2.344

Figure S.3.27: SEC analyses in THF of ferulic diol-based polyesters PFAD^{I} with and without excess of diol (curves were normalized by their area).

Annexes Chapitre 4 (supporting information)

NMR analyses of the p-acetyl ferulic acid (AcFA)

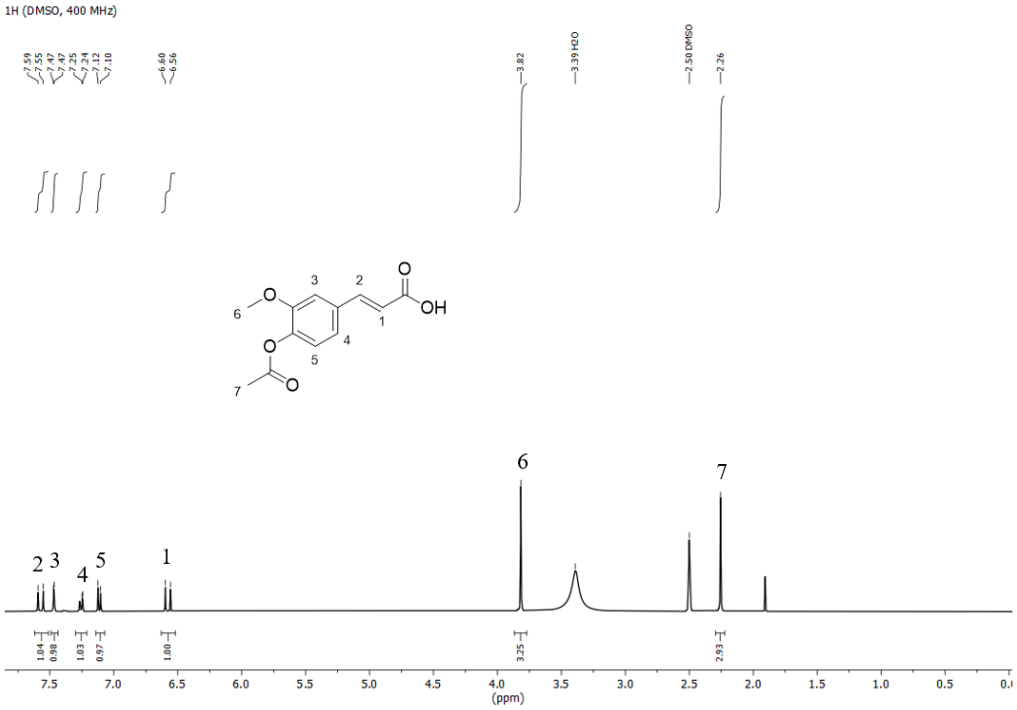

Figure S4.1: ^{1}H NMR analysis of the *p*-acetyl ferulic acid (AcFA).

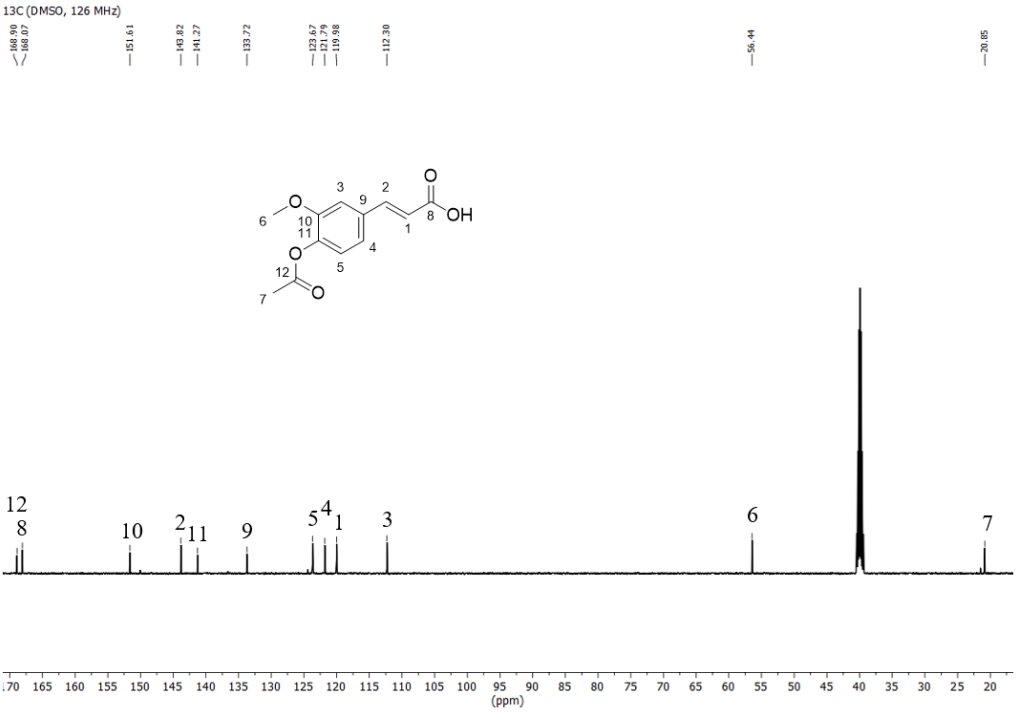

Figure S4.2: ^{13}C NMR analysis the *p*-acetyl ferulic acid (AcFA).

^{1}H NMR analysis of the p-acetyl ferulic acid (AcFA) dimerized in different solvents

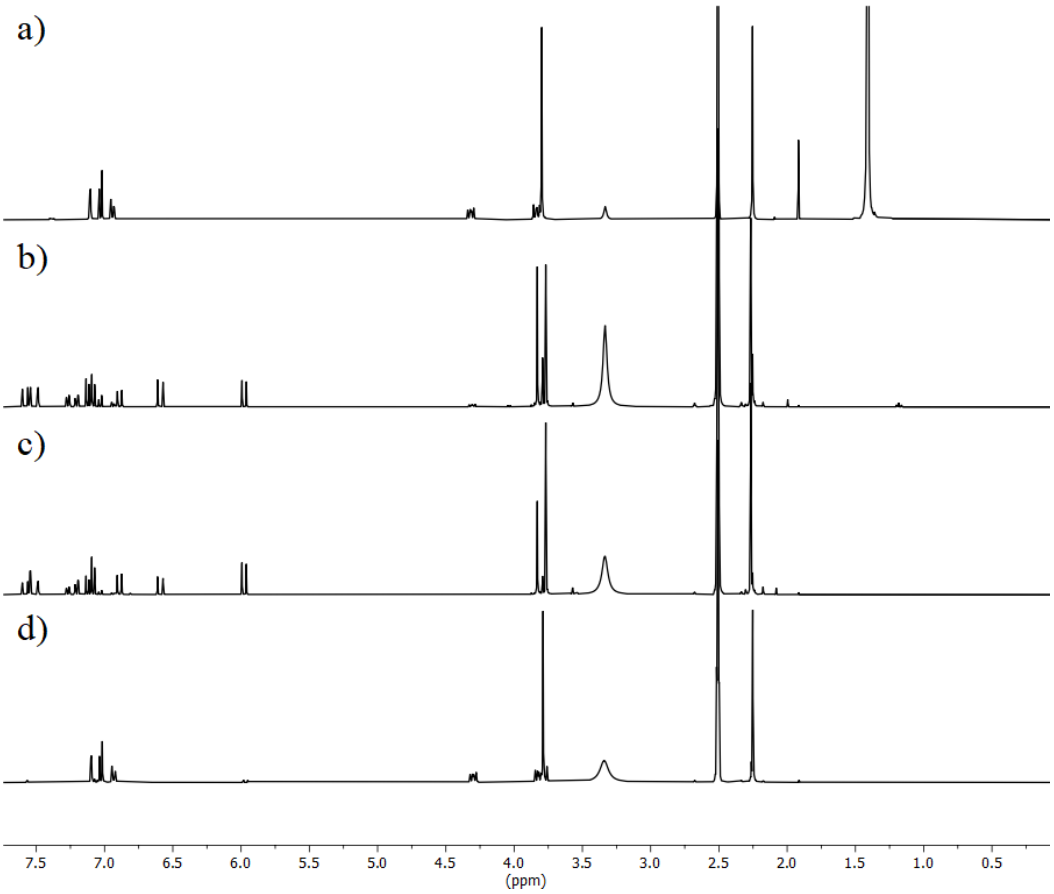

Figure S4.3: ^{1}H NMR analyses of AcFA exposed to UV light at a wavelength of 350 nm for 24 hours in different solvents. a) cyclohexane, b) ethyl acetate, c) acetonitrile, d) water.

NMR analyses of the dimer of p-acetyl ferulic acid (DAcFA)

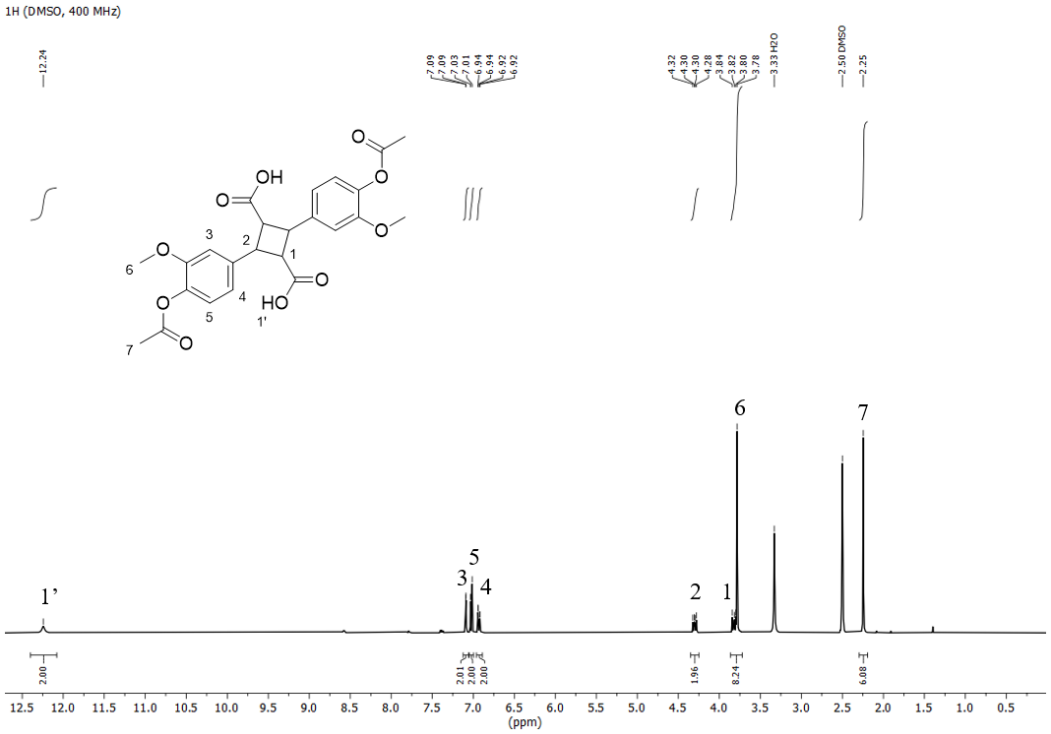

Figure S4.4: ^{1}H NMR analysis of the dimer of *p*-acetyl ferulic (DAcFA) synthesized in water.

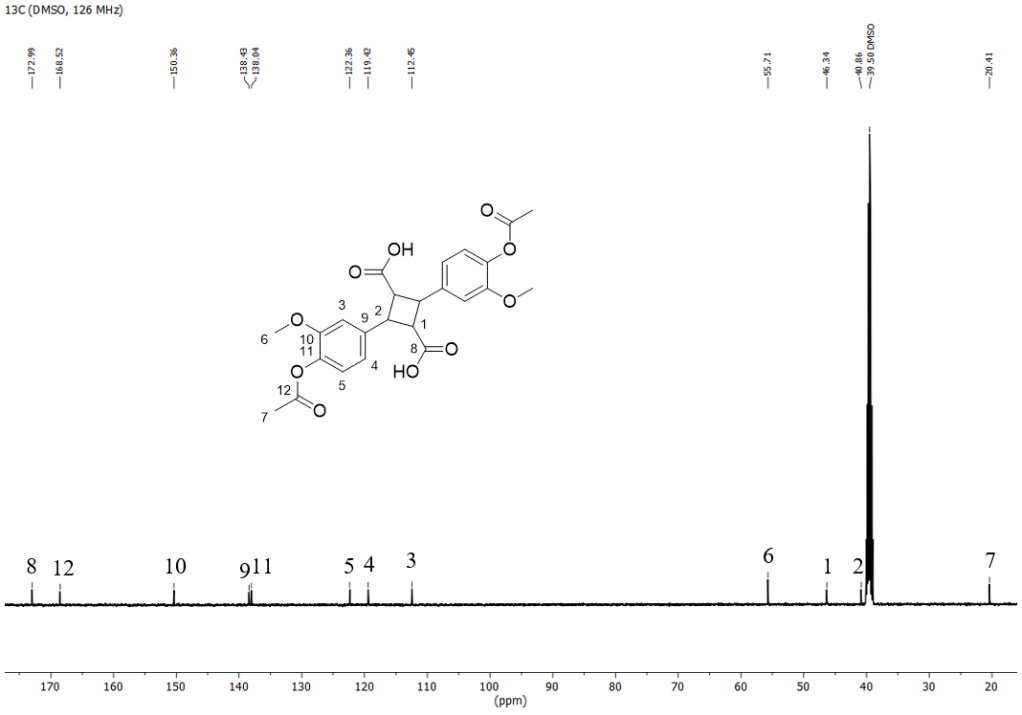

Figure S4.5: ^{13}C NMR analysis of the dimer of *p*-acetyl ferulic (DAcFA) synthesized in water.

NMR analyses of the dimer of ethyl ferulate (DeDFA)

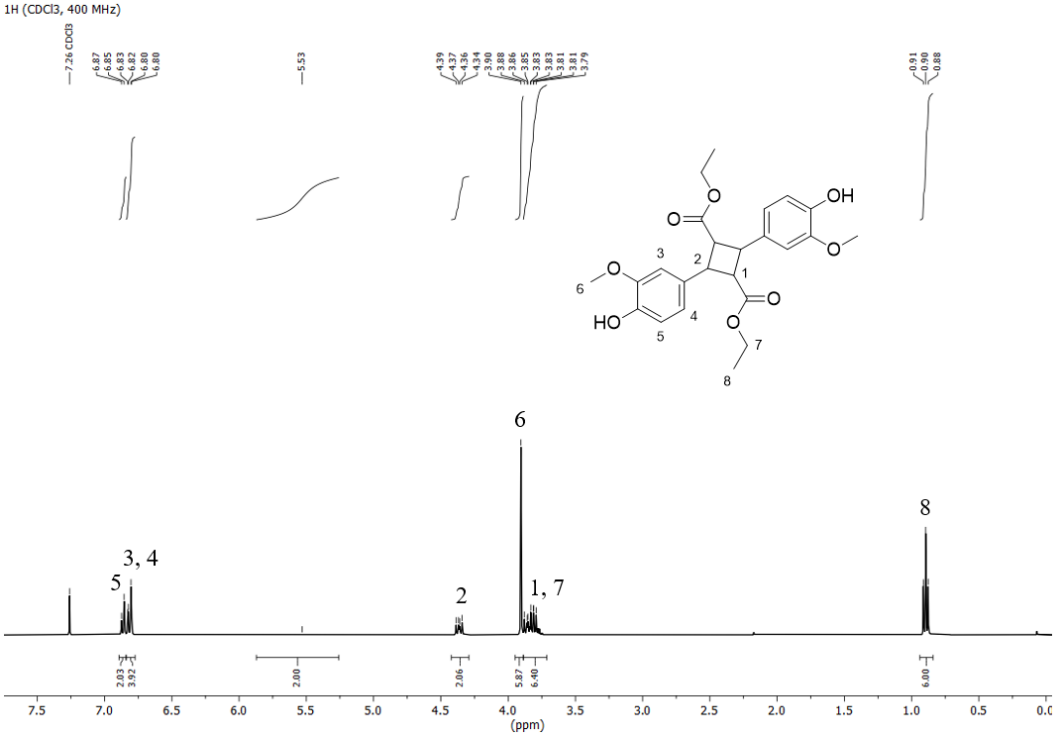

Figure S4.6: ^{1}H NMR analysis of the dimer of ethyl ferulate (DeDFA).

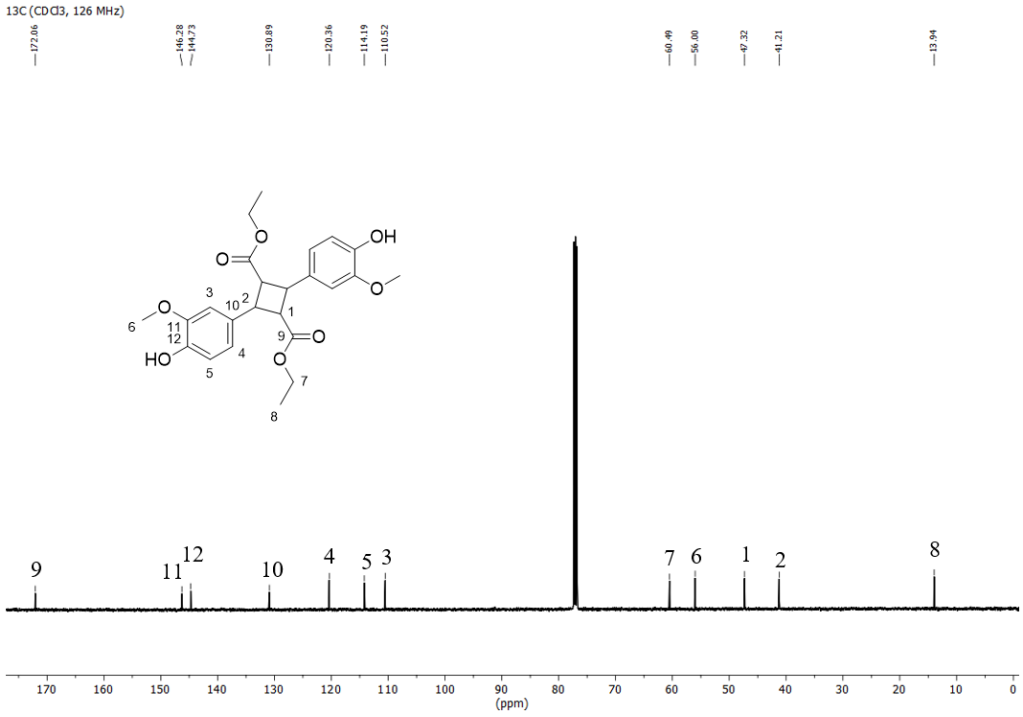

Figure S4.7: ^{13}C NMR analysis of the dimer of ethyl ferulate (DeDFA).

^{1}H NMR analyses of methyl 4-(methyl butanoate-oxy)-ferulate (DeFA^{II}) dimerized in different solvents.

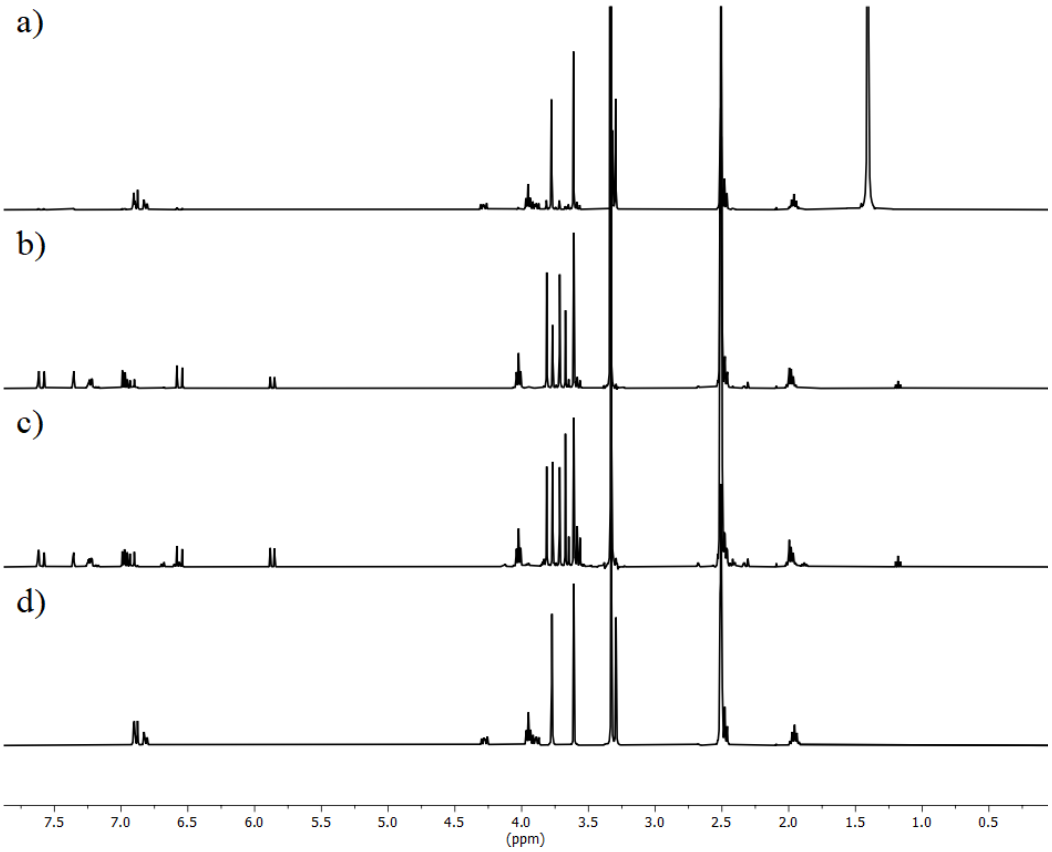

Figure S4.8: NMR analyses of methyl 4-(methyl butanoate-oxy)-ferulate (DeFA^{II}) exposed to UV light (350 nm) for 24 hours in different solvents. a) cyclohexane, b) ethyl acetate, c) acetonitrile, d) water.

Qualitative solubility determination of the methyl 4-(methyl butanoate-oxy)-ferulate (DeFA^{II})

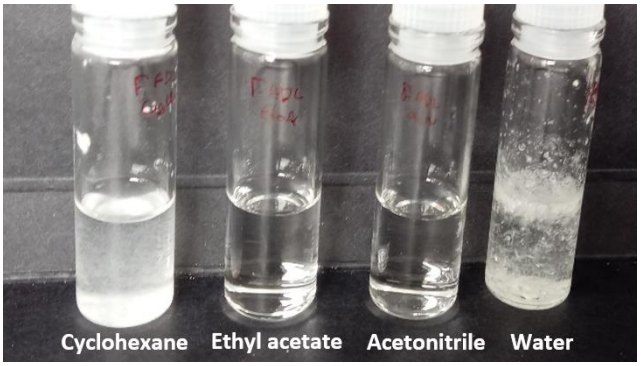

Figure S4.9: Vials containing DeFA^{II} solubilized or suspended is different solvent

NMR analyses of the dimer of methyl 4-(methyl butanoate-oxy)-ferulate (DDeFA^{II})

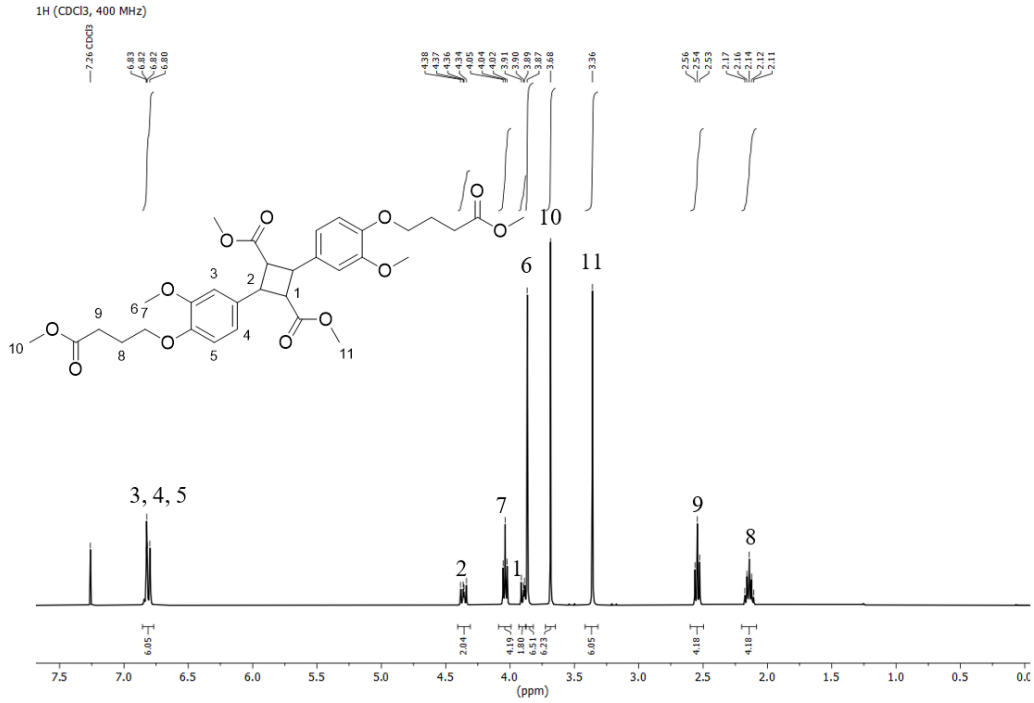

Figure S4.10: ^{1}H NMR analysis of the dimer of methyl 4-(methyl butanoate-oxy)-ferulate (DDeFA^{II}) synthesized in water.

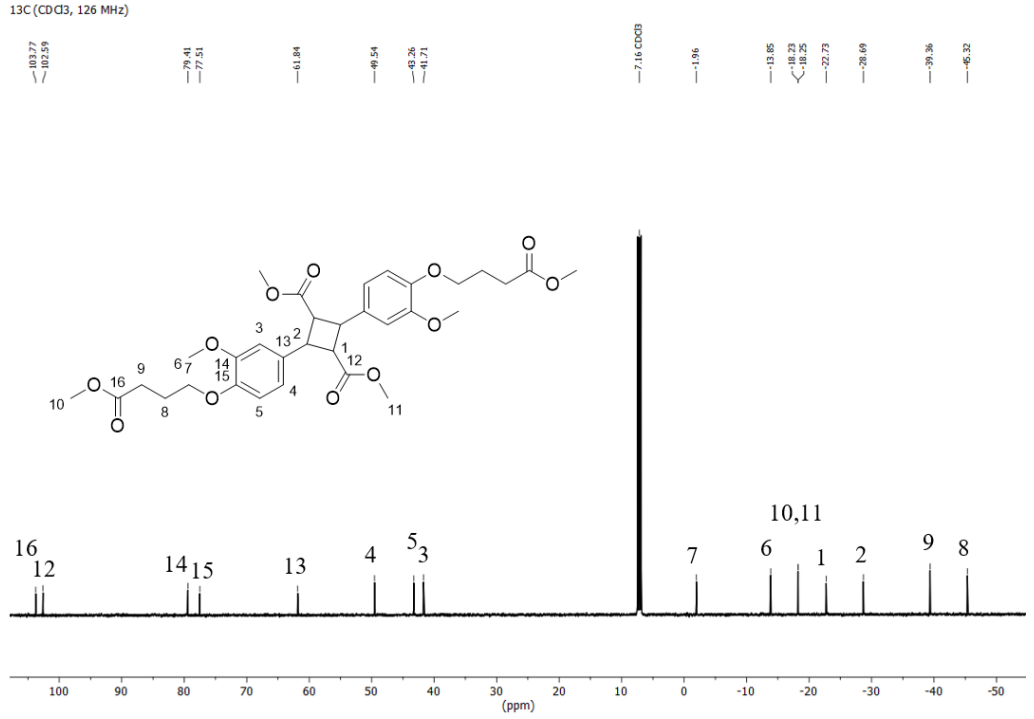

Figure S4.11: ^{13}C NMR analysis of the dimer of methyl 4-(methyl butanoate-oxy)-ferulate (DDeFA^{II}) synthesized in water

XRD analysis of the DeFA^{II} dimer (DDeFA^{II})

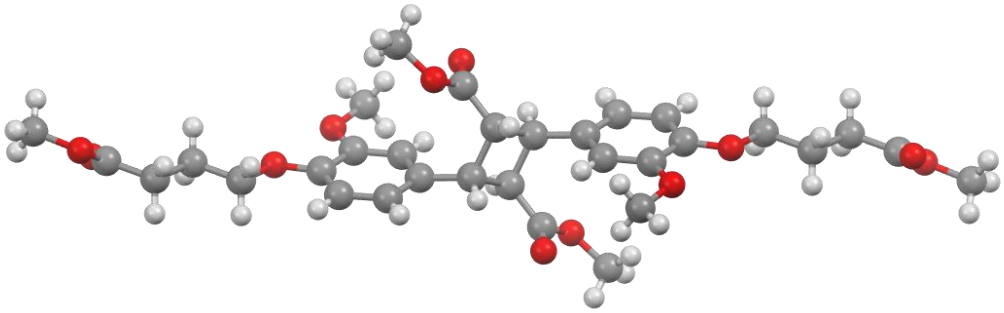

Formula	$C_{32}H_{40}O_{12}$
Space Group	$P\bar{1}$
a	5.9852
b	9.9087
c	13.4539
α	71.769
β	85.394
γ	80.079
Cell Volume	746.209
Z	1
Z'	0.5
R-Factor	4.6 %

Figure S4.12: XRD analysis of DDeFA^{II}

XRD analysis of the DeFA^{II}

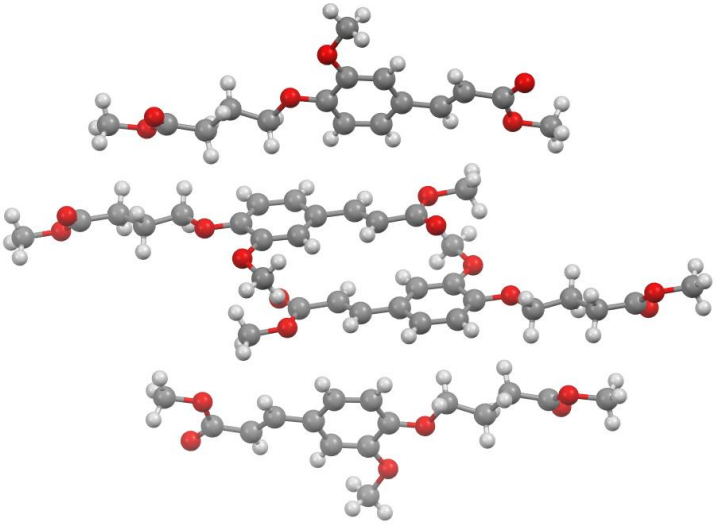

Formula	$C_{16}H_{20}O_6$
Space Group	P1
a	5.9824
b	14.9174
c	17.7484
α	74.564
β	81.164
γ	84.301
Cell Volume	1505.81
Z	4
Z'	2
R-Factor	10.92 %

Figure S4.13: XRD analysis of DeFA^{II}

Essay of reactivity of DDeFA^{II} with CALB

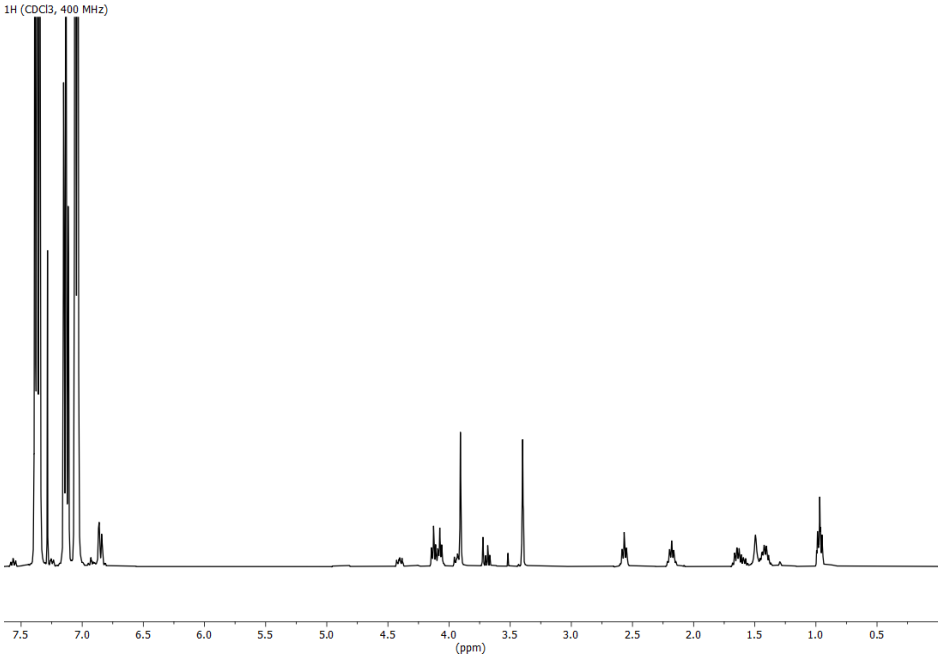

Figure S4.14: ^{1}H NMR analysis of the medium of reaction of DeDFA with an excess of butanol (CALB, in diphenyl ether, 90°C, 16 h).

^{1}H NMR analyses of the polyesters.

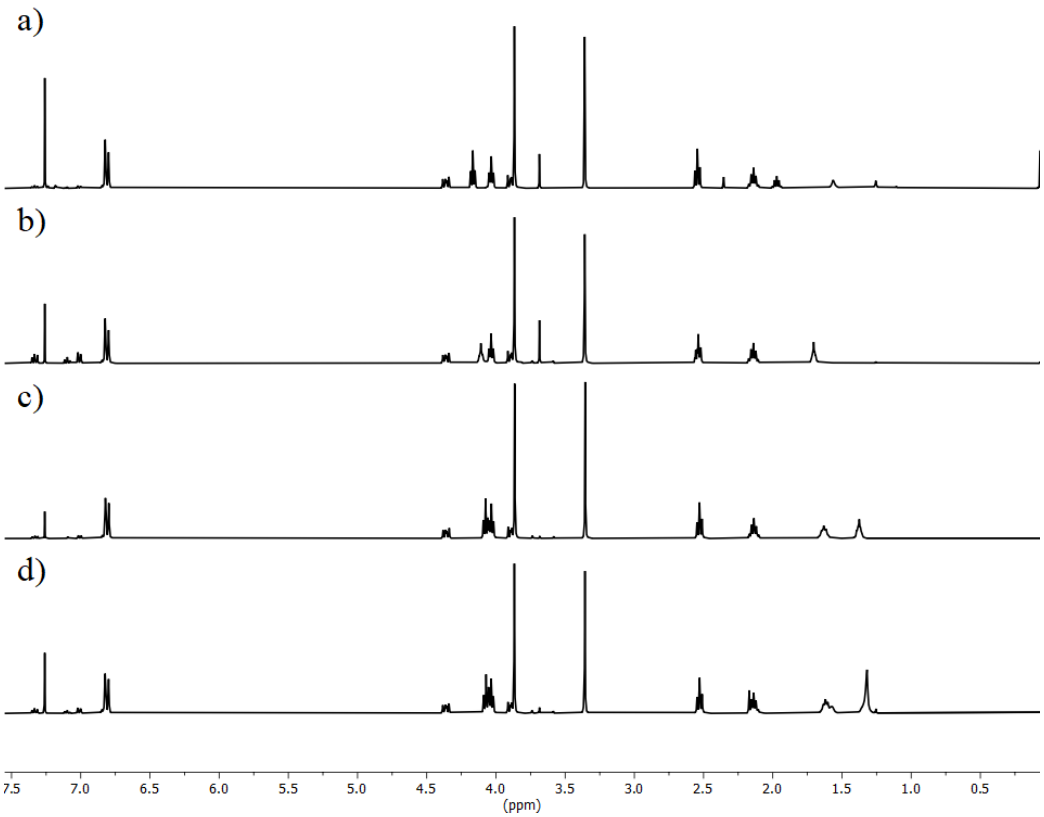

Figure S4.15: ^{1}H NMR analyses of polyesters synthesized from DDeFA^{II} and diols of different lengths through CALB-catalyzed polymerization (diphenyl ether, 90°C, 48h, partial vacuum). Diols employed for the reaction: a) PDO; b) BDO; c) HDO; d) ODO.

SEC analyses of the polyesters synthesized with PDO

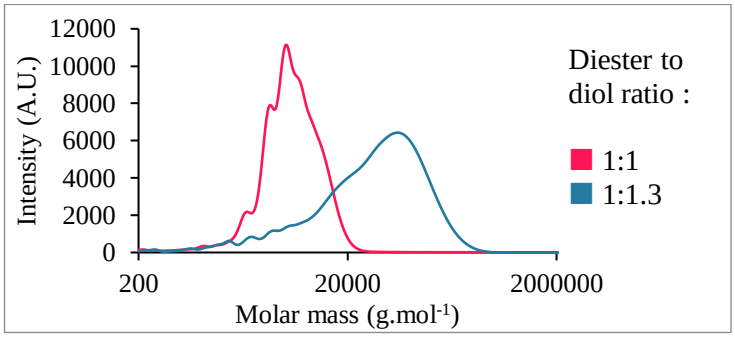

Figure S4.16: SEC chromatogram of polyesters synthesized from DDeFA^{II} with different ratio of PDO through CALB catalyzed polymerization (diphenyl ether, 90°C, 48h, partial vacuum)

^{1}H NMR analyses of polyesters synthesized from DDeFA^{II} and HDO after UV-C-induced photodepolymerization.

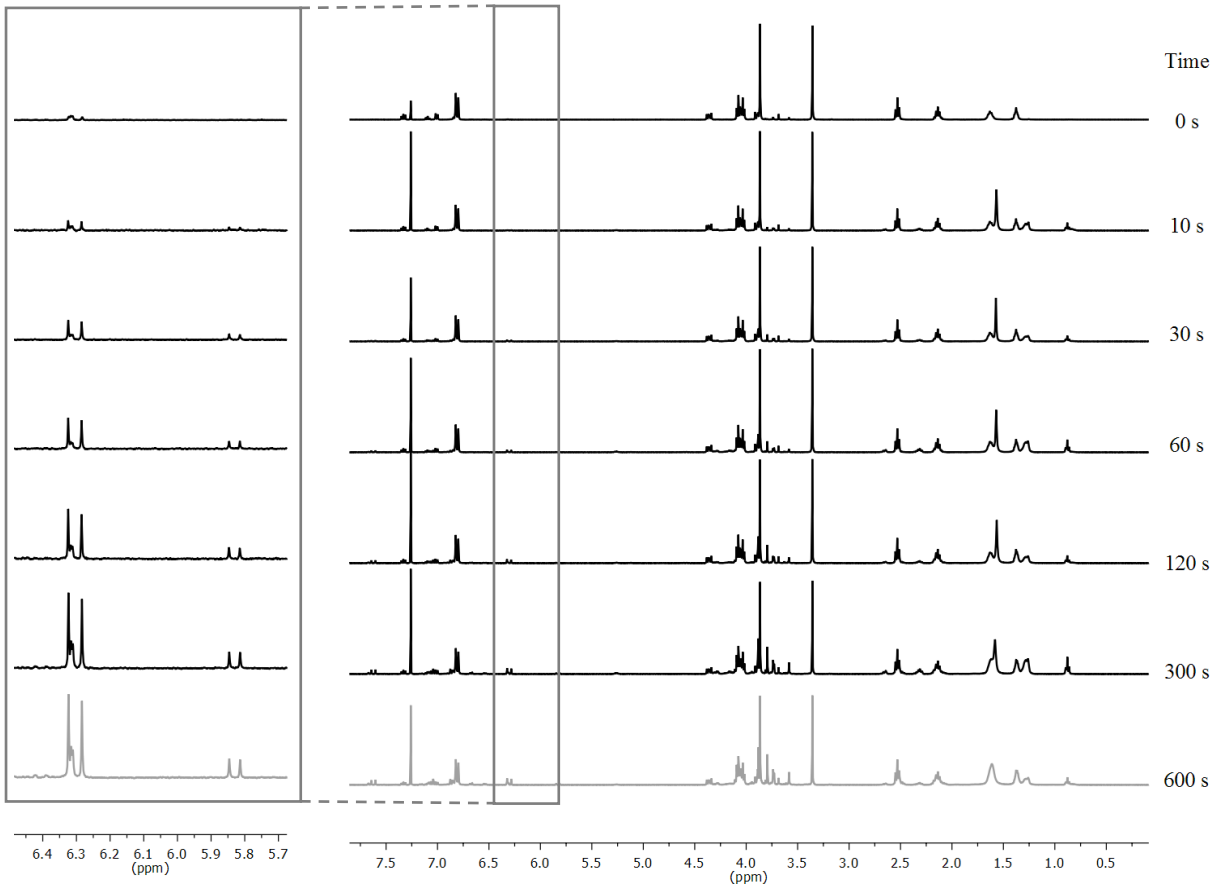

Figure S4.17: ^{1}H NMR analyses of the polyester synthesized from DDeFA^{II} and HDO after different times of UV-C light irradiation.

SEC and ^{1}H NMR analyses of the polyesters synthesized from ODO, BDO and PDO after UV-C-induced photodepolymerization.

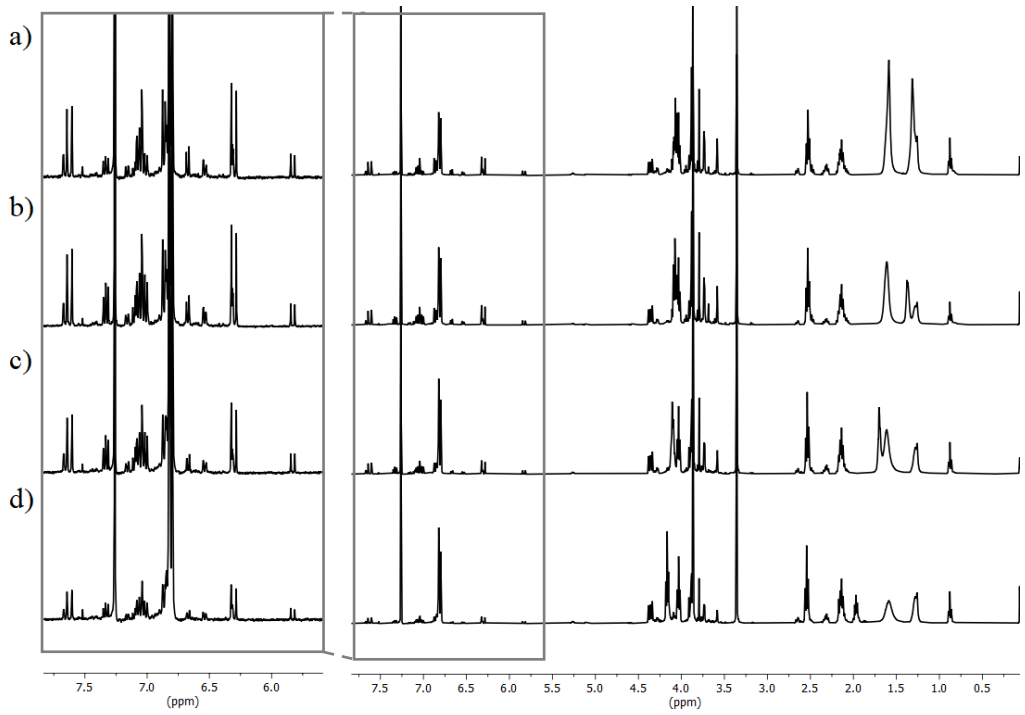

Figure S4.18: ^{1}H NMR analyses of polyesters synthesized from DDeFA^{II} and diols of different length after UV-C irradiation (600 seconds, RT) : a) PDO; b) BDO; c) HDO; d) ODO.

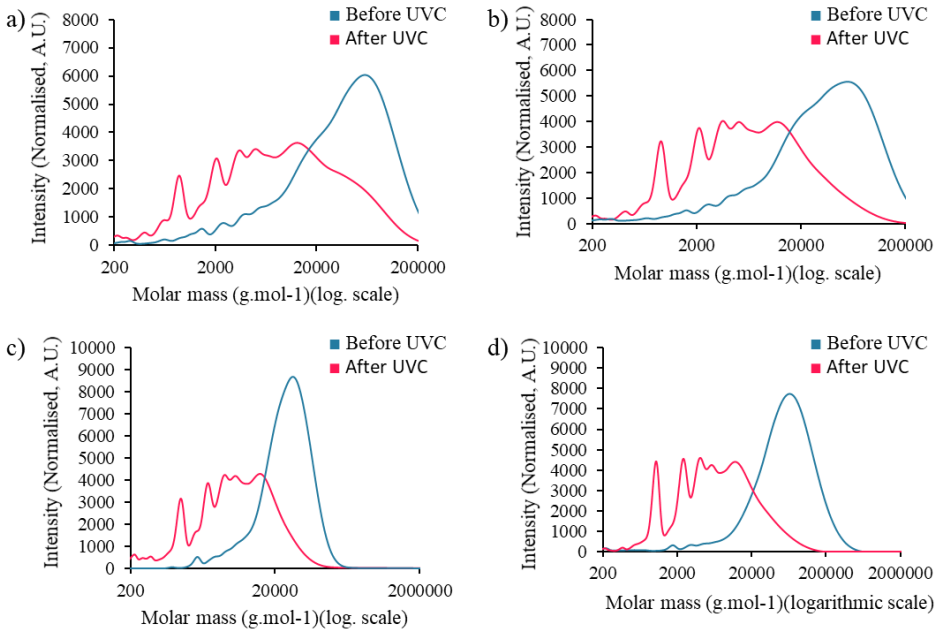

Figure S4.19: SEC chromatograms of polyesters synthesized from DDeFA^{II} and diols of different length after UV-C irradiation under (600 seconds, RT): a) PDO; b) BDO; c) HDO; d) ODO.

Details of the calculation of the DP_n of the $DDeFA^{II}$-based polyesters after photo-depolymerization

The DPn of a polymer distribution can be calculated as in Equation 2.a where n_{tot} is the total number of repeating unit and n_{chain} is the number of chains. As each chain contains two end-groups, n_{chain} is equal to half the number of end-groups $n_{end\text{-}groups}$ and Equation 2.a can be re-written as in Equation 2.b.

$$DP_n = \frac{n_{tot}}{n_{chain}} \quad \text{Eq. 2.a}$$

$$DP_n = \frac{n_{tot}}{0.5 * n_{end-groups}} \quad \text{Eq. 2.b}$$

The $n_{end\text{-}groups}$ at a given time is equal to the number of end-groups before photodepolymerization plus the number of double bonds, written n_{db}. If a single polymer chain is considered, the number of end-groups before photodepolymerization is 2 as shown in Equation 3.

$$n_{end-groups} = 2 + n_{db} \text{ (for a single polymer chain)} \quad \text{Eq. 3}$$

The number of double bonds can be calculated from the yield measured in NMR (written $\alpha_{(t)}$) as in the equation 4.

$$n_{db} = \alpha_{(t)} * n_{tot} \quad \text{Eq. 4}$$

Finally, considering again a single polymer chain, the total number of repeating units n_{tot} is equal to $DPn_{(t=0)}$, the degree of polymerization before photodepolymerization. Combining Equations 2.b, 3 and 4 gives Equation 5 that allows an estimation of the DPn of the polymer at a given time during the photodepolylerization ($DP_{n(t)}$).

$$DP_{n(t)} = \frac{DP_{n(t=0)}}{0.5 * (2 + \alpha_{(t)} * DP_{n(t=0)})} \quad \text{Eq. 5}$$

Figure S4.20: Detail of the calculation of the DP_n of the oligo-esters after photo-depolymerization.

^{1}H NMR analysis of the oligo-esters repolymerized under UV-A.

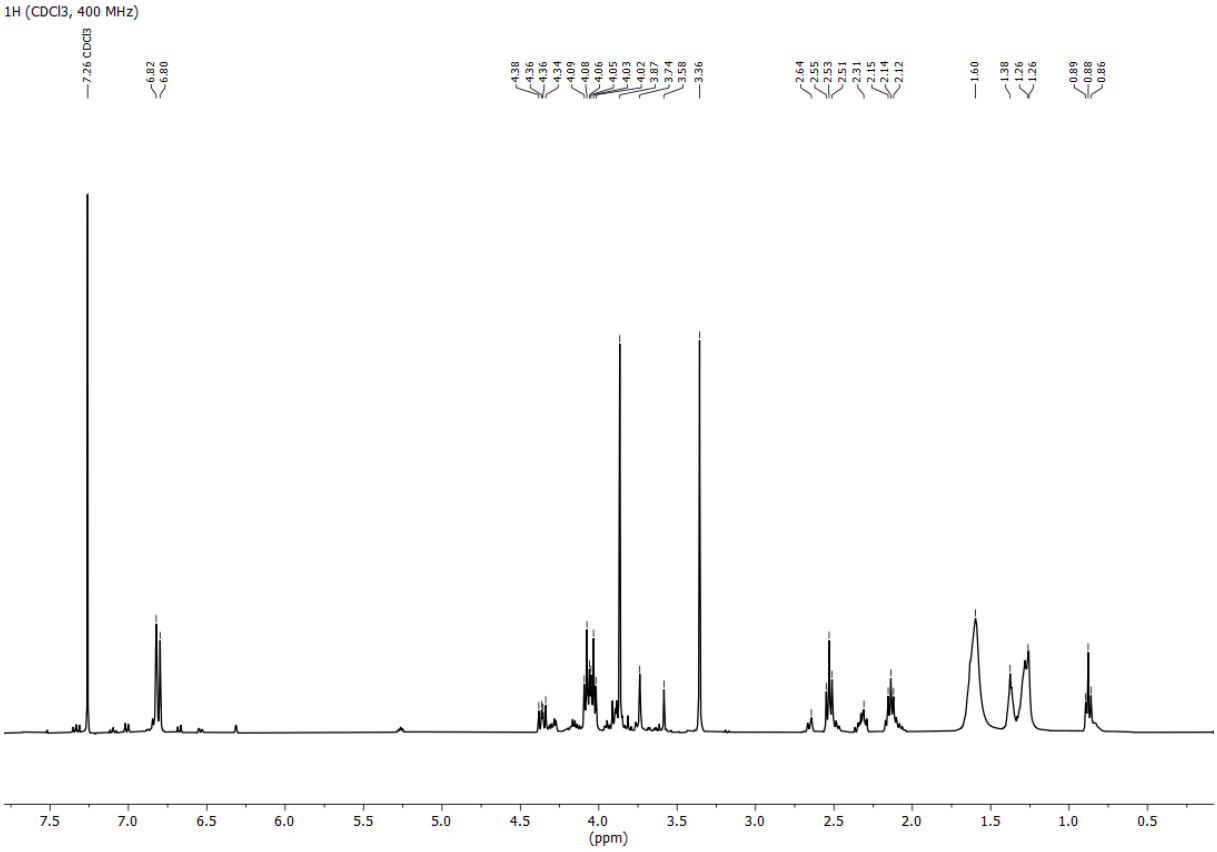

Figure S4.21: NMR analysis of the polyester synthesized from DDeFA^{II} and HDO, initially photodepolymerized under UV-C irradiation for 600s and subsequently repolymerized under UV-A light for 120 minutes.

Annexes Chapitre 5 (supporting information)

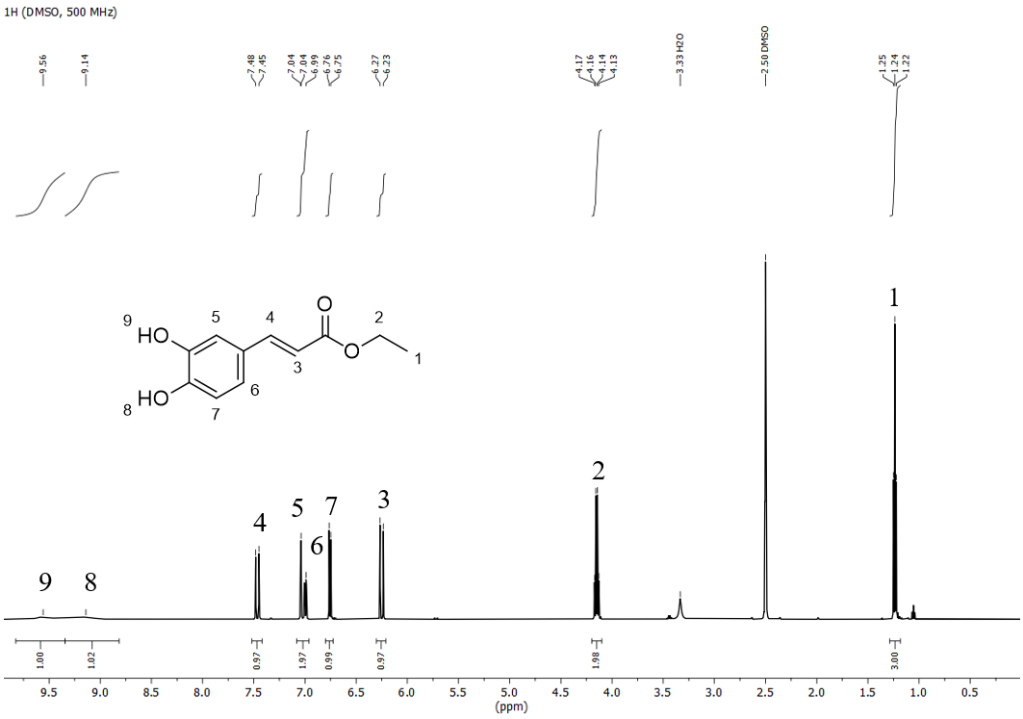

Figure S5.1: ^{1}H NMR analysis of ethyl caffeate.

Figure S5.2: ^{13}C NMR analysis of ethyl caffeate.

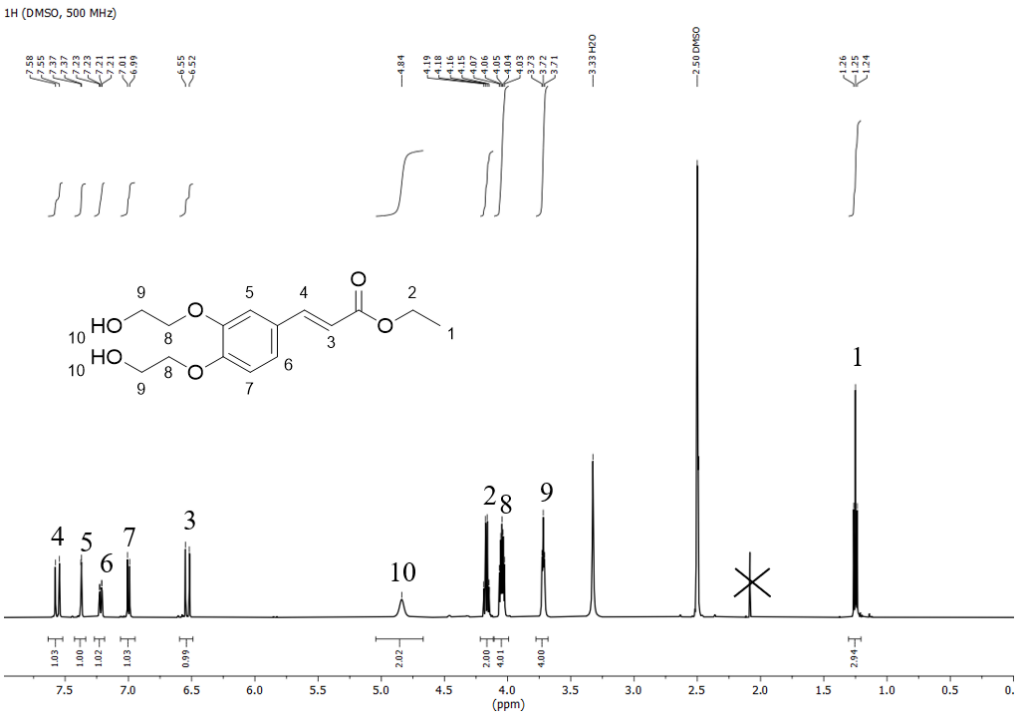

Figure S5.3: ^{1}H NMR analysis of ethyl 3,4-bis(hydroxyethyl) caffeate (CD).

Figure S5.4: ^{13}C NMR analysis of ethyl 3,4-bis(hydroxyethyl) caffeate (CD).

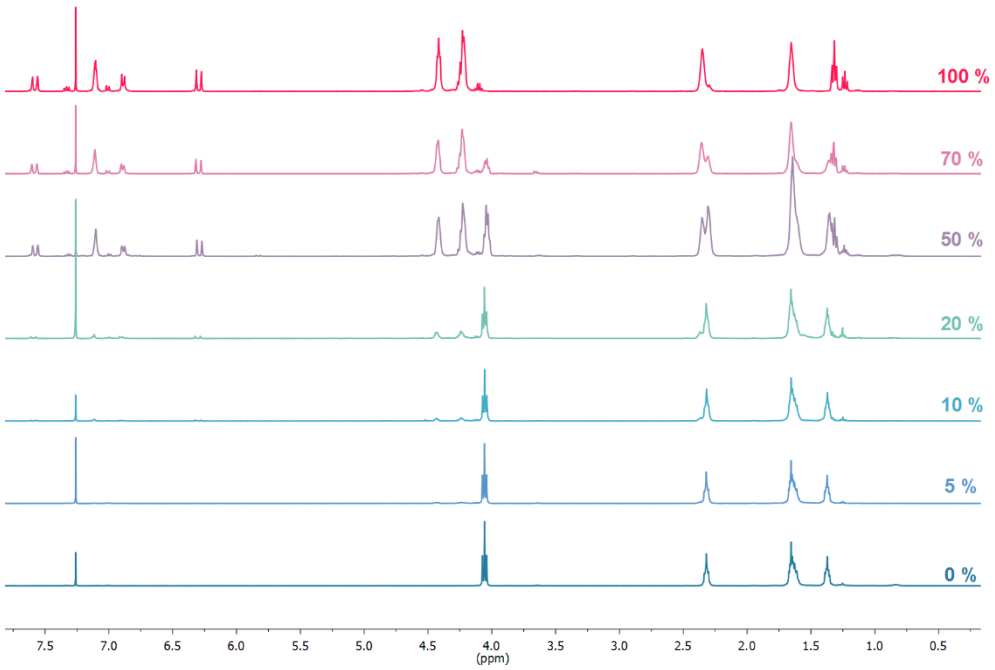

Figure S5.5: NMR analyses of polyesters synthesised with different CD ratios (CALB in diphenyl ether, 90 °C, 24 h under partial vacuum).

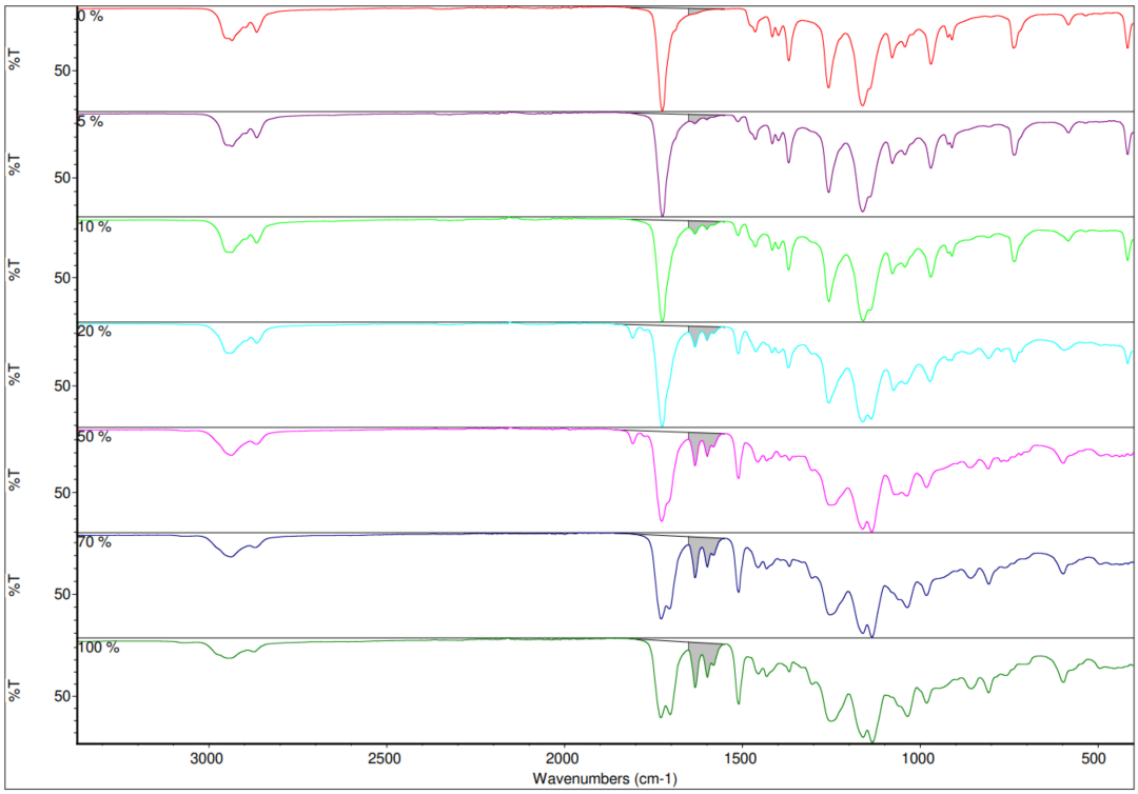

Figure S5.6: FTIR analyses of polyesters synthesised with different CD ratios (CALB in diphenyl ether, 90 °C, 24 h under partial vacuum).

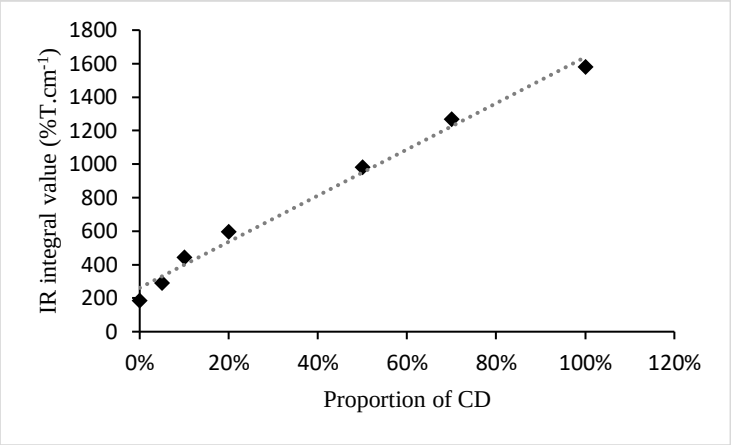

Figure S5.7: Integration of the FTIR bands attributed to the CD in the polyesters against the ratio of CD.

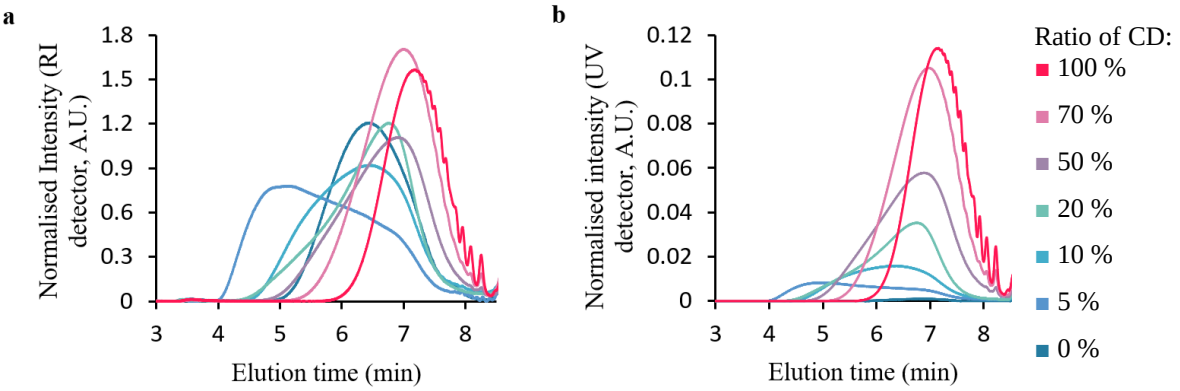

Figure S5.8:.SEC analyses of polyesters synthesised with different CD ratios (CALB in diphenyl ether, 90 °C, 24 h under partial vacuum). a: refractive index detector, intensity normalised by area, b: UV detector, intensity normalised according to area in RI detection.

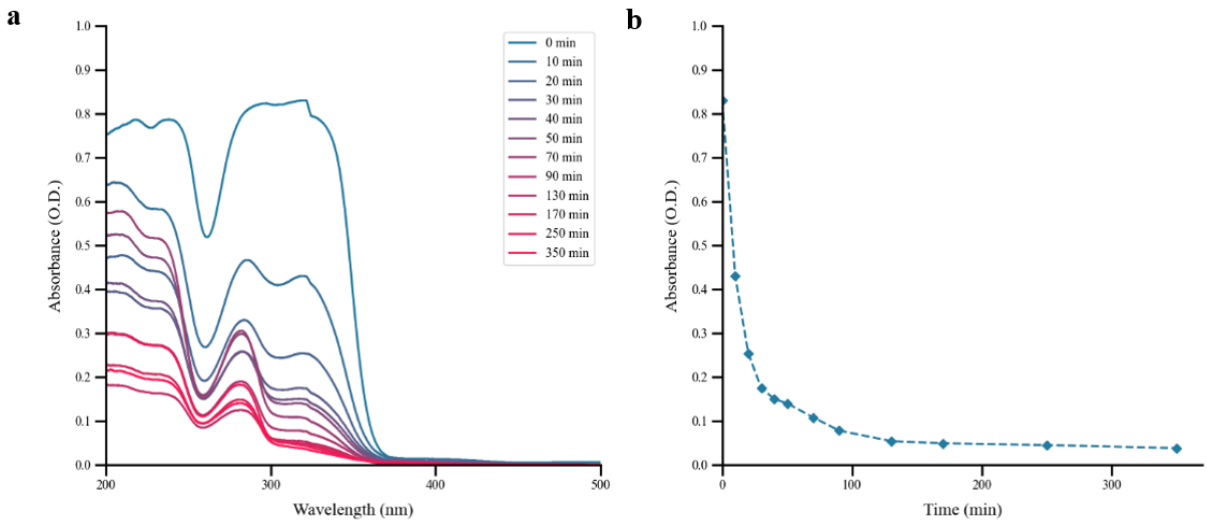

Figure S5.9: Measurement of the absorbance of the polyester containing 50 % of CD. a) Absorption spectra between 500 and 200 nm for various times of UV-A irradiation. b) Evolution of the maximum of absorption against UV-A irradiation time.

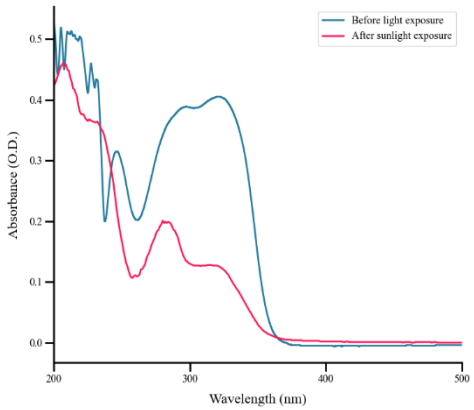

Figure S5.10: Absorption spectra of the polyester containing 10 % of CD before and after sunlight irradiation (7 h exposure).

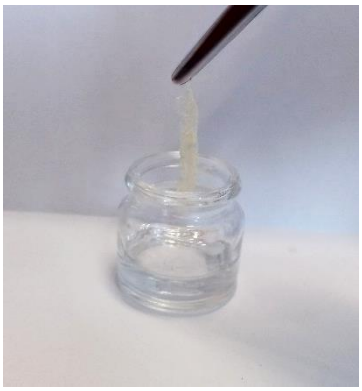

Figure S5.11: Visual aspect of the polyester containing 20 %CD irradiated under UV-A light after swelling in THF for 48 h.

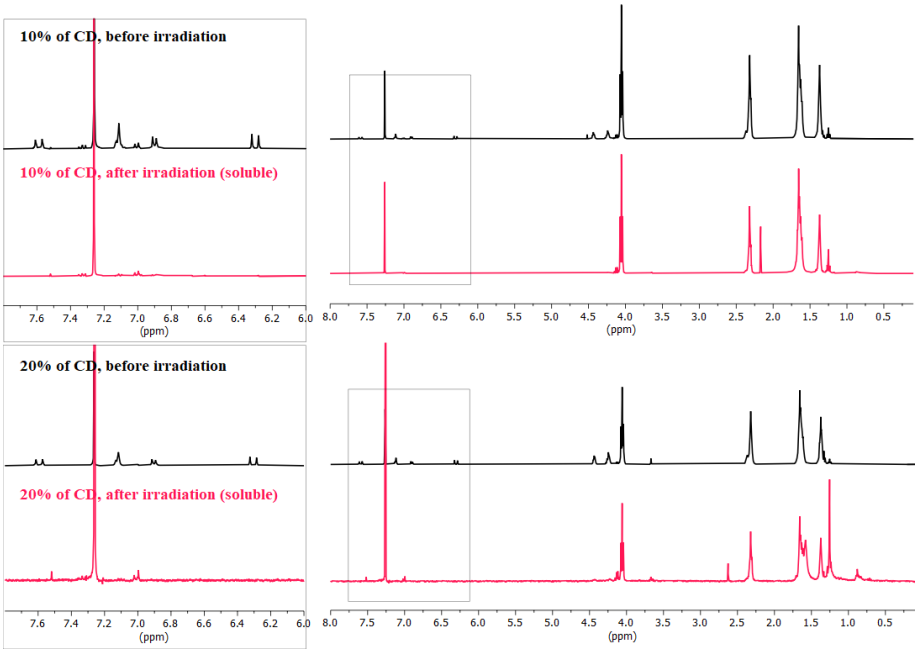

Figure S5.12: ^{1}H NMR analyses of the soluble fraction (in THF) recovered from gel content tests of the polyesters containing 10 % and 20 % of CD before and after irradiation under UV-A light.

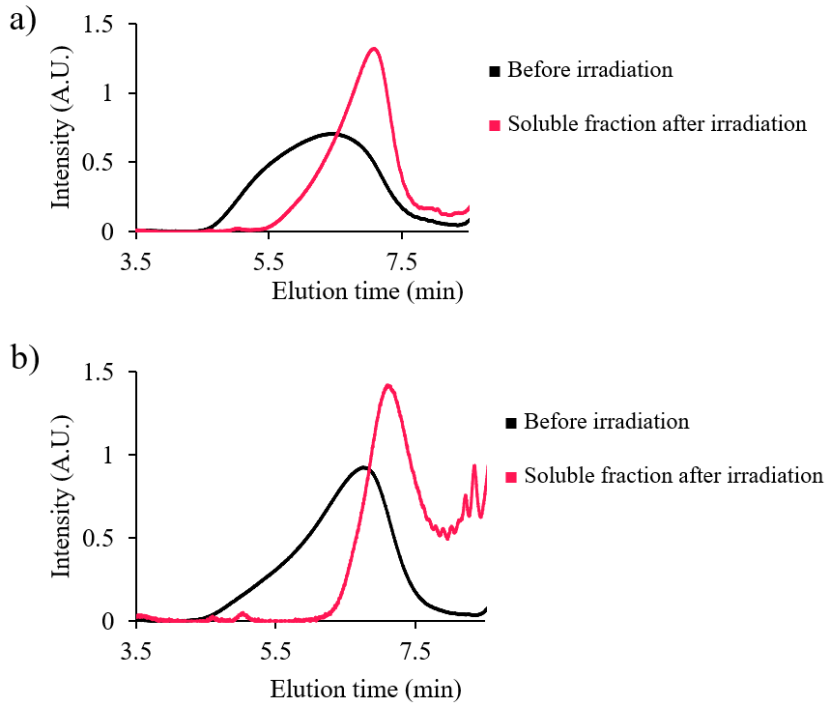

Figure S5.13: SEC analyses of the soluble fraction (in THF) recovered from the polyesters containing different ratio of CD before and after irradiation under UV-A light. a) 10 % of CD, b) 20 % of CD. Intensity normalised by the curve area.

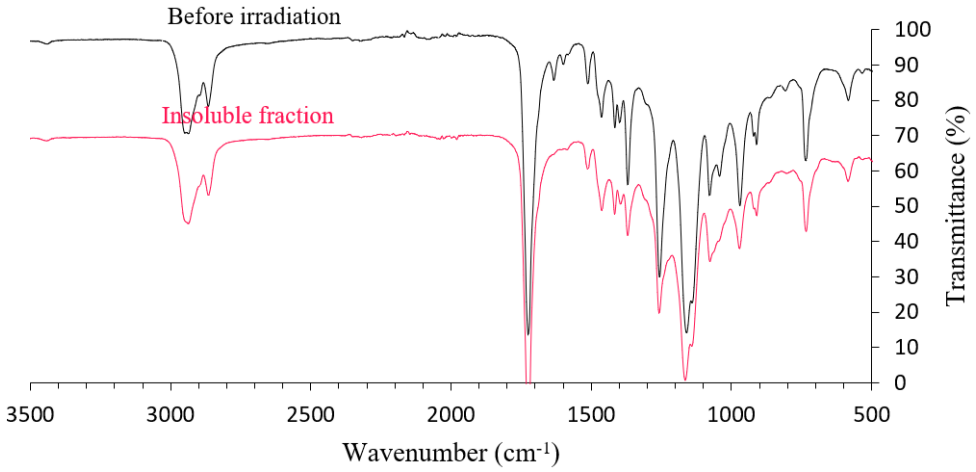

Figure S5.14: FTIR transmittance spectra of the polyester containing 10 % of CD before and after irradiation under UV-A (insoluble fraction), data offset by 30 % from each other.

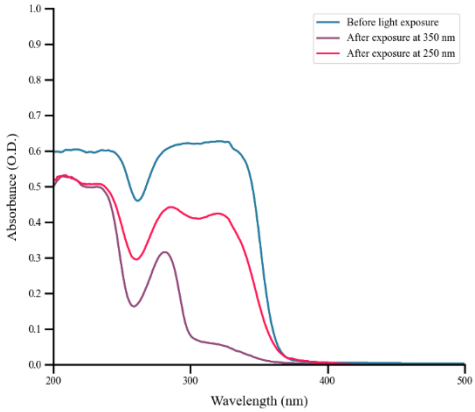

Figure S5.15: Absorption spectra of the polyester containing 50 % of CD before irradiation, after irradiation under UV-A (250 min at 350 nm) and after subsequent irradiation under UV-C (5 min at 254 nm).

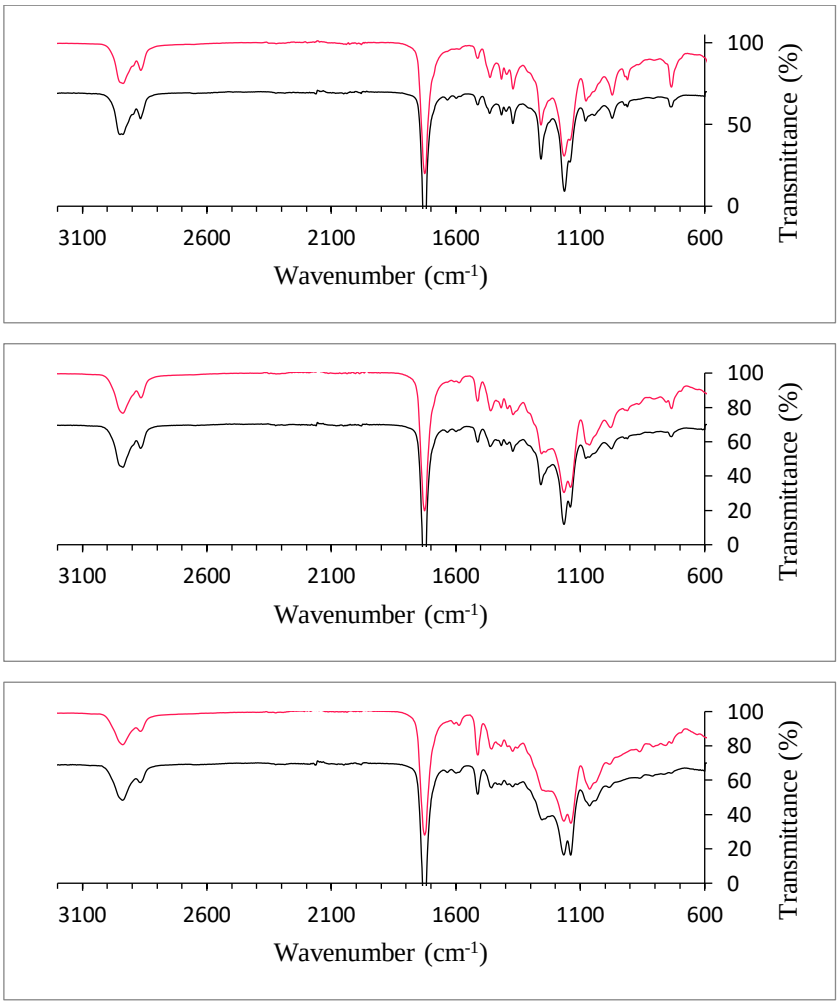

Figure S5.16: FTIR analyses of the insoluble fraction of the polyester containing 10, 20 and 50 % of CD induced by UV-A irradiation after exposure to UV-C light (10 minutes)

Alfred BAZIN

Développement de polyesters aromatiques biosourcés par catalyse enzymatique

Résumé

Le développement de polyesters aromatiques biosourcés via des procédés répondant aux principes de la chimie verte est aujourd'hui au cœur des préoccupations. Pour cela la catalyse enzymatique représente une voie très prometteuse. Néanmoins, la synthèse enzymatique de polyesters à partir de synthons aromatiques biosourcés reste encore peu développée. Dans un premier temps, la polymérisation enzymatique d'un diester de furane a donc été étudiée et a montré l'impact du solvant sur la réactivité du substrat et sur les propriétés du polyester obtenu. L'étude de la polymérisation enzymatique de synthons phénoliques a ensuite démontré la possibilité d'obtenir des polyesters de hautes masses molaires aux propriétés thermiques améliorées à partir de dérivés de l'acide férulique moyennant leur modification par hydrogénation, réduction ou photo-dimérisation. Enfin, la sélectivité de la catalyse enzymatique a été mise à profit pour la synthèse de polyesters issus de dérivés d'acide caféique présentant des propriétés de photo-réticulation réversible, ouvrant la voie vers l'obtention de polyesters aromatiques biosourcés aux propriétés innovantes.

Résumé en anglais

The development of biobased aromatic polyesters via processes in accordance with the principles of green chemistry is nowadays at the heart of the concerns. However, the enzymatic synthesis of polyesters from biobased aromatic building blocks is still a challenge. In a first step, the enzymatic polymerization of a furan-based diester was thus studied and showed the impact of the solvent on the reactivity of the substrate and on the properties of the obtained polyester. The study of the enzymatic polymerization of phenolic compounds then demonstrated the possibility of obtaining high molar mass polyesters with improved thermal properties from ferulic acid derivatives through their modification by hydrogenation, reduction or photodimerization. Finally, the selectivity of enzymatic catalysis was exploited on caffeic acid derivatives to synthesize polyesters with reversible photo-crosslinking properties, paving the way to the elaboration of biobased aromatic polyesters with innovative properties.